2013 Atomic, Molecular, and Optical Sciences Research Meeting

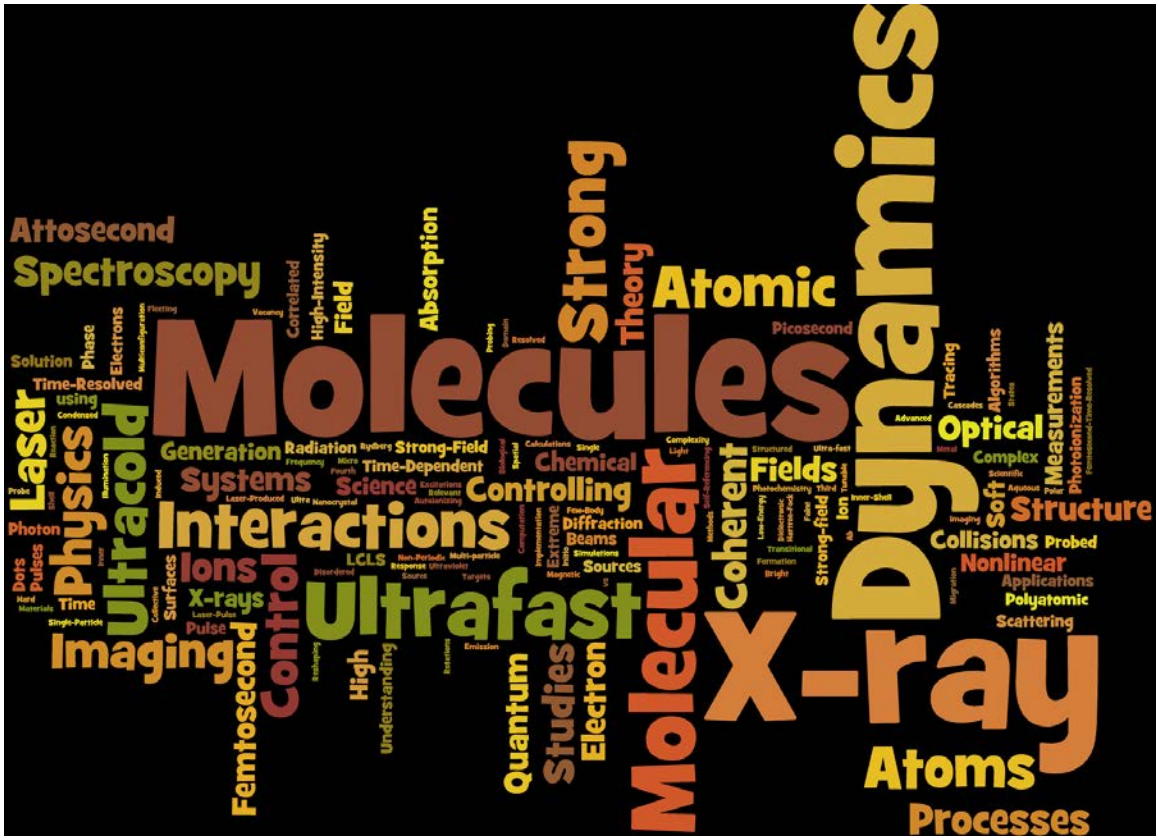

Bolger Conference Center
Potomac, Maryland
October 27-30, 2013

U.S. DEPARTMENT OF ENERGY | Office of Science

Office of Basic Energy Sciences
Chemical Sciences, Geosciences & Biosciences Division

Foreword

This volume summarizes the 33rd annual Research Meeting of the Atomic, Molecular and Optical Sciences (AMOS) Program sponsored by the U. S. Department of Energy (DOE), Office of Basic Energy Sciences (BES), and comprises descriptions of the current research sponsored by the AMOS program. The participants of this meeting include the DOE laboratory and university principal investigators (PIs) within the BES AMOS Program. The purpose is to facilitate scientific interchange among the PIs and to promote a sense of program identity.

The BES/AMOS program is vigorous and innovative, and enjoys strong support within the Department of Energy. This is due entirely to our scientists, the outstanding research they perform, and the relevance of this research to DOE missions. FY 2013 has been an exciting year for BES and the research community. Continuing initiatives included the Early Career Research Program, the Energy Frontier Research Centers and the Energy Innovation Hubs. As illustrated in this volume, the AMOS community continues to explore new scientific frontiers relevant to the DOE mission and the strategic challenges facing our nation and the world.

We are deeply indebted to the members of the scientific community who have contributed their valuable time toward the review of proposals and programs, either by mail review of grant applications, panel reviews, or on-site reviews of our multi-PI programs. These thorough and thoughtful reviews are central to the continued vitality of the AMOS program.

We are privileged to serve in the management of this research program. In performing these tasks, we learn from the achievements and share the excitement of the research of the scientists and students whose work is summarized in the abstracts published on the following pages.

Many thanks to the staff of the Oak Ridge Institute for Science and Education (ORISE), in particular Connie Lansdon and Tim Ledford, and to the Bolger Conference Center for assisting with the meeting. We also thank Diane Marceau, Robin Felder, and Michaelena Kyler-King in the Chemical Sciences, Geosciences, and Biosciences Division for their indispensable behind-the-scenes efforts in support of the BES/AMOS program.

Jeffrey L. Krause
Michael P. Casassa
Chemical Sciences, Geosciences, and Biosciences Division
Office of Basic Energy Sciences
Office of Science
Department of Energy

Cover Art Courtesy of Robin Krause

The input for this wordle was the titles of the abstracts for this year's meeting. The font is Grilled Cheese.

The research grants and contracts described in this document are supported by the U.S. DOE Office of Science, Office of Basic Energy Sciences, Chemical Sciences, Geosciences and Biosciences Division.

Agenda

2013 Meeting of the Atomic, Molecular and Optical Sciences Program

Office of Basic Energy Sciences
U. S. Department of Energy

Bolger Center, Potomac, Maryland, October 27-30, 2013

Sunday, October 27

3:00-6:00 pm	**** Registration ****
6:00 pm	**** Reception (No Host) ****
6:30 pm	**** Dinner ****

Monday, October 28

7:30 am	**** Breakfast ****
8:15 am	*Welcome and Introductory Remarks* **Jeff Krause**, BES/DOE
Session I	Chair: **Ali Belkacem**
8:30 am	*Capturing Electron Dynamics in Atoms and Molecules using VMI and COLTRIMS* **Henry Kapteyn and Margaret Murnane,** University of Colorado
9:00 am	*Inner-shell Transitions using Two Colors* **Steve Southworth,** Argonne National Laboratory
9:30 am	*High Harmonic Spectra and Isolated Attosecond Pulses with Intense Mid-infrared Lasers* **Carlos Trallero,** Kansas State University
10:00 am	**** Break ****
10:30 am	*Probing Complexity Using the ALS and LCLS* **Nora Berrah,** University of Western Michigan
11:00 am	*Breakup of Atoms and Molecules by Multiple Photoionization or Electron Attachment* **Bill McCurdy,** LBNL/University of California, Davis
11:30 am	*Molecular Dynamics with Ion and Laser Beams* **Itzik Ben-Itzhak,** Kansas State University
12:00 pm	*Atomic Electrons in Strong Radiation Fields* **Joe Eberly**, University of Rochester
12:30 pm	**** Lunch ****

Session II Chair: **Dan Haxton**

4:00 pm *Spatial Frequency X-ray Heterodyne Imaging of Micro and Nano Structured Materials and their Time-resolved Dynamics*
Christoph Rose-Petruck, Brown University

4:30 pm *Laser-Produced X-Ray Sources*
Don Umstadter, University of Nebraska

5:00 pm *Strong Field and Nonlinear X-ray Optical Science*
David Reis, SLAC Accelerator National Laboratory

5:30 pm *Probing Liquid Phase Molecular Dynamics with Ultrafast X-rays*
Bob Schoenlein, Lawrence Berkeley National Laboratory

6:00 pm **** Reception (No Host) ****

6:30 pm **** Dinner ****

Tuesday, October 29

7:30 am **** Breakfast ****

Session III Chair: **Phil Gould**

8:30 am *Electron/Photon Interactions with Atoms/Ions*
Alfred Msezane, Clark Atlanta University

9:00 am *Studies of Autoionizing States Relevant to Dielectronic Recombination*
Tom Gallagher, University of Virginia

9:30 am *Low-Energy Electron Interactions with Interfaces and Biological Targets*
Thom Orlando, Georgia Tech

10:00 am **** Break ****

10:30 am *Reactive Scattering of Ultracold Molecules*
John Bohn, University of Colorado

11:00 am *Interactions of Ultracold Molecules: Collisions, Reactions, and Dipolar Effects*
Dave DeMille, Yale University

11:30 am *Cold Molecules: Sensitive Detection and Chirality*
John Doyle, Harvard University

12:00 pm *Cold and Ultracold Polar Molecules*
Jun Ye, University of Colorado

12:30 pm **** Lunch ****

Session IV Chair: **Jim Feagin**

4:00 pm *Photoabsorption by Free and Confined Atoms and Ions*
Steve Manson, Georgia State University

4:30 pm *Electron Driven Processes in Polyatomic Molecules*
Vince McKoy, California Institute of Technology

5:00 pm *Algorithms for X-Ray Imaging of Single Particles*
Veit Elser, Cornell University

5:30 pm *Strong Field Rescattering Physics*
Chii-Dong Lin, Kansas State University

6:00 pm **** Reception (No Host) ****

6:30 pm **** Dinner ****

Wednesday, October 30

7:30 am **** Breakfast ****

Session V Chair: **Mette Gaarde**

8:30 am *Strong Field Ionization as a Probe of Molecular Dynamics and Structure*
Tom Weinacht, Stony Brook University

9:00 am *Tracing and Controlling Ultrafast Dynamics in Molecules*
Andreas Becker, University of Colorado

9:30 am *Structural Dynamics in Chemical Systems*
Kelly Gaffney, SLAC Accelerator National Laboratory

10:00 am **** Break ****

10:30 am *Molecular Response to X-ray Absorption and Vacancy Cascades*
Bob Dunford, Argonne National Laboratory

11:00 am *Time-Resolved Studies of Energy Transfer in Luminescent Lanthanide Complexes*
Jerry Seidler, University of Washington

11:30 am *Optical Two-Dimensional Fourier Transform Spectroscopy of Semiconductor Quantum Dots*
Steve Cundiff, JILA/University of Colorado

12:00 noon *Auger Decay Engineering in relation to Applications of Quantum Dots in Single-Photon Sources and LEDs*
Victor Klimov, Los Alamos National Laboratory

12:30 pm *Closing Remarks*
Jeff Krause, BES/DOE

12:45 am **** Lunch ****

1:00 pm Discussion

3:00 pm Adjourn

Table of Contents

Laboratory Research Summaries (by Institution)

University Research Summaries (by PI)

Laboratory Research Summaries
(by institution)

AMO Physics at Argonne National Laboratory

Gilles Doumy, Robert Dunford, Bertold Krässig,
Anne Marie March, Steve Southworth, Linda Young
X-ray Science Division
Argonne National Laboratory, Argonne, IL 60439
gdoumy@aps.anl.gov,dunford@anl.gov,kraessig@anl.gov
amarch@anl.gov,southworth@anl.gov,young@anl.gov

Norbert Scherer
Chemistry Department
University of Chicago, Chicago, IL 60637
nfschere@uchicago.edu

1 OVERVIEW

The Atomic, Molecular, and Optical Physics program aims at a quantitative understanding of x-ray interactions with atoms and molecules from the weak-field limit explored at the Advanced Photon Source (APS) to the strong-field regime accessible at the Linac Coherent Light Source (LCLS). Single photon x-ray processes can be dramatically altered in the presence of strong optical fields, and we exploit ultrafast x-ray sources to study these effects. Conversely, the atomic or molecular response to strong optical fields is itself of great interest due to the discovery of phenomena such as high-order harmonic generation and attosecond pulse generation. The use of tunable, polarized x-rays to probe such processes *in situ* can lead to new physical insights and quantitative structural information not accessible by other techniques. Optical lasers can also trap, orient, and order nanoparticles, providing a new route towards manipulation and assembly of nanomaterials. We are developing an optical trap for x-ray diffraction and spectroscopy measurements at the APS. Theory is a key component of our program by predicting phenomena that motivate experiments and by simulating and interpreting measured results. Nonlinear and multiple-photon phenomena in x-ray and inner-shell interactions are explored using the intense, femtosecond x-ray pulses generated at the LCLS free-electron laser. The APS remains our primary source of intense, tunable, polarized x rays both for time-resolved laser-pump/x-ray-probe experiments and for basic studies of x-ray interactions with atoms, molecules, and complex systems such as solvated molecules and nanoparticles. To exploit the full x-ray flux available at the APS, we are using high-repetition-rate laser systems for pump-probe experiments at MHz pulse rates. This capability enables measurements of laser-induced, transient electronic and atomic structures with high sensitivity.

2 INTENSE X-RAY PHYSICS

Pulse duration measurements at LCLS

(G. Doumy, A. L. Cavalieri,[1] M. Meyer,[2] and other collaborators)

The LCLS x-ray free electron laser is capable of producing very intense x-ray pulses believed to be as short as a few femtoseconds. Those properties have already revolutionized the field of ultrafast time resolved x-ray science, in spite of the current lack of exact determination of the pulse duration characteristics. Any measuring scheme is rendered even more challenging by the operating mode of

LCLS, called SASE (Self Amplified Spontaneous Emission), which makes it a purely chaotic source and ultimately requires a single shot measurement of every shot to get a full characterization of the source properties. In addition, the SASE operation produces an inherent temporal jitter between the x-ray pulses and any other laser source operating in parallel, which limits greatly the resolution of pump-probe techniques commonly used in time-resolved measurements.

The main route followed by our large collaboration to get a handle on those temporal properties consists in transferring the time properties of the x-ray pulses to electron wave-packets produced during ionization of a gas target or subsequent Auger decay. The simultaneous presence of a strong laser field (operating in the visible, IR or THz region) modifies the energy spectrum of those electrons wave-packets in a deterministic way. When the x-ray pulse duration is comparable with (or shorter than) the oscillation period of the laser, it becomes possible to use a streaking mode, where there is a one-to-one correspondence between the measured photoelectron energy and the time of emission. It is then possible to extract from the measured final energy distribution some of the properties of the x-ray pulses, as long as it is possible to ascertain the relative position between the x-ray pulse and the streaking ramp. This is readily done when using a long wavelength, THz laser pulse, since the half optical cycle is longer than the pulse duration and the timing jitter combined. However, this seriously limits the temporal resolution of the method, since the extent of the streaking in energy is limited by the need to get a good resolution over a large range of electron energies.

Several improvements have been proposed and tested. First, using a different method to generate the THz field (an organic crystal directly pumped in the IR), one can obtain a strong single cycle pulse with a 150 fs ramp. Combined with advanced methods to measure the arrival time of the x-ray pulses relative to the laser on a shot to shot basis with 25 fs resolution, a jitter correction of 10 fs fwhm, as well as a 25 fs time resolution between two successive x-ray pulses have been demonstrated. Progress in the shot to shot determination of the jitter correction allows us to use even faster ramps, provided in principle that the laser field has a fixed carrier-to-envelope phase. We have demonstrated, however, that this limitation can be lifted if simultaneous measurements of the streaking of photoelectron and delayed Auger electrons are performed (see next item). This new insight should allow performing those temporal measurements on ultrashort x-ray pulses with a resolution good enough to resolve the spiky structure associated with the SASE operating mode.

Self-referencing time domain measurements of femtosecond inner shell dynamics
(G. Doumy, L. F. DiMauro,[3] A. L. Cavalieri,[1], M. Meyer,[2] and other collaborators)

The availability of ultrashort x-ray laser pulses opens the potential of following ultrafast electronic and nuclear movements with atomic resolution. However, as was detailed before, the timing jitter between the x-ray pulses and any external source can dominate the temporal resolution of the measurements. New techniques to measure that jitter on a shot by shot basis allow for a $\sim$25 fs resolution correction, but this is still much longer that the shortest pulses created by the XFELs.

We propose a potentially very general technique to overcome this limitation when the observables are electrons (either photoelectrons or Auger electrons), by extending the laser streaking technique to measure simultaneously both the timing of direct photoionization from the x-ray pulse and the time dependent feature of interest. Measuring the photoionization event allows one to create, on a shot by shot basis, an absolute reference for the timeline of events being triggered by that pulse. Because this timing is extracted for every shot, events with low statistics can then be correctly added up to yield high quality data in the time domain. The objective is to measure, for every shot, the streaked energy spectra of both the photoelectron and the other electrons of interest. A streaked photoelectron spectrum collected with good statistics allows determining, for a particular shot, the relative position inside the streaking ramp. Then, determining the amount of

streaking experienced by the other electrons that are detected can directly indicate their emission time inside the ramp and relative to the x-ray pulse.

The concept is represented in Fig. 1, and some requirements for the parameters appear clearly. First, in order to observe, in the time domain, the emission times lasting a few femtoseconds, the streaking ramp needs to be much longer than the x-ray pulse, say at least 20 fs long, while increasing the wavelength of the laser too much limits the time resolution of the streaking technique, taking into account that the extent of the streaking in energy is limited by the resolution of the electron spectrometer. A good compromise is found using infrared light around 17-18 μm, with a 28-30 fs half cycle, easily obtained with optical parametric amplifiers. This does require being able to pinpoint the specific streaking ramp (i.e. half optical cycle) inside the IR pulse, a task that can be performed using the previously mentioned jitter correction techniques if the laser is CEP stable.

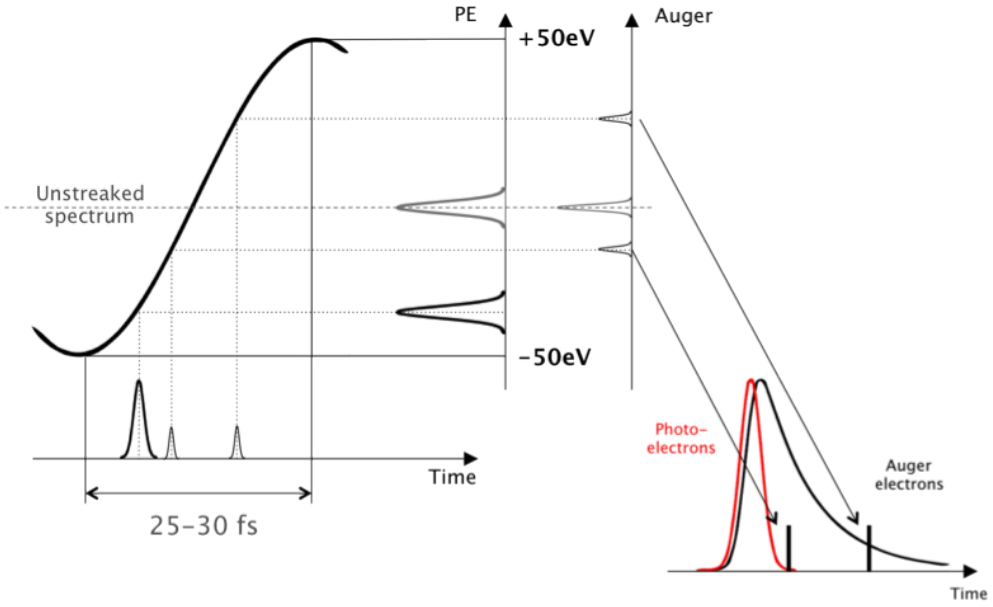

Figure 1: Concept for self-referenced timing measurement: inside the streaking ramp, the x-ray pulse emits photoelectrons whose energy is modified by the laser field, allowing referencing of the x-ray pulse inside the ramp. The electrons emitted by the process of interest (e.g. Auger decay) are also streaked and independently positioned relative to the ramp, and thus relative to this particular x-ray pulse. Statistics can then be accumulated to yield the time profile of the emission.

As a proof of principle, in an experiment at the LCLS, we tried to obtain time domain measurements of Auger decay lifetimes in atoms (Neon) and small molecules containing Carbon atoms (CO_2 and CF_4), in order to verify the influence of the chemical environment. Short x-ray pulses were obtained at 1keV (Neon) and 450 eV (Carbon) by using the low bunch charge mode of operation, in addition to the emittance spoiler in the bunch compressor. More than 20 μJ of 17 μm light was used to obtain a strong streaking field, allowing for measuring simultaneous streaking of the photoelectron and the Auger electrons. Unfortunately, the electron time-of-flight spectrometer designed to record the Auger electron spectrum with high resolution did not function properly. However, we were able to record both photo- and Auger-electrons with the same spectrometer, at the expense of resolution. In particular, we found that we were able to determine, for every shot, the position of the peak of the emission, in time, of both kinds of electrons, and the small delay between the two peaks due to the finite Auger lifetime can be used to extract the slope of the

streaking field. This allows determining the streaking conditions regardless of whether the laser field is CEP stable or not. Analysis of the data is ongoing.

Seeded vs SASE: ultra high-intensity, hard x-ray interactions with atoms
(L. Young, G. Doumy, R. W. Dunford, E. P. Kanter, B. Krässig, A. M. March, D. Ray, S. H. Southworth, J. Vila-Comamala, C. Buth, C. David,[4] D. Sokaras,[5] R. Alonso-Mori,[6] C. Bostedt,[6] H. Lemke,[6] D. Zhu,[6] M. Chollet,[6] R. Santra,[1,7] S.K. Son[1])

We are proposing an LCLS experiment to explore hard x-ray interactions in nickel atoms at intensities approaching 10^{20} W/cm^2 using near transform-limited and SASE pulses. Ultraintense x-ray interactions with transition metal atoms are of intrinsic interest as they are qualitatively different from those involving the second row elements, e.g. neon, in that intermediate electron shells can be addressed selectively. In this photon energy regime (7.4–9.4 keV) at ultrahigh intensities, broadband SASE pulses are predicted to initiate then facilitate chain reaction ionization via successive resonance excitation, whereas narrowband seeded pulses cannot. Understanding electron dynamics in transition metal atoms is also vital for establishing the reliability of multiple wavelength anomalous dispersion (MAD) phase retrieval methods at high intensity. Therefore, we plan to characterize ultraintense x-ray interactions with nickel atoms using ion time of flight and x-ray emission spectroscopies for three relevant photon energy regimes as a function of bandwidth, pulse energy and pulse duration. The nickel atom is an ideal target for self-seeded operation at LCLS.

The clean, atomic target will be provided by using a relatively simple laser ablation source. Using an ultrashort laser pulse, a dense target plume is created, containing atoms and nanoparticles that are well separated in time. To develop the ablation source and measure the density of the atomic plume, a first experiment will be performed at the Advanced Photon Source. An initial test of the atomic theoretical modeling will also be obtained by measuring the nickel charge-state distribution following K-shell ionization.

Hetero-site-specific femtosecond-time-resolved dynamics
(A. Picón, S. H. Southworth, P. J. Ho, G. Doumy, E. P. Kanter, B. Krässig, A. M. March, D. Ray, L. Young, S. T. Pratt,[8] J. R. Hammond,[9] Á. Vázquez-Mayagoitia,[9] N. Govind,[10] A. Rudenko,[11] C. Bostedt,[6] D. Rolles,[1] B. Erk,[1] and C. Bomme[1])

Core-hole decay in molecules is a fundamental process far less understood than in isolated atoms. When an x-ray photon is absorbed by a molecule, a core-shell electron can be promoted to an unoccupied valence orbital or to the continuum, leaving a core-hole in the molecule. The core-hole decay will trigger a cascade of processes all occurring at the same time: Auger electron emission, fluorescence photon emission, dissociation/fragmentation of the ion/neutral molecule, energy transfer, and charge transfer. The advent of XFELs and the concept of "diffract-before-destroy" for biomolecular coherent imaging [40] have created a significant need to understand molecular core-hole dynamics as it is responsible for radiation damage.

In a previous experiment we used synchrotron x rays to create deep core-holes in Xe both for the atom and for the XeF_2 molecule [14]. XeF_2 is a unique molecule as it allows to directly compare its dynamics induced by the core-hole decay in Xe with its atomic homologue. We measured charge states and fragmentation energies using x-ray/ion coincidence spectroscopy. The experimental results showed evidences of a strong charge/energy transfer during the core-hole decay. However, as we have access only to the final produced ions, it is difficult to track the intermediate induced dynamics.

A recently developed capability at LCLS allows the generation of two-color x-ray pulses with controlled delay on the femtosecond time scale [41]. With such capability we can perform pump-probe experiments to follow the intermediate hole-state dynamics. The level diagram sketched in

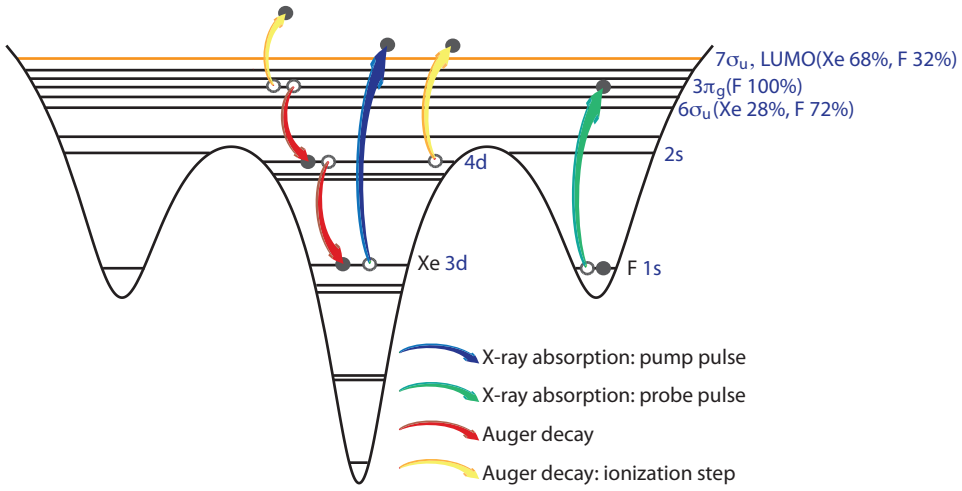

Figure 2: Sketch of the dynamics in XeF_2 triggered by a core-hole created in Xe. We show an example of how we can track a specific intermediate path by using the probe pulse to resonantly excite F to the induced holes.

Fig. 2 illustrates the two-pulse method. A pump pulse will create a 3d core-hole in Xe. During the core-hole decay, holes will be created in higher orbitals and reach the valence shells that form the molecular bonds. The probe-pulse time delay and energy will be tuned to resonantly excite transitions from F 1s to the time-dependent holes induced during the decay. With this approach we can identify specific intermediate paths and their formation time scales during the molecular core-hole dynamics. By using the LAMP chamber with a time and position sensitive detector (a "reaction microscope") to record the ion fragments in coincidence, we can characterize the ion-ion correlations and energetics. Our collaboration is also developing theoretical methods to simulate the dynamics.

3 X-RAY PROBES OF MOLECULAR DYNAMICS

Ultrastable, high-repetition rate, tunable picosecond x-ray pulses at the Advanced Photon Source

(R. Reininger, L. Young, A. M. March, G. Doumy, S. H. Southworth, P. Evans, D. Keavney, E. M. Dufresne, Y. Li, M. Beno, M. Borland, and collaborators)

The APS Upgrade project as described in the December 2012 CD-2 review had as a key component the worlds first ultra-stable, high-repetition-rate, high-average flux, widely tunable, and polarized ultrafast x-ray source (SPX). The pulses of 1-2 ps duration were to be generated from the Zholents scheme of chirping and unchirping electron bunches in the storage ring [42]. This class of x-ray source allows the full range of synchrotron characterization techniques (linear x-ray probes of matter) to be used with a time resolution improved from the current ∼100 ps to ∼1 ps, and thus be complementary to free-electron laser sources for investigating phenomena at timescales of 1-ps and longer. Gentle, linear x-ray probes at high-repetition-rate are preferable for systems where repetitive pump-probe cycles are used to monitor triggered/controlled dynamics. The few picosecond timescale is particularly relevant for nanoscale phenomena, where material and chemical dynamics can be governed by the speed of sound (∼ 1nm/ps), and molecular rearrangement of solvent and solute molecules.

In preparation for the SPX facility, a suite of three beamlines was fully designed with the

guiding principle of versatility of x-ray pulse parameters (pulse duration, repetition rate, bandwidth, polarization). Two insertion device beamlines served the hard x-ray regime and one the soft x-ray regime. The parameters of the beamlines are shown below.

Hard and Soft X-ray Beamlines	**Energy Range Bandwidth (ΔE/E)**	**Pulse duration, Repetition Rate Spot size, Flux, Comments**
SPX Spectroscopy & Scattering	4 - 35 keV 10^{-4} - 10^{-2}	2, 10, 100 ps; 6.5 MHz - 271 kHz C station: 6.4×6.4 μm^2, 2.2×0.06 mrad^2 D station: 2.7×3.4 μm^2, 4.0×0.02 mrad^2 10^{11}, 10^{12}, 10^{13} x-rays/s for 10^{-4} BW
SPX Imaging & Microscopy	7 - 14 keV 10^{-4}	2-80 ps; 6.5 MHz Sample: 33×14 μm^2, 0.9×1.3 mrad^2 Time dispersion at sample - 0.052 ps/μrad 50 nm @ zone plate microscope
SPX Soft X-ray Spectroscopy	200-2000 eV 5×10^{-4}, 2×10^{-4}	1.5-100 ps; 6.5 MHz Source Dispersion: 25 ps/mm Sample: 10×10 μm^2, 4×4 mrad^2 2×10^9 x-rays/s for 5×10^{-4} BW Linear and circular polarization

One publication describes ray tracing of the novel short pulse x-ray imaging and microscopy time-angle correlated diffraction beamline [28] where, in principle, the entire pulse could be dispersed on a standard area detector to achieve a time history with range 80 ps and resolution ∼2 ps. A second publication describes the complete design of a polarized soft x-ray beamline [29], where the bend magnet source is imaged, thus providing the possibility of rapid polarization switching by collecting radiation above and below the electron orbital plane. In addition, a document outlining First Experiments that could be done with the SPX was created [30] with the help of a significant outside user community with experiments in general areas: Ultrafast Dynamics in Nanoscale Materials and Nanodevices, Nanoscale Thermal Transport, Quantum Materials, Chemical Dynamics in Condensed Phases, Biological Sciences and Biomaterials.

Subsequent to the July 2013 BESAC report that encouraged the APS to incorporate a multibend achromat (MBA) lattice into the ring in order to yield much increased brightness and approach a diffraction-limited x-ray beam, significant effort has been devoted to the design of a new lattice. At this point, it appears that the time-structure of the present ring can be preserved with the present current per bunch, thus permitting time-resolved experiments [31]. Concomitantly, design and testing of alternative rf-delection cavities that could be used in the new MBA lattice is being carried out in collaboration with the Argonne Physics Division. It will be an exciting time as one explores the versatility of the next generation of storage ring with significantly enhanced brightness.

Time-resolved x-ray absorption and emission spectroscopy of photoexcited ferrocyanide ions in aqueous solution

(A. M. March, G. Doumy, S. H. Southworth, E. P. Kanter, B. Krässig, R. W. Dunford, D. Ray, L. Young, A. Galler,[2] A. Bordage,[12] C. Bressler,[2] G. Vankó,[12] and W. Gawelda[2])

Extending the well-developed x-ray techniques to the time domain has been at the forefront of research this last decade. The perspective to gain direct structural and electronic information on transient species is tantalizing, but a lot of development is still needed to bring those techniques to their full potential. We have continued our work with our international collaborators from the European XFEL and Budapest to further develop our high repetition rate setup at APS beamline 7ID-D for studies of photochemical processes in condensed phase molecular systems. With the aim of expanding the time-resolved x-ray emission spectroscopy (XES) techniques we demonstrated

with the measurements on Fe(II) spin-crossover complexes, namely $K\alpha$ (1s-2p) and $K\beta_{1,3}$ (1s-3p) spectroscopy, to include the even more flux demanding valence-to-core spectroscopies, $K\beta''/K\beta_{2,5}$, we have studied the model system $[Fe(II)(CN)_6]^{4-}$ (ferrocyanide) in an aqueous solution after laser excitation using x-ray absorption spectroscopy (XAS) and XES. We studied the system with 10 ps laser pulses at 355 nm, where the photoexcited state is believed to evolve into the pentacyano-aquo complex $[Fe(II)(CN)_5H_2O]^{3-}$ via ligand dissociation, and also at 266 nm where the excited state can also lead to photo-injection of an electron into the solvent, concomitant to the oxidation state change of the iron center, yielding $[Fe(III)(CN)_6]^{3-}$. XANES data and XES $K\beta_{1,3}$ (1s-3p) data were collected at both wavelengths and good statistics EXAFS data were collected at 355 nm. We also recorded the first picosecond transient valence-to-core XES spectrum, upon 266 nm excitation, although with very few points due to the long integration time that was required and the finite length of the beamtime. Initial analysis of the XANES and XES data indicates that the spectra at 266 nm excitation are due to the presence of both $[Fe(II)(CN)_5H_2O]^{3-}$ and $[Fe(III)(CN)_6]^{3-}$. As shown in Fig. 3, by comparison of the spectra at the two excitation wavelengths, we are able to quantify the contributions from each species and thus reconstruct the absorption spectrum of the pentacyano-aquo complex intermediate. EXAFS analysis should yield the structure of this intermediate. A manuscript for publication of these results is in preparation.

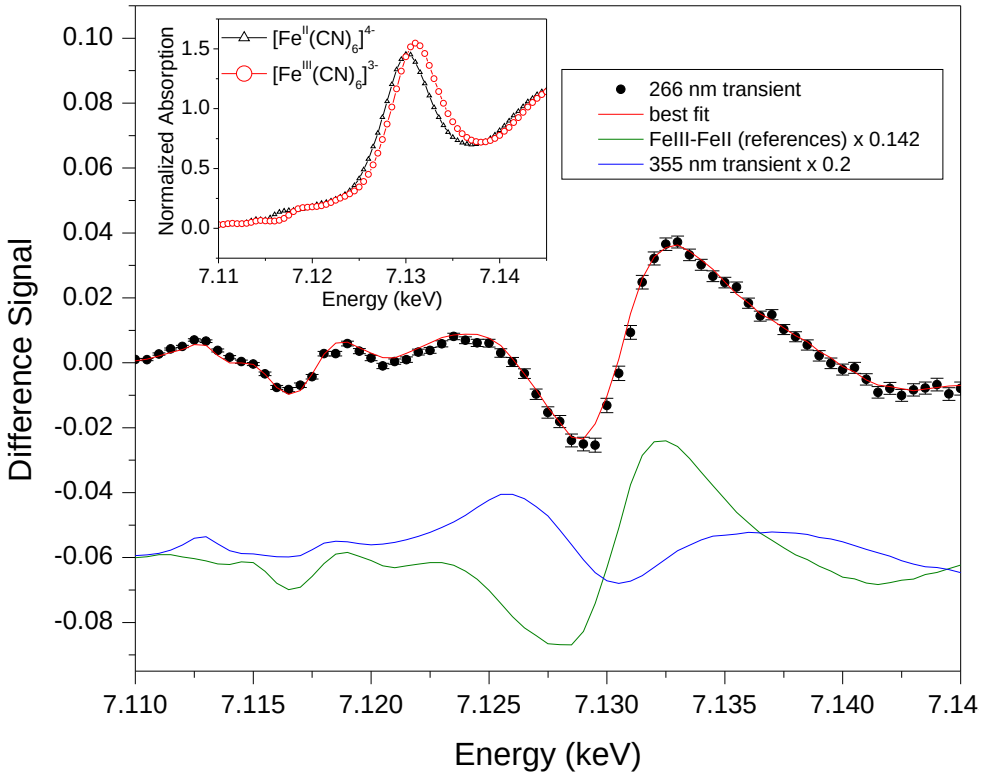

Figure 3: XANES transient signal obtained in $Fe(II)CN_6^{4-}$ after excitation at 266 nm. The red curve corresponds to the quantitative separation between the two competing processes: (1) oxidation with formation of $Fe(III)CN_6^{3-}$, with a difference spectrum measured using static references shown in the inset, and (2) ligand dissociation, with a difference spectrum obtained after excitation at 355 nm where it is the only process.

Molecular response to x-ray absorption and vacancy cascades

(R. W. Dunford, S. H. Southworth, E. P. Kanter, G. Doumy, B. Krässig, D. Ray, and Y. Gao)

This project aims to study decay processes in electronically excited molecules. Apart from the importance of these studies to extending our knowledge of molecular physics, there is strong motivation for more practical reasons. For example, recent cancer therapy in which iodinated compounds are inserted into tumorous regions and irradiated with high energy x-rays [43] appear promising, and a better understanding of the mechanisms of the decay processes following irradiation would allow an optimization of these techniques. One of the contributing mechanisms, Interatomic Coulombic decay (ICD), is also of interest. This is a fast decay mode (femtoseconds) and leads to the release of both low energy electrons and energetic free radicals arising from the Coulomb explosion following the vacancy decay process. Both the low-energy electrons and the ions can cause damage to biological systems [44]. The availability of high energy x-rays from the Advanced Photon Source provides the opportunity to study the relatively unexplored regime in which the initial molecular excitation occurs in a deep inner-shell of a heavy atom. With regard to the biological effects of ionizing radiation, it is interesting to note that while low-energy ($\sim$0-20 eV) secondary electrons are implicated in the breaking of DNA strands [45], the studies of Corde *et al.* [43] on radiotoxicity enhancement by x-ray absorption of tumors injected with iodine compounds find the best effects at an x-ray energy of 50 keV that generate 17 keV photoelectrons. This result is attributed to the increased penetration of high-energy electrons in tissue [46].

Our goal for this project is to understand the physics behind the molecular fragmentation probabilities and the kinetic energy release following ionization of a heavy atom component in a molecule. The proposed work includes a theoretical component to calculate the charge state distributions expected from vacancy decay following inner shell ionization of atomic Kr, Xe, Br, and I. These calculations will provide a benchmark of our atomic description for comparison with data for the molecular experiments in IBr and XeF_2. We also plan to explore the effect on these processes experimentally by changing the distance between atoms in the molecules. To do this we can choose molecules with low-Z spacer atoms between two heavy atoms in different molecules. The results of these studies, together with the theoretical calculation for the isolated atoms, will provide some insight into the mechanisms governing the final state distributions.

In recent work [14], we observed molecular effects in vacancy cascades of the molecule XeF_2. Our method was to compare the total charge produced in atomic Xe to that produced in XeF_2 following K-shell ionization of Xe. The yields of the final charge states were measured in coincidence with x-ray fluorescence. Since the x-ray detector was able to resolve the $K\alpha$ and $K\beta$ lines, this coincidence provided a tag on the initial state in these events. This work showed evidence that the total charge produced in the XeF_2 molecule was larger than that produced in the isolated Xe atom, an observation that has been attributed to an ICD-like effect. These results led to theoretical work in which the cascade decay from Xe following K-shell ionization was simulated, taking into account Auger and Coster-Kronig rates, fluorescence rates, and shake-off branching ratios. It was found that the appearance of 5p electrons signals the time scale for participation of the molecular orbitals and when ionization of F atoms is expected. The results of this analysis indicated that the F atoms participate in the decay cascade during the fragmentation process and this lowers the kinetic energy release (KER) in comparison to a model in which the KER is estimated based on the ground state Xe-F intermolecular distance. This reduction in KER is in qualitative agreement with experimental observations [14].

In order to explore the theoretical model further, the KER [14] associated with a given breakup mode must be known to good accuracy. In the initial XeF_2 experiment, we were only able to measure the KER averaged over all Xe charge states and this was not sufficient to make a detailed comparison with theory. So we set about making a new apparatus with a position-sensitive ion

detector, which allows a complete reconstruction of each ion fragmentation event, and we now have the capability to more fully test the theoretical calculations. In addition to gaining a further understanding of the molecular fragmentation process in the hard x-ray regime, the new apparatus is being used to explore the more general question of what are the most probable breakup modes and KERs for a molecule following deep inner-shell photoionization of a heavy atom constituent.

We have begun to study other systems starting with the simple binary molecule IBr. For IBr, the APS has the capability for creating K-shell holes in either the Br atom at 13 keV or on the I atom at 33 keV. These data will allow us to extract breakup probabilities and KERs for these molecules for two different excitation modes and compare with theoretical calculations based on atomic theory. The differences between the calculations and the data will provide insight into the molecular specific effects such as ICD. For comparison we have also used similar techniques to study the molecule CH_2BrI in order to begin to explore the effect of changing the separation between the I and Br atoms in a molecule. Data analysis is in progress, but it is already apparent that the improved apparatus with its faster electronics, multi-hit position-sensitive detector, and increased detection efficiency have removed the ambiguities in the charge-state distributions that plagued the earlier study of XeF_2.

A further upgrade to the apparatus in the near future would add the capability to trigger events on photoelectron/ion or Auger/ion coincidences in addition to the K-x-ray/ion coincidences being used currently. This improvement would allow the study of all the ions produced in an interaction, including those whose initial decay is via Auger emission. Data obtained with this improved apparatus would provide a more complete picture of the vacancy decay following inner shell ionization.

4 CONTROL OF X-RAY AND INNER-SHELL PROCESSES

X-ray scattering from laser-aligned molecules

(B. Krässig, G. Doumy, P. J. Ho, E. P. Kanter, A. M. March, D. Ray, S. H. Southworth, L. Young, R. W. Henning[13], I. Kosholeva[13])

This work builds upon our previous demonstration of an x-ray microprobe of laser-aligned bromotrifluoromethane (CF_3Br) molecules [62]. As in the previous work, the duration of the x-ray probe pulse is ∼100 ps, which is of similar magnitude as molecular rotational periods, and TW laser pulses with ∼120 ps duration are used to produce quasi-adiabatic molecular alignment in a gaseous sample cooled by supersonic expansion. Whereas in our previous work the x-ray probe was based on resonant x-ray absorption and fluorescence detection, the goal of this work is to collect diffraction patterns of coherently scattered x-rays from laser aligned ensembles of molecules, guided by theoretical predictions made in our group [61, 63, 64]. The successful demonstration of coherent x-ray scattering from a molecular beam requires significantly higher x-ray flux and sample density than in the work of Ref. [62]. We use beamline 14-ID-B at the Advanced Photon Source, which has two in-line undulators and produces x-ray pulses of 10^{10} photons per pulse in pink beam operation ($\Delta E/E$∼2%) and a pulsed Even-Lavie valve as the molecular beam source.

The focus of this work during the past year was still mainly on issues of instrumentation. We implemented the laser beam path and laser-x-ray overlap tools. In our current geometry the laser beam and x-ray beams copropagate collinearly to maximize overlap in the focal regions at the scattering center. The laser beam is coupled in at right angles to the x-ray beam using a 1" square mirror at 45° with a 300-μm diameter hole to pass the focussed x-rays. Downstream of the scattering center are the x-ray beam stop and on the front of it a small 4-mm diameter mirror, also with a 300 μm diameter center hole for the x-ray beam and tilted at ∼5° to back-reflect the laser beam onto a power meter. The laser beam is aligned to the centers of the two mirror holes to approximate collinearity, and the holes were chosen small so as to limit the loss of laser intensity

on the 45° mirror and the amount of laser power leaking onto the x-ray beam stop. The size of the beam stop mirror was chosen small to minimize its shadow on the x-ray area detector. In this setup we obtained a 28-μm laser focal waist with 4.5 mJ pulse energy in the interaction region. Spatial and temporal overlap can be adjusted and checked using a remote-controlled pinhole/knife edge/photodiode assembly. The laser beam components are mounted on dedicated pre-configured breadboards to facilitate the setup, alignment, spatial and temporal overlap, performed every beam time after the vacuum chamber has been aligned to the focussed x-ray beam at the experimental end station.

Optically-dressed resonant Auger processes induced by high-intensity x rays
(A. Picón, P. J. Ho, G. Doumy, and S. H. Southworth)

X rays interacting with atoms and molecules produce inner- or core-shell excitations, i.e. an x-ray photon is absorbed by the atom or molecule and an inner- or core-shell electron is promoted to an unoccupied valence orbital or to the continuum (ionization). A core-hole left by the x-ray absorption is unstable and decays very fast (for Ne it is 2.4 femtoseconds). During the decay the atom reorganizes itself by emitting a photon (fluorescence) or by emitting an electron (Auger decay). Therefore, the study of Auger processes constitutes the major cornerstone of light-matter interactions in the x-ray regime.

The combination of x-ray/XUV light with strong optical fields (10^{10}-10^{15}W/cm^2) introduces a new degree of controllability exceptionally beneficial for pump-probe experiments [47, 48, 49], optical control of x-ray absorption [37, 38, 24], and x-ray pulse characterization [3]. In these experiments inner- or core-shell holes are created, triggering the emission of electrons from Auger processes. However, the Auger electron is streaked by the optical field during the electron emission and a proper understanding of the light-matter interaction is needed to analyze the spectrum. In particular, when the Auger electron emission occurs during a significant change of the optical vector potential, the electron wavepacket interferences give rise to a multipeak structure in the spectrum; the so-called sidebands [50, 51, 10]. The sidebands are related to the above-threshold ionization (ATI) phenomenon, and analogously to ATI, every sideband-peak is separated by an optical photon energy.

In a previous work, see Ref. [26], we made an important contribution in the understanding of the Auger electron spectrum with strong optical fields. We developed a theoretical model for Ne atom, focusing on resonant Auger processes (when the core-shell electron is promoted to an unoccupied valence orbital) [52]. We unveiled the two main effects: 1) the envelope of the sidebands contain information about the angular emission asymmetry of the resonant Auger electron, and 2) the appearance of new peaks in the spectrum due to optical resonant couplings during the Auger decay (i.e. the electron in the valence orbital can be further resonantly coupled to other valence orbitals).

In a recent work [32], we used the theoretical model developed in Ref. [26] to study self-seeding high-intensity x rays for Ne^+. Free-electron lasers (FELs) can achieve very high intensities (more than 10^{15} W/cm^2), an important feature to produce nonlinear processes in the x-ray/XUV regime [39]. Self-seeding and optical-laser-seeding methods are being developed at FELs that produce x-ray/XUV pulses with high temporal coherence [53, 54]. The combination of high intensity and high coherence enables population control via Rabi oscillations [55, 2]. We observed that the high-intensity and coherent x rays control the core-shell state dynamics and therefore control when Auger decay occurs. In particular, allowing Auger decay only during the maxima of the optical vector potential, we observe a strong optical streaking that produces asymmetries in the energy emission of the Auger electron, see Fig. 4. In Ref. [32] we have studied such asymmetries in detail and our simulations show that they are very sensitive to the x-ray and optical parameters due to the intrinsic coherence of the whole process. We believe that these asymmetries have strong relevance

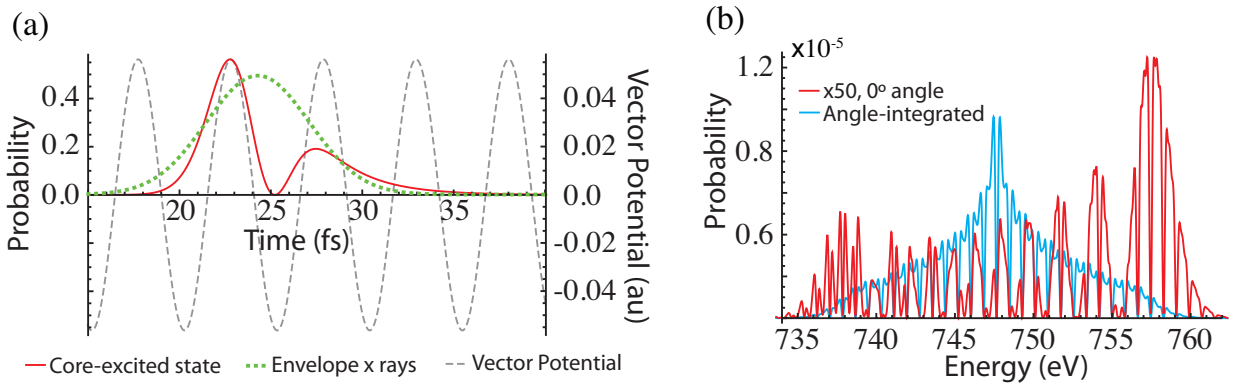

Figure 4: High-intensity x rays (gaussian profile, peak intensity 1.4×10^{16} W/cm^2 and FWHM 3.33 fs) resonant with the Ne^+ transition $2p^5 \leftrightarrow 1s^{-1}2p^6$ (decaying to the final ion $2s^{-2}(^1S)$). Ne^+ is under a strong optical field (continuous wave, λ=1.5 μm, and peak intensity 10^{11} W/cm^2). (a) Evolution of the core-excited state ($1s^{-1}2p^6$) population (red line) compared with the optical vector potential and x-ray envelope. Auger decay rate is maximum in the maxima of the optical vector potential. (b) Auger electron spectrum for the same case considered in (a). Strong asymmetries are shown in the spectrum measured in the 0° angle (parallel to the optical field polarization). No asymmetries are observed in the angle-integrated Auger electron spectrum, see Ref. [32] for further details.

for future pump-probe experiments, optical control schemes of x-ray absorption, and x-ray pulse characterization in FELs.

Attosecond extreme ultraviolet vortices from high-order harmonic generation
(A. Picón, C. Hernández-García,[14] J. San Román,[14] and L. Plaja[14])

Light beams can transport spin (SAM) and orbital (OAM) angular momentum, related to its polarization and spatial structure respectively. For infrared (IR) and optical wavelengths, light beams with well-defined OAM can be generated using diffractive masks to imprint a phase twist in the wavefront. Although in the x-ray regime similar methods can be found [56], high-quality diffractive masks are not so easy to produce.

In a recent collaboration with the Universidad of Salamanca, we have shown theoretically that it is possible to create x-ray vortices through high-harmonic generation (HHG) [33]. HHG is an extreme nonlinear process in which an electron is removed from an atom by an IR laser and subsequently driven back to the parent ion during the same laser field oscillation. Upon recollision, the electron recombines with the parent ion and emits ultrashort x-ray flashes at the attosecond timescale (10^{-18} s). Using HHG we have shown that it is possible to generate helical pulses in the x-ray regime that inherit the temporal and spatial coherence of the IR laser. The combination of OAM with the spatio-temporal characteristics of HHG leads also to the prediction of twisted attosecond pulse trains, see Fig. 5. Our work merges two distinct topics in Optical Science, a joining of fields with promising perspectives for nonlinear and attosecond physics, optical and quantum communications, ultrafast micromanipulation, microscopy, and spectroscopy, among others.

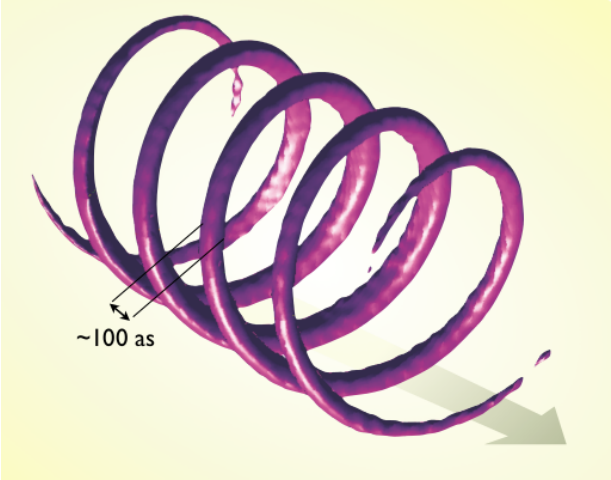

Figure 5: Numerical results of a twisted attosecond x-ray pulse train obtained through high-order harmonic generation. See Ref. [33]

5 OPTICAL CONTROL AND X-RAY IMAGING OF NANOPARTICLES

Optical control of metal nanowires and single-particle x-ray diffraction
(N. F. Scherer,[15] M. Pelton,[16] J. Guest,[17] Y. Gao, U. Manna,[15] S. H. Southworth, L. Young and collaborators)

We have built on our preliminary demonstration that silver nanowires could be stably trapped in three dimensions using appropriately shaped optical fields. We constructed a trapping configuration based on shaping a focused laser into the Fourier transform of a Bessel function, in order to obtain an extended focal spot and depth of focus, and reflecting this beam back onto itself, in order to cancel out radiation pressure. Using this interferometric Bessel-beam trap, we obtained stable three-dimensional trapping and orientation of individual silver wires for half an hour or longer. The position of single nanowires could be controlled with precision better than 100 nm, and the orientation could be controlled with precision better than 1°. The results were reported in Refs. [17, 18]. We performed theoretical simulations in order to explain the observed results, particularly the orientation of the wires perpendicular to the laser polarization. Although silver nanowires are more straightforward to synthesize and to trap optically, gold nanowires are more stable under x-ray illumination, and are thus more suitable for the eventual goal of measuring x-ray diffraction from a single, optically trapped nanoparticle. We therefore investigated the optical trapping of gold nanowires, and demonstrated the ability to hold them, as well, in appropriately shaped optical fields.

Having developed a sample preparation method that stabilizes individual gold nanowires on a surface when they are exposed to intense x-ray fluxes, we collected coherent-diffraction patterns from individual nanowires. Three-dimensional diffraction patterns were collected from single nanowires, including multiple Bragg peaks from the same wire. Unfortunately, the smallest of the coherent-diffraction fringes that resulted were beyond the resolution of the detector that was used. We were therefore unable to use inversion algorithms to reconstruct the structure of the wires. Nonetheless, the experiments demonstrated the feasibility of measuring coherent diffraction from single metal nanowires.

The central goal for the next year will be the final construction, commissioning, and demonstration of an optical-trapping apparatus capable of operating at the APS beamlines. We will then use

this apparatus to trap individual nanowires, and will measure coherent x-ray diffraction from the trapped nanowires. The apparatus will also be used for trapping other nanoparticles of interest. The custom-built, compact trapping apparatus will be designed to be compatible with the APS beamlines where coherent-diffraction imaging will be performed. The optical trapping components and laser were purchased and stored at the CNM, however the apparatus has been transferred to the AMO group who will assemble, test, and modify it for APS experiments.

We will first verify the feasibility of reconstructing the three-dimensional internal structure of nanowires from coherent x-ray diffraction. Numerical calculations, using our preliminary measurements as a guideline, indicate that available detectors in the APS detector pool will allow for the nanoscale structural reconstruction of nanowires with lengths up to 2 μm. These calculations also indicate the experimental conditions required to obtain the corresponding x-ray diffraction patterns. As well as proving the feasibility of single-nanowire diffraction measurements, these experiments will provide important structural information about nanowires, including internal strain distribution and localized defects, that is correlated to optical properties and that cannot be obtained using other methods.

The nanowire trapping will be based on the interferometric Bessel-beam configuration that we have developed. Preliminary results indicate that gold nanowires, which are more stable under x-ray illumination, interact in the trap in much the same way as silver nanowires. Semiconductor nanowires should also be readily trapped and oriented by the Bessel beam. The optical-trapping apparatus will include a spatial light modulator (SLM), in order to shape the optical fields as needed. This SLM will also make it possible to create multiple traps at the same time. This, in turn, will enable the simultaneous trapping of multiple nanowires, which can subsequently be manipulated and joined together into three-dimensional assemblies. These assemblies will address one of the key limitations of optical trapping of individual nanowires: although the long axis of a nanowire can be oriented relative to the trapping-laser polarization, the wire is still free to rotate about this axis. Asymmetric nanowire assemblies, by contrast, could be stably oriented in three dimensions, eliminating free rotational diffusion.

Radiation damage in nanoparticles by intense x-ray interactions
(P. J. Ho, W. Jiang,[9] and L. Young)

Intense, femtosecond x-ray pulses currently available at x-ray free-electron laser (XFEL) facilities have been shown to be useful for femtosecond serial crystallography [40], imaging biomolecular crystals of sub-micron dimensions [57, 58, 59], smaller than ever achieved at a synchrotron source. However, radiation damage induced by high intensity x-ray radiation in these crystals is unavoidable. In particular, x-ray photoionization, inner-shell transitions (Auger and fluorescence) and secondary ionization can take place with high probability within the pulse duration, and these processes can damage the structure of the molecules and potentially limit the usefulness of these intense x-ray pulses for molecular structural determination. We devised a theoretical model to investigate the fundamental mechanisms of the damage in clusters of varying size, with an ultimate aim of understanding phenomena from molecular to the nanometer scale, perhaps eventually approaching 1 MDa in size.

In order to obtain an atomistic view of the dynamical x-ray damage processes and the subsequent structural distortion on the target system throughout the x-ray pulse, we use a combined Monte-Carlo/Molecular-dynamics (MC/MD) computational model (see Fig. 6). At first, the rates of all inner-shell transitions and the cross sections of photoionization of each subshell will be obtained with Hartree-Fock-Slater calculations. During the x-ray pulse, the occurrences of the photoionization, inner-shell decay processes, electron-impact ionization and the site of their occurrences are treated by Monte-Carlo type methods. Subsequently, the dynamics of the photoelectrons,

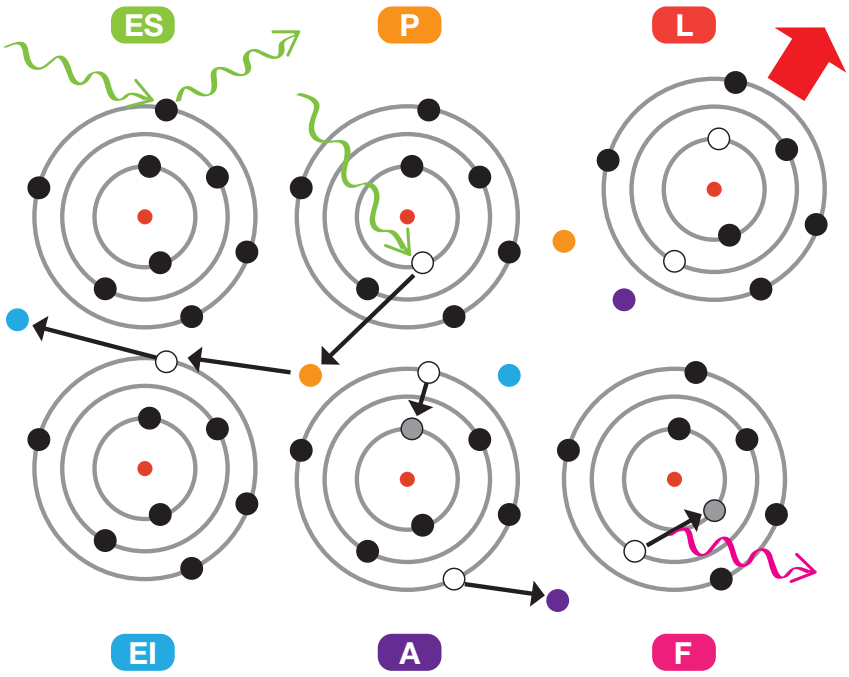

Figure 6: Processes in x-ray-nanoparticle interaction included in MC/MD model. ES: elastic x-ray scattering, P: photoionization, L: Lattice dynamics, EI: electron-impact ionization, A: Auger (Coster-Kronig) decay and F: fluorescence.

Auger electrons, secondary electrons and the atoms/ions in the systems are tracked using molecular dynamics methods. The advantage of this MC/MD model is that it allows us to compute the time-dependent coherent x-ray diffraction pattern of the target system by tracking the position of the delocalized electrons and the configuration (electronic configuration and charge state) and positions of atoms/ions. In addition, we can monitor the fluorescence spectrum, charge-state distribution, energy spectra, lattice dynamics, and dynamics of photoelectrons, Auger and secondary electrons.

Understanding photoelectron dynamics is critical: initial high-energy photoelectron escape leads to a charged cluster, which traps low-energy electrons that can, in turn, generate secondary ionization, hydrodynamic motion, and/or Coulomb explosion. One expects a transition from Coulomb explosion to hydrodynamic expansion as a function of size. Recently, we have extended the capability of our computational code by successfully integrating a modified LAMMPS code to perform MD calculations. LAMMPS is known to have good scalability with MPI/OpenMP parallelization on high-performance computing machines. More importantly, implementation of EAM potentials for metallic systems is straightforward in LAMMPS. Thus, with our MC/MD code, we can study x-ray damage processes in high-Z, metallic nanoparticles with sizes larger than 100 nm. We have begun to use our code on the high-performance IBM Blue Gene/Q systems at the Argonne Leadership Computing Facility (ALCF) to investigate the effects of x-ray energy, pulse duration, pulse fluence and particle size (1 to 100 nm) on the complex mechanism of radiation damage with nanoscale argon and nickel clusters as our first target systems.

Our choice of argon clusters is motivated by the recent experiments by Schorb and cowokers that measured the ionization dynamics of clusters of various sizes exposed to different x-ray pulse parameters [60]. We want to compare our calculated results with the measurements and shed light

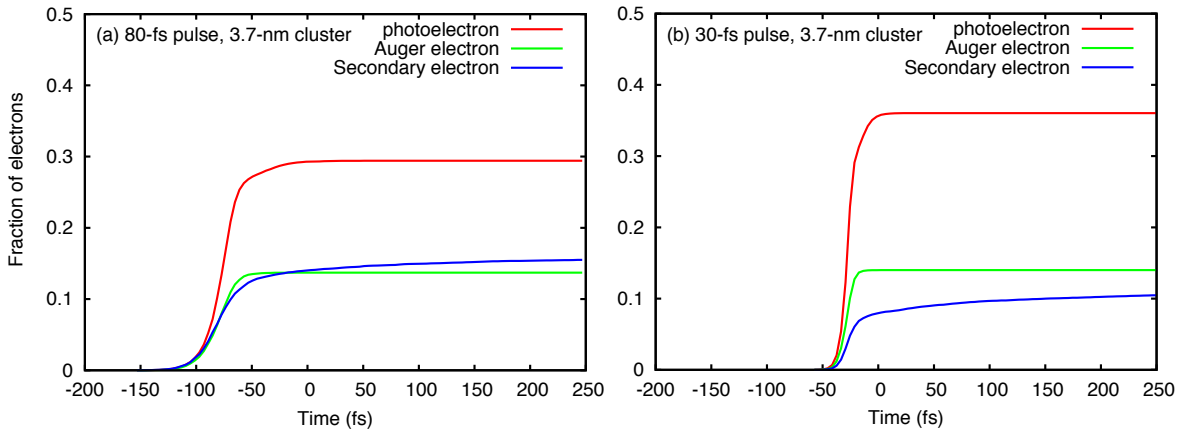

Figure 7: Generation of photoelectrons, Auger electrons, and secondary electrons in a 3.7-nm argon cluster throughout (a) an 80-fs x-ray pulse, and (b) a 30-fs x-ray pulse.

on the ionization dynamics of clusters. Our first argon calculations show that secondary ionization plays an important role in the ionization dynamics of clusters, especially in a large cluster. Fig. 7(a) shows that, for a 3.7-nm cluster exposed to a 480-eV, 0.015-mJ and 80-fs pulse, the process of electron-impact ionization accounts for more than 1/4 of the ionized electrons. In addition, pulse parameters are control knobs that can be used to control the ionization dynamics in clusters. By using a shorter pulse of 30-fs with the same pulse energy, Fig. 7(b) shows that the fraction of electron-impact ionization events can be suppressed and the fraction of the photoionization events is increased. More calculations are underway to provide new insights into the ionization dynamics of argon clusters.

Also, we have begun to examine the physics of nickel cluster interaction with ultrashort, intense x-ray pulses. This is motivated by the fact that the seeded XFEL pulses with predictable pulse shape are currently available at energies above and below the K-edges (near 8 keV) of the neutral nickel atom and the single-core-hole nickel ion. When nickel nanoparticles are exposed to 8-keV x-rays, the ionized electrons from photoionization, Auger decay and secondary ionization have a mean free path in the range of 1 nm to 10 nm. By studying nickel nanoparticles with sizes smaller and larger than the electron mean free path, we will gain a better understanding of the complex mechanisms of radiation damage in intense x-ray pulses.

6 Affiliations of collaborators

[1]Center for Free-Electron Laser Science, DESY, Hamburg, Germany
[2]European XFEL, Hamburg, Germany
[3]Ohio State University, Columbus, OH
[4]Paul Scherrer Institute, Villegen, Switzerland
[5]Stanford Synchrotron Radiation Laboratory, SLAC NAL, Menlo Park, CA
[6]Linac Coherent Light Source, SLAC National Accelerator Laboratory, Menlo Park, CA
[7]University of Hamburg, Germany
[8]Chemical Sciences & Engineering Division, Argonne National Laboratory, Argonne, IL
[9]Argonne Leadership Computing Facility, Argonne National Laboratory, Argonne, IL
[10]Pacific Northwest National Laboratory, Richland, WA
[11]Kansas State University, Manhattan, KS
[12]Wigner Research Centre for Physics, Hungarian Academy Sciences, Budapest, Hungary

[13]BioCARS, University of Chicago, IL
[14]Universidad de Salamanca, Salamanca, Spain
[15]University of Chicago, Chicago, IL
[16]University of Maryland, Baltimore County, MD
[17]Center for Nanoscale Materials, Argonne National Laboratory, Argonne, IL

References

Publications 2011–2013

[1] G. Doumy, C. Roedig, S.-K. Son, C. I. Blaga, A. D. Chiara, R. Santra, N. Berrah, C. Bostedt, J. D. Bozek, P. H. Bucksbaum, J. Cryan, L. Fang, S. Ghimire, J. M. Glownia, M. Hoener, E. P. Kanter, B. Krässig, M. Kuebel, M. Messerschmidt, G. G. Paulus, D. A. Reis, N. Rohringer, L. Young, P. Agostini, and L. F. DiMauro, "Nonlinear atomic response to intense ultrashort x rays," Phys. Rev. Lett. **106**, 083002 (2011).

[2] E. P. Kanter, B. Krässig, Y. Li, A. M. March, P. Ho, N. Rohringer, R. Santra, S. H. Southworth, L. F. DiMauro, G. Doumy, C. A. Roedig, N. Berrah, L. Fang, M. Hoener, P. H. Bucksbaum, S. Ghimire, D. A. Reis, J. D. Bozek, C. Bostedt, M. Messerschmidt, and L. Young, "Unveiling and driving hidden resonances with high-fluence, high-intensity x-ray pulses," Phys. Rev. Lett. **107**, 233001 (2011).

[3] S. Düsterer, P. Radcliffe, C. Bostedt, J. Bozek, A. L. Cavalieri, R. Coffee, J. T. Costello, D. Cubaynes, L. F. DiMauro, Y. Ding, G. Doumy, F. Grüner, W. Helml, W. Schweinberger, R. Kienberger, A. R. Maier, M. Messerschmidt, V. Richardson, C. Roedig, T. Tschentscher, and M. Meyer, "Femtosecond x-ray pulse length characterization at the Linac Coherent Light Source free-electron laser," New J. Phys. **13**, 093024 (2011).

[4] C. Buth, M. C. Kohler, J. Ullrich, and C. H. Keitel, "High-order harmonic generation enhanced by XUV light," Opt. Lett. **36**, 3530 (2011).

[5] S. Pabst, L. Greenman, P. J. Ho, D. A. Mazziotti, and R. Santra, "Decoherence in attosecond photoionization," Phys. Rev. Lett. **106**, 053003 (2011).

[6] S.-K. Son, L. Young, and R. Santra, "Impact of hollow-atom formation on coherent x-ray scattering at high intensity," Phys. Rev. A **83**, 033402 (2011); **83**, 069906(E) (2011).

[7] A. M. March, A. Stickrath, G. Doumy, E. P. Kanter, B. Krässig, S. H. Southworth, K. Attenkofer and C. A. Kurtz, L. X. Chen, and L. Young, "Development of high-repetition-rate laser pump/x-ray probe methodologies for synchrotron facilities," Rev. Sci. Instrum. **82**, 073110 (2011).

[8] E. Silver, J. D. Gillaspy, P. Gokhale, E. P. Kanter, N. S. Brickhouse, R. W. Dunford, K. Kirby, T. Lin, J. McDonald, D. Schneider, S. Seifert, and L. Young, "Work towards experimental evidence of hard x-ray photoionization in highly charged krypton," AIP Conference Proceedings **1336**, 146 (2011).

[9] R. W. Dunford and R. J. Holt, "Parity nonconservation in hydrogen," Hyp. Int. **Online**, (2011).

[10] M. Meyer, P. Radcliffe, T. Tschentscher, J. T. Costello, A. L. Cavalieri, I. Grguras, A. R. Maier, R. Kienberger, J. Bozek, C. Bostedt, S. Schorb, R. Coffee, M. Messerschmidt, C. Roedig, E. Sistrunk, L. F. Di Mauro, G. Doumy, K. Ueda, S. Wada, S. Düsterer, A. K. Kazansky, and N. M. Kabachnik, "Angle-resolved electron spectroscopy of laser-assisted Auger decay induced by a few-femtosecond x-ray pulse," Phys. Rev. Lett. **108**, 063007 (2012).

[11] C. Buth, J.-C. Liu, M. H. Chen, J. P. Cryan, L. Fang, J. M. Glownia, M. Hoener, R. N. Coffee, and N. Berrah, "Ultrafast absorption of intense x rays by nitrogen molecules," J. Chem. Phys. **136**, 214310 (2012).

[12] M. C. Kohler, C. Müller, C. Buth, A. B. Voitkiv, K. Z. Hatsagortsyan, J. Ullrich, T. Pfeiffer, C. H. Keitel, "Electron correlation and interference effects in strong-field processes," in Multiphoton Processes and Attosecond Physics, K. Yamanouchi and K. Midorikawa, Springer Proceedings in Physics **125**, Springer, Berlin, 2012.

[13] S. M. Cavaletto, C. Buth, Z. Harman, E. P. Kanter, S. H. Southworth, L. Young, and C. H. Keitel, "Resonance fluorescence in ultrafast and intense x-ray free-electron-laser pulses," Phys. Rev. A **86**, 033402 (2012).

[14] R. W. Dunford, S. H. Southworth, D. Ray, E. P. Kanter, B. Krässig, L. Young, D. A. Arms, E. M. Dufresne, D. A. Walko, O. Vendrell, S.-K. Son, and R. Santra, "Evidence for interatomic Coulombic decay in Xe K-shell-vacancy decay of XeF_2," Phys. Rev. A **86**, 033401 (2012).

[15] L. Fang, T. Osipov, B. Murphy, F. Tarantelli, E. Kukk, J. Cryan, P. H. Bucksbaum, R. N. Coffee, M. Chen, C. Buth, and N. Berrah, "Multiphoton ionization as a clock to reveal molecular dynamics with intense short x-ray free electron laser pulses," Phys. Rev. Lett. **109**, 263001 (2012).

[16] K. Haldrup, G. Vankó, W. Gawelda, A. Galler, G. Doumy, A. M. March, E. P. Kanter, A. Bordage, A. Dohn, T. B. van Driel, K. S. Kjaer, H. T. Lemke, S. E. Canton, J. Uhlig, V. Sundström, L. Young, S. H. Southworth, M. M. Nielsen, and C. Bressler, "Guest-host interactions investigated by time-resolved x-ray spectroscopies and scattering at MHz rates: solvation dynamics and photoinduced spin transition in aqueous $[Fe(bipy)_3]^{2+}$," J. Phys. Chem. A **116**, 9878 (2012).

[17] Z. Yan, J. E. Jureller, J. Sweet, M. J. Guffey, M. Pelton, and N. F. Scherer, "Three-dimensional optical trapping

and manipulation of single silver nanowires," Nano Lett. **12**, 5155 (2012).
[18] Z. Yan, J. Sweet, J. E. Jureller, M. J. Guffey, M. Pelton, and N. F. Scherer, "Controlling the position and orientation of single silver nanowires on a surface using structured optical fields," ACS Nano **6**, 8144 (2012).
[19] B. Krässig, E. P. Kanter, S. H. Southworth, L. Young, R. Wehlitz, B. A. deHarak, and N. L. S. Martin, "Dipole-quadrupole interference spectroscopy: the observation of an autoionizing He ^1D Rydberg series," Phys. Rev. A **86**, 053408 (2012).
[20] L. Young, "A comb in the extreme ultraviolet," Nature **482**, 45 (2012).
[21] S. Stoupin, A. M. March, H. Wen, D. A. Walko, Y. Li, E. M. Dufresne, S. A. Stepanov, K.-J. Kim, Yu. V. Shvyd'ko, V. D. Blank, and S. A. Terentyev, "Direct observation of dynamics of thermal expansion using pump-probe high-energy-resolution x-ray diffraction," Phys. Rev. B **86** 054301 (2012).
[22] W. Becker, X. J. Liu, P. J. Ho, and J. H. Eberly, "Theories of photoelectron correlation in laser-driven multiple atomic ionization," Rev. Mod. Phys. **84**, 1011 (2012).
[23] B. Adams, M. Borland, L. X. Chen, P. Chupas, N. Dashdorj, G. Doumy, E. Dufresne, S. Durbin, H. Drr, P. Evans, T. Graber, R. Henning, E. P. Kanter, D. Keavney, C. Kurtz, Y. Li, A. M. March, K. Moffat, A. Nassiri, S. H. Southworth, V. Srajer, D. M. Tiede, D. Walko, J. Wang, H. Wen, L. Young, X. Zhang, and A. Zholents, "X-ray capabilities on the picosecond timescale at the Advanced Photon Source," Synch. Rad. News **25**, 6 (2012).
[24] B. W. Adams, C. Buth, S. M. Cavaletto, J. Evers, Z. Harman, C. H. Keitel, A. Pálffy, A. Picón, R. Röhlsberger, Y. Rostovtsev, and K. Tamasaku,"X-ray quantum optics," J. Mod. Opt. **60**, 2 (2013).
[25] G. Vankó, A. Bordage, P. Glatzel, E. Gallo, M. Rovezzi, W. Gawelda, A. Galler, C. Bressler, G. Doumy, A. M. March, E. P. Kanter, L. Young, S. H. Southworth, S. E. Canton, J. Uhlig, V. Sundström, K. Haldrup, T. Brandt van Driel, M. M. Nielsen, K. S. Kjaer, and H. T. Lemke, "Spin-state studies with XES and RIXS: From static to ultrafast," J. Electron. Spectrosc. Relat. Phenom. **188**, 166 (2013).
[26] A. Picón, C. Buth, G. Doumy, B. Krässig, L. Young, and S. H. Southworth, "Optical control of resonant Auger processes," Phys. Rev. A **87**, 013432 (2013).
[27] C. Buth, F. He, J. Ullrich, C. H. Keitel, and K. Z. Hatsagortsyan, "Attosecond pulses at kiloelectronvolt photon energies from high-order harmonic generation with core electrons," Phys. Rev. A, in press (2013).
[28] R. Reininger, E. M. Dufresne, M. Borland, M. A. Beno, L. Young, K.-J. Kim, and P. G. Evans, "Optical design of the short pulse x-ray imaging and microscopy time-angle correlated diffraction beamline at the Advanced Photon Source," Rev. Sci. Instrum. **84**, 053013 (2013).
[29] R. Reininger, D. Keavney, M. Borland and L. Young, "Optical design of the Short Pulse Soft X-Ray Spectroscopy beamline at the Advanced Photon Source, J. Synch. Rad. **20**, 654 (2013).
[30] "SPX First Experiments, Contributors: D. Reis, A. Lindenberg, M. Trigo, M. DeCamp, C. Milne, A. M. March, G. Doumy, M. Borland, D. Keavney, R. Reininger, L. X. Chen, W.-S. Lee, Z. X. Shen, H. Ihee, J. Kim, K. Moffat, V. Srajer, R. Henning. Contacts: L. Young and P. Evans.
[31] "Preliminary Expected Performance Characteristics of an APS Multi-Bend Achromat Lattice, M. Borland for the APS Upgrade team.
[32] A. Picón, P. J. Ho, G, Doumy, and S. H. Southworth, "Optically-dressed resonant Auger processes induced by high-intensity x rays," New J. Phys. **15**, 083057 (2013).
[33] C. Hernández-García, A. Picón, J. San Román, and L. Plaja, "Attosecond extreme ultraviolet vortices from high-order harmonic generation," Phys. Rev. Lett. **111**, 083602 (2013).
[34] L. Young, "Ultra intense x-ray interactions at the Linac Coherent Light Source," in press, Attosecond and XUV Physics, Chapter 16. Editors: M. Vrakking and T. Schultz, Wiley-VHC Verlag GmbH & Co. KGaA
[35] C. Bostedt, J.D. Bozek, P.H. Bucksbaum, R.N. Coffee, J.B. Hastings, Y. Huang, R.W. Lee, S. Schorb, J.N. Corlett, P. Denes, P. Emma, R.W. Falcone, R.W.Schoenlein, G. Doumy, E. Kanter, B. Krässig, S. Southworth, L. Young, L. Fang, M. Hoener, N. Berrah, C. Roedig, L.F. DiMauro, "Ultra-fast and ultra-intense x-ray sciences: first results from the Linac Coherent Light Source free-electron laser," J. Phys. B **46**, 1 (2013).
[36] T. Osipov, L. Fang, B. Murphy, F. Tarantelli, E. R. Hosler, E. Kukk, J. D. Bozek, C. Bostedt, E. P. Kanter, and N. Berrah, "Sequential multiple ionization and fragmentation of SF_6 induced by an intense free electron laser pulse," J. Phys. B **46**, 164032 (2013).

Other cited references

[37] T.E. Glover, M.P. Hertlein, S.H. Southworth, T.K. Allison, J. van Tilborg, E.P. Kanter, B. Krässig, H.R. Varma, B. Rude, R. Santra, A. Belkacem, and L. Young, "Controlling X-rays with light," Nature Phys. **6**, 69 (2009).
[38] C. Buth, R. Santra, and L. Young, "Electromagnetically Induced Transparency for X Rays," Phys. Rev. Lett. **98**, 253001 (2007).
[39] L. Young, E. P. Kanter, B. Krässig, Y. Li, A. M. March, S. T. Pratt, R. Santra, S. H. Southworth, N. Rohringer, L. F. DiMauro, G. Doumy, C. A. Roedig, N. Berrah, L. Fang, M. Hoener, P. H. Bucksbaum, J. P. Cryan, S. Ghimire, J. M. Glownia, D. A. Reis, J. D. Bozek, C. Bostedt, and M. Messerschmidt, "Femtosecond electronic response of atoms to ultra-intense x-rays," Nature **466**, 56 (2010).
[40] R. Neutze, R. Wouts, D. van der Spoel, E. Weckert, and J. Hajdu, "Potential for bimolecular imaging with

femtosecond x-ray pulses," Nature **406**, 752 (2000).
[41] A. A. Lutman, R. Coffee, Y. Ding, Z. Huang, J. Krzywinski, T. Maxwell, M. Messerschmidt, and H.-D. Nuhn, "Experimental demonstration of femtosecond two-color x-ray free-electron lasers," Phys. Rev. Lett. **110**, 134801 (2013).
[42] A. Zholents *et al.*, "Generation of subpicosecond x-ray pulses using RF orbit deflection," Nucl. Instrum. Meth. A **425**, 385 (1999).
[43] S. Corde *et al.*, "Synchrotron radiation based experimental determination of the optimal energy for cell radiotoxicity enhancement following photoelectric effect on stable iodinated compounds," Brit. J. Cancer **91**, 544 (2004).
[44] S. D. Stoychev, *et al.*, "Intermolecular Coulombic decay in small biochemically relevant hydrogen-bonded systems," J. Am. Chem. Soc. **133**, 6817 (2011).
[45] L. Caron, "Low-energy electron scattering from DNA including structural water and base-pair irregularities," Phys. Rev. A **80**, 012705 (2009).
[46] J. Balosso, 2012, private communication.
[47] M. Drescher, M. Hentschel, R. Kienberger, M. Uiberacker, V. Yakovlev, A. Scrinzi, Th. Westerwalbesloh, U. Kleineberg, U. Heinzmann, and F. Krausz, "Time-resolved atomic inner-shell spectroscopy," Nature **419**, 803 (2002).
[48] P. Ranitovic, X. M. Tong, C. W. Hogle, X. Zhou, Y. Liu, N. Toshima, M. M. Murnane, and H. C. Kapteyn, "Laser-Enabled Auger Decay in Rare-Gas Atoms," Phys. Rev. Lett. **106**, 053002 (2011).
[49] W. A. Bryan, F. Frassetto, C. A. Froud, I. C. E. Turcu, R. B. King, C. R. Calvert, G. R. A. J. Nemeth, P. Villoresi, L. Poletto, and E. Springate, "Isolated high-harmonic XUV photon absorption and NIR strong-field tunnel ionization," New J. Phys. **14**, 013057 (2012).
[50] J. M. Schins, P. Breger, P. Agostini, R. C. Constantinescu , H. G. Muller, G. Grillon, A. Antonetti, and A. Mysyrowicz, " Observation of Laser-Assisted Auger Decay in Argon," Phys. Rev. Lett. **73**, 2180 (1994).
[51] A.K. Kazansky and N.M. Kabachnik, "On the gross structure of sidebands in the spectra of laser-assisted Auger decay," J. Phys. B: At. Mol. Opt. Phys. **43**, 035601 (2010).
[52] M.N. Piancastelli, "Auger resonant Raman studies of atoms and molecules," J. Electron Spectrosc. Relat. Phenom. **107**, 1-26 (2000).
[53] J. Amann *et al.*, "Demonstration of self-seeding in a hard-X-ray free-electron laser," Nature Photon. **6**, 693 (2012).
[54] E. Allaria *et al.*, "Highly coherent and stable pulses from the FERMI seeded free-electron laser in the extreme ultraviolet," Nature Photon. **6**, 699 (2012).
[55] N. Rohringer and R. Santra, "Resonant Auger effect at high x-ray intensity," Phys. Rev. A **77**, 053404 (2008).
[56] A. G. Peele, P. J. McMahon, D. Paterson, C. Q. Tran, A. P. Mancuso, K. A. Nugent, J. P. Hayes, E. Harvey, B. Lai, and I. McNulty, "Observation of an x-ray vortex," Opt. Lett. **27**, 1752 (2002).
[57] H. N. Chapman *et al.*, "Femtosecond X-ray protein nanocrystallography," Nature **470**,73-77 (2011).
[58] S. Boutet *et al.*, "High-Resolution Protein Structure Determination by Serial Femtosecond Crystallography," Science **337**, 362-364 (2012).
[59] A. Barty *et al.*, "Self-terminating diffraction gates femtosecond X-ray nanocrystallography measurements," Nat. Photon. **6**, 35-40 (2012).
[60] S. Schorb *et al.*, "Size-dependent ultrafast ionization dynamics of nanoscale samples in intense femtosecond x-ray free-electron-laser pulses," Phys. Rev. Lett. **108**, 233401 (2012).
[61] S. Pabst, P. J. Ho, and R. Santra, "Computational studies of x-ray scattering from three-dimensionally-aligned asymmetric-top molecules," Phys. Rev. A **81**, 043425 (2010).
[62] E. R. Peterson, C. Buth, D. A. Arms, R. W. Dunford, E. P. Kanter, B. Krässig, E. C. Landahl, S. T. Pratt, R. Santra, S. H. Southworth, and L. Young, "An x-ray probe of laser-aligned molecules," Appl. Phys. Lett. **92**, 094106 (2008).
[63] P. J. Ho, D. Starodub, D. K. Saldin, V. L. Shneerson, A. Ourmazd, and R. Santra, "Molecular structure determination from x-ray scattering patterns of laser-aligned symmetric-top molecules," J. Chem. Phys. **131**, 131101 (2009).
[64] P. J. Ho and R. Santra, "Theory of x-ray diffraction from laser-aligned symmetric-top molecules," Phys. Rev. A **78**, 053409 (2008).

Engineered Electronic and Magnetic Interactions in Nanocrystal Quantum Dots

Victor I. Klimov

Chemistry Division, C-PCS, MS-J567, Los Alamos National Laboratory
Los Alamos, New Mexico 87545, klimov@lanl.gov, http://quantumdot.lanl.gov

1. Program Scope

Using nanocrystal (NC) quantum dots one can produce extremely strong spatial confinement of electronic excitations not accessible with other types of nanostructures. Because of this confinement, electronic energies in nanocrystals are directly dependent upon their dimensions, which is known as the quantum-size effect. This effect has been a powerful tool for controlling spectral responses of NCs, enabling potential applications such as multicolor labeling, optical amplification and low-cost lighting. In addition to spectral tunability, strong spatial confinement results in a significant enhancement of carrier-carrier interactions that leads to a number of novel physical phenomena including large splitting of electronic states induced by electron-hole exchange coupling, ultrafast mutiexciton decay via Auger recombination, and direct generation of multiple excitons by single photons via carrier multiplication. Confinement-induced mixing between the conduction and the valence band can also lead to interesting peculiarities in magnetic interactions such as switching of the sign of the g-factor in magnetically doped NCs. The major thrust of this project is to understand the physics of electronic and magnetic interactions under conditions of extreme quantum confinement, and to develop methods for controlling these interactions. Research topics explored here include: control of Auger recombination via engineered exciton-exciton interactions in heterostructured and alloyed NCs with a goal of realizing the regime of continuous-wave lasing; new functional behaviors via NC-doping with optically active ions such as copper; control of single-exciton dynamics via tunable fine-structure excitonic splitting; and controlled exchanged interactions in magnetically doped NCs probed by steady state and time-resolved magneto-optical spectroscopies.

2. Recent Progress

Overview. During the past year, our work has focused on three major areas:

(i) NC doping with magnetic impurities and its effect on NC optical properties. As highlighted in the previous year's report, spectroscopic studies of Cu-doped ZnSe/CdSe core/shell NCs revealed the presence of Cu^{2+} ions, which with a valence configuration of $3d^9$, should exhibit magnetism, albeit weaker than that of NCs doped with Mn^{2+} ($3d^5$). Recently, we demonstrated that these NCs exhibit not only the classic signatures of diluted magnetic semiconductors, but also a unique, long-lived photoinduced enhancement of their magnetism.

(ii) Effect of intentional interfacial alloying on properties of single- and multi-exciton states. Spectroscopic[1] and theoretical[2] studies suggest that Auger suppression in CdSe/CdS NCs with especially thick shells arises from the uncontrolled formation of a $CdSe_xS_{1-x}$ alloy layer at the core/shell interface, which reduces the abruptness of the electronic confinement potential. Our recent development of a new synthetic strategy for creating alternately CdSe/CdS NCs with no alloy layer, or CdSe/$CdSe_xS_{1-x}$/CdS NCs featuring an alloy layer of controlled composition and thickness, has allowed us to unequivocally demonstrate that the structure of the core/shell interface has a significant effect on the rate of nonradiative Auger recombination.

(iii) Dual-color NCs with controlled statistical properties of emitted light. In another synthetic advance, we have created novel dot-in-bulk (DiB) NCs, which comprise a quantum-confined CdSe core overcoated with a thick, bulk-like CdS shell. Using these nanostructures, we have realized a new antibunching mechanism (dynamic Coulomb blockade), which allows for simultaneous generation of quantum and classical light from the same nanostructure. The unusual versatility of these novel nanoscale light sources, which allows for facile tunability of effective color, opens new interesting opportunities for a range of applications from quantum optics to sensing and nanoscale imaging. Below, we provide a highlight on these unique materials.

In the period of 2011-13, this project produced 14 papers published in top quality journals. These include 2 publications in *Nature* family journals, 3 *Phys. Rev. Lett.*, 7 *Nano Lett.,* 1 *JACS* report, and an invited review in the September 2013 issue of *MRS Bulletin,* which features studies of NC-LEDs. These papers have been referenced in the literature 316 times, which corresponds to ca. 26 citations per paper on average. Various aspects of this work were presented in more than 30 invited/keynote talks at major research forums such as APS March

meetings, Gordon Research Conferences, Spring and Fall MRS meetings, and ACS National meetings.

Two-Color Quantum and Classical Light Using Dot-in-Bulk Semiconductor Nanocrystals. Colloidal NCs are an emerging class of color-tunable, solution-processible, room-temperature single-photon sources. In conventional NCs, photon antibunching arises from suppression of multiphoton emission by nonradiative Auger recombination. In this project, we have demonstrated a new antibunching mechanism, dynamic Coulomb blockade, which allows for generating both quantum and classical light from the same NC without the detrimental effects of Auger decay. This mechanism is realized in DiB nanostructures comprising a quantum-confined CdSe core overcoated with a thick, bulk-like CdS shell. The presence of one hole in the core suppresses the transfer of a second hole, thus forcing it to recombine in the shell region. Under weak excitation, these NCs emit red antibunched light from core states. At higher pump levels, they exhibit an additional higher-energy band (green shell emission) with bulk-like, Poissonian photon statistics.

A well-known property of chemically synthesized NCs is a pronounced size dependence of their electronic structures, which has been widely explored for controlling emission color.[3] Much less work has been done on understanding, and especially controlling the statistical properties of the photon stream emitted by individual NCs. [4-6] In this project, we have explored a regime where two strongly correlated quantum and classical (bulk-like) light emission channels are engineered within a single colloidal nanoparticle. Compared to previously reported "giant" CdSe/CdS NCs (Figs. 1a, b),[1, 7, 8] the DiB nanostructures (Figs. 1 c, d) have an even thicker shell comprising ~25 CdS monolayers and are produced by a novel "fast-growth" method. The overall size of these new NCs is *ca*. 20 nm (Fig. 1d, inset), much larger than the Bohr exciton radius in bulk CdS (3 nm). As a result, while core emission is nonclassical, the emission from the shell region is bulk-like; therefore, these structures can be considered as having a "dot-in-bulk" (DiB) motif.

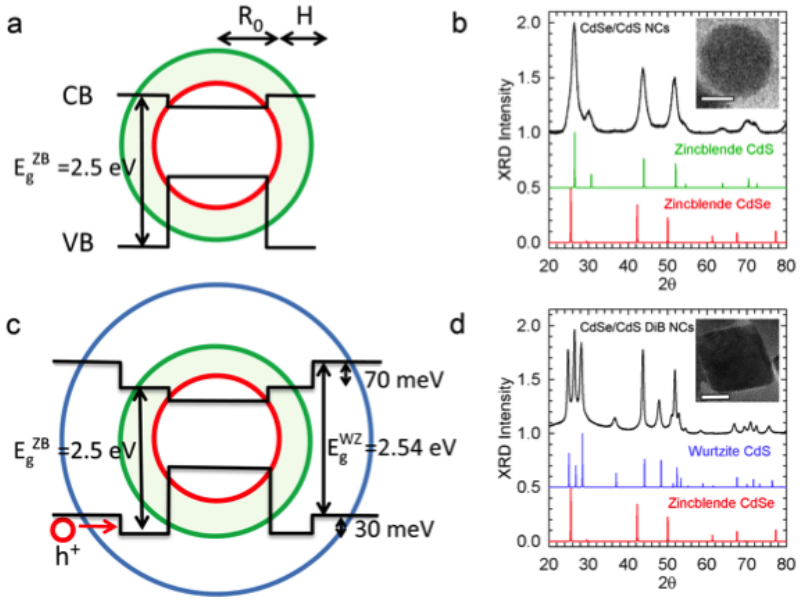

Fig. 1. Band structure of a standard core/shell CdSe/CdS NC vs. a dot-in-bulk NC. a, A schematic band structure of a NC with a small-to-intermediate shell thickness ($H \leq$ 3.5 nm). b, As inferred from the X-ray diffraction (XRD) measurements, for these thicknesses, the shell maintains the ZB structure of the core (top pattern); two lower patterns illustrate the positions of the XRD peaks in ZB bulk CdS (green) and CdSe (red). Inset: a TEM image of a NC with H = 3.5 nm (scale bar is 5 nm). c, The band structure of a DiB NC features an energetic barrier in the valence band associated with an interfacial ZB CdS layer, which separates a thick WZ CdS outer layer from the ZB CdSe core. (d) Due to its large volume, the final WZ CdS shell dominates the XRD spectrum of DiB NCs. Inset: a TEM image of a DiB NC (scale bar is 10 nm).

In Fig. 2a, we show a series of photoluminescence (PL) spectra from an individual NC under continuous-wave excitation with power increasing from 1.6 W/cm^2 to 1.5 kW/cm^2. The excitation energy is 3.1 eV, which is above the CdS band-edge; hence, both types of photogenerated carriers (electrons and holes) are initially in the shell, which has a much greater absorption cross-section than the CdSe core.[1] At low excitation levels (much less than one exciton per NC on average), we observe a single PL peak at 640 nm, which originates from radiative recombination of a delocalized electron with a core-localized hole (referred to as "core emission"). Remarkably, by increasing the pump power, we activate a new emission band at 515 nm, which is close to the bulk CdS PL wavelength. As illustrated on in Fig. 2b, by changing the pump power and thus modifying the relative intensities of the red and green bands, we can tune the effective color of our nanoscale emitter from red to yellow and then green.

In order to study the photon statistics of emitted light, we have performed measurements of the two-photon correlation function (g_2) using pulsed excitation (Figs. 2c-d). At low fluences, when only core emission is observed (Fig. 2c), we detect a vanishingly small central peak in the coincidence histogram, which indicates strong photon antibunching.[6] In Fig. 2d, the same measurement is performed on the green PL band, which appears at higher fluences, with the core emission blocked by a short-pass filter (see Fig. 2e). In sharp contrast

with the core PL, the statistics of the photons emitted from the shell of the same NC is Poissonian, as expected for emission from a bulk semiconductor. These results show that by varying excitation power one can control both the color and the photon statistics of light emitted by a single NC.

To explain this peculiar behavior, we have proposed a model, which assumes that hole relaxation from the shell into the core is hindered when the core is already occupied by a hole. This can occur due to the combined effect of Coulombic repulsion and an intrinsic potential barrier at the shell/core interface revealed by the XRD studies (see Fig. 1c, d). This new antibunching mechanism has several advantages over a traditional mechanism based on suppression of multiphoton emission by Auger recombination. Specifically, Auger decay is one of the pathways by which NCs become photocharged and, thus, essentially nonemissive (that is, "blink-off").[9] Further, a powerful approach to suppressing blinking in colloidal single-dot emitters is based on a growth of an ultra-thick shell.[7] This, however, is accompanied by suppression of Auger recombination[1, 10], which diminishes the quality of antibunching.[11] By offering a novel, non-Auger-decay related mechanism for antibunching the DiB NCs represent a new class of robust, room-temperature emitters of a high-purity stream of single photons that do not suffer from detrimental effects such as photocharging and blinking. Furthermore, an additional advantage of DiB NCs is associated with a co-existing channel for classical emission whose intensity and dynamics are controlled by core occupancy, which leads to a direct correlation between the two channels. This property can enable new applications that cannot be realized with traditional single-photon sources.

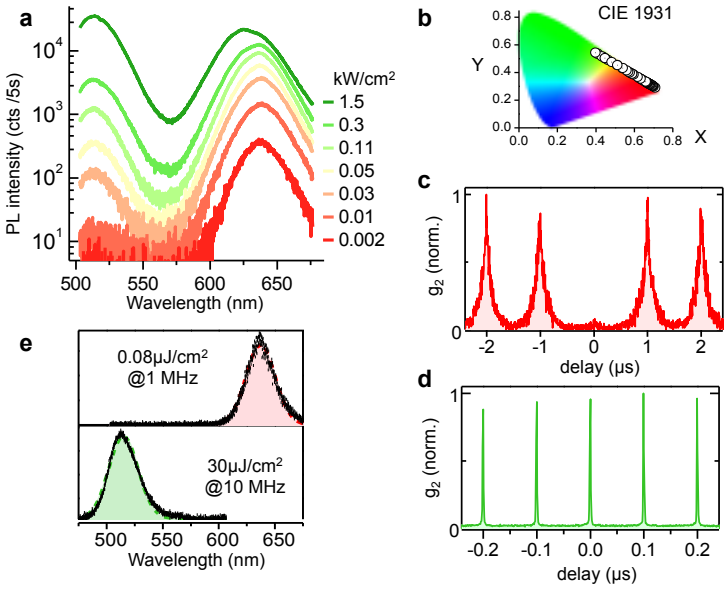

Fig. 2. Pump-power-controlled dual emission from an individual core/shell NC. a, PL spectra from an individual NC under 405 nm cw laser excitation for increasing pump power (semi-log representation). **b,** Color coordinates computed from the series of spectra shown in (**a**) and plotted on a CIE color chart. **c,** Two-photon correlation function (g_2) measured at very low pulsed excitation fluence of 0.08 μJ/cm^2 @ 1 MHz repetition rate. In this regime, about 0.02 excitons per NC per pulse is created on average (for an NC cross section of 10^{-13} cm^2); this corresponds to generation of one exciton every 50 μs, and the emission comes exclusively from the core. The probability of multi-photon emission is less than 5% without any background subtraction, demonstrating clear photon antibunching. **d,** The g_2 measurement for the same NC at a fluence of 30 μJ/cm^2 @ 10 MHz (one exciton is generated every 10-15 ns on average). The green shell emission is dominant and the residual red PL is blocked with a short-pass filter. The photon statistics is perfectly Poissonian as expected for a bulk emitter excited by a laser light. **e,** PL spectra corresponding to the conditions of the measurements reported in (e) and (f).

References

1. Garcia-Santamaria, F., Y. Chen, J. Vela, R.D. Schaller, J.A. Hollingsworth, and V.I. Klimov, *Nano Lett.* **9**, 3482 (2009).
2. Cragg, G.E. and A.L. Efros, *Nano Lett.* **10**, 313 (2009).
3. Qu, L. and X. Peng, *J. Am. Chem. Soc.* **124**, 2049 (2002).
4. Kiraz, A., M. Atatüre, and A. Imamoğlu, *Phys. Rev. A* **69**, 032305 (2004).
5. Michler, P., A. Imamoglu, M.D. Mason, P.J. Carson, G.F. Strouse, and S.K. Buratto, *Nature* **406**, 968 (2000).
6. Brokmann, X., G. Messin, P. Desbiolles, E. Giacobino, M. Dahan, and J.P. Hermier, *New J. Phys.* **6**, 99 (2004).
7. Chen, Y., J. Vela, H. Htoon, J.L. Casson, D.J. Werder, D.A. Bussian, V.I. Klimov, and J.A. Hollingsworth, *J. Am. Chem. Soc.* **130**, 5026 (2008).
8. Mahler, B., P. Spinicelli, S. Buil, X. Quelin, J.-P. Hermier, and B. Dubertret, *Nature Mater.* **7**, 659 (2008).
9. Galland, C., Y. Ghosh, A. Steinbruck, M. Sykora, J.A. Hollingsworth, V.I. Klimov, and H. Htoon, *Nature* **479**, 203 (2011).
10. Spinicelli, P., S. Buil, Qu, eacute, X. lin, B. Mahler, B. Dubertret, and J.P. Hermier, *Phys. Rev. Lett,* **102**, 136801 (2009).
11. Park, Y.S., A.V. Malko, J. Vela, Y. Chen, Y. Ghosh, F. Garcia Santamaria, J.A. Hollingsworth, V.I. Klimov, and H. Htoon, *Phys. Rev. Lett,* **106**, 187401 (2011).

3. Future Plans

In our future work in this project, we will explore applications for our newly developed DiB NCs and NCs with an interfacial alloy layer in LEDs. Using the first type of the NCs, we will attempt to realize dual-band LEDs with the effective color tunable by applied bias. The second type of nanostructures will be used to evaluate the effect of

Auger recombination on performance of NC-LEDs. In recent years the understanding of the physics underlying the operation of NC-LEDs, and specifically the factors that limit their performance, has greatly improved. However, the role of multicarrier effects including Auger recombination in operational devices is still largely unclear. It has been established that in traditional quantum-well based LEDs, Auger recombination is responsible for efficiency roll-off at high driving currents (also known as the "droop" effect). Some recent studies have suggested that a similar effect is also responsible for efficiency roll-off in NC-LEDs. However, this view is not universally accepted, as other works have attributed it to the effect of the applied electric field, which leads to spatial separation between electrons and holes that reduces the rate of radiative recombination. In this project, we will analyze the role of Auger recombination in NC-LEDs by conducting a systematic characterization of device performance in conjunction with studies of the dynamics of photoexcited carriers directly within the device structure. In our LEDs, we will use a series of structurally engineered core/shell nanostructures that are characterized by similar band gaps and valence/conduction band positions, but distinctly different rates of nonradiative Auger recombination. By correlating device performance with the photophysical properties of the NCs, we will elucidate the effect of multicarrier Auger recombination on LED efficiency and the onset for efficiency roll-off. We expect that these studies will allow us to develop a set of guidelines for optimal design of NCs for high-performance LEDs that feature both enhanced efficiency and also improved roll-off characteristics.

4. Publications (2011 - 2013)

1. Y.-S. Park, W. K. Bae, L. A. Padilha, J. M. Pietryga, V. I. Klimov, *Effect of the core/shell interface on Auger recombination evaluated by single-quantum dot spectroscopy,* Nano Lett.*,* in press (2013)
2. W. K. Bae, S. Brovelli, V. I. Klimov, *Spectroscopic insights into the performance of quantum dot light-emitting diodes*, MRS Bulletin*,* September (2013).
3. C. Galland, S. Brovelli, W.K. Bae, L.A. Padilha, F. Meinardi, V.I. Klimov, *Dynamic hole blockade yields two-color quantum and classical light from 'dot-in-bulk' nanocrystals*, Nano Lett. **13**, 321 (2013)
4. L.A. Padilha, W.K. Bae, V.I. Klimov, J.M. Pietryga, R.D. Schaller, *Response of Semiconductor Nanocrystals to Extremely Energetic Excitation*, Nano Lett. **13**, 925 (2013).
5. Y.-S. Park, Y. Ghosh, Y. Chen, A. Piryatinski, P. Xu, N. H. Mack, H. –L. Wang, V. I. Klimov, J. A. Hollingsworth and H. Htoon, *Super-Poissonian Statistics of Photon Emission from Single Core/Shell Nanocrystals Coupled to Metal Nanostructures*, Phys. Rev. Lett. **110**, 117401 (2013).
6. A. Pandey, S. Brovelli, R. Viswanatha, L. Li, J.M. Pietryga, V. I. Klimov and S. A. Crooker, *Long-lived photoinduced magnetization in copper doped ZnSe–CdSe core–shell nanocrystals*, Nature Nanotech.. **7**, 792 (2012).
7. S. Brovelli, C. Galland, R. Viswanatha, V. I. Klimov, Tuning Radiative *Recombination in Cu-Doped Nanocrystals via Electrochemical Control of Surface Trapping*, Nano Lett. **12**, 4327 (2012).
8. B. N. Pal, Y. Ghosh, S. Brovelli, R. Laocharoensuk, V. I. Klimov, Jennifer Hollingsworth, H. Htoon, *"Giant" CdSe/CdS core/shell nanocrystal quantum dots as efficient electroluminescent materials: Strong influence of shell thickness on light-emitting diode performance,* Nano Lett. **12**, 331 (2012).
9. R. Viswanatha, S. Brovelli, A. Pandey, S. A. Crooker, V. I. Klimov, *Copper-Doped Inverted Core/Shell Nanocrystals with "Permanent" Optically Active Holes*, Nano Lett. **11**, 4753 (2011).
10. R. Viswanatha, J. M. Pietryga, V. I. Klimov, and S. A. Crooker, *Circularly-polarized Mn^{2+} emission from Mn-doped colloidal nanocrystals*, Phys. Rev. Lett. **107**, 067402 (2011).
11. S. Brovelli, R. D. Schaller, S. A. Crooker, F. Garcia-Santamaria, Y. Chen, R. Viswanatha, J. A. Hollingsworth, H. Htoon, V. I. Klimov, *Nano-engineered electron-hole exchange interaction controls exciton dynamics in core-shell semiconductor nanocrystals*, Nature Comm. **2**, 280 (2011)
12. Y.-S. Park, A. V. Malko, J. Vela, Y. Chen, Y. Ghosh, F. Garcia-Santamaria, J. A. Hollingsworth, V. I. Klimov, H. Htoon, *Near-unity quantum yields of biexciton emission from CdSe/CdS nanocrystals measured using single-particle spectroscopy*, Phys. Rev. Lett. **106**, 187401 (2011).
13. L. Li, A. Pandey, D. J. Werder, B. P. Khanal, J. M. Pietryga, V. I. Klimov, *Efficient synthesis of highly luminescent indium sulfide based core/shell nanocrystals with surprisingly long-lived emission,* J. Am. Chem. Soc. **133**, 1176 (2011).
14. Garcia-Santamaria, F., S. Brovelli, R. Viswanatha, J. A. Hollingsworth, H. Htoon, S. Crooker, V. I. Klimov, *Breakdown of volume scaling in Auger recombination in CdSe/CdS heteronanocrystals: The role of the core-shell interface*, Nano Lett. **111**, 687 (2011).

J.R. Macdonald Laboratory Overview

The J.R. Macdonald Laboratory focuses on the interaction of intense laser pulses with matter with the goal of understanding — and eventually controlling — the resulting ultrafast dynamics. The dynamics studied occurs over a broad range of timescales from attoseconds, the natural timescale for electronic motion in matter, to femtoseconds and picoseconds for molecular vibration and rotation, respectively. While better understanding leads to better control, the reverse can also be true. Thus, we are currently harnessing the multi-timescale expertise within the Lab to enable deeper studies than would otherwise be possible. The synergy afforded by the close interaction of theory and experiment within the Lab further multiplies this effort. To achieve our goals, we are advancing theoretical modeling and computational approaches as well as experimental techniques, taking advantage of our expertise in particle imaging techniques.

Most of our research projects are associated with one of two themes: "Attosecond Physics" and "Control". The boundary between these themes, however, is not always well defined. A few examples from each are briefly mentioned below, while further details are provided in the individual abstracts of the PIs: I. Ben-Itzhak, B.D. Esry, M.F. Kling, V. Kumarappan, C.D. Lin, A. Rudenko , U. Thumm, and C. Trallero.

Attosecond physics: Attosecond science is motivated by the idea of observing electronic motion in atoms and molecules on its natural timescale. Light pulses whose duration approaches this timescale must thus be produced. Such pulses, however, can also serve as very precise triggers or probes of the femtosecond-scale nuclear motion in molecules. Moreover, the underlying high-harmonic generation (HHG) mechanism, used to create attosecond pulses, provides essential information about the target and has been the focus of some of our theoretical and experimental studies. Recent theoretical work from the Lab has shown, for instance, that optimizing the waveform of the driving infrared pulse can improve HHG by orders of magnitude. High-harmonics have also been used to experimentally uncover information about the structure of SF_6 and its shape resonances. Our ability to align molecules very well has also been combined with HHG to demonstrate the importance of molecular orbitals beyond the valence electron in strong-field ionization processes of molecules.

Control: Methods for controlling the motion of heavy particles in small molecules continue to be developed. Theoretically, our work shows that carrier-envelope phase (CEP) effects, two-color control, and the physics of overlapping attosecond pulse trains and infrared pulses are all manifestations of multi-color control and can all be treated with exactly the same analytical framework. In particular, our formulation shows that these effects arise from interference between different multiphoton pathways. Our experimental carrier-envelope phase control of strong-field dissociation of H_2^+ — the first such measurement directly on the ion — serves as a good demonstration of the theory. The measurement of the CEP dependence of D^* production in strong-field dissociation of D_2 further supports this formulation. Work in the Lab has also led to the imaging of structural rearrangement in small polyatomic molecules. Significant steps to improve impulsive alignment of symmetric top molecules — and even asymmetric top molecules — have also been taken in the Lab.

In addition to our laser-related research, we have conducted some studies using our high- and low-energy accelerators. Some of this work is conducted in collaboration with visiting scientists

(for example, S. Lundeen).

Like the visitors benefiting from the use of our facilities, we pursue several outside collaborations at other facilities and with other groups (*e.g.*, ALS, Århus, FLASH, University of Frankfurt, University of Jena, LBNL, Max-Planck Institutes for Quantum Optics and Kernphysik, Ohio State University, Texas A&M, Tokyo, Weizmann Institute, and others).

On the personnel side, Matthias Kling has left Kansas State, but a search for a new tenure-track experimentalist to join the Lab is already underway. And, while Itzik Ben-Itzhak takes his sabbatical during 2013–2014, Brett Esry is serving as Interim Director of the Lab with significant help from the Associate Director for Lab Operations, Kevin Carnes.

Finally, it is worth mentioning the ongoing changes in the Lab. The DOE-funded PULSAR laser, which provides about an order of magnitude improvement in count rate (10–20 kHz, 790 nm, 2 mJ/pulse, ~21 fs FWHM, CEP stable) over the typical Ti:sapphire laser system, is now operational and has been used for various coincidence imaging experiments whose results are beginning to appear in publication. In particular, the sub-5 fs pulses possible with it, combined with a CEP stereo phase meter now in the Lab, enable CEP studies on systems and processes not possible previously. The laser itself resides in newly renovated space funded by an investment from the University. A second room was renovated at the same time by the University and will house a second new laser system funded through NSF. This laser system, HITS, will feature high-power pulses at long wavelengths. It should be delivered in the very near future.

Combining the experimental and theoretical expertise within the Lab with the capabilities becoming available with the new laser facilities promises exciting physics from the Lab in the near future. We are also working to contribute to the community by co-hosting an ultrafast dynamics workshop with ITAMP to take place at Kansas State University in November, 2013.

Structure and Dynamics of Atoms, Ions, Molecules, and Surfaces:
Molecular Dynamics with Ion and Laser Beams

Itzik Ben-Itzhak, J. R. Macdonald Laboratory, Kansas State University
Manhattan, KS 66506; ibi@phys.ksu.edu

Scope: *The goal of this part of the JRML program is to study and control molecular dynamics under the influence of ultrashort intense laser pulses or the swift Coulomb field of ions. To this end we typically use molecular ion beams as the subject of our studies and have a close collaboration between theory and experiment.*[i] *Examples of our recent work are given below*.

Carrier-envelope phase (CEP) control over molecular dynamics – The phase between the carrier and the pulse envelope has been used in recent years to control atomic processes (Ref. [1] and Pub. 4,14,25) and molecular dissociation (Refs. [2-3] and Pub. 22). In the latter case, studies have focused mainly on spatial asymmetries along the laser polarization – a symmetry broken by the CEP, ϕ, in pulses approaching single cycle. We have been advancing the technologies needed to facilitate such measurements at JRML, including near one-cycle pulses (5 fs or shorter) and CEP tagging (Ref. [4] and Pub. 4), which, combined with our new 10 kHz PULSAR laser, have enabled first-of-a-kind CEP-dependence measurements on a thin ion-beam target.

CEP control over pathway interference in strong-field dissociation of H_2^+, *Nora G. Kling, K.J. Betsch, M. Zohrabi, S. Zeng, F. Anis, U. Ablikim, Bethany Jochim, Z. Wang, M. Kübel, M.F. Kling, K.D. Carnes, B.D. Esry, and I. Ben-Itzhak* – We have used the benchmark H_2^+ molecular-ion beam as the first subject of CEP-dependence studies to demonstrate that phase tagging combined with 5 fs laser pulses at a high repetition rate make such measurements possible in spite of the extremely low target density (equivalent to $\lesssim 10^{-12}$ Torr). Moreover, the study of H_2^+ enables direct quantitative comparison with state-of-the-art calculations including nuclear rotation and intensity averaging [5,6], which can now provide a nearly exact description of strong-field dissociation so long as ionization remains negligible. In contrast, to interpret the previous studies of CEP effects in the dissociative ionization of D_2 (or H_2) [2,3], one is forced to model the ionization step, as including it together with dissociation in *ab initio* calculations is beyond present theoretical capabilities. Therefore, quantitative agreement of accurate theoretical results and experimental data, which we set as one of our goals, has so far been missing.

In the experiment, shown schematically in Fig. 1(Left) a focused laser beam, providing 5 fs pulses at 10 kHz, was crossed with an H_2^+ beam from our ECR ion source. The crossing point was 2 mm in front of the laser focus, in order to take advantage of the larger volume and therefore higher count rate and to minimize the impact of the Gouy phase shift [7]. The dissociation into H^++H was measured by the coincidence 3D momentum imaging technique [8]. From the momenta of both fragments, the kinetic energy release (KER) upon dissociation and the angular distribution are determined. The CEP of each pulse was monitored by focusing about 10% of the same laser beam into a single-shot stereographic above-threshold-ionization (ATI) phase meter described in Refs. [4,9,10].

We define the spatial asymmetry as the difference between protons going up and down divided by their sum, namely $A(\mathrm{KER},\phi) = [N_u(\mathrm{KER},\phi) - N_d(\mathrm{KER},\phi)] / [N_u(\mathrm{KER},\phi) + N_d(\mathrm{KER},\phi)]$, where $N_{u,d}$ is the number of events in the two directions along the laser polarization. The measured and calculated asymmetry as a function of KER and CEP, shown in the middle and right panels of Fig. 1, look very similar to each other. To compare theory and experiment quantitatively, we show line outs of a couple of KER ranges in the same figure. It has been shown theoretically (e.g. Ref. [5]) that the dominant behavior of A is $A(\phi) = \alpha\cos(\phi + \phi_0)$ where α is the asymmetry amplitude and ϕ_0 is an offset. The data follow this prediction nicely. These

CEP effects are due to interference of different photon number pathways to $1s\sigma_g$ and $2p\sigma_u$ final states, having opposite nuclear parity, whose relative phase is controlled by the CEP [12].

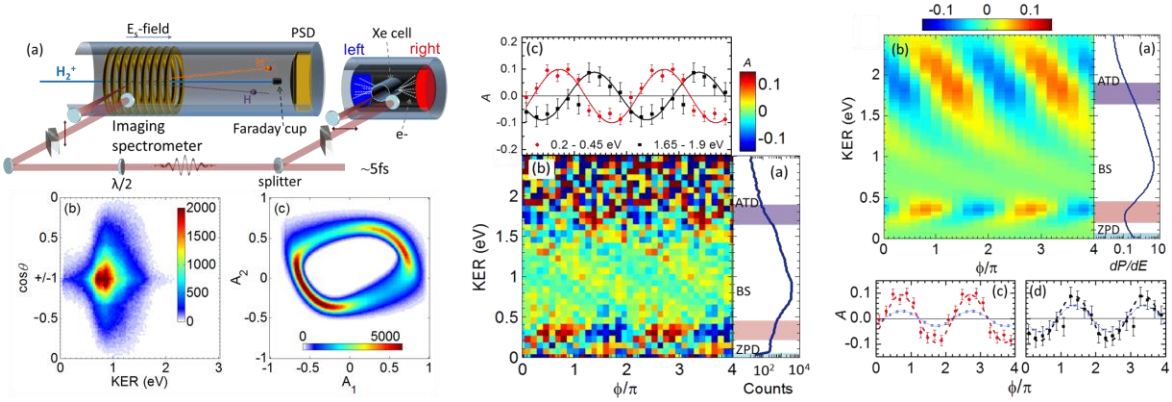

Figure 1. ***Left*****:** (a) Schematic view of the experimental setup. (b) CEP-integrated dissociation yield as a function of KER and cosθ, where θ is the angle between the H^+ momentum and the laser polarization. (c) Measured parametric asymmetry plot [4,10], from which the CEP is determined (linear color scale). ***Middle*****:** (a) KER spectrum of H_2^+ dissociation by 5 fs, 4×10^{14} W/cm^2 laser pulses, averaged over ϕ. The wide shaded regions indicate where the highest asymmetries are observed. (b) The corresponding asymmetry map showing the dependence of A(KER,ϕ) on KER and CEP. The data are shown for fragments within a cone, cosθ = 0.2, around the polarization axis. (c) The asymmetry parameter integrated over the indicated energy regions, fit to sinusoidal curves (see text). ***Right*****:** Calculated (a) ϕ-averaged dissociation probability, dP/dE, as a function of KER with the same shaded regions. (b) A(KER,ϕ) as a function of KER and ϕ for the dissociation of H_2^+, calculated for 5 fs, 1×10^{14} W/cm^2 pulses, averaged over the (c) low- and (d) high-KER regions. The solid light blue lines are theoretical predictions for the same KER regions, with the estimated theoretical error in dark blue. The calculations include Franck-Condon factors and intensity averaging. Adapted from Ref. [11].

As stated above the overall quantitative agreement is quite good, except for the underestimated asymmetry amplitude (by a factor of 3) for the low KER. Achieving better quantitative agreement will require further study (both experimental and theoretical), most likely addressing the theory limitation to lower intensities [11] and any non-Gaussian character of the laser pulse. We know from Ref. [5], for instance, that even a weak prepulse can substantially increase the asymmetry.

One further advantage of our method is that it facilitates the measurement of relative total dissociation yields as a function of CEP. However, we have found no discernible dependence of the total yield, integrated over all KER, on CEP within our error bars. In contrast, a similar study did recently report such a CEP dependence [13]. The dissimilar findings are most likely due to laser-field differences.

We plan to extend these studies and focus on CEP dependence of branching ratios, beginning with HD^+ dissociation to $H+D^+$ or H^++D and continuing with more complex diatomic molecules.

CEP control over D^* formation in strong-field dissociation of D_2, *M. Zohrabi, B. Berry, Nora G. Kling, U. Ablikim, Travis Severt, Bethany Jochim, K.D. Carnes, B.D. Esry, and I. Ben-Itzhak* – In a similar CEP control study we explored the formation of long-lived excited neutral fragments from D_2. The production of D^* fragments, associated with the "frustrated tunneling ionization" mechanism [14], vanishes for circular polarization [14] and decreases rapidly with increasing ellipticity (Pub. 10). The high- and low-KER D^* fragments are associated with D^+ and D fragments, respectively [14]. Preliminary results of D^* formation in 5 fs pulses, shown in Fig. 2(a), exhibit strong spatial-asymmetry oscillations with CEP at low KER, tentatively associated with D^*+D dissociation. The measured periodicity suggests a 1-photon difference between the involved dissociation pathways. Moreover, the D^* yield integrated over θ, shown in Fig. 2(b), oscillates as $Y(\phi) \propto \cos(2\phi + \phi_0)$, as predicted by theory [15].

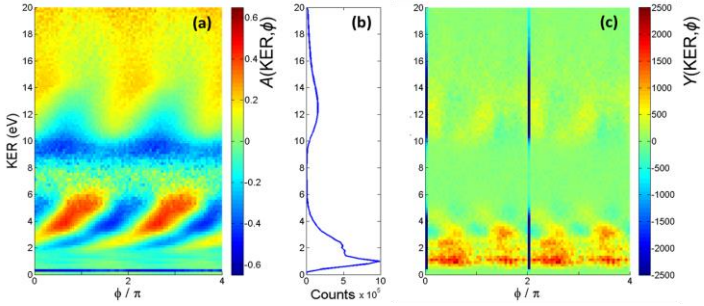

Figure 2. D^* from D_2 breakup in 5 fs, 3×10^{14} W/cm^2 laser pulses: (a) A(KER,ϕ), (b) Y(KER), and (c) Y(KER,ϕ) integrated over both directions along the laser polarization. The data are shown for fragments within a narrow cone, $\cos\theta = 0.993$ ($\theta = 7°$), around the polarization axis. The sharp blue "cuts" in the 2D plots are an artifact of the preliminary analysis.

Collisions: In addition to our laser studies, we have conducted a few collision experiments between keV molecular ion beams and atomic targets focusing on collision induced dissociation (CID). For example, we measured the angular dependence of $H_2^+ \rightarrow H^+ + H$ on the H_2^+ internuclear distance and isotopic effects in HD^+ dissociation – both presented at DAMOP 2013.

Future plans: We will continue to probe molecular-ion beams in a strong laser field, in particular taking advantage of the new capabilities of the PULSAR laser, specifically exploring challenging two-color, pump-probe, and CEP-dependence experiments. We will carry on our studies of more complex systems, including triatomic molecules, and also continue some collision studies that will merge with our laser studies in the near future.

References:

1. G.G. Paulus *et al*., Nature (London) **414**, 182 (2001)
2. M.F. Kling *et al*., Science **312**, 246 (2006)
3. M. Kremer *et al*., Phys. Rev. Lett. **103**, 213003 (2009)
4. T. Rathje *et al*., J. Phys. B **45**, 074003 (2012)
5. F. Anis and B.D. Esry, Phys. Rev. Lett. **109**, 133001 (2012)
6. F. Anis, Ph.D. thesis, Kansas State Univ. (2009)
7. F. Lindner, *et al*., Phys. Rev. Lett. **92**, 113001 (2004)
8. I. Ben-Itzhak *et al*., Phys. Rev. Lett. **95**, 073002 (2005)
9. G.G. Paulus *et al*., Phys. Rev. Lett. **91**, 253004 (2003)
10. T. Wittmann *et al*., Nat. Phys. **5**, 357 (2009)
11. Nora G. Kling *et al*., Phys. Rev. Lett. – submitted.
12. V. Roudnev and B.D. Esry, Phys. Rev. Lett. **99**, 220406 (2007)
13. T. Rathje *et al*., Phys. Rev. Lett. **111**, 093002 (2013)
14. B. Manschwetus *et al*., Phys. Rev. Lett. **102**, 113002 (2009)
15. J.J. Hua and B.D. Esry, J. Phys. B **42**, 085601 (2009)

Publications of DOE sponsored research in the last 3 years:

26. "Attosecond Control of electron emission from atoms", G. Laurent, W. Cao, I. Ben-Itzhak, and C.L. Cocke, *ICPEAC 2013 proceedings* – invited talk – accepted
25. "Nonsequential double ionization of N_2 in a near-single-cycle laser pulse", M. Kübel, Nora G. Kling, K.J. Betsch, N. Camus, A. Kaldun, U. Kleineberg, I. Ben-Itzhak, R.R. Jones, G.G. Paulus, T. Pfeifer, J. Ullrich, R. Moshammer, M.F. Kling, and B. Bergues, Phys. Rev. A **88**, 023418 (2013)
24. "Attosecond pulse characterization", G. Laurent, W. Cao, I. Ben-Itzhak, and C.L. Cocke, Opt. Exp. **21**, 16914 (2013)
23. "Charge asymmetric dissociation of CO^+ molecular ion beams induced by strong laser fields", Nora G. Kling, J. McKenna, A.M. Sayler, B. Gaire, M. Zohrabi, U. Ablikim, K.D. Carnes, and I. Ben-Itzhak, Phys. Rev. A **87**, 013418 (2013)
22. "Controlled directional ion emission from several fragmentation channels of CO driven by a few-cycle laser field", K.J. Betsch, Nora G. Johnson, B. Bergues, M. Kübel, O. Herrwerth, A. Senftleben, I. Ben-Itzhak, G.G. Paulus, R. Moshammer, J. Ullrich, M.F. Kling, and R.R. Jones, Phys. Rev. A **86**, 063403 (2012)
21. "Frustrated tunneling ionization during strong-field fragmentation of D_3^+ ", J. McKenna, A.M. Sayler, B. Gaire, Nora G. Johnson, B.D. Esry, K.D. Carnes, and I. Ben-Itzhak, New J. Phys. **14**, 103029 (2012)
20. "Quantum control of photodissociation by manipulation of bond softening", Adi Natan, Uri Lev, Vaibhav S. Prabhudesai, Barry D. Bruner, Itzik Ben-Itzhak, Oded Heber, Dirk Schwalm, Daniel Zajfman, and Yaron Silberberg, Phys. Rev. A **86**, 043418 (2012)
19. "Measurements of intense ultrafast laser-driven D_3^+ dynamics", A.M. Sayler, J. McKenna, B. Gaire, Nora G. Johnson, K.D. Carnes, and I. Ben-Itzhak, Phys. Rev. A **86**, 033425 (2012)
18. "Fragmentation of molecular-ion beams in intense ultrashort laser pulses", Itzik Ben-Itzhak, *Fragmentation Processes - Topics in Atomic and Molecular Physics*, edited by Colm T. Whelan (Cambridge University Press, 2012) p. 72 – *Invited*

17. "Attosecond control of orbital parity mix interferences and the relative phase of even and odd harmonics in an attosecond pulse train", G. Laurent, W. Cao, H. Li, Z. Wang, I. Ben-Itzhak, and C. L. Cocke, Phys. Rev. Lett. **109**, 083001 (2012)
16. "Study of asymmetric electron emission in two-color ionization of helium (XUV-IR)", G. Laurent, W. Cao, I. Ben-Itzhak, and C.L. Cocke, in *Multiphoton Processes and Attosecond Physics* (Proceedings of the 12th International Conference on Multiphoton Processes (ICOMP12) and the 3rd International Conference on Attosecond Physics, edited by K. Yamanouchi and K. Midorikawa, Springer Proceedings in Physics, Vol. **125** (2012) p. 173
15. "Tracing nuclear-wave-packet dynamics in singly and doubly charged states of N_2 and O_2 with XUV-pump–XUV-probe experiments", M. Magrakvelidze, O. Herrwerth, Y.H. Jiang, A. Rudenko, M. Kurka, L. Foucar, K.U. Kühnel, M. Kübel, Nora G. Johnson, C.D. Schröter, S. Düsterer, R. Treusch, M. Lezius, I. Ben-Itzhak, R. Moshammer, J. Ullrich, M.F. Kling, and U. Thumm, Phys. Rev. A **86**, 013415 (2012)
14. "Attosecond tracing of correlated electron-emission in nonsequential double ionization", B. Bergues, M. Kübel, N.G. Johnson, B. Fischer, N. Camus, K.J. Betsch, O. Herrwerth, A. Senftleben, A.M. Sayler, T. Rathje, I. Ben-Itzhak, R.R. Jones, G.G. Paulus, F. Krausz, R. Moshammer, J. Ullrich, and M.F. Kling, Nature Communications **3**, 813 (2012)
13. "Spectral splitting and quantum path study of high-harmonic generation from a semi-infinite gas cell", W. Cao, G. Laurent, Cheng Jin, H. Li, Z. Wang, C.D. Lin, I. Ben-Itzhak, and C.L. Cocke, J. Phys. B: At. Mol. Opt. Phys. **45**, 074014 (2012)
12. "Dynamics of D_3^+ slow dissociation induced by intense ultrashort laser pulses", B. Gaire, J. McKenna, M. Zohrabi, K.D. Carnes, B.D. Esry, and I. Ben-Itzhak, Phys. Rev. A **85**, 023419 (2012)
11. "Controlling strong-field fragmentation of H_2^+ by temporal effects with few-cycle laser pulses", J. McKenna, F. Anis, A.M. Sayler, B. Gaire, Nora G. Johnson, E. Parke, K.D. Carnes, B.D. Esry, and I. Ben-Itzhak, Phys. Rev. A **85**, 023405 (2012)
10. "Frustrated tunneling ionization during laser-induced D_2 fragmentation: Detection of excited metastable D^* atoms", J. McKenna, S. Zeng, J.J. Hua, A.M. Sayler, M. Zohrabi, Nora G. Johnson, B. Gaire, K.D. Carnes, B.D. Esry, and I. Ben-Itzhak, Phys. Rev. A **84**, 043425 (2011)
9. "Dynamic modification of the fragmentation of autoionizing states of O_2^+", W. Cao, G. Laurent, S. De, M. Schöffler, T. Jahnke, A.S. Alnaser, I.A. Bocharova, C. Stuck, D. Ray, M.F. Kling, I. Ben-Itzhak, Th. Weber, A.L. Landers, A. Belkacem, R. Dörner, A.E. Orel, T.N. Rescigno, and C.L. Cocke, Phys. Rev. A **84**, 053406 (2011)
8. "Effect of linear chirp on strong field photodissociation of H_2^+", Vaibhav S. Prabhudesai, Uri Lev, Oded Heber, Daniel Strasser, Dirk Schwalm, Daniel Zajfman, Adi Natan, Barry D. Bruner, Yaron Silberberg, and Itzik Ben-Itzhak, Journal of Korean Physical Society **59**, 2890 (2011)
7. "Following dynamic nuclear wave packets in N_2, O_2 and CO with few-cycle infrared pulses", S. De, M. Magrakvelidze, I.A. Bocharova, D. Ray, W. Cao, I. Znakovskaya, H. Li, Z. Wang, G. Laurent, U. Thumm, M.F. Kling, I.V. Litvinyuk, I. Ben-Itzhak, and C.L. Cocke, Phys. Rev. A **84**, 043410 (2011)
6. "Vibrationally resolved structure in O_2^+ dissociation induced by intense ultrashort laser pulses", M. Zohrabi, J. McKenna, B. Gaire, Nora G. Johnson, K.D. Carnes, S. De, I.A. Bocharova, M. Magrakvelidze, D. Ray, I.V. Litvinyuk, C.L. Cocke, and I. Ben-Itzhak, Phys. Rev. A **83**, 053405 (2011)
5. "Velocity map imaging as a tool for gaining mechanistic insight from closed-loop control studies of molecular fragmentation", Bethany Jochim, R. Averin, Neal Gregerson, J. McKenna, S. De, D. Ray, M. Zohrabi, B. Bergues, K.D. Carnes, M.F. Kling, I. Ben-Itzhak, and E. Wells, Phys. Rev. A **83**, 043417 (2011)
4. "Single-shot carrier-envelope-phase-tagged ion-momentum imaging of nonsequential double ionization of argon in intense 4-fs laser fields", Nora G. Johnson, O. Herrwerth, A. Wirth, S. De, I. Ben-Itzhak, M. Lezius, B. Bergues, M.F. Kling, A. Senftleben, C.D. Schröter, R. Moshammer, J. Ullrich, K.J. Betsch, R.R. Jones, A.M. Sayler, T. Rathje, K. Rühle, W. Müller, and G.G. Paulus, Phys. Rev. A **83**, 013412 (2011)
3. "Three-dimensional energy profile measurement of a molecular ion beam by coincidence momentum imaging compared to a retarding field analyzer", W. Wolff, J. McKenna, R. Vácha, M. Zohrabi, B. Gaire, K.D. Carnes, and I. Ben-Itzhak, Journal of Instrumentation **5**, 10006 (2010)
2. "Dynamic control of the fragmentation of CO^{q+} excited states generated using high-order harmonics", W. Cao, S. De, K.P. Singh, S. Chen, M. Schöffler, A. Alnaser, I. Bocharova, G. Laurent, D. Ray, M.F. Kling, I. Ben-Itzhak, I. Litvinyuk, A. Belkacem, T. Osipov, T. Rescigno, and C.L. Cocke, Phys. Rev. A **82**, 043410 (2010).
1. "Time-dependent dynamics in intense laser-induced above threshold Coulomb explosion", B.D. Esry and I. Ben-Itzhak, Phys. Rev. A **82**, 043409 (2010)

[i] In addition to the close collaboration with the theory group of *Brett Esry*, some of our studies are done in collaboration with *Lew Cocke*, *Matthias Kling's* group, *C.W. Fehrenbach*, and others

Strong-field coherent control

B.D. Esry
J. R. Macdonald Laboratory, Kansas State University, Manhattan, KS 66506
esry@phys.ksu.edu
http://www.phys.ksu.edu/personal/esry

Program Scope

One main component of my program is to quantitatively understand the behavior of simple benchmark systems in ultrashort, intense laser pulses. As we gain this understanding, we will work to transfer it to other more complicated systems. The second main component of my program is to develop novel analytical and numerical tools to more efficiently and more generally treat these systems and to provide rigorous, self-consistent pictures within which their non-perturbative dynamics can be understood. The ultimate goal is to uncover the simplest picture that can explain the most — ideally, without heavy computation being necessary.

Carrier-envelope phase effects in strong-field dissociation

Recent progress

One of our ongoing efforts shows that carrier-envelope phase (CEP) effects, two-color control, and the physics of overlapping attosecond pulse trains and infrared pulses are all manifestations of multi-color control and can all be treated with exactly the same analytical framework [1–3]. In particular, our formulation shows that these effects arise from interference between different multiphoton pathways.

In the last year, our picture has been put to the test through two different — but simultaneous — measurements of CEP effects on H_2^+ ion-beam targets [P10] [4]. Using an ion-beam target rather than generating the ion from H_2 within the laser pulse removes the need for *ad hoc* modeling of the ionization step. We contributed the theory for both measurements, carrying out essentially exact, full-dimensional solutions of the time-dependent Schrödinger equation (TDSE) for comparison with experiment. The calculations did neglect ionization, but this should be a good approximation at the intensities considered. In Pub. [P10], we used the measured pulse spectrum rather than the standard Gaussian, and in both Pub. [P10] and Ref. [4], we performed intensity and vibrational averages. While good agreement was found, the agreement was not great, suggesting that further quantitative investigation is needed.

In addition to full comparisons with solutions of the TDSE, we applied our analytical formulation of Ref. [2] and found good agreement with its qualitative — and computation-free — predictions. For instance, the CEP dependence of the spatial asymmetry

$$\mathcal{A}_s = \frac{P_{\rm up} - P_{\rm down}}{P_{\rm up} + P_{\rm down}}, \tag{1}$$

for H_2^+ dissociation can be explicitly calculated to be

$$\begin{aligned} P_{\rm up} - P_{\rm down} &= 4\pi {\rm Re} \sum_{\substack{J\,{\rm even}\\ n\,{\rm even}}} \sum_{\substack{J'\,{\rm odd}\\ n'\,{\rm odd}}} C^*_{n'J'u} C_{nJg} Y_{J'0} Y_{J0} e^{i(n-n')\varphi} \\ P_{\rm up} + P_{\rm down} &= 2\pi \sum_{\substack{J\,{\rm even}\\ n\,{\rm even}}} |C_{nJg} Y_{J0}|^2 + 2\pi \sum_{\substack{J\,{\rm odd}\\ n\,{\rm odd}}} |C_{nJu} Y_{J0}|^2 \\ &\quad + 4\pi {\rm Re} \sum_{\substack{J\,{\rm even}\\ n\,{\rm even}}} \sum_{\substack{J'\,{\rm even}\\ n'\,{\rm even}}} C^*_{n'J'g} C_{nJg} Y_{J'0} Y_{J0} e^{i(n-n')\varphi} \\ &\quad + 4\pi {\rm Re} \sum_{\substack{J\,{\rm odd}\\ n\,{\rm odd}}} \sum_{\substack{J'\,{\rm odd}\\ n'\,{\rm odd}}} C^*_{n'J'u} C_{nJu} Y_{J'0} Y_{J0} e^{i(n-n')\varphi}. \end{aligned} \tag{2}$$

In these expressions, J is the total orbital angular momentum, E is the kinetic energy release (KER), θ_K is the angle between the laser polarization and the relative momentum of the nuclei, $Y_{J0} = Y_{J0}(\theta_K)$ are the

spherical harmonics, and φ is the CEP. All of the details of the strong-field dynamics and the molecular structure are contained in the amplitudes

$$C_{nJp} = (-i)^J e^{-i\delta_{Jp}} \langle EJp | F_{nJp}(t_f) \rangle, \qquad p = g, u, \tag{3}$$

where δ_{Jp} is the scattering phase shift and $F_{nJp}(R,t)$ is the nuclear radial wave function for the Jp symmetry with n net photons.

Examination of Eq. (2) shows that $P_{\rm up} - P_{\rm down}$ must depend on the CEP as $\cos(\varphi + \varphi_1)$ for some energy-dependent phase $\varphi_1 = \varphi_1(E)$ to lowest order and that $P_{\rm up} + P_{\rm down}$ must behave as $a_0(E) + a_2(E)\cos(2\varphi + \varphi_2)$ to the lowest two terms. The periodicities observed for both the spatial asymmetry and the total yield in Pub. [P10] and Ref. [4] do indeed agree with these predictions. In fact, these periodicities turn out to be completely general for these observables, so that finding agreement for the periodicity is guaranteed so long as dipole selection rules are followed. The periodicity is thus, in a sense, the most trivial quantity to check. The real physics lies in the coefficients a_n and phases φ_n.

Another important point to emerge from Eq. (2) is that spatial asymmetry in strong-field H_2^+ dissociation is *not* due to controlling electron localization. Rather, one must control the nuclear degrees of freedom. To see this explicitly, we can calculate the electron density $\rho(\mathbf{r}, t)$ from the total wave function as

$$\begin{aligned} \rho(\mathbf{r}, t) &= \int d^3R \, |\Psi(\mathbf{R}, \mathbf{r}, t)|^2 \\ &= \int d^3R \left| \sum_{\alpha, J} F_{\alpha J}(R, t) Y_{J0}(\theta, \phi) \Phi_\alpha(R; \mathbf{r}) \right|^2 \end{aligned} \tag{4}$$

where Φ_α is the electronic wave function. Expanding the square and evaluating the integral gives

$$\rho(\mathbf{r}, t) = \sum_{\alpha, J} \int dR \, |F_{\alpha J}(R, t)|^2 |\Phi_\alpha(R; \mathbf{r})|^2. \tag{5}$$

Given that $\mathbf{r}$ is the molecular-frame electronic coordinate, the asymmetry we seek should appear as a function of $\tilde{z}$ where the tilde indicates a molecular-frame coordinate. Given that $\Phi_{1s\sigma_g}$ and $\Phi_{2p\sigma_u}$ are even and odd, respectively, under $\tilde{z} \to -\tilde{z}$, we see that $\rho(\mathbf{r}, t)$ displays no asymmetry. To find asymmetry, the integration over nuclear angles in Eq. (4) must be restricted to a domain asymmetric with respect to $\theta_K = \pi/2$. That is, the direction of the nuclei is critical.

The fact that CEP-dependent spatial asymmetry indicates control over the nuclear degrees of freedom rather than over electron localization is made perfectly clear by considering $\mathcal{A}_s$ for strong-field dissociation of HeH^+ at 4000 nm. For an intensity of 10^{14} W/cm^2 at this wavelength, only the $X^1\Sigma^+$ state is accessible [P6]. Consequently, there is only one way the electrons can localize — namely, as $He(1s^2)+H^+$. Nevertheless, Fig. 1 shows $\mathcal{A}_s$ for this case, revealing clear asymmetries. Thus, CEP-dependent spatial asymmetries is not equivalent to controlling the localization of the electron.

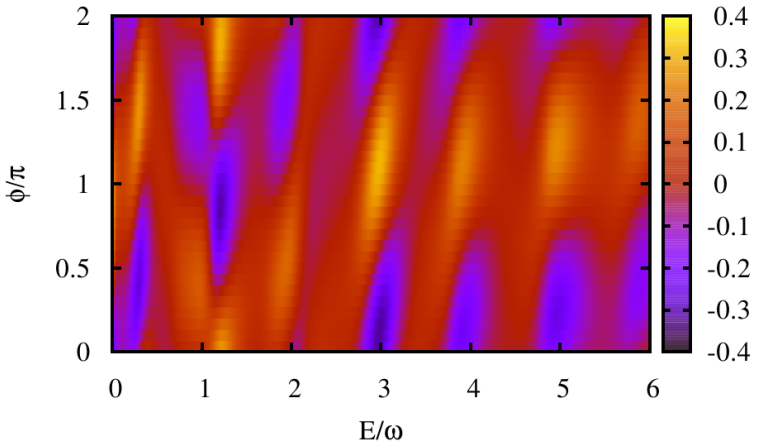

Figure 1: CEP-dependent spatial asymmetry for strong-field dissociation of HeH^+ into $He(1s^2)+H^+$ in a three-cycle, 10^{14} W/cm^2, 4000 nm laser pulse. (Adapted from Ref. [5].)

Future plans

We will continue to apply our formulation of strong-field coherent control to understand and predict which parameters lead to control over any given observable. Moreover, because our whole formulation is based upon a simple discrete Fourier transform of the wave function's φ dependence with the conjugate variable being the photon number, we can use this to define and extract the photon channel components of a calculated CEP-dependent wave function. The photon channels can provide considerable insight but have generally not been obtainable since they do not directly correspond to a physical observable. In practice, the photon index has simply been assigned based on the energy a state, but this technique is not reliable in strong fields. We hope to extend the formalism to extract the photon channels from an observable, in which case they could be extracted, in principle, from experimental data. Since our approach is independent of the system's complexity, it would apply to larger molecules as well.

Correlated electron-nuclear motion in strong-field dissociative ionization

Recent Progress

Based on preliminary calculations we did several years ago [6], we wanted to investigate the energy-sharing spectrum for strong-field dissociative ionization. We had seen the surprising — but in hindsight completely understandable — result that the total energy spectrum for dissociative ionization of H_2^+ looked very much like above threshold ionization. That is, it showed multiple peaks, each separated by one photon. This is the result one would expect from a simple energy conservation argument: $E_v + n\hbar\omega = E_N + E_e + U_p$, where E_v is the initial energy of the molecule, $n\hbar\omega$ is the multiphoton energy absorbed from the field, E_N is the final relative nuclear kinetic energy, E_e is the final energy of the electron relative to the nuclei, and U_p is the ponderomotive energy.

If one considers the individual nuclear and elecronic energies rather than their total, then the resulting joint energy spectrum looks like Fig. 2(a) [P8]. Multiphoton features are clearly seen, consistent with the energy conservation argument given above. The corresponding total energy spectrum is given in Fig. 2(b); and the energy-sharing spectra for each n-photon peak, in Fig. 2(c). These spectra clearly give access to more information than the projection to either the E_N or E_e axes as had been considered before our work. In particular, they show that the electron takes away the excess energy in most — but not all — cases.

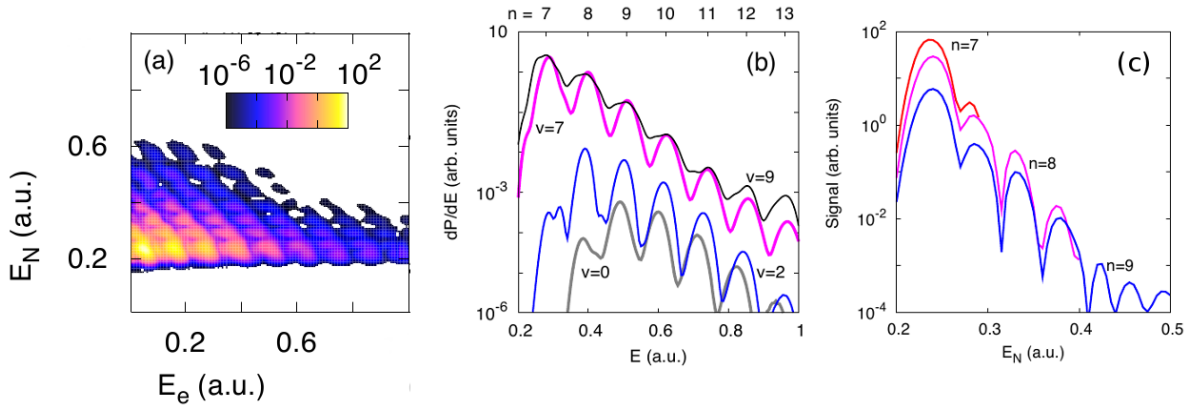

Figure 2: (a) Joint energy spectrum from a one-dimensional model H_2^+ TDSE for a 400 nm, 8.8×10^{13} W/cm^2, ten-cycle laser pulse starting from the $v = 7$ state. (b) Total energy spectra for several initial v. (c) Energy-sharing spectra for different n-photon peaks of $v = 7$. (Adapted from Pub. [P8].)

To measure a joint energy spectrum like Fig. 2(a), a coincidence measurement of all three particles in the continuum is needed. Such a measurement is possible, although a bit challenging, for a COLTRIMS apparatus. So, we discussed the idea with the main COLTRIMS groups. Reinhard Dörner's group "bit" first, and we suggested that they measure $H_2+n\hbar\omega \rightarrow p+H+e^-$. We further suggested that they do it with 400 nm to provide clear separation between the multiphoton peaks. And, taking all our suggestions, they obtained a spectrum that looked quite similar to Fig. 2(a). This work led to Pub. [P11].

Future Plans

We will continue using these observables to understand the energy sharing between electrons and nuclei. In particular, we want to use these to help us understand how to control the energy sharing. We know, for instance, that CEP effects require interference between n-photon channels. Since this observable clearly shows these channels, it is relatively clear that the CEP should not provide any substantial control over the energy sharing. We also want to explore such spectra for more complicated systems, including the three-body strong-field dissociation of triatomic molecules.

References

[1] V. Roudnev and B. D. Esry, "General theory of carrier-envelope phase effects," Phys. Rev. Lett. **99**, 220406 (2007).

[2] J. J. Hua and B. D. Esry, "The role of mass in the carrier-envelope phase effect for H_2^+ dissociation," J. Phys. B **42**, 085601 (2009).

[3] J. V. Hernández and B. D. Esry, "Attosecond pulse trains as multi-color coherent control," Phys. Rev. A (in preparation).

[4] N. G. Kling, K. J. Betsch, M. Zohrabi, S. Zeng, F. Anis, U. Ablikim, B. Jochim, Z. Wang, M. Kübel, M. F. Kling, K. D. Carnes, B. D. Esry, and I. Ben-Itzhak, "Carrier-envelope phase control over pathway interference in strong-field dissociation of H_2^+," Phys. Rev. Lett. (2013), (submitted), see I. Ben-Itzhak's abstract for more details.

[5] D. Ursrey and B. D. Esry, "Carrier-envelope phase effects for long wavelength HeH^+ dissociation," (in preparation).

[6] J. J. Hua and B. D. Esry, "Numerical explorations of above threshold Coulomb explosion for H_2^+ in an intense laser pulse," Bull. Am. Phys. Soc. **52**, abstract D1.76.

Publications of DOE-sponsored research in the last 3 years

[P11] "Electron-nuclear energy sharing in above-threshold multiphoton dissociative ionization of H_2," J. Wu, M. Kunitski, M. Pitzer, F. Trinter, L. Ph. H. Schmidt, T. Jahnke, M. Magrakvelidze, C. B. Madsen, L. B. Madsen, U. Thumm, and R. Dörner, Phys. Rev. Lett. **111**, 023002 (2013). Although my name does not appear, C. B. Madsen was in my group.

[P10] "Coherent control at its most fundamental: CEP-dependent electron localization in photodissoziation of a H_2^+ molecular ion beam target," T. Rathje, A. M. Sayler, S. Zeng, P. Wustelt, H. Figger, B. D. Esry, and G. G. Paulus, Phys. Rev. Lett. **111**, 093002 (2013).

[P9] "Frustrated tunnelling ionization during strong-field fragmentation of D_3^+," J. McKenna, A.M. Sayler, B. Gaire, N.G. Kling, B.D. Esry, K.D. Carnes, and I. Ben-Itzhak, New J. Phys. **14**, 103029 (2012).

[P8] "Multiphoton above threshold effects in strong-field fragmentation," C.B. Madsen, F. Anis, L.B. Madsen, and B.D. Esry, Phys. Rev. Lett. **109**, 163003 (2012).

[P7] "Enhancing the intense field control of molecular fragmentation," F. Anis and B.D. Esry, Phys. Rev. Lett. **109**, 133001 (2012).

[P6] "Multiphoton dissociation of HeH^+ below the $He^+(1s)$+H($1s$) threshold," D. Ursrey, F. Anis and B.D. Esry, Phys. Rev. A **85**, 023429 (2012).

[P5] "Dynamics of D_2^+ slow dissociation induced by intense ultrashort laser pulses," B. Gaire, J. McKenna, M. Zohrabi, K.D. Carnes, B.D. Esry, and I. Ben-Itzhak, Phys. Rev. A **85**, 023419 (2012).

[P4] "Controlling strong-field fragmentation of H_2^+ by temporal effects with few-cycle laser pulses," J. McKenna, F. Anis, A.M. Sayler, B. Gaire, N.G. Johnson, E. Parke, K.D. Carnes, B.D. Esry, and I. Ben-Itzhak, Phys. Rev. A **85**, 023405 (2012).

[P3] "Frustrated tunneling ionization during laser-induced D_2 fragmentation: detection of excited metastable D^* atoms," J. McKenna, S. Zeng, J.J. Hua, A.M. Sayler, M. Zohrabi, N.G. Johnson, B. Gaire, K.D. Carnes, B.D. Esry, and I. Ben-Itzhak, Phys. Rev. A **84**, 043425 (2011).

[P2] "Protonium formation in collisions of antiprotons with atomic and molecular hydrogen: A semiclassical study," R. Cabrera-Trujillo and B.D. Esry, Radiation Effects and Defects in Solids **166**, 346 (2011).

[P1] "Time-dependent dynamics of intense laser-induced above threshold Coulomb explosion," B.D. Esry and I. Ben-Itzhak, Phys. Rev. A **82**, 043409 (2010).

Controlling and tracing ultrafast processes in atoms and molecules in strong fields

Matthias F. Kling
James R. Macdonald Laboratory, Department of Physics
Kansas State University, Manhattan, KS 66506
Email: kling@phys.ksu.edu

Program Scope

The goal of our research is to gain deeper insight into ultrafast processes in atoms and molecules in strong laser fields. Our research is motivated by gaining fundamental insight into the real-time dynamics of many-electron systems and to gain control over more complex, highly-correlated systems.

Recent progress

We have continued our studies on the attosecond control of correlated electron dynamics in atoms and molecules. These studies are carried out in a large international collaboration involving several other JRML members (I. Ben-Itzhak, C.L. Cocke, and A. Rudenko), R.R. Jones (University of Virginia), G.G. Paulus (University of Jena, Germany), T. Pfeifer and R. Moshammer (MPI of Nuclear Physics, Heidelberg, Germany). We have used the developed carrier-envelope-phase (CEP)-tagging approach [Pub. [11]] in combination with cold-target-recoil-ion-momentum-spectroscopy (COLTRIMS) to study the non-sequential double ionization (NSDI) of Ar and N_2 under identical conditions to explore potential differences and their origin [Pub. [4]]. Furthermore, we have investigated correlated electron momentum spectra of Ar for different laser pulse durations to elucidate the rapid change in these spectra with pulse duration. These studies are currently extended to more complex molecular systems and dynamics.

Oriented and aligned molecules are of large importance in molecular physics. We have followed up on our initial demonstration of field-free orientation of heteronuclear molecules [De et al.(2009)] and investigated the orientation mechanisms in two-color laser fields as a function of the laser intensity [Pub. [1]]. The work was performed at JRML with theoretical support by the NRC group (M. Spanner and P. Corkum).

Finally, we have studied the photoionization of C_{60} in strong, ultrashort laser fields with a particular focus on the contribution of super-atomic molecular orbitals and Rydberg states to the photoionization.

Attosecond control of the correlated electron emission from N_2 molecules

We pioneered non-sequential double ionization (NSDI) in a single laser cycle for diatomic molecules, where N_2 serves as a test case. The first and second ionization potentials of N_2 with 15.58 eV and 27.12 eV, respectively, are very close to those of Ar with 15.76 eV and 27.63 eV, respectively. Similarities in the ionization behavior, particularly NSDI, of the two species have been reported (see e.g. [Uiterwaal et al.(2004)] and references therein). The fact that those similarities are not observed for all atom-molecule pairs with nearly equal ionization potentials (such as, for instance, Xe and O_2) (see e.g. [Grasbon et al.(2001)]) provides evidence, however, that this criterion is not sufficient to explain the resemblance in the ionization behavior.

It was shown recently that for NSDI of Ar, the transition to the single-cycle regime leads to dramatically different correlation spectra. There, the two electrons exhibit totally asymmetric rather than totally symmetric energy sharing, resulting in a characteristic cross-shaped pattern in the correlation momentum spectrum [Pub. [10]]. The theoretical interpretation of this experiment involves electron impact excitation of the Ar^+ ion. Since the excited-state spectra of Ar^+ and N_2^+ are significantly different from each other (the lowest excited energy of Ar^+ is 13.5 eV above the ground state, while N_2^+ has several excited states at much lower energy), there is no obvious reason to expect strong similarities between the two-electron momentum distributions of both species.

A remarkably high degree of similarity was observed in the CEP-resolved correlation spectra, which both exhibit totally asymmetric energy sharing between the electrons. Not only the striking similarities but also the differences in NSDI of the two studied species can be understood in terms of rescattering excitation with subsequent ionization (RESI) with sub-cycle depletion of the excited-state population [Pub. [4]]. The development of quantitative models for NSDI in molecules should benefit from both the many constraints imposed by our highly differential experimental data and the fact that a rigorous theoretical treatment of NSDI is significantly easier for an isolated recollision event than for the more complex long-pulse dynamics involving multiple recollisions.

Transition between field-free molecular orientation mechanisms

Laser-induced field-free molecular orientation had been demonstrated first in [De et al.(2009)], followed by [Oda et al.(2010)] and more recently [Frumker et al.(2012)]. These all-optical studies introduced a controversy into the literature. Although the experiments all made use of a similar two-color pump pulse, comprised of the fundamental frequency ω and its second harmonic 2ω, they invoked differing theoretical interpretations to explain the underlying mechanism leading to orientation. The first two studies [De et al.(2009), Oda et al.(2010)] attributed the orientation to the hyperpolarizability (HP) interaction [Kanai and Sakai(2001)], while the third [Frumker et al.(2012)] claimed that an ionization depletion (ID) mechanism [Spanner et al.(2012)] was active. The present work resolves this inconsistency by experimentally demonstrating that in fact either mechanism can be active depending on the intensity of the pump pulse, and therefore gives the complete and unified description of two-color laser-induced orientation. We

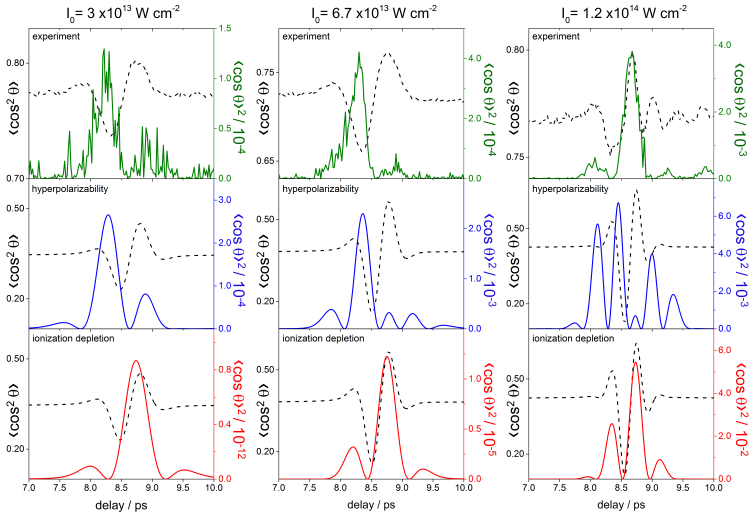

Figure 1: Comparison of experimental dynamic alignment and orientation data for CO at three selected intensities of the two-color field (top row) with theoretical predictions from the hyperpolarizability (middle row) and ionization depletion mechanisms (bottom row). The alignment (dashed black lines in all rows) is represented by the parameter $\langle\cos^2\theta\rangle$. The orientation is given by the parameter $\langle\cos\theta\rangle^2$.

recorded the field-free orientation of CO molecules as a function of the intensity of a two-color laser field (see Fig. 1). The experimental data is compared to recent theoretical predictions by Spanner *et al.*, considering both the HP and the ID mechanisms [Spanner et al.(2012)]. By comparing the measured and calculated temporal structures of the revivals of orientation, we unambiguously assign the regimes of the HP and ID mechanisms. This assignment based on the temporal structure of the revivals is further supported by the intensity dependence of the maximum orientation, which displays a sharp change in slope as the ID mechanism becomes active. For CO molecules, we find that at intensities below 8×10^{13} W/cm^2 the HP mechanism is responsible for orientation, while the ID mechanism becomes dominant at higher intensities. In addition, we find that the ID mechanism is responsible for generating the highest degrees of orientation we observe.

Ionization of C_{60} in ultrashort and intense laser fields

We have continued our investigations on the ionization of C_{60} molecules in strong laser fields. Recent VMI spectra of laser-ionized C_{60} have suggested that super-atomic molecular orbitals (SAMOs) in C_{60} can be

identified by using the energy and angular distributions of low energy electrons (below a photon energy) [Johansson et al.(2012)]. An earlier interpretation of low-energy structures was attributed to Rydberg states in C_{60} [Boyle et al.(2001)]. The studies in Ref. [Johansson et al.(2012)] have shown that even with 120 fs pulses thermal electron emission is largely dominating the spectra and only after subtraction of the thermal emission, structures which may be assigned to SAMOs become visible. We have thus investigated the electron emission from C_{60} with much shorter pulses of around 30 and 50 fs at 785 and 393 nm, respectively. Electrons from the ionization of C_{60} with the linearly polarized femtosecond laser pulses are recorded by a VMI spectrometer, giving access to the photoelectron angular distributions (PADs). The dependence of the electron PADs and kinetic energy spectra on laser intensity are studied for both wavelengths. In our studies at 785 nm, a previously unobserved six-lobe structure is seen in the low electron energy region (around 0.2 eV) for low laser intensities. In Ref. [Johansson et al.(2012)], a peak in the electron spectrum in this region is assigned to ionization from *p*-SAMOs. This assignment was confirmed by recent unpublished calculations by the Remacle group that take the interaction of the strong field with the molecule explicitly into account. Computation of PADs in strong fields will permit a more detailed comparison. At 393 nm we obtained similar results to those reported for 120 fs pulses at 400 nm [Johansson et al.(2012)]. We have further investigated the dependence of the photoionization of C_{60} on the laser pulse chirp. Both the spectra and the PADs are strongly modulated for the chirped pulses. Theoretical work is underway to understand the role of chirp in the population of excited states of C_{60} and their photoionization in strong fields.

Work in progress and outlook

We are currently finishing up studies on diatomic molecules in elliptically polarized pulses. NSDI proceeds via an inelastic recollision process, where the recollision is typically strongly suppressed in laser fields with elliptical polarization due to the transverse drift velocity of the electron. We experimentally investigated the effect of elliptical polarization on high-harmonic generation in NO in 4 fs laser fields at 750 nm. Even for high ellipticities, where HHG is suppressed for Ar, significant high-harmonic generation was found for NO.

With the recent move of the group to Munich, Germany, further activities at and with JRML are continued within the framework of an international collaboration.

Publications

1. I. Znakovskaya, M. Spanner, S. De, H. Li, D. Ray, P. Corkum, I.V. Litvinyuk, C.L. Cocke, M.F. Kling, **Transition between mechanisms of laser-induced field-free molecular orientation**, arXiv:1307.0303 (2013).
2. N.G. Kling, K.J. Betsch, M. Zohrabi, S. Zeng, F. Anis, U. Ablikim, B. Jochim, Z. Wang, M. Kbel, M.F. Kling, K. Carnes, B.D. Esry, I. Ben-Itzhak, **Carrier-envelope phase control over pathway interference in strong-field dissociation of H_2^+**, arXiv:1306.4010 (2013).
3. K. Schnorr, A. Senftleben, M. Kurka, A. Rudenko, L. Foucar, G. Schmid, A. Broska, T. Pfeifer, K. Meyer, D. Anielski, R. Boll, D. Rolles, M. Kübel, M.F. Kling, Y.H. Jiang, S. Mondal, T. Tachibana, K. Ueda, T. Marchenko, M. Simon, G. Brenner, R. Treusch, J. Ullrich, C.D. Schröter, R. Moshammer, **Time-resolved measurements of the interatomic Coulombic decay in Ne_2**, *Phys. Rev. Lett.* **111**, 093402 (2013).
4. M. Kübel, N.G. Kling, K.J. Betsch, N. Camus, A. Kaldun, U. Kleineberg, I. Ben-Itzhak, R.R. Jones, G.G. Paulus, T. Pfeifer, J. Ullrich, R. Moshammer, M.F. Kling, B. Bergues, **Nonsequential double ionization of N_2 in a near-single-cycle laser pulse**, *Phys. Rev. A* **88**, 023418 (2013).
5. Y.H. Jiang, A. Senftleben, M. Kurka, A. Rudenko, L. Foucar, O. Herrwerth, M.F. Kling, M. Lezius, J. van Tilborg, A. Belkacem, K. Ueda, D. Rolles, R. Treusch, Y.Zh. Zhang, Y.F. Liu, C.D. Schröter, J. Ullrich, R. Moshammer, **Ultrafast dynamics in acetylene clocked in a femtosecond XUV stopwatch**, *J. Phys. B* **46**, 164027 (2013).
6. M.F. Kling, P. von den Hoff, I. Znakovskaya, R. de Vivie-Riedle, **(Sub-)femtosecond control of molecular reactions via tailoring the electric field of light**, *Phys. Chem. Chem. Phys.* **15**, 9448 (2013).
7. K.J. Betsch, N. G. Johnson, B. Bergues, M. Kübel, O. Herrwerth, A. Senftleben, I. Ben-Itzhak, G.G. Paulus, R. Moshammer, J. Ullrich, M.F. Kling, R.R. Jones, **Controlled directional ion emission from multiple fragmentation channels of CO driven by a few-cycle laser field**, *Phys. Rev. A* **86**, 063403 (2012).
8. M. Kübel, K.J. Betsch, Nora G. Johnson, U. Kleineberg, R. Moshammer, J. Ullrich, G.G. Paulus, M.F. Kling, B. Bergues, **Carrier-envelope-phase tagging in measurements with long acquisition times**, *New J. Phys.* **14**, 093027 (2012).
9. M. Magrakvelidze, O. Herrwerth, Y.H.Jiang, A. Rudenko, M. Kurka, L. Foucar, K.U. Kühnel, M. Kübel, Nora G. Johnson, C.D. Schröter, S. Düsterer, R. Treusch, M. Lezius, I. Ben-Itzhak, R. Moshammer, J. Ullrich, M.F. Kling, U. Thumm, **Tracing nuclear wave packet dynamics in singly and doubly charged states of N_2 and O_2 with XUV pump XUV probe experiments**, *Phys. Rev. A* **86**, 013414 (2012).

10. B. Bergues, M. Kübel, N.G. Johnson, B. Fischer, N. Camus, K.J. Betsch, O. Herrwerth, A. Senftleben, A.M. Sayler, T. Rathje, T. Pfeifer, I. Ben-Itzhak, R.R. Jones, G.G. Paulus, F. Krausz, R. Moshammer, J. Ullrich, M.F. Kling, **Controlling and tracing correlated electron emission on attosecond timescales**, *Nature Communic.* **3**,813 (2012).

11. T. Rathje, N.G. Johnson, M. Möller, F. Süßmann, D. Adolf, M. Kübel, R. Kienberger, M.F. Kling, G.G. Paulus, A.M. Sayler, **Review of attosecond resolved measurement and control via carrier-envelope phase tagging with above-threshold ionization**, *J. Phys. B.* **45**, 074003 (2012).

12. I. Znakovskaya, P. von den Hoff, G. Marcus, S. Zherebtsov, B. Bergues, X. Gu, Y. Deng, M.J.J. Vrakking, R. Kienberger, F. Krausz, R. de Vivie-Riedle, M.F. Kling, **Sub-cycle controlled charge-directed reactivity with few-cycle mid-infrared pulses**, *Phys. Rev. Lett.* **108**, 063002 (2012).

13. W. Cao, G. Laurent, S. De, M. Schöffler, T. Jahnke, A.S. Alnaser, I.A. Bocharova, C. Stuck, D. Ray, M.F. Kling, I. Ben-Itzhak, Th. Weber, A.L. Landers, A. Belkacem, R. Dörner, A.E. Orel, T.N. Rescigno, C.L. Cocke, **Dynamic modification of the fragmentation of autoionizing states of O_2^+**, *Phys. Rev. A* **84**, 053406 (2011).

14. H. Li, D. Ray, S. De, I. Znakovskaya, W. Cao, G. Laurent, Z. Wang, M.F. Kling, A.T. Le, C.D. Lin, C.L. Cocke, **Orientation dependence of the ionization of CO and NO in an intense femtosecond two-color laser field**, *Phys. Rev. A* **84**, 043429 (2011).

15. A. Gzibegovic-Busuladzic, E. Hasovic, M. Busuladzic, D.B. Miosevic, F. Kelkensberg, W.K. Siu, M.J.J. Vrakking, F. Lepine, G. Sansone, M. Nisoli, I. Znakovskaya, M.F. Kling, **Above-threshold ionization of diatomic molecules by few-cycle laser pulses**, *Phys. Rev. A* **84**, 043426 (2011).

16. S. De, M. Magrakvelidze, I.A. Bocharova, D. Ray, W. Cao, I. Z nakovskaya, H. Li, Z. Wang, G. Laurent, U. Thumm, M.F. Kling, I.V. Litvinyuk, I. Ben-Itzhak, C.L. Cocke, **Following dynamic nuclear wave packets in N_2, O_2 and CO with few-cycle infrared pulses**, *Phys. Rev. A* **84**, 043410 (2011).

17. F. Süßmann, S. Zherebtsov, J. Plenge, Nora G. Johnson, M. Kübel, A.M. Sayler, V. Mondes, C. Graf, E. Rühl, G.G. Paulus, D. Schmischke, P. Swrschek, M.F. Kling, **Single-shot velocity-map imaging of attosecond light-field control at kilohertz rate**, *Rev. Sci. Instr.* **82**, 093109 (2011).

18. B. Jochim, R. Averin, N. Gregerson, J. McKenna, S. De, D. Ray, M. Zohrabi, B. Bergues, K.D. Carnes, M.F. Kling, I. Ben-Itzhak, E. Wells, **Velocity map imaging as a tool for gaining mechanistic insight from closed-loop control studies of molecular fragmentation**, *Phys. Rev. A* **83**, 043417 (2011).

19. D. Ray, Z.J. Chen, S. De, W. Cao, I.A. Bocharova, I.V. Litvinyuk, A.T. Le, C.D. Lin, M.F. Kling, C.L. Cocke, **Momentum spectra of electrons rescattered from rare gas targets following their extraction by one- and two-color short laser pulses**, *Phys. Rev. A* **83**, 013410 (2011).

20. S. Zherebtsov, A. Wirth, T. Uphues, I. Znakovskaya, O. Herrwerth, J. Gagnon, M. Korbman, V.S. Yakovlev, M.J.J. Vrakking, M. Drescher, M.F. Kling, **Attosecond imaging of XUV-induced atomic photoionization and Auger decay in strong laser fields**, *J. Phys. B.* **44**, 105601 (2011).

21. I. Znakovskaya, P. von den Hoff, N. Schirmel, G. Urbasch, S. Zherebtsov, B. Bergues, R. de Vivie-Riedle, K.-M. Weitzel, M.F. Kling, **Waveform control of orientation-dependent ionization of DCl in few-cycle laser fields**, *Phys. Chem. Chem. Phys.* **13**, 8653 (2011).

22. N.G. Johnson, O. Herrwerth, A. Wirth, S. De, I. Ben-Itzhak, M. Lezius, B. Bergues, M.F. Kling, A. Senftleben, C.D. Schröter, R. Moshammer, J. Ullrich, K.J. Betsch, R.R. Jones, T. Rathje, K. Rühle, W. Müller, G.G. Paulus, **Single-shot carrier-envelope-phase tagged ion momentum imaging of non-sequential double ionization of argon in intense 4-fs laser fields**, *Phys. Rev. A* **81**, 013412 (2011).

References

[De et al.(2009)] S. De et al., Phys. Rev. Lett. **103**, 153002 (2009).
[Uiterwaal et al.(2004)] C. J. G. J. Uiterwaal et al., Eur. Phys. J. D **30**, 379 (2004).
[Grasbon et al.(2001)] F. Grasbon et al., Phys. Rev. A **63**, 041402 (2001).
[Oda et al.(2010)] K. Oda et al., Phys. Rev. Lett. **104**, 213901 (2010).
[Frumker et al.(2012)] E. Frumker et al., Phys. Rev. Lett. **109**, 113901 (2012).
[Kanai and Sakai(2001)] T. Kanai and H. Sakai, J. Chem. Phys. **115**, 5492 (2001).
[Spanner et al.(2012)] M. Spanner et al., Phys. Rev. Lett. **109**, 113001 (2012).
[Johansson et al.(2012)] J. O. Johansson et al., Phys. Rev. Lett. **108**, 173401 (2012).
[Boyle et al.(2001)] M. Boyle et al., Phys. Rev. Lett. **87**, 273401 (2001).

Controlling rotations of asymmetric top molecules: methods and applications

Vinod Kumarappan
James R. Macdonald Laboratory, Department of Physics
Kansas State University, Manhattan, KS 66506
vinod@phys.ksu.edu

Program Scope

The goal of this program is to improve molecular alignment methods, especially for asymmetric top molecules, and then use well-aligned molecules for further experiments in ultrafast molecular physics. We use multi-pulse sequences for 1D alignment and orientation and 3D alignment of molecules.

Recent progress

Alignment assisted orientation of CO

(*X. Ren, V. Makhija, H. Li, M. F. Kling and V. Kumarappan*)

While field-free 1D alignment of molecules with intense non-resonant pulses has become a widely used tool, the same cannot be said for 1D orientation. Field-free orientation of CO was demonstrated with a phase-stable combination of two pulses (at 800 nm and 400 nm), the level of orientation obtained was rather weak ($\langle\cos\theta\rangle \sim 0.06$), even though the pulses where strong enough to produce significant amount of ionization. Subsequently, it was realized that in this measurement the orientation was produced primarily by the ionization depletion mechanism, in which molecules of one orientation are preferably ionized by the pump pulses and the remaining population becomes oriented in the opposite direction. The primary reason for the poor degree of orientation is the weak hyper-polarizability of CO. This constraint remains for most small molecules since large hyper-polarizability is typically accompanied by low ionization potentials and the field that can be applied without ionizing the molecules is correspondingly smaller. The second reason for poor orientation by two-color pulses is that the best orientation for any initial rotational eigenstate (as a function of time after the orienting pulse) is achieved after half the rotation period of the molecule, where states of opposite parity orient in opposite direction and cancel each other out. Only after a full rotational period do the even and odd parity states orient in the same direction, but at this time the orientation of both sets of states is weak.

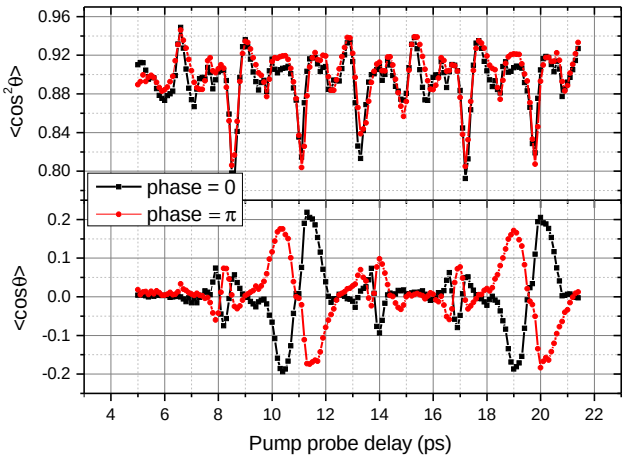

Figure 1: Alignment and orientation of CO, measured by $\langle cos^2\theta\rangle$ and $\langle cos\theta\rangle$, respectively, after a sequence of 800 nm and phase-locked 800+400 nm pulses. Pre-aligning the molecules at about $3/4^{th}$ of a revival period before the two-color pulse (at t=0 ps) significantly enhances the degree of orientation.

Following theoretical work by [2], we have shown experimentally that the orientation of CO can be substantially improved by aligning the molecules before orienting them. By applying the two-color pulse at $3/4^{th}$ of the rotational period after the a single color aligning pulse, the rotational wavepacket formed in odd initial-J states can be suppressed, leaving the high degree of orientation of the even initial-J states at the half-revival largely un-canceled. The molecules are cooled to ∼3 K, where the $J = 0$ population is about twice as much as the $J = 1$ population. By largely canceling the wavepacket launched from the $J = 1$

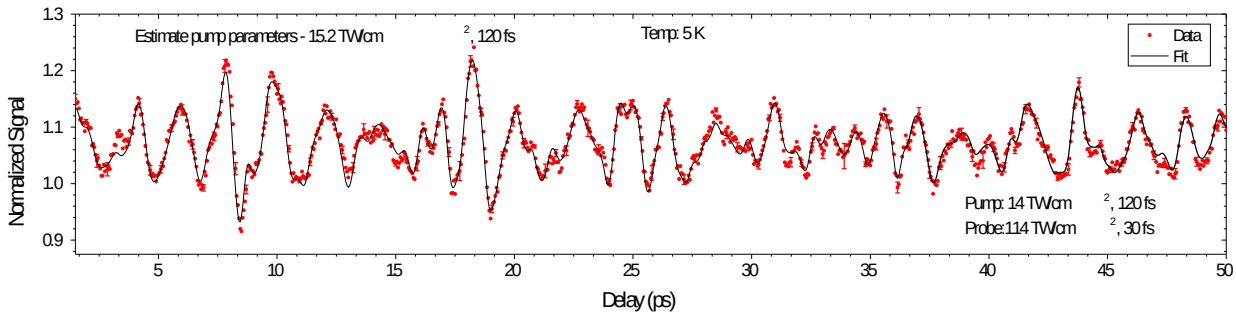

Figure 2: The delay dependence of the yield of $C_2H_4^+$ ion after alignment by a linearly polarized pulse at $t = 0$. Also shown is the fit obtained using 1.

states, the degree of field-free orientation can be boosted substantially when compared to previous two-color experiments. The measured $\langle cos^2\theta \rangle$ and $\langle cos\theta \rangle$ traces are shown in Fig. . These values were measured in the plane of the detector from the momentum distribution of C^{2+} ions. When the 2D momentum distributions are Abel inverted the peak value of $\langle cos\theta \rangle$ was 0.19, about a factor of three better than that reported by De *et al.*. A manuscript is under preparation.

Extracting 2D angular information from rotational wavepackets: Ionization

(*V. Makhija, D. Gockel, X. Ren and V. Kumarappan*)

Strong-field ionization of molecules in a linear polarized laser pulse depends on their orientation with respect to the field. For linear molecules this orientation can be specified by the polar angle θ between the laser polarization and the molecular axis, but for asymmetric tops two Euler angles are necessary. The second angle χ corresponds to the rotation of the molecule about its own axis. Linear molecules can be aligned with non-resonant laser pulses and the angle dependence of strong-field ionization can the be measured by scanning the angle between the aligning pump and the ionizing probe pulses. But this approach fails for asymmetric tops because although the pump pulse excites rotations in χ, the distribution of molecular axes remains cylindrically symmetric about the pump polarization axis and an angle scan for χ-dependence is not possible. Three-dimensional alignment appears to offer a way out, but it would be necessary to use non-collinear pump and probe pulses and to vary the angle between to two beams over at least zero to ninety degrees. Apart from the difficulty in getting good field-free 3D alignment, this would be an extremely challenging experiment.

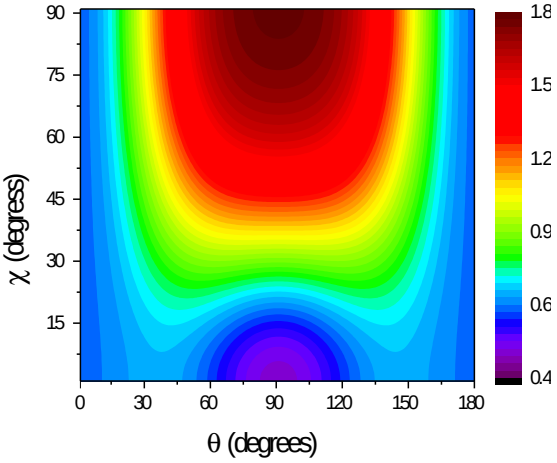

Figure 3: The 2D angle dependence of strong-field ionization of ethylene in a linearly polarized pulse obtained from the fit shown in Fig 2. The angle between the C-C bond and the laser polarization is θ. The angle χ corresponds to the rotation of the molecule about its own axis; for $\theta = 90°$, it is zero when the molecular plane is perpendicular to the laser polarization.

We show that it is possible to obtain the 2D angle dependence of strong-field ionization— and, by extension, other probe processes—from the delay dependence of the ionization yield in a pump-probe experiment. The signal due to any process that depends on these angles can be expanded in a basis set of Wigner functions. If the measurement is made from a rotational wavepacket $|\psi(t)\rangle$, the time-dependent expectation

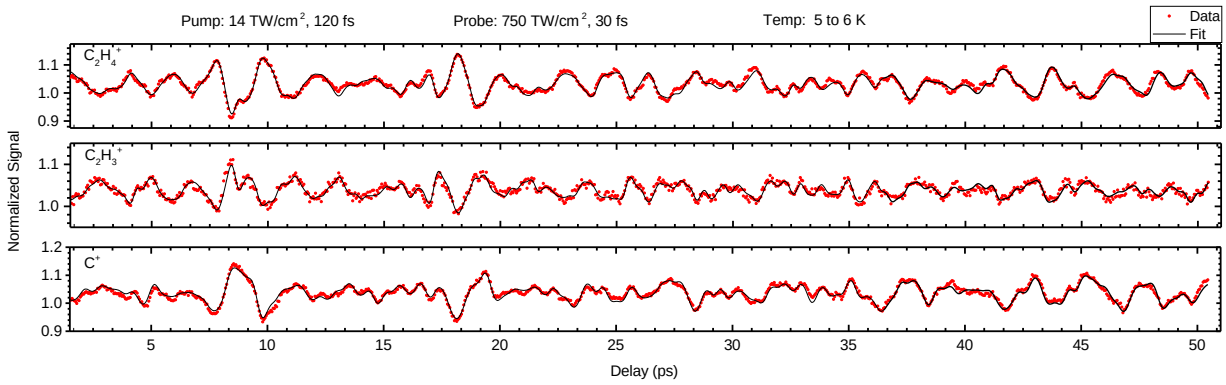

Figure 4: Left: Revivals in the yields of free species produced from ethylene by a probe pulse, which is delayed with respect to an aligning pump with the same linear polarization. The pump intensity and pulse duration extracted from the fitting procedure are 14 TW/cm^2 and 120 fs, respectively. Independently measured values were 15 TW/cm^2 and 120 fs, respectively.

value becomes

$$\langle I(t)\rangle = \sum_{jk} C_{jk} \left\langle \psi(t) \left| D^j_{k0} \right| \psi(t) \right\rangle . \tag{1}$$

Thus, the problem of finding $I(\theta, \chi)$, the molecular frame angle dependence of I, is reduced to determining the coefficients C_{jk} from the expansion of the measured $\langle I(t)\rangle$ in terms of $\left\langle \psi(t) \left| D^j_{k0} \right| \psi(t) \right\rangle$. The procedure is similar to that of Mikosch *et al.* [3], although we make no use of angle-scans and extend the method to asymmetric tops.

In the experiment, we measure the yield of $C_2H_4^+$ from supersonically cooled ethylene as a function of delay between the alignment pulse and the probe pulse, which is kept weak enough that very little fragmentation is observed. By varying both the pump laser parameters in the TDSE calculation and the C_{jk}'s, we find the best fit to the signal and extract the pump laser parameters (intensity and pulse duration), the target rotational temperature, and the 2D angle dependence of the strong-field ionization rate. The measured ion yield as a function of pump-probe delay (normalized to the yield obtained from unaligned molecules) and the fit are shown in Fig. 2. The corresponding extracted 2D angle dependence of the ionization rate are shown in Fig. 3. A comparison with a strong-field approximation (SFA) calculation by A. T. Le indicates that the HOMO and HOMO-1 orbitals contribute to the signal under these conditions. With lower probe intensity, the contribution we attribute to HOMO-1 goes away, as expected from calculations.

Angle-dependent fragmentation of asymmetric tops

(*V. Makhija, D. Gockel, X. Ren and V. Kumarappan*)

When the laser intensity is high enough, the mass spectrum of ethylene shows multiple fragments. A gated integrator was used to measure the yield of several of these fragments as a function of delay between the alignment pulse and the fragmenting probe. Three of these are shown in Fig. 4.

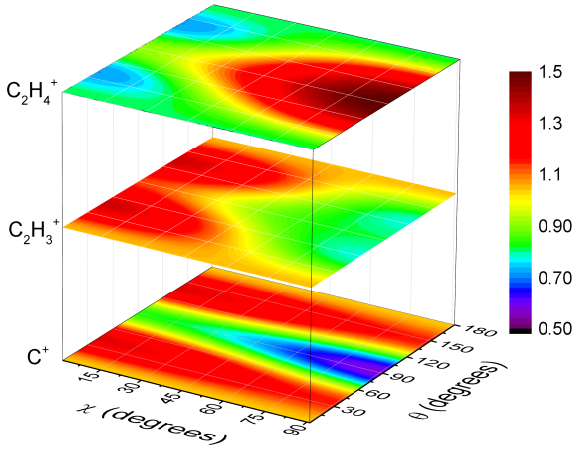

Figure 5: The 2D angle dependence of three ions obtained from the fits shown in Fig. 4.

The same alignment pulse was used for all three measurements, and the gas jet operating conditions were kept the same. The fitting procedure yields very similar results for the laser intensity, pulse duration and gas temperature, although the angular dependence, shown in Fig. for the three ions is quite different. This is an important check that the fit is unique. Note that the momentum distribution of the ions is not measured and this method does not rely of the axial recoil approximation. A manuscript reporting the results on ethylene ionization and fragmentation is in preparation.

High harmonic generation from asymmetric tops

(*V. Makhija, X. Ren, J. Tross, S. Mondal, A.T. Le, C. Trallero and V. Kumarappan*)

We have measured delay dependent HHG spectra from ethylene, but extraction of angle-dependent HHG amplitudes requires the assumption that the angle-dependent phase is zero. Calculations by A.T Le using the quantitative rescattering theory suggests that this is a good approximation for the contribution to HHG from the HOMO of ethylene, but not from HOMO-1. We found that some lower order harmonics ($<13^{th}$) yield angle dependences that compare well with theory, but the agreement is poor for higher orders. This may be due to the presence of HOMO-1 contributions that invalidate our zero assumption, or due to nuclear dynamics in the ion. Further experiments may be necessary to improve our understanding of the data.

Collaborations:

We have active collaborations with Carlos Trallero and Martin Centurion. Some of this collaborative work is reported in their contributions.

Outlook and Plans

A 20 mJ/pulse, 25 fs, 1 kHz repetition rate, carrier-envelop phase stable laser that we call HITS is expected to be installed in the Macdonald Lab within weeks. The system will include a high-energy OPA that will allow us to produce few-cycle, long wavelength (up to 2200 nm) pulses. The HHG experiments will then be capable of probing photo-ionization over a much larger energy range with smaller steps and, thus, higher resolution. The extraction of angle-dependent information from HHG spectra requires assumptions about the phase of the harmonics; this will be addressed by adding phase measurements.

The extraction of 2D angle dependence of probe processes from probe-probe delay scans is a powerful new tool for studying polyatomic molecules, especially for processes, that are not easily studied by coincidence techniques like COLTRIMS. Several experiments that seek to extract information about molecular ionization and fragmentation are now being planned.

Publications from DOE-funded research:

[P1] V. Makhija, X. Ren and V. Kumarappan, Phys. Rev. A 85 **85**, 033425 (2012).
[P2] X. Ren, V. Makhija and V. Kumarappan, Phys. Rev. A **85**, 033405 (2012).

References

[1] S. De *et al.*, Phys. Rev. Lett. **103** 153002 (2009).
[2] S. Zhang *et al.*, Phys. Rev. A **83**, 043410 (2011).
[3] J. Mikosch *et al.*, J. Chem. Phys. **139**, 024304 (2013).

Strong field rescattering physics and attosecond physics

C. D. Lin
J. R. Macdonald Laboratory, Kansas State University
Manhattan, KS 66506
e-mail: cdlin@phys.ksu.edu

Program Scope:

We investigate the interaction of ultrafast intense laser pulses, and of attosecond pulses, with atoms and molecules. Most notable accomplishments in the past year are: (1) Waveform synthesis for optimizing high-order harmonic generation, (2) High-order harmonic generation from polyatomic molecules by Mid-infrared lasers, (3) Photoelectron and transient absorption spectra in attosecond XUV pulses coupled to intense IR lasers. Additional results and plans for the coming year will be summarized.

Introduction

When an atom or molecule is exposed to an intense infrared laser pulse, an electron which was released earlier may be driven back by the laser field to recollide with the parent ion. The recollision of electrons with the ion can be described by the quantitative rescattering theory (QRS) established in 2009 under this program. The first two projects deal with high-order harmonic generation. In the third project we study the control of the dynamics of electrons exposed to attosecond pulses in the presence of strong coupling IR lasers and how the XUV pulses are shaped in the gaseous medium.

1. Waveform synthesis for optimizing high-order harmonic generation

Recent progress

Bright, coherent light sources over a broad electromagnetic spectrum are always in great demand for physical sciences. Today such sources are available only at large synchrotron and free-electron X-ray lasers facilities. Through high-order harmonics generation (HHG), a broadband coherent light can be generated with intense infrared and mid-infrared lasers, but conversion efficiency of HHG is quite small. To enhance HHG yields so far most of the experimental effort is to optimize phase-matching conditions. In this program we study how to optimize the HHG yields at the atomic level by manipulating the waveform of the laser pulse through synthesis of two- or three-color fields. Our simulations have shown that enhancement of the HHG yields by two-orders of magnitude or more. The optimized waveform also enhances HHG from the so-called short-trajectory electrons, thus additional enhancement is achieved after propagation in the gas medium. A manuscript based on this work is under preparation.

Ongoing projects and future plan

Experimentally waveform synthesis is being carried out at a number of laboratories, e.g., MIT, MPQ, Lund University, and Vienna Institute of Technology. To achieve optimal HHG enhancement, the amplitudes and phases of the two- or three-color fields should have definite values for each set of wavelengths that are to be synthesized. In particular, the phase of each elementary pulse should be stable to better than about 0.2π radians. All the reported waveform synthesis experiments so far have not pursued the optimization of HHG. We have been in contact with some laboratories about this work and more will be expected in the coming year. Additional simulations will be needed depending on the range of parameters of the lasers in each laboratory. Our simulation method is general and can accommodate the restrictions of parameter spaces imposed from each laboratory. This work will have great impact on the future of HHG as a tool for generating tabletop light sources.

2. High-order harmonic generation from polyatomic molecules

Recent progress

In the past year, we have extended the QRS theory to study HHG from polyatomic molecules by MIR lasers. HHG spectra contain structural information of the target molecules but the interpretation still needs a reliable theory. In the past three years HHG spectra from polyatomic molecules have been reported, e.g., Wong et al, Phys. Rev. A84, 051403 (2011). In these measurements the molecules are randomly distributed and MIR laser of wavelength of 1.7 μm was used. They also observed HHG spectra between isomers, e.g., for $C_2H_2Cl_2$ and for C_4H_8. The isomer dependence is of particular interest since photoionization cross sections are independent of isomers if the molecules are isotropically distributed. To extend QRS to study HHG from polyatomic molecules we need to calculate tunneling ionization rates and complex photoionization transition dipole moment for each orientation angle (Θ,ψ) over the 4π surface. The phase of the laser-induced dipole from each orientation angle has to be carefully taken into account. In paper A1 below, we showed that the experimentally observed difference in HHG between the two isomers has been well reproduced by the QRS theory. However, discrepancy in the spectra at the higher photon energy region was observed. We attributed the discrepancy to the high laser intensity used in the experiment where excessive ionization results in phase-mismatch from the electron plasma, where the effect is more important for higher harmonics. Due to the weak harmonic yields from MIR lasers, experiments tend to be carried out at intensities that are too high. Additional publications on HHG from polyatomic molecules are listed in A3, A7 and A9 below.

Ongoing projects and future plan

HHG from polyatomic molecules are best performed with MIR lasers due to the low ionization energies of these targets. Since the returning electron yields decrease quickly with the wavelength, intensities of the lasers used for existing experiments tend to be too high such that phase-mismatch due to plasma defocusing distorts the observed HHG spectra from the single-molecule predictions. Ideally this effect can be accounted for if propagation in the medium is included. Such calculations are quite time-consuming and thus had not been done yet. It is desirable that HHG from oriented/aligned polyatomic molecules be studied experimentally. Such data would provide a better verification of the QRS model and the related tunneling ionization rates and the dipole transition amplitudes. We comment that few photoionization cross section data are available for large molecules over an extended photon energy region and HHG data would provide useful information. In particular, HHG for isomers will be of great interest. We anticipate more theoretical work in this area will be carried out as experiments become available.

In the last year we also studied HHG from a molecule undergoing large vibrational motion (A9 below). We have been studying the isotope dependence of HHG using the same model and this work will be completed in the next few months. We then plan to look at HHG from a dynamic system consisting of two electronic states. This will be our first step toward a theory of HHG for "real" dynamic systems.

3. Attosecond Physics and transient absorption spectroscopy

At present, single attosecond pulses (SAP) and attosecond pulse trains (APT) in the XUV region are generated by the HHG processes. In the last few years, such pulses are becoming more widely available. Most of the experiments have been carried out using an attosecond (AS) pulse in the presence of an intense IR laser. The AS interacts weakly with the target, but the presence of an intense IR modifies the medium, such that the effect of XUV on the target can be controlled nonlinearly in the time domain, by changing the time delay between the two pulses. Most of the existing theoretical studies adopt the "brute-force" method by solving the time-dependent

Schrödinger Equation directly. We seek to identify situations where simpler models can be employed where the effect of the IR is most prominent.

In this work, we focus on Fano resonances. In a few-level model. We examined the electron spectra or the absorption spectra of the XUV in the presence of a near-resonant IR. In pub. A10 we studied the 2s2p (^{1}P) state of helium that is populated by an attosecond pulse from the ground state in the presence of an intense visible laser that can couple nearly resonantly with the $2s^2$ ^{1}S state. We showed that the Fano resonance profile of the 2s2p (^{1}P) state is modified, depending on the intensity of the visible laser and the time delay. If one measures the transmitted light in a gas medium, then the emerged XUV light can be manipulated by the intensity of the laser and the time delay. In other words, a laser can be used to control or shape the transmitted XUV light. The effect of propagation of the XUV light in a gas medium was considered in pub. A6. This general control of the absorption lineshape with an intense laser has been investigated experimentally for He by the group of Thomas Pfeiffer and their results were published in Science 340, 716 (2013). We were asked to provide a perspective article on that work, see Pub. A4.

Ongoing projects and future plan

The postdoc who was carrying out this work has left the group earlier in 2013. There are still a few projects that will be finished. One is to use our model to interpret the transient absorption spectra in N_2 by an attosecond pulse in the presence of an IR. This is in collaboration with G. Sansone of Milan and his group who performed the experiment. A joint manuscript is under preparation. Another collaboration is going on with Thomas Pfeiffer's group (Heidelberg) in order to explain some of their He experiment, to include the propagation effect in order to explain their absorption spectra. In another project, we are looking at the electron spectra of the dipole-forbidden states that are populated in the presence of the IR. The method allows one to extract the properties of such dipole-forbidden states that cannot be directly observed by the XUV alone.

Publications

A. Published and accepted papers (11papers from 2011 not listed)

A1. A. T. Le, R. R. Lucchese and C. D. Lin, "high harmonic generation from molecular isomers with mid-infrared intense laser pulses", accepted for Phys. Rev. A

A2. Toru Morishita and C. D. Lin, "Photoelectron spectra and high Rydberg states of lithium generated by intense lasers in the over-the-barrier ionization regime", Phys. Rev. A87, 063405 (2013).

A3. A.-T. Le, R. R. Lucchese and C. D. Lin, "Quantitative rescattering theory of high-order harmonic generation for polyatomic molecules", Phys. Rev. A87, 063406 (2013).

A4. C. D. Lin and Wei-Chun Chu, "Controlling atomic line shapes", Science, 340, 694 (2013)

A5. Wei-Chun Chu and C. D. Lin, "Probing and controlling the autoionization dynamics with attosecond light pulses", in *Progress in Ultrafast Intense Laser science IX.* Ed K. Yamanouchi and K. Midorikawa, Springer 2013.

A6. Wei-Chun Chu and C. D. Lin, " Absorption and emission of single attosecond light pulses in an autoionizing gaseous medium dressed by a time-delayed control field", Phys. Rev. A87, 013415 (2013)

A7. M. C. H. Wong, A.-T. Le, A. F. Alharbi, A. E. Boguslavskiy, R. R. Lucchese, J.-P. Brichta, C. D. Lin, and V. R. Bhardwaj, "High harmonic spectroscopy of the Cooper Minimum in Molecules", Phys. Rev. Lett. 110, 033006 (2013)

A8. Junliang Xu, Cosmin I Blaga, A. D. DiChiara, E. Sistrunk, K Zhang, Zhangjin Chen, A. T. Le, Toru Morishita, C. D. Lin, P. Agostini and L. F. DiMauro, “Laser-induced electron diffraction for probing rare gas atoms”, Phys. Rev. Lett. 109, 233002 (2012)

A9. A. T. Le, T. Morishita, R. R. Lucchese and C. D. Lin, “Theory of high harmonic generation for probing time-resolved large-amplitude molecular vibrations with ultrafast intense lasers”, Phys. Rev. Lett. 109, 203004 (2012)

A10. Wei-Chun Chu and C. D. Lin, “Spectral compression and enhancement of single attosecond pulses by time-delayed control field”, Fast track Communication, J. Phys. B45, 201002 (2012)

A11. C. D. Lin, Cheng Jin , Anh-Thu Le, and R. R. Lucchese, “ Probing molecular frame photoelectron angular distributions via high-order harmonic generation from aligned molecules”, J. Phys. B45, 194010 (2012).

A12. C. D. Lin and Junliang Xu, “Imaging ultrafast dynamics of molecules with laser-induced electron diffraction”, Perspective, PCCP 14, 13133-45 (2012)

A13. Guoli Wang, Cheng Jin, Anh-Thu Le and C. D. Lin, “Conditions for extracting photoionization cross sections from laser-induced high-order-harmonic spectra”, Phys. Rev. A86, 015401 (2012).

A14. Chen Jin and C. D. Lin, “Comparison of high-order harmonic generation of Ar using truncated Bessel and Gaussian beams”, Phys. Rev. A85, 033423 (2012).

A15. Wei Cao, Guillaume Laurent, Cheng Jin, Hui Li, Zhenghua Wang, C D Lin, I Ben-Itzhak and C L Cocke, “Spectral Splitting and quantum path study of high harmonic generation from a semi-infinite gas cell”, J. Phys. B 45, 074013 (2012).

A16. Cosmin I. Blaga, Junliang Xu, Anthony D. DiChiara, Emily Sistrunk, Kaikai Zhang, Pierre Agostini, Terry A. Miller, Louis F. DiMauro, C. D. Lin, “Observation of femtosecond, sub-Angstrom molecular bond relaxation using laser-induced electron diffraction”, Nature (Letter) 483, 194-197 (2012).

A17. Wei-Chun Chu and C. D. Lin, Photoabsorption of attosecond XUV light pulses by two strongly laser-coupled autoionizing states”, Phys. Rev. A85, 013409 (2012).

A18. Cheng Jin, Julien B. Bertrand, R. R. Lucchese, H. J. WÄorner, Paul B. Corkum, D. M. Villeneuve, Anh-Thu Le, and C. D. Lin, “ Intensity dependence of multiple-orbital contributions and shape resonance in high-order harmonic generation of aligned N_2 molecules”, Phys. Rev. A85, 013405 (2012).

A19. C. C. Trallero-Herrero, Cheng Jin, Bruno Schmidt, A. Shiner, D. M. Villeneuve, P. B. Corkum, C. D. Lin, F. Legare and A. T. Le, “Generation of broad XUV continuous high harmonic spectra and isolated attosecond pulses with intense mid-infrared lasers ,“, fast track communications, J. Phys. B45, 011001 (2012).

Time–resolved imaging of ultrafast light-induced dynamics

Artem Rudenko

J. R. Macdonald Laboratory, Department of Physics, Kansas State University, Manhattan, KS 66506

rudenko@phys.ksu.edu

Program scope: This program aims at studying basic physics of (non-linear) light-matter interactions in a broad span of wavelengths, from terahertz and infrared (IR) to XUV and X-ray domains, and applying the knowledge gained for real-time imaging of ultrafast photo-induced reactions. Two main directions of this research currently are (i) studies of the dynamics induced by inner-shell absorption of one or many photons, with the focus on charge and energy redistribution mechanisms in dissociating molecular systems; and (ii) imaging and control of light-induced structural rearrangement reactions in small polyatomic molecules.

Recent progress:

1. Multiple inner-shell ionization and interatomic relaxation processes

The development of high-intensity short-pulsed XUV and x-ray radiation sources promises revolutionary new techniques in diverse scientific fields, among others nurturing the vision of dynamic imaging of matter with angstrom spatial and femtosecond (or even sub-femtosecond) temporal resolution. In particular, the start-up of the first hard X-ray free-electron laser (FEL), the Linac Coherent Light Source (LCLS) triggered a variety of imaging experiments on small molecules, clusters, nanocrystals, and isolated bio- and nanoparticles [1-4, P1]. The basic prerequisite for designing these experiments is understanding the response of individual atoms, and tracing electronic and nuclear dynamics in the vicinity of the atom that absorbed X-ray photon(s), thus, revealing basic mechanisms of local radiation damage. Pursuing this goal, we have recently performed a series of experiments comparing multiphoton multiple ionization of isolated atoms and similar atoms in molecular systems. Measuring the charge states distributions for the ionization of heavy rare gases such as Kr and Xe [P2, P4,P5], for certain X-ray photon energies we observed the charge states well above the predictions of the simple sequential ionization model (up to 36+ instead of 27+ in Xe), which was very successful in explaining results of the earlier LCLS experiments on lighter elements [5,6]. Studying the wavelength dependence of inner-shell multiphoton ionization, we found that intermediate resonant excitations are responsible for the extremely high charge states observed. Simultaneous measurement of the X-ray fluorescence photons provided a direct evidence of the role of these bound-bound transitions [P2]. As a next step, we compared the ionization of the isolated Kr and Xe atoms with the ionization of molecules containing single Se (CH_3SeH, C_2H_5SeH) and I (ICl, CH_3I) atom, which have the electronic structure and the X-ray absorption cross sections very similar to Kr and Xe, respectively. For this systems, where the photoabsorption occurs almost exclusively by the single heavy atom, we exploit an ion-ion coincidence measurement scheme which allows us to define the total final charge state of the system as well as 3D momentum vectors of the emitted ions for a given final state. As illustrated in Fig, 1 for ICl molecule and described in [P6,P7] for Se-containing polyatomic systems, we find that while the total charge induced on the system is the same for both, the molecule and the isolated atom, the highest final charge state of the latter is considerably lower, pointing towards efficient charge redistribution within the molecular system. By measuring kinetic energy distribution of ionic fragments for a given final charge state and comparing them to the outcome of a simple Coulomb explosion (CE) model, we trace the evolution of the molecular geometry both, during and after the X-ray pulse and observe considerable displacement of the nuclei on the time scale of sequential multiple ionization and Auger decay, providing a quantitative measure of the radiation damage. For systems containing protons, we find surprisingly high fragment energies for channels where the measured charge of the non-absorbing C fragments is higher than that of Se, Analysis of the data along with the absence of these

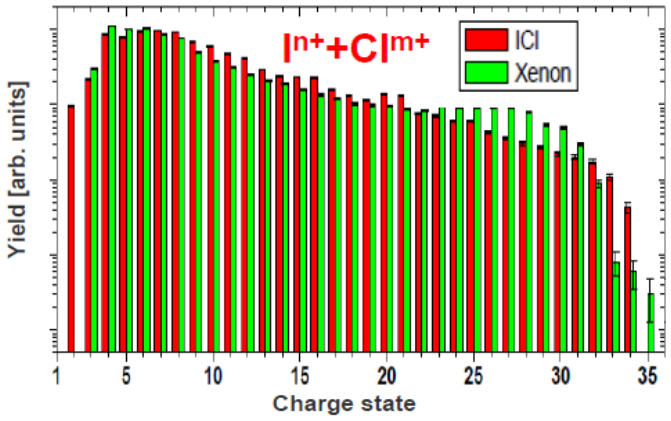

Fig. 1. Sum-charge of the measured yield of coincident I and Cl ion pairs created by 1500 eV, 80 fs, ~10^{17} W/cm^2 LCLS pulses compared to the charge state distribution observed in Xe atoms under the same conditions. Whereas the highest charge state of the individual I atoms is 28+ compared to Xe35+, the total charge of the molecule (sum over both fragments) is very similar to that of Xe.

anomalously high energies for the diatomic ICl molecule points towards ultrafast charge rearrangement occurring en route to these final states and involving highly charge transient complex with the excessive charge being taken away by the protons [P6,P7].

Following these initial results, we performed pump-probe experiments aimed to reveal the mechanisms as well as the time and length scales of the charge rearrangement processes similar to the ones described above. Such *interatomic* relaxation processes in core-shell ionized molecular or cluster systems, (e.g., molecular Auger, interatomic-Coulombic or electron-transfer mediated decay (ICD, ETMD)) represent some of the cleanest microscopic examples of charge and/or energy transfer reactions. However, explicit manifestations of the non-local interatomic phenomena in strongly bound molecules are typically entangled with the contributions of (often dominant) *intraatomic* channels, and, therefore, until now they were clearly identified in ionization of weakly bound extended systems like van der Waals clusters, where conventional "intra-atomic" Auger decay is energetically forbidden. We have recently succeeded in performing the first proof-of principle time-domain measurement on the ICD in the Ne_2 dimer exploiting our XUV-pump / XUV probe setup at FLASH and yielding the value of the ICD lifetime for this prototype system [P8]. In parallel to this, we performed an experiment at LCLS on X-ray ionization of the laser-dissociated CH_3I molecules aimed to unambiguously separate the contributions from the intra- and interatomic relaxation channels as the molecular system undergoes a transition towards isolated atoms. The preliminary results of this experiment are shown in Fig. 2. In Fig. 2a, where the kinetic energy of the created I^{6+} ions is shown as a function of the IR laser pump – X-ray probe delay, one can clearly see a broad, delay-independent band at high energies, a descending band reflecting the decrease of the CE energy of the dissociating fragments, and a very narrow band close to zero energy. Whereas the high-energy band reflects the CE of the molecules at the equilibrium internuclear distance R by the X-ray pulse (as can be seen in the single-pulse data of Fig, 2b), the descending band originate from the events where the 800 nm laser pulse dissociates the molecule into $CH_3^+ + I$ fragments, which are then multiply ionized by the X-ray pulse. At small delays (i.e., at small R) the events from the complementary $CH_3 + I^+$ channel also contribute to this band since upon the X-ray photoabsorption of the I^+ ion at least one charge is transferred to the CH_3 fragment. However, as R increases, the charge exchange channels between the two dissociating partners is closing, and the highly-charged iodine ions (I^{6+}) are detected in coincidence with the neutral CH_3, resulting in the appearance of the low-energy band in Fig. 2a. Considering the time-dependent yield of this low-energy band (Fig. 2c), we observe that its rise-time correlates with the decrease in the yield of the highly-charged carbon ions (C^{4+}), confirming that the latter obtain their charge mainly via charge exchange with the absorbing iodine fragment. From the measured asymptotic energy values describing the propagation of the laser-induced dissociating wave-packet, we conclude the characteristic distance at which charge exchange becomes small is ~7-8 Å, reflecting the transition from the bound molecule to the isolated atoms.

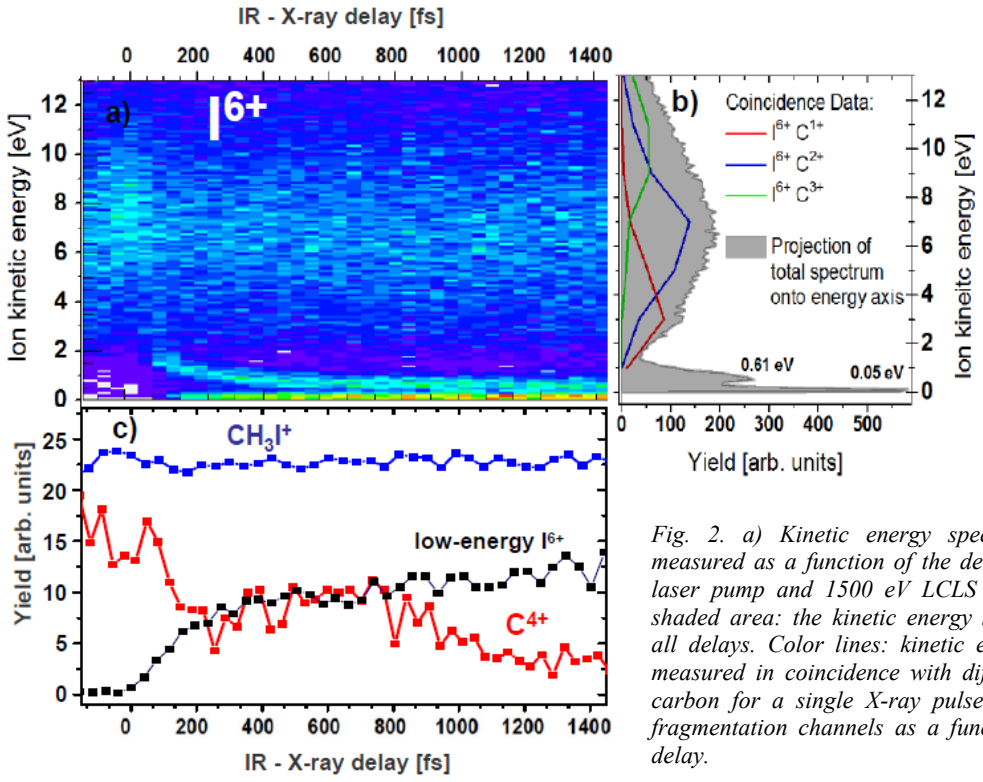

Fig. 2. a) Kinetic energy spectrum of the I^{6+} ions measured as a function of the delay between 800 nm IR laser pump and 1500 eV LCLS probe pulses. b) Gray shaded area: the kinetic energy spectra integrated over all delays. Color lines: kinetic energies of the I^{6+} ions measured in coincidence with different charge states of carbon for a single X-ray pulse. c) Yiedls of different fragmentation channels as a function of the IR / X-ray delay.

2. Imaging and control of light-induced structural rearrangement reactions in small polyatomic molecules.

This part of the program aims at real time imaging and control of prototypical photo-induced structural rearrangement reactions (isomerization, hydrogen migration, bond formation, H_2 / H_3 elimination etc.). Following up on our proof-of-principle measurements on XUV-induced isomerization in C_2H_2 cation [7,8], we performed elaborated measurements on this reaction at FLASH using our XUV-pump / XUV probe setup [P9]. The results exhibit good agreement with the theoretical predictions of O. Vendrell et al. [9], and a joint experimental and theoretical publication providing the first snapshots ofa femtosecond "molecular movie" is in preparation. Meanwhile, we have extended this kind of measurements to C_2H_4 molecule.

In parallel to continuing time-resolved isomerization experiments at FELs, we pursue similar type of studies at the JRML using ultrashort infrared laser pulses combined with ion-ion coincidence setup. One of the examples includes H_2^+ and H_3^+ formation in simple organic molecules. The preliminary results of such experiment on methane are presented in Fig. 3. There it can be clearly seen how the elimination of hydrogenic fragments evolves with the pulse duration. In Fig. 3a, where chirped 120 fs pulse was used, one observes a broad, flat-top structure for the H_2^+ emission, and detects considerable amount of H_3^+ ions. For 25 fs pulse the relative yield of the H_3^+ channel drops by more than two orders of magnitude, and is below our detection threshold for 8 fs pulses (Fig. 3b). The H_2^+ emission pattern also clearly changes, manifesting a sharp central peak. In Fig. 3c the results of the pump-probe experiment are shown, yielding the time-of-flight and, thus, kinetic energy spectra of H^+ and H_2^+ fragments as a function of the delay between two 8 fs pulses. One can clearly observe the signatures of molecular dissociation involving H_2^+ elimination.

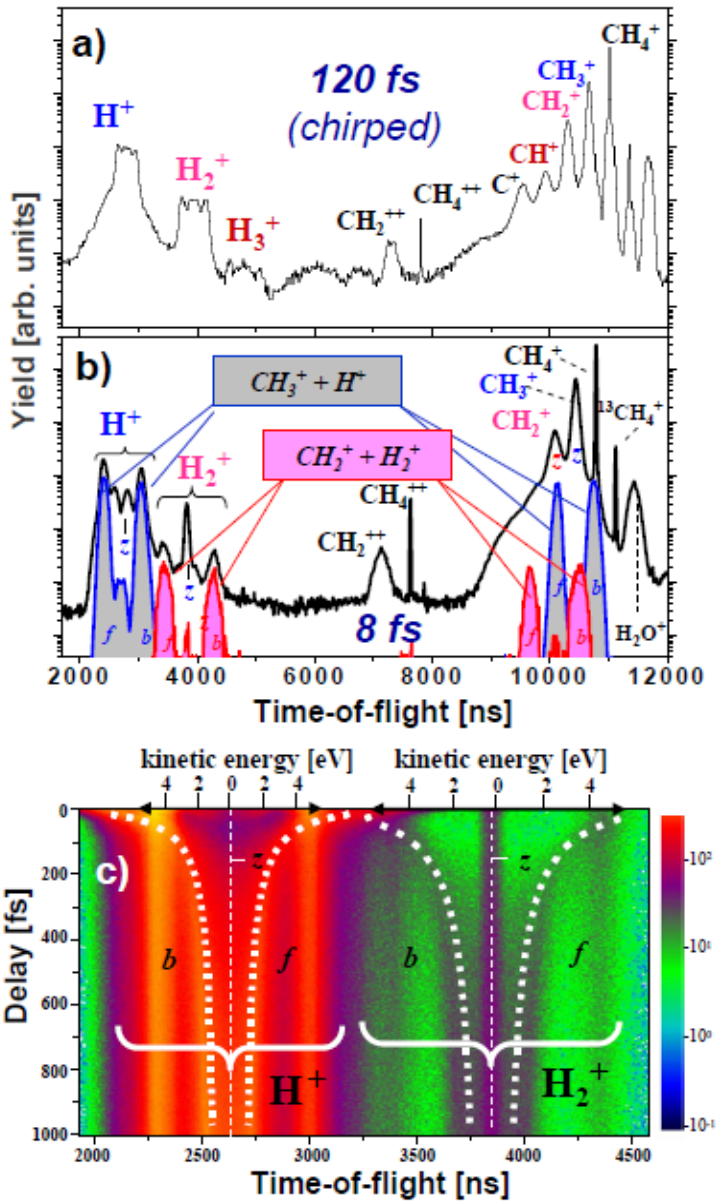

Fig. 3 (a,b). TOF spectra for CH_4 fragmentation by 120 fs (a) and 8 fs (b) 800 nm laser pulses at ~3 10^{14} W/cm^2. "b" and "f" indicate the backward and forward peaks, i.e., ion emission towards and away from the detector, respectively, whereas "z" denotes the TOF of the ion with zero momentum along the TOF axis. The shaded area in (b) shows ion pairs detected in coincidence. (c) TOF spectrum of light ionic fragments detected in a pump-probe experiment on CH_4 as a function of the delay between the two 8 fs laser pulses

Future plans:

We plan to continue research in both directions described above. For the inner-shell ionization of molecules we have obtained the first internuclear distance resolved Auger spectra for the laser dissociated CH_3I and CH_3F molecules, during our last LCLS run in summer 2013. The data, which are currently being analyzed, further highlight the transition between the bound systems and the isolated atoms, and the role of the interatomic decay channels. A couple of complementary synchrotron experiments will be performed by the collaborating groups at Soleil, France and at PETRA III in Hamburg, Germany. In the future we plan to extend these experiments towards larger systems, and will considerably improve time resolution using pump laser pulses comparable to Auger lifetimes. Beyond the continuation of the successful FEL experiments, preparations have been started for the built up of a new harmonic generation setup at JRML in order to perform experiments at the upper inner-shell levels (such as iodine 4d) at the JRML. This setup will be also used in the planned experiments on structural rearrangement

reactions, where we will combine it with the optical pump-probe arrangement used to obtain the above results on CH_4, finally aiming at the availability of the optimal pump and probe wavelengths for each of the reactions studied.

References

[1] M.M. Seibert et al., Nature 470, 78 (2011).
[2] H.N. Chapman et al., Nature 470, 73 (2011).
[3] T**.** Gorkhover et al., Phys. Rev. Lett*.* 108**,** 245005 (2012).
[4] D. Loh et al**.,** Nature 486**,** 513 (2012).
[5] L. Young et al., Nature 466, 56 (2010).
[6] M. Hoener et al., Phys. Rev. Lett. 104, 253002 (2010).
[7] Y. H. Jiang, A. Rudenko, O. Herrwerth *et al.*, Phys. Rev. Lett. 105, 263002 (2010).
[8] J. Ullrich, A. Rudenko and R. Moshammer, Annu. Rev. Phys. Chem. 63, 635 (2012).
[9] M. E. Madjet, O. Vendrell, and R. Santra, Phys. Rev. Lett. 107, 263002 (2011).

Publications from the DOE-funded research:

[P1] "*Single-particle structure determination by correlations of snapshot X-ray diffraction patterns"*, D. Starodub, A. Aquila, S. Bajt, M. Barthelmess, A. Barty, C. Bostedt, J. D. Bozek, N. Coppola, R.B. Doak, S.W. Epp, B. Erk, L. Foucar, L. Gumprecht, C.Y. Hampton, A. Hartmann, R. Hartmann, P. Holl, S. Kassemeyer, N. Kimmel, H. Laksmono, M. Liang, N. D. Loh, L. Lomb, A. V. Martin, K. Nass, C. Reich, D. Rolles, B. Rudek, A. Rudenko, J. Schulz, R. L. Shoeman, R.G. Sierra, H. Soltau, J. Steinbrener, F. Stellato, S. Stern, G. Weidenspointner, M. Frank, J. Ullrich, L. Strüder, I. Schlichting, H. N. Chapman, J.C.H. Spence, M. J. Bogan, *Nature Commun.* 3 1276 (2012).

[P2] "*Ultra-efficient ionization of heavy atoms by intense X-Rays*", B. Rudek, S.-K. Son, L. M. Foucar, S. W. Epp, B. Erk, R. Hartmann, M. Adolph, R. Andritschke, A. Aquila, N. Berrah, C. Bostedt, J. Bozek, N. Coppola, F. Filsinger, H. Gorke, T. Gorkhover, H. Graafsma, L. Gumprecht, A. Hartmann, G. Hauser, S. Herrmann, H. Hirsemann, P. Holl, A. Hömke, L. Journel, C. Kaiser, N. Kimmel, F. Krasniqi, K.-U. Kühnel, M. Matysek, M. Messerschmidt, D. Miesner, T. Möller, R. Moshammer, K. Nagaya, B. Nilsson, G. Potdevin, D. Pietschner, C. Reich, D. Rupp, G. Schaller, I. Schlichting, C. Schmidt, F. Schopper, S. Schorb, C.-D. Schröter, J. Schulz, M. Simon, H. Soltau, L. Strüder, K. Ueda, G. Weidenspointner, R. Santra, J. Ullrich, A. Rudenko, and D. Rolles, *Nature Photonics*, 6 858 (2012).

[P3] "*Tracing nuclear-wave-packet dynamics in singly and doubly charged states of N2 and O2 with XUV-pump – XUV-probe experiments*", M. Magrakvelidze, O. Herrwerth, Y.H. Jiang, A. Rudenko, M. Kurka, L. Foucar, K.U. Kühnel, M. Kübel, Nora G. Johnson, C.D. Schröter, S. Düsterer, R. Treusch, M. Lezius, I. Ben-Itzhak, R. Moshammer, J. Ullrich, M.F. Kling, and U. Thumm, *Phys. Rev. A*, 86, 013415 (2012).

[P4] "*Resonance-enhanced multiple ionization of krypton at an x-ray free-electron laser*", B. Rudek, D. Rolles, S.-K. Son, L. Foucar, B. Erk, S.W. Epp, R. Boll, D. Anielski, C. Bostedt, S. Schorb, R. Coffee, J. Bozek, S. Trippel, T. Marchenko, M. Simon, L. Christensen, S. De, S. Wada, K. Ueda, I. Schlichting, R. Santra, J. Ullrich and A. Rudenko, *Phys. Rev. A*., 87, 023413 (2013).

[P5] "*Strong-field interactions at EUV and X-ray wavelengths*", A. Rudenko, Chapter 15 in "Attosecond and Free-Electron Laser Physics", T. Schultz and M.J.J. Vrakking, Editors, Wiley (2013).

[P6] "*Ultrafast charge rearrangement and nuclear dynamics upon inner-shell multiple ionization of small polyatomic molecules*", B. Erk, D. Rolles, L. Foucar, B. Rudek, S.W. Epp, M. Cryle, C. Bostedt, S. Schorb, J. Bozek, A. Rouzee, T. Marchenko, M. Simon, F. Filsinger, L. Christensen, S. De, S. Trippel, J. Küpper, H. Stapelfeldt, S. Wada, K. Ueda, M. Swiggers, M. Messerschmidt, C.D. Schröter, R. Moshammer, I. Schlichting, J. Ullrich and A. Rudenko, *Phys. Rev. Lett*. 110, 053003 (2013).

[P7] "*Inner-shell multiple ionization of polyatomic molecules with an intense x-ray free-electron laser studied by coincident ion momentum imaging*", B Erk, D Rolles, L Foucar, B Rudek, S W Epp, M Cryle, C Bostedt, S Schorb, J Bozek, A Rouzee, A Hundertmark, T Marchenko, M Simon, F Filsinger, L Christensen, S De, S Trippel, J Küpper, H Stapelfeldt, S Wada, K Ueda, M Swiggers, M Messerschmidt, C D Schröter, R Moshammer, I Schlichting, J Ullrich and A Rudenko, *J. Phys. B: At. Mol. Opt. Phys.* 46 164031 (2013).

[P8] "*Time-Resolved Measurement of Interatomic Coulombic Decay in Ne_2*", K. Schnorr, A. Senftleben, M. Kurka, A. Rudenko, L. Foucar, G. Schmid, A. Broska, T. Pfeifer, K. Meyer, D. Anielski, R. Boll, D. Rolles, M. Kübel, M.F. Kling, Y.H. Jiang, S. Mondal, T. Tachibana, K. Ueda, T. Marchenko, M. Simon, G. Brenner, R. Treusch, S. Scheit, V. Averbukh, J. Ullrich, C.D. Schröter, R. Moshammer, *Phys. Rev. Lett*. 111, 093402 (2013).

[P9] "*Ultrafast dynamics in acetylene clocked in a femtosecond XUV stopwatch*", Y H Jiang, A Senftleben, M Kurka, A Rudenko, L Foucar, O Herrwerth, M F Kling, M Lezius, J V Tilborg, A Belkacem, K Ueda, D Rolles, R Treusch, Y Z Zhang, Y F Liu, C D Schröter, J Ullrich and R Moshammer, *J. Phys. B: At. Mol. Opt. Phys.* 46 164027 (2013).

Structure and Dynamics of Atoms, Ions, Molecules and Surfaces

Uwe Thumm
J.R. Macdonald Laboratory, Kansas State University, Manhattan, KS 66506, thumm@phys.ksu.edu

A. Theoretical analysis of dissociative ionization in diatomic molecules

Project scope: To develop numerical and analytical tools to (i) predict the effects of strong IR-laser and XUV fields on the bound and free electronic and nuclear dynamics in small molecules and (ii) fully image their laser-controlled nuclear and electronic dynamics.

Recent progress: Motivated by recent experiments, we extended our investigations of the dissociative ionization dynamics of diatomic molecules in several ways. For H_2 we (i) examined chemical-bond breaking in a single circularly polarized IR pulse and perfomed both classical and quantum calculations to simulate electron localization and kinetic energy release (KER) in a coincident angular streaking experiment [1] and (ii) investigated the electron-nuclear energy sharing in above-threshold multiphoton dissociative ionization [2]. For weakly bound noble gas dimers, we modeled the dissociation dynamics in intense two-color IR laser fields and revealed a distinguished "gap" in the KER spectra that was observed experimentally for Ar_2 targets. We traced this gap to a unique dissociation path along dipole-coupled Ar_2^+ potential curves [3]. Comparing pump-probe-delay dependent KER spectra for noble gas dimer cations of increasing mass, we found and quantified increasingly prominent (i) fine-structure effects in and (ii) classical aspects of the nuclear vibrational motion [4]. Further, we continued to examine KER spectra from heavier (than H_2) dimers as a function of pump-probe delay and vibrational quantum beat frequency and showed through specific examples how the complementray analysis of experimental and computed KER data in both, time and frequency regimes leads to a useful scheme for indentifying dissociation pathways [5].

Example 1: Attosecond timing of asymmetric chemical-bond breaking in H_2^+. We investigated a new route for ultrashort time-interval measurements that is based on the *coincident* detection of directions of particles emitted from the same molecule by a *single* circularly-polarized laser pulse. This approach combines angular streaking with coincident detection of an emitted photoelectron and molecular fragment [1]. This method uses the rotating electric field vector of the laser pulse as the hand of an ultrafast clock that measures the time elapsed between the detection of the photoelectron and nuclear fragment as the angle between the detected momenta of the electron (start signal) and fragment (stop signal) (Fig. 1). This technique enables the measurement of time intervals based on differences in particle momenta which can be detected with high precision, even for long pulses, thereby providing a powerful tool for ultrafast science.

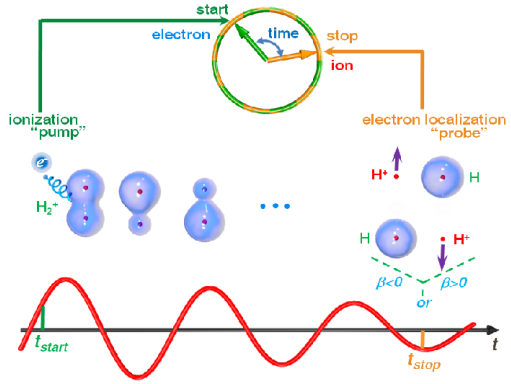

Fig.1: Time-resolved detection of chemical-bond breaking in H_2^+ using a single circularly-polarized multi-cycle IR pulse. Start and stop times are retrieved by coincident detection of the emitted electron (left) and ion (right) momenta. The laser field (red curve) continues to drive the remaining electron up and down and eventually leads to its localization at one nucleus.

We studied the attosecond dynamics of an electron in a breaking chemical bond of H_2^+ within semiclassical and quantum mechanical numerical models. In the semiclassical approach, we approximated the H_2^+ nuclear wave packet as a classical particle with reduced mass and solved Newton's equations for its motion on the two lowest adiabatic potential curves of H_2^+, starting on the $1s\sigma_g^+$ curve at the equilibrium distance of H_2, and continuing

along two possible dissociation pathways. Along path 1, the molecular ion moves outwards on the $1s\sigma_g^+$ curve, couples to the first excited $2p\sigma_u^+$ state by absorption of one laser photon, and dissociates on the $2p\sigma_u^+$ curve. Along the alternative path 2, the ion expands along the $1s\sigma_g^+$ curve until it transits to the $2p\sigma_u^+$ curve by absorption of three photons, followed by propagation on the $2p\sigma_u^+$ and coupling back to the $1s\sigma_g^+$ curve by emission of one photon, and dissociates along the $1s\sigma_g^+$ curve. The classically calculated phase accumulations along these two pathways for the net absorption of one and two photons, φ_1 and φ_2, yield reasonable approximations for the probabilities for electron localization at the left or right nucleus, P_l and P_r, and dissociation asymmetry $\beta = (P_l - P_r)/(P_l + P_r) \sim \cos(\varphi_1 - \varphi_2)$ as a function of the molecular-frame electron emission angle and fragment KER found in both, our quantum calculations and in the experiment [1].

Example 2: Electron-nuclear energy sharing in dissociative ionization of H_2. In above-threshold multiphoton dissociative ionization of H_2 by strong laser fields, the absorbed photon energy is shared between the ejected electron and nuclei in a correlated fashion, resulting in multiple diagonal lines in their joint energy spectrum governed by the energy conservation of all fragment particles (Fig. 2).

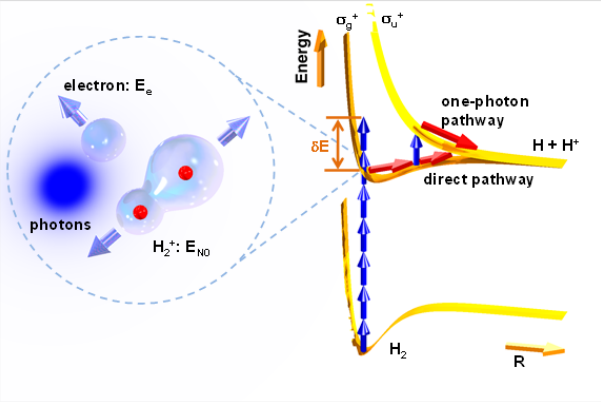

Fig.2: Illustration of the above-threshold multiphoton dissociative ionization of H_2. The blue vertical arrows stand for the photons of the driving 390 nm UV pulse. The absorbed excess photon energy δE is shared by the kinetic energies of the emitted electron (E_e) and the nuclei of H_2^+ (E_{N0}), which dissociate to $H + H^+$ through either direct or one-photon pathways as indicated by the red arrows.

To estimate how much photon energy is transferred to the nuclei, we use a two-step classical model in which the nuclei instantaneously acquire kinetic energy from their interaction with the outgoing electron in the first vertical ionization step, propagate on the H_2^+ potential curves, and dissociate to the nuclear continuum of the $1s\sigma_g^+$ (or $2p\sigma_u^+$) state, leading to the observable asymptotic nuclear KER. To validate this two-step scenario, we numerically propagated the nuclear wavepacket by solving the time-dependent Schrödinger equation (TDSE) in the subspace of the $1s\sigma_g^+$ and $2p\sigma_u^+$ states of H_2^+, modeling the ionization from the ground state of H_2 based on internuclear-distance-dependent molecular Ammosov-Delone-Krainov rates. Dipole coupling between the $1s\sigma_g^+$ and $2p\sigma_u^+$ states is allowed during wavepacket propagation. The nuclear KER spectrum was calculated after a sufficiently long propagation time past the end of the laser pulse and agrees well with the experimental data [2].

Example 3: Dissociation dynamics of noble gas dimers in intense two-color IR laser fields. We investigated the dissociation dynamics in noble gas dimers in two laser pulses of different wavelengths. The "delay gap" on the positive delay side (780 nm pump followed by 1450 nm probe pulse) in the KER spectra, observed previously for the Ar_2^+ dimer [3], we also found for He_2^+ and Ne_2^+ dimers. This striking feature can be explained within a wave packet propagation model that describes the motion of vibrational cation nuclear packets on two adiabatic potential curves that become dipole-coupled in the laser pulses. For Kr_2^+ and Xe_2^+ dimers the observed delay gap is tentatively explained by the same mechanism. Our study of the position and momentum variances and uncertainty products reveals increasing classical characteristics of the nuclear wave packet motion for increasingly massive dimers (Fig.3). In addition, comparing calculations with and without including spin-orbit coupling, we found that relativistic effects become noticeable and eventually crucial (for Kr_2^+ and Xe_2^+) in KER spectra as the mass of the dimer increases [4].

Future plans: The simultaneous study of measured and simulated KER spectra in both, time and energy domains provides a powerful tool that we intend to extend and refine in order to better understand the ro-vibrational nuclear dynamics of laser-excited (and ionized) molecules [1-5,7,8].

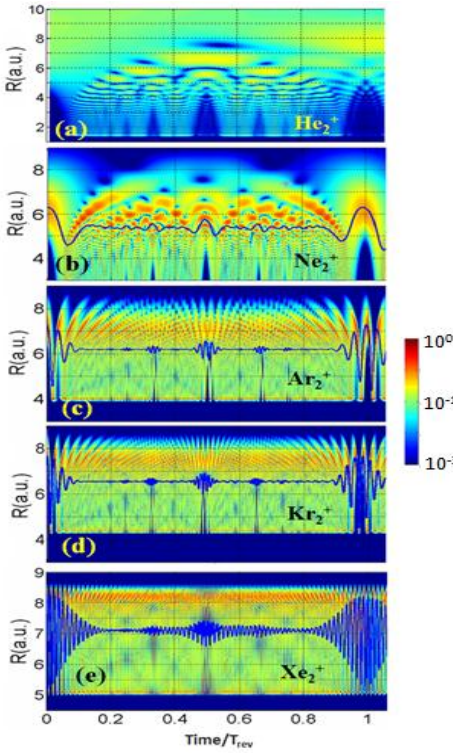

Fig.3: Probability density of nuclear vibrational wave packets in noble-gas dimer cations (Ng_2^+) as a function of the internuclear distance R for field-free propagation in the Ng_2^+ (I(1/2)u) state (including spin-orbit coupling). (a) He_2^+, (b) Ne_2^+, (c) Ar_2^+, (d) Kr_2^+, and (e) Xe_2^+ dimers. The propagation time is given in units of the respective revival times. The Ng_2^+ wave packets are launched by a 800 nm, 80 fs, 10^{14} W/cm^2 laser pulse. Noble gas dimers are weakly bound and have much larger vibrational periods than the diatomic molecules we studied so far. The dissociation energies of neutral noble gas dimers are in the 1-25 meV range, orders of magnitude below the dissociation energy of the corresponding dimer cations Ng_2^+. The vibrational periods of the dimer cations in their electronic ground states are of the order of hundreds of fs, an order of magnitude larger than those of H_2^+, O_2^+, N_2^+, and CO^+ [5,7]. The equilibrium distance of all neutral noble gas dimers is larger than for their cations. Dimer ions thus contract upon photoionization of the neutral parent molecule, before the molecular-ion nuclear wave packet reflects at the inner turning point of its adiabatic molecular state. These features, especially the comparatively slow nuclear motion and simple electronic structure, make noble gas dimers and their cations attractive targets for the detailed investigation of their bound and dissociative nuclear dynamics in pump-probe experiments [3,4].

B. Laser-assisted two-photon double ionization of He

Project scope: We developed a new finite-element discrete-variable-representation (FE-DVR) code for solving the full two-electron TDSE that we plan apply to examine correlation effects during the single and double ionization of He atoms exposed to short XUV and IR pulses.

Recent progress: IR-laser assisted XUV double ionization of helium. After validating our new FE-DVR code by comparing joint-angular distributions (JADs) for single-XUV-photon double ionization with published experimental and theoretical data, we studied N_{XUV}-photon double ionization with (for N_{XUV} =1) and without (for N_{XUV} =1,2,3) the presence of a short IR pulse (Fig. 4). We find that the assisting IR pulse promotes side-by-side emission (both electrons are emitted in almost the same direction along the polarization axis of the linearly polarized XUV and IR pulses) and enables back-to-back emission (electrons are emitted in the opposite directions).

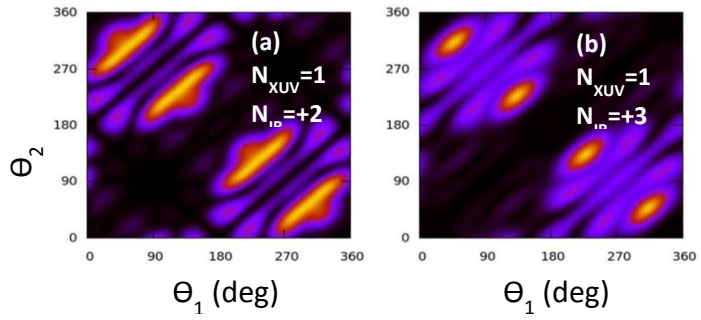

Fig.4: JADs for a 10^{14}W/cm^2, ω_{XUV} = 89 eV, 10 cycle XUV pulse and a $3x10^{12}$W/cm^2, ω_{IR} = 1.61 eV, 2.5 fs IR pulse for equal energy sharing of the emitted electrons. Single-XUV-photon double ionization for absorption of effectively (a) 2 and (b) 3 IR photons.

Future plans: We intend to (i) accurately calculate time-resolved IR Stark shifts for He and compare our results with recent transient absorption measurements, (ii) search for ideal laser parameters for the observation, with sub-IR-cycle resolution, of IR level shifts in delay-dependent single and non-sequential double-ionization probabilities, and (iii) explore this method as an ultrafast gate for double ionization. At a later stage, we intend to (iv) apply our new two-electron code to the laser-dressed autoionization of atoms (He) and compare its

numerical output with results we obtained within a technically simple heuristic model for the decay of laser-coupled autoionizing states [6].

Publications and manuscripts addressed in this abstract

[1] *Understanding the role of phase in chemical bond breaking with coincidence angular streaking*, J. Wu, M. Magrakvelidze, L. Ph. H. Schmidt, M. Kunitski, T. Pfeifer, M. Schöffler, M. Pitzer, M. Richter, S. Voss, H. Sann, H. Kim, J. Lower, T. Jahnke, A. Czasch, U. Thumm, R. Dörner, Nat. Commun. **4**, doi:10.1038/ncomms3177 (July 19, 2013).

[2] *Electron-nuclear energy sharing in above-threshold multiphoton dissociative ionization of H_2*, J. Wu, M. Kunitski, M. Pitzer, F. Trinter, L. Ph. H. Schmidt, T. Jahnke, M. Magrakvelidze, C. B. Madsen, L. B. Madsen, U. Thumm, R. Dörner, Phys. Rev. Lett. **111**, 023002 (2013).

[3] *Steering the nuclear motion in singly ionized argon dimers with mutually detuned laser pulses*, J. Wu, M. Magrakvelidze, A. Vredenborg, L. Ph. H. Schmidt, T. Jahnke, A. Czasch, R. Dörner, U. Thumm, Phys. Rev. Lett**. 110**, 033005 (2013).

[4] *Dissociation dynamics of noble-gas dimers in intense two-color IR laser fields*, M. Magrakvelidze and U. Thumm, Phys. Rev. A **88**, 013413 (2013).

[5] *Dissociation dynamics of diatomic molecules in intense laser fields: a scheme for selecting relevant molecular potential curves*, M. Magrakvelidze, C. Aikens, U. Thumm, Phys. Rev. A **86**, 023402 (2012).

[7] *Attosecond time-resolved autoionization of argon*, H. Wang, M. Chini, S. Chen, C.-H. Zhang, F. He, Y. Cheng, Y. Wu, U. Thumm, Z. Chang, Phys. Rev. Lett. **105**, 143002 (2010).

[8] *Tracing nuclear wave packet dynamics in singly and doubly charge states of N2 and O2 with XUV pump – XUV probe experiments*, M. Magrakvelidze, O. Herrwerth, Y.H. Jiang, A. Rudenko, M. Kurka, L. Foucar, K.U. Kühnel, M. Kübel, N. G. Johnson, C.D. Schröter, S. Düsterer, R. Treusch, M. Lezius, C.L. Cocke, I. Ben-Itzhak, R. Moshammer, J. Ullrich, M. F. Kling, U. Thumm, Phys. Rev. A **86**, 013415 (2012).

[9] *Laser-controlled vibrational heating and cooling of oriented H_2^+ molecules*, T. Niederhausen, U. Thumm, F. Martin, in, J. Phys. B: At. Mol. Opt. Phys. **45**, 105602 (2012).

Other recent publications and manuscripts (2011-13)

- *Attosecond Physics: Attosecond Streaking Spectroscopy of Atoms and Solids*, U. Thumm, Q. Liao, E. M. Bothschafter, F. Süßmann, M. F. Kling, R. Kienberger, Handbook of Photonics (Wiley), submitted.
- *H^- formation by electron capture in collision of H with an Al(100) surface*, B. Obreshkov and U. Thumm, Phys. Rev. A **87**, 022903 (2013).
- *Attosecond time-resolved photoelectron spectroscopy of surfaces*, U. Thumm and C.-H. Zhang, invited paper, Light at extreme intensities (Szeged, HU 2011), AIP Conf. Proc **1462**, 57 (2012).
- *Attosecond science – What will it take to observe processes in real time*, S. R. Leone, C. W. McCurdy, J. Burgdörfer, L. Cederbaum, Z. Chang, N. Dudovich, J. Feist, C. Greene, M. Ivanov, R. Kienberger, U. Keller, M. Kling, Z.-H. Loh, T. Pfeifer, A. Pfeiffer, R. Santra, K. Schafer, A. Stolow, U. Thumm, M. Vrakking, approved by Nature Photonics for publication on March 14, 2014.
- *Time-resolved Coulomb explosion imaging of nuclear wave-packet dynamics induced in atomic molecules by intense few-cycle laser pulses*, I.A. Bocharova, A. S. Alnaser, U. Thumm, T. Niederhausen, D. Ray, C.L. Cocke, I.V. Litvinyuk, Phys. Rev. A 83, 013417 (2011).
- *Following dynamic nuclear wave packets in N2, O2 and CO with few-cycle infrared pulses*, S. De, M. Magrakvelidze, I. Bocharova, D. Ray, W. Cao, I. Znakovskaya, H. Li, Z. Wang, G. Laurent, U. Thumm, M. F. Kling, I. V. Litvinyuk, I. Ben-Itzhak, C. L. Cocke, Phys. Rev. A 83, 013417 (2011).
- *Effects of wave-function localization on the time delay in photoemission from surfaces*, C.-H. Zhang and U. Thumm, Phys. Rev. A 84, 065403 (2011).
- *Probing dielectric response effects with attosecond time-resolved streaked photoelectron spectroscopy of metal surfaces*, C.-H. Zhang and U. Thumm, Phys. Rev. A 84, 063403 (2011).
- *Attosecond probing of instantaneous AC Stark shifts in helium atoms*, F. He, C. Ruiz, A. Becker, U. Thumm, J. Phys. B: At. Mol. Opt. Phys. 44, 211001 (2011).
- *Hydrogen-anion formation near (2x1) reconstructed Si (100) surfaces: Substrate-electronic-structure and trajectory dependence*, B. Obreshkov and U. Thumm, Phys. Rev. A 83, 062902 (2011).

Strong-Field Time-Dependent Spectroscopy

Carlos A. Trallero
J. R. Macdonald Laboratory, Kansas State University, Manhattan, KS 66506
trallero@phys.ksu.edu

Scope

The main scope of my program is to measure and control the state of molecular systems. In particular, I'm interested in observing molecules evolve with attosecond and/or femtosecond time resolution.

1 Coherent molecular spectroscopy using higher order harmonic generation

in collaboration with A.-T Le, V. Kumarappan, R. Lucchese and E. Poliakoff

1.1 Spectroscopy of large isotropic molecules

As mentioned in the introduction, one of our main research objectives under this grant is to create a solid frame for the utilization of HHG as a new tool for molecular spectroscopy. We continue the collaboration between Carlos Trallero, An-Thu Le, C.D. Lin, Vinod Kumarappan of the J. R. Macdonald Laboratory (JRML), Erwin Poliakoff from Louisiana State University and Robert Lucchese from Texas A& M University. In addition, while spectroscopic studies with HHG have been done already [1, 2], there is a large controversy on whereas the observed structure is stable or not to phase matching conditions [3, 4]. Therefore, one question we also intend to answer is how robust the HHG method is to macroscopic conditions. In this section we focus on extracting PICS from large molecules whose electron spatial distribution is close to isotropic and the role of the induced macroscopic wavepacket to the extracted cross sections. In Section 1.2 we focus on molecules with electronic density on the HOMO that is far from isotropic.

We investigate the relationship between the ionization cross section with the recombination cross section by studying harmonic generation from SF_6, one the of the most studied molecules in the photo-ionization literature. Since the the third step in HHG is dependent on the dipole moment of the target, HHG from a variety of targets can elucidate different aspects of the photo-recombination step. We specifically aim to determine if spectroscopic elements, such as shape resonances, persist in HHG. Molecular shape resonances occur as a result of the temporary trapping of the photoelectron and are extremely sensitive to the potential responsible for the quasi-binding of the photoelectron resulting in a less obvious effect on the harmonic signal than other spectroscopic features. SF_6 has a relatively high ionization energy and multiple shape resonances in the ionization continuum, which make it ideal for an initial study.

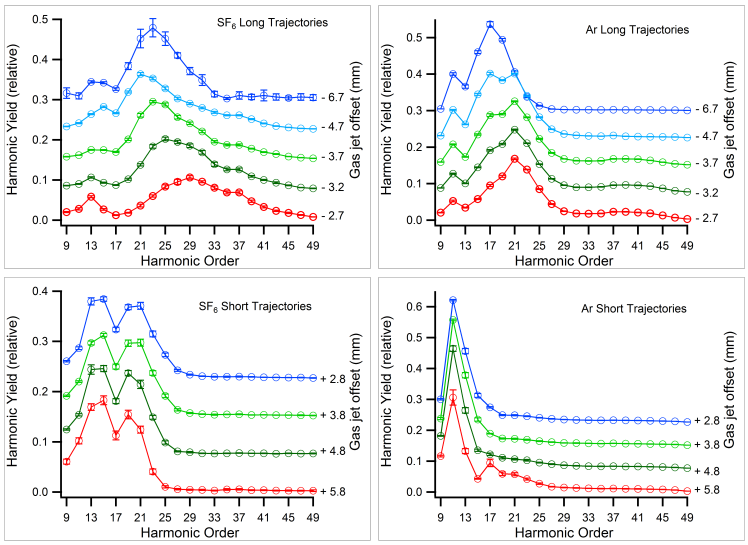

Figure 1: Position dependent envelopes representing long and short trajectories for SF_6 and Ar. The right axis represents the distance of the focal point from the center of the gas jet as determined by the ion signal. The laser intensity for each envelope presented is $1.32 \times 10^{14} W/cm^2$. The most significant details are observed in the long trajectory plots, particularly the minimum centered on the 31st harmonic in Ar, and the inflection in the 17th harmonic followed by a broad peak in SF_6.

Theoretical predictions concerning HHG in the presence of a resonance with an auto-ionizing state suggested an additional step to the classical three step model during which the wave packet is temporarily

trapped before recombination can complete . This temporary trapping results in an energy dependent population buildup and was later extended in theory to shape resonances. HHG-based spectroscopy is the perfect tool to study processes such as the time dependent trapping of the photoelectron in the vicinity of the shape resonance. So far our studies have shown that the energy range over which this increase in HHG efficiency occurs is blue shifted relative to ionization cross section theoretical predictions and previous experimental results. The similarities between the harmonic envelope and the ionization cross section appear to be most prevalent in long trajectories favoring recombination while short recombination trajectories do not contribute to the resonant enhancement.

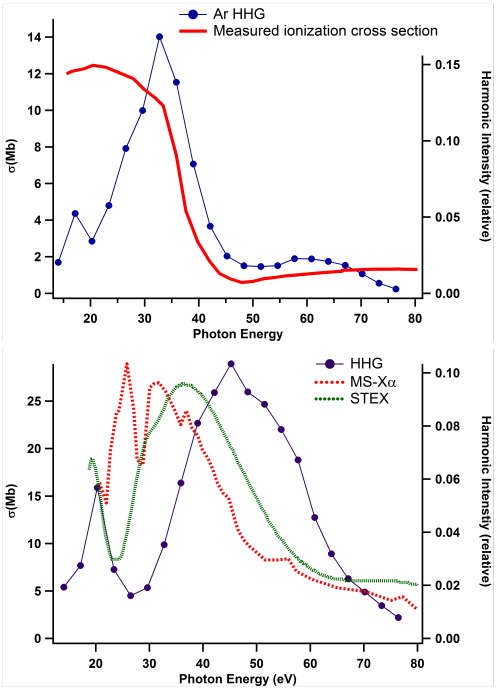

Figure 2: Comparison of the ionization cross section and harmonic envelopes for Ar and SF_6. In both samples, there is a noticeable blue shift for the spectroscopic features of interest.

Detailed focal position and intensity dependent spectra for the high harmonic generation from SF_6 are presented in figure 1. As the lens is moved such that the focus of the laser progresses through the gas jet, the primary quantum path is altered due to the change in phase matching conditions resultant from the axial divergence of the beam past the focal point. We differentiate long and short trajectories by the appearance in the raw images taken. The fact that the overall shape of the harmonic envelope, including what appears to be a resonant enhancement of plateau harmonics, is the key takeaway from this discussion. The bottom panel in figure 2 shows the HHG data for SF_6 against three different calculations for the ionization cross section. The light green line represents the static exchange method, the red line is the Schwinger Variational Theory, and the dark green line is the result of Quantitative Re-scattering Theory. With the energy shifted, the resonances occur in the plateau region of the harmonic envelope, making the increase from the population build up in the presence of a shape resonance clear.

The impact of the resonance is made clearer by comparing the long trajectory data to the short trajectory data, in agreement with former theoretical studies on the effect of resonances on HHG26. The resonance behaves as a trapping of the electron after it has returned to the ion. The duration of the short trajectory is less than the half cycle of the laser pulse which results in the resonance collapsing before the next electron returns, preventing a population buildup. The long trajectory is temporally longer than the half cycle of the laser pulse, allowing a rapid population buildup in the energy region of a resonance. A similar effect is observed in the lack of a Cooper minimum in Argon in the bottom panels of figures 2 and 3. The duration of the electron wave packet in the continuum, then, makes the long trajectories more significant in a spectroscopic sense while the short trajectories probe a different portion of the ionization continuum.

1.2 Measurement of multiorbital contributions to HHG

in collaboration with V. Kumarappan, A.-T Le and R. Lucchese

For this project we measure multi-orbital angular contributions to HHG from aligned N_2. We show that the change in revival structure in the cutoff harmonics, when HOMO-1 is present has a counterpart in the angular distribution. This angular distribution is directly observed in the lab without any further deconvolution. To achieve a clear picture of the angular dependent HOMO-1 contributions, we use a double pulse scheme to align rotationally cold N_2 molecules. Our multi-pulse technique, combined with an Evan-Lavie valve allows us to achieve degrees of alignment as high as $< cos^2\theta >= 0.82$. Finally, we developed a new fitting method to extract the spatial content of the HOMO-1 orbital as a function of harmonic. This fitting technique provides a clear indication of multi-orbital contributions. While for the moment we have to make very stringent assumptions about the relative phases of the harmonics, we expect to compliment our experiments with phase measurements. In this case, our fitting technique will yield phase and amplitude, angle-dependent, multi-orbital information of the bound-continuum dipole moment.

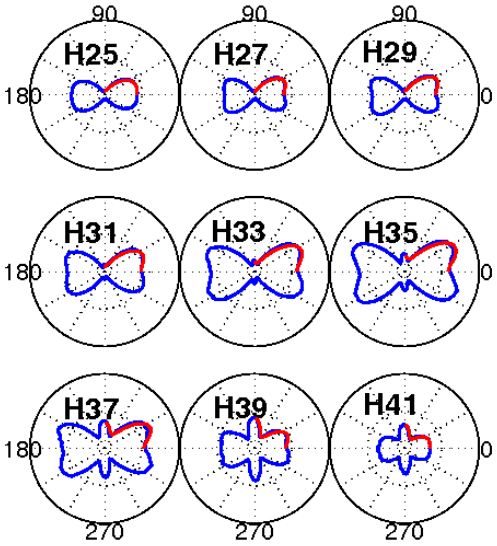

Figure 3: Harmonic yield of individual harmonics as a function of angle between pump and probe at the full revival. In red, the fit of our developed model. At 90 degrees, H25 shows a minimum whereas for higher harmonics we observe a maximum. The signal is normalized to an isotropic signal with no pump pulses present.

To further investigate the contribution from HOMO-1 in the HHG process, we perform an angle dependent measurement of the harmonic yield at the time of the full revival of nitrogen, and the peak in HHG signal, at 17.04 ps. At this time all molecules are aligned parallel to the harmonic generating beam when the pump polarization is parallel to the probe beam. We choose this time delay as a fixed delay and now change the angle between the pump pulses and the probe pulse. In doing so we acquire an angle dependent harmonic yield. In Figure 3, we plot the angle dependent yield for different harmonics. For lower order harmonic orders ¡ H29 the usual elongated yields, with a maximum at 0° is observed. The local minimum at 0° is due to the presence of the angle and energy dependent Cooper minimum in the N_2. However, for higher orders, a feature arises at 90 and 270 degrees. With increasing harmonic order, the relative contribution in the harmonic yield at pump and probe perpendicular to each other is increasing and reaches in the 39th harmonic the same peak value as at 30 degrees. However, the width of the perpendicular coil is smaller than for the parallel coil. Although the signals in Figure 3 are on the same scale for the pumps perpendicular and parallel to the probe, the total yield acquired from perpendicular components is lower by a magnitude than from the parallel components. Such difference in the angular dependence can only be explained by the presence of the HOMO-1 orbital. We have carried out several studies to establish this.

Among such studies we have investigated the influence of macroscopic conditions on the appearance of the HOMO-1 orbital. We have found out that we can turn on or off the contribution of this orbital in the revival structure [8]. Some of the macroscopic parameters that we investigated were the mode of the laser beam, the lens focal length, peak intensity, and focus position respect to the gas jet. Two manuscripts are currently being prepared. One on the multi-orbital angular contribution and the other on the macroscopic selectivity of HOMO-1 contributions to both angular yields and revival structures.

2 Strong field ionization of molecular isomers

in collaboration with A.-T Le

Recent results of HHG from isomer molecules indicate show large differences in the harmonic yield for different isomers of the the same molecular specie. In particular, [6] studies the isomers cis- and trans-1,2-dichloroethylene (DCE) and cis- and trans-2-butene. In their original publication, they attributed this differences to the ionization step, stating that the difference in the ionization yields for the cis-1,2-DCE is 7-9 times higher than for the trans-1,2-DCE, whereas they arrive to a factor of 5 higher for the cis-2-butene compared to the trans-2-butene. In a subsequent errata of the same publication [7], the authors claimed that the difference in ionization is only a factor of 2 between the cis and trans isomers. Besides the implications for HHG-based spectroscopic, such hypothesis are important because it also involves a comparison between polar (cis) and non-polar molecules. Our goal is to test the Keldysh interpretation of strong field ionization by comparing ionization yields from polar and non-polar which are isomers from each other and therefore have the same ionization potential. The above cited work [6, 7] suggests that the Keldysh parameter is not the characteristic parameter in the ionization of polar molecules since they calculate a very large change in the ionization yield while the difference in ionization potential of the isomers

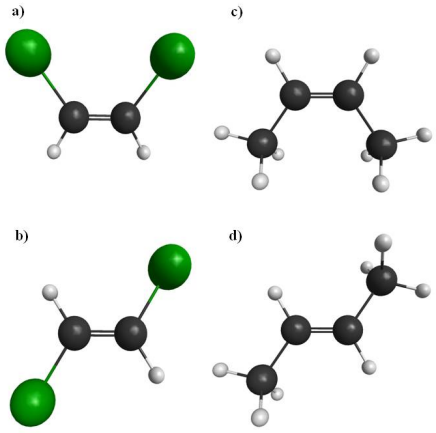

Figure 4: a) Cis-1,2-dichloroethylene, b) Trans-1,2-dichloroethylene, c) Cis-2-butene, d) Trans-2-butene

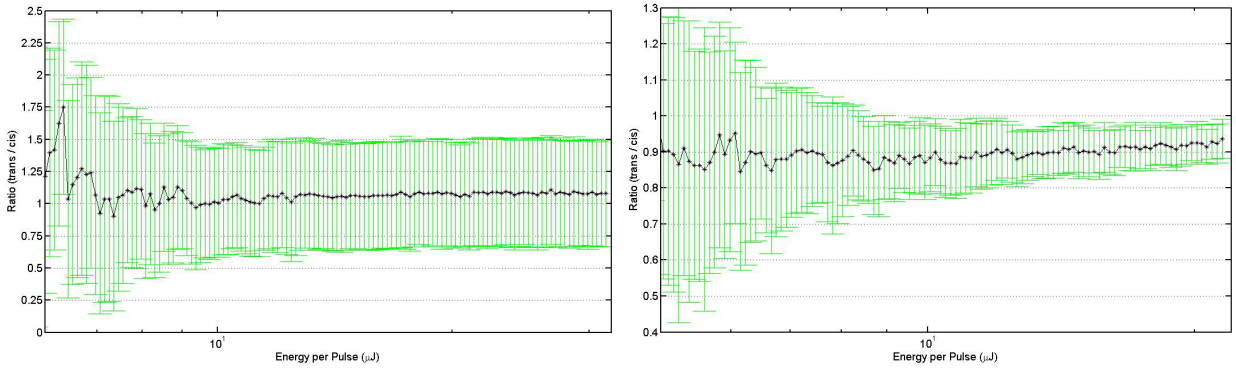

Figure 5: a) Isomer comparison of the first ion of cis- and trans-2-butene at low intensities. The ratio of trans- and cis-2-butene using the ionization yields of the first ion of each sample at low intensities b) Isomer comparison of the first ion of cis- and trans-1,2-DCE at low intensities. The ratio of trans- and cis-1,2-DCE using the ionization yields of the first ion of each sample at low intensities.

is very small.

The ratio, trans / cis, of the normalized ionization yield as a function of intensity for the first ion of 2-butene and 1,2-DCE can be seen in figure 5a) and figure 5b) respectively. Error bars in the graphs were calculated by the standard deviation over fifty plus scans. The range of energies shown here are at the low end, where there the appearance of secondary fragments is negligible. This range of energy per pulse is also far from the saturation regime, which is observed at two to three times the shown values. The first feature observed in the data is that both ratios remain almost constant for the shown range of pulse energies. Closer to saturation intensities, this trend changes. More relevant to this study is the fact that ratios for both isomers is very close to 1, in strong discrepancy with the predictions in [6, 7]. However, the error bars for 2-butene are quite large thus making it harder to conclude whereas the ionization of the trans-2-butene is smaller or higher than that of the cis-2-butene. However, what is conclusive from the experimental data is that the ionization ratio between trans and cis configurations is not 2 nor 5 as reported before. For 1,2-DCE there is a significant statistical difference between the cis and trans ionization. This ratio is around trans/cis=0.9, again far from the suggested value of 7 to 9. It should be noted that we are not suggesting that the ionization ratios are constant. It is clear that they change gradually with intensity and molecular orientation respect to the laser polarization.

The relatively low differences might indicate that molecular ionization has only a small dependence on atomic configuration with the same atomic composition. Such observations lead to the conclusion that for randomly aligned molecules, the Keldysh parameter is still the characteristic parameter for strong field ionization.

DOE Supported Publications

- C. Jin, A.-T. Le, C. A.Trallero-Herrero, and C. D. Lin. Generation of isolated attosecond pulses by far field spatial filtering high-order harmonic generation of Xe in an intense mid-infrared laser. *Phys. Rev. A*, 84:043411, 2011
- C. A. Trallero-Herrero, C. Jin, B. Schmidt, A. Shiner, D. M. Villeneuve, P. B. Corkum, C. D. Lin, F. Légaré and A. T. Le, Generation of broad XUV continuous high harmonic spectra with intense mid-infrared lasers. *J. Phys. B.*, 45:011001, 2011.

References

[1] A. D. Shiner, B. E. Schmidt, C. Trallero-Herrero, *et. al.* Nat. Phys., **7**, 464, 2011.
[2] H. J. Wörner, H. Niikura, J. B. Bertrand, *et. al.*. Phys. Rev. Lett., **102**, 103901, 2009.
[3] J. P. Farrell, L. S. Spector, B. K. McFarland, *et. al.* Phys. Rev. A, **83**, 023420, 2011.
[4] Cheng Jin, Anh-Thu Le, and C. D. Lin. Phys. Rev. A, **83**,023411, Feb 2011.
[5] Cheng Jin, Julien B. Bertrand, R. R. Lucchese, *et. al* Phys. Rev. A, , 013405, 2012.
[6] M. C. H. Wong *et al.*, Phys. Rev. A **84**, 051403(R) (2011).
[7] M. C. H. Wong *et al.*, Phys. Rev. A **85**, 049901(E) (2012).
[8] X. Ren, V. Makhija, A.-T. Le, *et. al.*. Phys. Rev. A, **submitted**, 2013.

Atomic, Molecular and Optical Sciences at LBNL

Ali Belkacem, Daniel J. Haxton, Clyde W. McCurdy, Thomas N. Rescigno and Thorsten Weber
Chemical Sciences Division, Lawrence Berkeley National Laboratory, Berkeley, CA 94720
Email: *abelkacem@lbl.gov, djhaxton@lbl.gov, cwmcurdy@lbl.gov, tnrescigno@lbl.gov, tweber@lbl.gov*

Objective and Scope

The AMOS program at LBNL is aimed at understanding the structure and dynamics of atoms and molecules using photons and electrons as probes. The experimental and theoretical efforts are strongly linked and are designed to work together to break new ground and provide basic knowledge that is central to the programmatic goals of the Department of Energy as formulated in the "*Grand Challenges*". The current emphasis of the program is in three major areas with important connections and overlap: inner-shell photo-ionization and multiple-ionization of atoms and small molecules; low-energy electron impact and dissociative electron attachment of molecules; and time-resolved studies of atomic processes using a combination of femtosecond x-rays and femtosecond laser pulses. This latter part of the program is folded in the overall research program in the Ultrafast X-ray Science Laboratory (UXSL).

The experimental component at the Advanced Light Source makes use of the Cold Target Recoil Ion Momentum Spectrometer (COLTRIMS) to advance the description of the final states and mechanisms of the production of these final states in collisions among photons, electrons and molecules. Parallel to this experimental effort, the theory component of the program focuses on the development of new methods for solving multiple photo-ionization of atoms and molecules. This dual approach is key to break new ground and provide a new understanding how electronic energy channels into nuclear motion and chemical energy in polyatomic molecules as well as unravel unambiguously electron correlation effects in multi-electron processes.

Inner-Shell Photoionization and Dissociative Electron Attachment to Small Molecules

Ali Belkacem and Thorsten Weber
Chemical Sciences Division, Lawrence Berkeley National Laboratory, Berkeley, CA 94720
Email: abelkacem@lbl.gov, tweber@lbl.gov

Objective and Scope: This experimental subtask is focused on studying photon and electron impact ionization, excitation and dissociation of small molecules and atoms. The first part of this project deals with the interaction of X-rays with atoms and simple molecules by seeking new insight into atomic and molecular dynamics and electron correlation effects. The second part of this project deals with the interaction of low-energy electrons with small molecules with particular emphasis on Dissociative Electron Attachment (DEA). Both studies are strongly linked to our AMO theoretical studies by C.W. McCurdy, D. Haxton and T.N. Rescigno. Both experimental studies (photon and electron impact) make use of the powerful COLd Target Ion Momentum Spectroscopy (COLTRIMS) method to achieve a high level of completeness in the measurements.

Photo double ionization of ethylene and acetylene near threshold

The PDI has been broadly explored in recent years by choosing simple targets with two electrons (e.g. H_2, He) or diatomic molecules involving both intra-shell and inter-shell electrons. The natural next step is to study polyatomic molecular targets in order to explore the difference between intra-shell and inter-shell electron correlation. With our COLTRIMS scheme we utilize a method that allows the coincident detection of both electrons and recoil ions produced during the double ionization that enables the kinematically complete study of the direct PDI of these molecules. Our initial goal is to identify the states that result from the removal of intra-shell and/or inter-shell electrons and to understand their role in the subsequent fragmentation process after the PDI. For this investigation it is essential to know the potential energy surfaces of the doubly charged molecular ions in order to shed light on the ionization mechanisms. D.J. Haxton performed calculations of the excited state dication potential energy surfaces, which allowed us to identify the states involved by comparison with our measured kinetic energies of the electrons and fragment ions. As an example that highlights the powerful combination of kinematically complete experiments and ab-initio calculations we focus on the asymmetric breakup channel. For the $H_2^+ + C_2H_2^+$ channel the energy map, shown in Fig. 1(c) above, indicates that the KER distribution peaks at around 4.4eV while the broad kinetic electron sum energy E_{sum} distribution has a peak at around 5eV. Hence the vertical energy is 35.5 eV which is similar to that of the symmetric channel. Several excited di-

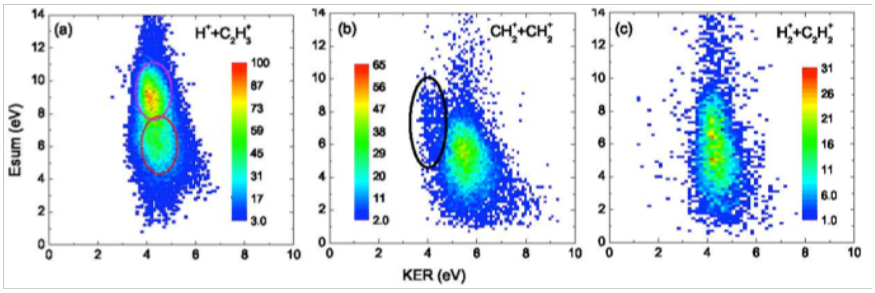

Energy correlation map between the ionic KER (horizontal axis) and the sum kinetic energy of the two electrons (vertical axis) for the (a) $H^+ + C_2H_3^+ + 2e$, (b) $CH_2^+ + CH_2^+ + 2e$, and (c) $H_2^+ + C_2H_2^+ + 2e$ channels of ethylene using 40.5eV photons.

cationic states are populated. The above observation is a strong indication that the asymmetric break up is caused by a transition from these initial singlet/triplet states to the singlet/triplet state that correlates with the lowest asymptote on the PES.

Hydrogen and fluorine migration in the photo double ionization of 1,1-diuoroethylene ($C_2H_2F_2$) near threshold

As a follow-up to the investigation of ethylene (C_2H_4) and acetylene (C_2H_2) we studied the non-dissociative and dissociative ionization of 1,1-difluoroethylene using single photons of energies from 40 to 70eV. While C_2H_4 is the simplest organic molecule containing a single π bond, two hydrogen atoms on one side of the C=C double bonding are replaced by fluorine atoms in 1,1-$C_2H_2F_2$. The dissociative ionization, channels with two ionic fragments is explored in detail by measuring the kinetic energy release and the sum of the kinetic energies of the two photo electrons simultaneously. The dissociative channel producing H_2^+ fragments (hydrogen elimination) has the smallest yield and suggests an interesting mechanism of the hydrogen atom migration: in order to form a molecular hydrogen ion (H_2^+), one could assume that the two hydrogen atoms simply bond together and leave the parent ion. By looking at the structure of 1,1-$C_2H_2F_2$ one can think that this may be a favorable process since the two hydrogen atoms are bonded to the same carbon atom. Instead, the low yield suggests that direct hydrogen elimination does not happen that way or possibly does not take place in the PDI of 1,1-$C_2H_2F_2$ at all. The channel that involves both the migration of hydrogen and fluorine species, i.e. the HF^+ fragment ion production, increases with the photon energy. In order to produce an HF^+ fragment a conformation change must have happened. However, there are at least three possibilities for this to proceed: a.) the hydrogen atom migrated to one side, b.) the fluorine atom moved to the opposite end, or c.) both constituents migrated towards each other along the C=C bond. The additional observation of the CF^++CH_2F^+ channel confirms the migration of fluorine. While the hydrogen atoms remain bound to their respective carbon atom, this channel clearly results from the migration of one of the F atoms followed by the central C=C bond breaking.

Dissociative electron attachment to carbon dioxide.

Low-energy electron scattering from CO_2 is dominated by the well-known $^2\Pi_u$ shape resonance at 4-eV collision energy and a dramatic rise in the total cross section below 1 eV that has been attributed to a $^2\Sigma^+$ virtual state. A temporary negative ion (TNI) CO_2^- is also formed at 8.2 eV due to a $^2\Pi_g$ electronic Feshbach resonance that can decay either by electron auto-detachment or dissociation into O^- and vibrationally hot CO in its electronic ground state. In the experimental part of this work the momentum of the final state anionic O^- fragment following DEA to single CO_2 molecules were measured using a momentum imaging negative ion spectrometer. A gaseous CO_2 beam was effused from a narrow stainless steel capillary to intersect with a magnetically collimated electron beam that was pulsed with a 50 kHz repetition rate. O^- anion momentum images were recorded from a position- and time-sensitive detector to an event list, so that 3-dimensional momentum distributions could be determined for a full 4Π solid angle of detection. The experimental measurement combined with theoretical calculations demonstrates that an understanding of anion dissociation dynamics beyond simple one-dimensional models is crucial in interpreting the measured angular distributions. Although several possible dissociation mechanisms involving conical intersections have been identified and discussed, the most likely scenario points to an initial linear asymmetric stretch motion followed by bending motion around a conical intersection.

Dissociative electron attachment to methanol.

A combined experimental and theoretical investigation of the dissociative electron attachment

(DEA) dynamics in methanol was performed for the Feshbach resonance at 6.5-eV incident electron energy . The measured 3-dimensional momentum spectra of H^- or D^- for the case of a deuterated methanol are shown in the figure. The distribution exhibits a wide peak in the backward with respect to the incident electron and the absolute momentum is found to be sharply peaked at 18 atomic units (a.u.). The absence of the low-energy H^- peak at the momentum of origin that was observed in undeuterated methanol clearly indicates that it is attributed entirely to C-H break within the methyl functional group. The outer high H^-/D^- momentum ring is due to the break-up of the OH/OD bond, respectively. In addition to the primary DEA fragmentation channel due to O-D bond break leading to a deuterium anion and a methoxy radical, we also measured the spectrum of the complementary channel producing atomic deuterium and the methoxide anion CH3O$^-$. The total ion yield of CH3O$^-$ in the present experiments was one to a few percent compared to the more favorable channel leading to D^-. These measurements are combined with calculations of the molecular frame electron attachment probability in order to investigate the dynamics of the dissociating methanol transient negative anion. In contrast to previous comparisons between water and methanol we find subtle differences in the dissociation dynamics of the two fragment channels that are direct evidence of planar symmetry-breaking of warm methanol in its electronic ground state. We also find that the DEA fragmentation does not strictly follow the axial recoil approximation and we describe the dynamics that enable an accurate prediction of the fragment angular distributions.

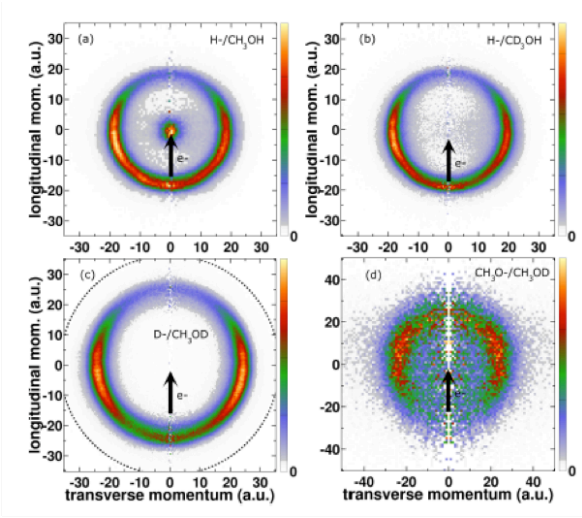

Momentum imaging of H- and D- in DEA to methanol.

Future Plans

We plan to continue application of the COLTRIMS approach to achieve complete descriptions of the single photon double ionization to polyatomic and dissociation dynamics. In particular we will investigate the particle migration and hydrogen elimination of small molecular chains like propadiene (C_3H_4). We plan to continue our on-going work using our Dissociative Electron Attachment modified-COLTRIMS to study DEA to uracil and pyrazine. This latter work will be done in close collaboration with Vincent McKoy from the theory side.

Recent Publications (2011-2013)

1. H. Sann, T. Jahnke, T. Havermeier, K. Kreidi, C. Stuck, M. Meckel, M. Schöffler, N. Neumann, R. Wallauer, S. Voss, A. Czasch, O. Jagutzki, Th. Weber, H. Schmidt-Böcking, S. Miyabe, D.J. Haxton, A.E. Orel, T. N. Rescigno, and R. Dörner, "Electron diffraction self imaging of molecular fragmentation in two step double ionization of water", Phys. Rev. Lett. **106**, 133001 (2011).
2. D.S. Slaughter, H. Adaniya, T.T. Rescigno, D.J. Haxton, A.E. Orel, C.W. McCurdy, A. Belkacem, "Dissociative electron attachment to carbon dioxide via 8.2 eV Feshbach resonance", J. Phys. B: At. Mol. Opt. Phys. **44** (2011) 205203.
3. D.J. Haxton, H. Adaniya, D.S. Slaughter, B. Rudek, T. Osipov, T. Weber, T.N. Rescigno, C.W. McCurdy, A. Belkacem, "Observation of the dynamics leading to a conical intersection in dissociative electron attachment to water", Phys. Rev. A **84** (2011) 030701.
4. H. Adaniya, B. Rudek, T. Osipov, D.J. Haxton, T. Weber, T.N. Rescigno, C.W. McCurdy, and A. Belkacem, "Comment on "Imaging the molecular dynamics of dissociative electron attachment to

water", Phys. Rev. Lett. **106**, (2011) 049302.
5. Schoffler M.S., Jahnke T., Titze J., Petridis N., Cole K., Schmidt L.P.H., Czasch A., Jagutzki O., Willams J.B., Cocke C.L., Osipov T., Lee S., Prior M.H., Belkacem A., Landers A.L., Schmidt-Bocking H., Dorner R., Weber T., "Matter wave optics perspective at molecular photoionization: K-shell photoionization and Auger decay of N2", New J. Phys. **13** (2011) 095013.
6. T. Jahnke, J. Titze, L. Foucar, R. Wallauer, T. Osipov, E.P. Benis, O. Jagutzki, W. Arnold, A. Czasch, A. Staudte, M. Schöffler, A. Alnaser, T. Weber, M.H. Prior, H. Schmidt-Böcking, R. Dörner, "Carbon K-shell Photo Ionization of CO: Molecular frame angular Distributions of normal and conjugate shakeup Satellites", J. Electron Spectroscopy and Related Phenomena, **183**, (2011), 48-52.
7. Adaniya H., Slaughter D.S., Osipov T. Weber T., Belkacem A., "A momentum imaging microscope for dissociative electron attachment", Rev. Scient. Inst. **83** (2012) 023106.
8. J.B. Williams, C.S. Trevisan, M.S. Schoffler, T. Jahnke, I. Bocharova, H. Kim, B. Ulrich, R. Wallauer, F. Sturm, T. N. Rescigno, A. Belkacem, R. Dorner, Th. Weber, C.W. McCurdy, A. L. Landers, "Imaging polyatomic molecules in three dimensions using molecular frame photoelectron angular distributions", Phys. Rev. Lett. **108** (2012) 233002.
9. F. Robicheaux, M.P. Jones, M. Schoeffler, T. Jahnke, K. Kreidi, J. Titze, C. Stuck, R. Doerner, A. Belkacem, Th. Weber and A.L. Landers, "Calculated and measured angular correlation between photoelectrons and Auger electrons from K-shell ionization ", J. Phys. B: At. Mol. Opt. Phys., **45**, (2012), 175001.
10. F. Trinter, L.Ph.H. Schmidt, T. Jahnke, M.S. Schöffler, O. Jagutzki, A. Czasch, J. Lower, T. A. Isaev, R. Berger, A.L. Landers, Th. Weber, R. Dörner, H. Schmidt-Böcking , Multi fragment vector correlation imaging: A search for hidden dynamical symmetries in many-particle molecular fragmentation processes,Molecular Physics, Vol. 110, Nos. 15-16, (2012), 1863-1872
11. J.B. Williams, C.S. Trevisan, M.S. Schoeffler, T. Jahnke, I. Bocharova, H. Kim, B. Ulrich, R. Wallauer, F. Sturm, T.N. Rescigno, A. Belkacem, R. Doerner, Th. Weber, C.W. McCurdy, and A.L. Landers, Probing the Dynamics of Dissociation of Methane Following Core Ionization Using Three-Dimensional Molecular Frame Photoelectron Angular Distributions, J. Phys. B: At. Mol. Opt. Phys., 45, (2012), 194003
12. D.S. Slaughter, D.J. Haxton, H. Adaniya, T. Weber, T.N. Rescigno, C.W. McCurdy, and A. Belkacem, Ion momentum imaging of dissociative electron attachment dynamics in methanol Phys. Rev. A, 87, (2013), 052711
13. M.S. Schoeffler, C. Stuck, M. Waitz, F. Trinter, T. Jahnke, U. Lenz, M. Jones, A. Belkacem, A. Landers, C. L. Cocke, J. Colgan, A. Kheifets, I. Bray, H. Schmidt-Boecking, R. Doerner, and Th. Weber, Ejection of quasi free electron pairs from the helium atom ground state by a single Photon, Phys. Rev. Lett., 111, (2012), 013003
14. F. Trinter, M. Schoeffler, H.K. Kim, F. Sturm, K. Cole, N. Neumann, A. Vredenborg, J. Williams, I. Bocharova, R. Guillemin , M. Simon , A. Belkacem, A. Landers, Th. Weber, H. Schmidt-Boecking, R. Doerner, and T. Jahnke, Resonant Auger decay driven intermolecular Coulombic decay as a tool for site-selective creation of low energy electrons in biological system, to be published in Nature
15. A. Moradmand, D.S. Slaughter, D.J. Haxton, T.N. Rescigno, C.W. McCurdy, Th. Weber, S. Matsika, A.L. Landers, A. Belkacem, and M. Fogle, Dissociative electron attachment to carbon dioxide via the ^2P_u shape resonance, accepted for publication in Phys. Rev. A, 88, (2013)
16. B. Gaire, D.J. Haxton, P. Braun, S.Y. Lee, I. Bocharova, F.P. Sturm, N. Gehrken, M. Honig, M. Pitzer, D. Metz, H-K. Kim, T. Jahnke, H. Gassert, S. Zeller, J. Voigtsberger, W. Cao, M. Zohrabi, J. Williams, A. Gatton, D. Reedy, C. Nook, Th. Mueller, A. Landers, C. L. Cocke, I. Ben-Itzhak, R. Doerner, A. Belkacem, and Th. Weber , Photo double ionization of ethylene and acetylene near threshold, Draft to be submitted to Phys. Rev. A, (2013)
17. Gaire, D.J. Haxton, P. Braun, S.Y. Lee, I. Bocharova, F.P. Sturm, N. Gehrken, M. Honig, M. Pitzer, D. Metz, H-K. Kim, T. Jahnke, H. Gassert, S. Zeller, J. Voigtsberger, W. Cao, M. Zohrabi, J. Williams, A. Gatton, D. Reedy, C. Nook, Th. Mueller, A. Landers, C. L. Cocke, I. Ben-Itzhak, R. Doerner, A. Belkacem, and Th. Weber , Hydrogen and Fuorine migration in the photo double ionization of 1,1-diuoroethylene ($C_2H_2F_2$) near threshold Draft to be submitted to Phys. Rev. A, (2013)

Electron-Atom and Electron-Molecule Collision Processes

T. N. Rescigno, D. J. Haxton and C. W. McCurdy
Chemical Sciences, Lawrence Berkeley National Laboratory, Berkeley, CA 94720
tnrescigno@lbl.gov, cwmccurdy@lbl.gov

Program Scope: This project seeks to develop theoretical and computational methods for treating electron processes that are important in electron-driven chemistry and physics and that are currently beyond the grasp of first principles methods, either because of the complexity of the targets or the intrinsic complexity of the processes themselves. A major focus is the development of new methods for solving multiple photoionization and electron-impact ionization of atoms and molecules. New methods are also being developed and applied for treating low- energy electron collisions with polyatomic molecules and clusters. A state-of-the-art approach is used to treat multidimensional nuclear dynamics in polyatomic systems during resonant electron collisions and predict channeling of electronic energy into vibrational excitation and dissociation.

Recent Progress and Future Plans:

Dissociative Electron Attachment

Dissociative electron attachment (DEA) plays a fundamental role in electron-driven chemistry. Its importance in radiation therapy, waste remediation, nanofabrication and planetary atmospheres provides an impetus for understanding the mechanism of DEA. Our earlier study of DEA to CO_2 (ref. 5), which focused on the main at 8.2 eV, has been extended to the 4 eV resonance, which feeds both vibrational excitation and dissociative electron attachment. Our *ab initio* calculations have shown that the topology of the CO_2 anion surfaces is quite complicated and have revealed three different conical intersections between shape resonance, Feshbach resonance and virtual anion states that can play a role in the dissociation dynamics. Earlier studies of the total dissociation cross sections belie the complexity of the dissociation dynamics, which is only revealed in angular distribution of the product anions. Our joint experimental/theoretical study will soon appear in Phys. Rev. A (ref. 20). We have completed a similar study on DEA to methanol, concentrating on the dynamics associated with the 6.5 eV $^2A''$ shape resonance (ref. 16). The angular distributions of the recoiling fragments were found to deviate significantly from the axial recoil approximation that was used previously to accurately describe the dynamics in the analogous $^2B_1$ resonance in water, primarily due to opening of the C-O-H bond angle in the transient methanol anion. Our calculated angular distribution of fragments from the two observed dissociation channels ($H_3CO + H^-$ and $H_3CO^- + H$) following an O-H break are in very good agreement with the measured ion-momentum distributions. Our future plans in this area include a study of DEA to ammonia, which has been measured in by our AMOS experimental group. We also plan to revisit our earlier study of the mechanism of DEA to formic acid, where substantial controversy about the attachment mechanism still exists. This work will be carried out in collaboration with the group of Prof. Ann Orel at UC Davis.

Molecular-Frame Photoelectron Angular Distributions (MFPADS)

The unexpected discovery, made in a joint experimental (COLTRIMS)/ theoretical study using methane as a probe (refs. 10 and 11), that the K-shell MFPAD, when averaged over all photon polarization directions, effectively images the geometry of the molecule, has prompted us to undertake theoretical studies on other target molecules to determine the possible generality of the effects initially observed for methane. We have found that other molecules containing hydrogen and a single heavy atom, namely H_2O and NH_3, show similar behavior (ref. 12). For molecules with more than one heavy atom, the situation can be more complicated. We found that for molecules possessing two or more degenerate or quasi-degenerate core orbitals, it is essential to

couple the different core-hole channels involved in order to describe the electron correlation properly. We discovered that the results of calculations without this coupling can, in many cases, produce MFPADs that do not even reflect the inherent symmetry of the molecule.

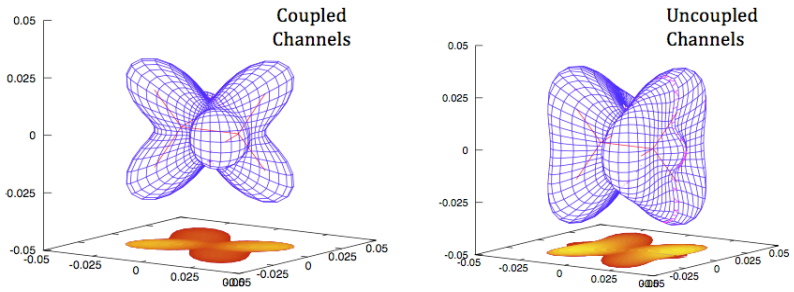

MFPADs for C_2H_6 at 3.27eV photoelectron energy computed with coupled channels (left) and uncoupled channels (right), averaged over polarization directions. The MFPAD directly reflects the geometry of the molecule only in the case of coupled-channel calculations.

K-shell MFPADs are very sensitive to nuclear geometry and relatively insensitive to the valence structure of the outer electrons, even in cases where they do not image the shape of the molecule. The suggests that such measurements might be taken into the time domain to image chemical reactions on their natural timescales. We demonstrated the idea for the case of isomerization of electronically excited ethylene, C_2H_4, which is being studied by our AMO experimental group. The results were recently published in *Phys. Rev. A* (ref. 18). Further studies will be aimed at looking for evidence of core-hole localization in targets with equivalent heavy atoms. We also plan to study molecules where the hydrogens are replaced by heavy atoms, such as CF_4. These studies will be done in collaboration with Prof. Cynthia Trevisan at CalState Maritime.

Photo-Double Ionization of Complex Targets

One-photon double photoionization (DPI) is a fundamental problem that has been the subject of significant investigation because of the explicitly correlated nature of the process. The simplest target where DPI can occur is helium, for which *ab initio* theory using advanced computational methods has produced results in excellent agreement with experiment. For more complex rare gas atoms, the volume of detailed experimental measurements of single-photon DPI greatly outweighs the theoretical data, which have been confined largely to simple parametrized model treatments. To be able to apply advanced grid-based techniques to such problems, we have developed an expanded frozen-core treatment which produces an effective 2-electron problem which we used to calculate fully differential DPI cross sections for neon and argon. Despite the relative simplicity of the approach, the accuracy of the results we obtained is comparable to that available for helium targets. This work, carried out in collaboration with the group of Prof. Fernando Martin in Madrid, was published in *Phys. Rev. Letters* (ref. 14). Encouraged by these results, we plan to extend this treatment to molecular targets in the future, to study DPI of N_2 and CO.

Electron-Impact Ionization of Molecular Targets

Very little has been done on the computation of fully differential cross sections for electron impact ionization of molecules beyond H_2. With polyatomic targets, even perturbative methods present formidable numerical challenges and the few distorted-wave studies that have appeared have had to rely on simplistic, unphysical approximations, such as the use of spherically averaged interaction potentials, in their implementation. A number of triply differential ionization cross section measurements have begun to appear in the past few years with electron impact energies in

the range of a few hundred eV. The collision energies are in the range where it would be reasonable to use the plane-wave Born approximation for the incident and scattered electron. The ejected electron, however, is slow, so a perturbative treatment would not be expected to be very reliable. In the limit where the fast incident and scattered electrons can be approximated by plane-waves and exchange between the fast and residual ion electrons can be ignored, the expression for the ionization amplitude is similar to the amplitude for photoionization, with the one-body dipole operator being replaced by $e^{i\mathbf{Q}\cdot\mathbf{r}}$, where **Q** is the momentum transfer vector. To treat the slow ejected electron which escapes in the field of the residual molecular ion, we can use the complex Kohn variational suite of codes we have developed for studying molecular photoionization, suitably modified to compute the ionization amplitude. Our initial efforts have been aimed at computing differential ionization cross sections for H_2O and CH_4 in the 200-500 eV range, where good experimental data exists. Our theoretical results for both molecules are in very good agreement with the measured values. We are currently preparing the results for publication. Our future plans in this area are to extend the treatment to study excitation-ionization. If the excitation produces a dissociative ion state, then COLTRIMS detection of the ejected electron and ion fragments in coincidence should allow observation of molecular ionization by electron impact in the body-frame which we will be able to calculate for comparison.

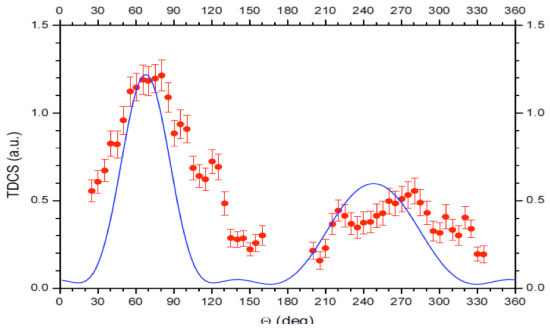

Triple-differential cross section for electron impact ionization of the $2a_1$ orbital of methane at 500 eV. The fast electron is scattered at 6 degrees and the ejected electron energy is 12 eV. Exp't data from Lahmam-Bennani et al. *J. Phys. B* **42**, 165201 (2009).

Electron-Molecule Scattering

There has been much recent interest in the interaction of low energy electrons with water, due in large part to the key role such interactions play in understanding and modeling radiation damage in biological environments. While much of the work in recent years, both experimental and theoretical, on electron-H2O scattering has been focused on resonant collisions resulting in dissociative electron attachment, non-resonant dissociation, which proceeds through direct excitation of low-lying electronic states, has received relatively less attention, because it presents some formidable challenges. The analysis of the electron energy loss spectra is complicated by the fact that the low-lying electronic states of water are dissociative and the profiles of the individual states are broad and strongly overlapped, making it difficult to extract a unique set of cross sections. On the theoretical side, one is faced with the problem of coupling between a number of relatively closely spaced states that have mixed valence-Rydberg character which is difficult to capture with simple, single-configuration wave functions. Prompted by the recent appearance of a new set of absolute differential cross sections measurements, we revisited the calculation of excitation cross sections, using correlated target wavefunctions in large-scale coupled-channel variational calculations. We found that earlier calculations at this level of theory were plagued by unphysical pseudo-resonances, so an extensive modification of our complex Kohn approach was needed to prevent their appearance. The results were published in *Phys. Rev. A* (ref. 17). Future work, to be carried out in collaboration with Prof. Ann Orel and the

experimental group of Prof. Morty Khakoo at Fullerton, will be directed at a similar study of dissociative excitation of methanol by electron impact.

Publications (2011-2013):

1. S. Miyabe, D. J. Haxton, T. N. Rescigno and C. W. McCurdy, "Role of nuclear dynamics in the Asymmetric molecular-frame photoelectron angular distributions for C 1s photoejection from CO_2 ", *Phys. Rev. A* **83**, 023404 (2011).
2. S. Miyabe, D. J. Haxton, K. V. Lawler, A. E. Orel, C. W. McCurdy and T. N. Rescigno, "Vibrational Feshbach resonances in near threshold $HOCO^-$ photodetachment; a theoretical study", *Phys. Rev. A* **83**, 043401 (2011).
3. H. Adaniya, B. Rudek, T. Osipov, D. J. Haxton, T. Weber, T. N. Rescigno, C. W. McCurdy, and A. Belkacem, "Reply to Comment on "Imaging the dynamics of dissociative electron attachment to water", *Phys. Rev. Lett.* **106**, 049302 (2011).
4. H. Sann, T. Jahnke, T. Havermeier, K. Kreidi, C. Stuck, M. Meckel, M. Schöffler, N. Neumann, R. Wallauer, S. Voss, A. Czasch, O. Jagutzki, Th. Weber, H. Schmidt-Böcking, S. Miyabe, D.J. Haxton, A.E. Orel, T. N. Rescigno and R. Dörner, "Electron diffraction self-imaging of molecular fragmentation in two-step double ionization of water", *Phys. Rev. Lett.* **106**, 133001 (2011).
5. D. S. Slaughter, H. Adaniya, T. N. Rescigno, D. J. Haxton, A. E. Orel, C. W. McCurdy and A. Belkacem, "Dissociative Electron Attachment to Carbon Dioxide via the 8.2eV Feshbach resonance", *Phys. Rev. A.* **44**, 205203 (2011).
6. D. J. Haxton, H. Adaniya, D. S. Slaughter, B. Rudek, T. Osipov, T. Weber, T. N. Rescigno, C. W. McCurdy and A.Belkacem, "Observation of the dynamics leading to a conical intersection in dissociative electron attachment to water", *Phys. Rev. A.* **84**, 030701(R) (2011).
7. W. Cao, G. Laurent, S. De, M. Schöffler, T. Jahnke, A. Alnaser, I. A. Bocharova, C. Stuck, D. Ray1, M. F. Kling, I. Ben-Itzhak, Th. Weber, A. Landers, A. Belkacem, R.Dörner, A. E. Orel, T. N. Rescigno and C. L. Cocke, "Dynamic modification of the fragmentation of autoionizing states of O_2^+", *Phys. Rev. A* **84**, 053406 (2011).
8. F. L. Yip, F. Martín, T. N. Rescigno and C. W. McCurdy, "Double *K*-shell photoionization of atomic beryllium", *Phys. Rev. A* **84**, 053417 (2011).
9. F. L. Yip, A. Palacios, C. W. McCurdy, T. N. Rescigno and F. Martín, " Time-dependent formalism of double ionization of multielectron atomic targets", *Chem. Phys.* **414**, 112 (2013).
10. J. B. Williams, C. S. Trevisan, M. S. Schöffler, T. Jahnke, I. Bocharova, H. Kim, B. Ulrich, R. Wallauer, F. Sturm, T. N. Rescigno, A. Belkacem, R. Dörner, Th. Weber, C. W. McCurdy and A. L. Landers, "Imaging Polyatomic Molecules in Three Dimensions using Molecular Frame Photoelectron Angular Distributions", *Phys. Rev. Lett.* **108**, 233002 (2012).
11. J. B. Williams, C. S. Trevisan, M. S. Schöffler, T. Jahnke, I. Bocharova, H. Kim, B. Ulrich, R. Wallauer, F. Sturm, T. N. Rescigno, A. Belkacem, R. Dörner, Th. Weber, C. W. McCurdy and A. L. Landers, "Probing the Dynamics of Dissociation of Methane Following Core Ionization Using Three-Dimensional Molecular Frame Photoelectron Angular Distributions", *J. Phys. B* **45**, 194003 (2012).
12. C. S. Trevisan, C. W. McCurdy and T. N. Rescigno, "Imaging Molecular Shapes with Molecular Frame Photoelectron Angular Distributions from Core Hole Ionization", *J. Phys. B* **45**, 194002 (2012).
13. T. N. Rescigno, N. Douguet and A. E. Orel, "Imaging Molecular Isomerization Using Molecular-Frame Photoelectron Angular Distributions", *J. Phys. B* **45**, 194001 (2012).
14. F. L. Yip, T. N. Rescigno, C. W. McCurdy and F. Martín, "Fully Differential Single-Photon Double Ionization of Neon and Argon", *Phys. Rev. Lett.* **110**, 173001 (2013).
15. N. Douguet, T. N. Rescigno and A. E. Orel, "Time-resolved molecular-frame photoelectron angular distributions: Snapshots of acetylene-vinylidene cationic isomerisation", *Phys. Rev. A* **86**, 013425 (2013).
16. D. S. Slaughter, D. J. Haxton, H. Adaniya, T. Weber, T. N. Rescigno, C. W. McCurdy and A. Belkacem, "Ion-momentum imaging of resonant dissociative-electron-attachment dynamics in methanol", *Phys. Rev. A* **87**, 052711 (2013).
17. T. N. Rescigno and A. E. Orel," A Theoretical Study of Excitation of the Low-Lying Electronic States of Water by Electron Impact", *Phys. Rev. A* **88**, 012703 (2013).
18. N. Douguet T. N. Rescigno and A. E. Orel, "Carbon K-shell molecular-frame photoelectron angular distribution in the photoisomerization of neutral ethylene", *Phys. Rev. A* **88**, 013425 (2013).
19. D. J. Haxton, "Breakup of H_2^+ by Photon Impact", Phys. Rev. A 88, 013415 (2013).
20. A. Moradmand, D. S. Slaughter, D. J. Haxton, T. N. Rescigno, C. W. McCurdy, Th. Weber, S. Matsika, A. L. Landers, A. Belkacem, and M. Fogle, "Dissociative electron attachment to carbon dioxide via the $^2\Pi_u$ shape resonance", *Phys. Rev. A* (in press).

Ultrafast X-ray Science Laboratory

C. William McCurdy (Director), Ali Belkacem, Oliver Gessner, Dan Haxton, Martin Head-Gordon, Stephen Leone, Daniel Neumark, Robert W. Schoenlein, Thorsten Weber

Chemical Sciences Division, Lawrence Berkeley National Laboratory, Berkeley, CA 94720

CWMcCurdy@lbl.gov, ABelkacem@lbl.gov, OGessner@lbl.gov, DJHaxton@lbl.gov, MHead-Gordon@lbl.gov, SRLeone@lbl.gov, DMNeumark@lbl.gov, RWSchoenlein@lbl.gov, TWeber@lbl.gov

Program Scope: This program exploits short pulses of X-rays to provide basic knowledge of ultrafast dynamics of photo-excited molecules in the gas phase and condensed phase from the natural time scale of electron motion to the time scale of the chemical transformations. There five subtasks in the UXSL effort, outlined below.

Recent Progress and Future Plans:

1. Soft X-ray high harmonic generation and applications in chemical physics -- *Oliver Gessner, Stephen Leone and Daniel Neumark*

This part of the laboratory is focused on the study of ultrafast chemical dynamics in molecules and clusters by means of novel femtosecond XUV and soft x-ray light sources. Laboratory based experiments using high-order harmonic generation (HHG) light sources are complemented by studies at the Linac Coherent Light Source (LCLS) free electron laser. Experimental techniques include time-resolved photoelectron spectroscopy, electron- and ion-imaging, transient absorption spectroscopy, and coherent diffractive imaging.

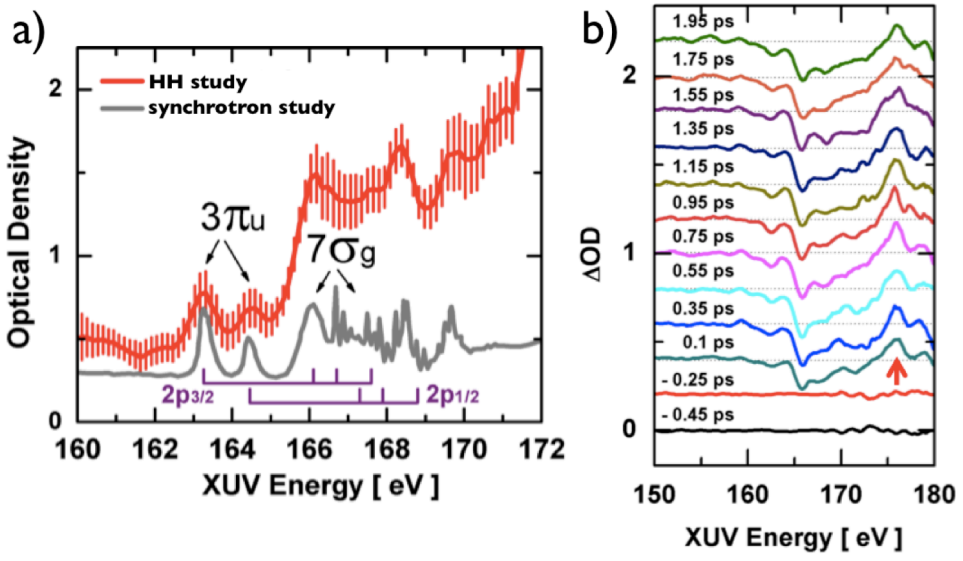

Fig. 1: High-harmonic generation based transient XUV absorption study of strong-field ionized CS_2 in the vicinity of the sulfur 2p edge. a) Static absorption spectrum (red) and reference spectrum from synchrotron-based study (gray, Hedin et al., J. Phys. B: At. Mol. Opt. Phys. **42,** 085102 (2009)). b) Femtosecond time-resolved XUV transient absorption spectra. The delay between the ionizing intense femtosecond IR pulse and the probing XUV pulse is noted beside each trace.

Significant progress has been made in extending the realm of laboratory-based ultrafast transient XUV absorption studies beyond the typical ~100 eV photon energy limit. Fig. 1 shows a) static and b) transient XUV absorption spectra of gas phase CS_2 molecules in the vicinity of the sulfur 2p absorption edge (~170 eV) recorded with a HHG based light source. Fig. 1a also shows a high-resolution spectrum from a recent synchrotron study for comparison. The laboratory based static absorption spectrum that has been acquired within ~50 s reproduces the dominant features of the accelerator-based data. In particular, the $2p \rightarrow 3\pi_u$ and $2p \rightarrow 7\sigma_g$ inner-shell to valence transitions can be discerned as marked in Fig. 1a. The time-resolved spectra in Fig. 1b show the change in XUV optical density (ΔOD) induced by strong-field ionization of CS_2 molecules with an intense (~10^{14} W/cm^2) femtosecond infrared (785 nm) laser pulse. The transient absorption spectra exhibit both negative and positive ΔOD's corresponding to the depletion of neutral ground state CS_2 molecules and the generation of excited/ionized transient molecular species, respectively. The spectroscopic interpretation of the transient spectra is ongoing.

Dynamics in superfluid helium nanodroplets are studied in two classes of experiments. Laboratory-based femtosecond time-resolved XUV photoelectron imaging experiments monitor transient electronic configurations induced by single-photon excitation in the ~20 eV – 24 eV range. An ultraviolet (400 nm) probing scheme has been implemented that accesses intermediately populated states, giving new insight into the intra- and interband relaxation cascades of electronically excited helium clusters. Exploratory experiments have been performed on helium droplets doped with noble gas atoms, paving the way toward the first direct time-domain study of solvent-solvate energy- and charge-transfer mechanisms inside the superfluid nano-matrix.

The second class of experiments on helium nanodroplets utilizes the unique single-shot X-ray diffractive imaging capabilities of the LCLS. Images of single pure and doped droplets reveal new details of the hydrodynamic properties of the superfluid clusters and the formation and characteristics of dopant nanoclusters. In particular, the studies give direct access to both the implementation of quantum rotation by the formation of vortex lattices and the corresponding shape variations of self-contained quantum droplets. The collaborative effort between UXSL, the University of Southern California, and SLAC National Accelerator Laboratory has been awarded a new LCLS beam time in January 2014. By employing the new X-ray pump / X-ray probe capability of the LCLS, a *transient* diffractive imaging study will monitor the correlated electronic and structural dynamics in noble gas clusters and test strategies for using helium droplets as a tamper material for ultrafast diffractive imaging studies of biological samples.

2. Ultrafast X-ray Studies of Condensed Phase Molecular Dynamics -- *Robert W. Schoenlein*

The objective of this UXSL subtask is to advance our understanding of solution-phase molecular dynamics using ultrafast X-rays as time-resolved probes of the evolving electronic and atomic structure of solvated molecules. Time-resolved XANES provide detailed information about dynamics of the valence charge structure, while time-dependent EXAFS provides information about changes in the local atomic structure. X-ray measurements on the time scale of a vibrational period reveal important new information about solution-phase chemical reactions including: charge transfer processes, changes in oxidation states, formation/dissolution of bonds, and conformational changes. One area of present focus is on solvated transition-metal complexes exhibiting strong coupling between molecular structure, charge transfer, and electronic properties arising from the ligand field. These include transition-metal polypyridyl compounds, metal-porphyrins, metal-carbonyls, and bridged heteronuclear metal-metal compounds. Understanding the fundamental dynamics in these classes of compounds is relevant for solar energy conversion schemes, photo-catalysis, and related processes. This subtask exploits two unique time-resolved X-ray beamlines at the ALS with the capability for generating ~200 fs X-ray pulses from 200 eV to 10 keV, as well as the recently operational LCLS X-ray laser, complemented by ultrafast optical spectroscopy studies.

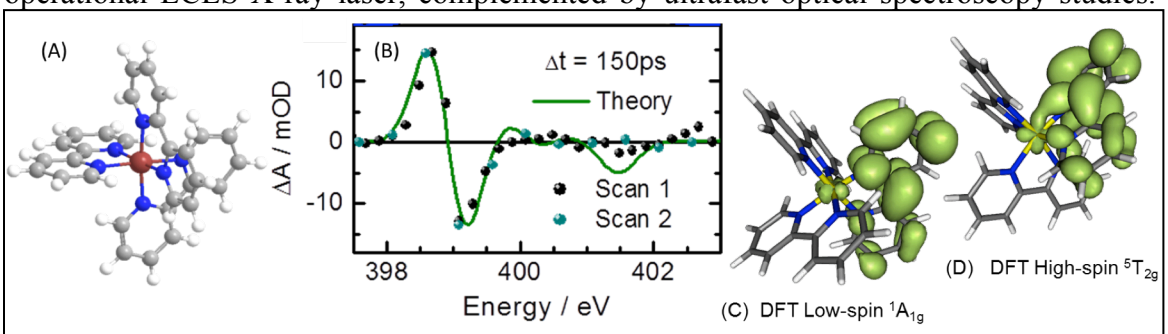

Fig. 2: (A) Molecular structure of the polypyridyl Fe^{II} compound with pseudo-octahedral arrangement of six nitrogen atoms (blue) around the central Fe^{II} ion (red). (B) Differential XAS at the N K-edge at 150 ps delay with DFT-based theoretical fit to the differential spectrum. (C, D) Charge distributions of the unoccupied N-*2p* DOS for the low-spin $^1A_{1g}$ ground state, and the high-spin $^5T_{2g}$ excited state.

Spin Transition in Fe^{II} Polpyridyl Complexes: This year we have focused on understanding changes of valence charge density in polypyridyl Fe^{II} complexes upon spin-crossover for different coordination environments of the metal center. One example are "ligand perspective" studies of the charge dynamics via transient spectroscopy of the N *1s*→*2p* core transition (K-edge XANES, ALS BL6.0.2), which provides important complementary information compared to transitions originating on the core ion. Fig. 2 shows differential N K-edge spectra of the Fe^{II} complex, and DFT calculations that well describe the high-spin/low-spin differential spectra. Importantly, this clearly reveals the enhancement of π-symmetry orbitals in the high-spin excited state.

Charge-transfer Dynamics in Ru-based "light-switch" Complexes: We have initiated new studies of the light the "light-switch" compound $[Ru(bpy)_2(dppp2)]^{2+}$ which exhibits photo-induced charge-transfer processes that are poorly understood, and yet are central for solar energy conversion (e.g. dye sensitized solar cells) and photo-catalysis. Time-resolved XAS at the Ru L-edge (ALS BL6.0.1) provide a quantitative understanding of

the charge transfer dynamics, transient electronic structures, and the solvent role in photo-excited complexes with dppz and dppp2 ligands. L-edge spectroscopy is particularly powerful for probing changes in the *3d*-orbital filling and mixing and the spin state of the complex. One important question to be addressed is the relative time-scale of both the triplet-state interconversion (the rate of which can be tuned over an order of magnitude via solvent stabilization) and the recovery of the ground state as a function of solvent properties. Future studies in Ru-based light harvesting complexes will focus of the "ligand-view" of the charge dynamics via time-resolved XANES at the N K-edge.

Electron Transfer Dynamics of Solvated Mixed Valence Photocatalyst: CN-bridged mixed-valence transition-metal complexes are prototypical models for homogeneous intramolecular photocatalysts for energy conversion. These consist of a visible-light harvesting moiety coupled to a photoredox-active center and a redox-active bridge. Using ALS BL6.0.1 we have initiated new time- X-ray spectroscopy studies of the Ru^{II}-CN-Cr^{III}-CN-Ru^{II} complex at the Ru L-edge and Cr K-edge. From experiments, spin multiplicity, oxidation state and symmetry of the donor-acceptor compounds are expected to change following charge transfer. Cr K-edge XANES reflects changes in electronic valency and the local chemical bonding geometry. Ru L-edge spectra provide specific information regarding changes in the *d*-orbital filling upon charge transfer. Coupling of the metal $d\pi$ orbitals to CN^- π and π^* orbitals can be formulated in terms of ligand to metal (LMCT) and metal-to-ligand (MLCT) charge transfer perturbations. Additionally, the EXAFS spectral region provides information about the structural changes upon MMCT. The FEFF code and charge-transfer multiple calculations will be used to simulate the X-ray absorption spectra of K- and L-edges, respectively.

3. Time-resolved studies and non-linear interaction of femtosecond x-rays with atoms and molecules -- *Ali Belkacem and Thorsten Weber*

This subtask of the UXSL is focused on using two-color Extreme Ultraviolet (XUV) pump and XUV probe to study non-Born-Oppenheimer dynamics in polyatomic molecules as well as non-linear x-ray processes. Higher-order harmonic generation has reached intensities high enough as to induce multiphoton ionization processes. This past year we focused on major laser upgrades and laboratory development. We upgraded our low repetition rate laser system from 10 Hz to 50Hz and to higher-pulse energy (>40 mJ per pulse). The design and construction of our intense XUV source is based on scaling-up in energy of the loose focusing high harmonic generation scheme. Pump/probe delay is achieved with a split mirror interferometer (SMI). VUV and XUV wavelength selection in each arm of the SMI is achieved through a combination of transmission filters and coatings on the two D-shaped mirrors. We applied our two-color VUV/XUV pump-probe system to the study non-Born-Oppenheimer dynamics in excited-state molecules. We continued our investigation of the nonadiabatic dynamics of the prototypical ethylene C_2H_4 molecule upon $\pi \rightarrow \pi^*$ excitation with 161 nm light. In particular we focused our study on the atomic and molecular hydrogen elimination by direct detection of $C_2H_3^+$ and $C_2H_2^+$ complementing our previous published work where we detected H^+ and H_2^+. Preliminary results appear to confirm that molecular hydrogen elimination (in the ground state) happens after transition through the "ethylidene-like" conical intersection (CI) instead of the "twist-pyramidalized" CI. Indications of this surprising result were already

seen in our previous work. We also applied our XUV pump-probe technique to study molecular dissociation of neutral CO_2 after excitation by a 7.75-eV photon. The CO_2* dissociation was probed with the 15^{th} harmonic (~23-eV). We monitored the production of CO^+ and O^+ as a function of the time delay between the 5^{th} pump and 15^{th} probe. We observed a time-dynamics of 250 fs that intuitively appears to be too long for direct dissociation and too short for singlet-triplet interstate-crossing. This work is ongoing and close theory-experiment effort is needed to unravel the surprisingly complex dynamics of excited CO_2.

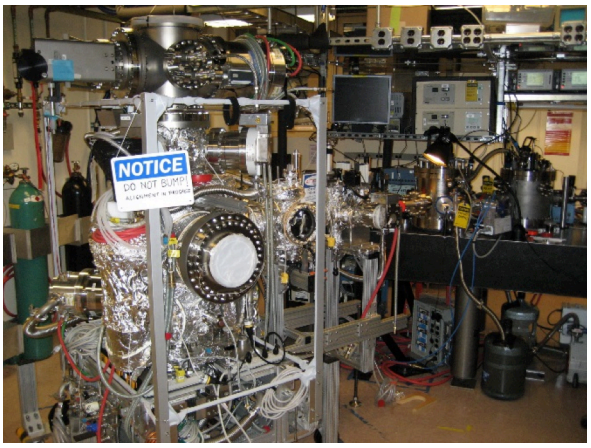

Fig. 3 MISTERS endstation (left) at the end of the 50Hz HHG beamline, followed by the XUV spectrometer (center glass flange), a differential pumping stage, the filter chamber, and the Split Mirror Interferometer (to the right).

We moved a newly constructed reaction microscope (MISTERS) end-station to the 50Hz HHG laser laboratory, shown in Fig. 3. While the laser light repetition rate is low we will aim for electron-ion coincidence measurements to extend our successful COLTRIMS projects to time resolved studies. The apparatus was set up aligned and equipped with a 3d-momentum imaging spectrometer and time and position large area sensitive detectors. Half of the existing beamline was replaced by a new layout consisting of a new Split Mirror Interferometer, a collimation section, a filter chamber, and the original silicon mirror. In an initial test phase these instruments will be optimized for a startup program on two-color two-photon single ionization of rare gas atoms like He, Ne and Ar followed by the investigation of small molecules like CO and O_2.

Parallel to the upgrade of the low repetition high harmonic system we commissioned a new state-of-the-art laser system (30 mJ, 1 kHz and 25fs) in an adjacent laboratory. A similar high harmonic generation scheme to the 50 Hz was constructed and commissioned. This latter system produces routinely in excess of 10^9 photons per harmonic at 1-kHz making it a one-of-a-kind source of high-intensity and high repetition rate XUV photons. In addition to ion fragmentation pathways, we will attempt photoelectron spectroscopy in the molecular frame. The angular distribution of photoelectrons in the molecular frame is directly related to the electronic state of the molecule at the time of ionization. By measuring these distributions as a function of pump/probe delay we should be able to directly measure when electronic state changes take place. In general there are two ways of finding the molecular frame: either one can know the orientation of a molecule *a priori* relative to the laboratory frame, or one can attempt to deduce what the orientation was during the photo--reaction by measuring the photo-fragments. This technique relies on coincidence detection of different ionic fragments created during the photo-reaction. These fragments are collected and momentum conservation is used to reconstruct the initial orientation of the molecule at

the time of ionization. The MISTERS reaction microscope installed at the 50 Hz system uses that approach. In the new laboratory instead of measuring the orientation after the fact, we intend to prepare ensembles of molecules using strong-field laser pulses. This technique is highly adaptable to many different molecular species and can be used to create rather high degrees of alignment that persist long after the aligning laser pulse is gone. To implement this technique we built a second beam line (4 mJ) along side our current XUV beam-line (26 mJ) which will deliver the aligning laser pulse – this set-up enables a multi-pulse capability as well (one IR/visible to be used for alignment, control, dump pulse, etc.. and two different XUV beams for pump-probe). Measurements made in the molecular frame will benefit greatly from other detection schemes, such as Velocity Map Imaging (VMI) spectroscopy, which we are also building.

4. Attosecond atomic and molecular science -- *Stephen Leone and Daniel Neumark*

The LBNL attosecond dynamics effort focuses on measuring attosecond timescales of electronic processes. Transient absorption spectroscopy with isolated attosecond pulses coupled with few cycle 800 nm pulses is used to measure laser-induced changes in the absorption of an atom or molecule on sub-femtosecond timescales. Isolated attosecond pulses in the spectral range of 15 to 80 eV are generated using high harmonic generation and Double Optical Gating. Several recent investigations utilize thin Sn foils to spectrally limit the attosecond pulses to 18-24 eV, with pulse durations of approximately 400 as.

In the past year, the vacuum system was redesigned and rebuilt. The new design uses a grazing incidence gold-coated toroidal mirror instead of specialized XUV multilayer optics, which results in significantly higher attosecond flux (factor of five) and a simpler geometry. The new design focuses on transient absorption measurements, while the capabilities for time–of-flight photoelectron spectroscopy and mass spectroscopy are retained. The spectral resolution after the interaction region, a critical parameter to investigate on line center for time-resolved measurements, was improved by a factor of 6 (now, 15 meV at 20 eV photon energy) and a new grating will soon be used to improve this spectral resolution by another factor of two or more. The rebuilt system has so far been used to generate isolated attosecond pulses around 20 eV photon energy, but producing pulses centered at higher photon energies requires minimal reconfiguration.
The broad bandwidth of the attosecond pulse allows simultaneous excitation of multiple

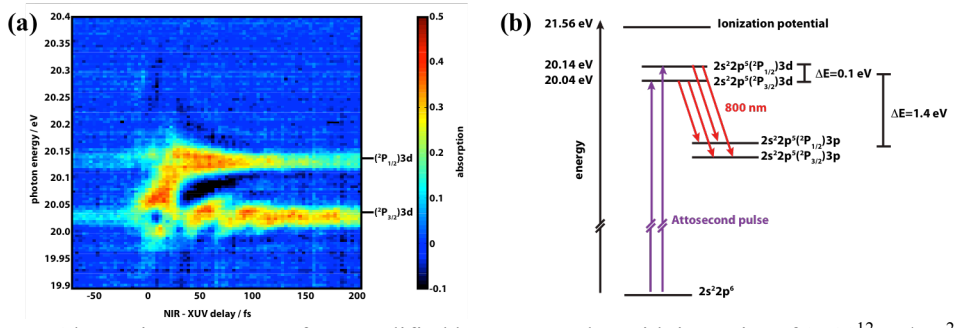

Fig. 4 **(a)** Absorption spectrum of Ne modified by a NIR pulse with intensity of $2x10^{12}$ W/cm^2 and duration of 11 fs. **(b)** Proposed mechanism for detection of quantum beating.

Rydberg states of neon below the first ionization potential at 21.56 eV. Simultaneous excitation of many Rydberg states creates electronic wavepackets and induces a polarization in the sample. Modifying the induced polarization with an 11 fs near-infrared (NIR) pulse results in changes in the measured absorption spectrum as a function of the relative time delay between the attosecond pulse and the NIR pulse, as shown in Fig. 4. Regions of enhanced absorption and emission are observed, with Lorentzian lines becoming Fano-shaped due to the effect of the NIR on the polarization of the medium. The high spectrometer resolution allows the spin-orbit splitting in neon states of 0.1 eV to be clearly resolved, and quantum beating in the spin-orbit split $2s^2 2p^5 3d$ Rydberg states is observed through the polarization of the medium. The beat period of 40 fs matches the spin-orbit splitting between these states. Additionally, higher frequency beats are observed in other Rydberg states, for example a 10 fs beat is observed in the $2s^2 2p^5 5s$ absorption feature located at 20.6 eV. Theoretical calculations by the group of Ken Schafer and Mette Gaarde at Louisiana State University reproduce the observed time dependent absorption lineshape changes and beat frequencies.

The improved spectrometer resolution allows new insights in the transient absorption studies of xenon. Isolated attosecond pulses have been used to excite the $5s5p^5 6p$, $5s5p^5 7p$, $5s5p^5 8p$ and $5s5p^5 9p$ autoionizing states of xenon, which appear as Fano window resonances in the XUV absorption spectrum. When a NIR few-cycle pulse interacts with the excited states before they decay, the Fano resonances are suppressed due to coupling of the population to neighboring states by the NIR laser field. This suppression recovers with the timescale of the autoionization, which is extracted in the measurement. In addition to obtaining the decay time of the autoionizing level $5s5p^5 6p$ (centered at 20.95 eV), coupling effects to neighboring states are resolved for the first time. This is revealed by an oscillatory contribution on top of the exponential decay of the $5s5p^5 6p$ state population. With the help of a theoretical model developed by Xuan Li and William McCurdy, this oscillation can be attributed to a neighboring two electron excited state centered at 21.35 eV. Furthermore, the model describes the experimentally observed changes in the decay time of the state population with spectral width and detuning from line center. At different energy positions across the resonance, the absorption strength decreases less quickly, which is attributed to a phase shift due to the energy detuning off resonance.

Future experiments will investigate short-lived states in molecular species using the theoretical understanding and experimental techniques developed in the xenon studies. The lifetimes of autoionizing 3d core-excited states of HBr around 70 eV will be determined using transient absorption. These measurements will be compared to those for the isoelectronic atomic species, krypton. The dissociation and autoionization dynamics of short-lived superexcited states of small molecules such as molecular nitrogen will also be studied.

5. Theory and computation -- *Martin Head-Gordon, Dan Haxton and C. William McCurdy*

This part of the program focuses on the theoretical description of the next generation of ultrafast XUV and X-ray experiments. To that end, we have completed an entirely new implementation of the Multiconfiguration Time-dependent Hartree Fock (MCTDHF) method with "all electrons active" based on finite-element grids in prolate spheroidal coordinates to represent the time-dependent orbitals.

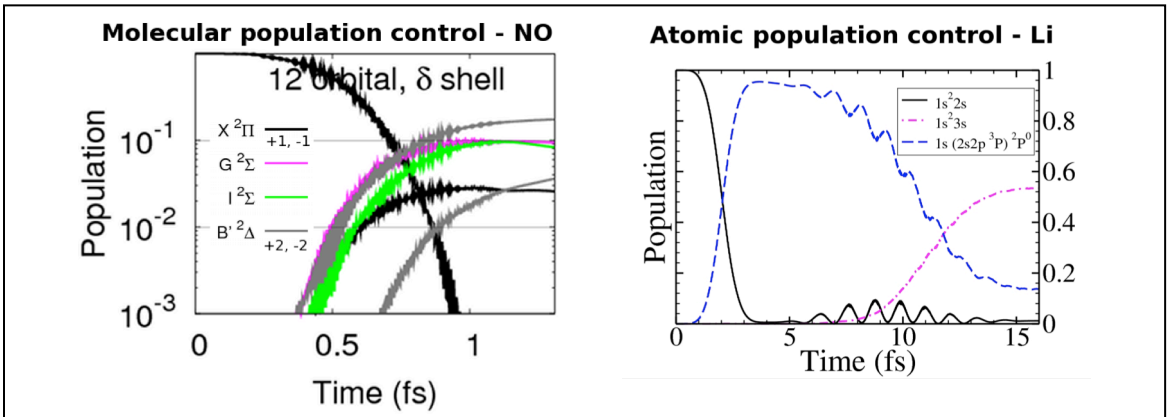

Fig. 5 MCTDHF calculations of ultrafast population control via core-hole states. Left: Transfer of 41% of NO ground state population to three valence excited states with two 1.3 femtosecond X-ray pulses at 402.6 and 393.3 eV near the nitrogen K-edge. Right: Li population transfer to the 3s state with two coincident π pulses at 58.9 and 55.5 eV. All electrons (15 and 3 respectively) are active in calculations.

The method treats general diatomics including for the the combination of (1) a rigorous representation of the ionization continuum via the method of exterior complex coordinate scaling, (2) an all-electrons-active treatment in which excitations are allowed from all orbitals and all orbitals are time dependent, and (3) the possibility of treating nuclear motion in diatomics on the same footing as electronic motion. This capability has opened the door to the complete *ab initio* simulation of both many-electron atoms and many-electron diatomic molecules in short, intense XUV and X-ray pulses.

In Fig. 5 we show two recent results from this newly developed capability. In nitric oxide stimulated X-ray Raman transfer of population from the ground state of NO to a wave packet of valence excited states using two 1.3 femtosecond pulses near the nitrogen K-edge moves 44% of the ground state population to these three valence excited states using intermediate Auger decaying core-hole intermediate states, with an ionization of about 30% of the initial population. This all-electrons-active calculation quantitatively demonstrates the feasibility of controlled population transfer among valence states using ultrafast X-ray pulses, and thus allows us to explore the possibility of site-selective nonlinear X-ray spectroscopy with new free electron laser facilities. Also in Fig. 5, from a study in which stimulated Raman adiabatic passage (STIRAP) was shown definitively to fail, we show population transfer between the ground state and $1s^2 3s$ of 55% is accomplished using femotosecond XUV π pulses with the population being transferred through an autoionizing state.

The crucial photochemical events in processes ranging from vision to light-harvesting to light emission involve ultrafast processes that involve multiple excited states. Experiments provide one window on the relevant states while first principles computations offers another, complementary, view. Recent work has relied on our development of spin-flipping methods to enable new calculations that provide fresh insight into the excited states relevant to the process of singlet fission in pentacene crystals. Our calculations on this process, where a single photon can yield two electron-hole pairs (via two triplets), suggest a crucial role for a conical intersection.

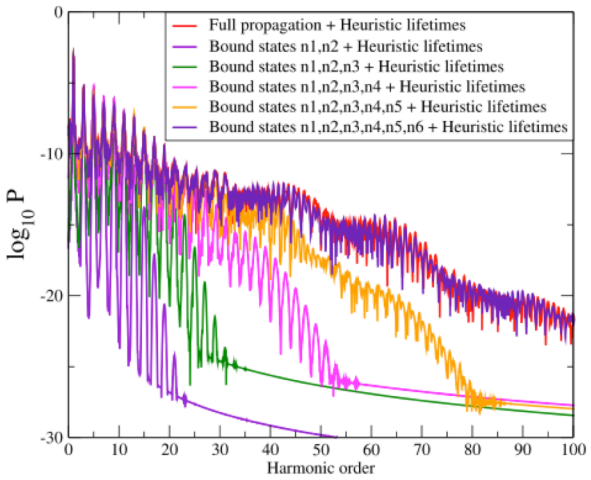

Fig. 6: Strong dependence of the H atom HHG signal on the inclusion or deletion of Rydberg states.

We are just finishing *ab initio* trajectory studies that explore post-electronic excitation dynamics of small helium clusters, as a simulation counterpart to UXSL experiments. The dynamics typically show dramatic cluster fragmentation, including a small fraction of dimers and an even smaller fraction of trimers. Additionally, the development of local excited state methods that are capable of treating much larger cluster sizes than standard algorithms is approaching production capability. Turning to the modeling of high harmonic generation, we have just completed a careful numerical study that illuminates the key role of Rydberg bound states in HHG generation in the H atom (see Fig. 6), that complements our previous work on the H_2 and N_2 molecules.

UXSL Publications, by Subtask (2011-2013)

1. O. Gessner, O. Kornilov, M. Hoener, L. Fang, and N. Berrah, "Intense Femtosecond X-ray Photoionization Studies of Nitrogen - How Molecules interact with Light from the LCLS" in Ultrafast Phenomena XVII, M. Chergui, D. M. Jonas, E. Riedle, R. W. Schoenlein, A. J. Taylor, Eds., Oxford University Press (2011).
2. Oleg Kornilov, Oliver Bünermann, Daniel J. Haxton, Stephen R. Leone, Daniel M. Neumark, and Oliver Gessner, "Femtosecond photoelectron imaging of transient electronic states and Rydberg atom emission from electronically excited He droplets", J. Phys. Chem. A **115**, 7891 (2011).
3. Oliver Bünermann, Oleg Kornilov, Stephen R. Leone, Daniel M. Neumark, and Oliver Gessner, "Femtosecond Extreme Ultraviolet Ion Imaging of Ultrafast Dynamics in Electronically Excited Helium Nanodroplets", IEEE J. Sel. Top. Quantum Electron. **18**, 308 (2012).
4. J. P. Cryan, J. M. Glownia, J. Andreasson, A. Belkacem, N. Berrah, C. I. Blaga, C. Bostedt, J. Bozek, N. A. Cherepkov, L. F. DiMauro, L. Fang, O. Gessner, M. Gühr, J. Hajdu, M. P. Hertlein, M. Hoener,

O. Kornilov, J. P. Marangos, A. M. March, B. K. McFarland, H. Merdji, M. Messerschmidt, V. Petrovic, C. Raman, D. Ray, D. Reis, S. K. Semenov, M. Trigo, J. White, W. White, L. Young, P. H. Bucksbaum, and R. N. Coffee, "Molecular Frame Auger Electron Energy Spectrum from N2", J. Phys. B: At. Mol. Opt. Phys. **45**, 055601 (2012).

5. Fabian Weise, Daniel M. Neumark, Stephen R. Leone, and Oliver Gessner, "Differential Near-Edge Coherent Diffractive Imaging for Element-Specific Contrast Enhancement in Ultrafast Imaging Applications", Opt. Express **20**, 26167 (2012).

6. Oliver Bünermann, Oleg Kornilov, Daniel J. Haxton, Stephen R. Leone, Daniel M. Neumark, and Oliver Gessner, "Ultrafast Probing of Ejection Dynamics of Rydberg Atoms and Molecular Fragments from Electronically Excited Helium Nanodroplets", J. Chem. Phys., **137**, 214302 (2012).

7. Ming-Fu Lin, Adrian N. Pfeiffer, Daniel M. Neumark, Stephen R. Leone, and Oliver Gessner, "Strong-Field induced XUV Transmission and Autler-Townes Multiplet Splitting in $4d^{-1}6p$ Core-excited Xe studied by Femtosecond XUV Transient Absorption Spectroscopy", J. Chem. Phys. **137**, 244305 (2012).

8. Olga Smirnova and Oliver Gessner, "Attosecond Spectroscopy", Chem. Phys. **414**, 1 (2013).

9. Andrey Shavorskiy, Amy Cordones, Josh Vura-Weis, Katrin Siefermann, Daniel Slaughter, Felix Sturm, Fabian Weise, Matthew Strader, Hana Cho, Ming-Fu Lin, Camila Bacellar, Champak Khurmi, Marcus Hertlein, Jinghua Guo, Hendrik Bluhm, Tolek Tyliszczak, David Prendergast, Giacomo Coslovich, Joseph Robinson, Robert Kaindl, Robert W. Schoenlein, Ali Belkacem, Thorsten Weber, Daniel M. Neumark, Stephen R. Leone, Dennis Nordlund, Hirohito Ogasawara, Anders R. Nilsson, Oleg Krupin, Joshua J. Turner, William F. Schlotter, Michael R. Holmes, Philip A. Heimann, Marc Messerschmidt, Michael P. Minitti, Martin Beye, Sheraz Gul, Jin Zhang, Nils Huse, and Oliver Gessner, "Time-Resolved X-Ray Photoelectron Spectroscopy Techniques for Real-Time Studies of Interfacial Charge Transfer Dynamics", Application of Accelerators in Research and Industry, AIP Conf. Proc. **1525**, 475 (2013).

10. Ming-Fu Lin, Daniel M. Neumark, Oliver Gessner, and Stephen R. Leone, "Ionization and Dissociation Dynamics of Vinyl Bromide Probed by Femtosecond Extreme Ultraviolet Transient Absorption Spectroscopy", J. Chem. Phys., *submitted* (2013).

11. N. Huse, H. Cho, T.K. Kim, L. Jamula, J.K. McCusker, F.M.F. de Groot, and R.W. Schoenlein, "Ultrafast spin-state conversion in solvated transition metal complexes probed with femtosecond soft x-ray spectroscopy," in **Ultrafast Phenomena XVII**, M. Chergui, D.M. Jonas, E.Riedle, R.W. Schoenlein, A.J. Taylor, Eds., Oxford University Press, New York, p. 370-372, (2011)

12. N. Huse, H. Wen, H. Cho, T.K. Kim, R.W. Schoenlein, and A.M. Lindenberg, "Ultrafast conversions of hydrogen-bonded structures in liquid water observed via femtosecond soft x-ray spectroscopy," in **Ultrafast Phenomena XVII**, M. Chergui, D.M. Jonas, E.Riedle, R.W. Schoenlein, A.J. Taylor, Eds., Oxford University Press, New York, p. 460-462, (2011)

13. H. Cho, M.L. Strader, K. Hong, L. Jamula, E.M. Gullikson, T.K. Kim, F.M.F. de Groot, J.K. McCusker, R.W. Schoenlein, and N. Huse, "Ligand-field symmetry effects in Fe(II) polypyridyl compounds probed by transient X-ray absorption spectroscopy," *Faraday Discuss*. **157**, 463-474 (2012).

14. B.E. Van Kuiken, N. Huse, H. Cho, M.L. Strader, M.S. Lynch, R.W. Schoenlein, and M. Khalil, "Probing the electronic structure of a photoexcited solar cell dye with transient X-ray absorption spectroscopy," *J. Phys. Chem. Lett*., **3**, 1695-1700 (2012).

15. B. Van Kuiken, M. Valiev, S. Daifuku, C. Bannan, M. Strader, H. Cho, N. Huse, R. Schoenlein, N. Govind, M. Khalil, "Simulating Ru L_3-edge X-ray Absorption Spectroscopy with Time-Dependent Density Functional Theory: Model Complexes and Electron Localization in Mixed-Valence Metal Dimers," *J. Phys. Chem. A*, **117**, 4444–4454 (2013).

16. H. Tao, T.K. Allison, T.W. Wright, A.M. Stooke, C. Khurmi, J. van Tilborg, Y. Liu, R.W. Falcone, A. Belkacem, and T.J. Martinez, "ultrafast internal conversion in ethylene. I. The excited state lifetime", J. Chem. Phys. **134**, 244306 (2011).

17. Cao W., Laurent G., De S., Schoffler M., Jahnke T., Alnaser A.S., Bocharova I.A., Stuck C., Ray D., Kling M.F., Ben-Itzhak I., Weber T., Landers A.L., Belkacem A., Dorner R., Orel A.E., Rescigno T.N., Cocke C.L., "Dynamics modification of the fragmentation of autoionizing states of O_2^+", Phys. Rev. A **84**, 053406 (2011).

18. R. Moshammer, Th. Pfeifer, A. Rudenko, Y.H. Jiang, L. Foucar, M. Kurka, K.U. Kuhnel, C.D. Schroter, J. Ullrich, O. Herrwerth, M.F. Kling, X.J. Liu, K. Motomura, H. Fukuzawa, A. Yamada, K. Ueda, K.L. Ishikawa, K. Nagaya, H. Iwayama, A. Sugishima, Y. Mizoguchi, S. Yase, M. Yao, N. Saito, A. Belkacem, M. Nagasono, A. Higashiya, M. Yabashi, T. Ishikawa, H. Ohashi, H. Kimura, T. Togashi, "second-order autocorrelation of XUV FEL pilses via time resolved two-photon single ionization of He", Optics Express **19**, 21698 (2011).

19. Allison T.K., Tao H., Glover W.J., Wright T., Stooke A.M., Khurmi C., van Tilborg J., Liu Y., Falcone R.W., Martinez T.J., Belkacem A., "Ultrafast internal conversion in ethylene. II. Mechanisms and pathways for quenching and hydrogen elimination", Jour. Chem. Phys. **136**, 124317 (2012).

20. Cryan, J.P., Glownia J.M., Andreasson J., Belkacem A., Berrah N., Blaga C.I., Bostedt C., Bozek J., Cherepkov N.A., Dimauro L.F., Fang L., Gessner O., Guhr M., Hajdu J., Hertlein M.P., Hoener M., Korlinov O., Marangos J.P., March A.M., McFarland B.K., Merdji H., Messerschmidt M., Petrovic V.S., Raman C., Ray D., Reis D.A., Semenov S.K., Trigo M., White J.L., White W., Young L., Bucksbaum P.H., Coffee R.N., "Molecular frame auger electron spectrum from N_2, Jour. Phys. B – At. Mol. Opt. Phys. **45**, 055601 (2012).

21. Y. Jiang, A. Senftleben, M. Kurka, A. Rudenko, L. Foucar, O. Herrwerth, M. Kling, M. Lezius, J. Tilborg, A. Belkacem, K. Ueda, D. Rolles, R. Treusch, Y. Zhang, Y. Liu, C. Schroeter, J. Ullrich and R. Moshammer, "Ultrafast dynamics in acetylene clocked in a femtosecond XUV stopwatch", *Accepted for publication Journal of Physics B.*

22. M. J. Abel, D. M. Neumark, S. R. Leone, and T. Pfeifer, "Classical and Quantum Control of Electrons using the Carrier-Envelope Phase of a Strong Field." Laser Photonics Rev. **25**, 1 (2011).

23. H. Mashiko, M. J. Bell, A. R. Beck, D. M. Neumark, and S. R. Leone, "Frequency tunable attosecond apparatus," ***Progress in Ultrafast Intense Laser Science X***, K. Yamanouchi, G. Paulus, D. Mathur, eds., Springer Science+Business Media, Inc.

24. S. Chen, M. J. Bell, A. R. Beck, H. Mashiko, M. Wu, A. N. Pfeiffer, M. B. Gaarde, D. M. Neumark, S. R. Leone, and K. J. Schafer, "Light-induced states in attosecond transient absorption spectra of laser-dressed helium." Phys. Rev. A **86**, 6 (2012).

25. M. J. Bell, A. R. Beck, H. Mashiko, D. M. Neumark, and S. R. Leone, "Intensity dependence of light induced states in transient absorption of laser dressed helium measured with isolated attosecond pulses." J. Mod. Opt. (in press) (2013).

26. A. N. Pfeiffer, M. J. Bell, A. R. Beck, H. Mashiko, D. M. Neumark, and S. R. Leone, "Alternating absorption features during attosecond pulse propagation in a laser-controlled gaseous medium." (Phys. Rev. A submitted).

27. D. J. Haxton, K. Lawler and C. W. McCurdy, "Multiconfiguration Time-dependent Hartree-Fock Treatment of Electronic and Nuclear Dynamics in Diatomic Molecules," Phys. Rev. A **83**, 063416 (2011).

28. D. J. Haxton, K. V. Lawler and C. W. McCurdy, "Single photoionization of Be and HF using the multiconfiguration time-dependent Hartree-Fock method," Phys. Rev. A **86**, 013406 (2012).

29. X. Li, C. W. McCurdy and D. J. Haxton, "Population transfer between valence states via core-hole states using ultrafast pulses: the limitations of adiabatic passage," Phys. Rev. A (Submitted).

30. D. J. Haxton and C. W. McCurdy, "Ultrafast population transfer among valence levels of a molecule with X-ray pulses," Phys. Rev. Letts. (Submitted).

31. J. Azar , W. Kurlancheek, and M. Head-Gordon, "Characterization of electronically excited states in anionic acetonitrile clusters," Phys. Chem. Chem. Phys. **13**, 9147-9154 (2011).

32. P.M. Zimmerman, F. Bell, D. Casanova, and M. Head-Gordon, "Mechanism for Singlet Fission in Pentacene and Tetracene: From Single Exciton to Two Triplets," J. Am. Chem. Soc **133**, 19944-19952 (2011).

33. E. Luppi and M. Head-Gordon, "Computation of high harmonic generation spectra of H_2 and N_2 due to intense laser pulses using quantum chemistry methods and time-dependent density functional theory," Mol. Phys. **110**, 909-923 (2012).

34. P.M. Zimmerman, C.B. Musgrave, and M. Head-Gordon, "A Correlated Electron View of Singlet Fission", Acc. Chem. Res. **46**, 1339-1347 (2013).

35. E. Luppi and M. Head-Gordon, "The role of Rydberg and continuum levels in computing high harmonic generation spectra of the hydrogen atom using time-dependent configuration interaction", J. Chem. Phys. (submitted, 2013).

Early Career: Ultrafast X-ray Studies of Intramolecular and Interfacial Charge Migration

Oliver Gessner

Chemical Sciences Division, Lawrence Berkeley National Laboratory, Berkeley, CA 94720

OGessner@lbl.gov

Program Scope: Intramolecular and interfacial charge-transport mechanisms in novel molecular devices for sustainable energy solutions are studied on their natural timescales and with atomic specificity by means of a new class of ultrafast X-ray experiments. The central motivation is to derive an accurate description, not only of the complex electronic structure that emerges from extended molecular and interfacial assemblies, but in particular of the dramatic changes in these electronic structures that, by definition, have to occur in order to enable, for example, long-range charge transfer and/or catalytic function. The combination of different X-ray techniques will provide the capability to test molecular level models of intramolecular and interfacial charge migration by a new set of molecular level probes.

This new initiative has been enabled by an Early Career Research Program Award of the DOE Office of Science. Time-resolved inner shell spectroscopy and time-resolved near-edge coherent diffractive imaging (CDI) techniques are developed to study charge-transfer processes in complex systems in real-time and with sub-micron spatial resolution. The program builds on a concerted effort of accelerator-based experiments at the Linac Coherent Light Source (LCLS) and the Advanced Light Source (ALS), and laboratory-based experiments driven by femtosecond high-harmonic generation (HHG) light sources.

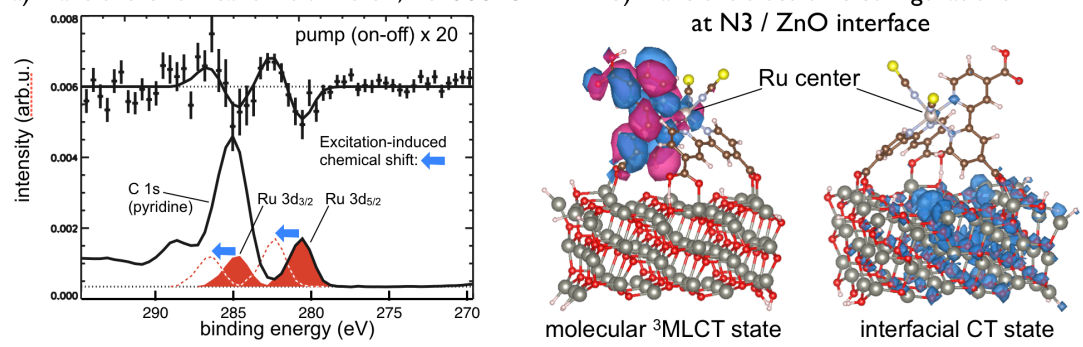

Fig. 1: Studying electronic dynamics at the interface between N3 dye molecules and ZnO semiconductor substrates. a) Transient chemical shift of the Ru $3d_{3/2,5/2}$ inner-shell levels detected by femtosecond time-resolved XPS at the LCLS. b) Ab-initio description of competing models for transient interfacial electron configurations using DFT calculations.

Recent Progress and Future Plans: A critical link between the experimental and theory efforts within the program has been established. The synthesis of femtosecond time-resolved X-ray photoelectron spectroscopy (tr-XPS) data recorded at the LCLS and state-of-the-art density function theory (DFT) calculations leads to new insights into the transient electronic configurations at the interface between a molecular dye (N3) and a nanocrystalline ZnO substrate. This type of interface is at the heart of emerging renewable energy technologies. The molecular dye acts as an antenna for visible/sun light and the relative alignment between the adsorbate and substrate energy levels facilitates efficient conversion of the absorbed photon energy into separate charge carriers.

The LCLS data provide an element-specific spectroscopic fingerprint of the transient valence electron configuration in the vicinity of the central Ru atom of the dye within the first picosecond after photoexcitation (Fig. 1a). A characteristic transient chemical shift of the Ru $3d_{3/2,5/2}$ doublet by 2 eV to higher binding energies is consistent with the removal of electron density in the central region of the dye induced by optical excitation. Ab-initio descriptions of competing models for the photoinduced transient electron configurations have been developed (Fig. 1b). The calculations have been extended to make the crucial link between the valence electron configurations and their inner-shell spectroscopic signatures. The completion of the calculations is imminent and current results show strong indications that the combined experimental/theory effort will provide new evidence in the decade-old controversy about the fundamental mechanisms that underlie the performance differences of ZnO and TiO_2 based dye-sensitized interfaces.

Significant progress has been made toward the implementation of picosecond time-resolved inner-shell spectroscopy techniques at the ALS that will complement the femtosecond domain studies at the LCLS. A new high-power picosecond laser system is currently commissioned for optical-pump/X-ray probe XPS experiments. First transient XPS spectra have been recorded indicating a sub-100 ps temporal resolution that will grant access to transient electronic configurations at molecule-semiconductor interfaces well below the critical time-scale for electron-hole recombination (~ns-ms). The high average power of the industrial-grade laser system and the built-in harmonics unit will provide the unique capability to perform picosecond time-resolved XPS studies in the principal excitation regime of photovoltaic systems with up to ~MHz repetition rates.

A new effort has been launched to extend the range of time-domain X-ray spectroscopy experiments on photoinduced interfacial charge transfer processes from isolated molecule-semiconductor interfaces to application-like assemblies of working photovoltaic and photoelectrochemical devices. The ultimate goal is to study key interfacial electronic processes in real-time and under real-world conditions with the superb element specificity of inner-shell transitions. The new initiative will take full advantage of the existing ambient-pressure XPS and *in-situ* XES/XAS capabilities at the ALS and translate them into the time-domain.

Many chemically engineered devices are marked by heterogeneous designs with nano- to micron-scale regions that differ in their electronic and chemical functions. Femtosecond X-ray CDI techniques may provide a route to monitor fundamental electronic processes

in molecular electronic devices simultaneously in space and time, while preserving the element-specific contrast mechanisms of inner-shell transitions. The near-edge CDI project of this program explores the potential of HHG-driven CDI setups to perform ultrafast imaging experiments with a particular emphasis on the capability to tune the imaging photon flux across characteristic inner-shell absorption edges. A recently constructed energy-tunable CDI setup is currently modified to optimize key characteristics such as the spatiotemporal coherence and, in particular, the energy-tunable XUV photon fluence at the sample for time-resolved imaging studies.

Publications

1. Andrey Shavorskiy, Amy Cordones, Josh Vura-Weis, Katrin Siefermann, Daniel Slaughter, Felix Sturm, Fabian Weise, Matthew Strader, Hana Cho, Ming-Fu Lin, Camila Bacellar, Champak Khurmi, Marcus Hertlein, Jinghua Guo, Hendrik Bluhm, Tolek Tyliszczak, David Prendergast, Giacomo Coslovich, Joseph Robinson, Robert A. Kaindl, Robert W. Schoenlein, Ali Belkacem, Thorsten Weber, Daniel M. Neumark, Stephen R. Leone, Dennis Nordlund, Hirohito Ogasawara, Anders R. Nilsson, Oleg Krupin, Joshua J. Turner, William F. Schlotter, Michael R. Holmes, Philip A. Heimann, Marc Messerschmidt, Michael P. Minitti, Martin Beye, Sheraz Gul, Jin Z. Zhang, Nils Huse, and Oliver Gessner, "Time-Resolved X-Ray Photoelectron Spectroscopy Techniques for Real-Time Studies of Interfacial Charge Transfer Dynamics", Application of Accelerators in Research and Industry, AIP Conf. Proc. 1525, **475** (2013).

Early Career Project: The Multiconfiguration Time-Dependent Hartree-Fock Method for Interactions of Molecules with Ultrafast X-Ray and Strong Laser Pulses

Daniel J. Haxton
Lawrence Berkeley National Laboratory MS2R0100
1 Cyclotron Road, MS 2R0100
Berkeley, CA 94720
djhaxton@lbl.gov

Program scope / definition

This project is based upon a computer code for solving the nonrelativistic Schrodinger equation for a small molecule, subject to arbitrarily strong laser fields, nonperturbatively. It is ab initio and includes correlated wave functions. The code was begun before the start of this project. It presently treats atoms and diatomic molecules, with an initial implementation of fully nonadiabatic motion in the internuclear degree of freedom.

The final goal of the project is a fully ab initio nonadiabatic treatment of a polyatomic molecules, electronic and nuclear degrees of freedom.

Several applications of the method will be pursued along the way, making use of the capabilities already implemented, and as additional capabilities are added.

Recent progress

Because of the synergy between this and another project for which I am funded, significant progress has already been made.

1) The necessary working equations for the Cartesian grid basis function treatment using the Discrete Variable Representation has been derived. This is a very important development, necessary for the polyatomic treatment.

The method performs very well. Sinc basis functions are used in the x, y, and z directions. The kinetic energy is computed exactly. An "approximation" to the one and two electron matrix elements is employed which renders their matrix elements diagonal in the sinc function basis. This method was originally derived using spherical polar coordinates and its extension to Cartesian coordinates has been a long range goal of mine. The crux is to find an expression for the inverse of an infinitely big matrix (the 3D kinetic energy matrix). This inverse gives the one and two electron matrix elements.

A) The exact mathematical form of the inverse would be nice to have. I still don't have it, but I found an extremely good way to approximate it.

B) The original method for interpolating the one body operator, as the nucleus moves within the Cartesian electronic grid, did not work with this basis, for some reason. It gave unphysical corrugations in the born oppenheimer eigenvalues. An alternate expression was

derived that does not suffer from this (and that may allow exotic calculations using coordinate scaling)

I find the performance of the method shocking. The ground state energy of Helium can be calculated to be -2.87 atomic units, double zeta quality (the exact is -2.903) using a grid spacing of 0.4 atomic units. On the to-do list is to calculate the variational result in this basis, which I expect to be a random number, due to the massive cusp error that the wave function, comprised of sinc functions, must have.

2) An implementation allowing restricted configuration spaces – that is, not full configuration interaction, spaces like those used in quantum chemistry like configuration interaction with singles and doubles (CISD) – is necessary in order to make the method scalable to bigger molecules. One way of doing this (in which the one electron density matrix is kept block diagonal) was already done before the project. I have finally correctly programmed up another way of doing it, arguably the best way, in which the variational principle that underlies the working equation is maintained. This paper will be submitted soon. Below I show a comparison between the method based on the variational principle (dots), the method based on density matrices (yellow), and the "dumb" way in which the working equations for full configuration interaction are used without accounting for the restricted configuration spaces (exes and black line). The figure shows the error, the Hilbert space angle between the full CI result and the restricted configuration result. As you can see, both methods produce far less error than the dumb way. The density matrix method, while by definition leading to more short term error than the variational method, does better in the long run, for this problem (this is beryllium in a very short very strong 100eV pulse)

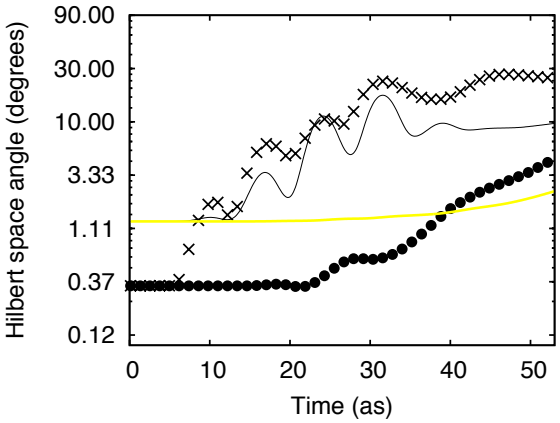

3) We have submitted to PRL our first paper on stimulated X-ray Raman within the NO molecule. I proposed a long line of research based on such transitions in NO and this is the first of that. Below I show the convergence of some results: this is the emission and absorption spectrum calculated, with varying numbers of orbitals. The result is essentially converged with 11 or 12 orbitals. Such convergence with a laser pulse of very high intensity (10^{18} watts per square centimeter) is a very promising result.

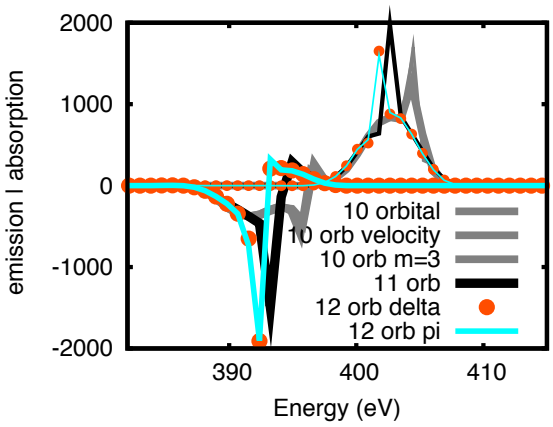

Future plans

Most of the project remains to be done, obviously. Right now I am doing a lot of code development, re-writing a bunch of stuff that needs to be rewritten before I hire any postdocs. The code needs to be in better form, in order for postdocs to be able to work with it efficiently.

Once that is done, we will proceed on other aspects of the proposal.

1) With the code ready to be added to, the implementation of nonadiabatic rotational motion for a diatomic molecule should be straightforward. We will proceed to study processes like light induced conical intersections.

2) Along with this, we need to change the prolate spheroidal coordinate system in a specific way so that it performs better within the MCTHDF ansatz. This will require quite a bit of algebra and code developm

3) Splitting of the orbital propagation. This is a long range, ambitious goal. In order for the method to be truly scalable to large molecules, the orbitals need to be propagated independently over short time steps. Several ways of doing this will be tried.

The applications that will be pursued include

1) An extensive study of NO, and stimulated X ray raman transitions in other molecules
2) Control of x ray processes in strong fields
3) Nonadiabatic processes in strong fields

PULSE Ultrafast Chemical Science Program

Philip Bucksbaum (spokesperson), David Reis, Kelly Gaffney, Markus Guehr, and Todd Martinez
Chemical Science Division, SLAC National Accelerator Laboratory, Menlo Park, CA

Science objectives: The PULSE Ultrafast Chemical Science Program at SLAC focuses on ultrafast chemical physics research enabled by LCLS, the world's first hard x-ray free-electron laser. Our overarching goal is to establish research at SLAC that makes optimal use of this new SLAC tool for fundamental discoveries and new insights in ultrafast science. The on-site presence of LCLS with its facilitating connections to our research is one of two distinguishing advantages of this program within the AMOS portfolio. Our other distinguishing advantage is our close connection to Stanford University maintained through the **Stanford PULSE Institute**. These help to keep us competitive on a national and international level.

Current and future progress: The specific progress of our individual research tasks will be laid out in separate abstracts. The successes of our program depends greatly on the cooperative and collaborative synergy made possible by our coordination and co-location in the PULSE Institute at SLAC. Here we will summarize the cross-cutting themes of our center. There are three major themes in the current program, which remain unchanged from last year**:**

• Imaging on the nanoscale in space and the femtoscale in time. Microscopy at its most essential level in both space and time is paramount to the BES mission to control matter. Non-periodic nano-structures and ultrafast timescales dominate the workings of biology and chemistry. To understand and control function we therefore must first observe structure and motion on these scales.

LCLS is a revolutionary x-ray source for investigations on the nanoscale, and our largest subtask is devoted to developing science using coherent x-ray imaging techniques at this and other x-ray free electron lasers. This work includes nanocrystal imaging on the few-Angstrom scale; nonperiodic imaging of single biomolecules; cell imaging; and imaging of aerosols.

Imaging of still smaller structures such as small molecules use other techniques, such as particle fragment velocity maps, and electron holography. Here we are exploring fundamental energy-relevant processes such as photo-induced isomerization, dissociation, and x-ray damage, using optical and x-ray probes, and a combination of linear and nonlinear spectroscopic methods.

Time scale measurements are a particular challenge at the femtosecond scale, but this is where chemistry happens and therefore we devote much of our effort to this range. Simple- "pump-probe" spectroscopy at visible and infrared wavelengths must be extended to the soft and hard x-ray range, and to new sources such as FELs.

• Light conversion chemistry. Light from the sun is the primary source of energy on earth, and so we are exploring its conversion to electron motion and then to chemical bonds. Some molecules are particularly adept at this conversion and we would like to understand how they work. For example, we are especially interested in the process of photocatalysis within coordination complexes and similar materials.

Energy conversion is initiated by charge separation, and we know that the charge distribution of the electron and hole, as well as the presence of low energy ligand field excited states greatly influence the lifetime of optically generated charge transfer excited states. Still, the detailed mechanism for the excited state quenching remains unclear. New methods of linear and nonlinear spectroscopy, and especially x-ray spectroscopy involving short-pulse FEL's, can help provide the answer.

An equally important problem is the protection of some chemical bonds, particularly in biology, from destruction in the presence of ultraviolet sunlight. Photoprotection is also an ultrafast process involving

charge transfer, and so these new techniques such as ultrafast x-ray absorption and Auger emission can show how critical bonds are protected.

The incorporation of theory within this program is critical for rapid progress in light conversion chemistry. The theory group helps us to focus our efforts in areas of greatest impact.

• **The eV scale in time, space, and field strength.** This is the fundamental scale that determines structure and dynamics of electrons in molecules, and motivates advances in sub-femtosecond time-resolution and Angstrom spatial resolution in theory and experiments. To achieve an adequate view of the molecular realm with at this level, we must interrogate atoms with fields comparable to Coulomb binding fields, and on time scales set by the electronic energy splittings in atoms.

One method to reach this scale is through high harmonic generation. We plan to extend our use of this technique to higher energies and with greater control over the target molecule, to interrogate the detailed motion of the electrons. We are particularly interested in coupled motion of multiple electrons, that goes beyond the "single active electron" approximation that has dominated thinking about strong field laser-atom physics. New theoretical approaches are also required for this, and we are tackling these as well.

LCLS is a source which is also capable of sub-femtosecond or few femtosecond pulses, and these have the unique property of wavelengths short enough to reach the most deeply bound electrons in first and second row atoms. Through the use of novel methods such as low bunch charge, double-slotted spoilers, strong laser fields, and novel data sorting methods, as well as future methods such as self-seeding, we will incorporate LCLS fully as a tool for sub-femtosecond spectroscopy.

Management structure: This research program is managed within the the Chemical Sciences Division, SLAC Photon Sciences Directorate. The current Division Director is Jens Norskov. Major changes in the organization at SLAC in the past year include a new Director and Associate Laboratory Director.

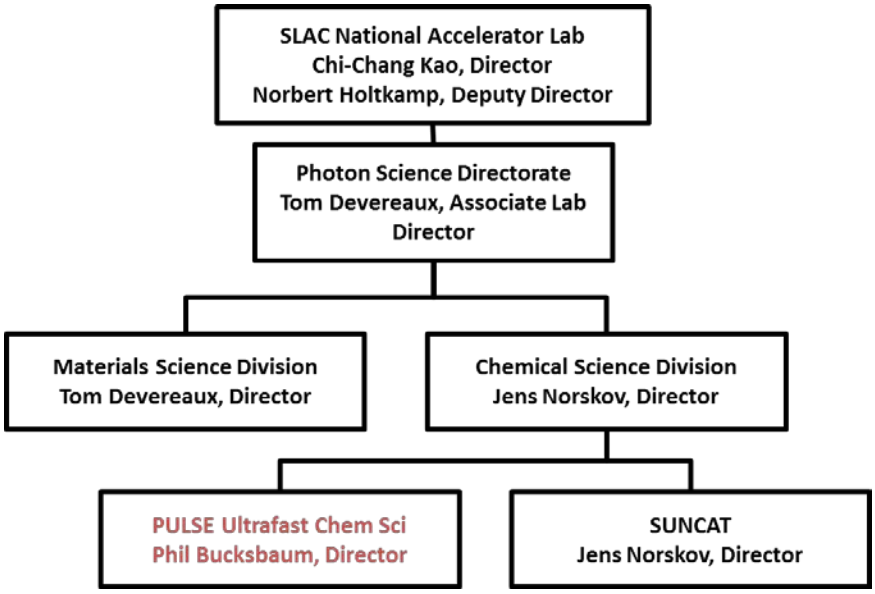

Figure 1: Partial organization chart for SLAC, showing the relation of the PULSE Ultrafast Chemical Science Program to other units with close research ties.

The Ultrafast Chemical Science program is the primary source of research funds and SLAC salary for five Principal Investigators, who are responsible for proposing and carrying out this science:

Professor Philip Bucksbaum, AMO Physics, Program Spokesperson;
Associate Professor David Reis, Nonlinear x-ray science, Deputy Spokesperson;
Assistant Professor Kelly Gaffney, Physical Chemistry;

Professor Todd Martinez, theory;
Senior Research Scientist Dr. Markus Guehr, AMO science.

In addition to these five, we also have a vacancy recently created by the departure of Mike Bogan, who directed the subtask on nonperiodic imaging. Three of our six PIs perform all of their SLAC effort in this program. Dr. Guehr splits his effort with his Early Career FWP, which is also managed within the Chemical Sciences Division. Prof. Reis splits his SLAC effort with a SIMES program, located in the Directorate's Materials Science Division. (His total SLAC effort is three-quarters time because of his one-quarter calendar year appointment with Stanford).

Subtasks: These six key personnel are responsible for six subtasks, which represent six different areas of expertise:

1. UTS: Ultrafast Theory and Simulation (Martinez)
2. ATO: Attoscience (Bucksbaum, Guehr)
3. SPC: Ultrafast Chemistry (Gaffney)
4. NPI: Non-periodic X-ray Imaging (Vacant)
5. SFA: Strong Field AMO Physics (Bucksbaum)
6. NLX: Strong Field and Nonlinear X-ray Optical Science (Reis)

The broad backgrounds of our PIs provide needed synergy for effective collaborations in cross-disciplinary projects.

Support operations (finance, HR, safety, purchasing, travel) are directed by the Photon Science Associate Laboratory Director and the Chemical Sciences Director and their staff. They provide oversight and delegate the work to appropriate offices in the SLAC Operations Directorate or to the staff of the Stanford PULSE Institute.

Connections to other units within the SLAC organizational structure: Close collaborations are maintained with the Science R&D Division within the LCLS Directorate; the Materials Science Division (SIMES) within the Photon Science Directorate; SSRL; and the SUNCAT Center within our own Chemical Sciences Division, as shown in figure 1. Our colocation with these facilities and research organizations at SLAC greatly aids collaboration.

Other important connections: The PIs have many separate affiliations with other Stanford University research and academic units: Most especially, all members of this program are members of the Stanford PULSE Institute. In addition, several are affiliated with the SIMES Institute, Bio-X, the Ginzton Laboratory, and the Departments of Chemistry, Physics, and Applied Physics.

Laser Research Coordination: Within the past year we have helped to start to organize a new coordinated laser research activity at SLAC and Stanford, in order to make more effective use of some of our state-of-the-art capabilities, both within DOE and in the larger international community. This activity has acquired special significance as plans for LCLS-II move forward, since this upgrade will benefit greatly from close coordination between laser-based research and x-ray science.

We also have collaborative connections to other outside research labs, including DESY, the Lawrence Berkeley Laboratory, the Center for Free Electron Lasers (CFEL) in Hamburg, and BES funded groups at the University of Michigan, the Ohio State University, Western Michigan University, LSU, Northwestern, and the University of Wisconsin Milwaukee.

Connections to LCLS: The transfer of knowledge and expertise to and from LCLS is extremely fluid and critical to our success. Much of our research creates benefits for LCLS by providing new research methods and research results, and in addition there are several more direct transfers of our research product to help LCLS:

- New in 2014, the PULSE Institute will take as new members two LCLS staff scientists: Ryan Coffee and Christoph Bostedt. They will both continue to have user support duties and be managed through LCLS, but will spend 25% of their effort building in-house science in PULSE. We anticipate that this will encourage even closer collaboration between scientists in the Photon Science and LCLS Directorates at SLAC, and that these individuals will help us build our science portfolio in the future in AMOS and the larger Chemical Sciences Division of DOE.
- Some of our graduate students provide user support through the LCLS laser group and various end station groups, and receive salary supplements for this work.
- We have assisted in the development of timing tools currently in use at LCLS.
- Some of our postdocs and students have transferred to permanent staff positions at LCLS.
- We connect LCLS to the Stanford PULSE Institute, since all of our staff are members of PULSE, and LCLS Director Jo Stohr is a member of PULSE as well. PULSE assists LCLS in several direct ways:
    - PULSE has helped LCLS to institute a Graduate Fellowship program, and PULSE manages LCLS graduate student campus appointments.
    - PULSE conducts an annual Ultrafast X-ray Summer School to train students and postdocs about LCLS science opportunities.

Advisory committee. The Ultrafast Chemical Science program receives valuable external advice from the External Advisory Board of the Stanford PULSE Institute. This board of advisors serves the PULSE Institute Director and meets annually. It reports to the PULSE Director and to the Stanford Dean of Research. The reports have also been forwarded to the SLAC Director, the ALD for Photon Science, and to the SLAC Science Policy Committee at their request.

Educational programs and outreach activities. We have an extremely active outreach and visitors program through our affiliation with the Stanford PULSE Institute. PULSE maintains a Stanford-funded visitors program, a website (ultrafast.stanford.edu) as well as an annual Ultrafast X-ray Summer School. This school, which was founded by the PIs of this program in 2006, continues to be a main mechanism for expanding the research community interested in using x-ray free electron lasers for their research. In 2011 we teamed up with CFEL in Hamburg and began to rotate the school between DESY and SLAC in alternate years. The school has received continued strong supported from BES, Stanford, and from CFEL. The school will be held at SLAC in 2014 and 2016.

Photographs from six Ultrafast X-ray Summer Schools that have been held at SLAC and organized by this program.

ATO: Attoscience

Principle Investigator: *Philip H. Bucksbaum, Markus Guehr (co-PI)*

Objective and Scope

We seek to observe and control sub-femtosecond electron dynamics in atoms and small molecules. Our discovery that multiple electron orbitals can contribute to HHG in molecules is now employed to investigate electronic structural symmetries and subfemtosecond dynamics in field-ionized molecules. It now appears likely that multiple orbital involvement in strong field processes ATI and HHG is the rule, not the exception.

Recent Progress

High harmonic generation from asymmetric top molecules. *(Collaboration with T. Seideman, A. Saenz, and T. Martinez)* Quantum asymmetric top systems comprise the widest and most general class of molecules, but are difficult to explore in strong field physics. Most progress in HHG has been limited to atoms and high symmetry diatomic molecules or symmetric tops, The dependence of HHG on molecular orientation in simple linear molecules shows how different molecular orbitals participate in this highly nonlinear process. This provides strong motivation for extending these studies to asymmetric tops. We have now introduced a method to extract axis-dependent information from asymmetric tops. We use the rotational revival structure of an impulsively excited molecule to decompose the angular contributions of HHG emission.

Our first investigation of structure dependence of HHG in an asymmetric top molecule is SO_2. This molecule has many compelling features, such as several molecular orbitals with different symmetries within a few eV of the highest occupied orbital (HOMO). It also has several unoccupied excited bound states that have been proposed for HHG studies of intramolecular dynamics. Our experimental scheme employs two pulses: one to deliver the impulse to the molecular gas, and one to produce HHG from the resulting rotational coherent states. We vary the time delay between the two pulses to record the variations of HHG during transient alignment. Since the SO_2 molecules are aligned with respect to the field polarization vector at a molecular revival, the harmonic signal is sensitive to the molecular structure along the aligned axis.

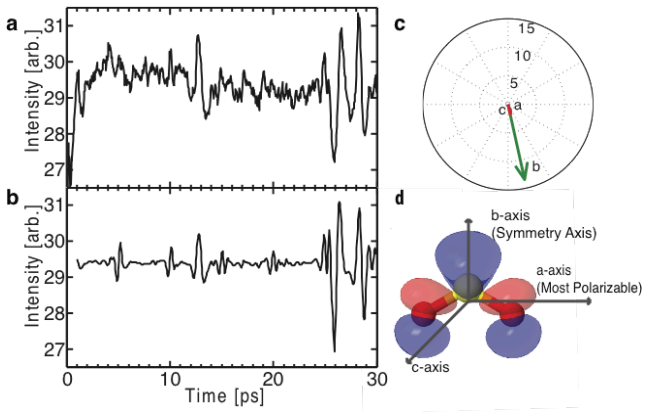

Fig. 1: (a) Data for high harmonic 19 (29.5 eV) for the first 30 ps following alignment of SO_2, and asymmetric top. All prolate-type asymmetric top revivals can be seen, including partial revivals and multiple revivals. (b) Best-fit theory curve fits all 3 single-axis alignment patterns to the data. The fit coefficients yield the orientational information corresponding to the high harmonic emission along each of the three molecular axes. (c) A phasor plot shows the magnitude and direction of HHG emission as extracted by this analysis. (d) An isosurface representation of the HOMO of SO_2, shown in red and blue to encode the phase, overlaid with a ball and stick model. We see highest electron density in the b-axis direction, in confirmation of our analysis.

The experimental signal is shown in Fig. 1a. We observe fractional revivals and multiple revivals to a sensitivity seen by high harmonic generation only in linear molecules in previous work. A complete set of asymmetric top revivals has not previously been recorded together in one trace. This shows the extreme sensitivity of HHG to small features in the alignment distribution.

To aid in the decomposition, we make use of calculations of the single-axis alignment patterns for SO_2, provided by the group of T. Seidemann. The single-axis alignment patterns are the set of molecular

alignments as viewed from a particular axis of the molecule. The pattern is the expectation value $\langle\cos^2\theta_i\rangle$ in the rotational wavepacket, where θ_i is the angle between the polarization direction of the HHG pulse and the molecular axis *i*. There is no simple correspondence between a particular axis and a particular revival feature. The molecular alignment is calculated with respect to all three molecular axes, a, b, and c, which are defined in Fig. 1d.

We can use the single-axis alignment patterns as basis vectors along which the data is decomposed. To extract the harmonic signal along each of the principal axes of the molecule, we combine the alignment patterns to fit the data to the form $\left|\sum_j c_j f_j\right|^2$, where f_j are the three alignment patterns and the $c_j = |c_j| e^{i\theta_j}$ are complex coefficients whose amplitudes $c_j = |c_j|$ and phases θ_j serve as six Nelder-Mead fit parameters.

The high contribution to harmonic emission from the b-axis shown in Fig. 1 could be due to either enhanced field ionization or enhanced recombination along this axis, according to the standard recollision mode. To provide a check for the method, we modeled the energy- and angle-dependent recombination dipole by calculating the VUV photoemission cross section of SO_2 in the molecular frame. We find that recombination is a major contribution to the magnitude of harmonic emission along different molecular axes. At our signal energy of 29.5 eV there is a large recombination probability along the molecular symmetry axis, but much less recombination along the other two axes.

We expect that alignment decomposition will be useful for other studies of angle-dependent molecular structure and dynamics as well.

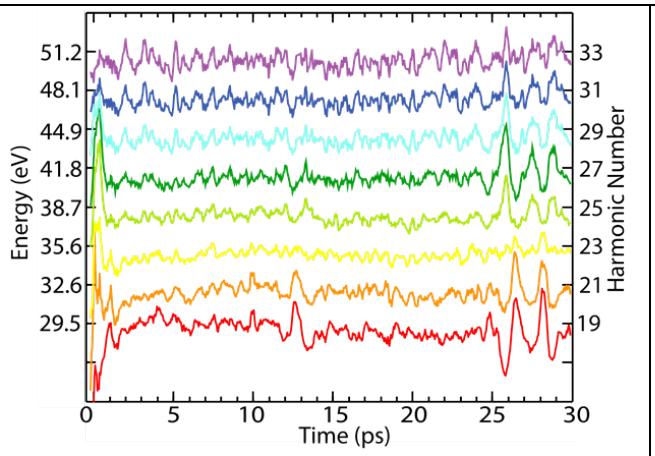

Fig. 2: Data from the 19th-33rd harmonic in SO_2 over the first 30 ps. At the full J-type and C-type rotational revivals of the molecule at 26 ps and 28 ps and at the half J-type rotational revival of the molecule at 13 ps, harmonic 19 and 27 display a harmonic modulation with the opposite sign in Fig. 2. At times when harmonic 19 is enhanced, harmonic 27 is suppressed. The full harmonic spectrum shows that this reversal in HHG efficiency happens gradually, over several harmonics. The modulation of the sign happens gradually, with a dampening of harmonic emission at the 23rd harmonic.

The full set of harmonics are shown in Fig. 2. At the full J-type and C-type rotational revivals of the molecule at 26 ps and 28 ps and at the half J-type rotational revival of the molecule at 13 ps, harmonic 19 and 27 display a harmonic modulation with the opposite sign in Fig. 2. At times when harmonic 19 is enhanced, harmonic 27 is suppressed. The full harmonic spectrum shows that this reversal in HHG efficiency happens gradually, over several harmonics. We quantify this effect by employing the alignment decomposition technique, which extracts the amplitude and phase of the HHG emission. Results show that different inner-valence orbitals are largely responsible for the higher harmonics in SO_2.

HHG dynamical studies of H_2O

In HHG, fast ionization of the molecular orbital from occupied valence orbitals launches a vibrational wave packet on multiple ionic electron potential energy surfaces. The harmonic light is emitted as the returning electron recombines with the molecular ion, thereby forming a molecule in its electronic and vibrational ground state. The efficiency of this process is governed by the spatial overlap of the ionic state nuclear wave

packet and the neutral vibrational ground state. As the ionic state nuclear wave packet moves, it loses overlap with the ground state. The nuclear wave packet for the heavy isotope is slow, thus maintaining a stronger overlap than the lighter, faster isotope. This gives a larger harmonic yield for the heavier isotope. The timescale of the nuclear motion is mapped onto the energy of different harmonics as shown by the Marangos group in 2006.

In water, the HOMO-1 ionization results in a fast nuclear motion since it is strongly repulsive. We have shown that the water HHG depends on the isotope, indicating that nuclear dynamics is imprinted on the harmonic yield. We deduce that a considerable amount of ionization stems from the lower lying HOMO-1 orbital, since only that ionic state produces a difference in harmonics from D_2O and H_2O.

We are currently working on extending this technique. Up to now, only so called short trajectories have been used to determine the HOMO/HOMO-1 ratio. We are extending the scheme to electron trajectories with much longer recollision times. One one hand, this improves the observable time window for the harmonic spectroscopy. On the other hand, this also increases the sensitivity for isotope differences, since the nuclear wavepackets for different isotopes will be acquiring a larger difference at longer propagation times.

Future Progress

We continue to extend the harmonic spectroscopy on asymmetric top molecules. We are currently implementing a UV preexcitation beam that will promote molecular population of SO_2 form the electronic ground state to covalent excited states. On those excited states, the molecule will undergo rapid electronic symmetry changes as a consequence of a conical intersection passage. We expect that the harmonic spectrum will contain information about the symmetry changes that reflect the conical intersection. Our past studies of transient gratings for the extreme UV domain and the alignment studies reported above provide the basis for contrast enhancement in the SO_2 experiments.

For water, we will try to implement alignment schemes similar to SO_2. We have also constructed THz alignment tools to take advantage of the dipole moment in water.

We will continue to be part and also take leadership in LCLS experiments in the future. Our strong contribution in the nucleobase photoprotection LCLS experiments gives us credibility in the field.

Publications

Bucksbaum, P. H. (2013). "Ultrafast quantum control in atoms and molecules." Ultrafast nonlinear optics, Springer: 105-128.

Bucksbaum, P. H., J. Farrell, L. Spector, B. McFarland, S. Wang and M. Guehr (2012). "High harmonic probes of inner electron sub-cycle dynamics in molecules." Laser Science, Optical Society of America.

Cryan, J., J. Glownia, J. Andreasson, A. Belkacem, N. Berrah, C. Blaga, C. Bostedt, J. Bozek, N. Cherepkov and L. DiMauro (2012). "Molecular frame auger electron energy spectrum from n2." Journal of Physics B: Atomic, Molecular and Optical Physics 45(5): 055601.

Doumy, G., C. Roedig, S.-K. Son, C. I. Blaga, A. DiChiara, R. Santra, N. Berrah, C. Bostedt, J. Bozek and P. Bucksbaum (2011). "Nonlinear atomic response to intense ultrashort x rays." Physical review letters 106(8): 083002.

Fang, L., T. Osipov, B. Murphy, F. Tarantelli, E. Kukk, J. Cryan, M. Glownia, P. Bucksbaum, R. Coffee and M. Chen (2012). "Multiphoton ionization as a clock to reveal molecular dynamics with intense short x-ray free electron laser pulses." Physical review letters 109(26): 263001.

Farrell, J., B. McFarland, N. Berrah, C. Bostedt, J. Bozek, P. Bucksbaum, R. Coffee, J. Cryan, L. Fang and R. Feifel (2012). "Ultrafast x-ray probe of nucleobase photoprotection." Quantum Electronics and Laser Science Conference, Optical Society of America.

Farrell, J., B. K. McFarland, L. S. Spector, P. H. Bucksbaum and M. Guehr (2011). "Isotope effect in the high harmonics of water." Quantum Electronics and Laser Science Conference, Optical Society of America.

Farrell, J., L. Spector, B. McFarland, P. Bucksbaum, M. Gühr, M. Gaarde and K. Schafer (2011). "Influence of phase matching on the cooper minimum in ar high-order harmonic spectra." Physical Review A 83(2): 023420.

Farrell, J. P., S. Petretti, J. Foerster, B. K. McFarland, L. S. Spector, Y. Vanne, P. Decleva, P. H. Bucksbaum, A. Saenz and M. Guehr (2011). "Ionic state superposition in the strong field ionization of water." Laser Science, Optical Society of America.

Farrell, J. P., S. Petretti, J. Förster, B. K. McFarland, L. S. Spector, Y. V. Vanne, P. Decleva, P. H. Bucksbaum, A. Saenz and M. Gühr (2011). "Strong field ionization to multiple electronic states in water." Physical Review Letters 107(8): 083001.

M. Gühr, “Perspective article: Getting molecular electrons into motion,” Science, 335, 1314 (2012)

McFarland, B., J. Farrell, N. Berrah, C. Bostedt, J. Bozek, P. Bucksbaum, R. Coffee, J. Cryan, L. Fang and R. Feifel (2013). "Probing nucleobase photoprotection with soft x-rays." EPJ Web of Conferences 41, 07004 (2013) 41: 07004.

McFarland, B., J. Farrell, N. Berrah, C. Bostedt, J. Bozek, P. H. Bucksbaum, R. Coffee, J. Cryan, L. Fang and R. Feifel (2012). "Ultrafast nucleobase photoprotection probed by soft x-rays." Laser Science, Optical Society of America.

McFarland, B., J. Farrell, S. Miyabe, F. Tarantelli, A. Aguilar, N. Berrah, C. Bostedt, J. Bozek, P. Bucksbaum and J. Castagna (2013). "Delayed ultrafast x-ray auger probing (duxap) of nucleobase ultraviolet photoprotection." arXiv preprint arXiv:1301.3104.

B. K. McFarland, J. P. Farrell, S. Miyabe, F. Tarantelli, A. Aguilar, N. Berrah, C. Bostedt, J. Bozek, P.H. Bucksbaum, J. C. Castagna, R. Coffee, J. Cryan, L. Fang, R. Feifel, K. Gaffney, J. Glownia, T. Martinez, M. Mucke, B. Murphy, A. Natan, T. Osipov, V . Petrovic, S. Schorb, Th. Schultz, L. Spector, M. Swiggers, I. Tenney, S. Wang, W. White, J. White, M. Gühr, “Experimental strategies for optical pump- soft x-ray probe measurements at the LCLS“submitted (2013)

Petrovic, V. S., S. Schorb, J. Kim, J. White, J. P. Cryan, J. M. Glownia, L. Zipp, D. Broege, S. Miyabe and H. Tao (2012). "High sensitivity of strong-field multiple ionization to conical intersections." arXiv preprint arXiv:1212.3728.

Petrović, V. S., M. Siano, J. L. White, N. Berrah, C. Bostedt, J. D. Bozek, D. Broege, M. Chalfin, R. N. Coffee and J. Cryan (2012). "Transient x-ray fragmentation: Probing a prototypical photoinduced ring opening." Physical Review Letters 108(25): 253006.

Spector, L., S. Wang, J. Farrell, B. McFarland, M. Guehr, P. Bucksbaum, M. Artamonov and T. Seideman (2012). "Field-free asymmetric top alignment and rotational revivals using high harmonic generation." CLEO: Applications and Technology, Optical Society of America.

Spector, L. S., M. Artamonov, S. Miyabe, T. Martinez, T. Seideman, M. Guehr and P. H. Bucksbaum (2012). "Quantified angular contributions for high harmonic emission of molecules in three dimensions." arXiv preprint arXiv:1207.2517.

Spector, L. S., J. P. Farrell, B. K. McFarland, P. H. Bucksbaum, M. B. Gaarde, K. J. Schafer and M. Guehr (2011). "Influence of phase matching of the cooper minimum in argon high harmonic spectra." Quantum Electronics and Laser Science Conference, Optical Society of America.

Spector, L. S., S. Miyabe, A. Magana, S. Petretti, P. Decleva, T. Martinez, A. Saenz, M. Guehr and P. H. Bucksbaum (2013). "Multiple orbital contributions to molecular high-harmonic generation in an asymmetric top." arXiv preprint arXiv:1308.3733.

NLX: Ultrafast X-ray Optical Science and Strong Field Control

David A. Reis*, Shambhu Ghimire

Stanford PULSE Institute
SLAC National Accelerator Laboratory, MS 59
2575 Sand Hill Rd.
Menlo Park, CA 94025

*dreis@slac.stanford.edu

Program Scope:

The goal of this subtask in the Ultrafast Chemical Sciences FWP at SLAC is to understand and control the fundamental processes that occur during the interaction of ultrafast and ultra-strong electromagnetic fields with matter, in these two important extreme and relatively unexplored regions of the electromagnetic spectrum. We are particularly interested in the discovery and development of fundamental ultrafast optical, coherent and nonlinear phenomena in the x-ray regime and investigation of the attosecond electronic response in dense optical media and its scaling with wavelength from THz to x-ray. We are focused on two major areas: (1) long-wavelength strong-field interactions in periodic media, including a detailed comparison of both the above an below threshold harmonics in gas and solid phase argon, exited state electronic structure, and the measurement and control of temporal coherence of high-order harmonics and (2) fundamental x-ray nonlinear optics including the measurement of two-photon inner-shell absorption cross-sections and non-resonant third harmonic generation that is expected to show an enhanced nonlinearity due to periodicity.

Progress Report

Under DOE Chemical Sciences support, we explored several fundamental strong-field effects in periodic optical media over the past three years. Notably, we observed the first nonperturbative high-order harmonics in crystals [10]. The harmonics were generated by a strong mid-infrared laser field that drives coherent Bragg scattering of electrons from the lattice potential. The crystalline HHG differs from nonperiodic atomic and molecular HHG in several key ways, including linear scaling of the cutoff with field, relative insensitivity to elliptical polarization, odd only or odd and even harmonics depending on symmetry. We also predict that the energy of the high harmonic cutoff will be insensitivity to wavelength [4]. The process occurs in a regime of tunnel ionization where the field competes with the interatomic bonding, and the electron wavepacket becomes increasingly localized. Here we have also shown that the electronic properties are altered dramatically but only transiently in the presence of the field—as evidenced by strong photon assisted tunneling of near band gap light [11]—all with no permanent damage. This has implications for both understanding the high-field electronic structure of solids and the possibility of extending the cutoff and efficiency of high harmonics. We have also recently observed that the high-harmonics in solids in a general behavior, at least in insulating materials, and in particular, we have been investigating the effect in thin rare gas solid films grown on silicon-nitride substrates. We have measured the coherence

length of below-band gap harmonics and compared the intensity and polarization dependence of above and below gap harmonics in gaseous and solid Ar [3,8]

We also collaborated on many of the first experiments on LCLS as reported in last years' progress report. More recently, we have begun to study nonlinear coherent x-ray processes in the hard x-ray regime (both resonant and non-resonant). This has been made possible by the unprecedented peak-brightness of x-ray free electron lasers such as the LCLS at SLAC and more recently the SACLA free electron laser in Japan which allows for focused intensities in excess of 10^{20} W/cm^2 and thus fields in excess of kilovolts/Å. Nonetheless, because of the high frequency (short wavelength) of the x-rays, the field reverses sign on a sub-attosecond time-scale and the subsequent ponderomotive energy is negligible compared to the photon energy. Thus, high-field and nonlinear processes in the hard x-ray regime operate in a very different regime than ordinary optics. Nonetheless we have observed the first phase-matched x-ray second harmonic generation (in diamond at 10^{16} W/cm^2) [1], two-photon Compton scattering (in beryllium at 10^{19}–10^{20} W/cm^2) and have evidence for below threshold two-photon inner shell absorption in the hard x-ray regime (Zr 1s). Notably, we have discovered an anomalously large red-shift in the Compton scattering experiment, whereby the energy of the outgoing photon is substantially smaller than kinematically allowed for a free-electron process or even a simple extrapolation of the linear scattering including known bound and conduction electron contributions.

The next three years: We will continue our research along two lines. (1) long-wavelength strong-field interactions in periodic media, including a detailed comparison of both the above and below threshold harmonics in gas and solid phase argon, excited state electronic structure, and the measurement and control of temporal coherence of high-order harmonics and (2) fundamental x-ray nonlinear optics including experiments aimed at understanding the anomalous red-shift measured in the two-photon Compton scattering experiments as well as non-resonant third harmonic generation that is expected to show an enhanced nonlinearity due to periodicity.

References to publications of DOE sponsored research

2013

[1] S. Shwartz, M. Fuchs, J. B. Hastings, Y. Inubushi, D. A. Reis, M. Yabashi, and S. E. Harris. Second harmonic generation at x-ray wavelengths. In *Nonlinear Optics*. Optical Society of America, 2013.

[2] A. D. DiChiara, S. Ghmire, D. A. Reis, L. F. DiMauro, and P. Agostini. Strong-field and attosecond physics with mid-infrared lasers. In *Attosecond Physics*, pages 81–98. Springer, 2013.

[3] G. Ndabashimiye, S. Ghimire, D. Reis, and D. Nicholson. Measurement of coherence lengths of below threshold harmonics in solid argon. In *CLEO: 2013*, page QW1A.7. Optical Society of America, 2013.

2012

[4] S. Ghimire, A. D. DiChiara, E. Sistrunk, G. Ndabashimiye, U. B. Szafruga, A. Mohammad, P. Agostini, L. F. DiMauro, and D. A. Reis. Generation and propagation of high-order harmonics in crystals. *Physical Review A*, 85:043836, 2012.

[5] T. E. Glover, D. M. Fritz, M. Cammarata, T. K. Allison, S. Coh, J. M. Feldkamp, H. Lemke, D. Zhu, Y. Feng, R. N. Coffee, M. Fuchs, S. Ghimire, J. Chen, S. Shwartz, D. A. Reis, S. E. Harris, and J. B. Hastings. X-ray and optical wave mixing. *Nature*, 488(7413):603–608, 08 2012.

[6] J. P. Cryan, J. M. Glownia, J. Andreasson, A. Belkacem, N. Berrah, C. I. Blaga, C. Bostedt, J. Bozek, N. A. Cherepkov, L. F. DiMauro, L. Fang, O. Gessner, M. Gühr, J. Hajdu, M. P. Hertlein, M. Hoener, O. Kornilov, J. P. Marangos, A. M. March, B. K. McFarland, H. Merdji, M. Messerschmidt, V. S. Petrović, C. Raman, D. Ray, D. A. Reis, S. K. Semenov, M. Trigo, J. L. White, W. White, L. Young, P. H. Bucksbaum, and R. N. Coffee. Molecular frame auger electron energy spectrum from n 2. *Journal of Physics B: Atomic, Molecular and Optical Physics*, 45(5):055601, 2012.

[7] D. Reis. Strong-field nonperturbative effects in solids. In *42nd Annual Meeting of the APS Division of Atomic, Molecular and Optical Physics*, volume 56, page T4.00001, 2012.

[8] S. Ghimire, G. Ndabashimiye, and D. A. Reis. High-order harmonic generation in solid argon. In *CLEO: QELS-Fundamental Science*, page QW1F.1. Optical Society of America, 2012.

[9] F. Krasniqi, Y.-P. Zhong, D. A. Reis, M. Scholz, R. Hartmann, A. Hartmann, D. Rolles, A. Rudenko, S. W. Epp, L. Foucar, M. Trigo, M. Fuchs, D. M. Fritz, M. Cammarata, D. Zhu, H. Lemke, M. Braune, M. Ilchen, J. Larsson, S. Techert, L. Strüder, I. Schlichting, and J. Ullrich. Resonant x-ray emission spectroscopy with free electron lasers: Nonequilibrium electron dynamics in highly excited polar semiconductors. In *Research in Optical Sciences*, page IW1D.2. Optical Society of America, 2012.

2011

[10] S. Ghimire, A. D. DiChiara, E. Sistrunk, P. Agostini, L. F. DiMauro, and D. A. Reis. Observation of high-order harmonic generation in a bulk crystal. *Nature Physics*, 7(2):138–141, 2011.

[11] S. Ghimire, A. D. DiChiara, E. Sistrunk, U. B. Szafruga, P. Agostini, L. F. DiMauro, and D. A. Reis. Redshift in the optical absorption of ZnO single crystals in the presence of an intense midinfrared laser field. *Physical Review Letters*, 107:167407, 2011.

[12] G. Doumy, C. Roedig, S.-K. Son, C. I. Blaga, A. D. DiChiara, R. Santra, N. Berrah, C. Bostedt, J. D. Bozek, P. H. Bucksbaum, J. P. Cryan, L. Fang, S. Ghimire, J. M. Glownia, M. Hoener, E. P. Kanter, B. Krässig, M. Kuebel, M. Messerschmidt, G. G. Paulus, D. A. Reis, N. Rohringer, L. Young, P. Agostini, and L. F. DiMauro. Nonlinear atomic response to intense ultrashort x rays. *Phys. Rev. Lett.*, 106(8):083002, 2011.

[13] D. Daranciang, J. Goodfellow, M. Fuchs, H. Wen, S. Ghimire, D. A. Reis, H. Loos, A. S. Fisher, and A. M. Lindenberg. Single-cycle terahertz pulses with >0.2*V*/Å field amplitudes via coherent transition radiation. *Appl. Phys. Lett.*, 99(14):141117, 2011.

[14] E. P. Kanter, B. Krässig, Y. Li, A. M. March, P. Ho, N. Rohringer, R. Santra, S. H. Southworth, L. F. DiMauro, G. Doumy, C. A. Roedig, N. Berrah, L. Fang, M. Hoener, P. H. Bucksbaum, S. Ghimire, D. A. Reis, J. D. Bozek, C. Bostedt, M. Messerschmidt, and L. Young. Unveiling and driving hidden resonances with high-fluence, high-intensity x-ray pulses. *Phys. Rev. Lett.*, 107:233001, 2011.

[15] G. Doumy, S.-K. Son, C. Roedig, C. I. Blaga, A. D. DiChiara, R. Santra, C. Bostedt, J. Bozek, P. Bucksbaum, J. Cryan, J. M. Glownia, S. Ghimire, L. Fang, M. Hoener, N. Berrah, E. Kanter, B. Krässig, D. Reis, N. Rohringer, L. Young, P. Agostini, and L. DiMauro. Nonlinear atomic response to intense, ultrashort x rays. In *42nd Annual Meeting of the APS Division of Atomic, Molecular and Optical Physics*, volume 56, page L1.00060, 2011.

[16] A. DiChiara, S. Ghimire, C. Blaga, E. Sistrunk, E. Power, A. March, T. Miller, D. Reis, P. Agostini, and L. DiMauro. Scaling of high-order harmonic generation in the long wavelength limit of a strong laser field. *Selected Topics in Quantum Electronics, IEEE Journal of*, PP(99), 2011.

[17] S. Ghimire, D. Reis, A. DiChiara, E. Sistrunk, L. F. DimMauro, and P. Agostini. Strong-field induced optical absorption in zno crystal. In *Quantum Electronics and Laser Science Conference*, page QMF6. Optical Society of America, 2011.

[18] D. Daranciang, J. Goodfellow, S. Ghimire, H. Loos, D. Reis, A. S. Fisher, and A. M. Lindenberg. Generation of >100 mJ Broadband THz Transients with >10 MV/cm Fields via Coherent Transition Radiation at the Linac Coherent Light Source. In *CLEO:2011 - Laser Applications to Photonic Applications*, page CMW7. Optical Society of America, 2011.

[19] C. Roedig, G. Doumy, S.-K. Son, C. I. Blaga, A. DiChiara, R. Santra, N. Berrah, C. Bosteadt, J. D. Bozek, P. H. Bucksbaum, J. P. Cryan, L. Fang, S. Ghimire, J. M. Glownia, M. Hoener, E. P. Kanter, B. Krassig, M. Kuebel, M. Messerschmidt, G. Paulus, D. A. Reis, N. Rohringer, L. Young, P. Agostini, and L. DiMauro. Multi photon physics at the lcls. In *Laser Science*, page LThE1. Optical Society of America, 2011.

NPI: Non-Periodic Imaging

Claudiu A. Stan, Raymond G. Sierra, N. Duane Loh, Dmitri Starodub, Hartawan Laksmono, Hasan Demirci, and Michael J. Bogan
Stanford PULSE Institute for Ultrafast Energy Science
SLAC National Accelerator Laboratory, Menlo Park, CA 94025
Email: cstan@slac.stanford.edu

PROGRAM SCOPE

The main goal of the Non-Periodic Imaging Task of the Ultrafast Chemical Science field work proposal is the determination of the dynamics and structure of matter that cannot be investigated with standard atomic-resolution techniques—disordered and biological systems, and materials undergoing fast structural transformations—taking advantage of the unprecedented brilliance, time resolution, and coherence of X-ray free-electron laser (XFEL) light sources such as the Linac Coherent Light Source (LCLS) at SLAC. To realize the full potential of XFELs for these tasks, it is critical to identify throughout science important systems and processes that can be investigated with X-ray lasers, and to develop a range of new techniques in two areas: (i) processing and interpretation of the scattered X-ray data and (ii) highly accurate and reliable preparation of the systems under investigation, on the timescales and lengthscales that are characteristic to them. The NPI group is active in all these areas, and we have pursued specific problems that have the potential to produce techniques that are useful to the general user community at LCLS, thus broadly supporting DOE's mission of understanding and controlling matter.

XFELs enable structural determinations on much smaller length scales and much faster timescales than it was previously possible; in addition, the extremely short duration of the pulses ensures that the atomic structure being probed is static during probing, even though it will often be damaged by radiation afterwards—the "diffract-before-destroy" technique to whose development we contributed. This powerful combination of characteristics comes at the cost of performing experiments serially, with one fresh sample brought at the interaction region for each pulse of photons. Much of our work focuses on different aspects of serial operation: extracting structural information from single-particle scattering experiments; handling efficiently the large data sets; and delivering micron- and nanometer-scale samples efficiently and with high accuracy.

This program's near-term goals include continued analysis of LCLS data collected in recent experiments, development of new algorithms for interpreting structure from single-shot diffraction patterns, solving time-resolved protein structures at atomic resolution using LCLS serial crystallography, and probing mesoscopic structure and dynamics of airborne particulate matter. A new research direction in our program is the investigation of chemical phenomena in the millisecond and microsecond timescale: to give just two examples, most enzymatic biochemical reactions occur in the millisecond timescale, and spontaneous disorder-to-order transitions, such as the nucleation of ice, are predicted to occur at the microsecond timescale. Although LCLS provides femtosecond pulses, the structural dynamics of these much slower phenomena cannot be currently investigated because experiments are limited by the temporal resolution of sample preparation.

RECENT PROGRESS

In the past three years our program has progressed from early experiments at the FLASH free electron laser facility in Hamburg to the Linac Coherent Light Source (LCLS) at SLAC. In FY 12–13 we led 2 LCLS experiments, were main collaborators in 4, and supported 7. We have scheduled 3 additional LCLS beamtimes where we are major collaborators, and more upcoming. The research conducted at LCLS led to 18 published and 3 submitted papers under review. The work described below represents a selection of recent work in which our lab had a leading or major role.

Single particle imaging of non-periodic systems. We are progressing from analysis of strong scattering periodic objects like protein crystals (Barty 2011; Chapman 2011; Lomb 2011; Aquila 2012; Boutet 2012; Johansson 2012; Kern 2012; Koopmann 2012) to large strong scattering non-periodic objects (soot, large viruses) (Martin 2011; Yoon 2011; Loh 2012a; Martin 2012a; Martin 2012b) to smaller weakly scattering non-periodic objects (small viruses, protein complexes, nanoparticles) (Kassemeyer 2012; Loh 2012b; Starodub 2012). We used XFELs to extract structural information from airborne particulate matter (Loh 2012a) such as soot, realizing the important health and climate goal of imaging airborne particulate matter smaller than 2.5 microns; previously, such information was either inferred from electron micrographs (with strong assumptions) or ensemble-averaged processes. In our

work, we resolved the fractal fingerprint of individual soot particles and determined their fractal length scale, which exposed the extent and nature of soot's random aggregation processes. Significant fluctuations in the fractal dimensions of individual soot particles were measured in our observations, suggesting variations in the conditions in which they were formed. We have developed a new darkfield approach to extend the imaging size limit of coherent X-ray diffraction from 0.5 to 2 micron objects (Martin 2012a), developed new algorithms to directly extract non-periodic structural information from single-shot x-ray diffraction data, including the fractal dimension of disordered particles (Bogan 2010c; Loh 2012a), and used for the first time speckle correlations to solve a structure of identical particles in random orientations (Starodub 2012). We have directly imaged the varied morphologies of self-assembled, 30nm aerosolized core-shell particles in-flight (Pedersoli 2013), uncovering structures that were invisible to techniques restricted to averaging over many particles (Fig. 1). This single-particle imaging effort also led to a method to characterize the wavefront of exceptionally intense light (which destroys conventional diagnostic instruments) through variations in the single diffraction patterns from single aerosolized 70-nm polystyrene spheres (Loh 2013).

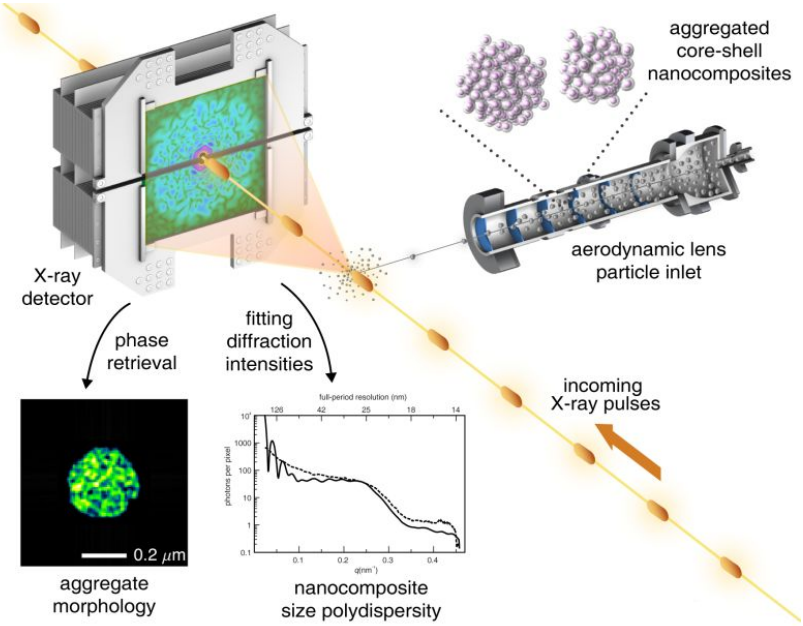

Figure 1: Schematic of non-periodic single particle imaging at the LCLS.

Time-resolved structures of photosensitive membrane proteins. Our work in non-periodic imaging has led to methods critical to serial femtosecond crystallography (SFX), where the structural information of micro- and nanocrystals is measured at near-physiological temperatures. We have developed (Sierra 2012) and received a provisional patent (Bogan 2012) for inventing a nanoflow micron-sized liquid jet in vacuo for SFX that consumes 60-100 times less sample than existing methods and has an open geometry ideal for optical pumping and spectroscopy. Both characteristics were critical to the LCLS study of large membrane protein, Photosystem II (Kern 2012), in which, for the first time, the structure of the protein and the electronic state of its metal center were determined simultaneously as the protein was photo-excited to different states.

Freezing in nanosized drops. In an experiment led by us at LCLS in collaboration with Barbara Wyslouzyl's group at Ohio State University, we have investigated the freezing of water and alkane droplets with radiuses around 10–20 nm using the nanofocus beam at the CXI endstation. The supersonic nozzle setup, developed by the Wyslouzyl group, is a promising systems for investigating structural changes during liquid-to-solid phase transitions, as it produces deeply supercooled liquid droplets of a size that is not much larger than the size of the critical nucleus; therefore, this is a system in which the signal from the critical nucleus would not be drowned in the background scattering from the surrounding supercooled liquid. Preliminary data from this experiment confirmed that in deeply supercooled state water freezes to metastable cubic ice.

FUTURE PLANS

As the XFEL field, and our own work within it, evolves from the first demonstration of foundational methods (such as the "diffract-before-destroy" technique) towards exploring new systems and increasingly complex experiments, we plan to devote a larger part of our efforts to investigate millisecond and microsecond structural dynamics. This task will require the development of more sophisticated and accurate sample delivery techniques applicable to a wide range of problems; we also intend to use this expertise to develop simple and robust methods that can be used by many XFEL users. In addition to the main focus on single-particle and disordered materials, we will continue to work on aspects of femtosecond X-ray crystallography; this field is one of the most important parts of XFEL science, and a stepping stone towards investigating disordered materials.

Non-periodic imaging. At the core of non-periodic structural studies with X-ray lasers are the algorithms necessary for the recovery of structural information from diffraction patterns characterized by low scattered intensity, multiple particles in random orientations per a shot, high extraneous noise, and fluctuating X-ray fluence. To date, we have published the only two demonstrations of 3D test structures recovered from experimental FEL data (Loh 2010; Starodub 2012). We will continue to adapt and improve imaging algorithms to make them applicable to biological samples of practical interest, and test them on both simulated and experimental data sets. We will also tackle the conditions necessary for studying sample heterogeneity. We believe the latter is necessary to open entirely new fields of non-periodic structural study with X-ray lasers. Another major algorithmic challenge at high repetition rate of FELs (while LCLS generates pulses at 120 Hz, the European XFEL will exceed 10 kHz) is the automated preprocessing and curating the many terabytes of data collected during beamtime. In this regard, we are designing algorithms towards fair, unsupervised and automated data processing and reduction, aiming to isolate the unbiased scattering information produced by the sample(s) of interest.

Structural dynamics of enzymatic reactions. We plan to approach an important open problem in biology—determining the structural changes of enzymes during their catalytic action—by X-ray diffraction of enzyme microcrystals suddenly exposed to substrate molecules in solution, a method known as kinetic crystallography. While photochemically-triggered kinetic crystallography has been demonstrated at LCLS (for example in the study of PS-II protein complex), chemical-binding-triggered kinetic crystallography was not attempted to date. Such an experiment is actually inconceivable if standard X-ray sources are used: the diffusion time of the substrate in a crystal large enough for standard X-ray diffraction is orders on magnitude larger than the millisecond timescale characteristic of enzymatic action. XFELs make such an experiment possible because diffusion times are proportional to the square of a crystal size; in micron-sized crystals, the diffusion of reagents should be faster than the binding kinetics. To conduct this type of experiments, we have built in our lab a state-of-the art facility for growing high-quality protein crystals. We are also designing microfluidic mixing devices that will combine the crystals and substrates in solution with high temporal resolution; these devices will be useful to study the millisecond kinetics of other chemical systems as well.

Sample delivery. Serial delivery of samples at XFELs requires accurate positioning and timing, reliable operation during hundreds of thousands of cycles, and low sample consumption. The best current techniques use micron and submicron liquid jets focused either aerodynamically or, in the system we developed, electrodynamically. We plan to advance sample delivery methods by continuing the development of our electrospun jet and by developing new "drop-on-demand" techniques based on two-phase (sample-containing droplets in a carrier liquid) microfluidic technology. For both directions, we will use high-speed imaging for development and online diagnostics, and we are currently installing at LCLS a prototype imaging setup that will be more than 1000 times faster than current endstation hardware. Improving the electrospun jet will include sample prescreening using nanoparticle tracking analysis, improved control and measurement of the liquid flow, and pulsed operation of the jet. We achieved periodic drop generation at the LCLS pulse frequency, we can control the timing of drops inside closed channels, and we are working on controlling jets containing drops in vacuum, where flow cannot be confined by walls or driven by positive hydrostatic pressure.

High-harmonic generation. We will participate in a project to develop a high-power, benchtop high-harmonic source. Our main role in this collaboration with David Ries's group at SLAC is to develop the conversion medium—-a "gas" of nanoparticles in vacuum—which is the central part of this new design.

COLLABORATIONS: This work is done with colleagues from SLAC, Stanford, LLNL, Uppsala, LBNL, Arizona State University, Max Planck Biomedical Heidelberg, CFEL@DESY, Brown University and others.

PUBLICATIONS WHICH NPI WAS PRIMARY AUTHOR

Bogan, M. J., *et al.* (2010a). " Single-shot femtosecond x-ray diffraction from randomly oriented ellipsoidal nanoparticles." *Phys. Rev. ST Accel. Beams* **13**, 094701.

Bogan, M. J., *et al.* (2010b). " Aerosol Imaging with a Soft X-Ray Free Electron Laser." *Aerosol Sci. Tech.* **44**, 1.

Bogan, M. J., *et al.* (2010c). " Single-particle coherent diffractive imaging with a soft x-ray free electron laser: towards soot aerosol morphology ." *J. Phys. B: At. Mol. Opt. Phys.* **43**, 194013.

Bogan, M. J. (2011). "Ultrafast X-ray Lasers Illuminate Airborne Nanoparticle Morphology." *MRS Proceedings* **1349**, mrss11-1349-dd1307-1305, doi:10.1557/opl.2011.1405.

Bogan, M. J., *et al.* (2012). "Apparatus and method for nanoflow serial femtosecond x-ray protein nanocrystallography", provisional patent.

Demirci, H., *et al.* (2013). " Serial femtosecond X-ray diffraction of 30S ribosomal subunit microcrystals in liquid suspension at ambient temperature using an X-ray free-electron laser." *Acta Crystallog.* **F69**, 1066.

Loh, N. D., et al. (2010). "Cryptotomography: reconstructing 3D Fourier intensities from randomly oriented single-shot diffraction patterns." *Phys. Rev. Lett.* **104**, 225501.

Loh, N. D., *et al.* (2012a). "Profiling structured beams using injected aerosols." *Proc. SPIE* **8504**, 850403.

Loh, N. D., *et al.* (2012b). "Fractal morphology, imaging and mass spectrometry of single aerosol particles in flight." *Nature* **486**, 513.

Loh, N. D., *et al.* (2013). “Sensing the wavefront of x-ray free-electron lasers using aerosol spheres.” *Opt. Express* **21**, 12385.

Pedersoli, E., *et al.* (2013) “Mesoscale morphology of airborne core–shell nanoparticle clusters: x-ray laser coherent diffraction imaging.”*J. Phys. B At. Mol. Opt. Phys.* **46**, 164033.

Sierra, R. G., *et al.* (2012). "Nanoflow electrospinning serial femtosecond crystallography." *Acta Crystallog.* **D68**, 1584.

Starodub, D., *et al.* (2010). " Reconstruction of the electron density of molecules with single-axis alignment." *Proc. SPIE* **7800**, 78000O.

Starodub, D., *et al.* (2012). "Single-particle structure determination by correlations of snapshot X-ray diffraction patterns" *Nat. Commun.* **3**, 1276.

SELECTED PUBLICATIONS IN WHICH NPI WAS A MAJOR COLLABORATOR

Alonso-Mori, R., *et al.* (2012). "Energy-dispersive X-ray emission spectroscopy using an X-ray free-electron laser in a shot-by-shot mode." *Proc. Natl. Acad. Sci.USA* **109**, 19103.

Aquila, A., *et al.* (2012). "Time-resolved protein nanocrystallography using an X-ray free-electron laser." *Opt. Express* **20**, 2706.

Barty, A., *et al.* (2011). "Self-terminating diffraction gates femtosecond X-ray nanocrystallography measurements." *Nat. Photonics* **6**, 35.

Boutet, S., *et al.* (2012). " High-resolution protein structure determination by serial femtosecond crystallography." *Science* **337**, 362.

Chapman, H., *et al.* (2011). "Femtosecond X-ray protein nanocrystallography." *Nature* **470**, 73.

Ekeberg, T., *et al.* (2012). "Three-dimensional structure determination with an X-ray laser." *Doctoral thesis preprint*, Uppsala Universitet.

Frank, M., *et al.* (2011). "Single-particle aerosol mass spectrometry (SPAMS) for high-throughput and rapid analysis of biological aerosols and single cells."In Rapid Characterization of Microorganisms by Mass Spectrometry. Demirev, American Chemical Society, pp161-166.

Hau-Riege, S. P., *et al.* (2010). "Sacrificial tamper slows down sample explosion in FLASH diffraction experiments." *Phys. Rev. Lett.* **104**, 064801.

Johansson, L. C., *et al.* (2012). "Lipidic phase membrane protein serial femtosecond crystallography." *Nat. Methods* **9**, 263.

Kassemeyer, S., *et al.* (2012). "Femtosecond free-electron laser x-ray diffraction data sets for algorithm development." *Opt. Express* **20**, 4149.

Kern, J., *et al.* (2012). "Room temperature femtosecond X-ray diffraction of photosystem II microcrystals." *Proc. Natl. Acad. Sci. USA* **109**, 9721.

Koopmann, R., *et al.* (2012). "In vivo protein crystallization opens new routes in structural biology." *Nat. Methods* **9**, 259.

Lomb, L., *et al.* (2011). "Radiation damage in protein serial femtosecond crystallography using an x-ray free-electron laser." *Phys. Rev. B* **84**, 214111.

Martin, A. V., *et al.* (2011). "Single particle imaging with soft x-rays at the Linac Coherent Light Source." *Proc. SPIE* **8078**, 807809.

Martin, A. V., *et al.* (2012a). "Femtosecond dark-field imaging with an X-ray free electron laser." *Opt. Express* **20**, 13501.

Martin, A. V et al. (2012b). "Noise-robust coherent diffractive imaging with a single diffraction pattern." *Opt. Express* **20**, 16650.

Pedersoli, E., *et al.* (2011). "Multipurpose modular experimental station for the DiProI beamline of Fermi@Elettra free electron laser." *Rev Sci. Instrum.* **82**, 043711.

Saldin, D. K., *et al.* (2010a). "Structure of a single particle from scattering by many particles randomly oriented about an axis: toward structure solution without crystallization? " *New J. Phys.* **12**, 035014.

Saldin, D. K., *et al.* (2010b). "Reconstruction from a single diffraction pattern of azimuthally projected electron density of molecules aligned parallel to a single axis." *Acta Crystallogr.* **A66**, 32.

Saldin, D. K., *et al.* (2011). "New light on disordered ensembles: ab-initio structure determination of one particle from scattering fluctuations of many copies." *Phys. Rev. Lett.***106**, 115501.

Seibert, M. M., *et al.* (2010). "Femtosecond diffractive imaging of biological cells." *J. Phys. B At. Mol. Opt. Phys.* **43**, 194015.

Seibert, M. M., *et al.* (2011). "Single mimivirus particles intercepted and imaged with an X-ray laser" *Nature* **470**, 78.

Yoon, C. H., et al. (2011). "Unsupervised classification of single-particle X-ray diffraction snapshots by spectral clustering." *Opt. Express* **19**, 16542.

SFA: Strong-Field Laser-Matter Interactions

P. Bucksbaum, A. Natan

PULSE Ultrafast Chemical Science Program

SLAC National Accelerator Laboratory, Menlo Park, CA 94025

Email: phb@slac.stanford.edu

Program Scope: The core issue under investigation in SFA is ***the nature of the short wavelength strong field interaction with bound and free electrons.*** We explore the femtosecond regime of bound electron dynamics in strongly driven molecules. We study both ***core-hole wavepacket dynamics (1-10 fs)*** and ***driven electron intramolecular dynamics (20-250 fs)*** in molecules, utilizing intense laser and x-ray fields and momentum and energy resolved multidimensional detection. Key questions concern the interplay between correlated electron motion and relaxation, nuclear motion, and photoabsorption when molecules are subjected to strong infrared, optical or x-ray fields. These are critical issues for strong-field imaging, molecular dynamics, and light source development.

Recent Progress:

Velocity Map Imaging for Ions*:* We have continued to develop velocity map imaging for ions. This has been used successfully to track transient ultrafast motion in molecules, not only for in own initial interest on LCLS-driven dissociation of oxygen and nitrogen, but also in a growing number of more complex experiments, including last year's observations of **LCLS-probed ring opening reactions in cyclohexadiene,** which was a collaboration led by Dr. Vladimir Petrovic from the coherent control program within the Bucksbaum lab. Our initial work on this has been published now in Physical Review Letters.

X-ray pump, x-ray probe experiment. A second collaboration with Dr. Petrovic at LCLS was just completed which incorporated a different kind of VMI detector together with the newly commissioned split and delay detector for soft x-rays. The goal is to capture the x-ray-induced motion of bonds in deuterated acetylene (D-C≡C-D) by coincidence detection of two-body or three-body fragmentation. We were actively involved in the design and operation of this, and also in the Pass I data analysis.

Other ion VMI Experiments: Our ion VMI detector platforms are designed for use either at LCLS or in our own lab in PULSE. We have now collected significant data sets for several experiments in the laboratory and at LCLS to exploit this capability. The following experiments are in the data analysis phase:

- Studies of dication dissociation nitrogen simultaneously exposed to strong laser fields and ultrafast x-rays;
- Iodine excited to vibrational wave packets, with light-induced conical intersections;
- Oxygen excited by pairs of ultrafast x-ray pulses.

Electron VMI experiments: We have developed a new capability for electron velocity map imaging, and have applied it to examine the strong field process in atoms and small molecules. There are a number of new and promising results from this.

Quantum phase metrology for ATI electrons: We have combined a strong-field ionizing 400nm laser with a weak 800nm field with good control over their relative phase in ATI experiments. We find that VMI momentum analysis can yield the initial quantum phase of the emitted electron wavepacket . We used the asymmetries and interferences of the electron momentum distribution as a function of relative phase between the two wavelengths. This represents a complete characterization of the emitted electronic wavefunction, up to the accuracy of the phase determination method. Unlike the RABBIT technique, were

high-harmonics sidebands are measured, we directly observe the interference of complex ATI transitions, with phases that depend on the quantum path followed by the photoelectrons. This technique may prove to be a very sensitive probe of atomic and molecular potentials that will give additional information beyond the usual methods of measuring electron momentum distributions in ATI processes.

We also see higher order phase interference features in when the second harmonic and the fundamental field have equal strengths (the Schumacher regime). We believe that the faster phase modulation arises from a different interference mechanism, which is still under investigation.

Freeman resonances as a tool for observing ultrafast electron dynamics: The electron VMI records Freeman resonances with full radial and angular resolution, yielding rich new information about the ultrafast dynamics of strong field ionization (se Fig. 1). We will extend these observations to chirped pulses to attempt to localize in time (hence in energy) the part of the pulse that contributes to the Freeman resonance. Accurately controlling Freeman resonances formation translates to spatiotemporal information on the velocity map image and can serve as a tool to capture transient phenomena such as, bond formation, as well as structure and symmetry of electrons undergoing non-Born Oppenheimer dynamics .

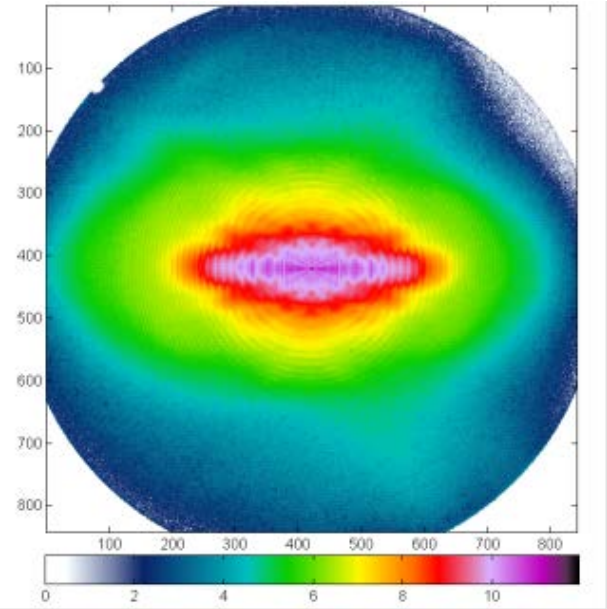

Fig 1. Raw electron VMI data from strong field ionization of N2. The color map represent the log number of counts. Multiple ATI rings, Freeman resonances and rescattering rings are evident.

Higher fidelity alignment features in electron VMI: Laser induced orbital projection and electron diffraction using electron velocity map imaging experiments are in progress. We are examining multiple orbital contributions to the rescattered electrons of aligned vs anti-aligned molecules such as N2, CO2, etc. We will use previous alignment techniques to obtain superior alignment. We will examine the modulation in the diffraction structure of the samples as function of the molecules alignment. For example, For N2 we expect to obtain contributions from the lower bound orbital HOMO-1 orbital that will be perpendicular to the HOMO orbital. The angular information available using the electron VMI would facilitate the observation of such contributions.

***Light-induced CI physics*:** Conical Intersections (CIs) are molecular transient structures where energy surfaces cross and the Born Oppenheimer approximation fails. We have new simulations of CI dynamics that include strong field non-adiabatic coupling between electronic vibration and rotation degrees of freedom in the vicinity of light-induced conical intersections of molecules. We will use this to extend previous work in I2. We seek to obtain three goals: (1) Controlling population transfer through the LICI will be attained by changing the crossing propertied by changing the orientation of the dressing laser polarization in relation to the molecular axis that is determined by the polarization of the light launching the vibrational wavepacket under study. (2) Observing Berry Phase: a hallmark of conical intersection is the Berry or geometric phase, where an adiabatic state changes sign when moved around the conical intersection. Although this phase change is predicted to happen around a LICI, the confirmation of its existence would validate the proposition that the LICI is directly analogous to a natural CI. To measure this experimentally we will measure the phase accumulated by a vibrational wavepacket that moves around the intersection using wavepacket interferometry. (3) The rotational degrees of freedom will evolve erratically around the CI due to the diverging coupling between rotational, vibrational, and electronic

levels in a molecule. Building upon the experience gained in measuring the Berry phase around the LICI we can use similar experimental methods in combination with molecular alignment detection to directly study the effects of the LICI on rotational states.

Going beyond the periodically kicked quantum rotor: Our work on multiply kicked quantum rotors has now been extended beyond simply control protocols to increase the quality of alignment. We have been working with Aberbukh and Floss at Weizmann to use this platform to study the more general problem of the quantum kicked rotor. This is a paradigm for studies of quantum disorder and quantum chaos. Our current efforts are to demonstrate disorder-induced localization, also known as Anderson Localization, in the quantum kicked rotor, in the presence of decoherence and finite temperatures.

We have also started a collaboration with the ATO subtask, who have been studying the evolution of kicked quantum asymmetric top molecules, whose Hamiltonian is non-separable and whose corresponding classical dynamics is chaotic, and have proposed extending these efforts to x-ray scattering experiments at LCLS. Our two goals are (1) to demonstrate that x-ray scattering from a coherently driven ensemble of molecular asymmetric rotors can be used to determine aspects of the three dimensional structure of these molecules, even when they are not assembled in a static crystal; and (2) to observe in the x-ray scattering images the quasiperiodic quantum trajectories that characterizes quantum chaos in impulsively driven asymmetric top systems, and measure the evolution to chaos.

Multi-configuration wave-packets experiment*:* We have recently conducted an LCLS experiment that investigated the formation and dynamics of multi-configuration wave packets in the acetylene dication via core-ionization of C2H2 and C2D2 by a short x-ray pulse (<5fs) followed by Auger relaxation that coherently populates multiple electronic states in the dication. Using Coulomb explosion by the second x-ray pulse or an IR pulse (in a different part of the experiment) we monitored the ensuing short-time electronic (<20fs) and subsequent nuclear dynamics (<100fs) that eventually lead to the isomerization into vinylidene dication (~60 fs). Acetylene, which has been a workhorse of molecular dynamics due to its diatomic like electronic structure, is the smallest hydrocarbon that can isomerize and permits ion-ion coincidence measurements at the current LCLS repetition rate. We selected two fragmentation channels in acetylene, in which previous experiments and calculations showed that single-state picture is incomplete. In two parts of the experiment we recorded the three-particle ion-ion coincidences as a function of the pump-probe delay. This experiment can open the door for the FEL studies of the strongly non-adiabatic regime on sub 5 fs timescales at which electron-electron, electron-nuclear interactions and proton migration occur leading to the breakdown of the molecular orbital picture. These experiments are in the data analysis phase.

Bostedt, C., J. Bozek, P. Bucksbaum, R. Coffee, J. Hastings, Z. Huang, R. Lee, S. Schorb, J. Corlett and P. Denes (2013). "Ultra-fast and ultra-intense x-ray sciences: First results from the linac coherent light source free-electron laser." *Journal of Physics B: Atomic, Molecular and Optical Physics* **46**(16): 164003.

Bucksbaum, P. (2012). "Atomic and molecular physics at the lcls x-ray laser." *Mexican Optics and Photonics Meeting Abstracts, San Luis Potosi*.

Bucksbaum, P. and J. Glownia (2013). "Ultrafast AMO physics at the LCLS x-ray FEL." *EPJ Web of Conferences* **57**: 04001.

Bucksbaum, P. H. (2013). "Ultrafast quantum control in atoms and molecules." Ultrafast nonlinear optics, Springer**:** 105-128.

Bucksbaum, P. H., R. Coffee and N. Berrah (2011). "The first atomic and molecular experiments at the linac coherent light source x-ray free electron laser." *Advances in Atomic Molecular and Optical Physics* **60**: 239-289.

Cryan, J., J. Glownia, J. Andreasson, A. Belkacem, N. Berrah, C. Blaga, C. Bostedt, J. Bozek, N. Cherepkov and L. DiMauro (2012). "Molecular frame auger electron energy spectrum from N_2." *Journal of Physics B: Atomic, Molecular and Optical Physics* **45**(5): 055601.

Cryan, J., J. Glownia, N. Cherepkov, P. Bucksbaum and R. Coffee (2011). "Angular dependance of auger electrons from n $ _ (*1*) $." *Bulletin of the American Physical Society* **56**.

Cryan, J. P., J. M. Glownia, D. W. Broege, Y. Ma and P. H. Bucksbaum (2011). "Ensemble of linear molecules in nondispersing rotational quantum states: A molecular stopwatch." *Physical Review X* **1**(1): 011002.

Doumy, G., C. Roedig, S.-K. Son, C. I. Blaga, A. DiChiara, R. Santra, N. Berrah, C. Bostedt, J. Bozek and P. Bucksbaum (2011). "Nonlinear atomic response to intense ultrashort x rays." *Physical Review Letters* **106**(8): 083002.

Fang, L., T. Osipov, B. Murphy, F. Tarantelli, E. Kukk, J. Cryan, M. Glownia, P. Bucksbaum, R. Coffee and M. Chen (2012). "Multiphoton ionization as a clock to reveal molecular dynamics with intense short x-ray free electron laser pulses." *Physical Review Letters* **109**(26): 263001.

Farrell, J., B. McFarland, N. Berrah, C. Bostedt, J. Bozek, P. Bucksbaum, R. Coffee, J. Cryan, L. Fang and R. Feifel (2012). "Ultrafast x-ray probe of nucleobase photoprotection." *Quantum Electronics and Laser Science Conference*, Optical Society of America.

Fung, R., J. Glownia, J. Cryan, A. Natan, P. Bucksbaum and A. Ourmazd (2012). "Towards extracting dynamics below timing jitter by manifold--based machine learning." *Signal* **1**: i2.

Glownia, J. M., A. Ourmazd, R. Fung, J. Cryan, A. Natan, R. Coffee and P. Bucksbaum (2012). "Sub-cycle strong-field influences in x-ray photoionization." *Quantum Electronics and Laser Science Conference*, Optical Society of America.

Kanter, E., B. Krässig, Y. Li, A. March, P. Ho, N. Rohringer, R. Santra, S. Southworth, L. DiMauro and G. Doumy (2011). "Unveiling and driving hidden resonances with high-fluence, high-intensity x-ray pulses." *Physical Review Letters* **107**(23): 233001.

McFarland, B., J. Farrell, N. Berrah, C. Bostedt, J. Bozek, P. Bucksbaum, R. Coffee, J. Cryan, L. Fang and R. Feifel (2013). "Probing nucleobase photoprotection with soft x-rays." *EPJ Web of Conferences 41, 07004 (2013)* **41**: 07004.

McFarland, B., J. Farrell, S. Miyabe, F. Tarantelli, A. Aguilar, N. Berrah, C. Bostedt, J. Bozek, P. Bucksbaum and J. Castagna (2013). "Delayed ultrafast x-ray auger probing (duxap) of nucleobase ultraviolet photoprotection." *arXiv preprint arXiv:1301.3104*.

Petrovic, V. S., S. Schorb, J. Kim, J. White, J. P. Cryan, J. M. Glownia, L. Zipp, D. Broege, S. Miyabe and H. Tao (2012). "High sensitivity of strong-field multiple ionization to conical intersections." *arXiv preprint arXiv:1212.3728*.

Petrović, V. S., M. Siano, J. L. White, N. Berrah, C. Bostedt, J. D. Bozek, D. Broege, M. Chalfin, R. N. Coffee and J. Cryan (2012). "Transient x-ray fragmentation: Probing a prototypical photoinduced ring opening." *Physical Review Letters* **108**(25): 253006.

Roedig, C., G. Doumy, S.-K. Son, C. Blaga, A. DiChiara, R. Santra, N. Berrah, C. Bosteadt, J. Bozek and P. H. Bucksbaum (2011). "Multi photon physics at the lcls." *Laser Science*, Optical Society of America.

Solution Phase Chemical Dynamics (SPC)

Principal Investigator: Kelly Gaffney

Program Scope: Understanding how molecular properties dictate the non-equilibrium dynamics of molecular excited states represents a critical step towards a better utilization of light triggered molecular phenomena. Our works emphasis on solution phase dynamics and more complex molecular systems complements the small molecule, gas phase chemical dynamics efforts in the *Ultrafast Chemistry* field work proposal at the SLAC National Accelerator Laboratory.

The development of the LCLS, an ultrafast x-ray free electron laser, presents a tremendous opportunity to harness the advantages of x-ray scattering and spectroscopy to investigate chemical dynamics (Kunnus 2012; Kunnus 2013; Lemke 2013; Zhang 2013). X-ray methods provide a novel approach to distinguishing electronic and nuclear dynamics in time resolved measurements, a central challenge in experimental studies of chemical dynamics. We complement these ultrafast x-ray studies with time resolved vibrational spectroscopy (Ji 2010; Ji 2010; Park 2010; Gaffney 2011; Hartsock 2011; Jha 2011; Ji 2011; Ji 2011; Jha 2012; Ji 2012; Zhang 2012; Zhang 2012; Sun 2013; Sun 2013) and steady state x-ray spectroscopy (Meyer 2010). Our current research focuses on the non-adiabatic dynamics of charge transfer excitations, primarily in, but not limited to, transition metal coordination compounds.

Recent Progress and Future Plans

Tracking Excited State Charge and Spin Dynamics in Iron Coordination Complexes: For transition metal containing molecular complexes, excited state electron transfer and spin crossover represent key phenomena for characterization and ideally control. Poly-pyridal iron complexes, such as $[Fe(2,2'\text{-bipyridine})_3]^{2+}$, provide archetypical coordination complexes where the excited state charge and spin dynamics involved in spin crossover have long been a source of interest and controversy. While experimental evidence supporting the ultrafast time scale for excited state charge and spin dynamics in these iron complexes has been accumulating, the spin crossover mechanism remains unclear. Mechanistic understanding has proven difficult because the generally complex electronic structure of coordination compounds make unambiguous theoretical and experimental studies of these chemical dynamics challenging. Most critically, robust determination of the ultrafast spin dynamics has been impeded by the indirect sensitivity of optical spectroscopy to spin dynamics, and the flux limitations of ultrafast x-ray sources.

We have used femtosecond resolution Fe K-edge XANES (Lemke 2013) and Kβ x-ray fluorescence (Zhang 2013) to study the ultrafast charge and spin dynamics of $[Fe(2,2'\text{-bipyridine})_3]^{2+}$ induced by metal to ligand charge transfer (MLCT) excitation. These measurements demonstrate the ability of x-ray fluorescence to robustly track the charge and spin dynamics of an electronically excited molecule. Our initial measurements demonstrate spin crossover in $[Fe(2,2'\text{-bipyridine})_3]^{2+}$ occurs step wise from both a spin and electron transfer perspective. At this point we have a firm handle of the electronic states involved in spin crossover and the transition rates between these states.

Our future work will focus of two objectives: (1) understanding how chemical changes, such as ligand substitution, influence the interaction between charge transfer and ligand field excited states and (2) determining the vibrational coordinates that govern the non-adiabatic electronic transitions involved in spin crossover. These efforts will focus on a series of mixed ligand complexes involving both 2,2'-bipyridine and cyanide ligands. Initial measurments demonstrate

that replacing two of the three 2,2'-bipyridine ligands with four cyanide ligands, greatly modifies the MLCT excited state dynamics of the molecule. Understanding these preliminary findings will be an emphasis of our future work.

Mapping the electronic density evolution of charge transfer excited states: The spatial extent of interacting electronic states significantly influences the non-adiabatic coupling and transfer rate between these states. Fast and efficient energy migration and charge separation represent essential steps in molecularly based light-harvesting materials. High symmetry and strong intermolecular coupling facilitate fast energy migration, while solvent disorder leads to the symmetry breaking that facilitates charge separation. The interplay of electronic coupling and disorder, both dynamic and static, has a critical impact on the electron mobility in molecular materials.

We have used time resolved vibrational anisotropy to study the dynamics of electron localization in the ligand-to-metal charge transfer (LMCT) excited state of $[Fe(CN)_6]^{3-}$ (Zhang 2012) and the dynamics of twisted intra-molecular charge transfer in julolidine malanonitrile (Zhang 2012). In previous work, we have used time resolved vibrational spectroscopy to determine the rate of excited state localization in $[Fe(CN)_6]^{3-}$. The single excited state vibrational absorption peak and the absence of excited state anisotropy for the initially generated LMCT excited state of $[Fe(CN)_6]^{3-}$ strongly indicate the ligand electron hole hops between the equivalent ligands with a rate too high to be resolved with the 200 fs time resolution of the measurement. On the picosecond time scale, we observe the excited state spectrum transition from one to two excited state absorptions with a solvent dependent rate. We attribute this to a reduction in molecular symmetry induced by hole localization. While vibrational spectroscopy has proven valuable for studying excited state charge dynamics, the interpretation has relied heavily on symmetry considerations and TDDFT calculations. Our future work will complement this vibrational spectroscopy studies with time resolved soft x-ray resonance Raman measurements – more commonly referred to as resonance inelastic x-ray scattering (RIXS). By resonantly exciting transitions associated with specific atoms in a molecule, such as the N K-edge of the ligand and the Fe L-edge of the metal center in $[Fe(CN)_6]^{3-}$, we will utilize the spatial localization of the 1*s* orbital of N and the 2*p* orbitals of Fe to provide an atom specific view of the molecular electronic structure. An initial experimental study of the photodissociation dynamics of $Fe(CO)_5$ with Fe L-edge RIXS has demonstrated the feasibility of the measurements at LCLS (Kunnus 2012; Kunnus 2013). These initial studies of CO photodissociation from $Fe(CO)_5$ demonstrate that the during the initial bond dissociation, the parent molecules fragment into both singlet and triplet spin configurations of the $Fe(CO)_4$ photoproduct. While the triplet state interacts weakly with the ethanol solvent, the singlet configurations exhibit strong ethanol-$Fe(CO)_4$ interactions on the 100 fs time scale. Whether the solute-solvent structure in the electronic ground state or the details of the non-adiabatic dynamics along dissociative potential energy surfaces governs the branching ratio for singlet and triplet photoproducts has yet to be determined.

Publications Supported by AMOS Program

Ji, M. B., M. Odelius and K. J. Gaffney (2010). Large Angular Jump Mechanism Observed for Hydrogen Bond Exchange in Aqueous Perchlorate Solution. *Science* **328**: 1003.

Ji, M. B., S. Park and K. J. Gaffney (2010). Dynamics of Ion Assembly in Solution: 2DIR Spectroscopy Study of LiNCS in Benzonitrile. *J. Phys. Chem. Lett.* **1**: 1771.

Meyer, D. A., X. N. Zhang, U. Bergmann and K. J. Gaffney (2010). Characterization of charge transfer excitations in hexacyanomanganate(III) with Mn K-edge resonant inelastic x-ray scattering. *J. Chem. Phys.* **132**.

Park, S., M. B. Ji and K. J. Gaffney (2010). Ligand Exchange Dynamics in Aqueous Solution Studied with 2DIR Spectroscopy. *J. Phys. Chem. B* **114**: 6693.

Gaffney, K. J., M. B. Ji, M. Odelius, S. Park, et al. (2011). H-bond switching and ligand exchange dynamics in aqueous ionic solution. *Chem. Phys. Lett.* **504**: 1.

Hartsock, R. W., W. K. Zhang, M. G. Hill, B. Sabat, et al. (2011). Characterizing the Deformational Isomers of Bimetallic $[Ir_2(dimen)_4]^{2+}$ (dimen=1,8-diisocyano-p-menthane) with Vibrational Wavepacket Dynamics. *J. Phys. Chem. A* **115**: 2920.

Jha, S. K., M. B. Ji, K. J. Gaffney and S. G. Boxer (2011). Direct measurement of the protein response to an electrostatic perturbation that mimics the catalytic cycle in ketosteroid isomerase. *Proc. Natl. Acad. Sci. U. S. A.* **108**: 16612.

Ji, M. B. and K. J. Gaffney (2011). Orientational relaxation dynamics in aqueous ionic solution: Polarization-selective two-dimensional infrared study of angular jump-exchange dynamics in aqueous 6M NaClO4. *J. Chem. Phys.* **134**: 044516.

Ji, M. B., R. W. Hartsock, Z. Sun and K. J. Gaffney (2011). Interdependence of Conformational and Chemical Reaction Dynamics during Ion Assembly in Polar Solvents *J. Phys. Chem. B* **115**: 11399.

Jha, S. K., M. B. Ji, K. J. Gaffney and S. G. Boxer (2012). Site-Specific Measurement of Water Dynamics in the Substrate Pocket of Ketosteroid Isomerase Using Time-Resolved Vibrational Spectroscopy. *J. Phys. Chem. B* **116**: 11414.

Ji, M. B., R. W. Hartsock, Z. Sung and K. J. Gaffney (2012). Influence of solute-solvent coordination on the orientational relaxation of ion assemblies in polar solvents. *J. Chem. Phys.* **136**: 014501.

Kunnus, K., I. Rajkovic, S. Schreck, W. Quevedo, et al. (2012). A setup for resonant inelastic soft x-ray scattering on liquids at free electron laser light sources. *Rev. Sci. Instr.* **83**: 123109.

Zhang, W. K., M. B. Ji, Z. Sun and K. J. Gaffney (2012). Dynamics of Solvent-Mediated Electron Localization in Electronically Excited Hexacyanoferrate(III). *J. Am. Chem. Soc.* **134**: 2581.

Zhang, W. K., Z. G. Lan, Z. Sun and K. J. Gaffney (2012). Resolving Photo-Induced Twisted Intramolecular Charge Transfer with Vibrational Anisotropy and TDDFT. *J. Phys. Chem. B* **116**: 11527.

Kunnus, K., P. Wernet, M. Odelius, I. Josefsson, et al. (2013). Observation of ultrafast ligand addition and spin crossover following Fe(CO)5 photodissociation in ethanol. in preparation.

Lemke, H. T., C. Bressler, L. X. Chen, D. M. Fritz, et al. (2013). Femtosecond X-ray Absorption Spectroscopy at a Hard X-ray Free Electron Laser: Application to Spin Crossover Dynamics. *J. Phys. Chem. A* **117**: 735.

Sun, Z., W. K. Zhang, M. B. Ji, R. W. Hartsock, et al. (2013). Aqueous Mg^{2+} and Ca^{2+} Ligand Exchange Mechanisms Identified with 2DIR Spectroscopy. *J. Phys. Chem. B*: accepted.

Sun, Z., W. K. Zhang, M. B. Ji, R. W. Hartsock, et al. (2013). Contact Ion Pair Formation between Hard Acids and Soft Bases in Aqueous Solutions Observed with 2DIR Spectroscopy. *J. Phys. Chem. B*: accepted.

Zhang, W. K., R. Alonso-Mori, U. Bergmann, C. Bressler, et al. (2013). Tracking Excited State Charge and Spin Dynamics in Iron Coordination Complexes submitted.

Ultrafast Theory and Simulation (UTS)

Todd J. Martínez
Department of Photon Science, SLAC National Accelerator Laboratory, Menlo Park, CA
Email: toddjmartinez@gmail.com

Objective and Scope

The goal of this subtask is to develop and apply the theoretical and computational tools needed to understand energy and charge flow in molecular systems. This goal is being pursued on several fronts: 1) improving the efficiency and accuracy of solutions to the electronic structure problem, especially for excited electronic states, 2) developing methods to determine the requisite potential energy surfaces by interpolation and/or direct computation during subsequent simulations of dynamics, 3) improving methods for dynamical propagation including quantum effects such as nonadiabatic transitions, and 4) applying these methods to novel ultrafast experiments, including those enabled by novel light sources such as LCLS.

Recent Progress

We have expanded our ability to combine ab initio multiple spawning (AIMS) treatments of nonadiabatic dynamics with photoionization probe pulses. We incorporated a description of the continuum ejected electron, going beyond previous descriptions in terms of Franck-Condon-like matrix elements. This will allow us to go beyond the prediction of energy-resolved photoelectron ejection intensities to also describe photoelectron angular distributions. These new methods were applied to the ultrafast dynamics of ethylene (a paradigmatic molecule for photoinduced isomerization),[5,7,8,9] as well as dynamics in the simplest conjugated molecules (butadienes).[12] We have been carrying out the first "on the fly" simulations of excited state dynamics using the multireference perturbation theory approach which is able to model both static and dynamic electron correlation effects (AIMS-MSPT2). Most electronic structure methods used in previous dynamics simulations are not able to provide a balanced treatment of static and dynamic correlation. This causes difficulties when valence and Rydberg states are involved in the dynamics or when multiple low-lying valence electronic states of widely differing character are involved. Thus, the AIMS-MSPT2 method allowed us to resolve long standing questions about the role of Rydberg states in ethylene photoisomerization[9] and the dynamics of butadiene photoisomerization[12] (where there are two low-lying valence excited states – with covalent and charge-transfer character).

In collaboration with the Vanicek group at EPFL in Switzerland, we have demonstrated the use of Gaussian wavepacket dynamics methods for ultrafast spectroscopy.[14] The accuracy of these methods can be improved by employing a "forward-backward" strategy, where one focuses on the accurate evolution of the relevant correlation function instead of the time-evolving wavefunction itself.

We developed a new approach to describe the topography of conical intersection seams that are critical to nonadiabatic effects. This new "seam space nudged elastic band" (SS-NEB) method[15] extends the NEB approach used for elucidating reaction pathways to one that can determine minimum energy paths connecting conical intersections. This will allow us to characterize excited state dynamics much more clearly, using minimal energy conical intersections (MECIs) as "signposts" on the potential energy surface and determining how these are related to each other.

We have developed the techniques to model Auger spectroscopy from excited electronic states in order to aid in the interpretation of femtosecond UV pump-Auger probe experiments that are now being pioneered at LCLS. We computed Auger spectra for various geometries and electronic states of thymine in order to compare to such a delayed ultrafast x-ray Auger probe (DUXAP) experiment led by M. Guehr at LCLS.

We have also added the ability to use effective core potentials (ECPs) in our graphical processing unit (GPU) based electronic structure and *ab initio* molecular dynamics code, TeraChem. This is enabling the calculation of excited state dynamics for molecules containing transition metal atoms. Such calculations are in the planning phases, and will be pursued once the ECP code is fully tested.

Future Plans

Work planned over the next funding period focuses on 1) developing methods to describe the detailed attosecond electron and nuclear dynamics in strong fields for high harmonic generation, 2) improving our methods for computing Auger spectra and applying these directly to the excited state dynamics of thymine, and 3) investigating the excited state dynamics of Fe- and Ru-based organometallic complexes which have promising uses in solar energy applications.

Publications (2010-2013):

1. S. A. Varganov and T. J. Martínez, *Variational Geminal Augmented Multireference Self-Consistent Field Theory: Two Electron Systems*, J. Chem. Phys. **132**, 054103 (2010).
2. T. J. Martínez, *Seaming is Believing*, Nature **467**, 412-413 (2010).
3. C. R. Evenhuis and T. J. Martínez, *A Scheme to Interpolate Potential Energy Surfaces and Derivative Coupling Vectors Without Performing a Global Diabatization*, J. Chem. Phys. **135**, 224110 (2011).
4. H. Tao, L. Shen, M. H. Kim, A. G. Suits and T. J. Martínez, *Conformationally Selective Photodissociation Dynamics of Propanal Cation*, J. Chem. Phys. **134**, 054313 (2011).
5. A. L. Thompson and T. J. Martínez, *Time-resolved Photoelectron Spectroscopy from First Principles*, Faraday Disc. **150**, 293-311 (2011).

6. S. Yang and T. J. Martínez, *Ab Initio Multiple Spawning: First Principles Dynamics Around Conical Intersections* in Conical Intersections: Theory, Computation and Experiment, Eds. W. Domcke and H. Koppel, World Scientific, Singapore, 2011.
7. H. Tao, T. K. Allison, T. W. Wright, A. M. Stooke, C. Khurmi, J. van Tilborg, Y. Liu, R. W. Falcone, A. Belkacem and T. J. Martínez, *Ultrafast Internal Conversion in Ethylene. I. The Excited State Lifetime*, J. Chem. Phys. **134**, 244306 (2011).
8. T. K. Allison, H. Tao, W. J. Glover, T. W. Wright, A. M. Stooke, C. Khurmi, J. Van Tilborg, Y. Liu, R. W. Falcone, T. J. Martínez and A. Belkacem, *Ultrafast Internal Conversion in Ethylene. II. Mechanisms and Pathways for Quenching and Hydrogen Elimination*, J. Chem. Phys. **136**, 124317 (2012).
9. T. Mori, W. J. Glover, M. S. Schuurman and T. J. Martínez, *Role of Rydberg States in the Photochemical Dynamics of Ethylene*, J. Phys. Chem. A **116**, 2808-2818 (2012).
10. V. S. Petrovic, M. Siano, J. L. White, N. Berrah, C. Bostedt, J. D. Bozek, D. Broege, M. Chalfin, R. N. Coffee, J. Cryan, L. Fang, J. P. Farrell, L. J. Frasinski, J. M. Glownia, M. Guehr, M. Hoener, D. M. P. Holland, J. Kim, J. P. Marangos, T. J. Martínez, B. K. McFarland, R. S. Minns, S. Miyabe, S. Schorb, R. J. Sension, L. S. Spector, R. Squibb, H. Tao, J. G. Underwood and P. H. Bucksbaum, *Transient X-Ray Fragmentation: Probing a Prototypical Ring-Opening,* Phys. Rev. Lett. **108**, 253006 (2012).
11. J. Kim, H. Tao, J. L. White, V. S. Petrovic, T. J. Martínez and P. H. Bucksbaum, *Control of 1,3-Cyclohexadiene Photoisomerization Using Light-Induced Conical Intersections*, J. Phys. Chem. A **116**, 2758-2763 (2012).
12. T. S. Kuhlman, W. J. Glover, T. Mori, K. B. Moller, and T. J. Martínez, *Between Ethylene and Polyenes – The Nonadiabatic Dynamics of cis-Dienes*, Faraday Disc. **157**, 193-212 (2012).
13. A. M. Virshup, J. Chen, and T. J. Martínez, *Nonlinear Dimensionality Reduction for Nonadiabatic Dynamics: The Influence of Conical Intersection Topography on Population Transfer Rates*, J. Chem. Phys. **137**, 22A519 (2012).
14. M. Sulc, H. Hernandez, T. J. Martínez, and J. Vanicek, *Relation of Exact Gaussian Basis Methods to the Dephasing Representation: Theory and Application to Time-Resolved Spectra*, J. Chem. Phys. **139**, 034112 (2013).
15. T. Mori and T. J. Martínez, *Exploring the Conical Intersection Seam: The Seam Space Nudged Elastic Band Method*, J. Chem. Theo. Comp. **9**, 1155-1163 (2013).

Understanding Photochemistry using

Extreme Ultraviolet and Soft X-ray Time Resolved Spectroscopy

Markus Gühr, SLAC National Accelerator Laboratory, 2575 Sand Hill Road, Menlo Park, CA 94025
mguehr@slac.stanford.edu

Scope of the program

The scientific scope of this early career program is the site specific probing of chemical processes. For this purpose, we use light in the extreme ultraviolet (EUV) and soft x-ray (SXR) spectral range providing the site specificity due to the distinct absorption and emission features of core electrons. We are especially interested in non-Born-Oppenheimer approximation (non-BOA) dynamics, because of its importance for light harvesting [1], atmospheric chemistry [2] and DNA nucleobases photoprotection [3]. We use three different technical approaches for our studies: Laboratory based high harmonic generation (HHG) sources in the range of 20-100 eV delivering pulses with a few femtoseconds duration, synchrotrons with a wide spectral range from the EUV to the high SXR and the Linac Coherent Light Source (LCLS) providing high pulse energy femtoseconds pulses in the soft and hard x-ray range.

Progress in 2012/2013

Interpretation of LCLS experiment on nucleobase photoprotection

(together with the nucleobase photoprotection collaboration [4], see refs. A, B, C)

We introduced a new experimental method called "delayed ultrafast x-ray induced Auger probing" (DUXAP) to monitor the photoprotection mechanism of isolated nucleobases. In this scheme, a molecule is photoexcited with an ultrashort laser pulse and subsequently core ionized by a soft x-ray (SXR) pulse. The latter leads to immediate Auger relaxation and we analyze the energy dispersed Auger electrons as a function of delay between the ultrashort UV excitation and the SXR probe pulses. The element and site specific probing by soft x-ray pulses in combination with Auger electron detection can resolve non-BOA processes in isolated molecules, even for cases that are not easily resolved by traditional ultrafast experiments. In addition, the DUXAP method is well suited for self amplified spontaneous emission (SASE) lasers like the LCLS, since Auger electrons kinetic energy does not fluctuate in correlation to the photon energy.

We prove the strength of the DUXAP method on the example of the nucleobase thymine. Thymine shows an electronic relaxation process out of the directly photoexcited $\pi\pi^*$ state. This relaxation contributes to the protection of DNA from damaging ultraviolet-induced chemistry. All optical, time-resolved ion and photoelectron measurements on isolated molecules aimed at attributing a time constant to the electronic relaxation. They all showed a very short, ~100 fs, decay constant followed by additional 5-7 ps decay [5]. The time constants are generally consistent with calculations of the potential energy surface [6]. However, the assignment of the transients in to electronic or nuclear relaxation varies among theoretical approaches, and it depends strongly on the reaction barrier in the $\pi\pi^*$ state which is particularly sensitive to the chosen quantum chemical details. The thymine photochemistry clearly represents a difficult case for theory and experiment, motivating further ultrafast experimental studies. The SXR pulses used in our investigation are capable of core-ionizing the molecule in any nuclear geometry and thus the integrated Auger signal persists upon nuclear relaxation on the $\pi\pi^*$ state. In addition, we show that Auger spectroscopy allows for experimental separation of electronic and nuclear relaxation. Nuclear relaxation on $\pi\pi^*$ shows a spectral shift towards higher Auger kinetic energies. In contrast, electronic relaxation (to the $n\pi^*$ state) manifests itself as a shift towards lower kinetic energies (see below).

We succeed to attribute different spectral regions to electronic states of the molecule. The fastest signals must be related to the depletion of the ground state and the creation of an initial wave packet in the $\pi\pi^*$ excited state. The fastest feature in the DUXAP spectrum in Fig. 1 shows a spectral shift from towards higher kinetic energies, and must be related to the population of the $\pi\pi^*$ state immediately after the interaction with the UV pulse. The subsequent signal ~200 fs decay in the 505-513 eV region reflects an electronic relaxation out of the $\pi\pi^*$ state. We exclude nuclear relaxation as the process behind this feature as nuclear relaxation lead would lead to a further blueshift, as shown by calculations as well as the following general arguments about the binding energy of dicationic states. Dicationic states (having two valence holes), as produced by Auger decay, generally have a lower bond strength and therefore a lowered energy for increasing bond lengths along the reaction coordinate. The decrease in energy during nuclear relaxation is weaker for core-ionized states with full valence population. Thus the energy difference between the core-ionized state and the dicationic final state

increases along the reaction coordinate. We attribute the redshift of the Auger spectrum setting in after 200-300 fs (see rise around 490 eV in Fig. 1) to a population of the $n\pi^*$ state, based on our Auger decay simulations from electronically excited states.

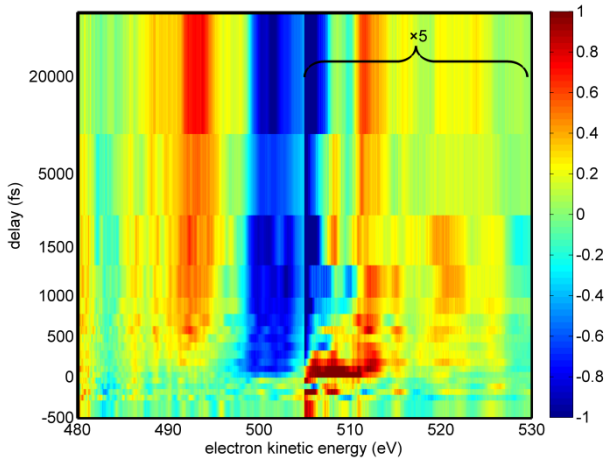

Fig.1: a) Difference Auger spectra $D(delay,E_{kin})=Signal(UV_{on})-Signal(UV_{off})$ as function of Auger electron kinetic energy and time delay between UV pump and soft x-ray probe pulse, color code: blue: UV induces less Auger decay, red: UV induces more Auger decay. The region between 505 and 530 eV is scaled by a factor of 5 for better visibility.

We have directly measured the product state for nucleobase photoprotection in the isolated molecule. We estimate the $\pi\pi^*$ non-BOA decay time to be 200 fs and from the comparison to simulations we deduce a transient increase in the $n\pi^*$ state on a similar timescale.

Determining the metal-ligand character of photolines in metalorganic complexes

(Emily Sistrunk, Jakob Grilj see ref. D)

Resonant photoemission in transition metal atoms and transition metal-containing molecules has been a topic of close study since the first observation of resonant photoemission in Ni metal. As the photon energy is swept through resonance with the np→nd absorption threshold, a Fano resonance is observed in the nd electron emission signal. This results from the interference of the Auger electron emitted in the np core hole decay with the photoelectron directly emitted from one of the nd states. We use the Fano modulation to quantify the degree of iron-ligand mixing in the molecular orbitals.

The photoelectron spectrum in Fig. 2a shows features associated with different electron continua, associated with orbitals in Koopmans approximation. Figure 2b and c show the Fano resonances in the photoelectron spectra at the iron M-edge of iron-pentacarbonyl ($FeCO_5$). We use a generalized resonant photoemission formulation whereby we extract the strength of the Auger process from the Fano resonances. Since the Auger matrix element is proportional to the overlap between the iron 3p core and the valence orbital showing the Fano resonance, we can deduce the iron character of the orbital. The large modulation in b) belongs to orbitals that are mostly of iron 3d character. The modulation in c) is much smaller, nevertheless we can deduce the amount of iron commixing in the respective orbitals. In that way we succeed to attribute the photolines to orbitals that were not previously considered in the literature.

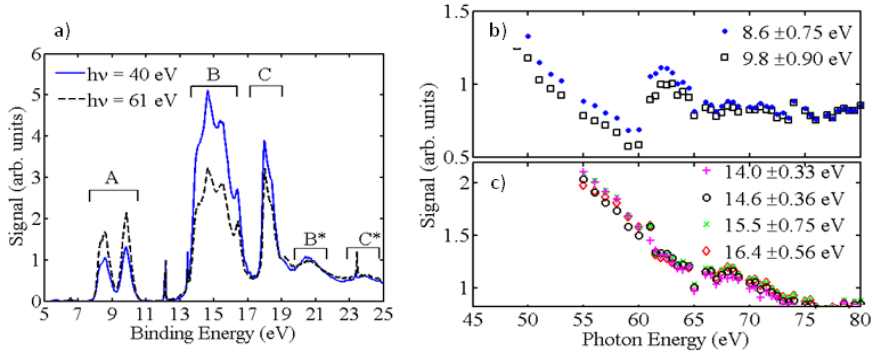

Fig. 2: a) Electron emission spectra of $Fe(CO)_5$ at photon energies of 40 and 61 eV, normalized to the Xe $5P_{3/2}$ line. The sharp peaks at 12.1, 13.4 and 23.3 eV are xenon lines used for calibration and normalization. The peaks in band A are mainly Fe 3d in character, while those in bands B and C are typically attributed to the ligands. Bands B* and C* correspond to shake-up satellites of bands B and C. **b,c)** . Integrated signal of photolines in each of the three bands as a

function of photon energy. The Fano resonance at 61 eV is clearly visible for band A in the photoelectron spectrum (shown in b). Band B in the photoelectron spectrum shows no or reduced Fano profiles (shown in c) which results from the iron character of the respective orbitals giving rise to the photoline. We use the Fano modulation to quantify the iron character in an orbital responsible for a photoline.

Transient grating spectroscopy in the extreme ultraviolet

(Jakob Grilj, Emily Sistrunk)

We have set up a new laser laboratory in Room 101, Bldg. 40 of the SLAC campus. In the past year we commissioned a high harmonic source and started first time resolved experiments.

We use pulses in the near ultraviolet range to excite molecular valence electrons which results in a coupled electron-nuclear dynamics. We are especially interested in compounds containing transition metals, as their photochemistry involves non-BOA dynamics relevant for light harvesting processes. The 3d transition metal M-edges are located in the EUV spectral region and allow us to probe the metal center view of the valence electron and nuclear dynamics via transient absorption spectroscopy.

Currently we are working on transient grating spectroscopy with EUV probe pulses. Transient gratings allow an alternative view on chemical processes compared to absorption spectroscopy because of its intrinsic sensitivity on additional *dispersive* properties of the sample. So far, there are no demonstrations of EUV diffraction from a transient grating.

a) b)

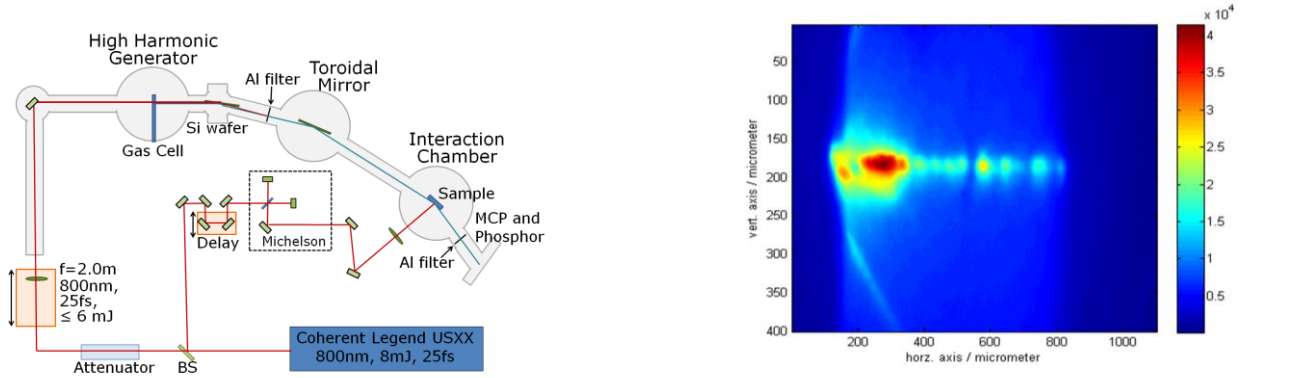

Fig. 3: a) Experimental setup for a transient grating experiment probed with EUV pulses. A pair of infrared pulses from a Michelson interferometer creates a transient grating on a semiconductor sample. The EUV pulse generated in a harmonic source is scattered off the grating and detected in a multi channel plate (MCP.) **b)** The image of the scattered EUV light from a *permanent* grating burnt on the sample by our laser, consisting of several harmonics and various diffraction orders.

Figure 3a shows an overview of the setup. We generate a transient grating on a vanadium dioxide (VO_2) sample by two pulses with slightly different angles from a Michelson interferometer. The VO_2 shows a laser induced insulator to metal transition (IMT) with controversial interpretations. For this sample we are collaborating with H. Durr/Alex Gray at PULSE/SIMES. We probe the IMT by diffracting a EUV pulse, generated in a high harmonic source. Figure 3b shows a permanent grating in a sample and we are currently recording first time resolved data.

Extreme ultraviolet time resolved photoion/electron spectroscopy

(Markus Koch)

In addition to the setup shown in Fig. 3a, we also have built a photoion/photoelectron spectrometer for time resolved spectroscopy. For unambiguous identification of ionization channels, the broadband harmonic continuum needs to be narrowed, which we accomplish using a combination of metal filters and mirrors. For isolation of the 9th harmonic (14 eV), we currently use a combination of an In filter with Al mirror. To reach higher photon energies, we specified multilayer optics.

The photoion spectrometer has been calibrated and tested with various atomic gases and perylene as a molecular species. The resolution of the spectrometer is better than 1/250 mass units when operated with 800 nm laser pulses in the multiphoton ionization regime.

Figure 4 shows first time resolved results obtained with the new extreme ultraviolet photoion spectrometer. We used 400 nm pulses to excite the S1 state of perylene (its geometry is shown in the inset). The 9th harmonic serves as the probe

pulse. We show parent ion and identify a transient rise in both channels demonstrating temporal and spatial overlap and allowing for determining the cross correlation time of the two pulses in the range of 100 fs. This can be improved by correct dispersion management in the future.

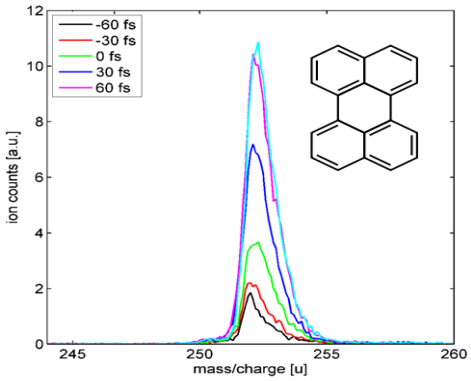

Fig. 4: Parent ion yield of perylene as a function of pump-probe delay between a 400 nm pulse exciting the S1 state and a 9th harmonic (hv=14eV) pulse ionizing the molecule. The parent ion transiently rises with increasing delay, indicating the cross correlation time of the two pulses of about 100 fs.
Smaller fragments (not shown here) show much less pump-probe modulation in the range of a few percent.

The photoelectron spectrometer is operated in a magnetic bottle mode with permanent magnet and solenoid coil. We have so far worked on its characterization and calibration using above threshold ionization (ATI) and photoemission of Xe with 14 eV radiation.

Future plans: We aim at investigating molecular non-BOA dynamics with time resolved photoion/electron spectroscopy using EUV pulses. Moreover we will use EUV transient grating/absorption spectroscopy for that purpose. In addition we apply for LCLS beamtime to perform SXR absorption spectroscopy on nucleobses.

Peer reviewed publications of this task:

A) Delayed Ultrafast X-ray Auger Probing (DUXAP) of Nucleobase Ultraviolet Photoprotection
B. K. McFarland, J. P. Farrell, S. Miyabe, F. Tarantelli, A. Aguilar, N. Berrah, C. Bostedt, J. Bozek, P.H. Bucksbaum, J. C. Castagna, R. Coffee, J. Cryan, L. Fang, R. Feifel, K. Gaffney, J. Glownia, T. Martinez, M. Mucke, B. Murphy, A. Natan, T. Osipov, V . Petrovic, S. Schorb, Th. Schultz, L. Spector, M. Swiggers, I. Tenney, S. Wang, W. White, J. White, M. Gühr, submitted (2013)
Earlier preprint of this paper on arXiv:1301.3104 [physics.chem-ph]
B) Experimental strategies for optical pump- soft x-ray probe measurements at the LCLS
B. K. McFarland, J. P. Farrell, S. Miyabe, F. Tarantelli, A. Aguilar, N. Berrah, C. Bostedt, J. Bozek, P.H. Bucksbaum, J. C. Castagna, R. Coffee, J. Cryan, L. Fang, R. Feifel, K. Gaffney, J. Glownia, T. Martinez, M. Mucke, B. Murphy, A. Natan, T. Osipov, V . Petrovic, S. Schorb, Th. Schultz, L. Spector, M. Swiggers, I. Tenney, S. Wang, W. White, J. White, M. Gühr, submitted to J. Phys. B Conference Proceedings (2013)
C) Probing nucleobase photoprotection with soft x-rays
B. K. McFarland, J. P. Farrell, S. Miyabe, F. Tarantelli, N. Berrah, C. Bostedt, J. Bozek, P.H. Bucksbaum, R. Coffee, J. Cryan, L. Fang, R. Feifel, K. Gaffney, J. Glownia, T. Martinez, M. Mucke, B. Murphy, A. Natan, T. Osipov, V . Petrovic, S. Schorb, Th. Schultz, L. Spector, I. Tenney, S. Wang, W. White, J. White, M. Gühr,
Ultrafast Proceedings, EJP Web of Conferences 41, 07004 (2013)
D) Resonant Photoemission at the iron M-edge of $Fe(CO)_5$, E. F. Sistrunk, J. Grilj, B. K. McFarland, J. Rohlen, A. Aguilar, M. Gühr, in review at J. Chem. Phys. (2013)
E) Getting molecular electrons into motion, M. Gühr, Science **335**, 1314 (2012)

References:

[1] C. C. Hu, and K. Schulten, Physics Today **50**, 28 (1997).
[2] Dermota T. E., A. P. Hydutsky, N. J. Bianco, et al., J. Phys. Chem. A **109**, 8259 (2005).
[3] C. E. Crespo-Hernandes *et al.*, Chem Rev **104**, 1977 (2004).
[4] LCLS Nucleobase photoprotection collaboration: J. P. Farrell[1,2], B. K. McFarland[1], N. Berrah[3], C. Bostedt[4], J. Bozek[4], P.H. Bucksbaum[1,2], R. Coffee[4], J. Cryan[1,2], L. Fang[3], R. Feifel[5], K. Gaffney[1], J. Glownia[1,2], T. Martinez[1,6], M. Mucke[5], B. Murphy[3], S. Miyabe[1,6], A. Natan[1], T. Osipov[3] , V . Petrovic[1,2], S. Schorb[4], Th. Schultz[7], L. Spector[1,2], F. Tarantelli[8], I. Tenney[1,2], S. Wang[1,2], W. White[4], J. White[1,2], M. Gühr[11] *PULSE, SLAC National Accelerator Lab, [2] Physics and Applied Physics, Stanford University, [3] Western Michigan University, [4] LCLS, SLAC National Accelerator Lab, [5] Uppsala University, Uppsala, Sweden, [6] Chemistry, Stanford University[7] Max-Born-Institut, Germany, [8]Universita di Perugia, Italy*
[5] Kang, H.et al. *J. Am. Chem. Soc.* 124, 12958 (2002); Canuel, C. *et al. J. Chem. Phys.* 122, 074316 (2005); Gonzalez-Vasquez, J.et al. *Phys. Chem. Chem. Phys.* 11, 3927 (2009); Ullrich, S., Schultz, T., Zgierski, M. Z. & Stolow, A, *Phys. Chem. Chem. Phys.* 6, 2796 (2004). [5] S. A. Trushin, K. Kosma, W. Fuss, and W. E. Schmid, Chem. Phys. **347**, 309 (2008).
[6] H. R. Hudock, B. G. Levine, A. L. Thompson, *et al.*, J. Phys. Chem. A **111**, 8500 (2007); M. Merchan, R. Gonzalez-Luque, T. Climent, L. Serrano-Andres *et al.*, J.Phys. Chem. B **110**, 26471 (2006); S. Perun, A. L. Sobolewski, and W. Domcke, J. Phys. Chem. A **110**, 13238 (2006).

University Research Summaries
(by PI)

Tracing and Controlling Ultrafast Dynamics in Molecules

Principal Investigator: Andreas Becker

JILA and Department of Physics, University of Colorado at Boulder,
440 UCB, Boulder, CO 80309-0440

andreas.becker@colorado.edu

Introduction

Recently, various sources of ultrashort intense laser pulse sources have been developed, which operate at wavelengths ranging from the ultraviolet to the X-ray regime. The laser fields are generated as isolated pulses or trains of pulses with durations as short as a few tens of attoseconds. This development enables us to monitor and control the coupled dynamics of electrons and nuclei in atoms and molecules and study how light can be used to control chemical reactions at the level of electrons. In this project we provide theoretical support for ongoing and future experimental studies of electron dynamics and the energy exchange between electronic and nuclear degrees of freedom on their natural time scale using the whole variety of laser light sources which are now available.

Recent Progress and Future Goals

Our activities in the project can be summarized in the following sub-projects.

A. Enhancement of vibrational excitation and dissociation of H_2^+ at infrared laser wavelengths

The recent development of intense laser systems operating in the infrared (up to about 5 μm) renewed the theoretical interest in exploring atomic and molecular strong-field phenomena in this wavelength regime. Since the corresponding photon energies are of the same order as the vibrational energy spacings in molecules, one can expect new insights into the coupling of electronic and nuclear dynamics from studies with infrared lasers. Based on earlier experimental observations [1,2], it was concluded that strong laser pulses cannot induce a significant vibrational excitation and dissociation of a diatomic molecule without ionizing the molecule, unless the laser pulse is chirped to account for the anharmonicity of the molecular vibrations [3].

We revisited this aspect of strong-field molecular dissociation and found the surprising result that the ratio of dissociation to ionization signals is reversible in certain wavelength and intensity regimes using a few-cycle laser pulse without any chirp [DOE1]. Results of our numerical simulations for the hydrogen molecular ion, supported by model calculations, revealed that there is an orders of magnitude enhancement of vibrational excitation and dissociation at certain (mid-)infrared wavelengths. In particular, at wavelengths of about 12 μm our theoretical predictions show a dissociation probability of 10% for laser intensities in the mid of 10^{13} W/cm^2. This signal exceeds the dissociation probabilities at near-infrared wavelengths and the ionization probabilities at the same laser parameters by orders of magnitude. The enhancement of the dissociation probability is accompanied by a strong population of the excited vibrational levels in the hydrogen molecular ion, which shows that the dissociation proceeds via vibrational excitation of the molecule and not via a transition from the ground state to the first excited electronic state at the equilibrium distance.

The origin of the enhancement of the vibrational excitation is related to two- and higher-order photon transitions between different vibrational levels of the molecular ion. As shown previously in this project [DOE2], such transitions between (Stark-shifted) vibrational states become effective and can be controlled at wavelengths, at which the energy difference between vibrational levels equals an even multiple of the photon energy. Correspondingly, we observe for the hydrogen molecular ion strong excitations at 5-6 μm and 10-12 μm. At the shorter wavelengths there is a strong coupling between the ground state and one of the excited vibrational state levels, but no further efficient transfer of the excitation energy to higher vibrational levels and, therefore, a rather small probability for dissociation is found. In contrast, at the longer wavelengths rapid excitation of several vibrational levels is found, in particular at about 12 μm, at which we also observe the largest dissociation probabilities. In view of the fact that the excitation occurs within a few cycles of the electric field of the laser we concluded that there has to be a transfer of energy directly from the ground state to several excited vibrational levels as well as an efficient energy transfer between the different vibrational excited levels, which results in a rapid excitation of high vibrational states and finally in the dissociation of the molecule.

Previously, we studied the mechanism of the rapid energy transfer within a two-level model [DOE1,DOE2]. Since the results of our numerical simulations indicate that several vibrational levels may be excited at the same time, we currently extend our model to incorporate more levels in the model calculations. This will provide us in future with the opportunity to further analyze the relative importance of adiabatic vs. nonadiabatic energy transfer as well as the role of the Stark shift on vibrational levels in an ultrashort laser pulse at infrared laser wavelengths. Furthermore, we currently extend our numerical code to include the calculation of higher-order harmonic generation. We are, in particular, interested in the question whether or not this rapid dissociation mechanism may prohibit the efficient generation of higher harmonics from molecules in certain wavelength and intensity regimes.

B. Analysis of time delays in light induced ionization

The development of attosecond laser pulse technology makes it possible to study the electron dynamics in quantum processes, such as photoionization, on an unprecented time scale. For example, in the attosecond streak camera technique [4] the momentum of the photoelectron, emitted due to the interaction with an ultrashort XUV pulse, is varied by superimposing a weak near-infrared laser field, which is applied at a variable time delay with respect to the ionizing XUV laser pulse. Observations of temporal offsets in streaking patterns, which are recorded as a function of time delay between the two pulses, for photoelectrons from different shells of an atom led to the question whether or not the photoemission occurs instantaneously upon application of the XUV laser pulse [5]. In the theoretical analysis the observed temporal offset is often related to the Wigner-Smith time delay [6,7], that measures the delay of an electron propagating in a potential towards infinity as compared to a freely propagating electron. Such an assumption however promptly provokes the concern that the Wigner-Smith time delay diverges for any long-range interaction [7], such as the Coulomb potential in the reported experimental studies.

We contributed to the ongoing theoretical debate by investigating the following two aspects. First, we presented a theoretical approach in which we extended the previous time-independent time delay concept to time-dependent applications in the analysis of ultrashort processes [DOE3,DOE4]. We further demonstrated how the concept can be applied in ab-initio numerical simulations to calculate time delays in photoionization. We have shown that

a time delay (for any potential) can be well-defined for the propagation of the electron over any finite region in space (in contrast to the Wigner-Smith time delay which may diverge). This time delay can be e.g. used to analyze the effect of a finite streaking pulse on the propagation of the photoelectron.

Besides the development of this general time-dependent time delay concept, which is however not directly related to the observed temporal offsets, we also studied the streaking measurements itself. We showed that the observed temporal offsets are accumulated over a finite range in space, which the emitted photoelectron probes after its transition into the continuum until the streaking pulse ceases [DOE5]. This finite-range time delay results from the coupling of the atomic potential and the streaking field and strongly depends on the parameters, in particular the duration, of the streaking field. We have further shown that the observed temporal offsets can be represented as an integral or sum over piecewise field-free time delays weighted by the ratio of the instantaneous streaking field strength relative to the field strength at the instant of ionization.

We currently study further aspects of the streaking time delay measurements, among these are the role of the shape of the streaking pulse on the observations as well as its application to image extended molecular systems. Furthermore, we plan to extend our studies to other processes, e.g. multiphoton ionization or the previously studied control schemes of few-photon ionization of atoms and molecules [DOE6].

C. Attosecond laser-driven intramolecular electron dynamics

We further continued our studies of the laser-driven electron dynamics in small molecules. Our previous studies of multiple ionization bursts in linearly polarized laser pulses [8] and a delayed photoemission of the electron in circularly polarized fields [DOE7] are now discussed together with a general overview in a review paper [DOE8]. The detailed analysis related these effects, observed and predicted for the hydrogen molecular ion, to a simple two-level model [9]. We therefore expect that the general features of the electron dynamics found for H_2^+ hold for other molecules with pair(s) of quasi-degenerate charge resonant states as well. In a linear H_3^{2+} model system, in which the electron dynamics is restricted along the molecular axis, there exists a pair of quasidegenerate charge resonant states, in which the electron is predominantly localized at the outer two of the three protons. Our results show that at low intensities the electron distribution is driven adiabatically between the two protons, while at higher intensities we observe a change to a nonadiabatic dynamics, which is in qualitative agreement with our expectations [DOE9].

Interestingly, we also observe a decrease in the amplitude of the oscillation of the electron distribution at higher intensities which is – according to preliminary results – accompanied with a suppression of the so-called enhanced ionization effect. We currently investigate this suppression systematically with the goal to make quantitative predictions for the ion yields and saturation intensities.

Publications of DOE sponsored research

[DOE1] A. Picon, A. Jaron-Becker, and A. Becker, *Enhancement of vibrational excitation and dissociation of H_2^+ in infrared laser pulses,* Phys. Rev. Lett. **109**, 163002 (2012)

[DOE2] A. Picon, J. Biegert, A. Jaroń-Becker, and A. Becker, *Coherent control of the vibrational state population in a nonpolar molecule,* Phys. Rev. A **83**, 023412 (2011).

[DOE3] J. Su, H. Ni, A. Becker and A. Jaron-Becker, *Numerical simulation of time delays in light induced ionization*, Phys. Rev. A **87**, 033402 (2013)

[DOE4] J. Su, H. Ni, A. Becker and A. Jaron-Becker, *Theoretical analysis of time delays and streaking effects in XUV photoionization*, Journal of Modern Optics (published online: http://www.tandfonline.com/doi/full/10.1080/09500340.2013.778342#.UjMtZD-Wk-A)

[DOE5] J. Su, H. Ni, A. Becker and A. Jaron-Becker, *Finite-range time delay in numerical streaking experiments*, Phys. Rev. A **88**, 023413 (2013)

[DOE6] J. Su, S. Chen, A. Jaroń-Becker and A. Becker, *Temporal analysis of nonresonant two-photon coherent control involving bound and dissociative molecular states*, Phys. Rev. A **84**, 065402 (2011).

[DOE7] M. Odenweller, N. Takemoto, A. Vredenborg, K. Cole, K. Pahl, J. Titze, L.Ph.H. Schmidt, T. Jahnke, R. Dörner and A. Becker, *Strong-field electron emission from fixed in space H_2^+*, Phys. Rev. Lett. **107**, 143004 (2011).

[DOE8] A. Becker, F. He, A. Picon, C. Ruiz, N. Takemoto and A. Jaroń-Becker, *Observation and control of electron dynamics in molecules* (invited), in *Attosecond Physics: Attosecond Measurements and Control of Physical Systems*, ed. by L.Plaja, R. Torres, and A. Zair, Springer Series in Optical Sciences Vol.177 (Springer, Berlin-Heidelberg, 2013) p. 207-229

[DOE9] A. Becker, N. Takemoto, A. Picon, and A. Jaron-Becker, *Attosecond intramolecular electron dynamics,* EPJ Web of Conferences **41**, 02008 (2013)

References

[1] S.L. Chin, Y. Liang, J.E. Decker, F.A. Ilkov, and M.V. Ammosov, J. Phys. B **25**, L249 (1992).

[2] N. Bloembergen and A.H. Zewail, J. Phys. Chem. **88**, 5459 (1984).

[3] S. Chelkowski, A.D. Bandrauk, and P.B. Corkum, Phys. Rev. Lett. **65**, 2355 (1990)

[4] J.Itatani, F.Quere, G. L. Yudin, M. Y. Ivanov, F. Krausz, and P. B. Corkum, Phys. Rev. Lett. **88**, 173903 (2002)

[5] M. Schultze et al., Science **328**, 1658 (2010).

[6] E. P. Wigner, Phys. Rev. **98**, 145 (1955).

[7] F. T. Smith, Phys. Rev. **118**, 349 (1960)

[8] N. Takemoto and A. Becker, Phys. Rev. Lett. **105**, 203004 (2010)

[9] N. Takemoto and A. Becker, Phys. Rev. A **84**, 023401 (2011)

Probing Complexity using the LCLS and the ALS

Nora Berrah
Physics Department, Western Michigan University, Kalamazoo, MI 49008
e-mail:nora.berrah@wmich.edu

Program Scope

The goal of our research program is to investigate *fundamental interactions between photons and molecular systems* to advance our quantitative understanding of electron correlations, charge transfer and many body phenomena. Our research investigations focus on probing on femtosecond time-scale multi-electron interactions and tracing nuclear motion in order to understand and ultimately control energy and charge transfer processes from electromagnetic radiation to matter. Most of our work is carried out in a strong partnership with theorists.

Our current interests include: **1)** The study of non linear and strong field phenomena in the x-ray regime using the linac coherent light source (LCLS), ultra-fast x-ray free electron laser (FEL) facility at the SLAC National Laboratory. Our experiments center on probing physical and chemical processes that happen on ultrafast time scales. This is achieved by measuring and examining both electronic and nuclear dynamics subsequent to the interaction of molecules and clusters with LCLS pulses of various intensity and pulse duration. **2)** The study of dynamics and correlated processes in select molecules as well as anions with vuv-soft x-rays from the Advanced Light Source (ALS) at Lawrence Berkeley Laboratory. We present here results completed and in progress this past year and plans for the immediate future.

Recent Progress

1) Multiphoton Ionization as a Clock to Reveal Molecular Dynamics with Intense Short X-ray Free Electron Laser Pulses from the LCLS.

We have used the intensity of the LCLS X-FEL as well as its time structure to probe molecular dynamics. We have used *multi-photon* ionization, and in particular, multiple Photoionizaton (P) and Auger decay (A) cycles as an "intrinsic" clock to probe the development of the ionization and fragmentation dynamic of molecules. In other words, we can regard the multiple PA cycles as a pump-multiple probe scheme, by sequential absorption, within one single x-ray pulse. This scheme should be applicable for any system and used this methodology in the case of N_2.[1] We measured multiple ionization leading to molecular fragmentation and fully stripped N atom, through multiple core-level photoabsorption and subsequent Auger decay processes induced by intense, short x-ray free electron laser pulses. The timing dynamics of the photoabsorption and dissociation processes is mapped onto the kinetic energy of the measured atomic fragments ions. The latter allow us to map out the average internuclear separation for every molecular photoionization sequence step and obtain the average time interval between the photoabsorption events. Using multiphoton ionization as a tool of the multiple-pulse pump-probe scheme, we demonstrated the modification of the ionization dynamics as we vary the x-ray laser pulse duration from 280, 110 and 80 fs. We also examined the ionization of the molecules throughout the spatial FEL beam profile [1].

2) Single-Photon Multiple Detachment in Fullerene Negative Ions: Absolute Ionization Cross Sections and the Role of the Extra Electron

Anions are strongly correlated systems presenting differences both qualitatively and quantitatively compared to neutral and positive ions. This sometimes dramatic difference in

behavior arises from the different binding potential in negative ions. In contrast to the Coulomb potential (proportional to r^{-1}, with r being the distance from the nucleus) that binds the electrons in neutral and positive atoms, negative ions are bound by an induced-dipole potential (proportional to r^{-4}) which results in dramatic differences, such as resonance structures, in the electronic structure and photodetachment dynamics.

We have measured the *singe-photon* multiple ionization of fullerene anions and compared our data to ionization of neutral fullerene. Our absolute photo-double- and photo-triple-detachment cross sections was obtained using the Ion-Photon-Beamline (IPB) at the Advanced Light Source and covered the photon energy range of 17–90 eV. The measured absolute photodetachment cross sections of C_{60}^- were found to be 2 and 2.5 times larger than those for C_{60} and appear to be compressed and shifted in photon energy as compared to neutral C_{60} ionization. Our analysis reveals that the additional electron in C_{60} primarily produces screening which is responsible for the modification of the spectrum. Both screening effects, the shift and the compression, can be quantitatively accounted for by a linear transformation of the energy axis. Applying the transformation allows us to map the neutral and negative ion cross sections onto each other, pointing out to the close relationship of correlated few-electron dynamics in neutral and negatively charged extended systems such as C_{60} molecule. In contrast, dynamics of neutral and negatively charged atoms or small molecules are typically not closely related. They have so far always shown drastic dissimilarities [2].

3) Multi-photon ionization of H_2S and fragmentation of SF_6

Sequential multiphoton *L*-shell ionization of H_2S molecule has been carried out using intense 1.25-keV x ray pulses. In the most intense part of the x-ray focal volume, an average molecule can absorb more than five photons, producing multiple *L*-shell ionization followed by the Auger process. We have treated the ionization of H_2S molecule as the photoionization of sulfur atomic ion and ignored the hydrogen atoms when predicting contributions to Auger and photoelectron spectra from charge states above S^{2+}. At the 1.2–1.3-keV x-ray photon energy used in our experiments, photoabsorption by hydrogen atoms is negligible. The pulse duration of 280 fs and an approximate 10^{17} Wcm^{-2} focal intensity, results in ion charge state up to S^{14+}. We do not however observe S^{15+}, which would have been the non-linear signature of the absorption of 2 photons by one electron [3].

We have also investigated multiphoton ionization of larger molecules, SF_6, and its subsequent fragmentation under intense x-ray FEL pulses. In this case, we observe as anticipated, highly-charged molecular and atomic ions which were absent in previous single-photon absorption experiments with synchrotron light source. We have observed fully stripped fluorine ions resulting from sequential multiphoton ionization processes with intermediate 1s electron excitation. We measured the average momentum and kinetic energy of each fragment which points toward many-body fragmentation pathways of the molecular SF_6 ions. We observed non-monotonic dependence of the kinetic energy on F charge states indicating multiphoton ionization of isolated atomic neutral fluorine or fluorine ions resultant from bond cleavages. Our results imply that the fragmentation of highly-charged molecular ions are produced at a later time during a single FEL pulse [4].

Future Plans.

The principal areas of investigation planned for the coming year are:

1a) Analyze the recent data generated during our June 2013 beamtime at the LCLS regarding the ionization of encapsulated molecules inside C_{80} cages. **1b)** Finish the analysis and interpretation of the data generated during October-November 2012 LCLS beamtimes. The experiments

consisted of measuring molecular dynamics using IR pump-XFEL probe as well as measuring double core holes in large molecules as a means to determine the structure of large molecules. **2a)** Carry out and analyze new experiment on the photodetachment of H^- using single photon ionization from the ALS. The previous data was contaminated with higher order effects from the beamline. **2b)** Carry out photodetachment experiments on the carbon anions chain.

Publications from DOE Sponsored Research

1. L. Fang, T. Osipov, B. Murphy, F. Tarantelli, E. Kukk, J.P. Cryan, M. Glownia, P.H. Bucksbaum, R.N. Coffee, M. Chen, C. Buth, and N. Berrah, "Multiphoton Ionization as a Clock to Reveal Molecular Dynamics with Intense Short X-ray Free Electron Laser Pulses", Phys. Rev. Lett., **109**, 263001 (2012).
2. R. C. Bilodeau, N. D. Gibson, C. W. Walter, D. A. Esteves-Macaluso, S. Schippers, A. Muller, R. A. Phaneuf, A. Aguilar, M. Hoener, J. M. Rost, and N. Berrah, "Single-Photon Multiple- Detachment in Fullerene Negative Ions: Absolute Ionization Cross Sections and the Role of the Extra Electro, Phys. Rev. Lett. **111**, 043003 (2013).
3. B. F. Murphy, L. Fang, M.-H. Chen, J. D. Bozek, E. Kukk, E. P. Kanter, M. Messerschmidt, T. Osipov, and N. Berrah," Multiphoton L-Shell Ionization of H2S using Intense X-ray Pulses from the LCLS Free Electron Laser" Phys. Rev. A 86, 053423 (2012).
4. T Osipov, L Fang, B Murphy, F Tarantelli, E R Hosler, E Kukk, J D Bozek, C Bostedt, E P Kanter and N Berrah, " Multiphoton ionization and fragmentation of SF_6 induced by intense free electron laser pulses", J. Phys. B: At. Mol. Opt. Phys. **46** , 164032 (2013).
5. L.J. Frasinski, V. Zhaunerchyk, M. Mucke, R.J. Squipp, M. Siano, J.H.D. Eland, P. Linusson, P.v.d. Meulen, P. Salén, R.D. Thomas, M. Larsson, L. Foucar, J. Ullrich, K. Motomura, S. Mondal, K. Ueda, T. Osipov, L. Fang, B.F. Murphy, N. Berrah, C. Bostedt, J.D. Bozek, S. Schorb, M. Messerschmidt, .M. Glownia, J.P. Cryan, R.N. Coffee, O. Takahashi, S. Wada, M.N. Piancastelli, R. Richter, K.C. Prince, and R. Feifel Phys. Rev. Lett. 111, 073002 (2013).
6. V. Zhaunerchyk, M. Mucke, P. Salén, P.v.d. Meulen, M. Kaminska, R.J. Squipp, L.J. Frasinski, M. Siano, J.H.D. Eland, P. Linusson, R.D. Thomas, M. Larsson, L. Foucar, J. Ullrich, K. Motomura, S. Mondal, K. Ueda, T. Osipov, L. Fang, B.F. Murphy, N. Berrah, C. Bostedt, J.D. Bozek, S. Schorb, M. Messerschmidt, J.M. Glownia, J.P. Cryan, R.N. Coffee, O. Takahashi, S. Wada, M.N. Piancastelli, R. Richter, K.C. Prince, and R. Feifel J. Phys. B: At. Mol. Opt. Phys. 46, 164034 (2013).
7. Bostedt, J. D. Bozek, P. H. Bucksbaum, R. N. Coffee, J. B. Hastings, Z. Huang, R. W. Lee, S. Schorb, J. N. Corlett, P. Denes, P. Emma, R. W. Falcone, R. W. Schoenlein, G. Doumy, E. P. Kanter, B. Kraessig, S. Southworth, L. Young, L. Fang, M. Hoener, N. Berrah, C. Roedig, and L. F. DiMauro, J. Phys. B: At. Mol. Opt. Phys. 46, 164003 (2013).
8. M Larsson, P Salén, P van der Meulen, H T Schmidt, R D Thomas, R Feifel, M N Piancastelli, L Fang, B Murphy, T Osipov, N Berrah, E Kukk, K Ueda, J D Bozek, C Bostedt, S Wada, R Richter, V Feyer and K C Prince "Double core-hole formation in small molecules at the LCLS free electron laser" (accepted J. Phys. B)
9. J.C. Castagna, B. Murphy, J. Bozek, and N. Berrah, "X-ray split and delay for soft x-rays at LCLS". Journal of Physics:Conference Series 425 152021, (2013).
10. 10. B. Rudek, S. Kil Son, L. Foucar, S. W. Epp, B. Erk, R. Hartmann, M. Adolph, R. Andritschke, A. Aquila, N. Berrah, et al."Ultra-Efficient Ionization of Heavy Atoms by Intense X-Ray Free-Electron Laser Pulses, Nature Photonics **6**, 865 (2012).
11. N. Berrah, L. Fang, T. Osipov, B. Murphy, E. Kukk, K. Ueda, R. Feifel, P. van der Meulen, P. Salen, H. Schmidt, R. Thomas, M. Larsson, R. Richter, K. C. Prince, J. D. Bozek, C. Bostedt, S. Wada, M. Piancastelli, M. Tashiro, M. Ehara, "Double Core-Hole Spectroscopy

for Chemical Analysis with an Intense X-Ray Femtosecond Laser" Proc. Natl. Acad. Sci., PNAS **108**, issue 41, 16912 (2011).
12. P. Salen, P. van der Meulen, H.T. Schmidt, R.D. Thomas, M. Larsson, R. Feifel, M.N. Piancastelli, L. Fang, B. Murphy, T. Osipov, N. Berrah, E. Kukk, K. Ueda, J.D. Bozek, C. Bostedt, S. Wada, R. Richter, V. Feyer and K.C. Prince, "X-ray FEL-induced Two-Site Double Core-Hole Formation for Chemical Analysis", Phys. Rev. Lett. PRL 108, 153003 (2012)
13. James P. Cryan, J. M. Glownia, Andreasson, A. Belkacem, N. Berrah, C. I. Blaga, C. Bostedt, J. Bozek, N. A. Cherepkov, L. F. DiMauro, L. Fang, O. Gessner, M. Guehr, J. Hajdu, M. P. Hertlein, M. Hoener, O. Kornilovy, J. P. Marangos, A. M. March, B. K. McFarland, H. Merdji, M. Messerschmidt, V. Petrovic, C. Raman, D. Ray, D. Reis, S. K. Semenov, M. Trigo, J. L. White, W. White, L. Young,P. H. Bucksbaum, and R. N. Coffee, **"**Molecular frame Auger electron energy spectrum from N_2" J. Phys. B: At. Mol. Opt. Phys. 45, 055601 (2012).
14. H. Thomas, A. Helal, K. Hoffmann, N. Kandadai, J. Keto, J. Andreasson, B. Iwan, M. Seibert, N. Timneanu, J. Hajdu, M. Adolph, T. Gorkhover, D. Rupp, S. Schorb, T. Möller, G. Doumy, L.F. DiMauro, M. Hoener, B. Murphy, N. Berrah, M. Messerschmidt, J. Bozek, C. Bostedt and T. Ditmire, "Explosions of Xe-clusters in ultra-intense femtosecond x-ray pulses from the LCLS Free Electron Laser", Phys. Rev. Lett. **108**, 133401 (2012).
15. Christian Buth, Ji-Cai Liu, Mau Hsiung Chen, L. Fang, M. Hoener, N. Berrah, "Ultrafast absorption of intense x rays by nitrogen molecules", J. Chem. Phys. J. Chem. Phys.136, 214310 (2012).
16. B.F. Murphy, L. Fang, T.Y. Osipov, M. Hoener, and N. Berrah, "Intense X-ray FEL-Molecule Physics: Highly Charged Ions", the American Institute of Physics (AIP) Conference Proceedings of ICAPiP, **1438**, 249 (2012).
17. V. S. Petrović, M. Siano, J.L. White, N. Berrah, C. Bostedt, J. D. Bozek, D. Broege, M. Chalfin, R. N. Coffee, J. Cryan, L. Fang, J. P. Farrell, L. J Frasinski, J. M. Glownia, M. Gühr, M. Hoener, D.M. P. Holland, J. Kim, J. P. Marangos[3], T. Martinez, B. K. McFarland, R. S. Minns, S. Miyabe, S. Schorb, R. J. Sension, L. S. Spector, R. Squibb, H. Tao, J. G. Underwood, and P. H. Bucksbaum "Transient X-ray fragmentation: Probing a prototypical photoinduced ring opening", Phys. Rev. Lett. Phys. Rev. Lett. **108**, 253006, (2012).
18. N. Berrah, R.C. Bilodeau, I. Dumitriu, D. Toffoli, and R. R. Lucchese, "Shape and Feshbach Resonances in Inner-Shell Photodetachment of Negative Ions, J. Elect. Spectr. and Relat. Phen. Kai Siegbahn Memorial Volume **183,** 64 (2011)
19. G. Doumy, C. Roedig, S.-K. Son, C. I. Blaga, A. D. DiChiara, R. Santra, N. Berrah, C. Bostedt, J. D. Bozek, P. H. Bucksbaum, J. P. Cryan, L. Fang, S. Ghimire, J. M. Glownia, M. Hoener, E. P. Kanter, B. Krässig, M. Kuebel, M. Messerschmidt, G. G. Paulus, D. A. Reis, N. Rohringer, L. Young, P. Agostini, and L. F. DiMauro, Phys. Rev. Lett. **106**, 083002 (2011).
20. E. P. Kanter, B. Krassig, Y. Li, A. M. March, N. Rohringer, R. Santra, S. H. Southworth,L. F. DiMauro, G. Doumy, C. A. Roedig, N. Berrah, L. Fang, M. Hoener, P. H. Bucksbaum, S. Ghimire, D. A. Reis, J. D. Bozek, C. Bostedt, M. Messerschmidt, L. Young, "Modifying Auger Decay with Femtosecond X-ray Pulses" Phys. Rev. Lett. **107**, 233001 (2011).
21. L. Fang, M. Hoener, N. Berrah, "Ultra intense x-ray induced non-linear processes in Molecular nitrogen", J. of Physics, **288,** 012019 (2011)
22. N. Berrah, R.C. Bilodeau, I. Dumitriu, D. Toffoli, and R. R. Lucchese, "Shape and Feshbach Resonances in Inner-Shell Photodetachment of Negative Ions, J. Elect. Spectr. and Relat. Phen., Kai Siegbahn Memorial Volume **183** pp 64-69. (2011)
23. Philip H. Bucksbaum, Ryan Coffee, and Nora Berrah, "The First Atomic and Molecular Experiments at the Linac Coherent Light Source X-Ray Free Electron Laser" Book Chapter, Advances in Atomic, Molecular, and Optical Physics, Volume 60, p. 240, (2011).

Ultracold Collisions of Complex Atoms and Molecules

Principal Investigator: John Bohn, JILA, NIST and University of Colorado
Address: UCB 440, University of Colorado, Boulder, CO 80305
Phone: 303-492-5426 Email: bohn@murphy.colorado.edu

1 Program Scope

In an effort to probe ever deeper into the fundamental dynamics of chemical reactions, one is faced these days with two options. One may either increase resolution in the time domain and deliberately push around molecular constituents, as in the rapidly maturing field of ultrafast dynamics; or else increase resolution in the energy domain by effectively slowing the beams, as is done in the nascent field of cold and ultracold molecules. This program is concerned with the latter approach. It seeks to address what new chemical information may be afforded by molecular gases cooled to sub-milliKelvin temperatures. In these experiments, the incident channel of the reactants can be completely specified in terms of the internal state, as well as an extremely low relative translational energy that, in favorable cases, allows probing the reactivity of a single partial wave in the incident channel.

One essential aspect that emerges with extreme energy resolution (of order peV in μK gases) is an increase in *complexity* of scattering observables. Molecules colliding in these circumstances may possess an enormous density of extremely narrow resonant states, as we will show below. In principle, these many resonances provide a wealth of information on energy transfers between the constituent atoms of the complex. This may, indeed, prove to be too much information to use meaningfully. A main goal of this program is to explore the complexity of ultracold collisions. We explore two aspects of this goal. In one, we adapt flexible methods of scattering theory to help explore and characterize resonant scattering in detail, seeking to find order and simplicity within the complexity. In a second, we embrace the complexity, seeking information not from individual resonances but rather from statistical aspects of their distribution. Essential to this goal is to understand which collision partners would benefit from which theoretical treatment.

2 Recent Progress

An exact numerical treatment of Fano-Feshbach resonances in ultracold scattering has been possible for some time, for "simple" collision partners such as alkali atoms or alkaline earth

atoms. These calculations have been made many times more efficient, and their underlying analytical structure laid bare, by applications of multichannel quantum defect theory (MQDT). Previously, this theory has been well-established for s-waves, but proved problematic for the higher partial waves that surely will be necessary for more highly anisotropic collision partners. In a recent collaboration with C. H. Greene, we have established a version of MQDT that is ideally suited to ultracold temperatures and high partial waves. An example is shown in Fig. 1.

Armed with the fast and accurate MQDT theory, we were able for the first time to identify *all* the Fano-Feshbach resonances of a given partial wave in a given magnetic field range. For example, we unearthed 31 d-wave resonances in a range 1 -1000 Gauss for collisions between potassium and rubidium atoms. Using MQDT, these resonances can be identified even though their widths may be extremely narrow. This breakthrough allows us to tabulate large datasets of resonances in realistic systems, which will in turn provide benchmarks for our statistical studies of resonance distribution.

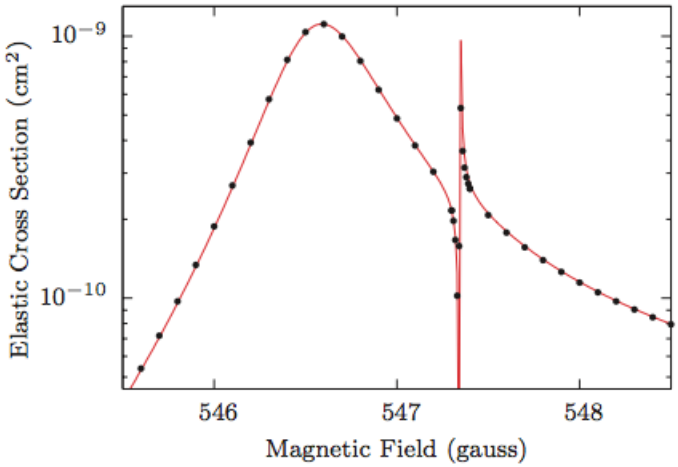

Figure 1: A triumph of the quantum defect theory. Shown is the elastic scattering cross section of K atoms and Rb atoms, as a function of magnetic field, and a collision energy of 1 μK. The solid points represent a full close-coupling calculation involving 67 coupled channels, repeated separately at each field. By contrast, the solid red curve was computed by performing *two* such calculations, at $B = 500$ Gauss and $B = 600$ Gauss. The resulting short-range scattering matrix was interpolated between these fields, and the red curve computed by trivial linear algebra. The broad feature is an s-wave resonance, while the narrow feature is a d-wave resonance. Figure from Ref. [P5].

Complementing this exact treatment, we have developed statistical viewpoints for scattering of much more complicated objects, such as alkali dimers. The significant new feature here is that these molecules are believed to possess a very high density of ro-vibrational resonance states, estimated to be of order mK^{-1} for atom-molecule, and of order nK^{-1} for molecule-molecule scattering. The resonances are sufficiently numerous that a direct calculation, no matter how thorough, is unlikely to describe these states accurately. However, given a model that incorporates the density of states and appropriate energy-level statistics, the MDQT

theory provides a means of faithfully turning these into real scattering observables. In this way we applied, for the first time, statistical resonance theories familiar in nuclear physics to the ultracold regime. For example, individual resonances were shown to meld into "Ericson fluctuations" by the simple expedient of altering a single nuclear spin.

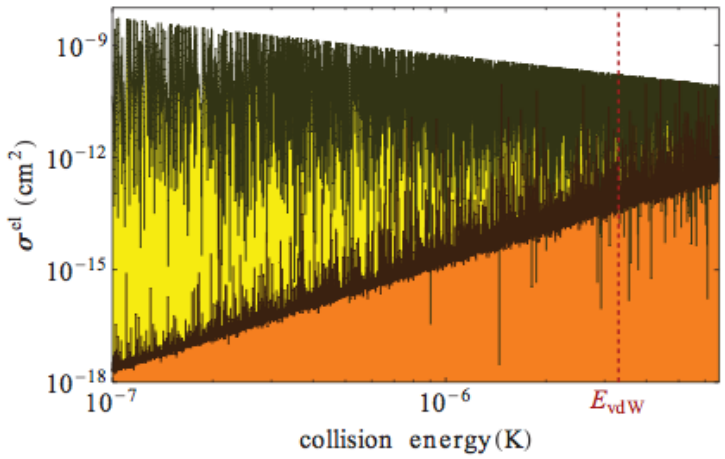

Figure 2: Simulated resonance spectrum of cold collisions of RbCs molecules with each other. Shown is the elastic scattering cross section versus collision energy in s-wave (yellow) and d-wave (orange) channels. These resonances should not be experimentally resolvable, even in an ultracold gas. Observables are therefore necessarily averages over many such resonances, leading to a mean "sticking rate" of the molecules. Figure from Ref. [P4].

For the case of molecule-molecule scattering, we predict that the density of states is far too high to be experimentally resolved, see Figure 2. However, a striking observable effect should nevertheless emerge. Namely, in a dense forest of extremely narrow resonances such as this, resonant collisions should lead to a "sticking rate" whereby molecules cling together in a four-body complex for some mean lifetime τ (inversely proportional to resonance width) before falling apart again into molecules. For heavier alkali atoms such as RbCs, this time can be of order tens of milliseconds. At any given time, therefore, some fraction of the molecules are locked away in these complexes, and can serve as an novel objects of study themselves. Additionally, these complexes, if struck by another molecule, will likely relax by a kind of delayed three-body-recombination mechanism, leading to trap loss.

This is an entirely unanticipated and vital prediction for the field of ultracold molecules. Heretofore it was assumed that if the molecules are not chemically reactive, then they are stable against two-body collisions in a trap. The sticking argument implies, to the contrary, that such molecules are not as safe as once believed. Interestingly, preliminary data from the Nagerl group at Innsbruck has seen loss of Cs_2 molecules on precisely the tens of msec time scale predicted by the theory, which may be evidence for the highly resonant scattering we predict.

3 Future Plans

Both areas of exploration will continue in the near future. On the MQDT side, we have developed and are implementing a perturbation theory that will enable us to include the effect of long-range forces such as dipole-dipole or quadrupole-quadrupole forces. This is expected to make the MQDT theory completely quantitative for a wide variety of collision partners. An initial goal will be to exploit the theory to interpret scattering data in ultracold erbium, where Fano-Feshbach rseonances have been observed with an enormous density of states, of order 1 per Gauss (F. Ferlaino, private communication). An accurate MQDT treatment will enable detailed studies of statistics of these resonance, and their reliance on details on the underlying potential energy surface. In a new development, we are also opening a collaboration with B. Naduvalath at UNLV, to apply MQDT to ultracold collisions of H_2 molecules. This work will serve as a prototype for understanding magnetic-field manipulation of energy transfer in molecular scattering.

On the side of statistical analysis, we will begin to explore classical and semiclassical approaches to resonant scattering. Rather than track and label each individual resonance, this approach will explore the information content of the overall structure of the density of states. Using as a link the Gutzwiller trace formula, this approach will connect large-scale features of the density of states function to short-time classical orbits on the potential energy surface, and thereby illuminate this surface itself and the motion on it. Initial studies of this sort will also apply to erbium collisions, with an eye soon thereafter to molecular scattering.

4 DOE-supported Publications in the last three years

[P1] Anisotropic Superfluidity in a Dipolar Bose Gas
C. Ticknor, R. M. Wilson, and J. L. Bohn, Phys. Rev. Lett. 106, 065301 (2011).

[P2] Emergent Structure in a Dipolar Bose Gas in a One-Dimensional Lattice
R. M. Wilson and J. L. Bohn, Phys. Rev. A 83, 023623 (2011).

[P3] Statistical Aspects of Ultracold Resonant Scattering
M. Mayle, B. P. Ruzic, and J. L. Bohn, Phys. Rev. A 85, 062712 (2012).

[P4]Scattering of Ultracold Molecules in the Highly Resonant Regime
M. Mayle, G. Quéméner, B. Ruzic, and J. L. Bohn, Phys. Rev. A 87, 012709 (2013).

[P5] Quantum Defect Theory for High Partial Wave Cold Collisions
B. P. Ruzic, C. H. Greene, and J. L. Bohn, Phys. Rev. A 87, 032706 (2013).

Ultrafast Electron Diffraction from Aligned Molecules

Martin Centurion
Department of Physics and Astronomy, University of Nebraska, Lincoln, NE 68588-0299
mcenturion2@unl.edu

Program Scope

The aim of this project is to record time-resolved electron diffraction patterns of aligned molecules and to reconstruct the 3D molecular structure. The molecules are aligned non-adiabatically using a femtosecond laser pulse. A femtosecond electron pulse is then used to record a diffraction pattern while the molecules are aligned. The experiment consists of a laser system, a pulsed electron gun, a gas jet that contains the target molecules and a detector to capture the diffraction patterns. The diffraction patterns are processed to obtain the molecular structure.

Introduction

The majority of known molecular structures have been determined using either x-ray diffraction for crystallized molecules or Nuclear Magnetic Resonance (NMR) spectroscopy for molecules in solution. However, for isolated molecules there has been no method demonstrated to measure the three dimensional structure. Electron diffraction has been the main tool to determine the structure of molecules in the gas phase[1] and also to investigate ultrafast changes in structure[2-4]. In this method the diffraction pattern is compared with a calculated structure iteratively until an appropriate match between experiment and theory is found. Diffraction patterns from randomly oriented molecules contain only one-dimensional information, and thus input from theoretical models is needed to recover the structure. We propose to use pulsed electron diffraction from aligned molecules to recover the three dimensional structure, and to investigate molecular dynamics.

In previous experiments, electron diffraction patterns of aligned molecules have been recorded using adiabatic alignment with long laser pulses (in this case the laser is longer than the rotational period and is present during the alignment)[5], and by selective alignment in a photo-dissociation reaction[6]. However, in both cases the degree of alignment was found to be too weak to extract structural information. Additionally, in adiabatic alignment the presence of a strong laser field can distort the molecular structure, while selective alignment relies on a change in the structure. In our experiments, the molecules are impulsively aligned with a femtosecond laser pulse and probed with femtosecond electron pulses in a field-free environment at the peak alignment. This ensures that the molecules are not distorted by the laser field when the structure is probed by the electron pulse.

Recent Progress

We have recently demonstrated, for the first time, three dimensional imaging of isolated molecules. The structure was retrieved from diffraction patterns of laser-aligned molecules [7], assuming only that the constituent atoms are known, but not their spatial distribution. In order to reach this goal, we had to overcome two major obstacles: 1. Sub-picosecond resolution was needed to capture the diffraction pattern while the molecules were aligned. Previously, the highest temporal resolution for gas phase diffraction experiments was about 3 ps [6]. We were able to reach a resolution of 850 fs by simultaneously improving on several parts of the experiments. 2. Retrieving the structure from diffraction of partially aligned molecules. Previously, all existing phase retrieval methods, to our knowledge, could only be applied to perfectly aligned molecules. Experimentally it is very difficult to achieve very high degrees of alignment, particularly because the densities needed for diffraction are higher than those of molecular beams with the sub-Kelvin temperatures needed for strong alignment. We developed a new algorithm that combines several diffraction patterns corresponding to different projections of partially aligned molecules, and then retrieves the structure.

In the experiments, the direction of the alignment laser, electron pulse and gas jet are all mutually orthogonal. A supersonic gas jet is produced by flowing a mixture of CF_3I and helium through a convergent-divergent nozzle. The laser pulses are split in two for alignment and triggering the electron pulse. A small fraction of the laser pulse energy is frequency tripled and focused on a photocathode to trigger the emission of electrons. The electrons are accelerated to 25 keV using a static electric field and collimated by a magnetic lens. The diffraction patterns are captured with the electron pulse arriving 2 ps after the laser pulse, at the peak of the alignment. The overall resolution of the experiment is 850 fs, considering velocity mismatch in the finite size interaction volume and the duration of the pulses.

First results were achieved with trifluoroiodomethane (CF_3I), a symmetric top molecule. This molecule was chosen because it has a simple 3D structure and because the presence of the iodine (high scattering cross section) makes the phase retrieval simpler. In our experiments, the laser impulsively aligns the long axis (along the C-I bond) of the molecule along the direction of laser polarization. The molecule rotates freely about the perpendicular axis, so an average over many molecules results in a cylindrically symmetric structure. It has been shown that if a diffraction pattern from perfectly aligned molecules is captured, the structure of such a molecule can be retrieved directly with a Fourier-Hankel transform [8]. This is possible because the iodine atom scatters much more strongly than the others, and the diffraction pattern can be reconstructed using a holographic approximation. However, if the degree of alignment is not perfect, this phase retrieval method method fails to reconstruct the molecule.

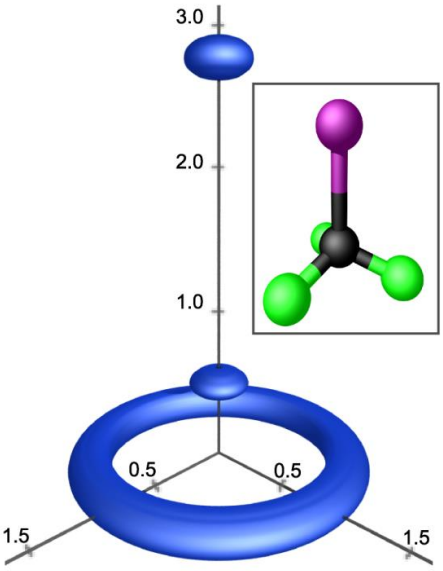

Figure 1. Experimental reconstruction of the CF_3I molecule. The CF_3I molecules rotate freely about the C-I axis, which results in a cylindrically symmetric structure. The units are in angstroms. See Methods section for details on the reconstruction. The inset shows a theoretical model of the CF_3I molecule for comparison. The fluorine atoms are colored green, carbon is black and the iodine atoms is purple.

We have developed a genetic algorithm that combines several diffraction patterns (from different orientations of the alignment axis) with a low degree of alignment to reconstruct the diffraction pattern corresponding to perfect alignment. The direction of the alignment axis can be changed continuously by rotating the direction of the linear polarization of the alignment laser. In our experiments, the degree of alignment was $\langle \cos^2 \alpha \rangle = 0.5$, where α is the angle between the long axis of the molecule and the laser polarization. Once the single-molecule diffraction pattern is constructed, we use the holographic algorithm of Ho et al. [8] to retrieve an image of the molecule. Figure 1 shows the retrieved molecular structure. The inset is a model of the molecule using the known interatomic distances. The three fluorine atoms appear as a band on the experimental reconstruction because the molecule rotates freely along the long axis. Additional knowledge, such as the number of fluorine atoms would be sufficient to fully determine the structure. All the retrieved distances and angles are accurate to better than 10%.

With this initial experiment, we showed that the diffraction patterns, even with partial alignment, contain enough information for retrieving the structure. The retrieval method, however, assumed that one of the atoms scatters much more strongly than the others and cannot be generalized easily. Other methods require a known symmetry of the molecule, and all require that the molecules be perfectly or almost perfectly aligned. We have extended our retrieval algorithm, and we have shown in simulations that we can retrieve the 3D structure of molecules with unknown symmetries from diffraction patterns of partially aligned molecules [manuscript in preparation]. This is a crucial development that will allow us to study a larger class of molecules.

We are also studying the limits of the impulsive laser-alignment method. It is known that as the intensity is increased, molecules will first be aligned, then enter a regime where there might be deformation and/or dissociation, and finally ionization and Coulomb explosion. However, there are no sharp boundaries between these regimes, and in most cases there are probably several of these effects happening simultaneously. Traditionally, different measurement would be needed to

determine the angular distribution and the changes in molecular structure. We use an intense laser pulse to align carbon disulfide (CS_2) molecules, and use short electron pulses to probe. Using diffraction to probe the molecules allows us to determine both the angular distribution and molecular structure simultaneously. We are currently taking and analyzing data to determine what is the maximum laser intensity that can be used for alignment, and what are the limiting mechanisms.

Future Plans

After this first demonstration of three-dimensional imaging we plan to apply the method to more complex molecules. The new phase retrieval method that we developed will allow us to study larger molecules. We are also constructing a new device that will produce shorter pulses and increased electron current. This will give us better signal to noise and allow us to work with lower gas densities. We also plan to use our imaging method to investigate time-resolved dynamics in molecules. An additional improvement to the setup will be a new method to deliver the target molecules. The new device will include a heater to create a molecular beam for molecules with a low vapor pressure.

References

[1] P. W. Allen and L. E. Sutton, Acta Crystallogr. 3, 46 (1950).
[2] H. Ihee, V. A. Lobastov, U. M. Gomez, B. M. Goodson, R. Srinivasan, C. Y. Ruan, and A. H. Zewail, Science 291, 458 (2001).
[3] C. I. Blaga, J. Xu, A. D. DiChiara, E. Sistrunk, K. Zhang, P. Agostini, T. A. Miller, L. F. DiMauro, and C. D. Lin, Nature 483, 194 (2012).
[4] R. Srinivasan, J. Feenstra, S. Park, S. Xu, and A. Zewail, Science 307, 558 (2005).
[5] K. Hoshina, K. Yamanouchi, T. Ohshima, Y. Ose, and H. Todokoro, J. Chem. Phys. 118, 6211 (2003).
[6] P. Reckenthaeler, M. Centurion, W. Fuss, S. A. Trushin, F. Krausz, and E. E. Fill, Phys. Rev. Lett. 102, 213001 (2009).
[7] C. J. Hensley, J. Yang, M. Centurion, Phys. Rev. Lett. 109, 133202 (2012)
[8] P.J. Ho, D. Starodub, D.K. Saldin, V.L. Shneerson, A. Ourmazd, and R. Santra, J. Chem. Phys. 131, 131101 (2009).

.

Publications of DOE sponsored research in the past 3 years

1. “Imaging of Isolated Molecules with Ultrafast Electron Pulses”, Christopher J. Hensley, Jie Yang, and Martin Centurion, Phys. Rev. Lett. 109, 133202 (2012). *This paper was featured in APS Physical Review Focus on 9/28/2012*
2. “Dispersion Compensation for Attosecond Electron Pulses”, Peter Hansen, Cory Baumgarten, Herman Batelaan, Martin Centurion, Appl. Phys. Lett. 101, 083501 (2012)

Atomic and Molecular Physics in Strong Fields

Shih-I Chu
Department of Chemistry, University of Kansas
Lawrence, Kansas 66045
E-mail: sichu@ku.edu

Program Scope

In this research program, we address the fundamental physics of the interaction of atoms and molecules with intense ultrashort laser fields. The main objectives are to develop new theoretical formalisms and accurate computational methods for *ab initio* nonperturbative investigations of multiphoton quantum dynamics and very high-order nonlinear optical processes of one-, two-, and many-electron quantum systems in intense laser fields, taking into account detailed electronic structure information and many-body electron-correlated effects. Particular attention will be paid to the exploration of the effects of electron correlation on high-harmonic generation (HHG) and multiphoton ionization (MPI) processes, multi-electron response and underlying mechanisms responsible for the strong-field ionization of diatomic and small polyatomic molecules, time-frequency spectrum, coherent control of HHG processes for the development of tabletop x-ray laser light sources, and for the exploration of attosecond AMO processes, etc.

Recent Progress

1. Coherent Control and Giant Enhancement of Multiphoton Ionization and High-Order-Harmonic Generation Driven by Intense Frequency-Comb Laser Fields

We present an *ab initio* theoretical investigation of the coherent control and significant enhancement of multiphoton ionization (MPI) and high-order-harmonic generation (HHG) of atoms and molecules by means of intense frequency-comb laser fields [1]. We show that the nonperiodically or quasi-periodically time-dependent Schrödinger equation for the frequency-comb laser excitation problem can be transformed exactly into a *time-independent* non-Hermitian generalized Floquet matrix eigenvalue problem by means of the many-mode Floquet theory [2,3] and the complex-scaling transformation. The generalized Floquet Hamiltonian can be optimally discretized and the complex quasienergy eigenvalues and eigenfunctions can be solved accurately and efficiently by means of the generalized pseudospectral method. The procedure is applied to a case study of the resonance-enhanced MPI and HHG of atomic hydrogen driven by an intense frequency-comb laser field. Our study shows that both the MPI and HHG rates can be coherently controlled by tuning the laser parameters such as the pulse-to-pulse carrier-envelope-phase (CEP) shift. In particular, both the MPI and HHG rates exhibit dramatic enhancement by tuning the CEP shift, due to the phenomenon of simultaneous multiphoton resonances [1].

2. Generation and Coherent Control of Even-Order Harmonics Driven by Intense Frequency-Comb and Cavity-Mode Fields Inside a fsEC

We present a theoretical investigation of the multiphoton resonance dynamics driven by intense frequency-comb and cavity-mode fields inside a femtosecond enhancement cavity (fsEC) [4]. The many-mode Floquet theorem [2,3] is employed to provide a nonperturbative and exact treatment of the interaction between a quantum system and laser fields. The quasienergy structure driven by the frequency-comb laser field is modified by coupling the cavity-mode field and the multiphoton resonance processes between modified quasienergy states, resulting in the generation of even-order harmonics. The high-order harmonic generation (HHG) from a two-level system driven by the laser fields can be coherently controlled by tuning the laser parameters. In particular, the tuning intensity of the cavity-mode field allows one to coherently control the HHG power spectra without changing the absolute positions of comb frequencies.

3. Precision Calculation of Above-threshold Multiphoton Ionization in Intense Short-wavelength Laser Fields: The Time-dependent Generalized Pseudospectral Method in Momentum-space

We develop a new approach in momentum (P) space for the accurate study of multiphoton and abovethreshold ionization (ATI) dynamics of atomic systems driven by intense laser fields [5]. In this approach, the electron wave function is calculated by solving the P-space time-dependent Schrödinger equation (TDSE) in a finite P-space volume under a simple zero asymptotic boundary condition. The P-space TDSE is propagated accurately and efficiently by means of the time-dependent generalized pseudospectral method (TDGPS) with optimal momentum grid discretization and a split-operator time propagator in the *energy* representation. The differential ionization probabilities are calculated directly from the continuum-state wave function obtained by projecting the total electron wave function onto the continuum-state subspace using the projection operator constructed by the continuum eigenfunctions of the unperturbed Hamiltonian. As a case study, we apply this approach to the nonperturbative study of the multiphoton and ATI dynamics of a hydrogen atom exposed to intense ultrashort wavelength laser fields. High-resolution photoelectron energy-angular distribution and ATI spectra have been obtained. We find that with the increase of the laser intensity, the photoelectron energy-angular distribution changes from circular to dumbbell shaped and is squeezed along the laser field direction. We also explore the change of the maximum photoelectron energy with laser intensity and strong-field atomic stabilization phenomenon in detail [5].

More recently, we further extend the TDGPS method in the momentum space [5] to the exploration of ATI processes of atomic H in super-intense free-electron x-ray laser fields beyond the dipole approximation [6]. We find that, compared to results of the dipole approximation, the nondipole ATI spectra are enhanced substantially in the high-energy regime, and the photoelectron angular distributions are distorted significantly in higher-intensity and/or longer-pulse laser fields. In particular two lobes are induced, one along and one against the laser propagation direction. The origin of these phenomena has been explored in detail.

4. Recent Development of Fast Algorithms for Searching Optimal Control Fields

(a) We present a general method to formulate monotonically convergent algorithms for identifying optimal control fields to manipulate quantum dynamics phenomena beyond the linear dipole interaction. The method, facilitated by a field-dependent dipole moment operator, is based on an integral equation of the first kind arising from the Heisenberg equation of motion for tracking a time-dependent, dynamical invariant observable associated with a reference control field [7].

(b) We develop a fast-kick-off two-point boundary-value quantum control paradigm (TBQCP) search algorithm for quickly finding optimal control fields in the state-to-state transition probability control problems, especially those with poorly chosen initial control fields [8] . Specifically, the local temporal refinement of the control field at each iteration is weighted by a fractional inverse power of the instantaneous overlap of the backward-propagating wave function, associated with the target state and the control field from the previous iteration, and the forward-propagating wave function, associated with the initial state and the concurrently refining control field.

(c) Recently, a single-cycle THz pulses have been demonstrated in the laboratory to induce field-free orientation in gas-phase polar molecules at room temperature [9]. In a recent article [10], we explore the maximum attainable field-free molecular orientation with optimally shaped linearly polarized near–single-cycle THz laser pulses of a thermal ensemble. Large-scale benchmark optimal control simulations are performed, including rotational energy levels with the rotational quantum numbers up to $J = 100$ for OCS linear molecules. The simulations are made possible by an extension of the recently formulated fast search algorithm, the two-point boundary-value quantum control paradigm [8], to the mixed-states optimal control problems in the present work. It is shown that a very high degree of field-free orientation can be achieved by strong, optimally shaped near–single-cycle THz pulses.

5. Coherent Control of the Electron Quantum Paths for the Optimal Generation of Single Ultrashort Attosecond Laser Pulse

We report a new mechanism and experimentally realizable approach for the coherent control of the generation of an isolated and ultrashort attosecond (*as*) laser pulse from atoms by means of the optimization of the two-color laser fields with a proper time delay [11]. Optimizing the laser pulse shape allows the control of the electron quantum paths and enables high-harmonic generation from the long- and short-trajectory electrons to be enhanced and split near the cutoff region. In addition, it delays the long-trajectory electron emission time and allows the production of extremely short attosecond pulses in a relatively narrow time duration. As a case study, we show that an isolated 30 *as* pulse with a bandwidth of 127 eV can be generated directly from the contribution of long-trajectory electrons alone.

We have then explored the optimization of three-color laser field for the generation of single ultrashort attosecond pulse [12]. We show that the plateau of high-order harmonic generation is extended dramatically and a broadband supercontinuum spectra is produced. As a result, an isolated 23 *as* pulse with a bandwidth of 163 eV can be obtained directly by superposing the supercontinuum harmonics near the cutoff region. We show that such a metrology can be realized experimentally.

More recently, we have further investigated the effect of macroscopic propagation on the supercontinuum harmonic spectra and the subsequent attosecond-pulse generation [13]. The effects of macroscopic propagation are investigated in near and far field by solving Maxwell's equation. The results show that the contribution of short-trajectory electron emission is increased when the macroscopic propagation is considered. However, the characteristics of the dominant long-trajectory electron emission (in the single-atom response case) are not changed, and an isolated and shorter *as* pulse can be generated in the near field. Moreover, in the far field, the contribution of long-trajectory electron emission is still dominant for both on-axis and off-axis cases. As a result, an isolated and shorter *as* pulse can be generated directly. Similar results are obtained when the atomic target position is changed.

6. *Ab Initio* Precision Study of High-Lying Doubly Excited States of Helium in Static Electric Fields: Complex-Scaling Generalized Pseudospectral Method in Hyperspherical Coordinates

We develop a complex-scaling (CS) generalized pseudospectral (GPS) method in hyperspherical coordinates (HSC) for *ab initio* and accurate treatment of the resonance energies and autoionization widths of two-electron atomic systems in the presence of a strong dc electric field [14]. The GPS method allows nonuniform and optimal spatial discretization of the two-electron Hamiltonian in HSC with the use of only a modest number of grid points. The procedure is applied for the first precision calculation of the energies and autoionization widths for the high-lying $^1S^e$, $^1P^o$, $^1D^e$, and $^1F^o$ (n = 10–20) doubly excited resonance states of He atoms. In addition, we present a theoretical prediction of the energies and widths of high-lying doubly excited resonance states of $^1P^o$ (n = 8–15) in external dc electric field strengths of 3.915–10.44 kV/cm. The calculated dc-field perturbed high-lying resonance energies are in good agreement with the latest experimental data.

7. Sub-cycle Oscillations in Virtual States Brought to Light

Understanding and controlling the dynamic evolution of electrons in matter is among the most fundamental goals of attosecond science. While the most exotic behaviors can be found in complex systems, fast electron dynamics can be studied at the fundamental level in atomic systems, using moderately intense ($\leq 10^{13}$ W/cm^2) lasers to control the electronic structure in proof-of-principle experiments. In cooperation with the experimental group led by Zenghu Chang, we probe the transient changes in the absorption of an isolated attosecond extreme ultraviolet (XUV) pulse by helium atoms in the presence of a delayed, few-cycle near infrared (NIR) laser pulse, which uncovers absorption structures corresponding to laser-induced ''virtual'' intermediate states in the two-color two-photon (XUV + NIR) and three-photon (XUV+ NIR + NIR) absorption process [15]. These previously unobserved absorption structures are modulated on half-cycle (~1.3

fs) and quarter-cycle (~ 0.6 fs) time scales, resulting from quantum optical interference in the laser-driven atom.

8. We have completed three invited book chapters on the recent development of *self-interaction-free* time dependent density functional theory (TDDFT) for the nonperturbative treatment of atomic and molecular multiphoton processes in intense ultrashort laser fields in the past 3 years [16-18].

Future Research Plans

In addition to continuing the ongoing researches discussed above, we plan to initiate the following several new project directions: (a) Development of time-dependent (TD)-Voronoi-cell finite difference (VFD) method for the study of MPI/HHG processes in triatomic and small polyatomic molecular systems. (b) Extension of the TDGPS method in momentum space to the study of HHG/ATI processes in intense ultrashort laser fields. (c) Development of *self-interaction-free* TDDFT with proper *derivative discontinuity* for the treatment of double ionization of complex atoms in intense laser fields [19]. (d) Development of nonperturbative methods for the accurate treatment of transient absorption and subcycle dynamics in MIR+ attosecond pulses.

References Cited (***** Publications supported by the DOE program in the period of 2011-2013).

*[1] D. Zhao, F. l. Li, and S.I. Chu, Phys. Rev. A **87**, 043407 (2013).
[2] S. K. Son and S. I. Chu, Phys. Rev. A **77**, 063406 (2008).
[3] S. I. Chu and D. A. Telnov, Phys. Rep. **390**, 1-131 (2004).
*[4] D. Zhao, F. l. Li, and S.I. Chu, J. Phys. B: At. Mol. Opt. Phys. **46**, 145403 (2013).
*[5] Z. Y. Zhou and S. I. Chu, Phys. Rev. A **83**, 013405 (2011).
*[6] Z. Y. Zhou and S. I. Chu, Phys. Rev. A **87**, 023407 (2013).
*[7] T. S. Ho, H. Rabitz, and S. I. Chu, Comput. Phys. Comm. **182**, 14 (2011).
*[8] S. L. Liao, T. S. Ho, S. I. Chu, and H. Rabitz, Phys. Rev. A **84**, 031401 (2011).
[9] S. Fleischer, Y. Zhou, R. W. Field, and K. A. Nelson, Phys. Rev. Lett. **107**, 163603 (2011).
*[10] S. L. Liao, T. S. Ho, H. Rabitz, and S. I. Chu, and, Phys. Rev. A **87**, 013429 (2013).
*[11] I. L. Liu, P.-C. Li, and S.I. Chu, Phys. Rev. A **84**, 033414 (2011).
*[12] P. C. Li, I. L. Liu, and S.I. Chu, Opt. Express **19**, 23857 (2011).
*[13] P. C. Li and S.I. Chu, Phys. Rev. A **86**, 013411 (2012).
*[14] J. Heslar and S. I. Chu, Phys. Rev. A**86**, 032506 (2012).
*[15] M. Chini, X. Wang, Y. Cheng, Y. Wu, D. Zhao, D.A. Telnov, S.I. Chu, and Z. Chang, Nature Sci. Rep. **3**, 1105-1 (2013).
*[16] S. I. Chu and D. A. Telnov, in *Computational Studies of New Materials II: From Ultrafast Processes and Nanostructures to Optoelectronics, Energy Storage and Nanomedicine*, edited by T.F. George, D. Jelski, R.R. Letfullin, and G. Zhang (World Scientific, 2011), pp. 75–101.
*[17] D. A. Telnov, J. Heslar, and S.I. Chu, in *Theoretical and Computational Developments in Modern Density Functional Theory*, edited by Amlan K. Roy (Nova Science Publishers, Inc., Hauppauge, NY (USA), 2012), pp. 357- 390.
*[18] J. Heslar, D. A. Telnov, and S. I. Chu, in *Concepts and Methods in Modern Theoretical Chemistry: Statistical Mechanics,* Volume 2, edited by S.K. Ghosh and P.K. Chattaraj (Taylor & Francis Inc., Bosa Roca, USA, 2013), pp. 37-55.
*[19] J. Heslar, D. A. Telnov, and S. I. Chu, Phys. Rev. A**87**, 052513 (2013).

Formation of Ultracold Molecules

Robin Côté

Department of Physics, U-3046
University of Connecticut
2152 Hillside Road
Storrs, Connecticut 06269

Phone: (860) 486-4912
Fax: (860) 486-3346
e-mail: rcote@phys.uconn.edu
URL: http://www.physics.uconn.edu/∼rcote

Program Scope

Current experimental efforts to obtain ultracold molecules (*e.g.*, photoassociation (PA), buffer gas cooling, or Stark deceleration) raise a number of important issues that require theoretical investigations and explicit calculations.

The main aims of this Research Program are to identify efficient approaches to obtain ultracold molecules, and to understand their properties. To that end, we often need to calculate the electronic properties (energy surfaces, dipole and transition moments, ro-vibrational states, etc.), as well as the interaction of the molecules with their environment (surrounding atoms, molecules, or external fields).

Recent Progress

During FY 2013, we have made progress on 4 main axes of research: 1) Rydberg-Rydberg interactions, 2) Energy surfaces and reactions, 3) Long-range interaction between diatomic (homonuclear and heteronuclear) molecules, and 4) Formation of dimers and tetramers. Below, we refer to DOE supported articles during the last four years only; new articles published since the last annual report filling (August 2012) are listed as [N...], while those of the prior years since 2009 by [P...].

1) Rydberg-Rydberg interactions

We extended our previous work on Rydberg-Rydberg interactions explaining spectral features observed in ^{85}Rb experiments, namely resonances correlated to the $69p_{3/2} + 71p_{3/2}$ asymptote [J. Stanojevic *et al.*, Eur. Phys. J. D **40**, 3 (2006)], and to $69d + 70s$ asymptote [J. Stanojevic *et al.*, Phys. Rev. A **78**, 052709 (2008)], to investigate the existence of potential wells of doubly-excited atoms due to ℓ-mixing, first for the 0_g^+ symmetry [P1], and then for other molecular symmetries (0_u^- and 1_u) of Rb_2 Rydberg macrodimers [P2]. We showed that these wells are robust against small electric fields, and support many bound states.and how these vibrational levels could be populated via photoassociation.

In [N1], we have started to explore the possibility of forming metastable long-range *macrotrimers* made of three Rydberg. Our calculations show the existence of shallow (roughly 20 MHz deep) long-range wells for three Rydberg atoms forming a linear molecule. Finally, we recently started to investigate a possible new chemical bound between ground state atoms using Rydberg dressing of the atoms [N2]. The molecular bound states would be extremely long-range, roughly 500 bohr radii, and very weakly bound.

2) Energy surfaces and reactions

A recent effort in my group towards reactive scattering involving cold molecules and molecular ions has started with the calculation of potential energy surfaces (PES). In our previous work, we studied PES for trimers, such as the lowest doublet electronic state of Li_3 ($1^2A'$) [P3], or the lowest $^2A''$ surface arising from the $Li_2[X^1\Sigma_g^+]$+$Li^*[^2P]$ interaction [P4]. In [P5], we extended this work to obtain accurate long-range *ab initio* PES for the ground state X^2A' of Li_3, the van der Waals dispersion coefficients and three-body dispersion damping terms for the atom-diatomic dissociation

limit. We recently computed the surfaces for $RbOH^-$ and RbOH [N3] to model the associative detachment reaction, paying special attention to the angular dependence of the PES.

Together with my collaborators, we have studied the collisions of trapped molecules with slow beams, particularly of $OH(J = \frac{3}{2}, M_J = \frac{3}{2})$ molecules with ^{4}He atoms [P6], and demonstrated the importance of including the effects of non-uniform trapping fields. More recently, we computed rate coefficients for reaction and vibrational quenching of the ultracold collision D + $H_2(v, j = 0)$ for a wide range of initial vibrationally excited states v [P7]. The v-dependence of the zero-temperature limit shows two distinct regimes: a barrier dominated regime for $0 \leq v \leq 4$, and a barrierless regime for $v \geq 5$. We extended our study of atom-diatom reactive scattering to H_2+Cl to investigate the effect of resonances near the scattering threshold [N4]. We find a new universal behavior of the inelastic cross section in the s-wave regime scaling as k^{-3}, which can be explained by the proximity of a pole in the complex k-plane.

We extended our previous work on the structure of K_2Rb_2 tetramers and thermochemistry relevant to KRb+KRb collisions and reactions [P8] to all possible alkali tetramers formed from X_2+X_2 $\rightarrow X_4$, X_2+Y_2 $\rightarrow X_2Y_2$, and XY+XY$\rightarrow X_2Y_2$ association reactions [P9], and found two stable structures for the tetramers, rhombic (D_{2h}) and planar (C_s), and that there are barrier-less pathways for the formation of tetramers from dimer association reactions. We are still exploring these systems.

Finally, we have continued our new effort on molecular ions, carefully calculating their energy surface and transition dipole moments. We started with alkaline-earth elements, since they can be cool to very low temperatures. In [P10], we reported *ab initio* calculations of the $X^2\Sigma_u^+$ and $B^2\Sigma_g^+$ states of Be_2^+, and found two local minima, separated by a large barrier, for the $B^2\Sigma_g^+$, and extended this work to Ca_2^+ in [P11]. We are in the process to complete two other systems: Mg_2^+ [N5] and Sr_2^+ [N6].

3) Long-range interaction between diatomic molecules

In our previous work on K_2Rb_2 [P8], we calculated the minimum energy path for the reaction KRb+KRb$\rightarrow$$K_2$+$Rb_2$ and found it to be barrierless. However, we recently showed that long-range barriers originating from the anisotropic interaction due to higher electrostatic, induction, and dispersion contributions could exist and stabilize a molecular sample [N7]. In addition, we showed that by changing the orientation of the molecules using an external DC electric field, and by varying its strength, one could control the effective inter-molecular interaction, switching it from attractive to repulsive (and vice-versa). Recently, we generalized our treatment to the long-range interaction between homonuclear alkali dimers [P12], where there are still anisotropic interactions (e.g. due to quadrupolar terms). and extended this work to the case of heteronuclear diatomic alkali molecules [N8]; in addition to the multipole expansion and van der Waals terms, we also give an analytic expression for molecules in an external (weak) DC electric field. Finally, we summarized some of this work in a book chapter on ultracold molecules for quantum information processing [N9].

4) Formation of dimers and tetramers

In previous papers sponsored by DOE [E. Juarros *et al.*, PRA **73**, 041403(R) (2006), E. Juarros *et al.*, JPB **39**, S965 (2006), N. Martinez de Escobar *et al.*, PRA **78**, 062708 (2008)], we explored the formation of homo- and hetero-nuclear diatomic molecules in their ground electronic state from one- and two-photon photoassociative processes [P13]. We also worked on using many coherent laser pulses [E. Kuznetsova *et al.*, PRA **78**, 021402(R) (2008)], and Feshbach resonances [P. Pellegrini *et al.*, PRL **101**, 053201 (2008)] to increase the formation rate of ultracold diatomic molecules [P14, P15, P16]. We recently started to explore how Feshbach resonances could enhance the pump-dump scheme to produce ground state molecules [N10], and we are using the same approach to investigate

the possible formation of tetramers [N11]. In fact, by controlling the long-range interaction between polar diatomic molecules using external DC electric field [N9], we could increase the shorter-range overlap of the continuum and excited states (as in FOPA [P14, P15]), and thus the formation rate of tetramers.

Future Plans

In the coming year, we expect to carry more calculations on Rydberg-Rydberg interactions, especially the possibility of forming metastable long-range *macrotrimers* made of three Rydberg. We will continue and extend our work on computing electronic properties of molecules (PES and moments), especially for the molecular ions, where not much is available. We plan to extend our work on the long-range interaction between molecules to more complex systems (e.g. diatomic + triatomic molecules, etc.). Finally, we will investigate in detail paths to form larger ultracold molecules by controlling the inter-molecular interactions in order to enhance formation rate.

New DOE sponsored publications since August 2012

N1. Nolan Samboy and Robin Côté, *Rubidium Rydberg linear macrotrimers.* Phys. Rev. A **87**, 032512 (2013).

N2. Jia Wang and Robin Côté, *A new long-range chemical bound using Rydberg-dressing.* In preparation: to be submitted to Phys. Rev. Lett.

N3. Jason N. Byrd, H. Harvey Michels, John A. Montgomery, Jr., and Robin Côté, *Associative detachment of rubidium hydroxide.* Submitted to Phys. Rev. A: see `arXiv:1307.4125`.

N4. Ion Simbotin, Subhas Ghosal, and Robin Côté, *Threshold resonance effects in reactive processes*, In preparation: to be submitted to Phys. Rev. Lett..

N5. Sandipan Banerjee, John A. Montgomery, Jr., H. Harvey Michels, and Robin Côté, *Comparison of the Alkaline Earth diatomic homonuclear molecular ions.* In preparation: to be submitted to J. Chem. Phys.

N6. Sandipan Banerjee, John A. Montgomery, Jr., H. Harvey Michels, and Robin Côté, *Ab initio potential curves for the* $X\ ^2\Sigma_u^+$, $A\ ^2\Pi_u$, *and* $B\ ^2\Sigma_g^+$ *states of* Sr_2^+. In preparation: to be submitted to Chem. Phys. Lett.

N7. Jason N. Byrd, John A. Montgomery, and Robin Côté, *Controllable Binding of Polar Molecules and Metastability of One-Dimensional Gases with Attractive Dipole Forces*, Phys. Rev. Lett. **109**, 083003 (2012)..

N8. Jason N. Byrd, John A. Montgomery, and Robin Côté, *Long-range forces between polar alkali-metal diatoms aligned by external electric fields.* Phys. Rev. A **86**, 032711 (2012).

N9. Robin Côté, *Ultracold molecules: their formation and application to quantum computing.* Advances of Chemical Physics **154**, Chap. 7, John Wiley and Sons (New York). Accepted.

N10. M. Gacesa, I. Simbotin, J.N. Byrd, S. Ghosal, and R, Côté, *Enhanced formation of alkali dimers using a pump-dump scheme near a Feshbach resonance: the case of LiRb.* In preparation (to be submitted to Phys. Rev. A).

N11. J.N. Byrd, S. Ghosal, and R, Côté, *The formation of tetramers of alkali metals by controlling inter-molecular interactions.* In preparation (to be submitted to Phys. Rev. Lett.).

Prior DOE sponsored publications since 2009

P1. N. Samboy, J. Stanojevic, and R. Côté, *Formation and properties of Rydberg macrodimers*, Phys. Rev. A 83, 050501(R) (2011).

P2. Nolan Samboy and Robin Côté, *Rubidium Rydberg macrodimers*, J. Phys. B **44**, 184006 (2011).

P3. J.N. Byrd, J.A. Montgomery (Jr.), H.H. Michels, and and R. Côté, *Potential energy surface of the* $1^2A'$ *Li_2+Li doublet ground state*, Int. J. of Quantum Chem., **109**, Issue 13, pp. 3112-3119, 5 November (2009).

P4. J.N. Byrd, J.A. Montgomery (Jr.), H.H. Michels, and R. Côté, *Electronic Structure of the* Li_2 $[X^1\Sigma_g^+] + LI^*[P_2]$ *Excited* A'' *Surface*, Int. J. of Quantum Chem **109**, 3626 (2009).

P5. Jason N. Byrd, H. Harvey Michels, John A. Montgomery, Jr., and Robin Côté, *Long-range three-body atom-diatom potential for doublet* Li_3, Chem. Phys. Lett. **529**, 23 (2012).

P6. T. V. Tscherbul, Z. Pavlovic, H. R. Sadeghpour, R. Côté, and A. Dalgarno, *Collisions of trapped molecules with slow beams*, Phys. Rev. A **82**, 022704 (2010).

P7. Ion Simbotin, Subhas Ghosal, and Robin Côté, *A case study in ultracold reactive scattering:* $D + H_2$, Phys. Chem. Chem. Phys. **13**, pp. 19148-19155 (2011).

P8. J.N. Byrd, J.A. Montgomery (Jr.), and R. Côté, *Structure and thermochemistry of* K_2Rb, KRb_2 *and* K_2Rb_2, Phys. Rev. A 82, 010502 (2010).

P9. Jason N. Byrd, H. Harvey Michels, John A. Montgomery, Robin Côté, and William C. Stwalley, *Structure, energetics, and reactions of alkali tetramers*, J. Chem. Phys. **136**, 014306 (2012).

P10. S. Banerjee, J. N. Byrd, R. Côté, H. H. Michels, J. A. Montgomery, Jr. *Ab initio potential curves for the* $X^2\Sigma_u^+$ *and* $B^2\Sigma_g^+$ *states of the* Be_2^+*: Existence of a double minimum*, Chem. Phys. Lett. **496**, 208 (2010).

P11. Sandipan Banerjee, John A. Montgomery, Jr., Jason N. Byrd, H. Harvey Michels, and Robin Côté, *Ab initio potential curves for the* $X\ ^2\Sigma_u^+$, $A\ ^2\Pi_u$, *and* $B\ ^2\Sigma_g^+$ *states of* Ca_2^+, Chem. Phys. Lett. **542**, 138-142 (2012).

P12. Jason N. Byrd, Robin Côté, and John A. Montgomery, *Long-range interactions between like homonuclear alkali metal diatoms*, J. Chem. Phys. **135**, 244307 (2011).

P13. E. Juarros, K. Kirby, and R. Côté, *Formation of ultracold molecules in a single pure state: LiH in* $a^3\Sigma^+$. Phys. Rev. A **81**, 060704 (2010).

P14. P. Pellegrini, and R. Côté, *Probing the unitarity limit at low laser intensities.* New J. Phys. **11**, 055047 (2009).

P15. E. Kuznetsova, M. Gacesa, P. Pellegrini, S.F. Yelin, and R. Côté, *Efficient formation of ground state ultracold molecules via STIRAP from the continuum at a Feshbach resonance.* New J. Phys. **11**, 055028 (2009).

P.16 J. Deiglmayr, A. Grochola, M. Repp, R. Wester, M. Weidemüller, O. Dulieu, P. Pellegrini, and R. Côté, *Influence of a Feshbach resonance on the photoassociation of LiCs.* New J. Phys. **11**, 055034 (2009).

Optical Two-Dimensional Spectroscopy of Disordered Semiconductor Quantum Wells and Quantum Dots

Steven T. Cundiff
JILA, University of Colorado & NIST, Boulder, CO 80309-0440
cundiff@jila.colorado.edu

September 6, 2013

Program Scope: The goal of this program is to implement optical 2-dimensional coherent spectroscopy and apply it to electronic excitations, including excitons, in semiconductors. Specifically of interest are quantum wells that exhibit disorder due to well width fluctuations and quantum dots. In both cases, 2-D spectroscopy will provide information regarding coupling among excitonic localization sites.

Progress: During the prior grant year, we reported that we had obtained optical two-dimensional spectra from a sample containing InAs quantum dots. Our spectra allowed the biexciton binding to be determined as a function of dot size, and showed that it was independent of dot size. In addition, our results showed that the biexciton transition energy was highly correlated with the exciton energy. These results were surprising because they did not correspond to single dot studies.

To additionally support our conclusions, during this grant year we performed similar measurements on a second InAs QD sample that had a different annealling temperature as well as on a sample with interface fluctuation dots (we reported on this sample in an earlier grant cycle). The results on the second InAs QD sample confirmed the results from the first one. On the other hand, the interface fluctuation dots clearly showed a variation in the biexciton binding energy. These results were published (items 2 and 6 below).

We also used a different type of two-dimensional spectrum, known as a zero-quantum spectrum, to study exchange-mediated fine-structure splitting of bright excitons in an ensemble of InAs quantum dots. By monitoring the non-radiative coherence between the bright states, we found that the fine-structure splitting decreases with increasing exciton emission energy at a rate of 0.1 μeV/meV. Dephasing rates were compared to population decay rates to reveal that pure dephasing causes the exciton optical coherences to decay faster than the radiative limit at low temperature, independent of excitation density. Fluctuations of the bright state transition energies are nearly perfectly correlated, protecting the non-radiative coherence from interband dephasing mechanisms. This work was published during the grant year (item 3 below).

We returned to studying quantum wells to look at two samples. One contained a pair of coupled InGaAs quantum wells. The other was a lightly n-doped CdTe quantum well.

We studied an asymmetric double InGaAs quantum well using a collection of zero-quantum, one-quantum and two-quantum two-dimensional spectra to provide a unique and comprehensive picture of the double well coherent optical response. Coherent and incoherent contributions to the coupling between the two quantum well excitons are revealed. Excellent agreement with density matrix calculations was obtained and shows that many-body interactions play an essential role in the coherent inter-well coupling. The dominance of many-body effects may explain discrepancies in previous transient four-wave-mixing studies of double quantum wells, which typically did not consider many-body effects. Coupled semiconductor quantum wells are an interesting model system to understand the coupling of excitonic states because the have

a fixed barrier thickness, as opposed to molecular systems where vibrations can confuse the results. This is particularly true in the current discussion of energy transfer mechanisms in light harvesting systems. This work has been submitted for publication.

We used a similar collection of zero-, one- and two-quantum two-dimensional coherent spectra to study excitons and trions in a CdTe/(Cd,Mg)Te quantum well. The set of spectra provides a unique and comprehensive picture of the exciton and trion nonlinear optical response. Exciton-exciton and exciton-trion coherent coupling is manifest as distinct peaks in the spectra, whereas signatures of trion-trion interactions are absent. Excellent agreement using density matrix calculations is obtained, which highlights the essential role of many-body effects on coherent interactions in the quantum well. The presence of exciton-trion coherent coupling is surprising because they are thought to be spatially separated, with trions forming in regions where a resident electron is present while excitons form elsewhere. The absence of trion-trion interactions is expected due to their Coulomb repulsion. This work has been submitted for publication.

Future Plans: Currently we are trying to exploit the ability of two-dimensional spectroscopy to make size resolved measurements to observe Rabi oscillations in the quantum dot samples. Typically Rabi oscillations are obscured in ensemble measurements because different members of the ensemble have different detunings from the laser field, and thus different generalized Rabi frequencies. We plan to excite the sample with a pre-pulse that will coherently drive the quantum dots into the excited state. We will then measure the two-dimensional spectrum. Simulations show that the relative strength of the diagonal excitonic peak and the off-diagonal biexcitonic peak can be used to determine the relative populations of the ground and excitonic states.

We have also begun working on collodial quantum dots provide by Victor Klimov's group at Los Alamos. As an initial "warm-up" we are looking at CdTe/ZnS core-shell dots. While these dots have been extensively studied in the past, they are bright and thus provide a system for which we expect to get strong signals. These studies will allow us to try out our technique on collodial dots and understand issues such as the effect of photocharging of the dots. We plan to follow these initial studies with work on newer and more exotic materials and structures.

Publication during the current grant year:

1. S.T. Cundiff and S. Mukamel, "Optical multidimensional coherent spectroscopy," Physics Today **66**, number 6, p. 44-49 (2013).

2. G. Moody, R. Singh, H. Li, I.A. Akimov, M. Bayer, D. Reuter, A.D. Wieck, A.S. Bracker, D. Gammon and S.T. Cundiff, "Biexcitons in semiconductor quantum dot ensembles," Physica Status Solidi B **250**, 1753-1759 (2013).

3. G. Moody, R. Singh, H. Li, I.A. Akimov, M. Bayer, D. Reuter, A.D. Wieck and S.T. Cundiff, "Correlation and dephasing effects on the non-radiative coherence between bright excitons in an InAs QD ensemble measured with 2D spectroscopy," Solid State Commun. **163**, 65-69 (2013).

4. G. Moody, R. Singh, H. Li, I.A. Akimov, M. Bayer, D. Reuter, A.D. Wieck and S.T. Cundiff, "Fifth-order nonlinear optical response of excitonic states in an InAs quantum dot ensemble measured with 2D spectroscopy," Phys. Rev. B **87**, 045313 (2013).

5. H. Li, G. Moody, S.T. Cundiff, "Reflection optical two-dimensional Fourier-transform spectroscopy," Opt. Express **21**, 1687-1992 (2013).

6. G. Moody, R. Singh, H. Li, I.A. Akimov, M. Bayer, D. Reuter, A.D. Wieck, A.S. Bracker, D. Gammon and S.T. Cundiff, "Influence of confinement on biexciton binding in semiconductor quantum dot ensembles measured with 2D spectroscopy," Phys. Rev. B **87**, 041304(R) (2013).

Publication during the prior 2 years from this project:

1. G. Moody, M. E. Siemens, A. D. Bristow, X. Dai, D. Karaiskaj, A. S. Bracker, D. Gammon, and S.T. Cundiff, "Spectral broadening and population relaxation in a GaAs interfacial quantum dot ensemble and quantum well nanostructure," Phys. Stat. Sol. (b) **248**, 829-832 (2011).

2. G. Moody, M. E. Siemens, A. D. Bristow, X. Dai, D. Karaiskaj, A. S. Bracker, D. Gammon, and S. T. Cundiff, "Exciton-exciton and exciton-phonon interactions in an interfacial GaAs quantum dot ensemble," Phys. Rev. B **83**, 115324 (2011). [This paper was selected as an "**Editors Suggestion**" in Physical Revew B]

3. A.D. Bristow, T. Zhang, M.E. Siemens, S.T. Cundiff and R.P. Mirin, "Separating homogeneous and inhomogeneous line widths of heavy- and light-hole excitons in weaklydisordered semiconductor quantum wells," J. Phys. Chem. B **115**, 5365-5371 (2011).

4. G. Moody, M. E. Siemens, A. D. Bristow, X. Dai, A. S. Bracker, D. Gammon, and S. T. Cundiff, "Exciton relaxation and coupling dynamics in a GaAs/AlGaAs quantum well and quantum dot ensemble," Phys. Rev. B **83** 245316 (2011).

5. S.T. Cundiff, "Optical two-dimensional Fourier transform spectroscopy of semiconductor nanostructures," J. Opt. Soc. Am. B **29**, A69-A81 (2012).

6. S.T. Cundiff, A.D. Bristow, M. Siemens, H. Li, G. Moody, D. Karaiskaj, X. Dai and T. Zhang, "Optical Two-Dimensional Fourier Transform Spectroscopy of Excitons in Semiconductor Nanostructures (Invited)," IEEE J. Spec. Topics Quantum Electr. 18, 318-328 (2012).

7. D. B. Turner, P. Wen, D. H. Arias, K. A. Nelson, H. Li, G. Moody, M. E. Siemens, and S. T. Cundiff, ”Measuring many-body interaction dynamics in GaAs quantum wells using two-dimensional electronic correlation spectroscopy,” Phys. Rev. B **85**, 201303(R) (2012).

SISGR: Understanding and Controlling Strong-Field Laser Interactions with Polyatomic Molecules

DOE Grant No. DE-SC0002325

Marcos Dantus, dantus@msu.edu
Department of Chemistry and Department of Physics and Astronomy, Michigan State University, East Lansing MI 48824

1. Program Scope

When intense laser fields interact with polyatomic molecules, the energy deposited leads to fragmentation, ionization and electromagnetic emission. The objective of this project is to determine to what extent these processes can be controlled by modifying the phase and amplitude characteristics of the laser field according to the timescales for electronic, vibrational, and rotational energy transfer. Controlling these processes will lead to order-of-magnitude changes in the outcome from laser-matter interactions, which may be both of fundamental and technical interest.

The proposed work is unique because it seeks to combine knowledge from the field of atomic-molecular-optical physics with knowledge from the fields of analytical and organic ion chemistry. This multidisciplinary approach is required to understand to what extent the shape of the field affects the outcome of the laser-molecule interaction and to which extent the products depend on ion stability. The information resulting from the systematic studies will be used to construct a theoretical model that tracks the energy flow in polyatomic molecules following interaction with an ultrafast pulse.

2. Recent Progress

In the field of Coherent Control, there has always been some uncertainty and ambiguity regarding the extent coherence plays a role in the various laser control experiments. When a laser pulse interacts with a molecule, the coherent response of the molecule may include rotational, vibrational and electronic quantum state coherence. Determining if electronic coherence plays a role in Coherent Control experiments has been very difficult because of the short timescales for electronic coherence, and because it is difficult to unravel the interference between the electric fields of the pump and probe laser pulses. For example, when two ultrashort pulses are scanned collinearly, they interfere, and this linear optical interference dominates the short time response of the molecule with the laser field in the timescale of the pulse duration.

Our work has focused on two types of projects. (a) We have been studying isolated molecules under strong fields with the goal of exploring the extent of electronic and vibrational coherence. (b) We have been exploring electronic coherence in large organic molecules in solution.

(a) Coherent dynamics in molecules resulting from strong-field interactions.

We have focused on the fragmentation of substituted acetophenones, in particular the coherent dynamics found in the first 3ps following strong-field excitation. As found by us (Zhu 2011), the molecular ion formed by field induced ionization undergoes torsional motion in the 0.5-1ps time scale. The carbonyl group is conjugated with the benzene pi-electrons; therefore, the torsion modulates the polarizability of the cation and makes it sensitive to the probe laser. In principle, we have a good understanding of the process; however, when we explore methyl substitution in the benzene ring we find significant changes in the modulation depth and torsional frequency. Ortho, meta and para substitution effects on benzene rings have been the subject of organic chemists for as much as a hundred years. Organic chemists have derived their knowledge indirectly from product distributions and rationalize their findings by drawing resonance structures; we have the opportunity to directly observe how substitution affects the potential energy surface and the ensuing dynamics. Given the bandwidth of ultrafast laser pulses ionization leads to coherent excitation of two or more electronic states, therefore, it can be expected that the coherence observed involves two or more electronic states in addition to vibrational states involved with the torsion. Here we illustrate a small fraction of our experiments on acetophenone, o, m & p-acetophenone, benzophenone and fluorenone (see Fig. 1). W include the natural orbitals calculated for acetophenone and m-acetophenone. The red circle shows the stabilization of the positive charge by the methyl substituent for m-acetophenone, which shows only one very weak oscillation with a period of about1.5ps. Ab-initio calculations are being carried out in collaboration with Prof. B. Levine (MSU). In addition to determining the potential energy surface for these molecules, Prof. Levine is running molecular dynamics calculations. He has found that the ground electronic state of the ion undergoes torsional motion to reach a minimum energy near 37^{o}. He has also found

that the first and second excited states of the cation are strongly coupled to the ionic ground state. The goal of our research is to elucidate the benzene ring substitution rules from our direct time-resolved measurements and to determine if the dynamics observed are associated with slightly different electronic configurations that can be correlated to the resonance structures used by organic chemists to rationalize their findings.

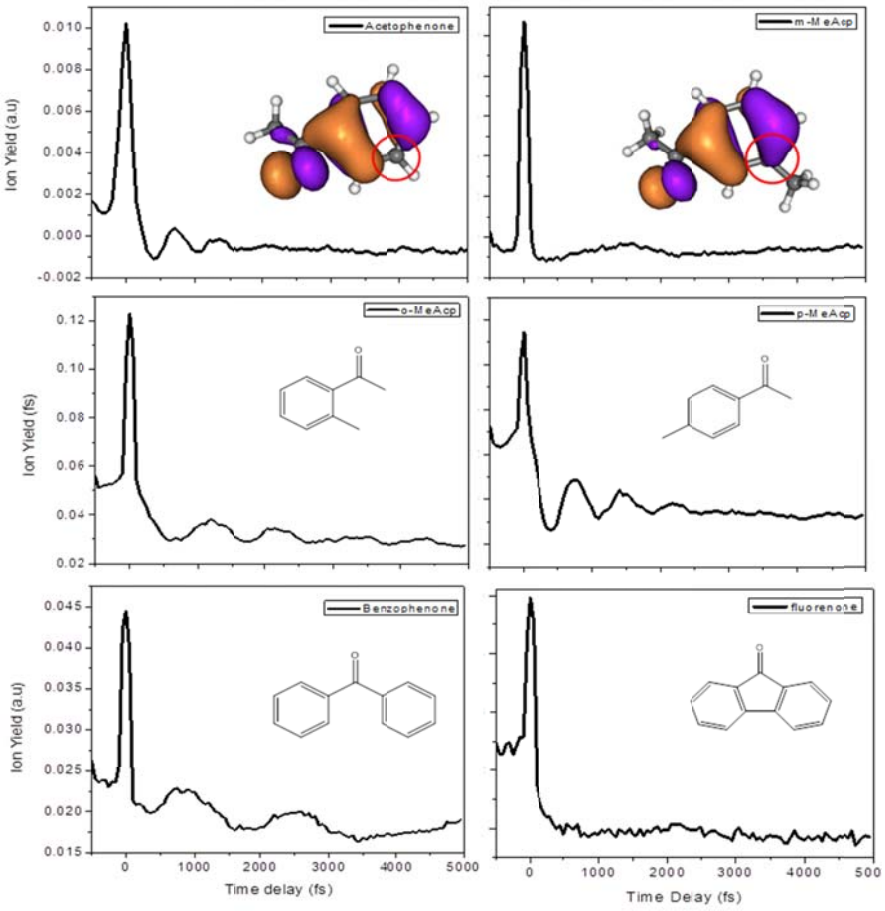

Figure 1: Time resolved dynamics following strong-field ionization (pump 800nm, 10^{14} W/cm^2) as a function of time delay (probe 800nm, 10^{12} W/cm^2) for acetophenone, o, m & p-acetophenone, benzophenone and fluorenone. Insets: The natural orbital with occupation number equals to 1 in D0 state from SA3-CAS5/8 for acetophenone and m-acetophenone (data from Prof. B. Levine).

(b) Electronic coherence in large organic molecules in solution.

This line of research was started as a reference point, assuming that everything related to the optical response of large organic molecules in condensed phase was well understood. We find the first few hundred femtosecond involve a number of inter- and intra-molecular processes that are not very well understood. While powerful nonlinear measurements such as three-pulse photon echo peak shift (3PEPS) have been considered to provide clear cut data that could be used to elucidate the role of inhomogeneous broadening, solvatochromic shift, and electronic coherence, the reality is that these aspects are still far from being clearly understood. Therefore, there is a need for the development of methods that are sensitive, provide high temporal resolution and yet provide complementary information to other experiments such as transient absorption or 3PEPS. Here we illustrate how the use of chirped laser pulses may be a powerful approach to extract the early optical response of large organic molecules in solution. The fluorescence and stimulated emission yield results shown are obtained from two related compounds (IR125 and IR144), in two solvents (methanol and ethylene glycol) at three temperatures. We find: i. Negative chirps are insensitive to changes in viscosity; ii. Positive chirps are very sensitive to viscosity; iii. Large changes are observed within the first 100fs; iv. The response for IR144 returns to TL values within the first 2ps, however, for IR125 there is no such relaxation. This is particularly visible when looking at the stimulated emission results for IR144 negative chirp. The full interpretation of this data is included in the manuscript we plan to submit later in September.

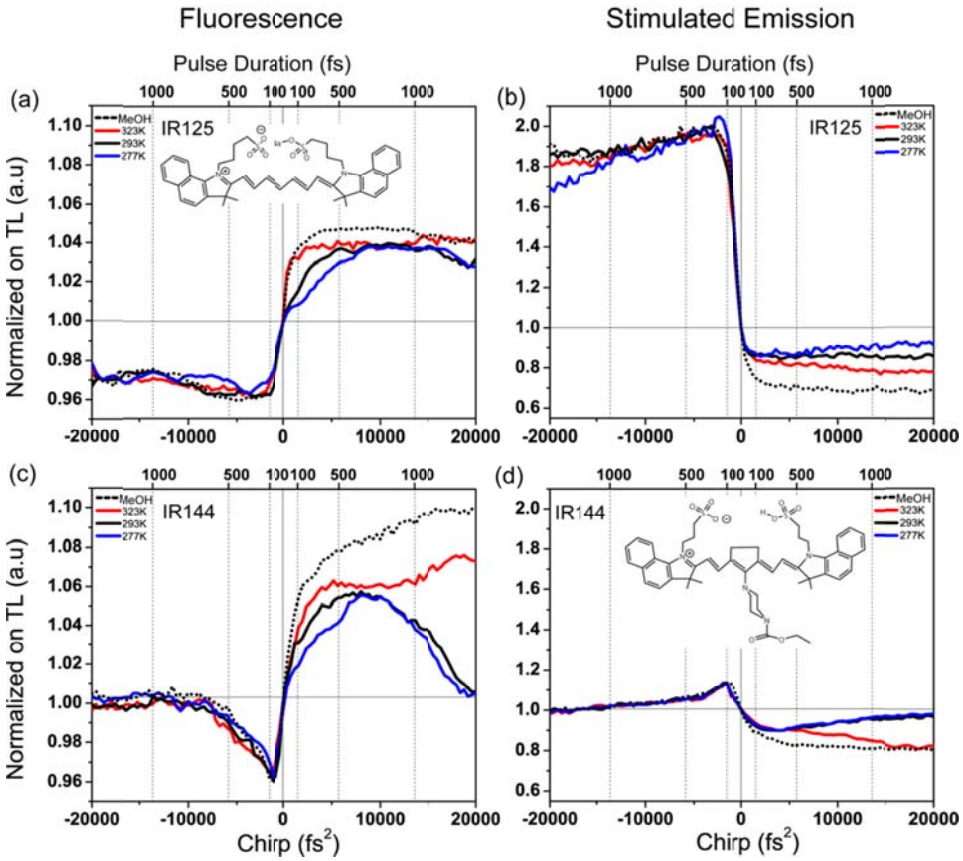

Figure 2: Fluorescence and stimulated emission response to chirped pulses for IR125 (a) and (b) and for IR144 (c) and (d) respectively in methanol (dashed) and ethylene glycol at three temperatures 323K (red), 293K (black), and 277K (blue). The plots have been normalized on the value of fluorescence and stimulated emission for transform limited pulses.

We have confirmed the longer electronic coherence for IR125 compared with IR144 by carrying out interferometric measurements while detecting the nonlinear stimulated emission. The results, presented in Fig. 3, show the slightly saturated fluorescence (red), the fundamental laser light (black) and the non-linear stimulated emission (blue). Note that electronic coherence in IR125 appears to decay in about 130fs, a value that is very different than what is normally quoted (<30fs).

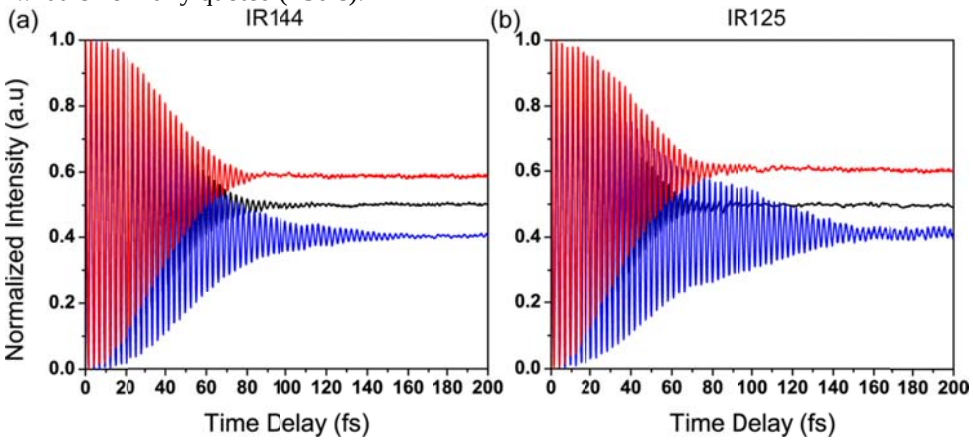

Figure 3. Experimental interferometric time-delay scans for integrated fluorescence (red), the laser fundamental (black) and forward emission (blue) signals obtained using pair of transform limited pulses generated using phase amplitude modulation normalized on TL pulses.

Summary:

(a) We are developing new methods to explore electronic coherence in gas, liquid, solid and plasma states of matter.
(b) We have found a way to measure resonance-structure dynamics in substituted benzene compounds. This is a very significant observation that represents the first direct measurement of resonance structures as have been postulated by chemists for over 100 years. Resonance structures involve flow of electron density that is schematically shown as changes in the electronic structure of molecules.
(c) Our experiments on IR125 and IR144 have led to detailed understanding of the early optical response of large organic molecules in solution, including the solvation Stokes shift. Our results have been confirmed through additional experiments as a function of temperature and molecular structure. Further studies involving pairs of phase-locked pulses have also been carried out to study the mechanism of decoherence in solution and a manuscript reporting the results is currently in preparation. Additional experiments using chirped pulses have led to a new theoretical model to interpret the early solvation dynamics. These results complete some of the earliest results in the field of laser control using chirped pulses. In particular we found that the magnitude of the chirp effect on fluorescence intensity and stimulated emission is a second order process on laser intensity but the shape of the chirp dependence is independent of laser intensity.
(d) We are building a photoelectron and photoion coincidence (PEPICO) instrument that will give us additional information about the electronic states involved in the strong field experiments.

3. Future Plans

(a) We plan to complete the studies of IR144, and IR125 in solution, these studies should provide an independent method to measure electronic coherence, dephasing and solvation effects using shaped pulses.
(b) We plan to report on the electronic coherence involved in laser control of chemical reactions, in particular intense non-resonant fields.
(c) We plan to complete a set of measurements for a number of substituted acetophenones with electron withdrawing and electron donating groups in order to ascertain the observation of resonance structure dynamics as observed by pump-probe measurements.

One of the important goals of our proposed work was to upgrade our molecular beam in order to be able to carry out experiments taking advantage of PEPICO detection, to determine how much energy was deposited in the molecule by the laser field to produce each of the different fragment ions. We will also be able to correlate the origin of the ejected electron with a specific fragment. All parts for that instrument have arrived, machining is almost complete and we have started the construction of the system.

4. Publications

1. X. Zhu, V. V. Lozovoy, J. D. Shah and M. Dantus, "Photodissociation dynamics of acetophenone and its derivatives with intense nonresonant femtosecond pulses," *J. Phys. Chem. A* **115**, 1305–1312 (2011)

2. A. Konar, V. V. Lozovoy and M. Dantus, "Solvation Stokes-Shift Dynamics Studied by Chirped Femtosecond Laser Pulses", *J. Phys. Chem. Lett.* **3**, 2458-2464 (2012)

3. A. Konar, J. D. Shah, V. V. Lozovoy and M. Dantus, "Optical Response of Fluorescent Molecules Studied by Synthetic Femtosecond Laser Pulses", *J. Phys. Chem. Lett.* **3**, 1329–1335 (2012)

4. A. Konar, V. V. Lozovoy and M. Dantus, "Long-Lived Electronic Polarization and Nonlinear Optical Effects of Fluorescent Molecules in Solution", *J. Phys. Chem. Lett.* Submitted (2013)

5. A. Konar, V. V. Lozovoy and M. Dantus, "Probing Stokes Shift Dynamics and Electronic Coherence using Femtosecond Chirped-Pulse Spectroscopy," *J. Phys. Chem. Lett.* In preparation (2013)

Picosecond x-ray diagnostics for third and fourth generation synchrotron sources

Matthew F. DeCamp
Department of Physics and Astronomy
University of Delaware, Newark, DE 19716
mdecamp@udel.edu
DOE Grant No: DE-FG02-11ER46816

1 Program Scope

The objective of this research program is to design and implement a series of experiments utilizing, or improving upon, existing time-domain hard x-ray diagnostics at a third generation synchrotron source. Specifically, the research program aims at three experimental projects to be explored in the grant cycle: 1) implementing a picosecond x-ray Bragg switch using a laser excited nano-structured metallic film, 2) designing a robust x-ray optical delay stage for x-ray pump-probe studies at a hard x-ray synchrotron source, and 3) building/installing a laser based x-ray source at the Advanced Photon Source for two-color x-ray pump-probe studies.

2 Recent Progress

During this first two years of this three year grant, we have studied the ultrafast dynamics of photoexcited metallic thin films using both optical and hard x-ray probes. In particular, we have studied the generation of picosecond acoustic pulses with a gold photo-acoustic transducer as well as the ultrafast dynamics of optical phonons in a 20nm bismuth film.

Time-resolved x-ray diffraction of acoustic pulses

The first goal of this research plan is the use of an ultrafast photo-acoustic transducer to efficiently switch x-ray radiation on a picosecond timescale. In particular, we are trying to implement the phonon "Bragg switch" using a lithographically printed metallic grating on a crystalline substrate. This method has the potential of producing sub-picosecond x-ray bursts from a third generation synchrotron sources or it could be used to measure the hard x-ray pulse length of fourth generation x-ray synchrotron sources. We have recently published work in *Applied Physics Letters* [1] and *Physical Review B*[3], studying the generation and structure of a coherent acoustic pulse generated by a laser excited metallic film on a germanium substrate.

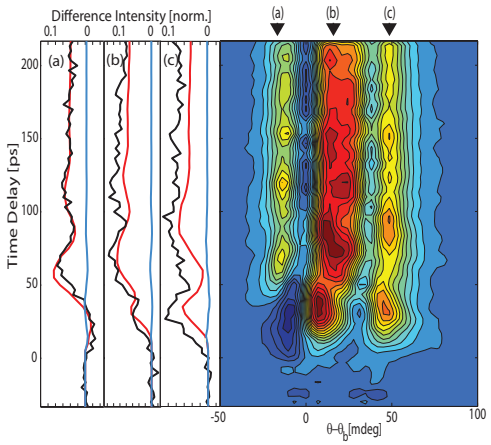

Figure 1: Differential time-resolved x-ray diffraction of a gold coated Germanium crystal. Experiment: black. Simulation: 100 nm (15 nm) strain pulse red (blue).[1]

Upon ultrafast optical excitation, photo-electrons are generated in a layer consistent with the optical penetration depth ($\sim$15nm) and then rapidly diffuse through out the entire 100nm thick film. In less than 5ps, the hot-electrons cause the gold film to heat up in excess of 200K degrees which results in ultrafast expansion of the film and the creation of a coherent acoustic pulse to propagate into the crystalline substrate. To probe the picosecond lattice dynamics, a time-resolved x-ray diffraction experiment was performed on the substrate crystal. The gold film is sufficiently thin to effectively be transparent to the incoming x-ray radiation, making it possible to directly probe the propagating acoustic pulse in the substrate.

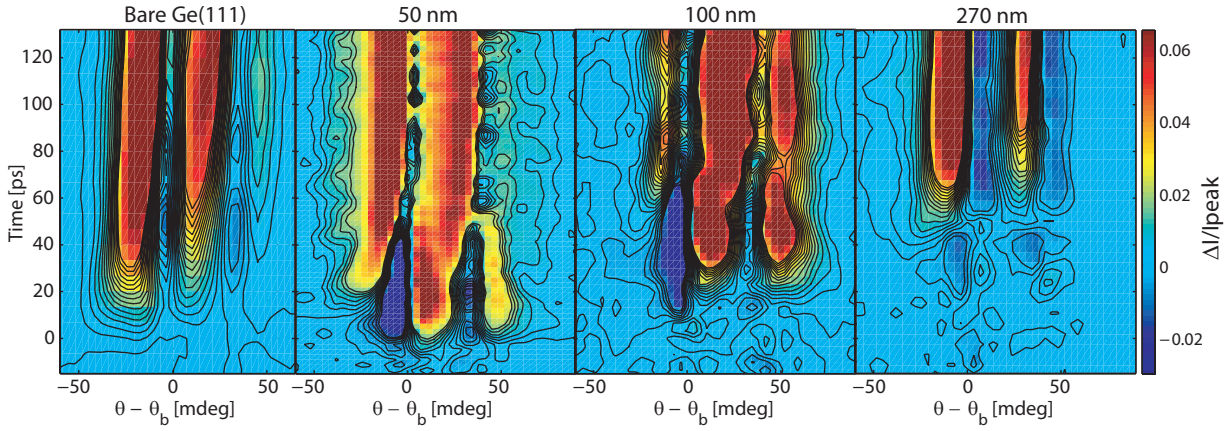

Figure 2: From left to right, the differential time-resolved x-ray diffraction of a bare germanium crystal, 50nm gold film on Ge, 100nm gold film on Ge, and 200nm gold film on Ge. [3]

In figure 1, we show the results of the time-resolved x-ray diffraction experiment. Upon the generation of the acoustic pulse, we see significant sidebands on the x-ray diffraction peak, corresponding to the generation of acoustic wavevectors in crystalline substrate. In addition, we see no evidence of crystalline heating (i.e. peak shift), indicating that the diffraction sidebands are solely due to the generation and transmission of an isolated acoustic pulse from the laser excited gold film. This was confirmed by directly comparing the experimental results with x-ray diffraction simulations. The resulting diffraction sidebands have significant amplitude, indicating that the proposed "picosecond Bragg switch" could have efficiencies as large as 10%, sufficient for picosecond x-ray experiments at the APS.

In an effort to better understand the dynamics of the generated acoustic pulses for use in the photo-acoustic Bragg switch, we also studied acoustic phonon generation process from a series of transducer geometries. In particular, we have utilized differing thickness gold films to generate acoustic phonons with a distinct spatio-temporal structure, as well as measuring the absolute efficiency of the process by directly measuring the dynamics generated by the metallic films (see figure 2).

As the x-ray diffraction peak is in "reciprocal space", we have shown that a Fourier transform of the time-resolved x-ray diffraction measurement allows a direct reconstruction of the acoustic pulse shape [3]. In particular, we determine the shape of the generated acoustic pulse that propagates into the substrate with spatial resolution in excess of 20nm (see figure 3). These experiments confirm that the acoustic pulse shape is primarily determined by the film thickness, (i.e. the generated wavevectors are directly proportional to the film thickness) but the width of the acoustic pulse is larger than anticipated by an order of magnitude.

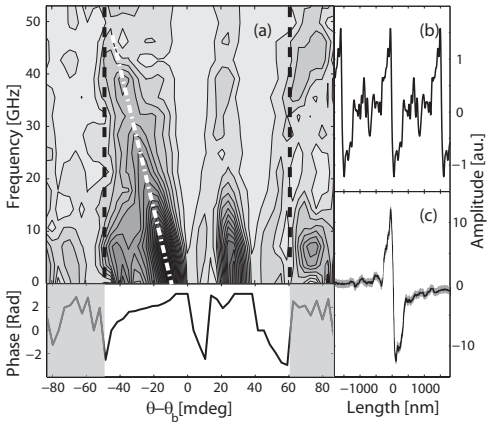

Figure 3: Spectral amplitude and phase of sidebands retrieved form the TRXRD patterns observed for the 50 nm thick gold film. Dashed line is a guide to the eye. (b) The reconstructed spatial profile of the acoustic pulse using the data as shown. (c) The reconstructed spatial profile of the acoustic pulse obtained by adding 9 interpolated points for each data point [3]

Optical pump-probe studies of bismuth thin films

While an acoustic phonon Bragg switch has the potential of producing a picosecond x-ray pulse at a conventional third generation synchrotron source, the time-scale of the switch will be limited to the acoustic velocity in the substrate. To overcome this physical limitation, one can use a coherent optical phonon. These transitions can have vibrational periods in the 10s of femtoseconds, providing the potential of generating femtosecond x-ray pulses through the Bragg switch. We are investigating the possibility of using a nano-structured bismuth film as an optical phonon Bragg switch.

Prior experiments performed by the PI have demonstrated the possibility of generating high-wavevector optical phonons in Bismuth using a photolithographic engineered structure. To efficiently utilize the bismuth for an x-ray switch, because the optical penetration depth of the semi-metal is so small ($\sim$20nm), it will be necessary to excite the large amplitude optical phonon in a thin film. In work recently published in the *Journal of Applied Physics* [2], we studied the dynamics of optical phonon generation in thin Bismuth films. In particular, although the we excited a "fully symmetric" optical phonon mode, we reported results indicating the phase and amplitude of the phonon is highly sensitive to the polarization states and incident angle of the pump-probe pulses. This is due to the presence of a surface plasmon resonance within the bismuth thin film, which significantly changes the dielectric properties and therefore the excitation mechanism of the optical phonon mode. These result may have implications on the use of metallic crystals in the use of the Bragg switch.

3 Work in Progress

Currently we are working on several parallel tracks towards the development of ultrafast x-ray tools at the APS. This includes designing a photolithographic mask for the acoustic phonon Bragg switch and construction of an x-ray delay line and pulsed x-ray source for x-ray pump/x-ray probe experiments. In addition, we are currently measuring the phonon generation in a variety of metallic thin films, paving a way to optimizing the Bragg switch.

Time-resolved x-ray diffraction of a photo-acoustic transducer

In addition, during our first run at the APS in February 2013, we extended our previous work to the higher optical excitation energies and saw some previously undetected "ringing" of the laser driven film which induces a periodic acoustic wave to propagate into the crystalline substrate (see figure 4). This period is directly proportional to the ratio of the sound speed to the film thickness. In addition, we see a clear signal for a ringing at wavevector at twice the film thickness, corresponding to periods less than 10ps. The transient superlattice has x-ray scattering amplitudes of greater than 10% of the main Bragg peak, with lifetimes exceeding 500ps, providing a method of efficiently modulating the x-ray intensity of the synchrotron pulse on a picosecond timescale. Further investigations are currently planned with the picosecond x-ray streak camera located at the APS for detailed temporal studies of this ultrafast modulation. In addition we plan to a coherent control experiment on the laser induced superlattice in an effort to efficiently slice the 100ps x-ray pulse of the APS.

In addition to homogenous thin film samples, we have recently printed nanoscale structures using the Center for Nanoscale Materials at Argonne National Lab to construct the prototype photoacoustic Bragg switch. The generated mask will allow us to generate a series of metallic gratings with differing wavevectors (spatial periods of 25nm-1μm) on a crystalline substrate, making it possible to have a tunable acoustic phonon switch.

Construction of a time-domain x-ray tools for Argonne National Labs

In addition to the construction of the x-ray Bragg switch, we are currently developing a series of pulsed x-ray tools for the APS for x-ray pump/x-ray probe spectroscopy. This includes the design and testing of a delay

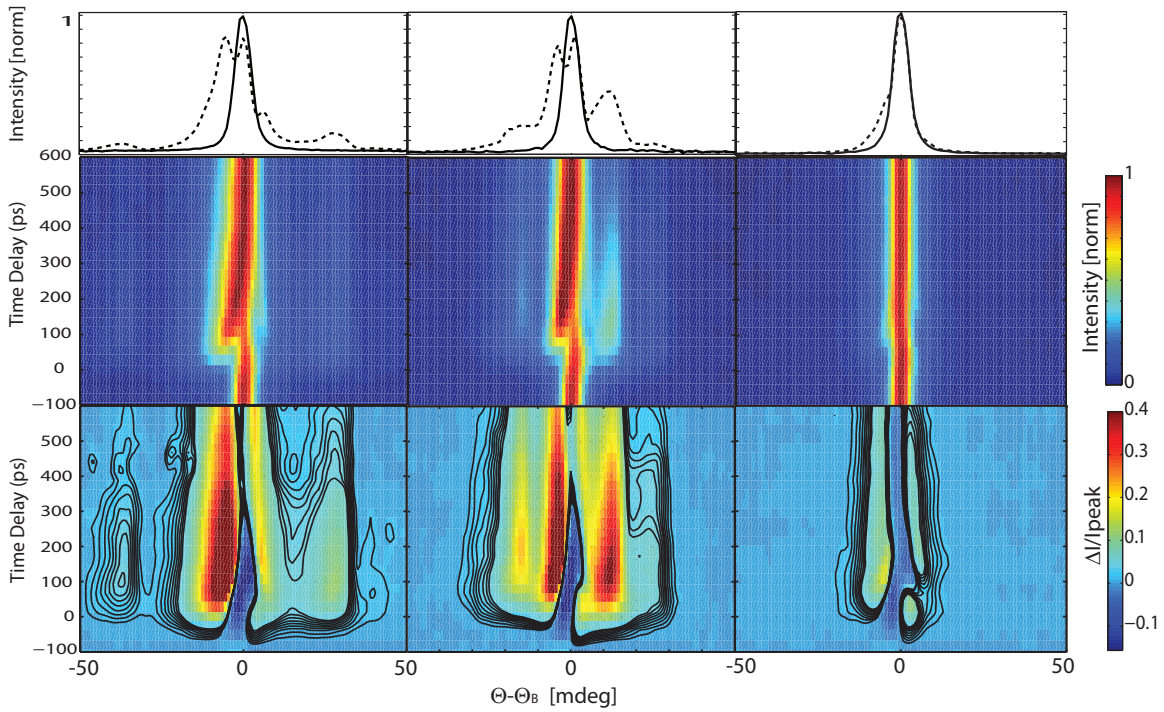

Figure 4: Top: Diffraction intensities before (solid) and 120ps (dashed) after after laser excitation. Left 50nm sample, center 100nm sample, right 270nm sample. Center: TRXRD surfaces of the Ge(111) peak. Bottom: Differential diffraction intensity as a function of time. Contours levels represent changes in x-ray intensity of 0.5% of the main Bragg peak.*In preparation*.

line for an x-ray pump-probe spectrometer and the construction of a laser-driven x-ray diode. The laser-driven diode is currently being tested at the University of Delaware. This diode will generate sufficient hard x-ray flux to have a viable x-ray probe of picosecond crystalline dynamics at the APS. When completed, we plan on installing this device at the APS for testing of an x-ray pump/x-ray probe experiment. In particular, the tunable x-ray pump pulse will be generated by the APS. Any x-ray dynamics will be probed using the picosecond x-ray diode and a conventional x-ray CCD camera.

In addition, we have constructed an x-ray diffraction delay line for testing at the APS. This delay line is constructed of a series of Bragg crystals oriented such that the x-ray beam is retro reflected back to the x-ray source. Initial testing of this device will commence during a November 2013 beamtime at the APS.

Publications related to DOE funding

- "Generation of acoustic pulses from a photo-acoustic transducer measured by time-resolved x-ray diffraction," Y. Gao and **M.F. DeCamp** *Applied Physics Letters* **100** 191903 (2012).
- "Measurement of optical phonon dynamics in a bismuth thin film through a surface plasmon resonance" Z. Chen and **M.F. DeCamp**, *Journal of Applied Physics* **112** 013527 (2012).
- "Reconstructing longitudinal strain pulses using time-resolved x-ray diffraction" Y. Gao, Z. Chen, Z. Bond, A. Loether, L.E. Howard, S. LeMar, S. White, A. Watts, B.C. Walker, and M. F. DeCamp, *Phys. Rev. B* **88** 014302 (2013).
- "Transient crystalline superlattice generated by a photoacoustic transducer" A. Loether, Y. Gao, Z. Chen, E.M Dufresne, D. Walko, and M.F. DeCamp *In Preparation* (2013)

Production and trapping of ultracold polar molecules

D. DeMille
Physics Department, Yale University, P.O. Box 208120, New Haven, CT 06520
e-mail: david.demille@yale.edu

Program scope: The goal of our project is to produce and trap polar molecules in the ultracold regime. Once achieved, a variety of novel physical effects associated with the low temperatures and/or the polar nature of the molecules should be observable. We recently discovered and characterized a simple and efficient method to produce and accumulate ultracold RbCs in its absolute rovibronic ground state, and have used our findings to predict the properties of trapped samples produced using this technique. Molecules in such a sample will be stable against inelastic collisions and hence suitable for further study and manipulation. Once in place, we will study chemical reactions at ultracold temperatures, dipolar effects in collisions, etc.

Our group earlier pioneered techniques to produce and state-selectively detect ultracold heteronuclear molecules. These methods yielded RbCs molecules at translational temperatures $T < 100$ μK, in any of several desired rovibronic states—including the absolute ground state, where RbCs has a substantial electric dipole moment. Our previous method for producing ultracold, ground state RbCs consisted of several steps. First, laser-cooled and trapped Rb and Cs atoms were bound into an electronically excited state via photoassociation (PA).[1] These states decayed rapidly into weakly bound vibrational levels in the ground electronic state manifold.[2] We demonstrated the ability to transfer population from one high vibrational levels into the lowest vibronic state $X\ ^1\Sigma^+(v=0)$ of RbCs using a laser "pump-dump" scheme.[3,4] We detect ground-state molecules with vibrational-state selectivity with a resonantly-enhanced multiphoton ionization process (1+1 REMPI) followed by time-of-flight mass spectroscopy. Subsequently, we incorporated a CO_2-laser based 1D optical lattice into our experiments. This made it possible to trap vibrationally-excited RbCs molecules as they were formed. The precursor Rb and Cs atoms could also be trapped with long lifetimes (>5 s). We used this capability to measure inelastic (trap loss) cross-sections for individual RbCs vibrational levels on both Rb and Cs atoms in the ultracold regime, and also developed a simple theoretical model for these collisions.[5]

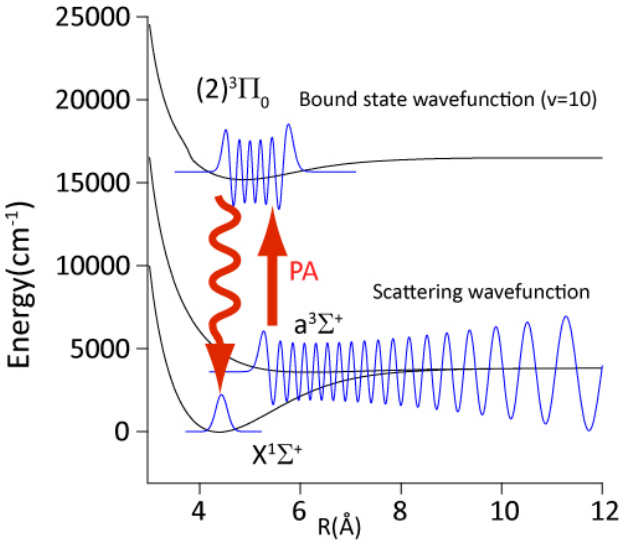

Fig. 1: Scheme for ground state molecule formation via direct short-range photoassociation.

We have focused recently on a new method to directly create rovibronic ground-state $X\ ^1\Sigma^+(v=0,\ J=0)$ RbCs molecules (Fig. 1). The approach is to drive PA transitions into tightly-bound states of excited electronic potentials. Such states can in principle decay with substantial probability to the $X\ ^1\Sigma^+(v=0,\ J=0)$ absolute ground state, which also has small internuclear separation. PA to short-range states was previously believed to be impractical: in the WKB approximation, the scattering-state wavefunction of two colliding atoms has negligible amplitude at distances comparable to the separation of atoms in the

molecular ground state,[6] so Franck-Condon factors (FCFs) for the free-to-bound PA transition were expected to be too small to drive efficiently.

Nevertheless, recent observations from groups working on similar heteronuclear bi-alkali systems has shown that it is sometimes possible to drive PA transitions into tightly-bound states. These include observations of short-range PA transitions in LiCs,[7] NaCs,[8] and RbCs.[9,10] In all cases the PA rate was larger than the naïve expectation, although the underlying mechanisms were sometimes unclear. For LiCs and NaCs it was found that PA to J=1 levels was strongly suppressed; hence production of the rovibronic $X\,^1\Sigma^+(v=0, J=0)$ ground state via decay of a PA level could not be performed efficiently. In RbCs, the J=1 PA resonance was not suppressed; however, the state assignment of the short-range PA level was unclear, and thus so was the question of whether it could decay to the $X\,^1\Sigma^+(v=0)$ vibronic ground state.

In our recent work, we have demonstrated that formation of rovibronic ground-state RbCs via short-range PA is indeed viable, and in fact more favorable than any previously found case in other species.[11] We first used our REMPI detection method to show that the short-range PA level of Ref. [9] indeed results in population of the $X\,^1\Sigma^+(v=0)$ state. Using existing spectroscopic data on RbCs,[12] we were able to assign the PA level definitively to the $(2)^3\Pi(0^-)$ state, which can decay to $X\,^1\Sigma^+$ only via a two-photon cascade. This led us to speculate that more efficient routes for population of $X\,^1\Sigma^+(v=0)$ could be found by using PA through the neighboring $(2)^3\Pi\,(0^+)$ state, which can decay to $X\,^1\Sigma^+$ directly via single photon emission. Again using existing spectroscopic data for state identification, we demonstrated PA into several vibrational levels of $(2)^3\Pi\,(0^+)$ state, with larger rates of $X\,^1\Sigma^+(v=0)$ formation than using the previously known resonance (Fig. 2).

We subsequently compared the rates of formation of $X\,^1\Sigma^+(v=0)$, via PA through different $(2)^3\Pi\,(0^+)[v']$ subelevels, to expectations based on FCFs for the free-bound and bound-bound transitions. We found excellent qualitative agreement, indicating that our description of excitation and decay processes in terms of simple FCFs is valid. This model relies on no unusual circumstances such as resonant coupling between bound states or scattering resonances. Rather, it simply takes advantage of the fact that the triplet-state scattering wavefunction is considerably larger than would be expected based on the WKB approximation; and that (non-resonant) spin orbit coupling is strong in bi-alkali molecules containing Cs. We also demonstrated that the PA transition could be saturated under typical experimental conditions, in rough agreement with calculated PA rates based on the FCFs. This means that formation of rovibronic ground state molecules can proceed at a rate given by the unitarity-limited scattering rate (i.e., the theoretical maximum PA rate), times the branching ratio b~0.2% for decay of the J = 1 PA resonance into the $X\,^1\Sigma^+(v=0,J=0)$ state. In the course of this work, we also developed a straightforward and general method for predicting and analyzing rotational line

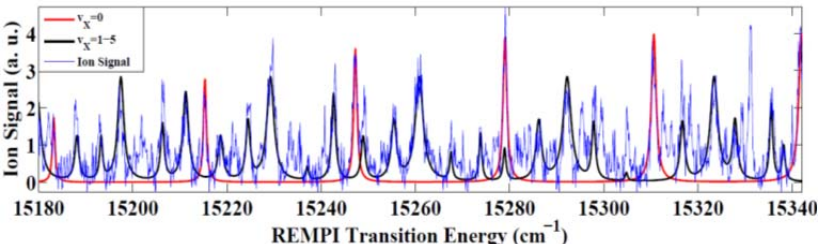

Fig. 2: Population of $X\,^1\Sigma^+(v=0)$ via short-range PA. Plotted is signal (blue) vs. detection laser frequency, with the PA laser tuned to the short-range $(2)^3\Pi_{0+}[v'=10]$ state. Red and black curves are simulated spectra, based on known energies and FCFs of the $X\,^1\Sigma^+(v'')\rightarrow(2)^1\Pi\,[v']$ states transitions. The black [red] curve is for transitions from $X(v''=0)$ [sum of signals from all excited levels $X(v''=1$-$5)$]. The only free parameters in the fit are an overall scale, and the relative populations of the $X\,^1\Sigma^+(v'')$ levels. Here the relative population of $X(v''=0)$ is ~20%.

strengths in PA spectra. This method makes it possible to assign the electronic symmetry of the excited state in a PA spectrum simply, and also to determine the temperature of the trapped atomic sample, as well as the presence of any scattering resonances between atoms. A publication describing this method and its application to previous PA spectra is near completion. We are now undertaking high-resolution "depletion spectroscopy" measurements[13] to explicitly verify that the $X\,^1\Sigma^+(v=0,J=0)$ is populated by the decay of the $J = 1$ PA resonance.

This method should make it possible to continuously produce and accumulate $X\,^1\Sigma^+(v=0,J=0)$ RbCs molecules into an optical trap. This is fundamentally different from existing approaches to form similar molecular samples, which use Feshbach-resonance association followed by stimulated optical transitions to the ground state.[14] Here the dissipation associated with decay of the PA resonance allows irreversible accumulation. Key to this approach is that, unlike many heteronuclear bialkali species, RbCs is immune to inelastic, chemically-reactive collisions with itself, and with Cs atoms. Hence, molecule production in the presence of dense Rb and Cs vapors can allow the accumulation of large molecular samples. Once the molecule density reaches equilibrium (due to destructive collisions with Rb atoms and residual rovibrationally-excited RbCs* molecules), removal of Rb and continued co-trapping with Cs atoms can "scrub" the sample of RbCs* via inelastic collisions. We have simulated the properties of a trapped sample of $X\,^1\Sigma^+(v=0,J=0)$ RbCs molecules produced using this approach, based on simple rate equation arguments, and have concluded that it opens a pathway to trapping molecules at sufficient density and number to study collisions and reactions. We plan to experimentally explore the dynamics of the accumulation and scrubbing processes in an optical trap next.

Along with this main focus of our work, we recently completed an analysis of the full set of Cs_2 two-color PA data (previously described in part in Ref. [15]), with the goal to provide a more complete description of the coupled a $^3\Sigma_u^+$ and X $^1\Sigma_g^+$ ground state potentials in Cs_2.[16]

References

[1] A.J. Kerman *et al.*, Phys. Rev. Lett. **92**, 033004 (2004).

[2] A.J. Kerman *et al.*, Phys. Rev. Lett **92**, 153001 (2004).

[3] J.M. Sage, S. Sainis, T. Bergeman, and D. DeMille, Phys. Rev. Lett. **94**, 203001 (2005).

[4] T. Bergeman *et al.*, Eur. Phys. J. D **31**, 179 (2004).

[5] E. R. Hudson, N.B. Gilfoy, S. Kotochigova, J.M. Sage, and D. DeMille, Phys. Rev. Lett. **100,** 203201 (2008). [DOE SUPPORTED]

[6] W.C. Stwalley and H.J. Wang, J. Mol. Spectrosc. **195**, 194 (1999)

[7] J. Deiglmayr *et al.*, Phys. Rev. Lett. **101**, 133004 (2008)

[8] P. Zabawa, A. Wakim, M. Haruza, and N. P. Bigelow, Phys. Rev. A **84**, 061401(R) (2011).

[9] C. Gabbanini and O. Dulieu, Phys. Chem. Chem. Phys. **13**, 18905 (2011).

[10] Z. Ji *et al.*, Phys. Rev. A **85**, 013401 (2012).

[11] C.D. Bruzewicz, M. Gustavsson, T, Shimasaki, and D. DeMille, arXiv:1308.2613v1 [physics.atom-ph]; submitted to New J. Phys (2013). [DOE SUPPORTED]

[12] Y. Lee, Y. Yoon, S. Lee, J.-T. Kim, and B. Kim, J. Phys. Chem. A **112**, 7214 (2008).

[13] D. Wang *et al.*, Phys. Rev. A **75**, 032511 (2007).

[14] S. Ospelkaus *et al.*, Science **327**, 853 (2010).

[15] D. DeMille *et al.*, Phys. Rev. Lett. **100**, 043202 (2008). [DOE SUPPORTED]

[16] S. Sainis, J. Sage, E. Tiesinga, S. Kotochigova, T. Bergeman, and D. DeMille, Phys. Rev. A **86**, 022513 (2012). [DOE SUPPORTED]

SPATIAL-TEMPORAL IMAGING DURING CHEMICAL REACTIONS

Louis F. DiMauro
Co-PI: Pierre Agostini
Department of Physics
The Ohio State University
Columbus, OH 43210
dimauro@mps.ohio-state.edu
agostini@mps.ohio-state.edu

1.1 PROJECT DESCRIPTION

This document describes the BES funded project (grant #: DE-FG02-06ER15833) entitled "Spatial-temporal imaging during chemical reactions" at The Ohio State University. Imaging, or the determination of the atomic positions in molecules is of central importance in physical, chemical and biological sciences. X-ray and electron diffraction are well-established method to obtain static images with sub-Angstrom spatial resolution. However their temporal resolution is limited to picoseconds. This proposal builds on the "molecule self-imaging" approach, based on bursts of strong-field driven coherent electron wave packets emitted by the molecule under interrogation. We are investigating two complementary self-imaging methods: Laser-Induced Electron Diffraction (LIED) [1] and high harmonic tomography [2, 3]. Both thrust utilize the wavelength scaling of strong-field interactions to improve the imaging capabilities.

Over the past year, our efforts have focused on the LIED approach: (1) verify the principles of the quantitative rescattering theory using atomic ionization, (2) demonstrate that LIED at long wavelength provides femtosecond resolution together with atomic spatial precision [4] and (3) a proof of principle for determining the atomic positions by Fourier transform of the energy dependent differential cross-section.

1.2 PROGRESS IN FY13: THE LASER INDUCED ELECTRON DIFFRACTION

The LIED approach is one of the variants of molecular self-probing techniques, which has a simple analog to conventional electron diffraction (CED). In CED, an external multi-kilovolt electron beam elastically scatters from a molecular gas sample and the resulting small-angle, forward-scattering, diffraction pattern conveys information on the molecular structure. The bond-length information can be retrieved from the pattern, assuming some approximations. One key ansatz is that the high-energy electrons penetrate the core and thus, the short range atomic-like potential dominates the electron-molecule scattering, while the bonding valence electrons look transparent. This allows use of the independent atom model (IAM) approximation, which describes the scattering as the contribution from individual atoms and an interference term between atoms (molecular term).

In LIED, one simply records the photoelectron momentum distribution produced by the molecule irradiated by a strong mid-infrared laser. Although the electron return energies (typically 100-300 eV) employed are lower than in CED case, LIED can measure large angle scattering (large momentum transfer). Ultimately, the momentum transfer determines the spatial resolution, which for LIED and CED can be comparable. Furthermore, the DCS can be retrieved for different scattering energies by measuring a single momentum distribution. Most importantly, LIED contains information on the time difference between the instant the electron is promoted into the continuum and the instant when it rescatters with the molecule. This time difference (propagation time) is easily derived from the classical equation of motion of a field-driven electron.

The QRS model [5] postulates that the measured DCS is the product of the *field-free* DCS, which contains the angular dependence, and an angle-independent factor, which contains all the effects of the field. Thus, the model provides the connection between the photoelectron momentum distribution and the scattering cross-section. Conceptually LIED can be viewed as follow: the laser acts, first, as a source of photoelectrons and second as a clock that controls the emission and scattering times.

ATOMIC DCS OBTAINED FROM LIED MEASUREMENTS. LIED experiments on atoms establish an important benchmark for using LIED for time-resolved imaging of molecular dynamics. In this study [6],

we showed that *field-free* electron differential cross sections (DCS) of rare gas atoms could be extracted from measurements of the angular-resolved high-energy above-threshold ionization electron momentum distributions generated by mid-infrared lasers.

Figure 1(a) present results for the relative DCS retrieved from argon for different laser parameters for a 100 eV recollision energy. The figure shows that irrespective of the laser parameters, the extracted DCS are identical and agree with the CED measurements. In contrast to the typical monochromatic electron beam used in CED experiments, the laser-driven returning wave packet is broadband, ranging from 0 to $3.2U_p$. Thus, a series of DCS for different returning energies can be extracted from a *single* measured momentum distribution. Figure 1(b) and (c) depicts two additional DCS at 150 eV and 200 eV energies, respectively, extracted from the same 2 μm experiment. Similar measurements were also performed using krypton and xenon. All the extracted DCS faithfully reproduce the evolution in the shape seen in the *e*-neutral measurements and *e*-ion calculations as a function of electron energy. These results clearly support the validity of the QRS model but also demonstrate two important assumptions essential for imaging. First, above 100 eV recollision energies the DCS at large angles are nearly the same for neutral atoms and singly-charged ions, *i.e.* core-penetrating hard collisions. Second, the DCS extracted at different laser intensities and wavelengths are nearly identical for a fixed electron return energy in the strong field limit.

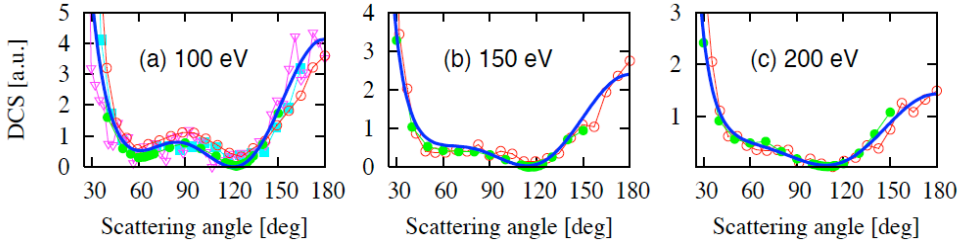

Figure 1: Comparison of LIED retrieved (open symbols), theoretical (solid line) and CED (green circles) measurements of the angular dependent DCS at three electron energies. The LIED DCS is extracted from electron momentum distributions emitted by argon at different laser wavelengths (1.7-2.3 μm) and intensities.

ULTRA-FAST MOLECULAR IMAGING. The initial investigations were performed on N_2 and O_2 using intense, ultra-short pulses over the wavelength range of 1.7 - 2.3 μm. Angle-resolved (collection angle 1.6°) momentum distributions were recorded by focusing the laser in a field-free time-of-flight (TOF) electron spectrometer. At each wavelength, the momentum distribution was obtained by rotating the laser polarization with respect to the spectrometer axis in 2° steps. For each angle, data was collected for approximately 10^6 laser shots, thus ensuring the necessary dynamic range while providing a low count rate to minimize space-charge effects. A typical N_2 momentum distribution for 260 TW/cm^2, 2.0 μm pulses has a classical cutoff energy of 900 eV and corresponds to return energies in excess of 250 eV. These energies exceed previous 0.8 μm studies by an order of magnitude, a critical element for producing core-penetrating collisions needed to validate the IAM approximation. In addition, our investigation does drive the ionization into the strong-field limit ($\gamma \sim 0.3$).

The control for our LIED investigation was ionization of the highest occupied molecular orbital (HOMO) of N_2, the bonding σ_g orbital. Removal of the σ_g electron results in a small change in the equilibrium N-N distance from 1.10 Å (neutral) to 1.12 Å (ion). The extracted DCS is matched to an IAM calculation by fitting the normalization constant and the internuclear separation. Figure 2(a) shows the best fit (red line) molecular contrast factor (MCF) retrieved from the 2 μm experiment (symbols), yielding a N-N distance of 1.14 Å. Comparing CED data at the same collision energy (120 eV), we estimate a 5 pm error on the retrieved bond length. For contrast, we also plot in Fig. 2(a) the theoretical MCF calculated for N-N distances deviating from the fitted value by ±5 pm (dashed lines) and equal to that of neutral N_2 (dotted line). Fig. 2(c) shows the similar analysis performed for a collision momentum of 4.11 *au* (230 eV energy) using 290 TW/cm^2, 2.3 μm pulses. The retrieved N-N distance is 1.12 Å. LIED measurements were also performed at 1.7 μm, resulting in a retrieved length of 1.15 Å. These three retrieved bond lengths are plotted in Fig. 2(e) as a function of time, using the classical correspondence with wavelength. The retrieved bond lengths agree, within a 5 pm uncertainty, with the accepted N_2

equilibrium value. However, the experiment cannot resolve the small N-N bond motion (~0.02 Å) during the 4-6 fs time interval following strong-field tunnel ionization.

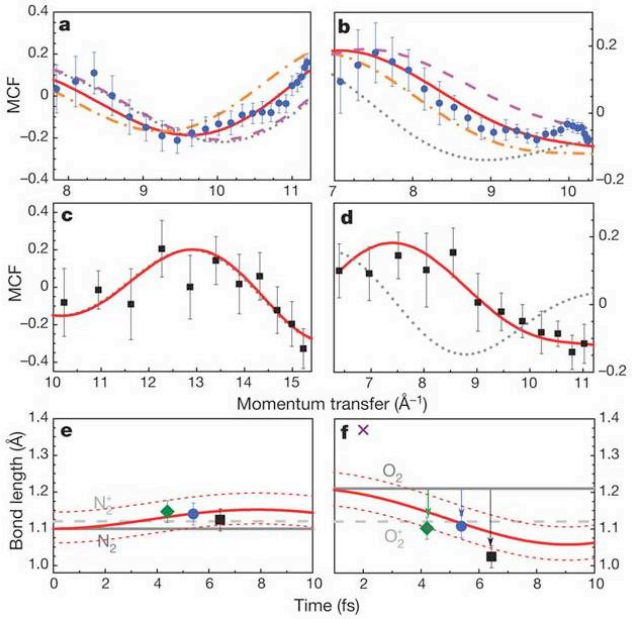

Figure 2: LIED for unaligned N_2 and O_2 molecules. (a)-(d), MCF extracted from the experimental data (scattered symbols) in comparison with theoretical predictions. The best-fit bond lengths are obtained by fitting the DCS extracted directly from the measurement. (a) N_2 data with 260 TW/cm^2, 2.0 μm pulses and (c) N_2 data taken with 290 TW/cm^2, 2.3 μm pulses. (b) O_2 data taken with 133 TW/cm^2, 2.0 μm pulses and (d) O_2 data taken with 150 TW/cm^2, 2.3 μm laser. Illustration of bond change for (e) N_2 and (f) O_2 following ionization. The bond lengths extracted from the LIED measurements at each wavelength (squares: 2.3 μm, circles: 2μm, diamonds: 1.7 μm) are plotted. The associated error bars represent the IAM standard deviation resulting from experimental uncertainties. The time and wavelength correspondence is based on a classical return analysis. The equilibrium bond length is indicated by the solid (neutral) and dashed grey (ion) lines. For O_2, the vertical arrows indicate that the measured bond lengths for all three wavelengths are consistently shorter (~ 0.1 Å) than the neutral's equilibrium length and statistically meaningful. The plot suggests that this is a consequence of the 4-6 fs bond evolution following ionization. The bond length reported in Ref [1] (cross symbol) was extracted from a 0.8 μm laser experiment on aligned O_2 molecules. The Meckel experiment did not achieve the strong-field limit, thus complicating the interpretation and analysis of the momentum distribution, ultimately producing larger systematic error in bond length.

In contrast to N_2, the O_2 HOMO is an anti-bonding π_g orbital and ionization results in a large change in the O-O equilibrium distance from 1.21 Å (neutral) to 1.10 Å (ion). Following the same procedure as above, the extracted O-O distances for 1.7, 2.0 and 2.3 μm LIED measurements are 1.10, 1.11 and 1.02 Å, respectively. Figures 2(b) and (d) present the MCF analysis at the two longest wavelengths, again by comparing experimentally determined MCF values against the theoretical best-fit and theoretical curves obtained for a bond length that differs from the best fit by ±5 pm or is equal to that of neutral O_2. In contrast to the N_2 results, the O_2 MCF curve calculated using the neutral equilibrium distance does not fit the experiment at either wavelength. The O-O distances derived from the best fits deviate by 2-4 standard deviations from the equilibrium value, providing a high degree of confidence (> 99.9%) that the bond has shortened in the 4-6 fs interval after ionization. The Franck-Condon curves in Fig. 2(f) show the free time evolution of the center of the nuclear wave packet (O-O distance, solid red line) whereas red dotted lines indicate its width (FWHM). The three experimental data points in Fig. 2(f) clearly show a statistically significant reduction (0.1 Å) in the O-O bond length from its initial, neutral equilibrium distance of 1.21 Å, as illustrated by the vertical arrows. However, the spatial resolution of the experiment is insufficient to track the much smaller bond length change (~5 pm resolution) occurring within the 4-6 fs time window spanned by the three measurement points. Regarding temporal resolution, we estimate a 2-3 fs uncertainty in assigning a return time for each wavelength.

1.3 Future Plans

LIED: Our current efforts are focused on both fundamental and applied tests of the LIED method: 1) the limits of spatial precision, the influence of multiple trajectories (long versus short and higher-order returns) on temporal precision, the dependence of the ionization rate on molecular alignment and the applicability of theoretical tools developed for CED analysis to LIED. 2) Applications of LIED to determine or observe structural changes in more complex systems; studies on isomeric systems and pump-probe interrogations. Larger molecules pose new challenges on experimental precision and theoretical methods in LIED. The inverse Fourier transform of the LIED image is being explored as an alternate structural retrieval method along with coordinated efforts to improve the data statistics using a VMI spectroscopy.

Tomography: Long wavelength tomography measurements of N_2 and CO_2 are being analyzed and should provide a benchmark for future efforts.

A strategy for imaging chemical dynamics using LIED and/or Tomography is being evaluated: the aim is to follow unimolecular dissociation using pump-probe schemes in which the LIED/Tomography is the probe. A potential candidate is the breaking of the I-C bond in aligned ICN (I_p = 10.8 eV) by exciting from its ground state to its lowest excited, repulsive **A** state.

1.4 References Cited

[1] M. Meckel *et al.*, "Laser-induced electron tunneling and diffraction", Science **320**, 1478-1482 (2008).

[2] J. Itatani *et al.*, "Tomographic imaging of molecular orbitals", Nature **432**, 867-871 (2004).

[3] S. Haessler *et al.*, "Attosecond imaging of molecular electronic wavepackets", Nat. Phys. **6**, 200 (2010).

[4] C. I. Blaga *et al.* "Imaging ultrafast molecular dynamics with laser-induced electron diffraction", Nature **483**, 194 (2012).

[5] C. D. Lin *et al.*, "Strong-field rescattering physics—self-imaging of a molecule by its own electrons", J. Phys. B **43**, 122001 (2010).

[6] Junliang Xu *et al.*, "Laser-induced electron diffraction for probing rare gas atoms", Phys. Rev. Lett. **109**, 233002 (2012).

1.5 Publication Resulting from this Grant in 2011

1. "Observation of high-order harmonic generation in a bulk crystal'', S. Ghimire *et al.*, Nat. Phys. **7**, 138 (2011).
2. "Redshift in the optical absorption of ZnO single crystals in the presence of an intense mid-infrared field", S. Ghimire *et al.*, Phys. Rev. Lett. **107**, 167407 (2011).
3. "Imaging ultrafast molecular dynamics with laser-induced electron diffraction", C. I. Blaga *et al.*, Nature **483**, 194 (2012).
4. Generation and propagation of high-order harmonics in crystals", S. Ghimire *et al.*, Phys. Rev. A **85**, 043836 (2012).

1.6 Review Articles Acknowledging this DOE Award

1. "Scaling of high-order harmonic generation in the long wavelength limit of a strong laser field", A. D. DiChiara *et al.*, IEEE J. Select. Topics Quan. Electro. **18**, 419-433 (2012).
2. "Atomic and molecular ionization dynamics in strong laser-fields: from optical to X-rays", P. Agostini and L. F. DiMauro, in Atomic, Molecular, and Optical Physics, v.61, eds. P. Berman, E. Arimondo and Chun Lin (Elsevier, Maryland Heights, 2012) pp. 117-158.

ATTOSECOND AND ULTRA-FAST X-RAY SCIENCE

Louis F. DiMauro
Co-PI: Pierre Agostini
Department of Physics
The Ohio State University
Columbus, OH 43210
dimauro@mps.ohio-state.edu
agostini@mps.ohio-state.edu

1.1 PROJECT DESCRIPTION

This report summaries the BES funded project (grant #: DE-FG02-04ER15614) entitled "Attosecond & Ultra-Fast X-ray Science" at The Ohio State University (OSU). Attosecond light pulses from gases offer a transition to a novel time-scale and open new avenues of science while complementing and directly contributing to the efforts at the LCLS. The main objectives of this grant is the development of competency in generation and metrology of attosecond pulses using mid-infrared drivers and a strategy of employing these pulses for studying multi-electron dynamics in atomic systems. It focuses on applications in which attosecond pulses are produced and transported to a different region of space and applied to a specific target, thus providing the greatness degree of spectroscopic flexibility. The proposal has also a strong thrust at the LCLS XFEL for studying the scaling of strong-field interactions into a new regime of x-ray science and the metrology of ultra-fast x-ray pulses.

Progress over the past year includes (1) measurement of the wavelength dependence of the attochirp, (2) attosecond shaping near a Cooper minimum and (3) streaking measurements at the LCLS XFEL.

1.2 PROGRESS IN FY13: THE ATTOSECOND PROGRAM

The OSU attosecond beamline/end-station began operations at the start of the current grant cycle and is routinely used to perform attosecond spectroscopy and tomographic molecular imaging experiments, both funded by DOE. The ultimate objective is to create sufficiently short wavelength attosecond pulses to allow access to core level transitions. This is accomplished by exploiting the favorable λ^2 wavelength scaling of the harmonic cutoff energy, which yields attosecond pulses with higher central frequency. An additional benefit is the scaling of the attochirp $\propto \lambda^{-1}$, which leads to inherently shorter attosecond pulses at longer wavelength. Using this approach, the OSU group has the ability to produce ~100 *as* pulses spanning 20-200 eV photon energies.

RABBITT MEASUREMENTS USING LONG WAVELENGTH DRIVING LASERS. The OSU beamline was developed with an approach analogous to synchrotron beamlines and thus is capable of supporting different experimental end-station configurations. The attosecond experiments discussed in this report are focused on studying electron interferometry, so a gas-phase end-station based on electron energy analysis is used. In the future, we would like to add a condensed-phase experimental end-station for performing time-resolved x-ray absorption measurements.

Figure 1 illustrates several features of our RABBITT measurement capability. Each set of points are measurements of the argon HHG phase driven by 0.8, 1.3 and 2 μm pulses. Obviously at the longer wavelengths, the HHG process produces higher energy photons (broader bandwidth) but equally important a finer frequency sampling for higher precision HHG spectroscopy. The significance of this result, which is unpublished, is an independent verification of the reduced attochirp with increasing wavelength. The only previous experiment, performed by our group [1], was based on an all-optical technique [2], which is prone to systematic errors and a model-dependent interpretation [3]. The inset shows the RABBITT measured (symbols) wavelength dependence of the attochirp along with a λ^{-1} curve.

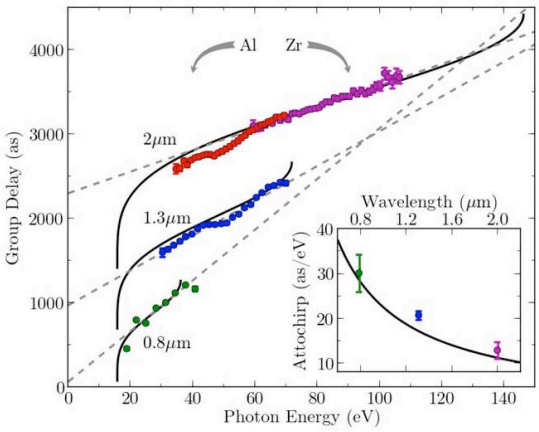

Figure 1: *Experimental argon RABBITT group delay measurements using 0.8 μm, 1.3 μm and 2.0 μm driving lasers.* Solid lines are quasi-classical calculation of the emission times and the dashed lines are linear fits to the experiment. The inset plots the experimental attochirp measurements extracted from the linear fits as a function of wavelength.

ATTOSECOND PULSE SHAPING AROUND A COOPER MIMINUM. The Cooper minimum [4] is a local minimum in the total photoionization (PI) cross section caused by a sign change of the bound-free transition dipole in one angular momentum channel. John W. Cooper showed that its existence could be explained within the Single Active Electron approximation using wave functions that are nonhydrogenic. Several decades of studies ensued using traditional frequency-domain photoionization spectroscopy but the rapid phase change (~π) of the dipole associated with the Cooper minimum (CM) could not be directly measured although its influence strongly affects the spectral shape of the electron angular distribution and spin polarization [5]. Alternately, the inverse process, field-driven strong-field photorecombination, responsible for production of coherent broadband XUV high harmonic radiation provides contact to both the amplitude and phase and a time domain measurement of the CM. Thus, the CM is a key paradigm for establishing the connection between photoionization and recombination because it is a signature of atomic structure that does not depend on the parameters of the driving laser. The argon CM has been observed to produce a minimum in the harmonic yield for energies above the *d*-channel sign change (48 eV) but the phase remained unexplored. We have, to the best of our knowledge, made the first measurement of the frequency-dependent phase around a CM.

In order to understand the influence of the Cooper minimum on the recombination dipole (RDM) and equally important on the attosecond shaping, we conducted a study that measures in argon the derivative of the spectral phase, the group delay, using the RABBITT method. This experiment exemplifies the utility of the long wavelength approach for attosecond precision. First, for a 0.8 μm driver the position of the Cooper minimum (antiresonance) occurs near the HHG cutoff energy (~ 50 eV). Second, the change in the Cooper phase occurs over a broad bandwidth thus requiring a fine frequency sampling. For 0.8 μm the sampling is ~3 eVs while it increases in resolution at 2 μm by a factor of 2.6.

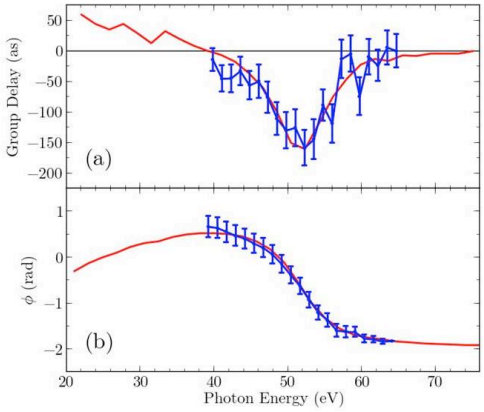

Figure 2: *Argon measurements (symbols with error bars) and the TDSE-MWE calculation (solid line) of* ***(a)*** *the group delay and* ***(b)*** *the spectral phase of the total recombination dipole matrix element (RDM).* Although the *d*-channel RDM undergoes a sharp π-phase shift at the Cooper minimum (48 eV), the phase shift of the total RDM is closer to 2.6 radians and spread over 20 eV.

The measured RABBITT phase is equal to the sum contributions of the recombination dipole phase, the wave packet phase of the continuum electron, and the macroscopic contributions including neutral-atom dispersion, the metal filter dispersion and the geometric (Gouy) phase of the harmonic wave fronts. The RABBITT measurement is performed at various wavelengths from 1.3-2 μm, *e.g.* raw data in Fig. 1. We find that the characteristic phase modulation (2.6 radians) due to the CM can be extracted from the RABBITT signal, as shown in Fig. 2. We obtain qualitative agreement

with a simple model based on the scattering phases and amplitudes of the interfering *s*- and *d*-channel contributions to the complementary PI process. In addition, we also find very good agreement with more comprehensive calculations that include both the single atom and macroscopic harmonic generation response (see curves in Fig. 2).

Most importantly, our results allow us to address on the relation between the measured group delay and the timing of harmonic emission in the presence of antiresonance. Since the CM is purely quantum mechanical, its main effect is to reshape the temporal envelope of the dipole response thus disconnecting the usefulness of an interpretation as an emission time. This work was performed in collaboration with the theory support of Mette Gaarde and Ken Schafer (LSU). A manuscript has been submitted to PRL.

1.3 Progress in FY13: Investigations at the LCLS XFEL

Since 2009, the OSU group has been involved in several experimental campaigns at the LCLS XFEL at SLAC. The OSU group was involved in the early commissioning, the design and construction of the magnetic bottle photoelectron spectrometer for the initial LCLS AMOS end-station and directly involved in several experimental runs. All the experiments reported here were conducted on the LCLS AMOS end-station in collaboration with other institutions. The following highlights only some of these efforts.

X-RAY PULSE CHARACTERIZATION USING TWO-COLOR FIELDS. Part of the group's LCLS activities is to exploit known attosecond techniques for characterization of femtosecond x-ray pulses. The SASE lasing process of the LCLS XFEL poses some significant challenges in this regard. First, the pulses have poor longitudinal coherence (~ 1 fs) and second, the uncertainty in the SASE buildup results in (a) large timing jitter with respect to a stable external clock (~ 100 fs) and (b) fluctuations in the x-ray pulse duration and energy. Consequently, the approach is to treat the data as single shot experiments which are tagged with various measurable quantities, e.g. central frequency, pulse energy, for post-processing. One obvious measurement absent from the diagnostic suite is the x-ray pulse duration.

Our expertise in ultra-fast metrology, particularly for soft x-ray attosecond pulses, supported by this grant translates into viable means for characterizing LCLS pulses. The approach is to use an external low-frequency laser reference field for (1) sideband AM dressing or (2) FM streaking. This is analogous to RABBITT or the attosecond streaking techniques used in a laboratory HHG experiment. However there is one major technical barrier, unlike an HHG experiment where the attosecond pulse(s) are precisely phase-locked to the fundamental dressing field, the LCLS x-rays jitter, ~ 50-100 fs, with respect to an external clock, *e.g.* optical laser, by several pulse widths (10-100 fs) depending on the mode of operation. A standard LCLS online diagnostic is the shot-to-shot arrival time of the electrons, which provides a timing tag with ~30 fs precision but the SASE contribution is random and large.

Our general approach is to use variants of two-color fields (x-ray + optical field) and single-shot time-of-flight electron spectroscopy. Depending on the objectives, we have used different variations of the dressing field from 0.8 μm to terahertz. For example, in one run the neon K-shell is ionized by 1 keV x-ray pulse in the presence of an intense optical field (1 TW/cm^2, 0.8 μm field). The resulting dressed photoelectron provides a straightforward, non-invasive and on-line means of determining the duration of femtosecond (> 40 fs) x-ray pulses [6]. It was found that the experimental measurement was systematically smaller than the electron bunch length. Nominal electron pulse durations of 175 and 75 fs yielded x-ray pulse durations of 120 ± 20 fs FWHM and 40 ± 20 fs FWHM, respectively.

1.4 Future Plans

Attosecond probing of below-threshold harmonics. The lowest energy harmonics probed by a typical RABBITT or streaking experiment is determined by the ionization potential of the detector atom, which is satisfactory for obtaining phase information in the HHG plateau region. The plateau region is usually explained using the semi-classical model. However, the classical model is not applicable for

harmonic orders produced below the ionization potential of the generation atom/molecule. To probe this region a RABBITT detector atom is used that has a lower ionization potential than the HHG source atom. We are making RABBITT measurements near threshold in order to gain some insight into the classical/quantum correspondence.

Auger decay and x-ray pulse measurements. We are trying to improve our earlier LCLS measurements on the time-resolved Auger decay and x-ray metrology by using the Streaking method employing 18 μm pulses instead of 2.3 μm. The advantage is that the long period of the reference field will be less sensitive to the jitter of the LCLS timing system. We are currently analyzing data from a run period in February 2013.

1.5 References Cited

[1] G. Doumy *et al.*, "Attosecond synchronization of high-order harmonics from midinfrared drivers", Phys. Rev. Lett. **102**, 093002 (2009)

[2] N. Dudovich *et al.*, "Measuring and controlling the birth of attosecond XUV pulses", Nat. Phys. **2**, 781 (2006).

[3] J. M. Dahlström *et al.*, "Atomic and macroscopic measurements of attosecond pulse trains", Phys. Rev. A **80**, 033836 (2009)..

[4] J. W. Cooper, "Photoionization from outer atomic subshells. A model study" Phys. Rev. **128**, 681 (1962).

[5] D. J. Kennedy & S. T. Manson, "Photoionization of the noble gases: cross sections and angular distributions", Phys. Rev. A **5**, 227 (1972).

[6] S. Düsterer *et al.*, "Femtosecond x-ray pulse length characterization at the Linac Coherent Light Source free-electron laser", *New J. Physics* **13**, 093024 (2011).

1.6 Publication Resulting from this Grant

1. "Observation of high-order harmonic generation in a bulk crystal'', S. Ghimire *et al.*, Nat. Phys. **7**, 138 (2011).
2. "Redshift in the optical absorption of ZnO single crystals in the presence of an intense midinfrared field", S. Ghimire *et al.*, Phys. Rev. Lett. **107**, 167407 (2011).
3. "Scaling of high-order harmonic generation in the long wavelength limit of a strong laser field", A. D. DiChiara *et al.*, IEEE J. Select. Topics Quan. Electro. **18**, 419 (2012).
4. "Nonlinear atomic response to intense ultrashort x-rays", G. Doumy *et al.*, Phys. Rev. Lett. **106**, 083002 (2011) (L. DiMauro [OSU], spokesperson).
5. "Unveiling and driving hidden resonances with high-fluence, high-intensity x-ray pulses", E. P. Kanter *et al.*, Phys. Rev. Lett. **107**, 233001 (2011) (E. Kanter [ANL], spokesperson).
6. "Angle-resolved electron spectroscopy of laser-assisted Auger decay induced by a few-femtosecond x-ray pulse", M. Meyer *et al.*, Phys. Rev. Lett. **108**, 063007 (2012) (L. DiMauro [OSU], spokesperson).
7. "Generation and propagation of high-order harmonics in crystals", S. Ghimire *et al.*, Phys. Rev. A **85**, 043836 (2012).
8. "Atomic and molecular ionization in strong laser fields: from optical to x-rays", P. Agostini and L. F. DiMauro, in Advs. In Atomic, Molecular and Optical Physics, vol. **61**, eds. E. Arimonda, P. R. Berman and C. C. Lin (Elsevier, Amsterdam), 118-158.
9. "Driving-frequency scaling of quantum paths", T. Auguste, P. Salieres, F. Catoire, P. Agostini and L. F. DiMauro, New J. Phys. **14**, 103014 (2012).

High Intensity Femtosecond XUV Pulse Interactions with Atomic Clusters

Project DE-FG02-03ER15406

Principal Investigator:
Todd Ditmire

Co-Investigator
John Keto

The Texas Center for High Intensity Laser Science
Department of Physics
University of Texas at Austin, MS C1600, Austin, TX 78712
Phone: 512-471-3296
e-mail: tditmire@physics.utexas.edu

Program Scope:

The nature of the interactions between high intensity, ultrafast, near infrared laser pulses and atomic clusters of a few hundred to a few thousand atoms have been well studied by a number of groups world wide. Such studies have found that these interactions are more energetic than interactions with either single atoms or solid density plasmas and that clusters explode with substantial energy when irradiated by an intense laser. Under the previous phase of BES funding we extended investigation in this interesting avenue of high field interactions by undertaking study of the interactions of intense extreme ultraviolet (XUV) pulses with atomic clusters, and more recently, interactions with intense x-ray pulses from the Linac Coherent Light Source (LCLS). Our current work builds on our previous work with a high energy high harmonic (HHG) femtosecond XUV source and seeks to study these XUV/cluster interactions at two to three orders of magnitude higher XUV intensity than we obtained in the last phase. This is being accomplished by upgrading our HHG beam line to much higher drive energies on our new THOR Petawatt laser.

The goal of our experimental program has been to extend experiments on the explosion of clusters irradiated at 800 nm to the short wavelength regime (1 to 50 nm). The clusters studied range from a few hundred to a few hundred thousand atoms per cluster (i.e. diameters of 1-30 nm). Our studies with XUV light are designed to illuminate the mechanisms for intense pulse interactions in the regime of high intensity but low ponderomotive energy by measurement of electron and ion spectra. This regime of interaction is very different from interactions of intense IR pulses with clusters where the laser ponderomotive potential is significantly greater than the binding potential of electrons in the cluster. Soon we will be able to generate short wavelength pulses with up to 1 J of laser drive energy in a much longer focal length geometry than previously employed.

The goal of our program is to extend this class of experiments to higher XUV intensity and a greater range of wavelengths. In particular we plan to perform experiments to confirm our hypothesis about the origin of the high charge states in these exploding clusters, an effect which we ascribe to plasma continuum lowering (ionization potential depression) in a cluster nanoplasma. This effect, which is well known in plasma physics, leads to a depression of the ionization potential enabling direct photo-ionization of ion charge states which would otherwise have ionization energies which are above the photon energy employed in the experiment. To do this we will perform experiments in which XUV pulses of carefully chosen wavelength irradiate clusters composed of only low-Z atoms and clusters with a mixture of this low-Z atom with higher Z atoms (eg. SiO_2 and SnO_2). Experiments on clusters from solids will be enabled by development during the past grant period in which we constructed and tested a cluster generator based on the Laser Ablation of Microparticles (LAM) method. Using a LAM device we will explore oxide clusters as well as metal clusters chosen such that the intense XUV pulse rests at a wavelength that coincides with the giant plasma resonance of the metallic cluster. The latter clusters will exhibit higher electron densities and will serve to lower the ionization potential further than in the clusters composed only of low Z atoms. This should have a significant effect on the charge states produced in the exploding cluster.

We will also explore the transition of explosions in these XUV irradiated clusters from hydrodynamic expansion to Coulomb explosion. We observed hints of this transition in our recent work on THOR in which we compared explosions of Xe and Ar clusters irradiated at 38 nm. The work to be performed with the upgraded beamline will explore clusters of a wide range of constituents, including not only clusters from gases (Xe, Kr, Ar, Ne, N_2 and CH_4) but also clusters from solids.

Progress During the Past Year

Work during this past year has concentrated in two areas. First we have completed construction of the high energy HHG beam line on the upgraded THOR Petawatt laser. Second, we have performed an experiment on the Texas Petawatt laser which measured XUV pulse production drive laser pulse energy of up to 100 J.

Upgrade of the HHG XUV beamline

Our principal work in the past year has been in the construction of a high energy HHG XUV beam line. In our past experiments on intense XUV irradiation of noble gas clusters we produced harmonic radiation by loosely focusing 40 fs pulses with a MgF f/60 lens from our THOR Ti:sapphire laser into an Ar gas jet. These data showed that we were able to produce an 8μm spot with the 38 nm pulse, yielding a focal intensity of ~ 10^{11} W/cm^2 assuming an XUV pulse duration of 20 fs. These harmonics were then focused into the plume of a second, low density cluster jet. The main limitation of this apparatus was that pulse energy was limited to ~ 30 mJ by the use of lens and focal geometry constrained by the lab space. This greatly limit the XUV energy produced to only ~ 10 nJ.

We have now improved this beamline in new expanded lab space. This new beamline is illustrated in figure 1. It is an all reflective design where the THOR laser sends its full energy (~1 J) into a long, loosely-focused (*f*/75), beamline which contains a gas jet to produce HHG of significant intensity. The XUV is sent to the interaction chamber where one of the harmonics is selected and focused using a Sc/Si mirror into gas, clusters or nanoparticles for HED studies.

Figure 1: THOR XUV beamline spanning across two laboratory spaces.

Figure 2 shows a top view of the XUV beamline and the compressor chamber. The beamline is divided in three stages: 1- Focusing, 2- HHG, 3-XUV interaction. In the first stage the compressed 7.5 cm diameter beam is steered 90º in the focusing chamber, sent to a 0º mirror in the retro chamber. There, the beam reflects back onto a *f* =5500 mm concave spherical mirror that focuses the beam under a gas jet in the HHG stage at intensities up to 3x10^{15} W/cm^2. The jet is moved out of the focus to keep the intensity below this transition for relativistic motion of quiver electrons. The angle of incidence in the focusing mirror is about 1º which makes spherical aberrations at focus negligible. The 1/e^2 spot diameter of 76 μm is entirely determined by diffraction with a 5.5 mm Rayleigh length. Once in the HHG stage the beam interacts with the gas jet to generate harmonics that travel down the beamline with the fundamental light. At a distance approximately one focal length from the gas jet the fundamental and low harmonics are filtered out and sent to the XUV interaction chamber. A Sc/Si mirror picks a particular harmonic in the 10-30 nm range and will focuses it on a gas jet.

Separation of the XUV pulses from the fundamental and low harmonics is done in a two-step process. Initially, the pulse before leaving the compressor goes through a 1 cm diameter circular disk mask in the center of the beam that creates a donut shape spatial beam profile. This disk is at approximately two focal lengths upstream from the focusing mirror and its image is located at two focal lengths downstream from the mirror with a magnification of -1. At this location, right before entering the interaction chamber, an aperture with the size of the circular disk blocks most of the infrared donut shape profile. The XUV, having a much shorter wavelength, diffracts much less and goes through the center of the aperture with a small fraction of the fundamental light that was scattered by the gas jet. Following the aperture, a free-standing 100 nm aluminum foil, with approximately 20-50% transmission in the XUV range, filters the remaining of the fundamental light and low harmonics.

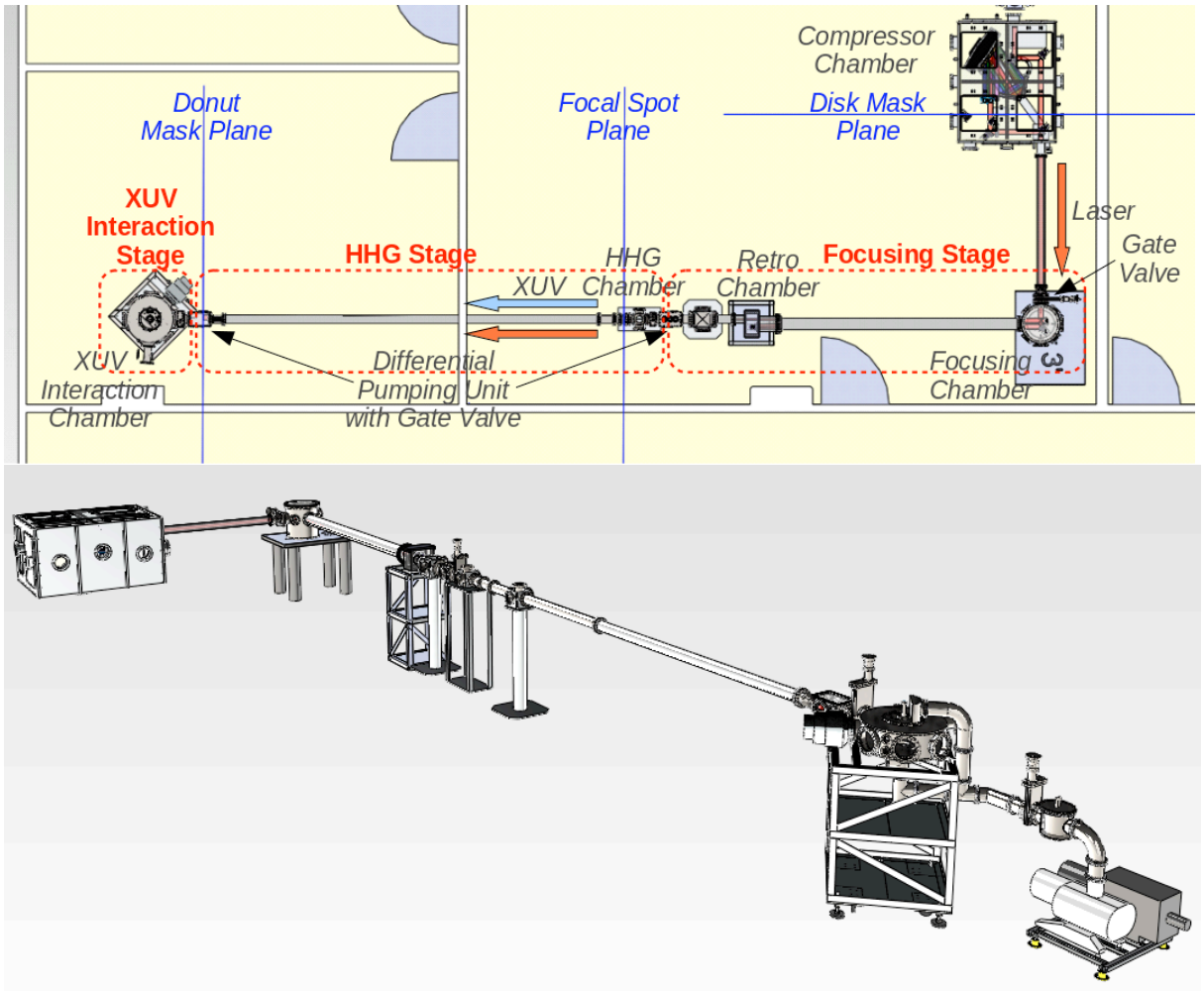

Figure 2: Top view schematics of the XUV beamline (top) and model rendering (bottom).

Optimization of the HHG yield is mainly achieved by varying the location of the gas jet with respect to the laser focus. A series of vacuum tubes with different length (1", 3", 6", 9" and 16") are swapped before or after the HHG chamber to produce the coarse positioning (1" steps) along the laser beam while a 1"-micrometer xyz-manipulator in the chamber creates the fine tuning. The combination of tubes and translation stage allow a total scan distance of 36". The alignment of the laser beam under vacuum starts with a pair of cross hairs that define the injection of the beam into the compressor chamber. An iris between the cross hairs apodizes the beam to a few millimeters diameter. After compression, a mirror on a rotation stage with motorized tip and tilt sends the beam into the XUV beamline. The small fraction of the beam that is transmitted by the dielectric focusing mirror is transported outside the chamber to a camera with a cross hair in front of it. The motorized mirror is adjusted to align the apodized beam with the cross hair behind the focusing mirror, as seen by the camera. The tip and tilt of the focusing mirror is also motorized and used to align the beam under the gas jet as seen by the ionized plume. Also, a window at the location of the aperture used to filter the fundamental light downstream allows viewing of the beam for alignment.

High Energy XUV pulse production by HHG on the Texas Petawatt Laser

A secondary thrust in the past year has been in the measurement of XUV pulse energies when the entire 100J pulses of the Texas Petawatt laser (150 J, 150 fs at wavelength of 1057 nm) is focused into a large aperture gas jet. We performed one 4-week run on the Texas Petawatt. The set-up for the experiment is illustrated in figure 3. We focused the laser with an f/40 mirror into a specially built slit gas jet which produced nearly a cm of gas for a target. The laser light was filtered away with expendable Al filters. The XUV light was incident on a XUV sensitive window which had a calibrated yield. A window could be

inserted to ascertain if through light from the laser was responsible for the observed signal. The inset to figure 3 shows an HHG beam partially obscured by the window proving that the signal was not IR or optical light. Estimates on the per harmonic yield indicate that we produced 30 – 100 μJ of energy per harmonic in the transmission window of the Al filter.

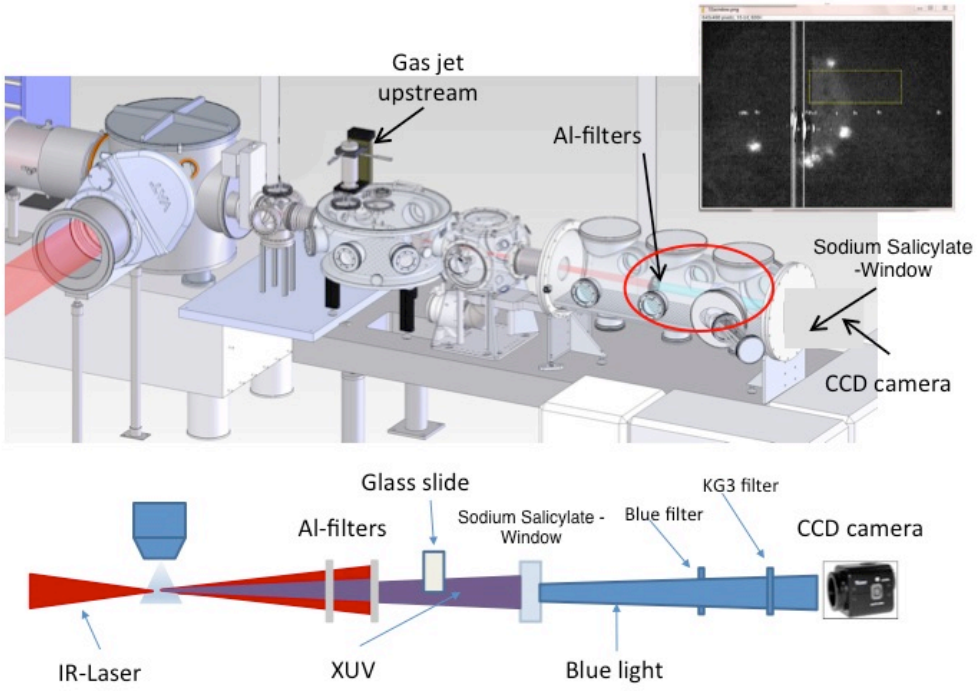

Figure 3: Layout of the HHG conversion experiment on the Texas Petawatt Laser. Inset, image of XUV light partially obscured on the Salicylate detector.

Future Research Plans

Our future plans involve studying continuum lowering in mixed species clusters. We have previously finished the construction of a micro-particle laser ablation beam to be installed on the beam line in figure 2. This will allow us to study continuum lowering in mixed low and high Z clusters. These new experiments are beginning on the upgraded THOR laser at the ~ 1 J level this month.

Refereed papers published or submitted on work supported by this grant during the past three years

1) W. Bang, M. Barbui, A. Bonasera, G. Dyer, H. J. Quevedo, K. Hagel, K. Schmidt, F. Consoli, R. De Angelis, P. Andreoli, E. Gaul, A. C. Bernstein, M. Donovan, M. Barbarino, S. Kimura, M. Mazzocco, J. Sura, J. B. Natowitz, and T. Ditmire, "Temperature Measurements of Fusion Plasmas Produced by Petawatt-Laser-Irradiated D-2-He-3 or CD4-He-3 Clustering Gases" *Phys. Rev. Lett.* **111**, 055002 (2013).
2) W. Bang, G. Dyer, H. J. Quevedo, A. C. Bernstein, E. Gaul, M. Donovan, and T. Ditmire, "Optimization of the neutron yield in fusion plasmas produced by Coulomb explosions of deuterium clusters irradiated by a petawatt laser" *Phys. Rev. E* **87**, 023186 (2013).
3) W. Bang, H. J. Quevedo, G. Dyer, J. Rougk, I. Kim, M. McCormick, A. C. Bernstein, A. and T. Ditmire, "Calibration of the neutron detectors for the cluster fusion experiment on the Texas Petawatt Laser" *Rev. Sci. Instruments* **83**, 063504 (2012).2)
4) H. Thomas, N. Kandadai, K. Hoffmann, A. Helal, J. Keto, B. Iwan, N. Timneanu, J. Andreasson, M. Seibert, D. van der Spoel, J. Hajdu, S. Schorb, T. Gorkhover, D. Rupp, M. Adolph, T. Möller, G. Doumy, L.F. DiMauro, C. Bostedt, J. Bozek, M. Hoener, B. Murphy, N. Berrah and T. Ditmire "Explosions of Xe-clusters in ultra-intense femtosecond x-ray pulses from the LCLS X-ray Free Electron Laser" *Phys. Rev. Lett.* **108**, 133401 (2012).
5) K. Hoffmann, B. F. Murphy, N. Kandidai, B. Erk, A. Helal J. Keto, and T. Ditmire, "Rare-gas-cluster explosions under irradiation by intense short XUV pulses" *Phys. Rev. A*, **83**, 043203 (2011).
6) B. Erk, K. Hoffmann, N. Kandadai, A. Helal, J. Keto, and T. Ditmire "Observation of shells in Coulomb explosions of rare-gas clusters" *Phys. Rev. A* **83**, 043201 (2011).
7) K. Hoffmann, B. Murphy, B. Erk, A. Helal, N. Kandadai, J. Keto, and T. Ditmire "High intensity femtosecond XUV pulse interactions with atomic clusters" *J. of High En. Den. Phys.*, **6**, 185 (2010).

Ultracold Molecules: Physics in the Quantum Regime

Senior Investigator: John Doyle, Harvard University
17 Oxford Street. Cambridge MA 02138
doyle@physics.harvard.edu
Research Project Abstract 2013

1. Overview of Project

Our research encompasses a unified approach to the cooling and detecting, and in many cases trapping, a diverse set of chemical species of both atoms and molecules, and study of their collisions. We have developed lasers and apparatus for trapping both CaH and CaF molecules and have trapped both using our new method. We have also cooled a large variety of large molecules and developed a new, definitive, large signal method for determining chirality. We have also demonstrated a method for trace detection with high specificity of small organic molecules in a mixture.

Publications from this period are:

[1] *Buffer Gas Cooling and Intense, Cold, Slow Molecular Beams*, N.R. Hutzler, Hsin-I Lu, J.M. Doyle, Chemical Reviews Special Issue on Ultracold Molecules **112** 4803 (2012)

[2] *Cooling molecules in a cell for FTMW spectroscopy*, D. Patterson and J.M. Doyle, Molecular Physics **110** 1757 (2012)

[3] *Enantiomer-Specific Detection of Chiral Molecules via Microwave Spectroscopy*, D. Patterson, M. Schnell and J.M. Doyle, Nature, **497** 475-477 (2013)

[4] *Sensitive Chiral Analysis via Microwave Three-wave Mixing*, D. Patterson and J.M. Doyle, Physical Review Letters **111** 023008 (2013)

[5] *Magnetic Trapping of Molecules via Optical Loading and Magnetic Slowing*, Hsin-I Lu, I. Kozyryev, B. Hemmerling, J. Piskorski, and J.M. Doyle, preprint (2013)

Work to date: demonstration of general trap loading for molecules

A simple optical pumping process with the scattering of two photons is employed to achieve magnetic slowing and irreversible trap loading. Fig. 1(a) depicts the apparatus, which consists of a two-stage beam source [1], a magnetic lens, and a superconducing magnetic trap. A cryogenic shutter after the magnetic lens can be closed after trap loading. CaF molecules are created by laser ablation inside the 1st cell at 1.3 K and thermalize with cold ^{3}He. The 2nd cell is designed such that there are sufficient collisions inside for additional slowing while He-molecules collisions in the beam can be suppressed. The slow CaF beam created in both $N = 0$ and $N = 1$ states has a peak forward velocity of 55 m/s with a velocity spread of 45 m/s (brightness of 3×10^9 molecules/sr/pulse).

Low-field seekers (LFS) are collimated by the magnetic lens into a quadrupole magnetic trap with a maximum field strength of 4.9 T. When entering the trap, the LFS lose their kinetic energy while climbing up the potential hill, as illustrated in Fig. 1(b). The first optical pumping laser (OPL), resonant with the LFS near the saddle (B_1), optically pumps CaF to high field seekers (HFS) via the $X^2\Sigma^+(v = 0) \rightarrow A^2\Pi_{1/2}(v' = 0)$ transition at 606 nm. The HFS proceed to the trap center, get further decelerated, and are pumped by the 2nd OPL to the trappable state (LFS) at B_2. Scattering two photons is sufficient for trap loading. The efficiency of transferring between the LFS and HFS is limited by the leakage to dark rotational excited states.

The capture energy of this loading scheme can be understood as follows. Only molecules with enough kinetic energy to climb up two potential hills can reach the trap center, setting the lower bound of

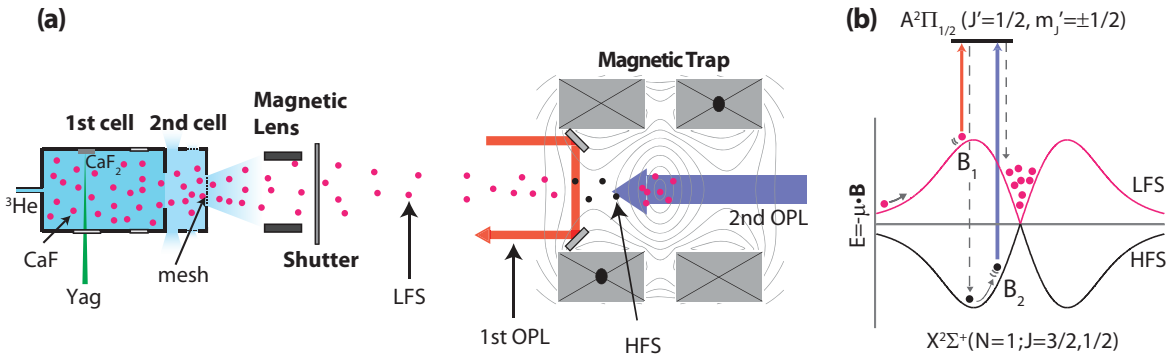

Figure 1: (a) Schematic of the direct trap loading of CaF apparatus. A slow CaF beam produced from a two-stage buffer-gas cell is focused by a magnetic lens and then enters a magnetic trap. Two optical pumping lasers are used to irreversibly transfer molecules into the trap. A cryogenic shutter between the magnetic lens and trap blocks the buffer gas after trap loading, providing a high vacuum in the trap region. (b) Optical loading scheme for $^2\Sigma^+$ ($N = 1$) molecules into a magnetic trap. Potentials experienced by the low field seekers and high field seekers are represented in pink and black curves respectively.

the capture energy to be $E_L = \mu_B \times (2B_1 - B_2)$. After deceleration, molecules with kinetic energy lower than the trap depth, $E_D \sim \mu_B \times (B_1 - B_2)$, can remain trapped.

State transfer of CaF during the optical pumping process is experimentally demonstrated with an efficiency of 15% for transferring LFS $\rightarrow$ HFS $\rightarrow$ LFS. We successfully load 2×10^4 CaF ($N = 1$) molecules/pulse into the trap with a decay time of 90 ms without the cryogenic shutter. After incorporating the shutter, we observe trapped CaF ($N = 1$) for longer than 1 s (decay time > 500 ms). The observed trap lifetime is limited by elastic collisions with the background buffer gas at a density of 5×10^{10} cm^{-3} according to the Monte Carlo trajectory simulations.

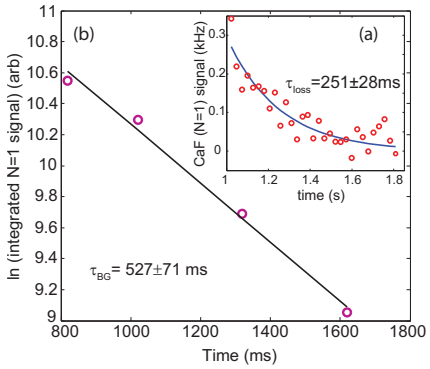

Figure 2: (a) Trapped CaF signal after the shutter is closed. The detection laser is turned on at 1 s. (b) Signal integrated over 210 ms as a function of time after ablation at which the detection laser is switched on. A decay time of 530 ms is limited by collisions with the background gas.

Magnetic trapping of CaF in $N = 0$ and CaH are also realized by simply changing the frequency of the pumping laser and ablation target, showing the generality of this loading method. Co-loading atomic species with molecules appears straightforward, yielding a platform for studying cold atom-molecule collisions.

Work to date: buffer gas cooling of large molecules We create a novel, continuous source of large molecules and demonstrate this on a diverse set of species. We as use a variation of this source to form a cold, continuous beam with a far lower forward velocity than seeded supersonic jets, which to date have been the only source for polyatomic, internally cold molecules. The modest forward velocity of the source ($\approx$ 70 m s^{-1}) makes it an attractive starting point for further manipulation and trapping.

Figure 3 shows the low temperature portion of the experimental apparatus. A hot injection tube is held $\approx$ 2 cm away from a circular aperture in a cold cell, which is anchored to the cold stage of a commercial pulse tube refrigerator. Cold (7K) fill lines deliver helium gas to the cold cell. A large flow (typically 2×10^{18} molecule s^{-1}, or 3 standard cm^3 minute^{-1}) of warm molecules exits the injection tube and flies ballistically towards the cell. As the molecules travel, the they collide with helium atoms exiting the cell. The collisions both cool and slow the incoming molecules. 10-20% of the molecules emitted from the hot tube end up thermalized within the cell. The flow rate of cold helium is tuned to a level high enough to give the molecules an in-cell diffusion time of a few msec, but low enough that molecules are not stopped close to the aperture, where they would be pushed away from the cell and lost.

Once molecules enter the cell, they continue to thermalize with the cold helium gas, which in turn thermalizes with the cell walls. At this point, the cold molecules can be detected spectroscopically, either via Fourier Transform Microwave Spectroscopy as demonstrated to date, or via optical/UV spectroscopy (demonstrated) or IR spectroscopy (proposed). Extensions to FTMW spectroscopy developed in our lab also allow us to perform enantiomer-specific spectroscopy of chiral species, identifying both chemical species and enantiomer simultaneously[2].

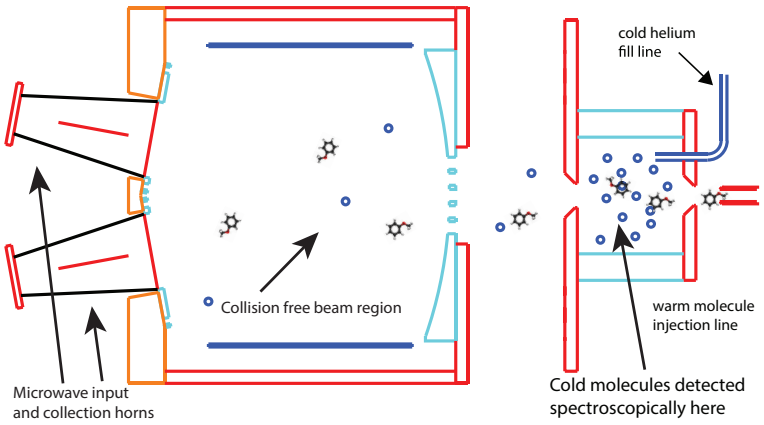

Figure 3: The apparatus to produce a cold, continuous samples and slow beams of larger molecules. Molecules are introduced to a cold cell via a warm injection tube. The molecules cool in the cell via collisions with cold helium buffer gas, and can be sensitively detected via microwave or other types of spectroscopy. A fraction of the cold molecule/helium mixture escapes through the exit aperture and sprays towards a second aperture, which leads into a separately cryopumped chamber where they realize a collision free beam.

2. Future Plans

We are planning on further exploring molecular detection of realistic mixtures into our large molecule cooling apparatus for demonstration of trace detection, including simultaneous species and enantiomer identification of complex chiral mixtures and biomolecules. We are also continuing to investigate fundamental He-molecule sticking (clustering) processes.

3. Other information

There are 2 graduate students working at least 50% of the time on these experiments.

References

[1] H.-I. Lu, J. Rasmussen, M. J. Wright, D. Patterson, and J. M. Doyle, "A cold and slow molecular beam.," *Physical chemistry chemical physics : PCCP*, vol. 13, pp. 18986–90, 2012.

[2] D. Patterson, M. Schnell, and J. Doyle, "Enantiomer-specific detection of chiral molecules via microwave spectroscopy," *Nature*.

Electron Correlation in Strong Radiation Fields

J. H. Eberly
University of Rochester, Rochester, NY 14627
eberly@pas.rochester.edu

Introduction

We are interested to understand how very intense laser pulses, with intensities above and well above 10^{13} W/cm^2, excite electrons in atoms and molecules. The combination of phase-coherent character and short-time nature of laser pulses in experimental use creates substantial challenges to theoretical study in this domain. The intensities in this regime correspond to a force on an electron from the laser's electric field that approaches the atomic Coulomb forces experienced by atomic and molecular electrons. This prevents treating the $e\vec{p}\cdot\vec{A}$ interaction in the traditional perturbative fashion and mandates development of one or more non-perturbative approaches to understand an electron's dynamics under rapidly ionizing conditions. Challenging complications of great interest arise when more than one electron is dynamically active in response to the laser excitation.

Here we report two developments: a recent advance in creating correlation control [1] and a new approach in theoretical methodology [2].

Controlling Angular Correlation

A lesson of the past 20 years is that ionized-electron correlation under strong fields arises non-sequentially as a consequence of recollision [3]. Outgoing electron correlations can thus be controlled by controlling the recollision process. But a slight ellipticity is capable of eliminating most recollision events [4, 5], so correlation between two ionized electrons cannot be expected if they are emitted *sequentially* under a circularly polarized (CP) laser pulse in the absence of recollision [6]. This is consistent with the results shown in Fig. 1.

However, we have obtained simulation results that revise this conventional conclusion and thus improve understanding of the emission process. We have found that two electrons ionized with-

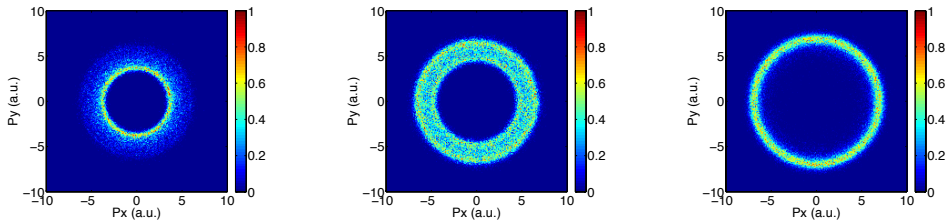

Figure 1: Rotationally invariant momentum distributions of doubly charged ions obtained for sequential double ionization at three intensities (in PW/cm^2): 5.7 (left), 7.7 (center), and 11.0 (right) under circular polarization.

out recollision by a short CP pulse can be strongly angularly correlated. Further, their preferred correlation angle can be controlled continuously from 0° (parallel) to 90° (perpendicular) to 180° (antiparallel), by just changing the laser intensity. This is illustrateed by results shown in Fig. 2. The angular correlations shown there are hidden in the momentum distributions of Fig. 1.

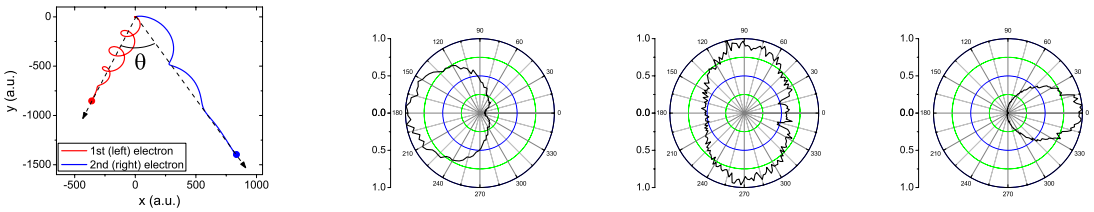

Figure 2: Two electrons may be emitted in any direction, as indicated in Fig. 1, but this ignores information about θ, their relative angle, which is shown here in the first panel. On the right, rotationally very non-symmetric distributions are shown of the angle θ for the same three laser intensities as in Fig. 1: 5.7 PW/cm^2 (left), 7.7 PW/cm^2 (center), and 11.0 PW/cm^2 (right).

We have found that the orientation of a relative angle distribution can be explained with attention to two time scales, the cycle time of the circular polarization and the time interval between ionizations. The latter is controlled closely by peak laser intensity, as one sees from a combined analytic-numerical examination of electron trajectory behavior [7, 8].

New Method for Calculating Momentum Distributions

Several high-field theoretical methods are of course well known. The Volkov-extended version of radiative perturbation theory, the strong field approximation (SFA), has been employed for decades. But for treatment of atomic processes under irradiation with intensities on the order of 1 PW/cm^2, three other methods have mainly been used to describe and evaluate atomic ionization dynamics. These are: (A) direct numerical solution of the time-dependent Schrödinger equation, (B) direct numerical solution of the time-dependent Newton equation, and (C) a semi-classical approach in which quantum tunneling is assumed to release the electron from its binding potential, after which it is treated classically for the remainder of the laser pulse. For the advantages and disadvantages of each of these approaches, see the recent review by Becker, et al. [9]. Approach (C) is probably most often used (see [10] for an early example), and it has an extensive record of semi-quantitative success. It is much simpler than (A), and its tunneling formulas contain important initial state parameters that are not available to (B). Unfortunately, (C) becomes progressively less reliable as the laser field strength approaches or exceeds the over-barrier level [11].

We have developed and tested a new approach (see [2]) that combines the best features of (A) and (B), and avoids the assumptions of (C) about the action of tunneling or its initiation. It is labelled SENE to indicate its use of both Schrödinger and Newtonian dynamics. It coordinates exact TDSE solutions in the pre-ionization regime with very convenient TDNE solutions during the main portion of the laser pulse by placing an extended "virtual detector" network [12] in the emission pathway. The virtual detectors, and their operation, are described in the caption of Fig. 3.

The necessary formulas are easily constructed. Given a numerical wave function $\Psi(\vec{r},t)$, the probability flux at the position of a virtual detector ($\vec{r}_d$) can be calculated:

$$\vec{j}(\vec{r}_d,t) = \frac{i\hbar}{2m}\left[\Psi(\vec{r}_d,t)\nabla\Psi^*(\vec{r}_d,t) - c.c.\right]. \qquad (1)$$

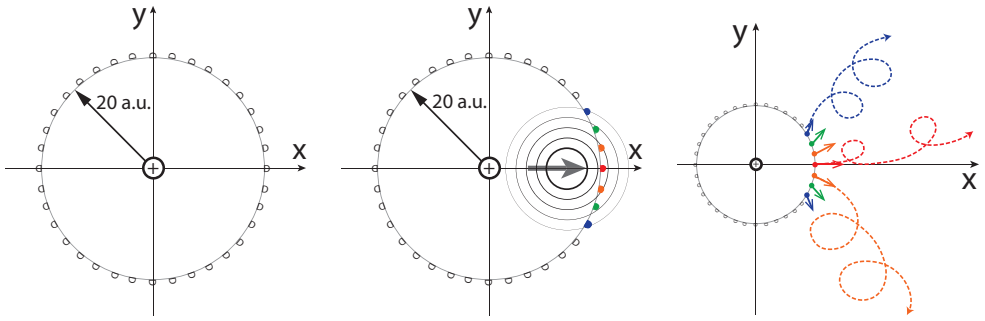

Figure 3: Illustration of the new SENE approach. Left: virtual detectors [12] are positioned along a circle of radius 20 a.u. from the atom. The actual number of detectors is much denser. Middle: A TDSE wave packet moving rightward is likely to trigger detectors near the +x axis, with the on-axis detector receiving the strongest signal. Right: Each triggered detector will immediately initiate an electron trajectory at the same position, with its momentum determined by Eq. (2), and a relative weight determined by the probability flux (1). The subsequent motion of each electron trajectory is determined by TDNE dynamics in the spatial zone wheree its results are highly accurate.

If one rewrites the wave function in terms of its amplitude and phase: $\Psi(\vec{r},t) = F(\vec{r},t)\exp[i\phi(\vec{r},t)]$ and substitutes this expression into Eq. (1), one gets the momentum from the gradient of the phase:

$$\vec{k}(\vec{r}_d,t) \equiv \nabla\phi(\vec{r}_d,t) = \frac{m\vec{j}(\vec{r}_d,t)}{|F(\vec{r}_d,t)|^2}. \tag{2}$$

Virtual detection has no effect on electron motion and provides a reliable starting point for outgoing classical trajectories, which are strongly influenced by the rest of the laser pulse. The outgoing electron could also be modeled by matching to quantum rather than classical outgoing waves [13] but classical modeling has a significant advantage in its ability to include outgoing strong-field Coulomb effects, something not yet possible with Volkov waves. Fig. 4 shows a comparison of SENE against fully TDSE solutions, with very satisfactory SENE results.

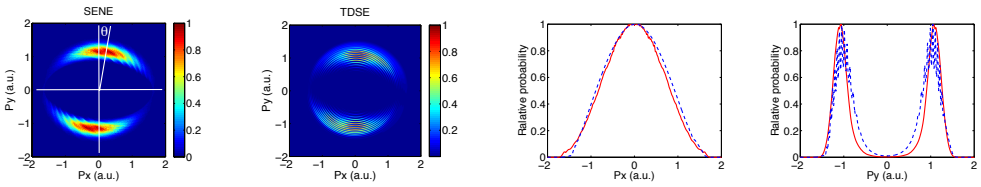

Figure 4: Electron momentum distribution obtained from the SENE approach (first panel) and from exact TDSE calculations (second panel) under exactly the same conditions [2]. The laser intensity is 0.4 PW/cm ^{2}. The first two panels have been further compared by projecting onto the P_x axis (third panel) and onto the P_y axis (fourth panel). The red solid curves are for SENE and the blue dashed curves for TDSE. The momentum tilt angle θ has been marked on the first panel as the angle between the P_y axis and the most probable direction of distribution.

The following references that were supported by DOE Grant DE-FG02-05ER15713 are marked with * in the listing below.**

References

[1] ***Xu Wang, J. Tian and J.H. Eberly, *Phys. Rev. Lett.* **110**, 073001 (2013). See also ***Xu Wang and J.H. Eberly, *J. Chem. Phys.* **137**, 22A542 (2012).

[2] ***Xu Wang and J.H. Eberly, *Phys. Rev. Lett.* **110**, 243001 (2013). See also ***Xu Wang, J. Tian and J.H. Eberly, *Phys. Rev. Lett.* **105**, 083001 (2010).

[3] P. B. Corkum, *Phys. Rev. Lett.* **71**, 1994 (1993).

[4] P. Dietrich, N.H. Burnett, M. Ivanov, and P.B. Corkum, *Phys. Rev. A* **50**, R3585 (1994).

[5] N.H. Burnett, C. Kan, and P.B. Corkum, *Phys. Rev. A* **51**, R3418 (1995).

[6] For exceptional recollision with elliptical or circular polarization, see ***X. Wang and J. H. Eberly, *New J. Phys.* **12**, 093047 (2010) and F. Mauger, C. Chandre and T. Uzer, *Phys. Rev. Lett.* **105**, 083002 (2010).

[7] See [1] and also ***Xu Wang and J.H. Eberly, *J. Chem. Phys.* **137**, 22A542 (2012).

[8] Phay J. Ho, R. Panfili, S. L. Haan and J. H. Eberly, *Phys. Rev. Lett.* **94**, 093002 (2005). See also Phay J. Ho, *Phys. Rev. A* **74**, 045401 (2005), ***Phay J. Ho and J.H. Eberly, *Phys. Rev. Lett.* **95**, 193002 (2005), ***Phay J. Ho and J.H. Eberly, *Phys. Rev. Lett.* **97**, 083001 (2006), and ***S.L. Haan, L. Breen, A. Karim, and J. H. Eberly, *Phys. Rev. Lett.* **97**, 103008 (2006).

[9] ***W. Becker, X.J. Liu, P.J. Ho and J.H. Eberly, *Rev. Mod. Phys.* **84**, 1011-1043 (2012).

[10] T. Brabec, M. Yu. Ivanov, and P. B. Corkum, *Phys. Rev. A* **54**, R2551 (1996).

[11] See evaluation in X. M. Tong and C.D. Lin, *J. Phys. B* **38**, 2593 (2005).

[12] Our virtual detectors were inspired by B. Feuerstein and U. Thumm, in *J. Phys. B* **36**, 707 (2003), where virtual detectors intercepted ionic fragments of a one-dimensional model dissociation of He_2^+.

[13] L. Tao and A. Scrinzi, *New J. Phys.* **14**, 013021 (2012).

Algorithms for X-ray Imaging of Single Particles

Office of Basic Energy Sciences
Division of Chemical Sciences, Geosciences, and Biosciences
Program in Atomic, Molecular, and Optical Sciences

Veit Elser, Department of Physics
PSB 426, Cornell University
Ithaca, NY 14853
(607) 255-2340
ve10@cornell.edu

Program Scope

The many-orders-of-magnitude gains in X-ray brightness achieved by free-electron laser sources such as the LCLS are driving a fundamental review of the data analysis methods in X-ray science. It is not just a question of doing the old things faster and with greater precision, but doing things that previously would have been considered impossible. My group at Cornell is working closely with experimental groups at LCLS and FLASH to develop data analysis tools that exploit the full range of opportunities made possible by the new light sources. More recently we have begun collaborations with David Mueller's electron microscopy group and Sol Gruner's detector group, both at Cornell.

Ultra-low flux experiments

While a reconstruction might succeed with *simulated* data at very low signal-to-noise, a more critical test lies in the detector's fidelity at such low signal levels. Prompted in part by reports of strong electronic noise in the Cornell Pixel Array Detector (PAD) at LCLS, we collaborated with Sol Gruner's group on proof-of-principle experiments that demonstrated both the fidelity of the detector and the noise tolerance of our reconstruction algorithm [1]. The detector comprised one module identical to those installed at LCLS, and the signal was formed by sending a highly attenuated beam from a table-top source through a mask that was given a random rotation for each of a half-million recordings. Our algorithm was able to accurately reconstruct the mask, without knowledge of the rotations, even for average photon counts as low as 2.5 per frame.

More recently [2] an extension of these experiments demonstrated 3D tomographic reconstruction of an object from its very low signal attenuation contrast, again under conditions where the algorithm had to discover the rotation for each frame of data. These experiments used six modules of the PAD; data statistics and a reconstruction are shown in Figure 1. Because of the much larger data volume of the 3D reconstructions, Kartik Ayyer, the student leader of this part of the project, first had to develop multi-processor software that could run on the SLAC Linux cluster.

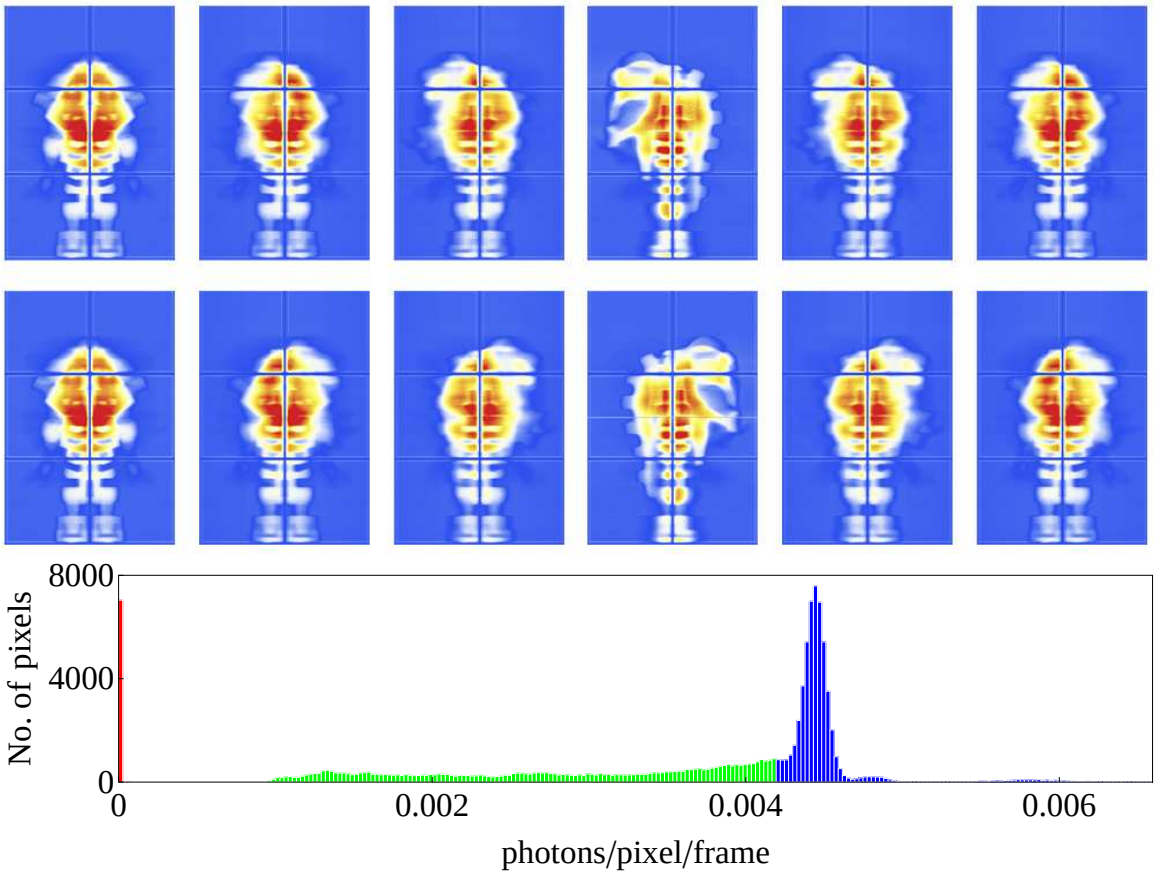

Figure 1: *Top*: Tomographic reconstruction of a Lego "Ninjago" figure from 3.8 million frames of low signal x-ray data and unknown orientations [2]. *Bottom*: Statistics of photons recorded by the PAD. The peak at high photon counts corresponds to rays that completely miss the figure and are therefore unattenuated.

Unsupervised particle reconstruction

Practitioners of diffraction imaging know all too well the numerous details that need to be overseen in a successful reconstruction. Saturated or otherwise compromised detector pixels must be eliminated, the support should be tight but not too tight, residual phase fluctuations caused by noise need to be averaged, etc. In any given imaging project these details are manageable, if tedious. But suppose one is faced with hundreds of data, each with unique corruption problems, and of objects spanning a wide range of sizes and shapes? This was the situation confronting us when we were asked to process some single-particle LCLS data of soot particles.

The soot-study team had produced a half dozen reconstructions for their main publication [3], but devoting the same style of analysis to the entire body of data seemed out of the question. This challenge was taken up by Hyung Joo Park, a new member to the Cornell group. He developed a completely automated protocol for processing the huge data set and also set high standards for reliability and reproducibility [4]. A selection of his soot particles are shown in Figure 2. The images are the subject of a separate study (to be published) and are accessible online.

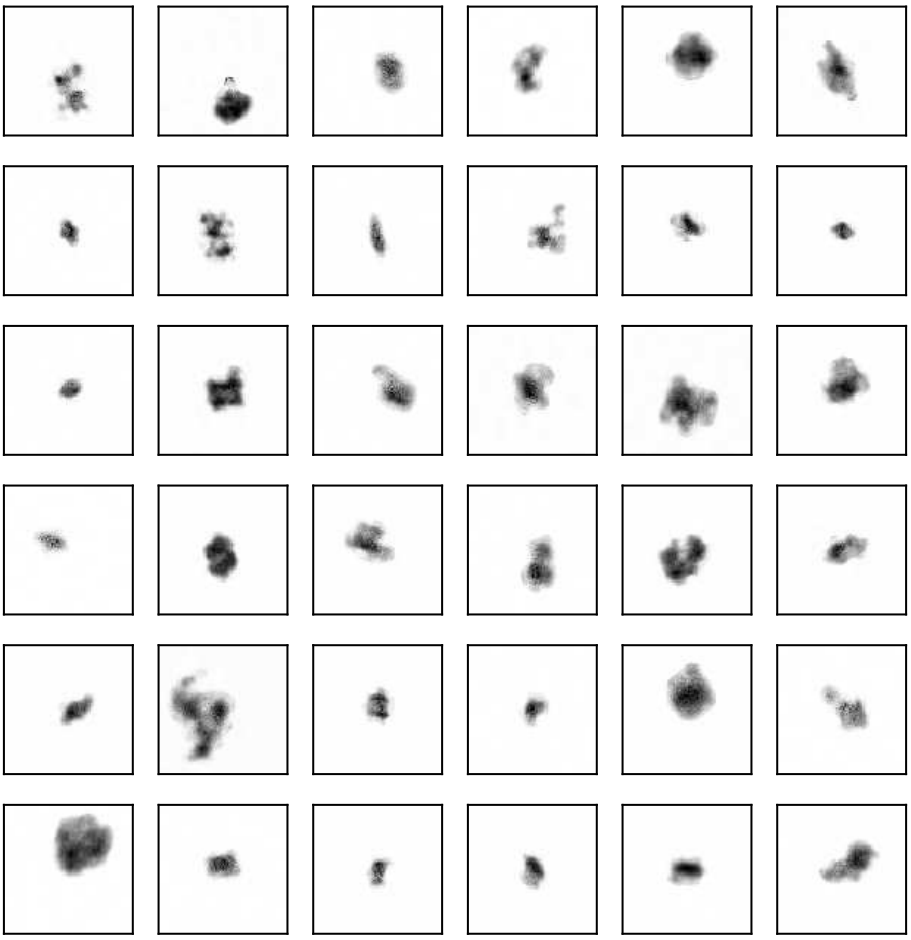

Figure 2: Sampling of soot particle reconstructions from LCLS data [4]. Each frame measures $752 \times 752\ \mathrm{nm}^2$.

Direct phasing of nanocrystal data

Recent experiments at LCLS have been able to resolve the intensity distributions about Bragg peaks in nanocrystals of large biomolecules [5]. Information derived from small shifts in the peak positions augment the Bragg samples of the particle intensity with samples of its *gradients*. Working on the assumption that the nanocrystal is entirely generated by lattice translations of a particle, the PI developed an algorithm that reconstructs the particle from intensities and intensity gradients [6]. Unlike traditional direct phasing methods that require very high resolution data in order to exploit sparsity of the electron density, the new method imposes no constraints on the contrast other than positivity and works well at low resolution. Reconstructions were demonstrated with simulated *P1* lysozyme nanocrystal data down to a signal-to-noise ratio of 2 in the intensity gradients. Some details of this work are shown in Figure 3.

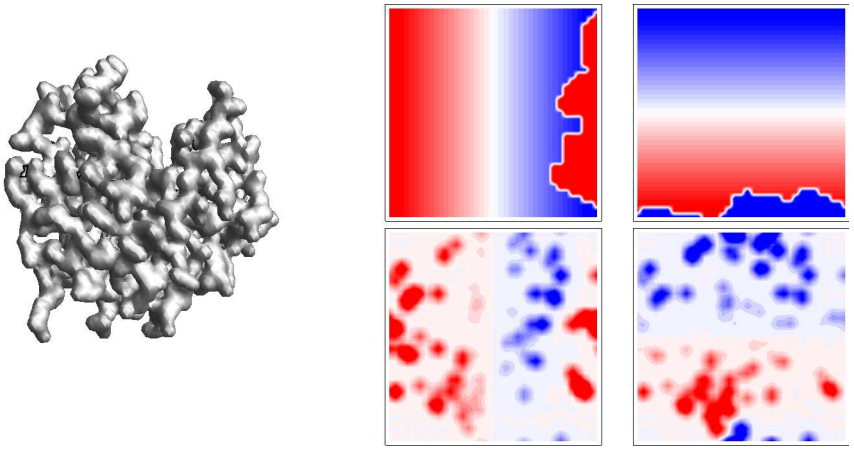

Figure 3: *Left*: Lysozyme molecule at the resolution for which direct phasing was demonstrated with simulated intensity and intensity-gradient data [6]. *Right*: In addition to reconstructing the electron density ρ, the algorithm must reconstruct linear functions (top panels) that describe how the molecule wraps around the unit cell; intensity-gradient data relates to the product of ρ and these linear functions (lower panels).

References

[1] H. T. Philipp, K. Ayyer, M. W. Tate, V. Elser & S. M. Gruner, *Solving structure with sparse, randomly-oriented x-ray data*, Opt. Express **20** 13129 (2012).

[2] K. Ayyer, H. T. Philipp, M. W. Tate, V. Elser & S. M. Gruner, *Real-space x-ray tomographic reconstruction of randomly oriented objects with sparse data frames*, submitted to Opt. Express (2013).

[3] N. D. Loh *et al.*, *Fractal morphology, imaging and mass spectrometry of single aerosol particles in flight*, Nature **486**, 5137 (2012).

[4] H. J. Park *et al.*, *Unsupervised single-shot diffractive imaging of heterogeneous particles using X-ray free-electron lasers*, submitted to Opt. Express (2013).

[5] H. N. Chapman *et al.*, *Femtosecond X-ray protein nanocrystallography*, Nature **470**, 73-77 (2011).

[6] V. Elser, *Direct phasing of nanocrystal diffraction*, accepted for publication in Acta Cryst. A (2013).

Collective Coulomb Excitations and Reaction Imaging

Department of Energy 2012-2013

James M Feagin
Department of Physics
California State University–Fullerton
Fullerton CA 92834
jfeagin@fullerton.edu

We continue with the basic science of electron and molecular reactions inherent to the ongoing global effort to secure sustainable energy resources. Although the work described in this report is theoretical, our interest in these topics remains motivated by the success of experiments involving few-body atomic and molecular fragmentation and the collection of all the fragments. We accordingly continue two parallel efforts with (i) emphasis on *reaction imaging* while (ii) pursuing longtime work on *collective Coulomb excitations*.

Electron-Pair Vortex Kinematics

Murray and Read[1] pioneered the detection of electron pairs scattered by incident electrons fired obliquely to the detection plane. At various energies and for certain electron gun angles and relative angular separation of the scattered electron pair, they observed pronounced minima in the cross section, which over the years have stubbornly resisted a consistent theoretical interpretation, although modern close-coupling calculations can accurately describe their structure and pinpoint their location.[2] Very recently, however, Macek and Ovchinnikov[3] have traced these observed $(e, 2e)$ deep minima to the occurrence of vortices in the wavefunction of the continuum electron pair. They have thus demonstrated the existence of nonzero electron-pair angular momentum about a line through the singularity and out of the detection plane.

We have worked to establish the analytic form of the cross section near a vortex in the electron-pair continuum by connecting with the angular momentum of the electron-pair center of mass (CM) about the vortex singularity. Following closely our electron-pair excitation work described above, we thus introduce the relative momentum wavevectors $\mathbf{k}_- = (\mathbf{k}_1 - \mathbf{k}_2)/2$ and $\mathbf{k}_+ = \mathbf{k}_1 + \mathbf{k}_2$ to describe the relative and center of mass (CM) motion, respectively, of the outgoing electron pair. Here, $\mathbf{k}_1$ and $\mathbf{k}_2$ are the electron wavevectors relative to the ion. We do not predict where a vortex is, or why, but given that it exists provide instead a compact description of its *kinematics*. In the equal-energy sharing experiments of Murray and Read, one has that $\mathbf{k}_+ \cdot \mathbf{k}_- = E_1 - E_2 = 0$, and the vortex line establishes itself along the relative momentum axis $\mathbf{k}_-$ through a point $\mathbf{k}_{+v}$. Accordingly, we also introduce the projection $\hbar\,\lambda = \mathbf{L} \cdot \hat{\mathbf{k}}_-$ of the electron-pair total angular momentum $\mathbf{L} = \mathbf{l}_1 + \mathbf{l}_2$ along $\mathbf{k}_-$ and use $\mathbf{k}'_+ \equiv \mathbf{k}_+ - \mathbf{k}_{+v}$ to describe the momentum of the electron-pair CM relative to the vortex singularity.

Our key notion is to move the angular-momentum origin from the helium ion to the vortex singularity with a momentum boost.[4] Since the scattering amplitude is a momentum-space function, the boost is trivially introduced by the replacement $\mathbf{k}_+ \to \mathbf{k}'_+ \equiv \mathbf{k}_+ - \mathbf{k}_{+v}$. However, a shift of angular-momentum origin changes $\mathbf{L} \to \mathbf{L}'$ and moves the centrifugal barrier along

---

[1] A. J. Murray and F. H. Read, Phys. Rev. A**47**, 3724 (1993).
[2] J. Colgan, O. Al-Hagan, D. H. Madison, A. J. Murray, and M. S. Pindzola, J. Phys. B: At. Mol. Opt. Phys. **42**, 171001 (2009).
[3] J. H. Macek, J. B. Sternberg, S. Y. Ovchinnikov, and J. S. Briggs, Phys. Rev. Lett. **104**, 033201 (2010).
[4] J. M. Feagin, J. Phys. B: At. Mol. Opt. Phys. **44**, 011001 (2011).

with it, and the centrifugal barrier dominates the analytic form of the amplitude near the new origin. We thus derive a threshold-like analytic expansion of the scattering amplitude in cylindrical partial waves $\lambda = 0, 1, 2, ...$ of the electron-pair about the vortex

$$f \sim c_0 + c_1\, k'_+ \cos\psi' + c_2\, k'^2_+ \cos 2\psi' + ..., \tag{1}$$

where ψ' is the angle $\mathbf{k}'_+$ makes with incident electron beam and the coefficients c_λ are undetermined but otherwise independent of the momenta. We thus demonstrate good fits to the $(e, 2e)$ cross section near the vortex can be obtained with just the lowest two partial waves about the vortex.

Momentum vs Spatial Reaction Imaging

The momentum vortices just described beg the question: Where are the corresponding vortices in the coordinate-wavefunction representation and how do they evolve into their asymptotic momentum representation? In calculations, usually the idealization that momentum can be measured to infinite accuracy is assumed. Then, for the simplest case of detection of a single particle in a momentum (plane wave) eigenstate with a well defined wave vector $\boldsymbol{k}$, the exact scattering amplitude is given to within a phase factor by

$$T_{\boldsymbol{k}}(t) \propto \langle\, \boldsymbol{k}\,|\,\Psi(t)\,\rangle = \tilde{\Psi}(\boldsymbol{k}, t), \tag{2}$$

where $\tilde{\Psi}(\boldsymbol{k}, t)$ is the Fourier transform (momentum-space wavefunction) of the exact spatial scattering state. For the case of many-particle fragmentation, the difficulty with this asymptotic numerical projection onto momentum eigenstates is that a many-dimensional integral, often with strongly oscillatory phase factors, must be performed.

A simple and effective solution that mostly circumvents this problem has emerged in recent years. The so-called *imaging theorem* (IT) establishes a relation between the asymptotic momentum and coordinate wavefunctions describing the multi-fragment dissociation of a complex system as $t \to \infty$. Thus, the IT provides an enormously practical method for extracting scattering amplitudes directly from the asymptotic form of numerically computed multidimensional coordinate wavefunction. Furthermore, the IT opens up the possibility of direct *experimental* imaging of collision wavefunctions via the measurement of the momentum distribution of the outgoing fragments. This is an aspect we have emphasized recently.[5]

Historically it appears that the IT was alluded to at least as far back as 1937 in the quantum mechanics text by Kemble. Kemble was concerned with the process of the measurement of linear momentum and how one can extract free-particle momentum probabilities from the coordinate wavefunction. Invoking a stationary-phase approximation, he thus derived a connection relating $\boldsymbol{r}$ of the coordinate wavefunction in the limit of large time to $\boldsymbol{k}$ of a momentum wavefunction via the stationary-phase condition $\boldsymbol{k} = \mu\,\boldsymbol{r}/\hbar t$, where μ is the particle mass. In atomic and molecular collisions the earliest applications have been to electron emission. Applications of the IT have appeared in various papers of Macek and Ovchinnikov for the past 15 years. In a recent review, Macek has given a full discussion of the IT in a general context.[6]

Our goal has been to give a simple alternative derivation designed to emphasize the application to a real detector having finite resolution in both position and momentum space. In addition our derivation shows under what limits of simultaneous position and momentum specification is the IT valid. We also show that the time dependent phase factors on the final state wavefunction of the detected fragment arise as the remnants of entanglement with a classical detector. We have begun a review of the theory of detection and imaging of fragmentation

---

[5] J. S. Briggs and J. M. Feagin, J. Phys. B: At. Mol. Opt. Phys. **46**, 025202 (2013).

[6] J. H. Macek in *Dynamical Processes in Atomic and Molecular Physics*, (Bentham Science Publishers, ebook.com, 2012), G. Ogurtsov and D. Dowek, eds.

reactions emphasizing the quantum vs classical aspects, which we hope will shed light on the spatial imaging of electron-pair vortices.[7]

Loss of Wavepacket Coherence

Schulz and coworkers have considered the transverse coherence length of a nearly monochromatic beam of protons, deBroglie wavelength λ, passing through a collimator aperture and scattered by a crossed beam of molecular hydrogen.[8] The two-center nature of the molecular scattering gives rise to a well-established 'double-slit interference' effect, which these investigators were able to suppress by reducing the distance L of the target volume to the collimator aperture. A decrease in L increases the angular width $\alpha \simeq a/L$ the collimator aperture subtends at the target, where $a \ll L$ is the aperture width in the scattering plane. They demonstrated that the corresponding decrease in the transverse coherence length λ/α of the scattered protons relative to the two-center molecular bond length suppresses as expected the observed interference effects in the scattering cross section.

While we feel these experiments demonstrate the role of transverse coherence in establishing

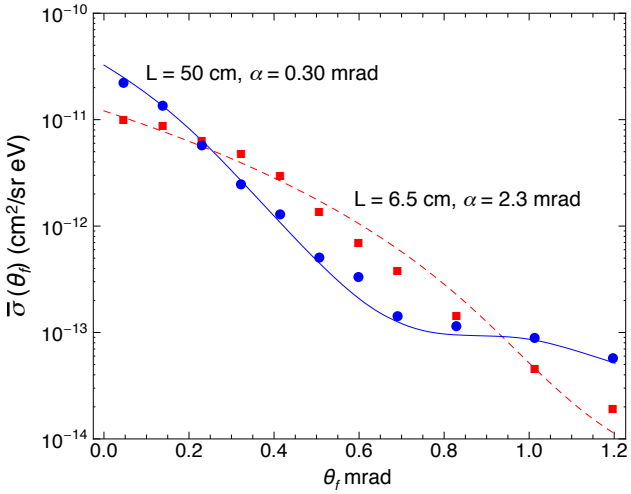

FIG. 1: The proton scattering cross section for ionization of H_2 as a function of proton scattering angle as in Fig. 1 of Schulz et al. The round (blue) and square (red) points are the $L = 50$ cm and $L = 6.5$ cm measurements, respectively, while the solid (blue) and the dashed (red) curves show the calculated cross section Madison and coworkers *averaged* over a small angular spread of the incident beam. The size of the data points corresponds roughly to the error bars in the data, and differences in the blue and red measurements are well outside the statistical error.

---

[7] J. S. Briggs and J. M. Feagin, in preparation, October (2013).
[8] K. N. Egodapitiya, S. Sharma, A. Hasan, A. C. Laforge, D. H. Madison, R. Moshammer, and M. Schulz, Phys. Rev. Lett. **106**, 153202 (2011).
[9] See for example C. Keller, J. Schmiedmayer, and A. Zeilinger, Opt. Commun. **179**, 129 (2000), and also J. M. Feagin, Phys. Rev. A**73**, 022108 (R) (2006).
[10] J. M. Feagin and L. Hargreaves, Phys. Rev. A, in press, September (2013).
[11] E. H. Wichmann, Am. J. Phys. **33**, 20 (1965).

collimated incident wavepackets with mean centroid momenta off axis relative to the incident-beam axis. Thus we show that the static energy-conserving scattering reactions with steady beam currents considered here will distinguish neither wavepacket structure nor coherence in the incident beam. Instead, we account for the loss of interference observed by Schulz et al. as simply an incoherent average over the poorly collimated ensemble of incident-beam momenta.

It is natural to debate the size and coherences of supposed wavepackets of particles in an incident beam. Such debates, however, will remain unresolved when extracting cross sections from the results of familiar static (energy-conserving) experiments with steady beam currents. One can consider each particle to be emitted as (i) a wavepacket with an energy spread equal to the energy spread of the beam ensemble, or (ii) a free-particle planewave with an energy that varies from one planewave to the next. Both of these rather disparate beam profiles lead to the same ensemble-averaged cross sections. In the end, all that one can say is that a static scattering reaction selects effectively a random (planewave) momentum eigenstate of the incident beam, and the usual theoretical cross sections between momentum eigenstates of the incident and target particles will account for experimental results.

If the collimation is weak, the cross section must be further averaged incoherently over off-axis incident-beam directions. These off-axis contributions to the beam ensemble can be regarded as incoherent—while defining a transverse coherence. Each individual scattering distribution produced by a particular incident direction combines incoherently with the other distributions, and each distribution is slightly shifted in scattering angle by the angle of incidence. Overall, observable interference effects will be diminished to some degree depending on the degree to which the beam is uncollimated. The transverse coherence gives a rule of thumb for estimating the degree to which an interference effect is washed out.

Recent Publications and Invited Talks

Theory of the Detection and Imaging of Fragmentation Reactions: Quantum vs Classical Aspects, J. S. Briggs and J. M. Feagin, Phys. Rev. A, in preparation (2013).

On the Loss of Wavepacket Coherence in Stationary Scattering Experiments, J. M. Feagin and L. Hargreaves, Phys. Rev. A, in press, September (2013).

Momentum and Spatial Imaging of Multi-Fragment Dissociation Reactions, J. S. Briggs and J. M. Feagin, J. Phys. B: At. Mol. Opt. Phys. **46**, 025202 (2013).

Vortex Kinematics of a Continuum Electron Pair, J. M. Feagin, J. Phys. B: At. Mol. Opt. Phys. **44**, 011001 (2011).

Vortices in the Electron-Pair Continuum or Deep Bubbles in My Guinness?, J. M. Feagin, Invited Talk to the International Symposium on $(e, 2e)$, Double Photoionization, and Related Topics, Dublin, Ireland, July (2011).

Electron Pairs in the Molecular Coulomb Continuum, J. M. Feagin, Invited Talk to the International Symposium on $(e, 2e)$, Double Photoionization, and Related Topics, Lexington, KY, July (2009).

Electron-Pair Excitations and the Molecular Coulomb Continuum, J. M. Feagin, J. Colgan, A. Huetz, and T. J. Reddish, Phys. Rev. Lett. **103**, 033002 (2009).

Transient Absorption and Reshaping of Ultrafast Radiation

Kenneth J. Schafer and Mette B. Gaarde
Department of Physics and Astronomy, Louisiana State University, Baton Rouge, LA 70803

Scope of Project and Future Work

This program was funded as of July 2013 so this report will largely be about the scope of our project. Our program will be centered around the theoretical study of transient absorption of ultrafast extreme ultraviolet (EUV) radiation by atoms and materials interacting with a precisely synchronized near-to-mid infrared (IR) laser pulse. Transient absorption spectroscopy can in principle provide high spectral resolution and high (attosecond) time resolution simultaneously, by spectrally resolving the light transmitted through a sample as a function of delay between the dressing laser pulse and the broadband attosecond EUV probe. We will study attosecond transient absorption (ATA) using a versatile theoretical treatment that takes account of both the strong laser-atom interaction at the atomic level, as well as propagation of the emitted radiation in the non-linear medium. Our current theoretical treatment of ATA, which includes first-principles calculations of the microscopic and the macroscopic response of atoms to ultrafast laser fields, in the single-active electron approximation, is described in detail in [1].

Our long-term goal is to build up a time-dependent picture of absorption at EUV and soft X-ray wavelengths. The problems we will study fall into three categories:

(i) Studies of atomic systems, mostly with single excitations. This work will build directly on our preliminary studies [2,3]. We will explore how the delay-dependent features in ATA spectra, including interference fringes and laser-induced states, can be interpreted in terms of the underlying electron dynamics; how choosing the intensity, polarization and frequency characteristics of the dressing IR pulse can be used to study and control excited wave packet motion on the attosecond time scale; how the phase of intermediate resonances can be studied by multiphoton processes that give rise to interference features in the ATA spectrum. We will also investigate the possibility of using ATA to measure the amplitude and phase of quantum wave packets, in analogy to electron wave packet interferometry.

(ii) Extension of ATA studies to two-electron systems. We will extend our studies of one-electron absorption and emission to two-electron excitations. This can be done in a variety of ways, for instance by using few state models of the Fano type [4], reduced dimensionality calculations [5], or large-scale ab-initio calculations [6]. We will couple the two-electron model to our propagation code in order to study the effects of propagation (absorption, reshaping) on the observed signal, using realistic parameters that give measurable effects.

(iii) Studies of ATA in condensed matter systems. We will collaborate with the Reis group at Stanford University that has recently demonstrated strong field, ultrafast transient absorption in zinc-oxide crystals [7]. We will construct computer codes to study transient absorption in solid systems subject to strong mid-infrared laser pulses. Our goal is to construct models that allow us to study electronic structure in the non-perturbative limit. We will also address the need for ultrafast propagation calculations in thin crystals.

Recent progress

(i) In collaboration with the Leone/Neumark experimental group at UC Berkeley we are studying ATA in neon.

(iii) We have developed a primitive code that incorporates both the microscopic and the macroscopic response for the interaction of a strong MIR field and a ZnO crystal, for comparison with the experimental results in [8]. The microscopic atomic response in this version of the code is based on the model proposed by Ghimire and collaborators. Future work on this project will be in two directions: (I) expand the current, simple, code to look at transient absorption of incoming EUV and MIR light, (II) develop a more sophisticated model for the microscopic response

[1] M. B. Gaarde *et al*, Phys. Rev. A **82**, 023401 (2011)
[2] S. Chen, M. J. Bell *et al*, Phys. Rev. A **86**, 063408 (2012)
[3] S. Chen *et al*, Phys. Rev. A **87**, 013828 (2013)
[4] Z.-H. Loh, C. H. Greene, and S. R. Leone, Chem. Phys. **350**, 7 (2008)
[5] J. Zhao and M. Lein, New J. of Phys. **14**, 065003 (2012)
[6] J. Feist *et al*, Phys. Rev. A **77**, 043420 (2008).
[7] S. Ghimire *et al*., Phys. Rev. Lett. **107**, 167407 (2011)
[8] S. Ghimire *et al*., Nature Physics **7**, 138 (2011)

Studies of Autoionizing States Relevant to Dielectronic Recombination

T.F. Gallagher
Department of Physics
University of Virginia
P.O. Box 400714
Charlottesville, VA 22904-4714
tfg@virginia.edu

With DOE support we have studied doubly excited autoionizing atomic states, the high angular momentum bound states of two electron atoms, and the effects of intense low frequency radiation on atomic photoionization. A systematic study of autoionization allows us to understand the reverse process, dielectronic recombination (DR), the recombination of ions and electrons via intermediate autoionizing states. DR provides an efficient recombination mechanism for ions and electrons in astrophysical and laboratory plasmas.[1-4] In fusion plasmas impurity ions from the wall of the containment vessel capture electrons and radiate power from the plasma, negating efforts to heat the plasma. The most important pathway for DR is through the autoionizing Rydberg states converging to the lowest lying excited states of the parent ion. Because Rydberg states are involved, DR rates are profoundly influenced by other charged particle collision processes and any small electric and magnetic fields in the plasma.[5,6] Consequently, a major thrust of this program has been understanding how autoionization rates, and thus DR, are affected by external fields. This understanding is broadly useful since DR exhibits similar physics to that found in other contexts, notably zero kinetic energy electron (ZEKE) spectroscopy,[7] dissociative recombination,[8] and fluorescence yield spectroscopy.[9] The isolated core excitation (ICE) method we have used to study autoionizing states provides a new tool for the spectroscopy of the bound high angular momentum states of alkaline earth atoms. From their energy separations one can determine the polarizabilities and radial matrix elements of the ionic cores.[10-13] These quantities are important in determining the blackbody frequency shifts of trapped ion based clocks and for parity nonconservation measurements.[14] The use of a microwave field to mimic the rapidly varying fields which occur in electron collisions has led quite naturally to laser photoionization of atoms in strong microwave fields, and we are exploring this problem to understand it more fully. An atom in a strong microwave field exposed to visible radiation is very similar to an atom in an intense infrared field exposed to a train of attosecond xuv pulses, a problem currently under investigation by many research groups.[15-19]

During the past year we have worked on two projects. First, we have demonstrated a novel technique to detect microwave transitions between high angular momentum states of alkaline earth atoms. As stated above, these spectroscopic intervals can be used to extract the polarizabilities of alkaline earth ions. Specifically, we have shown that it is possible to use ICE to detect microwave transitions between high ℓ states. The essential idea is easily understood using Ba as an example. The ICE transition from the bound $6sn\ell$ state to the autoionizing $6p_{1/2}n\ell$ state is the $6s\text{-}6p_{1/2}$ transition of the ion with a spectator $n\ell$ electron.[20] The width of the transition is determined by the autoionization rate of the Ba $6p_{1/2}n\ell$ state, and the ICE photoexcitation cross section is inversely proportional to this rate. Since the autoionization rates of the high angular momentum states decrease by a factor of five for each increase in ℓ of one,[21] the ICE cross

section increases by a factor of five for each increase in ℓ of one. It is possible to use this difference in the cross sections to detect the 6sng-6snℓ microwave transitions for $\ell>4$, even if the ICE transitions from the 6sng and 6snℓ states are centered at the same frequency, by using a narrow band laser to drive the ICE transition.

As proof of principle we have measured the Ba 6sng-6snh-6sni-6snk intervals for $15\leq n\leq 18$. In Ba the ICE transitions for different ℓ do not occur at the same frequency, which is a slight complication. Nonetheless, we have extracted new values for the Ba^+ dipole and quadrupole polarizabilities, 124.84(13) a_0^2 and 2613(24) a_0^5, respectively. We are preparing a report of this work for publication. We have started the analogous experiment with Ca, since Ca^+ is a promising clock candidate.[14] We have found a workable laser excitation scheme to produce the Ca 4sng states, and we have detected several microwave resonances.

The second project is motivated by experiments done with a combined xuv attosecond pulse train (APT) and infrared laser field.[15-16] These experiments show that the energy transfer to the electrons produced by the APT is dependent on the phase of the infrared field at which the excitation occurs.[15-16] We have done analogous experiments in which we excited atoms in a microwave field phase locked to a mode locked ps laser.[22,23] Our experiments showed that the electrons produced by the ps laser can be transferred to higher or lower energy when the ps laser excitation occurs at the correct phase of the microwave field. Unfortunately, the 250 GHz spectral width of the ps laser pulse is comparable to the energy transfer due to the microwave field, reducing the size of the signal. In addition, we are unable to see coherence in the excitation analogous to that seen with an APT.[15]

For both the above reasons we are altering the experimental approach to have better laser resolution. We are planning to excite Li atoms in the presence of a strong microwave field phase locked to an amplitude modulated laser field. Specifically, we are planning to excite atoms with an amplitude modulated 819 nm laser beam to which a strong microwave field will be phase locked. The frequency spectrum of the 819 nm light consists of two peaks 18 GHz apart, each having a width of 1 MHz. The width will increase to 100 MHz after pulse amplification. We are optimistic that this approach will have the advantages of both narrow band and phase dependent excitation. At this point we have verified that, using two continuous wave diode lasers we can generate amplitude modulated 819 nm light and detect a clean beat note to which we can lock the microwave oscillator. The experimental layout and the vacuum system have been substantially improved, and we now have the requisite two dye lasers running. We plan to begin taking data in the next few months.

References

1. A. Burgess, Astrophys. J. 139, 776 (1964).
2. A.L. Merts, R.D. Cowan, and N.H. Magee, Jr., Los Alamos Report No. LA-62200-MS (1976).
3. S. B. Kraemer, G. J. Ferland, and J. R. Gabel, Astrophys. J. 604 556 (2004).
4. N. R. Badnell, M. G. O'Mullane, H. P. Summers, Z. Altun, M. A. Bautista, J. Colgan, T. W. Gorczyca, D. M. Mitnik, M. S. Pindzola, and O. Zatsarinny, Astronomy and Astrophysics, **406**, 1151 (2003).

5. A. Burgess and H. P. Summers, Astrophysical Journal **157**, 1007 (1969).
6. V. L. Jacobs, J. L. Davis, and P. C. Kepple, Phys. Rev. Lett. 37, 1390 (1976).
7. E. W. Schlag*, ZEKE Spectroscopy* (Cambridge University Press, Cambridge, 1998).
8. V. Kokoouline and C. H. Greene, Phys. Rev. A **68**, 012703 (2003).
9. C. Sathe, M. Strom, M. Agaker, J. Soderstrom,J. E. Rubenson, R. Richter, M. Alagia, S. Stranges, T. W. Gorczyca, and F. Robicheaux, Phys. Rev. Lett. 96, 043002 (2006).
10. J. E. Mayer and M. G. Mayer, Phys. Rev. 431, 605 (1933).
11. J. H. Van Vleck and N. G. Whitelaw, Phys. Rev. 44, 551 (1933).
12. S. R. Lundeen, in Advances in Atomic , Molecular, and Optical Physics, edited by P. Berman and C. Lin (Elsevier Academic Press, San Diego, 2005).
13. E. S. Shuman and T. F. Gallagher, Phys. Rev. A **74**, 022502 (2006).
14. M. S. Safronova and U. I. Safronova, Phys. Rev. A **83**, 013406 (2011).
15. P. Johnsson, R. Lopez-Martens, S. Kazamias, J. Mauritsson, C. Valentin, T. Remetter, K. Varju, M. B. Gaarde, Y. Mairesse, H. Wabnitz, P. Salieres, Ph. Balcou, K. J. Shafer, and A. L'Huillier, Phys. Rev. Lett. **95**, 013001 (2005).
16. P. Ranitovic, X. M. Tong, B. Gramkow, S. De, B. DePaola, K. P. Singh,. W. Cao, M. Magrakelidze, D. Ray, I. Bocharova, H. Mashiko, A. Sandhu, E. Gagnon, M. M. Murnane, H. C. Kapteyn, I. Litvinyuk, and C. L. Cocke, New J. Phys. **12**, 013008 (2010).
17. P. Johnsson, J. Mauritsson, T. Remetter, A. L'Huillier, and K. J. Schafer, Phys. Rev. Lett. **99**, 233001 (2007).
18. X. M. Tong, P. Ranitovic, C. L. Cocke, and N. Toshima, Phys. Rev. A **81**, 021404 (2010).
19. P. Riviere, O. Uhden, U. Saalmann, and J. M. Rost, New J. Phys. **11**, 053011 (2009).
20. W. E. Cooke, T. F. Gallagher, R. M. Hill, and S. A. Edelstein, Phys. Rev. Lett. **40**, 178 (1978).
21. R. R. Jones and T. F. Gallagher, Phys. Rev. A **38**, 2846 (1988).
22. K. R. Overstreet, R. R. Jones, and T. F. Gallagher, Phys. Rev. Lett. **106**, 033002 (2011).
23 K. R. Overstreet, R. R. Jones, and T. F. Gallagher, Phys. Rev. A **85**, 055401 (2012).

Publications 2011-2013

1. K. R. Overstreet, R. R. Jones, and T. F. Gallagher, "Phase-Dependent Electron-Ion Recombination in a microwave field," Phys. Rev. Lett. **106**, 033002 (2011).
2. J. Nunkaew and T. F. Gallagher, "Spectroscopy of barium 6p1/2nk autoionizing states in a weak electric field," Phys. Rev. A **86**, 013401 (2012).
3. K. R. Overstreet, R. R. Jones, and T. F. Gallagher, "Phase-dependent energy transfer in a microwave field," Phys. Rev. A **85**, 055401 (2012).

Experiments in Ultracold Molecules

Phillip L. Gould
Department of Physics U-3046
University of Connecticut
2152 Hillside Road
Storrs, CT 06269-3046
<phillip.gould@uconn.edu>

Program Scope:

In recent years, there has been a great deal of progress in the production and manipulation of ultracold atoms and molecules. These advances have certainly benefited atomic, molecular and optical (AMO) physics, but they have also impacted a variety of other fields, including quantum information, condensed-matter physics, plasma physics, fundamental symmetries, and chemistry. Compared to atoms, molecules have a rich level structure which can complicate their manipulation. Nevertheless, molecules have attracted increasing interest because they have multiple internal degrees of freedom: electronic, vibrational, rotational, electron spin, and nuclear spin. These span a wide range of energy scales, allowing interactions with a variety of other systems. Furthermore, heteronuclear molecules can have permanent electric dipole moments, whose long-range and anisotropic potentials lead to novel interactions. Molecule cooling methods include "direct" techniques, such as buffer gas cooling, electrostatic slowing, and laser cooling. Ultracold molecules can also be produced "indirectly" by binding together cold atoms via the processes of photoassociation and magnetoassociation. The resulting samples can be confined and compressed using optical, magnetic, and electrostatic traps. The numerous applications of ultracold molecules include: quantum computation; simulations of condensed-matter systems; quantum degenerate gases; novel quantum phases of dipolar gases; tests of fundamental symmetries and fundamental constants; ultracold chemistry; and ultracold collisions. The main thrust of our experimental program is to coherently control the dynamics of colliding ultracold atoms using nanosecond-time-scale pulses of frequency-chirped light. Of particular interest is coherent control of photoassociative formation of ultracold molecules with chirped light.

Our experiments employ laser-cooled Rb atoms confined in a magneto-optical trap (MOT). Rb has a number of practical advantages: 1) its D_2 and D_1 resonance lines, at 780 nm and 795 nm respectively, are conveniently matched to available diode lasers; 2) it has two naturally occurring isotopes, ^{85}Rb and ^{87}Rb; 3) ^{87}Rb is the workhorse atom for BEC studies; and 4) the photoassociative formation of Rb_2, as well as its state-selective ionization detection, have been extensively investigated here at UConn and elsewhere. In our experiments, we load a phase-stable MOT with cold atoms from a separate "source" MOT. The phase-stable geometry provides reduced fluctuations in the atomic density. For molecule formation, we illuminate the cold trapped atoms with a sequence of pulses of frequency-chirped light. These pulses are typically 40 ns FWHM and the chirps typically cover 1 GHz in 100 ns. The ground-state Rb_2 molecules formed by photoassociation are directly detected by ionization with a tunable pulsed dye laser. The resulting Rb_2^+ ions are distinguished from Rb^+ by their time-of-flight to the detector.

Recent Progress:

We have made recent progress in several areas: formation of ultracold ground-state molecules by photoassociation with both positively- and negatively-chirped light; quantum simulations of this chirped photoassociation; and calculations of Raman transfer in 3- and 4-level systems with chirped pulses.

In earlier experiments, we used frequency-chirped light to induce excited-state collisions between pairs of atoms. If these collisions were sufficiently inelastic, or resulted in bound molecules, the involved atoms would be lost from the trap, allowing these "trap-loss" processes to be measured. The chirping of the light caused the excitation radius to change on a time scale similar to that of the collision, which can be quite long for cold atoms. We found that, under some conditions, the rate of trap-loss collisions depended strongly on the chirp direction. This was explained by a fundamental asymmetry in the system: an excited wavepacket always moves inward on the attractive molecular potential, while the excitation radius can move either outward (for a positive chirp) or inward (for a negative chirp). When the wavepacket and the excitation radius both move inward, and do so on similar time scales, there can be multiple interactions between the wavepacket and the light. This can coherently return the excited wavepacket to the ground state, resulting in a reduced rate of trap-loss collisions, as was observed for the negative chirp. We also investigated the effects of nonlinear frequency chirps and found that the detailed shape only mattered for negative chirps, as expected by the above argument. In collaboration with Shimshon Kallush at ORT Braude and Ronnie Kosloff at Hebrew University (both in Israel), we developed quantum dynamical calculations of these chirped-light-induced collisions, both for linear and nonlinear chirps. The agreement between these simulations and the experiments was generally quite satisfying.

More recently, we have switched our emphasis from trap-loss collisions to the formation of ultracold molecules using chirped photoassociation light. In this case, the central frequency of the chirp is shifted farther below the excited atomic asymptote, where the individual vibrational levels are well resolved. The range of the chirp covers a small number of these vibrational lines. We directly detect the resulting ground-state Rb_2 molecules using resonance-enhanced multiphoton ionization (REMPI) with a pulsed dye laser at ~600 nm. As in our earlier trap-loss collision experiments, we see a significant dependence of the molecule formation rate on chirp direction. With the chirps centered on a photoassociation resonance detuned 7.8 GHz below the atomic asymptote, the positive chirp forms more ground-state molecules than the negative chirp.

In order to understand this dependence on chirp direction, we have extended our quantum simulations to include the bound vibrational levels in both the ground- and excited-state molecular potentials. In our case, the 0_g^- and 1_g excited states are relevant, and these can populate high vibrational levels of the $a^3\Sigma_g^+$ triplet ground state, either by spontaneous (incoherent) or stimulated (coherent) emission. In general, the simulations reproduce the trends of the experiment, most significantly the dependence on chirp rate. Examining the time evolution of the various state populations in the simulations, we find that the positive chirp first passes through a photoassociation (free-bound) resonance, which produces excited molecules from free atoms, and then through a bound-bound resonance, which causes stimulated emission of the excited-state molecules into a bound

ground-state vibrational level. For the negative chirp, this sequence would occur in reverse, but it can't because the initial state is free ground-state atoms, not bound ground-state molecules. Therefore, the efficiency of producing ground-state molecules is reduced for the negative chirp. It is interesting that in both trap-loss collisions and molecule formation, an asymmetry is responsible for the dependence on chirp direction. In the former case, it is an asymmetry in the dynamics (inward vs. outward motion), while in the latter, it is an asymmetry in the energy levels (bound molecules vs. free atoms).

We are collaborating with Svetlana Malinovskaya (Stevens Institute of Technology) on calculations of Raman transfer in 3- and 4-level systems using a single chirped pulse on the nanosecond time scale. So far, the calculations have been done for atoms, but they can be adapted to describe the transfer of population between vibrational levels of an ultracold molecule.

Future Plans:

We will extend our chirped molecule formation experiments to faster time scales, increasing our chirp rates and reducing our pulse widths by at least a factor of 10. This will allow us to better match the dynamics of the formation process and avoid the effects of spontaneous emission. Since these faster chirps and shorter pulses require higher intensities, we will incorporate a tapered amplifier to amplify the modulated pulses. To go beyond linear chirps and Gaussian pulses, we will use our arbitrary waveform generator to control laser frequency and amplitude on the nanosecond time scale. With guidance from our quantum simulations, we will optimize the production of ground-state molecules in a target vibrational level.

Recent Publications:

"Characterization and Compensation of the Residual Chirp in a Mach-Zehnder-Type Electro-Optical Intensity Modulator", C.E. Rogers III, J.L. Carini, J.A. Pechkis, and P.L. Gould, Opt. Express **18**, 1166 (2010).

"Coherent Control of Ultracold ^{85}Rb Trap-Loss Collisions with Nonlinearly Frequency-Chirped Light", J.A. Pechkis, J.L. Carini, C.E. Rogers III, P.L. Gould, S. Kallush, and R. Kosloff, Phys. Rev. A **83**, 063403 (2011).

"Creation of Arbitrary Time-Sequenced Line Spectra with an Electro-Optic Phase Modulator", C.E. Rogers III, J.L. Carini, J.A. Pechkis, and P.L. Gould, Rev. Sci. Instrum. **82**, 073107 (2011).

"Quantum Dynamical Calculations of Ultracold Collisions Induced by Nonlinearly Chirped Light", J.L. Carini, J.A. Pechkis, C.E. Rogers III, P.L. Gould, S. Kallush, and R. Kosloff, Phys. Rev. A **85**, 013424 (2012).

"Production of Ultracold Molecules with Chirped Nanosecond Pulses: Evidence for Coherent Effects", J.L. Carini, J.A. Pechkis, C.E. Rogers III, P.L. Gould, S. Kallush, and R. Kosloff, Phys. Rev. A **87**, 011401(R) (2013).

Physics of Correlated Systems

Chris H. Greene
Department of Physics, Purdue University, West Lafayette, IN 47907-2036
chgreene@purdue.edu

Program Scope

A longstanding challenge in atomic, molecular, and optical physics is developing methods that can describe quantum mechanical correlated systems, both in their own right and also in the context of their interactions with time-dependent or static external fields. Although standard theories in atomic and molecular physics frequently treat the electrons as though they are moving independently of one another, many phenomena of interest involve their correlated motion which is in concert. This effort is particularly concentrated in the development of new theoretical techniques or novel combinations of previously used techniques that can handle these nonperturbative correlations.. Recently, we have been studying the effects of a dressing laser field on electron collisions and photoionization processes. In addition, studies have continued in the area of electron collisions with a molecular ion that triggers dissociation and vibrational excitation, especially the process of dissociative recombination (DR), which is one of the most fundamental reactive chemical processes yet one of the most difficult for theory to handle. Our work involves the development of formal theoretical and intuitive ideas as well as detailed numerical computations for target species of interest. This abstract concentrates primarily on work performed and papers published during the past year[1-6], with some discussion of future directions and a summary of publications dating back within two years prior to that.

Recent Progress and Immediate Plans

(i) Strong-field physics that ensues when an intense light pulse from a laser strikes an atom, molecule, or cluster.

A ubiquitous feature in the spectroscopy of bound states that are embedded in a continuum, as in familiar autoionizing resonances of atomic and molecular physics, is the Fano lineshape which was first interpreted by Fano in his 1935 article, but more famously in his elegant and highly-cited 1961 reformulation. A collaboration carried out with the Heidelberg experimental group of Thomas Pfeifer and Christian Ott and the theory group of Jörg Evers and Christoph Keitel led to a publication this year in Science [1]. This study was able to show a general theoretical connection between the Fano lineshape asymmetry parameter q and the phase φ of the dipole oscillations that are created by a short pulse excitation of any Fano resonance. This simple relationship, namely $q = -\cot(\varphi/2)$, had surprisingly not been identified previously, but it emerges as a simple consequence of causality and the Kramers-Kronig relation between the real and imaginary parts of the index of refraction. In parallel with this theoretical demonstration of the relationship between q and φ there are two notable experimental demonstrations in [1] that first of all confirm this theoretical relationship and secondly show its potential for enabling quantum control of resonant light absorption. In their experiment, the team of Pfeifer *et al.* were able to imprint an additional phase intentionally, and use this to modify the Fano lineshape q parameter, thereby turning an asymmetric line shape into a symmetrical Lorentzian. The reverse was also demonstrated, by using this phase imprinting method to change symmetrical line shapes into asymmetrical Fano lineshapes. This technique has significant potential for extending quantum control into new regimes and different types of systems in the future.

During the past year, this grant supported research with graduate student Nathan Morrison on the effect of laser-dressing on negative ion photodetachment and electron-atom scattering processes. This work continues to build on the recent work carried out in this project on the subject of helium photoionization near laser-dressed autoionization levels. The study published in the past year explored the system of an argon atom that is struck by an electron in the presence of a cw CO_2 laser field. Since the laser light in this case is monochromatic, the study adopted a mixed-gauge R-matrix formulation in the Floquet representation. The main conclusion of that study is that photon absorption and emission during the collision is almost negligible once the electron is beyond 10 to 15 Bohr radii from the atomic nucleus. Our investigation [2] provides independent confirmation of previous work carried out on this problem by Francis Robicheaux's group. There is further evidence that experimental measurements on this system dating back to the late 1980s are incompatible with the then-stated assumption that electron collisions in those experiments were occurring with single atoms. In the coming year we are investigating another class of laser-dressing phenomena. A major difference from that previous study of the transient absorption spectrum of helium, however, is that in the coming year we will examine the situation in which monochromatic dressing lasers are used to couple the degenerate threshold levels of atomic hydrogen in an H^- photodetachment process near excited thresholds H(n>1), rather than directly coupling the autoionizing levels as was explored in the Leone group experiment with helium.

***(ii)* Low energy electron collisions with a molecule, ionized or neutral.**

Off and on for a number of years, we have attempted to bootstrap from our improved understanding of dissociative recombination processes to make a first prediction of the rate of dissociative recombination (DR) for low energy electron collisions with the NO_2^+ molecule. This is one of the few important atmospheric molecular ions for which no DR rate has previously been measured or calculated. A major difference between this system and other species considered so far is the fact that there are tight chemical bonds and numerous strongly coupled electronic potential surfaces. Our study, published as a collaborative effort with Dan Haxton at LBNL,[XX] suggests that indirect Rydberg state pathways play a comparatively small role.

During the past year a study with postdoc Michal Tarana implemented an extension of the UK electron-molecule R-matrix suite maintained by Jonathan Tennyson, which should allow the suite to handle much larger and more sophisticated basis sets. The concept of this study is to change the R-matrix calculation strategy. In particular it is possible to solve for the R-matrix as an inhomogeneous linear system at each energy separately, as opposed to the usual route which requires a full diagonalization that obtains all eigenvalues and eigenvectors of the Hamiltonian matrix and allows the R-matrix to then be constructed at all energies in the range of interest. The concept of this alternative method has been known for some years but rarely applied to problems with many-electron molecules that require complicated multi-configuration basis sets. Of course it must be kept in mind that his method has a disadvantage in requiring a new full linear solve at each desired scattering energy, but it has the advantage of being able to treat far larger basis sets in principle, i.e. larger than can be readily solved by full diagonalization. A demonstration calculation for electron scattering from the O_2 molecule is encouraging and was published during the past year. [4]. Although Michal Tarana has now moved on to a permanent position in

Prague, we hope in the coming year to collaborate and develop this calculation further to treat the photodetachment of the negative ion O_2^-, in particular the photoelectron angular distribution which has been studied in recent experiments. A specific goal is to compute the photoelectron angular distributions with a vibrational frame transformation treatment. While such frame transformations are well known to be effective for describing electron interactions with positive molecular ions, very few studies exist for electron interactions with neutral species, and it is expected to elucidate the strengths and limitations of this theoretical technique.

A collaborative project with former graduate student Jia Wang [5] was also able to predict Rydberg spectra of H_3 and D_3 that are of current experimental interest, especially in low temperature supersonic discharges of the type that have been studied in Rich Saykally's group at Berkeley. These Rydberg spectra exhibit Jahn-Teller physics and they continue to generate experimental and diagnostic interest.

Finally, with John Bohn and his graduate student Brandon Ruzic, we also completed and published an extension of generalized quantum defect theory that makes it far more powerful and applicable to low energy collisions involving higher orbital angular momenta L>0, even in the presence of long range interactions.[6]

It is not anticipated that there will remain unexpended funds at the end of this year of the funding cycle. There have been one postdoc and two part-time graduate students supported during the past year by this grant.

Papers published since 2011 that were supported at least in part by this grant.

[1] *Lorentz Meets Fano in Spectral Line Shapes: A Universal Phase and Its Laser Control*, C Ott, A Kaldun, P Raith, K Meyer, M Laux, J Evers, C H Keitel, C H Greene, and T Pfeifer, Science **340**, 716-720 (2013).

[2] *Laser-assisted electron-argon scattering at small angles*, N Morrison and C H Greene, Phys. Rev. A **86**, 053422-1 to -6 (2012).

[3] *Estimates of rates for dissociative recombination of* NO_2^+ *+ e via various mechanisms,* D J Haxton and C H Greene, Phys. Rev. A **86**, 062712-1 to -5 (2012).

[4] *Low-energy electron collisions with* O_2*: Test of the molecular R-matrix method without diagonalization,* M Tarana and C H Greene, Phys. Rev. A **87**, 022710-1 to -13 (2013).

[5] *Rydberg states of triatomic hydrogen and deuterium,* Jia Wang and C H Greene, J. Phys. Chem. A **ASAP**, DOI: 10.1021/jp312462a, pp1-5 (2013).

[6] *Quantum defect theory for high-partial-wave cold collisions,* B P Ruzic, C H Greene and J L Bohn, Phys. Rev. A **87**, 032706-1 to -14 (2013).

[7] *Femtosecond transparency in the extreme-ultraviolet region,* M Tarana and C H Greene, Phys. Rev. A **85**, 013411-1 to -11 (2012).

[8] *Dissociative recombination of highly symmetric polyatomic ions,* N Douguet, A E Orel, C H Greene, and V Kokoouline, Phys. Rev. Lett. **108**, 023202-1 to -5 (2012).

[9] *Dissociative electron attachment and vibrational excitation of CF_3Cl: Effect of two vibrational modes revisited,* M Tarana, K Houfek, Jiri Horacek, and I I Fabrikant, Phys. Rev. A **84**, 052717-1 to -9 (2011).

[10] *Resonant structure of low-energy H_3^+ dissociative recombination*, A Petrignani, S Altevogt, M H Berg, D Bing, M Grieser, J Hoffmann, B Jordon-Thaden, C Krantz, M B Mendes, O Novotny, S Novotny, D A Orlov, R Repnow, T Sorg, J Stuetzel, A Wolf, H Buhr, H Kreckel, V Kokoouline, C H Greene, Phys. Rev. A **83**, 032711-1 to -10 (2011). See also the Publisher's Note, Phys. Rev. A **83**, 049906 (2011).

[11] *Breaking bonds with electrons: Dissociative recombination of molecular ions*, V Kokoouline, N Douguet, and C H Greene, Chem. Phys. Lett. (Frontiers Article) **507**, 1-10 (2011).

[12] *The role of the Jahn-Teller coupling in dissociative recombination of H_3O^+ and H_3^+ ions,* N. Douguet, A. Orel, I. Mikhailov, I. F. Schneider, C. H. Greene, and V. Kokoouline, J. Phys. Conf. Ser. **300**, 012015-1 to -13 (2011).

Using Strong Optical Fields to Manipulate and Probe Coherent Molecular Dynamics

Robert R. Jones, Physics Department, University of Virginia
382 McCormick Road, P.O. Box 400714, Charlottesville, VA 22904-4714
bjones@virginia.edu

I. Program Scope

This project focuses on the exploration and control of dynamics in atoms and small molecules driven by strong laser fields. Our goal is to exploit strong-field processes to implement novel ultrafast techniques for manipulating and probing coherent electronic and nuclear motion within molecules. Ultimately, through the application of these methods, we hope to obtain a more complete picture of the non-perturbative response of molecules to intense laser pulses.

II. Recent Results and Progress

During the past year we have: (i) continued our exploration of strong-field ionization of excited atoms by single-cycle THz pulses, focusing on novel effects associated with directional ionization in the asymmetric field; (ii) demonstrated a substantial degree of field-free orientation in polar molecules exposed to a combination of ultra-short laser and intense THz pulses; and (iii) enhanced our experimental capabilities to enable new and/or improved measurements. Brief summaries of completed and on-going projects are provided below.

(i) Strong-Field Ionization with Single-Cycle THz Pulses

Last year we began an investigation of the ionization of Rydberg atoms in intense, single-cycle THz fields in the low-frequency limit. The intense THz pulses are produced using optical rectification of tilted pulse-front, 150 fs, 790nm laser pulses in MgO doped stoichiometric Li:NbO3 [1,2]. We find that adiabatic ionization is suppressed due to the large distance that the weakly bound electrons must travel to pass over the saddle-point in the field-dressed Coulomb potential. In addition, contrary to standard tenets of energy transfer in a multi- or few-cycle field, electrons liberated at the peak of the THz field acquire a substantial energy, $\sim 2U_p$ (rather than 0), and energies approaching $8U_p$ (rather than $2U_p$) can be achieved without rescattering from the ion core. Accordingly, but non-intuitively, for a given single-cycle field strength, electrons with the greatest energy are produced during the ionization of the most tightly bound states. A manuscript describing these results was recently submitted to PRL.

We have extended these preliminary studies to the ionization of oriented Stark states by an asymmetric single-cycle pulse in which the maximum electric field in one direction is substantially greater than in the other. We find a significant variation in the ionization probability as a function of the relative orientation of the peak field and the atomic dipole moment. A manuscript on this work is in preparation.

As described briefly in Sect. III, we are now attempting to use these oriented electrons as initial states for "recollision" experiments.

(ii) Transient Field-Free Orientation of OCS using Intense Single-Cycle THz Pulses

We have demonstrated that polar molecules can be effectively oriented in a field free environment after coherent preparation using a combination of short optical and intense single-cycle THz pulses. In our experiment, rotationally cooled OCS molecules in a pulsed supersonic

expansion are first exposed to a short optical-frequency pulse. The pulse creates a rotational wavepacket in each molecule via stimulated Raman redistribution. This wavepacket exhibits transient alignment but no orientation. However, subsequent THz exposure leads to the creation of a mixed parity wavepacket that exhibits transient head vs. tail orientation in the lab frame. The optical preparation improves the level of orientation since the energy differences between excited states in the rotational wavepacket more closely match the frequency spectrum of the available THz pulses, facilitating transitions between adjacent rotational states [3,4]. Moreover, by choosing the appropriate delay between the optical and THz pulses, coherences between the rotational states can be exploited to optimize the population redistribution and the orientation. The optimum delay is found to be (N ± ¼)T where N is an integer and T is the fundamental rotational period. Coulomb explosion in an intense probe laser measures the delay-dependent alignment/orientation of the molecules. The standard metric for orientation, $\langle\cos\theta\rangle$ is found to be ±0.10.

This level of field-free orientation is an order of magnitude greater than that optically inferred for THz orientation of room temperature OCS [4] and comparable to that achieved through two-color ionization depletion [5]. While the optical+THz method is more complicated to implement, it has substantial advantages over the two color depletion technique for sample preparation in strong field experiments. Namely, by avoiding the use of an intense ionizing pulse, problems associated with high free-electron densities and/or vibrational/electronic excitation can be eliminated. A manuscript describing our result is nearly ready for submission to PRL. We plan to soon use the technique to explore HHG and controlled few-cycle ionization/dissociation from oriented molecular targets.

(iii) Facility Improvements

We have recently completed the move of our large, multi-user ultra-fast laser facility from its previous home in the Chemistry building to improved laboratory space in the new Physical and Life Sciences research building. The basement laboratories feature vibrationally isolated slabs, cleaner power, and better temperature control. Our initial measurements indicate that the laser stability is greatly improved in the new space.

Additionally, we have been working with Gerhard Paulus' group in Jena to obtain a single-shot carrier envelope phase (CEP) meter based on a stereo-ATI electron spectrometer [7]. The instrument is currently en route from Germany to Virginia. We will use it to both optimize the generation of few-cycle pulses in our lab and to measure the CEP of those pulses in experiments on directional dissociative ionization.

III. Future Plans

First, we are currently exploring the possibility of using oriented Stark states for studies of controlled, THz-induced, collisions between electrons and their parent ions. Here, field-driven electrons from well-defined Rydberg wave-functions will replace tunnel-ionized electrons for elastic and inelastic electron scattering, potentially enabling time-resolved molecular imaging. Second, we have begun to investigate the use of single-cycle THz pulses to induce and probe electron emission from wire tips. Third, using the phase-meter as a diagnostic, we hope to soon initiate pump-probe experiments that will utilize asymmetric few-cycle pulses to explore time-dependent electron localization resulting in asymmetric, multi-electron dissociative ionization.

IV. Publications from Last 3 Years of DOE Sponsored Research

(i) M. Kubel, Nora G. Kling, K. J. Betsch, N. Camus, A. Kaldun, U. Kleineberg, I. Ben-Itzhak, R.R. Jones, G.G. Paulus, T. Pfeifer, J. Ullrich, R. Moshammer, M.F. Kling, and B. Bergues, "Non-Sequential Double-Ionization of N2 in a Near Single-Cycle Laser Pulse," Physical Review A **88**, 023418 (2013).

(ii) K. J. Betsch, Nora G. Johnson, B. Bergues, M. Kubel, O. Herrwerth, A. Senftleben, I. Ben-Itzhak, G. G. Paulus, R. Moshammer, J. Ullrich, M. F. Kling, and R. R. Jones, "Controlled directional ion emission from the dissociative ionization of CO over multiple charge states in a few-cycle laser field," Physical Review A **86**, 063403 (2012).

iii) K.R. Overstreet, R.R. Jones, and T.F. Gallagher, "Phase dependent energy transfer in a microwave field," Physical Review A 85, 055401 (2012).

iv) Boris Bergues, Matthias Kübel, Nora G. Johnson, Bettina Fischer, Nicolas Camus, Kelsie J. Betsch, Oliver Herrwerth, Arne Senftleben, A. Max Sayler, Tim Rathje, Itzik Ben-Itzhak, Robert R. Jones, Gerhard G. Paulus, Ferenc Krausz, Robert Moshammer, Joachim Ullrich, and Matthias F. Kling, "Attosecond Control and Real-Time Observation of Electron Correlations," Nature Communications 3, 813 (2012).

v) K.R. Overstreet, R.R. Jones, and T.F. Gallagher, Phase-dependent Electron-Ion Recombination in a Microwave Field," Phys. Rev. Lett. **106**, 033002 (2011).

vi) Nora G. Johnson, O. Herrwerth, A. Wirth, S. De, I. Ben-Itzhak, M. Lezius, B. Bergues, M.F. Kling, A. Senftleben, C.D. Schröter, R. Moshammer, J. Ullrich, K.J. Betsch, R.R. Jones, A.M. Sayler, T. Rathje, Klaus Rühle, Walter Müller, and G. G. Paulus, "Single-shot Carrier-Envelope-Phase Tagged Ion-momentum Imaging of Non-sequential Double Ionization of Argon in Intense 4-fs Laser Fields," Phys. Rev. A **83**, 013412 (2011).

vii) K.J. Betsch, D.W. Pinkham, and R.R. Jones, "Directional Emission of Multiply-Charged Ions During Dissociative Ionization in Asymmetric Two-Color Laser Fields," Phys. Rev. Lett. **105**, 223002 (2010).

V. References

[1] For a recent review see: Janos Hebling, Ka-Lo Yeh, Matthias C. Hoffman, Balazs Bartal, and Keith A. Nelson, "Generation of High-Power Terahertz Pulses by Tilted-Pulse-Front Excitation and Their Application Possibilities," J. Opt. Soc. Am. B **25**, B6 (2008).

[2] H. Hirori, A. Doi, F. Blanchard, and K. Tanaka, "Single-cycle Terahertz Pulses with Amplitudes Exceeding 1MV/cm Generated by Optical Rectification in LiNbO3," Appl. Phys. Lett. **98**, 091106 (2011).

[3] K. Kitano, N. Ishii, and J. Itatani, "High Degree of Molecular Orientation by a Combination of THz and Femtosecond Laser Pulses," Phys. Rev. A **84**, 053408 (2011).

[4] C.-C. Shu and N.E. Henriksen, " Field-free Molecular Orientation Induced by Single-Cycle THz Pulses: The Role of Resonance and Quantum Interference," Phys. Rev. A **87**, 013408 (2013).

[5] Sharly Fleischer, Yan Zhou, Robert W. Field, and Keith A. Nelson, “Molecular Orientation and Alignment by Intense Single-Cycle THz Pulses,” Phys. Rev. Lett. **107**, 163603 (2011).

[6] E. Frumker *et al*., "Probing Polar Molecules with High Harmonic Spectroscopy," Phys. Rev. Lett. **109**, 233904 (2012).

[7] T. Wittman *et al*., "Single-shot Carrier-Envelope Phase Measurement of Few-Cycle Laser Pulses," Nat. Phys. 5, 357 (2009).

Molecular Dynamics Probed by Coherent Soft X-Rays

Henry C. Kapteyn and Margaret M. Murnane
University of Colorado at Boulder, Boulder, CO 80309-0440
Phone: (303) 210-5193; E-mail: kapteyn@jila.colorado.edu

The goal of this work is to develop novel short wavelength probes of molecules and to understand the response of atoms and molecules to strong laser fields, in particular mid-infrared (mid-IR) laser fields. We made exciting advances in several experiments. We also have very productive collaborations with chemistry colleagues including Tamar Seideman (Northwestern), Keith Nelson (MIT), and Gordana Dukovic and Jose L. Jimenez (CU Boulder).

1. Photoelectron spectroscopy of CdSe nanocrystals in the gas phase: a direct measure of the evanescent electron wavefunction of quantum dots

We performed the first photoelectron spectroscopy measurements of quantum dots (semiconductor nanocrystals) in the gas phase.[1] By coupling a nanoparticle aerosol source to a femtosecond velocity map imaging photoelectron spectrometer, we applied robust gas-phase photoelectron spectroscopy techniques to colloidal quantum dots, which typically must be studied in a liquid solvent or while bound to a surface. Working with a flowing aerosol of quantum dots allows us to isolate the intrinsic properties of quantum dots *independent of coupling to a host or substrate*, and also has the advantages of providing fresh nanoparticles for each laser shot to avoid degradation or charging effects.

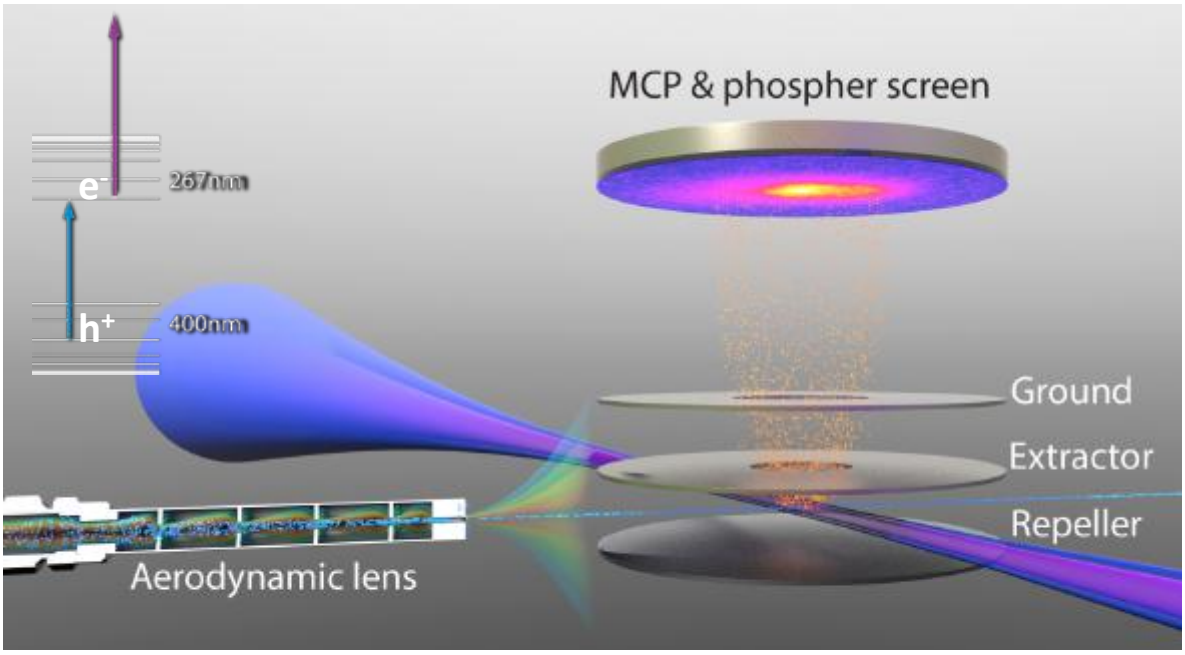

Fig. 1. Velocity map imaging photoelectron spectrometer coupled to a nanoparticle aerosol source to measure the evanescent electron wavefunction in QDs. Clusters of quantum dots are focused into the interaction region by an aerodynamic lens, where they are then excited to an exciton state by the pump pulse (400 nm) and later ionized by the probe pulse (267 nm). Insert: Energy diagram for two-photon photoelectron spectroscopy (2PPE) scheme (right) for capturing the evanescent wavefunction of the electron (left).

In our first work using this setup, we carefully measured a simple two-photon photoelectron yield, and showed that the yield per exciton depends on the physical size of the quantum dot, increasing for smaller dots. Next, using effective mass modeling, we showed that the extent to which the electron wavefunction of the exciton extends from the quantum dot, the so-called "evanescent electron wavefunction", increases as the size of the quantum dot decreases. This is

the most direct evidence yet of the quantum-confined nature of the quantum dot excited state wave function, since the photoelectron yield is dominated by the evanescent electron density that extends outside the physical confines of the QD. Our analysis took into account quantum confinement effects, the difference in the density of states inside and outside of the quantum dots, and the transmission factor for electrons through the surface of the quantum dot. Our conclusion is that the photoelectron yield nearly directly reflects the fraction of evanescent electron wavefunction that extends outside of the quantum dot. This work shows that gas-phase photoelectron spectroscopy is a robust and general probe of the electronic structure of quantum dots. We are now extending these studies to other quantum dot systems, including core-shell quantum dots, multiple excitons systems, as well as charge transfer to ligands on quantum dots.

2. Strong field ionization using mid-IR driving lasers: beyond the 3-step model

The favorable λ^2 scaling of the ponderomotive energy and resulting cutoff photon energy in high harmonic emission has motivated studies of strong field ionization of atoms and molecules with mid-IR driving pulses. However, until recently, the very different physics associated with mid-IR strong field ionization was not well understood. One reason for this is that the advanced (and very computationally intensive) numerical models required to model strong field ionization in the mid-IR make it challenging to develop a good physical insight.

In work published in PRL in 2012, [6] we showed that when an atom is irradiated by an intense mid-IR femtosecond laser pulse, the simple semi-classical 3-step model often used to describe how an atom ionizes needs to be extended to include the fact that the electron can re-encounter the ion many times before finally ionizing. This work also, to our knowledge, was the first to be able to show that an electron ionized from an atom with a strong field emerges into the continuum at the far side of the quantum tunneling barrier, several Å from the atomic core. We are now extending these studies to longer and shorter wavelength driving lasers.

3. X-ray driven dynamics in triatomic molecules: radiation femtochemistry

In past work, we combined HHG with a COLTRIMS momentum imaging apparatus to directly observe the chemical dynamics initiated by ionizing radiation i.e. *radiation femtochemistry.* This work immediately yielded new and unanticipated findings - exploring which shake-up states are responsible for dissociation of N_2, and explaining why autoionization is delayed in O_2.

In more recent work published in Nature Physics,[4] we explored how to use laser pulses to control non-Born-Oppenheimer dynamics in x-ray driven triatomics. N_2O is a simple linear triatomic molecule with an asymmetric bond. Using a few-femtosecond 43 eV XUV pulse, we can create an exotic excited-state target where a simple Born-Oppenheimer picture breaks down. The resultant decay dynamics involves a competition between two decay channels that occur on very fast, 20 fs, timescales: molecular autoionization by ejecting a second electron ($N_2O^{+*} \rightarrow N_2O^{2+} + e^-$), or dissociation without electron emission - including two-body dissociation to one singly charged atomic (molecular) ion plus another molecular (atomic) neutral fragment, or 3-body dissociation to one singly charged atomic ion and two atomic neutral fragments. In the presence of an intense IR field, we can interrupt the neutral-ion dissociation channel and strongly enhance the double-ion channel yield, because the excited N_2O^{+*} is very fragile in the laser field and can easily lose a second electron. Moreover, with the addition of an IR field, breaking the N-O bond can be enhanced more than breaking the N-N bond, indicating the presence of laser-induced non-adiabatic electron motion. We are now extending these studies to other molecules.

4. Understanding high harmonic generation from molecules

High harmonic generation (HHG) from atoms has been studied for about 25 years, and this area of research continues to yield surprising new physics. In contrast, high harmonic generation from molecules has been studied only in the past 10 years, and the richer nature of the molecular orbital structure provides both challenges and opportunities. We reported several new findings about HHG from molecules, many in collaboration with Tamar Seideman's group.[2, 5]

In our most recent work studying HHG from molecules, we made a surprising new finding - that the maximum in HHG emission from a molecule does not occur when the molecule is driven by linear polarized laser beams (as is the case for atoms), but rather for a non-zero value of the ellipticity of the driving laser. Moreover, the two polarization states that contribute to the elliptically polarized HHG beam behave very differently. To put this finding in context: for a long time it was known that HHG from atoms is brightest when driven by linearly polarized fields. As the driving laser becomes more elliptically polarized, the electron will simply not recollide with the ion. Thus, any ellipticity in the driving laser reduces the HHG emission in atoms. Clearly this is not the case for molecules.

At first we thought that an advanced and complex model would be needed to explain these surprising results. However, fortunately, we are able to fully interpret them using a simple and intuitive two-charge center model that gives great insight into the physics of HHG from molecules. Our work clearly demonstrates how to use molecular structure and alignment to manipulate the polarization state of high-order harmonics, and also presents a potential new attosecond probe of the underlying molecular dynamics. Specifically, information about molecular orbital structure is contained both in the value of the HHG dichroism as a function of laser ellipticity and laser-molecule angle, and in the variations with harmonic order. The use of an elliptically polarized laser field also provides new insights into the journey of the continuum electron and the underlying bound states of the molecular ion. In the future, our findings will provide useful insights into fundamental coupled electron-ion-structural dynamics in molecules. Moreover, the ability to control the polarization properties of HHG using an elliptical driving field is unique and provides a very valuable tool for the production and tuning of attosecond pulses that are recently finding broad applications in nanoscience.

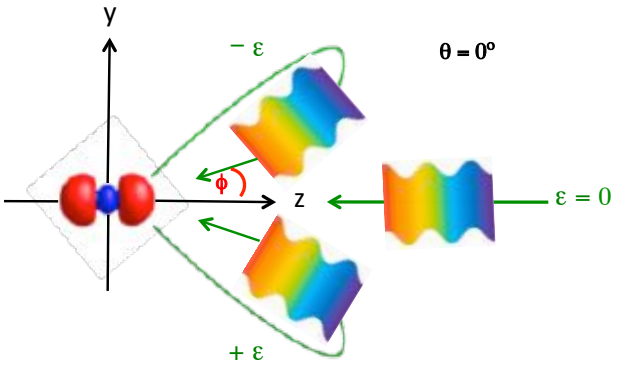

Fig. 2. Schematic illustration of the geometric roles played by the aligning pump pulse and HHG probe angles and the probe ellipticity in tuning the recollision dynamics in HHG from molecules.

Publications and patents as a result of DOE AMOS support since 2010

1. W. Xiong, D. Hickstein, K. Schnitzenbaumer, J. Ellis, B. Palm, K. Keister, L. Miaja-Avila, G. Dukovic, J. Jimenez, M. Murnane, H. Kapteyn, "Photoelectron spectroscopy of CdSe nanocrystals in the gas phase: a direct measure of the evanescent electron wavefunction of quantum dots", Nano Letters **13**, 2924 (2013).
2. P. Sherratt, R. Lock, X. Zhou, H. Kapteyn, M. Murnane, T. Seideman, "Ultrafast elliptical dichroism in high-order harmonics as a dynamic probe of molecular and electronic structure", submitted (2013).
3. T. Popmintchev, M. Chen, A. Bahabad, M. Murnane, H. Kapteyn, "Method for phase-matched generation of coherent soft and hard x-rays using IR lasers," US Patent # 20110007772, Notice of Allowance March 2013.
4. X. Zhou, P. Ranitovic, C. Hogle, H.C. Kapteyn and M.M. Murnane, "Probing and Controlling non-Born-Oppenheimer Dynamics in Super-Excited Triatomic Molecules", Nature Physics **8**, 232 (2012).
5. R. Lock, X. Zhou, H. Kapteyn, M. Murnane, S. Ramakrishna, T. Seideman, "Extracting continuum electron dynamics from high harmonic emission from molecules, " Physical Review Letters **108**, 133901 (2012).
6. D. Hickstein, P. Ranitovic, S. Witte, X. Tong, Y. Huismans, P. Arpin, X. Zhou, B. Zhang, C. Ding, K. Keister, P. Johnsson, N. Toshima, M. Vrakking, H. Kapteyn, M. Murnane, "Direct visualization of laser-driven electron multiple-scattering and tunneling distance using velocity-map imaging," Phys. Rev. Lett. **109**, 073004 (2012).
7. M. Spanner, J. Mikosch, A. Boguslavskiy, M. Murnane, A. Stolow, S. Patchkovskii, "Strong Field Ionization and High Harmonic Generation during Polyatomic Molecular Dynamics," Phys. Rev. A **85**, 033426 (2012).

8. Qing Li et al., “Generation and Control of Ultrashort-Wavelength 2D Surface Acoustic Waves at Nano-interfaces”, Phys. Rev. B **85**, 195431 (2012).
9. P. Ranitovic, X. M. Tong, C. W. Hogle, X. Zhou, Y. Liu, N. Toshima, M. M. Murnane, and H. C. Kapteyn, "Laser-Enabled Auger Decay in Rare-Gas Atoms," Physical Review Letters **106**, 053002 (2011).
10. D. Nardi et al., “Probing Thermomechanics at the Nanoscale: Impulsively Excited Pseudosurface Acoustic Waves in Hypersonic Phononic Crystals”, Nano Letters **11**, 4126 (2011).
11. T. Popmintchev, M.C. Chen, P. Arpin, M. M. Murnane, and H. C. Kapteyn, "The attosecond nonlinear optics of bright coherent X-ray generation," Nature Photonics **4**, 822 (2010). *Featured on cover.*
12. W. Li, A. Becker, C. Hogle, V. Sharma, X. Zhou, A. Becker, H. Kapteyn, M. Murnane, "Visualizing electron rearrangement in space and time during the transition from a molecule to atoms," PNAS **107**, 20219 (2010).
13. K. P. Singh et al., "Control of Electron Localization in Deuterium Molecular Ions using an Attosecond Pulse Train and a Many-Cycle Infrared Pulse," Phys. Rev. Lett. **104**, 023001 (2010).
14. P. Ranitovic et al, “IR-Assisted Ionization of He by Attosec XUV Radiation,” New J. Phys. **12**, 013008 (2010).
15. K. S. Raines, S. Salha, R. L. Sandberg, H. D. Jiang, J. A. Rodriguez, B. P. Fahimian, H. C. Kapteyn, J. C. Du, and J. W. Miao, "Three-dimensional structure determination from a single view," Nature **463**, 214 (2010).
16. M. Siemens, Q. Li, R. Yang, K. Nelson, E. Anderson, M. Murnane, H. Kapteyn, “Measuring quasi-ballistic heat transport across nanoscale interfaces using ultrafast coherent soft x-rays”, Nature Materials **9**, 26 (2010).

Imaging Multi-particle Atomic and Molecular Dynamics

Allen Landers landers@physics.auburn.edu
Department of Physics
Auburn University
Auburn, AL 36849

Program Scope

We are investigating phenomena associated with ionization of an atom or molecule by single photons (weak field) or low energy electrons with an emphasis on ionization-driven atomic and molecular dynamics. Of particular interest is untangling the complicated electron-correlation effects and molecular decay dynamics that follow an initial photoionization or electron attachment event. We perform these measurements using variations on the well-established COLTRIMS technique. The experiments take place at the Advanced Light Source at LBNL as part of the ALS-COLTRIMS collaboration with the groups of Reinhard Dörner at Frankfurt and Ali Belkacem and Thorsten Weber at LBNL and at Auburn University. Because the measurements are performed in "list mode" over a few days where each individual event is recorded to a computer, the experiments can be repeated virtually with varying gate conditions on computers at Auburn University over months. We continue to collaborate closely with theoreticians also funded by DOE-AMOS including most recently the groups of F. Robicheaux and C.W. McCurdy.

Publication Highlights from past year

We had a strong year for high impact publications resulting from work initiated by the Auburn part of the international ALS-COLTRIMS collaboration. We published in Physical Review Letters our measurement that used three-dimensional coincident imaging to demonstrate that low energy photoelectrons ejected from the core of a methane molecule emerge along the bond axes.
In addition, two of our papers were featured in the "highlights 2012" for the Journal of Physics B (one featured on the cover at left). The first was an extension of the work published in PRL, where we showed that these imaging experiments allowed us to trace decay dynamics at an unprecedented level of detail. The second was a collaborative paper with Francis Robicheaux, where his calculation coupled with our new measurements explained a previously not-understood phenomenon in the angular correlation of electrons ejected from the same atom with very different energies. Finally, we have performed a number of dissociative electron attachment measurements on small molecules in collaboration with Prof. Mike Fogle at Auburn, where we have used momentum imaging of the resulting anion in order to explore the dissociation dynamics. We summarize these articles here.

(1) Imaging polyatomic molecules in three dimensions using molecular frame photoelectron Angular Distributions, *Phys. Rev. Lett.* **108,** 233002 (2012)
Here we demonstrated a method for determining the full three-dimensional molecular-frame photoelectron angular distribution in polyatomic molecules using methane as a prototype. Simultaneous double Auger decay and subsequent dissociation allowed measurement of the initial momentum vectors of the ionic fragments and the photoelectron in coincidence, yielding full orientation by observing a three-ion decay pathway, (H^+, H^+, CH_2^+). We found the striking

result that at low photoelectron energies the molecule is effectively imaged by the focusing of photoelectrons along bond directions. The figures below show the momentum spectra of the ions (left) and the photoelectrons (right), both in the molecule frame.

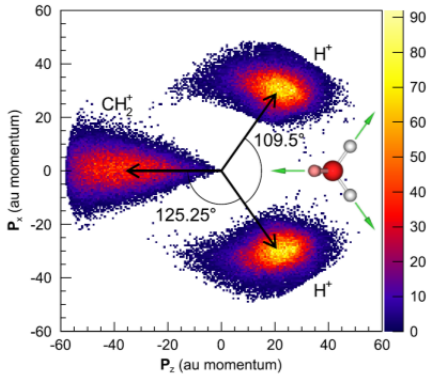

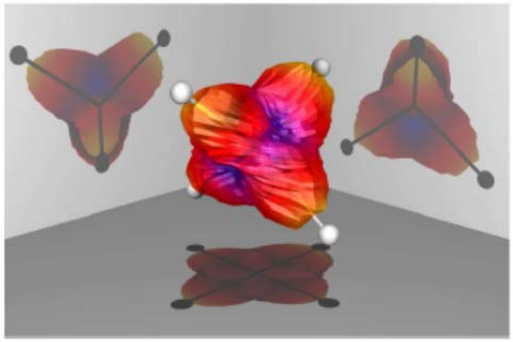

(2) Probing the dynamics of dissociation of methane following core ionization using three-dimensional molecular-frame photoelectron angular distributions, *J. Phys. B: At. Mol. Opt. Phys.* **45** 194003 (cover, and highlight 2012)
Here we presented experimental measurements and theoretical calculations for the photoionization of CH_4 at the carbon K-edge. Measurements performed using cold target recoil ion momentum spectroscopy (COLTRIMS) combined with complex Kohn variational calculations of the photoelectron in the molecular frame verified the surprising result that the low energy photoelectrons effectively image the molecule by emerging along the bond axes. Furthermore, we observed a dynamic breakdown of axial recoil behavior in one of the dissociation pathways of the intermediate dication, which were interpreted using electronic structure calculations. This investigation was driven in large part by the observation of the strong influence of the ion fragment kinetic energies on the photoelectron angular distributions found in our initial analysis.

(3) Calculated and measured angular correlation between photoelectrons and Auger electrons from K-shell ionization, *J. Phys. B: At. Mol. Opt. Phys.* **45** 175001 (highlight 2012)
Here we repeated and improved measurements to provide experimental support to calculations performed by Francis Robicheaux, who applied a recently developed computational method to an experimental puzzle that involves a slow outgoing electron that is scattered by a high-energy Auger electron. Although the experiment seemed to be in a regime accurately described by classical mechanics, such classical calculations could not accurately model the angular distribution of the electron pair. Using the wavefunction from his calculations to generate the energy and angular distributions of the two electrons, we compared his results to our measurements performed at the Advanced Light Source. We obtained good agreement between the experiment and our quantum results, attributing the poor classical result to the small number of angular momenta in the wavefunction.

(4) Dissociative electron attachment to small molecules (references 1-4 below)
We have employed a momentum imaging technique to measure the dissociative electron attachment to a number of small molecules including O_2, CO_2, and N_2O. By measuring the momentum distribution of the anion produced we are able to determine the kinetic energy release in the reaction as a function of emission angle over the full 4π solid angle of acceptance. This allows, for example, a comparison with theory that calculates the entrance amplitudes leading to

the dissociative resonance being studied. We have found that the high angular resolution of our supersonic crossed-beam experiment has provided new insights into previous measurements of some systems, and has opened the door to fruitful collaboration with the LBNL theoretical and experimental group also funded within the DOE-AMOS program.

Future Plans:

We intend to pursue additional experiments as part of our work within the ALS-COLTRIMS collaboration and expand our efforts at Auburn to study electron driven phenomena. Here are some examples:

- Study core-photoionization in similar systems to methane to explore whether or not the imaging effect observed in methane occurs elsewhere (e.g. H_20, NH_3).
- Measure the Auger electrons in coincidence with fragments to produce molecular frame angular distributions for Auger electrons in order to better identify dissociative pathways following photoionization.
- Measure methane analogues with substitutions for hydrogen (e.g. difluoromethane CH_2F_2) to study the influence of different electron density distributions along the bond axes.
- Study core-hole localization in C_2H_6 using 3D MFPADS.
- Use larger polyatomic molecules (e.g. allene) to probe the limits of extending these measurements to systems of increasing complexity.
- Extend DEA measurements to include liquid targets (e.g. alcohols, formic acid)
- Continue to be guided by and partner with theoreticians to study these fundamental processes.

Refereed Publications: Supported by DOE-AMOS (2010-present)

1. **Dissociative electron attachment to carbon dioxide via the $^2\Pi_u$ shape resonance,** A. Moradmand, D.S. Slaughter, D.J. Haxton, A.L. Landers, C.W. McCurdy, T.N. Rescigno, M. Fogle, A. Belkacem *Phys. Rev. A* **88** 032703 (2013).
2. **Dissociative-electron-attachment dynamics near the 8-eV Feshbach resonance of CO_2,** A. Moradmand, D. Slaughter, A.L. Landers, M. Fogle, *Phys. Rev. A* **88** 022711 (2013).
3. **Momentum imaging of dissociative electron attachment to N_2O,** A. Moradmand, A.L. Landers, M. Fogle, *Phys. Rev. A* **88** 012713 (2013).
4. **Momentum-imaging apparatus for the study of dissociative electron attachment dynamics** A. Moradmand, J. Williams, A. Landers, M. Fogle, *Review of Scientific Instruments* **84**, 033104 (2013).
5. **Ejection of quasi free electron pairs from the helium atom ground state by a single photon,** M. S. Schöffler, C. Stuck, M. Waitz, F. Trinter, T. Jahnke, U. Lenz, M. Jones, A. Belkacem, A.L. Landers, C.L. Cocke, J. Colgan, A. Kheifets, I. Bray, H. Schmidt-Böcking, R. Dörner, and Th.Weber *Phys. Rev. Lett*, **111** 013003 (2013).
6. **Probing the Dynamics of Dissociation of Methane Following Core Ionization Using Three-Dimensional Molecular Frame Photoelectron Angular Distributions**, J. B. Williams, C. S. Trevisan, M. S. Schöffler, T. Jahnke, I. Bocharova, H. Kim, B. Ulrich, R. Wallauer, F. Sturm, T. N. Rescigno, A. Belkacem, R. Dörner, Th. Weber, C. W. McCurdy, and A.L. Landers, *J. Phys. B: At. Mol. Opt. Phys.,* **45** 194003 (2012).

7. **Calculated and measured angular correlation between photoelectrons and Auger electrons from K-shell ionization**, F. Robicheaux, M. P. Jones, M. S. Schöffler, T. Jahnke, K. Kreidi, J. Titze, C. Stuck, R. Dörner, A. Belkacem, Th. Weber, and A.L. Landers *J. Phys. B: At. Mol. Opt. Phys*., **45** 175001 (2012).
8. **Multi fragment vector correlation imaging - A proposal to search for hidden dynamical symmetries in many-particle molecular fragmentation processes**, F. Trinter, L. Ph. H. Schmidt, T. Jahnke, M. S. Schöffler, O. Jagutzki, A. Czasch, J. Lower, T. A. Isaev, R. Berger, A. L. Landers, Th. Weber, R. Dörner, H. Schmidt-Böcking *Molecular Physics* **110** 1863 (2012).
9. **Imaging polyatomic molecules in three dimensions using molecular frame photoelectron angular distributions**, J. B. Williams, C. S. Trevisan, M. S. Schöffler, T. Jahnke, I. Bocharova, H. Kim, B. Ulrich, R. Wallauer, F. Sturm, T. N. Rescigno, A. Belkacem, R. Dörner, Th. Weber, C. W. McCurdy, and A.L. Landers, *Phys. Rev. Lett.* **108** 233002 (2012).
10. **Dynamic modification of the fragmentation of autoionizing states of O+2**, W. Cao, G. Laurent, S. De, M. Schöffler, T. Jahnke, A. S. Alnaser, I. A. Bocharova, C. Stuck, D. Ray, M. F. Kling, I. Ben-Itzhak, Th. Weber, A. L. Landers, A. Belkacem, R. Dörner, A. E. Orel, T. N. Rescigno, and C. L. Cocke, *Phys. Rev. A* **84** 053406, (2011).
11. **Matter wave optics perspective at molecular photoionization: K-shell photoionization and Auger decay of N_2**, M. Schöffler, T. Jahnke, J. Titze, N. Petridis, K. Cole, L. Ph. H. Schmidt, A. Czasch, O. Jagutzki, J.B. Williams, C.L. Cocke, T. Osipov, S. Lee, M.H. Prior, A. Belkacem, A.L. Landers, H. Schmidt-Böcking, R. Dörner, and Th. Weber, *New Journal of Physics* **13** 095013 (2011).
12. **Production of excited atomic hydrogen and deuterium from H_2, HD and D_2 photodissociation** R Machacek , V M Andrianarijaona , J E Furst , A L D Kilcoyne , A L Landers , E T Litaker , K W McLaughlin and T J Gay *J. Phys. B: At. Mol. Opt. Phys.* **44** 045201 (2011).
13. **Auger decay of $1\sigma_g$ and $1\sigma_u$ hole states of N_2 molecule: II. Young type interference of Auger electrons and its dendence on internuclear distance** N. A. Cherepkov, S. K. Semenov, M. S. Schöffler, J. Titze, N. Petridis, T. Jahnke, K. Cole, L. Ph. H. Schmidt, A. Czasch, D. Akoury, O. Jagutzki, J. B. Williams, T. Osipov, S. Lee,M. H. Prior, A. Belkacem, A. L. Landers, H. Schmidt-Böcking, R. Dörner and Th. Weber, *Phys. Rev. A* **82**, 023420 (2010).
14. **Auger decay of $1\sigma_g$ and $1\sigma_u$ hole states of the N_2 molecule: Disentangling decay routes from coincidence measurements** S. K. Semenov, M. S. Schöffler, J. Titze, N. Petridis, T. Jahnke, K. Cole, L. Ph. H. Schmidt, A. Czasch, D. Akoury, O. Jagutzki, J. B. Williams, T. Osipov, S. Lee, M. H. Prior, A. Belkacem, A. L. Landers, H. Schmidt-Böcking, Th. Weber, N. A. Cherepkov, and R. Dörner, *Phys. Rev. A* **81**, 043426 (2010).
15. **Carbon K-shell photoionization of fixed-in-space C_2H_4** T. Osipov, M. Stener, A. Belkacem, M. Schöffler, Th. Weber, L. Schmidt, A. Landers, M. H. Prior, R. Dörner, and C. L. Cocke, *Phys. Rev. A* **81**, 033429 (2010) .
16. **Formation of inner-shell autoionizing CO^+ states below the CO_2^+ threshold** T. Osipov, Th. Weber, T. N. Rescigno, S. Y. Lee, A. E. Orel, M. Schöffler, F. P. Sturm, S. Schössler, U. Lenz, T. Havermeier, M. Kühnel, T. Jahnke, J. B. Williams, D. Ray, A. Landers, R. Dörner, and A. Belkacem, *Phys. Rev. A* **81**, 011402 (2010).

Molecular photoionization studies of nucleobases and correlated systems

Erwin Poliakoff, Department of Chemistry, Louisiana State University, Baton Rouge, LA 70803, epoliak@lsu.edu

Robert R. Lucchese, Department of Chemistry, Texas A&M University, College Station, TX, 77843, lucchese@mail.chem.tamu.edu

Program Scope

Molecular photoionization is a process that allows one to probe fundamental electron scattering dynamics in complex systems. We use powerful experimental and theoretical tools for illuminating the microscopic details of the scattering dynamics. We focus on two primary areas. The first focus is to use vibrationally resolved photoelectron spectroscopy to probe the correlated motions of electrons and nuclei. This allows us to disentangle the geometry and energy dependence of the dipole matrix elements that couple the initial bound state to the continuum scattering state. The experimental approach is to obtain vibrationally resolved photoelectron spectra over a broad range of incident photon energies by exploiting the high brightness capabilities at the Advanced Light Source. On the theory side, we explicitly solve the electron-molecular ion scattering equations to compute the corresponding vibrationally specific matrix elements using the adiabatic approximation. The second major direction is to explore applications of single-photon molecular photoionization transition amplitudes to high harmonic generation (HHG) and related processes. We have made considerable progress, in collaboration with Profs. Trallero and Lin at the McDonald Laboratory. We have initiated studies of high harmonic generation in relatively complex molecules, and this work is progressing very well. We have also begun a collaboration with Bill McCurdy and Tom Rescigno of the Atomic, Molecular, and Optical Theory group at Lawrence Berkeley National Laboratory (LBNL) with the objective of applying the complex Kohn method developed at LBNL to the problems that we are studying and to a develop modified version of our electron-molecule scattering codes using the complex Kohn approach for solving the scattering equations. All of these research efforts benefit the Department of Energy because the results elucidate structure/spectra correlations that will be indispensable for probing complex and disordered systems of interest to DOE such as clusters, catalysts, reactive intermediates, transient species, and related species.

Recent Progress

Non-Franck-Condon Vibrational Branching Ratios

In the simplest view of molecular photoionization, one assumes that vibrational and photoelectron motion are decoupled, which leads to the Franck-Condon approximation. Nonresonant and resonant processes can result in coupling molecular vibration and photoelectron motion, with the result that vibrational branching ratios become dependent on photon energy, and that forbidden vibrations can be excited. A convenient way to express the extent of the breakdown of the Franck-Condon approximation for a given mode, represented by the variable q, is via the electronic factor F which is just the logarithmic derivative of the cross section with respect to changes in the coordinate q. This quantity, in the harmonic approximation, can be related to the vibrational branching ratio.

We are working with a wide variety of molecular targets, including nucleobases, substituted thiophenes, and acrolein (C_3H_4O). Experimentally, we have made considerable

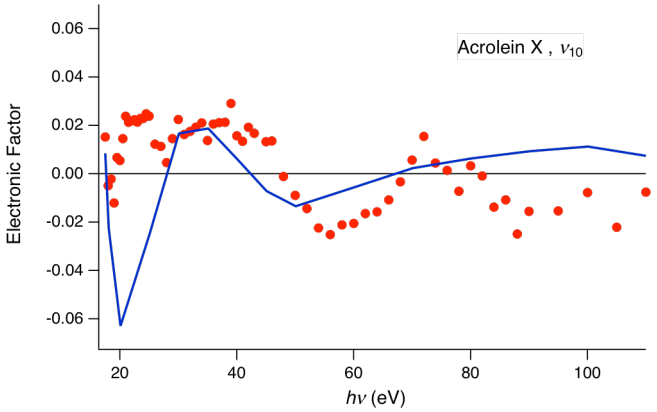

Figure 1. Computed (line) and measured (dots) F factors for the excitation of the ν_{10} fundamental in the ionization of acrolein leading to the $X\,A'$ state of the ion, computed using an assumed Franck-Condon branching ration of 0.18

progress on acrolein, which is the simplest unsaturated aldehyde, and for which we have obtained vibrationally resolved photoionization data. In this system there are 18 normal vibrational modes with 13 in-plane vibrations that have non-zero Franck-Condon factors. In the observed spectrum, the intensity of the excitation of seven of those modes can seen, although deriving intensities of individual lines requires curve fitting that introduces additional uncertainties.

One of the most prominent features in the photoelectron spectrum of acrolein is due to the excitation of the fundamental of the ν_{10} vibrational mode. This mode is primarily the stretching mode of the C-C single bond in the molecule which occurs at 1158 cm^{-1} in the neutral molecule. In Fig. 1, we present measured and computed F factors for the ν_{10} vibrational mode which are derived assuming a Franck-Condon vibrational branching ration of 0.18. The oscillations seen in the experiment and calculations around 50 eV indicate that there is a weak feature in the cross section. We are also analyzing features seen in the branching ratios for excitation of the ν_6, ν_9, ν_{11}, and ν_{13} modes.

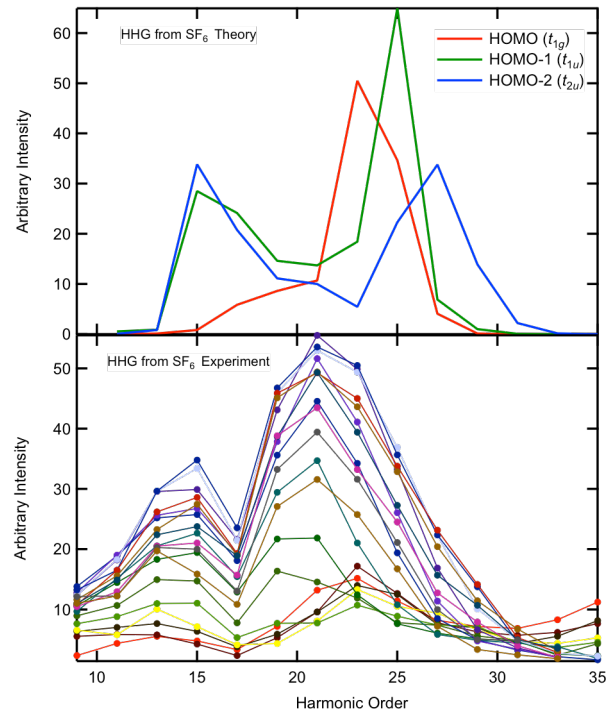

Figure 2. Comparison of computed and measured HHG spectra for SF_6.

We have obtained photoelectron spectra of cytosine, thymine, and uracil, where we do not find significant non-Franck-Condon behavior. However the increase in resolution in the present studies when compared to previous published work is noteworthy. In particular, it allows for a better comparison between experiment and theory leading to important conclusions about the tautomerization of cytosine, as well as the electronic structure of cytosine, thymine and uracil.

Molecular aspects of HHG

A major component of our recent work has been to develop connections between molecular high harmonic generation and photoionization dynamics. The two phenomena are intimately connected because a central step of high harmonic generation, within in three step model, is the photorecombination of an

electron with the ion from which it was ejected by tunnel ionization and to which it is then driven back by the oscillating strong field. Photorecombination is the conjugate process to photoionization and is governed by the same transition amplitudes. We have performed experiments on a series of molecules, including SF_6, $SiCl_4$, and CF_4. This work is done collaboratively with Kansas State researchers, primarily Profs. Carlos Trallero and C.D. Lin. Representative results are shown in Fig. 2 for SF_6 where we compare measured and computed theoretical HHG spectra. In the experimental data, the different curves correspond to different positions of the gas jet relative to the position of the laser focus. Changing the gas jet position changes the macroscopic propagation and the effective trajectories of the returning electron. The one feature that is consistently present in the experimental data is the minimum in the HHG spectrum at the 17^{th} harmonic. In the theory we have applied the quantitative rescattering (QRS) theory to isolated molecules and considered the ionization of the electrons from the three most weakly bound orbitals, i.e. the highest occupied molecule orbital (HOMO), the HOMO-1, and the HOMO-2. These three orbitals have ionization potentials that are all within 1.5 eV of each other. The structures in the computed HHG are related to shape resonant peaks in the photoionization cross section. The main conclusion from this comparison is that the two peaks in seen in the experiment are probably due to shape resonances in the electron-molecule scattering dynamics. Additionally, there is strong evidence that the HOMO-1 and HOMO-2 orbitals contribute to the measured HHG spectrum. We have seen similar, albeit less dramatic effects, in the other molecules studied.

Future Plans

We have a number of systems, studied at the ALS, where the analysis needs to be completed. These systems include several nucleobases and 2-bromothiophene. We will continue to expand our efforts on the studies of molecular HHG. In addition to considering new target molecules, we will also consider variations in parameters that affect the HHG spectrum including laser power, polarization (i.e., ellipticity), and focal position within the target molecular beam. We are also planning to incorporate pump-probe capabilities into our HHG work. Theoretically we will pursue the use of grid methods compatible with the complex Kohn method for solving the electron-molecule scattering equations. This approach should facilitate the implementation of these methods using parallel algorithms and allow for the routine treatment of electron scattering in larger molecular systems.

Publications in 2011-2013 Acknowledging Support from DOE

1. Misaki Okunishi, Hiromichi Niikura, R. R. Lucchese, Toru Morishita, and Kiyoshi Ueda, Extracting electron-ion differential scattering cross sections for partially aligned molecules by laser-induced rescattering photoelectron spectroscopy, *Phys. Rev. Lett.* **106**, 063001:1-14 (2011).
2. N. Berrah, R. C. Bilodeau, I. Dumitriu, D. Toffoli, R. R. Lucchese, Shape and Feshbach Resonances in Inner-Shell Photodetachment of Negative Ions, *J. Electron Spectrosc. Relat. Phenom.* **183**, 64-9 (2011).
3. Song-Feng Zhao, Cheng Jin, R. R. Lucchese, Anh-Thu Le, and C. D. Lin, High-order-harmonic generation using gas-phase H_2O molecules, *Phys. Rev. A* **83**, 033409:1-7 (2011).
4. Cheng Jin, Hans Jakob Wörner, V Tosa, Anh-Thu Le, Julien B. Bertrand, R. R. Lucchese, P. B. Corkum, D. M. Villeneuve, and C. D. Lin, Separation of target structure and medium propagation effects in high-harmonic generation, *J. Phys. B* **44**, 095601:1-5 (2011).

5. Bérenger Gans, Séverine Boyé-Péronne, Michel Broquier, Maxence Delsault, Stéphane Douin, Carlos E. Fellows, Philippe Halvick, Jean-Christophe Loison, Robert R. Lucchese, and Dolores Gauyacq, Photolysis of methane revisited at 121.6 nm and at 118.2 nm: quantum yields of the primary products, measured by mass spectrometry, *Phys. Chem. Chem. Phys.* **13**, 8140-52 (2011).
6. F. Kelkensberg, A. Rouzée, W. Siu, G. Gademann, P. Johnsson, M. Lucchini, R. R. Lucchese, M. J. J. Vrakking, XUV ionization of aligned molecules, *Phys. Rev. A* **84**, 051404(R):1-4 (2011).
7. Cheng Jin, Julien B. Bertrand, R. R. Lucchese, H. J. Wörner, Paul B. Corkum, D. M. Villeneuve, Anh-Thu Le, and C. D. Lin, Intensity dependence of multiple orbital contributions and shape resonance in high-order harmonic generation of aligned N_2 molecules, *Phys. Rev. A* **85**, 013405:1-7 (2012).
8. Hong Xu, U. Jacovella, B. Ruscic, and S. T. Pratt, and R. R. Lucchese, Near-Threshold Shape Resonance In The Photoionization Of 2-Butyne, *J. Chem. Phys.* **136**, 154303:1-10 (2012).
9. Arnaud Rouzée, Freek Kelkensberg, Wing Kiu Siu, Georg Gademann, R. Lucchese, Marc J. J. Vrakking, Photoelectron kinetic and angular distributions for the ionization of aligned molecules using a HHG source, *J. Phys. B* **45**, 074016:1-11 (2012)
10. C. Wang, M. Okunishi, R. R. Lucchese, T. Morishita, O. I. Tolstikhin, L. B. Madsen, K. Shimada, D. Ding, K. Ueda, Extraction of Electron-Ion Differential Scattering Cross Sections for C_2H_4 by Laser-Induced Rescattering Photoelectron Spectroscopy, *J. Phys. B* **45**, 131001:1-5 (2012).
11. J. A. Lopez-Dominguez, D. Hardy, A. Das, E. D. Poliakoff, A. Aguilar, and R. R. Lucchese, Mechanisms of Franck-Condon breakdown over a broad energy range in the valence photoionization of N_2 and CO, *J. Electron Spectrosc. Relat. Phenom.* **185**, 211 (2012).
12. C. D. Lin, Cheng Jin, Anh-Thu Le, and R. R. Lucchese, Probing molecular frame photoelectron angular distributions via high-order harmonic generation from aligned molecules, *J. Phys. B* **45**, 194010:1-9 (2012).
13. R. R. Lucchese, H. Fukuzawa, X.-J. Liu, T. Teranishi, N. Saito, and K. Ueda, Asymmetry in the molecular-frame photoelectron angular distribution for oxygen 1*s* photoemission from CO_2, *J. Phys. B* **45**, 194014:1-11 (2012).
14. Anh-Thu Le, T. Morishita, R. R. Lucchese, and C. D. Lin, Theory of high harmonic generation for probing time-resolved large-amplitude molecular vibrations with ultrashort intense lasers, *Phys. Rev. Lett.* **109**, 203004:1-5 (2012).
15. M. C. H. Wong, A.-T. Le, A. F. Alharbi, A. E. Boguslavskiy, R. R. Lucchese, J.-P. Brichta, C.D.Lin, and V.R.Bhardwaj, High Harmonic Spectroscopy of the Cooper Minimum in Molecules, *Phys. Rev. Lett.* **110**, 033006:1-5 (2013).
16. Anh-Thu Le, R. R. Lucchese, and C. D. Lin, Quantitative rescattering theory of high-order harmonic generation for polyatomic molecules, *Phys. Rev. A* **87**, 063406:1-9 (2013).
17. Ralph Carey, Robert R. Lucchese, and F. A. Gianturco, Electron scattering from gas phase cis-diamminedichloroplatinum(II): quantum analysis, *J. Chem. Phys.* **138**, 204308:1-10 (2013).
18. S. Marggi Poullain, K. Veyrinas, P. Billaud, M. Lebech, Y. J. Picard, R. R. Lucchese and D. Dowek, The role of Rydberg states in Photoionization of NO_2 and (NO^+, O^-) Ion Pair Formation induced by One VUV Photon, *J. Chem. Phys.* **139**, 044311:1-12 (2013).

Program Title:

"Properties of actinide ions from measurements of Rydberg ion fine structure"

Principal Investigator:

Stephen R. Lundeen
Dept. of Physics
Colorado State University
Ft. Collins, CO 80523-1875
lundeen@lamar.colostate.edu

Program Scope:

This project determines certain properties of chemically significant Uranium and Thorium ions through measurements of fine structure patterns in high-L Rydberg ions consisting of a single weakly bound electron attached to the actinide ion of interest. The measured properties, such as polarizabilities and permanent moments, control the long-range interactions of the ion with the Rydberg electron or other ligands. The ions selected for initial study in this project, U^{6+},U^{5+}, Th^{4+}, and Th^{3+}, all play significant roles in actinide chemistry, and are all sufficiently complex that *a-priori* calculations of their properties are suspect until tested. The measurements planned under this project serve the dual purpose of 1) providing data that may be directly useful to actinide chemists and 2) providing benchmark tests of relativistic atomic structure calculations. In addition to the work with U and Th ions, which takes place at the J.R. Macdonald Laboratory at Kansas State University, a parallel program of studies with stable singly-charged ions takes place at Colorado State University. These studies are aimed at clarifying theoretical questions connecting the Rydberg fine structure patterns to the properties of the free ion cores, thus directly supporting the actinide ion studies. In addition, they provide training for students who can later participate directly in the actinide work.

Recent Progress:

Over the past year, we have completed and published the study of two of the most complex ions ever studied with our Rydberg spectroscopy technique, Ni^{+} and Th^{3+}. Both ions have J_c=5/2 in their ground state, leading to a high-L Rydberg structure consisting of six eigenstates for each value of L. The Th^{3+} ion, Fr-like Thorium, was one of the key targets of our project. The Ni^{+} ion was selected for study because the similar complexity of its Rydberg states offered an opportunity to test and develop the necessary theoretical framework for interpreting the spectroscopy. Both studies are now complete, and the numerous ion property measurements derived from them are reported in publications [9] and [10] listed below. A separate paper deriving the theoretical framework used for both studies has also been published, and is represented by publication [7] listed below. With the previous completion of our studies of the Rn-like Th ion, Th^{4+}, represented in publication [8] below, we have successfully achieved more than half of the initial goals of this project.

What remains are the so far unsuccessful studies of the two Uranium ions, Rn-like U^{6+} and Fr-like U^{5+}. Both have proved to be much more difficult than expected. The difficulty is partially that the resolved RESIS signals, from which we extract information about the core ions, appear to be much smaller than expected. In the case of U^{6+},

extensive effort showed only that any resolved signals were at least a factor of five smaller than expected. The other source of difficulty is the presence of a large background signal which greatly reduces the signal to noise ratio, and makes observing small signals very time-consuming. One hypothesis that could explain both difficulties is the presence of a significant fraction of metastable excited levels in the Uranium ion beams extracted from the ECR source. These would reduce the size of resolved RESIS signals, since only Rydberg electrons bound to ground state ions would contribute to them. They could also contribute to background by auto-ionizing within our Stark ionization detector.

We have recently made some dramatic progress in combating the problem of the large background levels. Relying on the hypothesis that the background source is metastable Rydberg levels stable enough to survive to the detector, but undergoing Stark-induced auto-ionization within the detector, thus mimicking our signal, we redesigned our detector to minimize the time in the Stark ionization region. We also incorporated a region of weaker electric field intended to pre-ionize metastable Rydberg ions before they can contribute to the background. Both devices were fully successful, reducing the background to the lower levels that were usual in the successful Thorium experiments. We are still hoping to reduce the background further with an additional pre-ionization device now being constructed.

With these improvements in background levels, we have some indication of resolved RESIS structure in Rydberg ions bound to Fr-like U^{5+}, giving us optimism that that study can proceed successfully. The size of the signals observed to date suggests that the total metastable content in the U^{5+} beams is substantially less than in the U^{6+} beams.

Immediate Future Plans

Depending on the success of continuing efforts to reduce background levels, and parallel efforts to modify the metastable content of the ion beams extracted from the ECR, we remain hopeful that both Uranium ions can eventually be successfully studied with our technique.

Recent Publications:

1) "Optical spectroscopy of high-L Rydberg states of nickel", Julie A. Keele, Shannon L. Woods, M.E. Hanni, S.R. Lundeen, and W.G. Sturrus, Phys. Rev. A 81, 022506 (2010)

2) "Polarizabilities of Pb^{2+} and Pb^{4+} and Ionization Energies of Pb^{+} and Pb^{3+} from spectroscopy of high-*L* Rydberg states of Pb^{+} and Pb^{3+}. M.E. Hanni, Julie A. Keele, S. R. Lundeen, C.W. Fehrenbach, and W.G. Sturrus, Phys. Rev. A 81, 042512 (2010)

3) "Dipole transition strengths in Ba^{+} from Rydberg fine structure measurements in Ba and Ba^{+}, Shannon L. Woods, M.E. Hanni, S.R. Lundeen, and Erica L. Snow, Phys. Rev. A 82, 012506 (2010)

4) "Polarizabilities of Rn-like Th^{4+} from spectroscopy of high-L Rydberg levels of Th^{3+}", M.E. Hanni, Julie A. Keele, S.R. Lundeen, and C.W. Fehrenbach, Phys. Rev. A 82, 022512 (2010)

5) "Properties of Fr-like Th^{3+} from spectroscopy of high-L Rydberg levels of Th^{2+}", Julie. A. Keele, M.E. Hanni, Shannon L. Woods, S.R. Lundeen , and C.W.

Theory of Atomic Collisions and Dynamics

J. H. Macek

Department of Physics and Astronomy,
University of Tennessee, Knoxville, Tennessee and
Oak Ridge National Laboratory, Oak Ridge, Tennessee
email:jmacek@utk.edu

1 Program scope

One can characterize atomic dynamics by the exchange of physical quantities such as energy, momentum, and angular momentum between various constituents of atoms, molecules and ions. Our recent projects have concentrated on the exchange of angular momentum. Such exchanges leads to vortices in the velocity fields of atomic wave functions.

Vortices in the velocity field of atomic wave functions cannot be viewed experimentally, but, associated with each vortex there is an isolated zero in the wave function which can be observed. The imaging theorem shows that such zeros appear as zeros in the electron momentum distribution $P(\boldsymbol{k})$, where k is proportional to the ejected electron momentum. These zeros are difficult to observe, but our collaboration with the Frankfurt COLTRIMS group has successfully seen zero's in electron distributions produced by ion-atom collisions. Our computer simulations of the processes observed, verify that the zero's in the electron momentum distribution correspond to vortices in the velocity field of the atomic wave functions of the final state electrons.

The projects listed in this abstract are sponsored by the Department of Energy, Division of Chemical Sciences, through a grant to the University of Tennessee. The research is is carried out in cooperation with Oak Ridge National Laboratory under the ORNL-UT Distinguished Scientist program.

2 Recent progress

2.1 Ion-atom collisions: Our Previous work with the Regularized Lattice-Time-Dependent-Schrödinger equation (RLTDSE) method has shown that time dependent wave functions $\psi(\boldsymbol{r}, t)$ have zeros at isolated points in coordinate space where the real and imaginary parts of the wave function vanish.

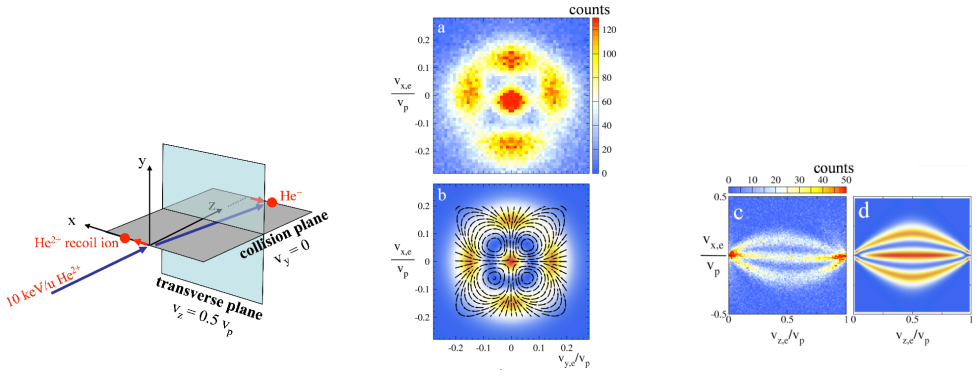

Figure 1: Coordinate system and contour plots of electron counts measured for the process $He^{++}+He \rightarrow He^{+}+e^{-}+He^{+}+$. Figs. (a) and (b) are counts registered for electrons ejected in the transverse plane, while Figs. (c) and (d) are counts registered for electrons ejected the y-z plane passing through the incident velocity

Using vortex theory, we have shown that if atomic wave functions have non-zero mean angular momentum $< \boldsymbol{J} >$, where the average is taken over a small region of coordinate space, then the velocity fields show vortices. The vortex structures are observable as zeros of electron momentum distributions $P(\boldsymbol{k})$ since such distributions image *coordinate* space wave functions according to the imaging theorem [2].

It may be possible to observe the vortices predicted by our time-dependent RLTDSE calculations [4]. It turns out that the COLTRIMS technique is sufficiently sensitive that the zeros in the transfer ionization electron distributions in collisions of alpha particles with He may be observed. Our experimental colleagues have recently made electron momentum distributions of extremely high quality as shown in Fig. 1.

Transverse slices of the electron momentum distributions are shown in Fig.1a The high resolution of the measurements make it possible to identify four regions surrounding a central on-axis maxima where the electron counts are nearly zero. Our computer simulation of the distribution is shown in Fig. 1b, and it reproduces the four minima surrounding a central maxima. In the computations the four minima are exact zeros. Arrows are drawn to show the direction of the velocity field $\boldsymbol{v}(\boldsymbol{r}) = -i\boldsymbol{\nabla} \ln \psi(\boldsymbol{r})$. Further considerations of the theoretical distribution show that the vortex lines pass through each

of the zeros. These vortex lines are approximately parallel to the internuclear axis in the final state. Figures 1c and 1d show the distribution in the collision plane and the two minima seen in the banana-shaped distribution approximately parallel the vortex lines. In effect, the vortex lines line in the two nodal planes of the $d_{x^2-y^2}$ diatomic molecular state and are parallel to the internuclear axis.

2.2 Electron-atom collisions: Unexplained minima for *electron* impact ionization of He have been identified as zeros associated with vortex structure in (e,2e) wave functions. This is the only observation to date that clearly shows vortex structure, therefore we investigate zeros in electron-impact-ionization amplitudes.

For ionization of K-shells of atoms, we have shown that the effective photons are actually elliptically polarized indicating that some vector angular momentum is transferred to the ejected electron. The Coulomb Born approximation is used to compute the effective elliptical polarization β for electron impact ionization of carbon K-shells . For the ejection of 7 eV electrons from the carbon K-shell by 1801 eV electrons $\beta = 0.25$ is found for a scattered electron angle of 6^o. Since β is non-zero, the electron spectra must have a vortex in the region near $k = 0$.

3 Publications in the 2011-2013 period.

1. Ionization in simple quasimolecules:$HeH_2{}^2+$ ($He^2+ + H_2$), G. N. Ogurtsov, S. Yu. Ovchinnikov, J. H. Macek, and V. M. Mikoushkin, J. Phys. B: At. Mol. Opt. Phys. 46 (2013) 175203.

2. Peripheral collisions of fast electrons with highly charged ions, J. H. Macek, Contributed Talk, CAARI 2012 Conference Proceedings . Accepted for publication, AIP conference proceedings (2012).

3. Vortices in Atomic Processes, Joseph H. Macek, in Dynamical Processes in Atomic and Molecular Physics, ed. by Gennadi Ogurtsov and Danielle Dowek, Bentham ebooks, 2012 pp 3-28.

4. Ionization processes in small quasimolecules: $He_2^{2+}(He^{2+} + He)$ G. N. Ogurtsov, S. Yu. Ovchinnikov, J. H. Macek, and V. M. Mikoushkin Phys. Rev. A **84**, 032706 (2011).

5. Theoretical demonstration of the feasibility of observing vortices in the ejected-electron spectrum in two-electron-atom collisions, S. Y. Ovchinnikov, J. H. Macek, L.. Ph. H. Schmidt, *et. al.*, Phys. Rev. A, **83**, 060701 (2011).

Photoabsorption by Free and Confined Atoms and Ions

Steven T. Manson, Principal Investigator
Department of Physics and Astronomy, Georgia State University, Atlanta, Georgia 30303
(smanson@gsu.edu)

Program Scope

The goals of this research program are: to provide a theoretical adjunct to, and collaboration with, the various atomic and molecular experimental programs that employ latest generation light sources, particularly ALS, APS and LCLS; to generally enhance our understanding of the photoabsorption process; and to study the properties (especially photoabsorption) of confined atoms and ions. To these ends, calculations are performed employing and enhancing cutting-edge methodologies to provide deeper insight into the physics of the experimental results; to provide guidance for future experimental investigations; and seek out new phenomenology, especially in the realm of confined systems. The main areas of programmatic focus are: manifestations of nondipole effects in photoionization; photodetachment of inner and outer shells of atoms and atomic ions (positive and negative); studies of atoms endrohedrally confined in buckyballs, C_{60}, particularly dynamical properties. Flexibility is maintained to respond to opportunities.

Highlights of Recent Progress

1. Confined Atoms

The study of confined atoms is still new. There are a number of theoretical investigations of various atoms endohedrally confined in C_{60} [1,2] , but experimental studies are sparse [3-6]. Thus, we are conducting a program of calculations at various levels of approximation, aimed at delineating the properties of such systems, especially photoionization, to guide the experimental community. Among our recent results, we have found that a huge transfer of oscillator strength from the C_{60} shell, in the neighborhood of the giant plasmon resonance, to the encapsulated atom for both $Ar@C_{60}$ [7] and $Mg@C_{60}$ [8]. In addition, confinement resonances [9], oscillations that occur in the photoionization cross section of an endohedral atom owing to the interferences of the photoelectron wave function for direct emission with those scattered from the surrounding carbon shell have been predicted in a broad range of cases; recently, the existence of confinement resonances has been confirmed experimentally [5,6]. In addition, the photoionization of endohedral atoms within nested fullerenes, called buckyonions, has shown that, as a result of the multi-walled confining structures, the confinement resonances become considerably more complicated [10].

Considering a Xe atom endohedrally confined in C_{60} the formation of a new type of atom-fullerene hybrid state was discovered [11]. These dimer-type states arise from the near-degeneracy of inner levels of the confined atom and the confining shell, in contrast to the known overlap-induced hybrid states around the Fermi level of smaller compounds, and are found to occur in confined noble gas, alkali-earth atoms [12] and the Zn series [13]. The photoionization cross sections of these hybrid states exhibit rich structures and are radically different from the cross sections of free atomic or fullerene states. This also occurs in buckyonions, nested fullerenes. A study of $C_{60}@C_{240}$ reveals strong hybridization between the plasmon excitations of the individual fullerenes leading

to a photoionization cross section of the nested system being dramatically different from the sum of the individual constituents [14]. This result suggests the possibility of creating buckyonions with plasmons of specified character, i.e., *designer resonances*.

We have also extended the Belfast R-matrix codes (both LS and Breit-Pauli versions) to include an external attractive spherical annular well to simulate the effect(s) of a fullerence cage encapsulating an atomic system. This methodology has been employed to look at trapped Ca [15] and Xe [6, 16]. In the latter case, the results show excellent agreement of the structure of the confinement resonances with recent experiment [5, 6]. We are presently exploring confined Mg [17], within the R-matrix framework, to begin to understand how the doubly-excited resonances, ubiquitous in the photoionization spectrum of Mg, react to confinement. To ameliorate this difficulty we are developing

2. Atomic/Ionic Photoionization

The study of photoionization of atoms/ions at high resolution leads to results of great complexity. Our effort is to perform state-of-the-art calculations, in concert with high-resolution synchrotron experiments, to understand this complexity. Using our upgraded relativistic Breit-Pauli R-matrix methodology we have performed studies of inner-shell photoionization of atomic Cl and the results are presented along with new experimental cross sections [18]. The spectrum exhibits enormous complexity in the vicinity of the 2p thresholds and reasonable agreement between experiment and theory. Of importance in this project is that we were able to separate dynamics from (angular momentum) geometry and arrive at a general rule for the widths of the resonances which is satisfied by both theory and experiment. Such general rules are very likely operative in most other cases of inner shell ionization of open-shell atoms.

We have also found significant structure in subshell photoionization cross sections many keV above their thresholds induced by interchannel coupling with inner-shell ionization channels, in the vicinity of the inner-shell thresholds [19]. This structure is nonresonant and about 50 eV wide. Using a relativistic random phase approximation calculation, we were able to explain the structure seen in Ag both qualitatively and quantitatively. We believe that this kind of structure should be a general phenomenon in photoionization throughout the Periodic Table.

The photoionization of Ba 5s in the vicinity of the high-energy Cooper minimum, induced by interchannel coupling, has been studied [20]. Our relativistic random-phase-aprpoximation with relaxation (RRPA-R) gives quite good agreement with recent cross section measurements [21]. In addition, the deviation of the photoelectron angular distribution parameter, β, from 2, which is an explicitly relativistic effect [22], is reproduced qualitatively, but only semi-quantitatively, by the calculation. What is missing is evidently coupling with the ionization plus excitation channels from the 4d subshell; two-electron excitations are explicitly excluded from RPA.

Future Plans

Our future plans are to continue on the paths set out above. In the area of confined atoms, we will look at the possibilities of interatomic Coulomb decay (ICD) of resonances. We will also work on ways to enhance the time-dependent local-density approximation to make it more accurate in our calculations of confined atoms. In

addition, we shall work towards upgrading our theory to include relativistic interactions to be able to deal with heavy endohedrals with quantitative accuracy. We will also look at the attosecond time delay in photoionization that has been found in various experiments, and we shall try to get some idea of how confinement might affect this time delay. Developmental work on enhancing our relativistic muticonfiguration Tamm-Damcoff (MCTD) theory shall continue with an eye towards dealing more accurately with situations like Ba 5s (discussed above). In addition, the search for cases where nondipole effects are likely to be significant, as a guide for experiment, and quadrupole Cooper minima, will continue. And we shall respond to new experimental results that are in need of interpretation as they come up.

Publications Citing DOE Support Since 2012

● "Interference in Molecular Photoionization and Young's Double-Slit Experiment," A. S. Baltenkov, U. Becker, S. T. Manson, and A. Z. Msezane, J. Phys. B **45**, 035202-1-12 (2012).

● "A Mathematical Model of Negative Molecular Ions," A. S. Baltenkov, S. T. Manson, and A. Z. Msezane, *Proceedings of Dynamic Systems and Applications 6* (Dynamic Publishers, Atlanta, Georgia, 2012), pp. 53-57.

● "Valence photoionization of small alkaline earth atoms endohedrally confined in C_{60}," M. H. Javani, M. R. McCreary, A. B. Patel, M. E. Madjet, H. S. Chakraborty and S. T. Manson, Eur. Phys. J. D **66**, 189-1-7 (2012).

● "Radiation Damping in the Photoionization of Fe^{14+}," M. F. Hasoglu, T. W. Gorczyca, M. A. Bautista, Z. Felfli, and S. T. Manson, Phys. Rev. A **85**, 040701(R)-1-4 (2012).

● "Photoionization of atomic krypton confined in the fullerene C_{60}," J. George, H. R. Varma, P. C. Deshmukh and S. T. Manson, J. Phys. B **45**, 185001-1-6 (2012).

● "Photoionization of ground and excited states of Ca^+ and comparison along the isoelectronic sequence," A. M. Sossah, H.-L. Zhou, S. T. Manson, Phys. Rev. A **86,** 023403-1-10 (2012).

● "Photoionization of Endohedral Atoms Using R-matrix Methods: Application to $Xe@C_{60}$, T. W. Gorczyca, M. F. Hasoğlu, and S. T. Manson, Phys. Rev. A **86**, 033204-1-9 (2012).

● "Atom-fullerene hybrid photoionization mediated by coupled *d*-states in $Zn@C_{60}$," Jaykob N. Maser, Mohammad H. Javani, Ruma De, Mohamed E. Madjet, Himadri S. Chakraborty, and Steven T. Manson, Phys. Rev. A **86**, 053201-1-5 (2012).

● "Photoionization of Confined Ca in a Spherical Potential Well," M. F. Hasoğlu, H.-L. Zhou, T. W. Gorczyca, and S. T. Manson, Phys. Rev. A **87**, 013409-1-5 (2013).

● "Core Correlation Effects in the Valence Photodetachment of Cu^-," J. Jose, H. R. Varma, P. C. Deshmukh, S. T. Manson, and V. Radojević, *Proceedings of the 26th Summer School and International Symposium on the Physics of Ionized Gases (SPIG 2012), 27th-31st August 2012, Zrenjanin, Serbia, Book of Contributed Papers & Abstracts of Invited Lectures and Progress Reports*, editors:, M. Kuraica and Z. Mijatović (University of Novi Sad, Novi Sad, Serbia, 2012), pp. 39-42.

● "Photoionization of Endohedrally Confined Ca ($Ca@C_{60}$)," M. F. Hasoglu, P. Prabha, M. H. Javani, H. L. Zhou, and S. T. Manson, J. Phys. Conf. Ser. **388**, 022026 (2012).

● "Dipole and Quadrupole Photoionization of Intermediate Subshells of Atomic Mercury," T. Banerjee, Hari R. Varma, P. C. Deshmukh, and S. T. Manson, J. Phys. Conf. Ser. **388**, 022076 (2012).

● "Dipole and quadrupole photodetachment/photoionization studies of the Ar isoelectronic sequence," J. Jose, G. B. Pradhan, V. Radojević, S. T. Manson and P. C. Deshmukh, J. Phys. Conf. Ser. **388**, 022098 (2012).

● "Effect of Interchannel Coupling and Confinement on the Photoionization of Kr," J. George, Hari R. Varma, P. C. Deshmukh and S. T. Manson, J. Phys. Conf. Ser. **388**, 022009 (2012).

● "Pronounced Effects of Interchannel Coupling In High-Energy Photoionization," W. Drube, T.M. Grehk, S. Thiess, G. B. Pradhan, H. R. Varma, P. C. Deshmukh and S. T. Manson, Phys. Rev. A (submitted).

● "A New Explanation for the Differences in Double Ionization by Particle and Antiparticle Impact," Phys. Rev. Letters (submitted).
● "Innershell Photoionization of Atomic Chlorine," W. C. Stolte, Z. Felfli, R. Guillemin, G. Ohrwall, S.–W. Yu, J. A. Young, D. W. Lindle, T. W. Gorczyca, N. C. Deb, S. T. Manson, A. Hibbert, and A. Z. Msezane, Phys. Rev. A (submitted).
● "Photoionization of the 5s subshell of Ba in the region of the second Cooper minimum: cross sections and angular distributions," A. Ganesan, S. Deshmukh, G. B. Pradhan, V. Radojevic, S. T. Manson and P. C. Deshmukh, J. Phys. B (in press).
● "Photoionization of Xe inside a C_{60}^{+} cage: a single-molecule electron interferometer," R. A. Phaneuf, A. L. D. Kilcoyne, N. B. Aryal, K. K. Baral, D. A. Esteves-Macaluso, C. M. Thomas, J. Hellhund, R. Lomsadze, T. W. Gorczyca, C. P. Ballance, S. T. Manson, M. F. Hasoglu, S. Schippers, and A. Müller, Nat. Phys. (submitted).
● "A Comprehensive X-ray Absorption Model for Atomic Oxygen," by T. W. Gorczyca, M. Bautista, C. Vries, M. Hasoglu, J. Garcia, E. Gatuzz, J. Kaastra, T. Kallman, S. Manson, C. Mendoza, and T. Raassen, Astrophys. J. (submitted).
● "Photoionization study of Xe 5s: Ionization Cross Sections and Photoelectron Angular Distributions,"A. Ganesan, J. Jose, S. Deshmukh, V. Radojevic, P .C. Deshmukh and S. T. Manson, J. Phys. B (submitted).

References

[1] V. K. Dolmatov, A. S. Baltenkov, J.-P. Connerade and S. T. Manson, Radiation Phys. Chem. **70**, 417 (2004) and references therein.
[2] V. K. Dolmatov, Advances in Quantum Chemistry, **58**, 13 (2009) and references therein.
[3] A. Müller *et al*, Phys. Rev. Lett. **101**, 133001 (2008).
[4] R. Phaneuf *et al*, Bull. Am. Phys. Soc. **55**(5), 40 (2010) and private communication.
[5] A. L. D. Kilcoyne, A. Aguilar, A. Müller, S. Schippers, C. Cisneros, G. Alna'Washi, N. B. Aryal, K. K. Baral, D. A. Esteves, C. M. Thomas, and R. A. Phaneuf, Phys. Rev. Lett. **105**, 213001 (2010).
[6] R. A. Phaneuf, A. L. D. Kilcoyne, N. B. Aryal, K. K. Baral, D. A. Esteves-Macaluso, C. M. Thomas, J. Hellhund, R. Lomsadze, T. W. Gorczyca, C. P. Ballance, S. T. Manson, M. F. Hasoglu, S. Schippers, and A. Müller, Nat. Phys. (submitted).
[7] M. E. Madjet, H. S. Chakraborty and S. T. Manson, Phys. Rev. Letters **99**, 243003 (2007).
[8] M. E. Madjet, H. S. Chakraborty, J. M. Rost and S. T. Manson, Phys. Rev. A **78**, 013201 (2008).
[8] V. K. Dolmatov and S. T. Manson, J. Phys. B **41**, 165001 (2008).
[10] V. K. Dolmatov and S. T. Manson, J. Phys. Rev. A **78**, 013415 (2008).
[11] H. S. Chakraborty, M. E. Madjet, T. Renger, J.-M. Rost and S. T. Manson, Phys. Rev. A **79**, 061201(R) (2009).
[12] M. H. Javani, M. R. McCreary, A. B. Patel, M. E. Madjet, H. S. Chakraborty and S. T. Manson, Eur. Phys. J. D **66**, 189 (2012).
[13] J. N. Maser, M. H. Javani, R. De, M. E. Madjet, H. S. Chakraborty, and S. T. Manson, Phys. Rev. A **86**, 053201 (2012).
[14] M. A. McCune, R. De, M. E. Madjet, H. S. Chakraborty, and S.T. Manson, J. Phys. B **44**, 241002 (2011).
[15] M. F. Hasoğlu, H.-L. Zhou, T. W. Gorczyca, and S. T. Manson, Phys. Rev. A **87**, 013409 (2013).
[16] T. W. Gorczyca, M. F. Hasoğlu, and S. T. Manson, Phys. Rev. A **86**, 033204 (2012).
[17] P. Padukka, H.-L. Zhou and S. T. Manson, Bull. Am. Phys. Soc. **58** (6) 168 (2013).
[18] W. C. Stolte, Z. Felfli, R. Guillemin, G. Ohrwall, S.–W. Yu, J. A. Young, D. W. Lindle, T. W. Gorczyca, N. C. Deb, S. T. Manson, A. Hibbert, and A. Z. Msezane, Phys. Rev. A (submitted).
[19] W. Drube, T.M. Grehk, S. Thiess, G. B. Pradhan, H. R. Varma, P. C. Deshmukh and S. T. Manson, Phys. Rev. A (submitted).
[20] A. Ganesan, S. Deshmukh, G. B. Pradhan, V. Radojevic, S. T. Manson and P. C. Deshmukh, J. Phys. B (in press).
[21] S. B. Whitfield, R. Wehlitz and V..K. Dolmatov, J. Phys. B **44**, 165002 (2011).
[22] S. T. Manson and A. F Starace, Rev. Mod. Phys. **54**, 389 (1982).

Combining High Level *Ab Initio* Calculations with Laser Control of Molecular Dynamics

Thomas Weinacht
Department of Physics and Astronomy
Stony Brook University
Stony Brook, NY
thomas.weinacht@stonybrook.edu

and

Spiridoula Matsika
Department of Chemistry
Temple University
Philadelphia, PA
smatsika@temple.edu

1 Program Scope

This program aims to develop our understanding of the ultrafast relaxation of small polyatomic molecules of chemical and biological interest as well as the interaction of these systems with strong laser fields.

2 Recent Progress

Our accomplishments in the past three years of DOE support are detailed in the 12 papers which we have written.[1–12] Ten of these have been published, and two are currently under review. Our principal findings/accomplishments are:

- *Development of time resolved strong field dissociative ionization spectroscopy for probing and interpreting excited state molecular dynamics*
- *Studying neutral to ionic state correlations in strong field molecular ionization*
- *Observing strong field molecular ionization from multiple orbitals*

Our main results from the past year have focused on understanding better strong field ionization (SFI) and combining electronic structure calculations, strong field ionization calculations and dissociative ionization pump probe measurements to unveil a detailed picture of excited state relaxation in uracil.

2.1 Uracil Relaxation Dynamics

We use a strong field ionization based pump probe approach, which coupled with *ab initio* electronic structure calculations and strong field ionization calculations can yield detailed insight into the relaxation dynamics of molecules after excited with a UV pulse. Our approach makes use of an ultrafast laser pulse in the deep UV (at 260 nm) to pump the molecules to the first bright excited state (S_2). The pump pulse is followed by a time delayed intense near infrared probe pulse, which ionizes the molecules to multiple states of the molecular cation, producing many fragments in a time of flight mass spectrometer. The electronic structure and strong field ionization calculations allow us to associate different molecular fragment ions with different relaxation pathways. We have used this approach on several molecules in the past, and most recently we were able to study the relaxation dynamics in uracil yielding a detailed picture of the relaxation dynamics which was not available before. In this work we used this approach to get insight into the excited state dynamics, paying particular attention to the extent to which population remains on the S_2 surface.[11] Figure 1 summarizes our findings.

The basic picture which emerges from our calculations and measurements is that the wavepacket initially launched on S_2 after UV excitation branches, with a portion spending a few ps trapped near the minimum on S_2 and another portion moving fast through the S_2/S_1 Conical Intersection(CI). This second portion further branches after passing through the CI and part of it is trapped near the minimum on S_1 while another part can reach the S_1/S_0 CI and decay to the ground state. If the

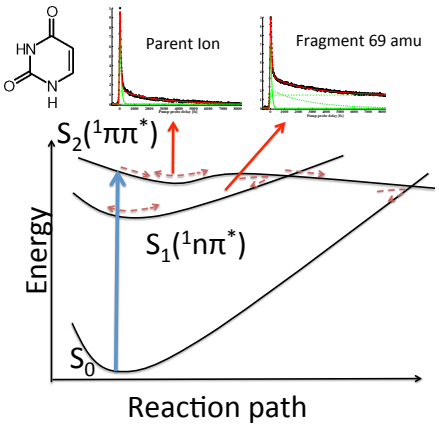

Figure 1: Cartoon showing the excited state dynamics in uracil after UV absorption and our approach to measuring these dynamics.

evolution on S_2 and S_1 proceeded purely sequentially, then we would observe a rise in the 69 signal mirroring the decay of the parent ion. However, both signals rise near time zero with a very small delay between their maxima (less than 50 fs). Our results for the first time give an experimental observable that can be directly related to the S_2 population, allowing us to experimentally verify the existence of a barrier on the S_2 surface. Population trapped on S_1 can spend a long time there - much more than 10 ps, based on our measurements. This is consistent with other measurements of ns lifetimes for the S_1 state. The fact that the parent and 69 signals also have a fast decay component is also consistent with a portion of the wavepacket going rapidly to S_0, yielding a picture of multiple bifurcations in the relaxation dynamics.

2.2 Understanding neutral to ionic state correlations in strong field molecular ionization

Our pump probe measurements described above rely on SFI in order to probe the dynamics on the neutral excited state. The ionization of these excited state molecules is interesting both as a probe of the neutral excited state dynamics and as a fundamental issue in strong field ionization - in particular as a probe of correlations between initial and final states in SFI. In collaboration with Michael Spanner and Sergeui Patchovskii at the National Research Council of Canada, who have carried out detailed calculations of strong field ionization for the molecules we are working on, we have studied the role of Dyson orbitals in strong field molecular ionization. The calculations suggest that the Dyson orbital description, which is central to the strong field approximation, is violated substantially.[8;9] Our experimental measurements are in qualitative agreement with the Spanner-Patchkovskii calculations.[9]

2.3 Strong Field Ionization: More than the orbital matters

Angle-dependent strong field ionization yields can give additional information about the ionization step, and the symmetry of the orbitals ionized. We compared the time and angle-dependent strong field ionization yields of three molecules with very similar electronic structure.[10] A pump pulse in the deep ultraviolet excites 1,3-cyclohexadiene, α-terpinene, and α-phellandrene to their first excited state. The latter two molecules are alkyl-substituted 1,3- cyclohexadiene systems (see Figure 2). We then measure the SFI yield due to a near infrared probe pulse as a function of delay and angle between pump and probe polarization vectors. *ab initio* electronic structure calculations allow us to associate the parent ion yields with removal of an electron from a LUMO orbital (occupied after excitation by the pump). Despite the fact that the LUMO orbitals for these molecules are very similar, the angle-dependent yields are very different (see Figure 3), indicating that it is not the orbital shape alone which determines angle-dependent ionization yields.

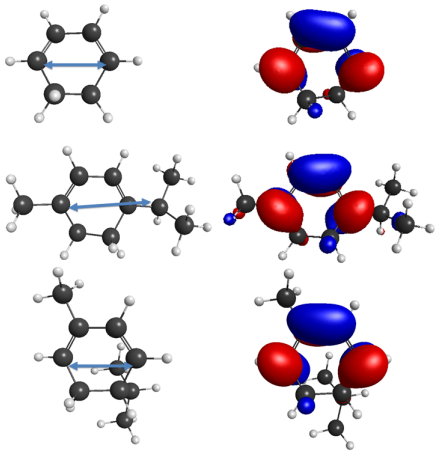

Figure 2: Ground state equilibrium structure and transition dipole moment (column 1) along with the LUMO orbital (column 2) for CHD (top row) α-terpinene (middle row) and α-phellandrene (bottom row).

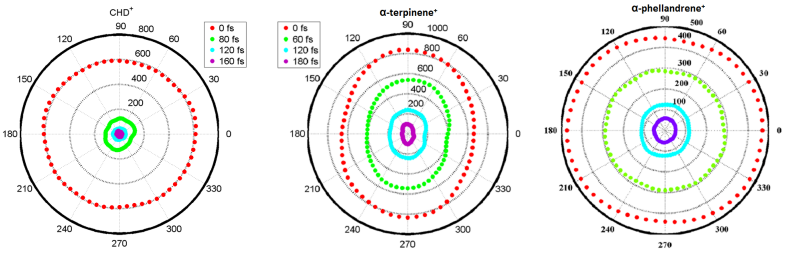

Figure 3: Angle dependent yields for CHD (left panel), α-terpinene (middle panel) and α-phellandrene (right panel). The radius is proportional to ion yield. The polar angle is the angle between pump and probe polarization vectors. CHD and phellandrene show no angular dependence, while α-terpinene shows an enhancement in the ionization yield when the pump and probe are orthogonal to each other.

3 Future Plans

We have several goals for the immediate future:

1. *Correlation between initial and final states in strong field ionization.* Recent work has demonstrated that the role of orbital symmetry in SFI might be qualitatively different for larger polyatomic molecules than has been observed for diatomic systems. We would like to probe and understand this. Also, Dyson orbital norms, which provide an accurate multielectron prediction of which cationic states are produced via single photon ionization from a given neutral state, do not serve as a good predictor of final state yields for SFI. Recent calculations suggest that there are multiple reasons for this. We would like to explore these findings and the underlying reasons both experimentally and theoretically. Finally, we have found that ionization from excited states where an electron is excited from a π to a π^* orbital ($\pi\pi^*$ states) is enhanced by a factor of 5-10 over excited states where lone pair n electrons are excited ($n\pi^*$ states) in two molecules, cytosine and uracil. We would like to understand if this is a general phenomenon and also whether it teaches us about electron correlation in SFI. We are planning to carry out systematic studies on a series of molecules of different sizes in different states in order to explore the effect of molecular size and state character on SFI.

2. *Ultrafast relaxation in molecular cations.* We are interested in how ultrafast relaxation of excited state molecular cations competes with direct dissociation. In molecular SFI several

excited ionic states are typically created, and it is not clear whether the fragments are produced directly in the excited ionic states or fast relaxation to the ground ionic state occurs first and fragmentation follows - i.e. does fragmentation of an excited molecular cation with energy above the dissociation barrier take place on the excited or ground state of the cation? Theoretically, we will employ a combination of trajectory surface hopping molecular dynamics calculations combined with high level electronic structure in order to track the evolution of excited molecular cations. Experimentally, we will use photoelectron and photoion coincidence velocity map imaging in order to determine whether relaxation precedes dissociation. Measurements of the photoelectron energy resulting from ionization can be used to label the initial electronic state of the cation immediately after ionization. Measuring the kinetic energy release of the fragment ions will allow us to determine how much energy went into kinetic energy during the dissociation process.

3. *Pulse shape correlation spectroscopy.* We would like to examine whether control can be used to further enhance our understanding of excited state dynamics. We will use pulse shape correlation spectroscopy to distinguish between different inter- and intra-molecular relaxation pathways in DNA and RNA bases excited by shaped ultrafast laser pulses in the deep UV. Preliminary measurements on cytosine indicate that there are interesting correlation patterns amongst different fragments in the time of flight mass spectrum as the shape of the pump pulse is varied and strong field ionization is used to probe the relaxation dynamics. We will compare measurements of the fragment ion yields using shaped laser pulses with pump probe measurements that we routinely carry out. This approach requires some degree of control, so we would also like to get a better understanding of when to expect control over the dynamics. In order to do that we will use simple models to check whether we can establish simple rules about how the shape of the potential energy surfaces affects the outcome of control, and what pulse shape parameterizations are most effective in discriminating between pathways and driving control.

4 Publications of DOE Sponsored Research

References

[1] M. Kotur, T. C. Weinacht, C. Zhou, K. Kistler and S. Matsika, *J. Chem. Phys.*, 2011, **134**, 184309.

[2] P. Krause, S. Matsika, M. Kotur and T. Weinacht, *J. Chem. Phys.*, 2012, **137**, 22A537.

[3] M. Kotur, T. C. Weinacht, C. Zhou and S. Matsika, *Phys. Rev. X*, 2011, **1**, 021010.

[4] S. Matsika, C. Zhou, M. Kotur and T. C. Weinacht, *Faraday Discussions*, 2011, **153**, 247 – 260.

[5] C. Zhou, S. Matsika, M. Kotur and T. C. Weinacht, *J. Phys. Chem. A*, 2012, **116**, 9217–9227.

[6] M. Kotur, T. C. Weinacht, C. Zhou and S. Matsika, *IEEE J. Sel. Topics Quantum Electron.*, 2012, **18**, 187–194.

[7] C. Tseng, P. Sandor, M. Kotur, T. C. Weinacht and S. Matsika, *J. Phys. Chem. A*, 2012, **116**, 2654.

[8] M. Spanner, S. Patchkovskii, C. Zhou, S. Matsika, M. Kotur and T. C. Weinacht, *Phys. Rev. A*, 2012, **86**, 053406.

[9] M. Kotur, C. Zhou, S. Matsika, S. Patchkovskii, M. Spanner and T. C. Weinacht, *Phys. Rev. Lett.*, 2012, **109**, 203007.

[10] O. Njoya, S. Matsika and T. Weinacht, *ChemPhysChem*, 2013, **14**, 1451–1455.

[11] S. Matsika, M. Spanner, M. Kotur and T. C. Weinacht, *J. Chem. Phys. (submitted)*, 2013, **x**, x.

[12] A. Moradmand, D. S. Slaughter, D. J. Haxton, T. N. Rescigno, C. W. McCurdy, T. Weber, S. Matsika, A. L. Landers, A. Belkacem and M. Fogle, *Phys. Rev. A, submitted, (http://arxiv.org/abs/1305.5002)*, 2013.

ABSTRACT

ELECTRON-DRIVEN PROCESSES IN POLYATOMIC MOLECULES

Investigator: Vincent McKoy

A. A. Noyes Laboratory of Chemical Physics
California Institute of Technology
Pasadena, California 91125

email: mckoy@caltech.edu

PROJECT DESCRIPTION

The focus of this project is the development, extension, and application of accurate, scalable methods for computational studies of low-energy electron–molecule collisions, with emphasis on larger polyatomics relevant to electron-driven chemistry in biological and materials-processing systems. Because the required calculations are highly numerically intensive, efficient use of large-scale parallel computers is essential, and the computer codes developed for the project are designed to run both on tightly-coupled parallel supercomputers and on workstation clusters.

HIGHLIGHTS

During the year we achieved significant milestones in our work on low-energy collisions with biological molecules and maintained strong collaborations with leading experimental groups. Highlights include:

- Completed a major study of low-energy electron-impact excitation of water
- Completed a study of elastic electron scattering from acetylene
- Obtained initial results for angle-resolved dissociative attachment to uracil

ACCOMPLISHMENTS

The most fundamental and abundant biomolecule is, of course, water. For that reason, understanding the interaction between radiation and living matter requires, above all, detailed knowledge of water's collision cross sections, both elastic and inelastic. Through cascades of ionizing collisions, mostly with water molecules, the energy contained in ionizing radiation is quickly converted into the kinetic energy of a shower of low-energy secondary electrons. The further collisions of these secondary electrons with water and other molecules can in turn drive chemistry leading to radiation damage. In particular, because the low-lying excited electronic states of water are dissociative, electronically inelastic e^-–H_2O collisions cause dissociation into reactive H and OH fragments.

Although one might expect the electron cross sections for such a fundamental molecule as water to be well established, that has not been the case. Only one set of absolute, differential measurements for low-energy electron-impact excitation had been reported [1–3], and those data were inconsistent with the few theoretical results in the literature [4–9], which were themselves in poor mutual agreement. In the past year, however, we completed and published [10,11] a major experimental and computational study, undertaken in collaboration with the group of Murtadha Khakoo (California State University, Fullerton), that established some of these important electron-impact excitation cross sections on a solid footing. In particular, we obtained good agreement between measurement and calculation for the $\tilde{a}\,^3B_1$, $\tilde{A}\,^1B_1$, and $\tilde{B}\,^1B_1$ states. Moreover, these results were subsequently supported by the calculations of Rescigno and Orel [12], obtained from an independent computational procedure, which were in overall excellent agreement with our Schwinger Multichannel calculations. Discrepancies between the calculations and the Khakoo group's measurements persist for higher-lying excitation channels, pointing to the need for further refinements; however, agreement is good enough for the lowest-lying transitions to stongly suggest that the current measurements are reasonably accurate, while previous measurements [1–3] appear to have large errors due at least in part to the unfolding procedure used in the data analysis.

Our second major focus in the past year was on extending our electron scattering codes to compute the transition amplitudes that describe resonant attachment of slow electrons to molecules, and that thereby give insight into angle-resolved dissociative attachment experiments. We also carried out our initial practical application of this new procedure by computing transition amplitudes for a $(\pi_3)^1(\sigma^*)^2$ Feshbach resonance near 6.3 eV in the RNA nucleobase uracil. Measurements carried out by Daniel Slaughter and Ali Belkacem of Lawrence Berekley Laboratory indicate a propensity for dissociative attachment to uracil to proceed through collisions in which the electron is incident at an oblique angle to the ring. Our results, although still preliminary, are consistent with this result, showing (as required by symmetry) zero amplitude in the ring plane, but also a minimum in the perpendicular direction, resulting in maxima at oblique angles.

As part of our ongoing collaboration with the Khakoo group, we also carried out calculations on low-energy elastic electron scattering by the prototypical hydrocarbon acetylene, C_2H_2. Our results were in good overall agreement with the measurements, especially in the region of the 2.5 eV π^* resonance; moreover, they indicated the presence of a broad C–C σ^* resonance centered at about 8.5 eV that was also observed in the Khakoo group's measurements.

PLANS FOR COMING YEAR

Our first priority in the coming year will be to finalize results for the transition amplitudes describing resonant electron attachment to uracil. Besides repeating our calculations on a larger scale as a check, we will also look at the amplitudes describing attachment via the three low-lying π^* shape resonances, in addition to the Feshbach resonance on which we have concentrated to date. Although corresponding angle-resolved experimental data are not yet available for the π^* resonances, they are known to play a role in dissociative attachment to uracil, and calculations of the detailed attachment dynamics may be a spur to future measurements.

We will also look at angle-resolved dissociative attachment in some or all of the DNA nucleobases. Here the two pyrimidine bases, thymine and cytosine, are of special interest because of their direct comparability to uracil. As with uracil, this work will be collaborative, with experiments being carried out by the Belkacem group at LBL.

We will continue our studies of electron-impact excitation of biomolecules by examining low-lying dissociative transitions in methanol, CH_3OH. Methanol is both a significant potential biofuel and an analogue of water, and thus a natural extension of our just-completed study of H_2O. This work will again be carried out in collaboration with the Khakoo group, with corresponding experiments being performed in the Fullerton laboratory.

Further, we will complete an ongoing study of elastic scattering by the acetaldehyde molecule, CH_3HCO, that is again being carried in collaboration with the Khakoo group.

REFERENCES

[1] P. A. Thorn, M. J. Brunger, P. J. O. Teubner, N. Diakomichalis, T. Maddern, M. A. Bolorizadeh, W. R. Newell, H. Kato, M. Hoshino, H. Tanaka, H. Cho, and Y.-K. Kim, J. Chem. Phys. **216**, 064306 (2007).

[2] P. A. Thorn, M. J. Brunger, H. Kato, M. Hoshino, and H. Tanaka, J. Phys. B **40**, 697 (2007).

[3] M. J. Brunger, P. A. Thorn, L. Campbell, N. Diakomichalis, H. Kato, H. Kawahara, M. Hoshino, H. Tanaka, and Y.-K. Kim, Int. J. Mass Spectrom. **271**, 80 (2008).

[4] H. P. Pritchard, V. McKoy, and M. A. P. Lima, Phys. Rev. A **41**, 546 (1990).

[5] M.-T. Lee, S. E. Michelin, and L. M. Brescansin, J. Phys. B **26**, L203 (1993).

[6] M.-T. Lee, S. E. Michelin, T. Kroin, L. E. Machado, and L. M. Brescansin, J. Phys. B **28**, 1859 (1995).

[7] T. J. Gil, T. N. Rescigno, C. W. McCurdy, and B. H. Lengsfield III, Phys. Rev. A **49**, 2642 (1994).

[8] L. A. Morgan, J. Phys. B **31**, 5003 (1998).

[9] J. D. Gorfinkiel, L. A. Morgan, and J. Tennyson, J. Phys. B **35**, 543 (2002).

[10] L. R. Hargreaves, K. Ralphs, G. Serna, M. A. Khakoo, C. Winstead, and V. McKoy, J. Phys. B **45**, 201001 (2012).
[11] K. Ralphs, G. Serna, L. R. Hargreaves, M. A. Khakoo, C. Winstead, and V. McKoy, J. Phys. B **46**, 125201 (2013).
[12] T. N. Rescigno and A. E. Orel, Phys. Rev. A **88**, 012703 (2013).

PROJECT PUBLICATIONS AND PRESENTATIONS, 2011–2013

1. "Absolute Angle-Differential Elastic Cross Sections for Electron Collisions with Diacetylene," M. Allan, C. Winstead, and V. McKoy, Phys. Rev. A **83**, 062703 (2011).

2. "Collisions of Low-Energy Electrons with Isopropanol," M. H. F. Bettega, C. Winstead, V. McKoy, A. Jo, A. Gauf, J. Tanner, L. R. Hargreaves, and M. A. Khakoo, Phys. Rev. A **84**, 042702 (2011).

3. "Low Energy Elastic Electron Interactions with Pyrimidine," P. Palihawadana, J. Sullivan, M. Brunger, C. Winstead, V. McKoy, G. Garcia, F. Blanco, and S. Buckman, Phys. Rev. A **84**, 062702 (2011).

4. "Low-Energy Electron Scattering by Tetrahydrofuran," A. Gauf, L. R. Hargreaves, A. Jo, J. Tanner, M. A. Khakoo, T. Walls, C. Winstead, and V. McKoy, Phys. Rev. A **85**, 052717 (2012).

5. "Electron-Biomolecule Collision Studies Using the Schwinger Multichannel Method," C. Winstead and V. McKoy, in *Radiation Damage in Biomolecular Systems,* G. García Gómez-Tejedor and M. C. Fuss, editors (Springer, Dordrecht, 2012), p. 87.

6. "Excitation of the $\tilde{a}\,^3B_1$ and $\tilde{A}\,^1B_1$ States of H_2O by Low-Energy Electron Impact," L. R. Hargreaves, K. Ralphs, G. Serna, M. A. Khakoo, C. Winstead, and V. McKoy, J. Phys. B **45**, 201001 (2012) *(Fast-Track Communication)*.

7. "Low-Energy Electron Collisions with Biomolecules," C. Winstead and V. McKoy, J. Phys. Conf. Ser. **388**, 012017 (2012).

8. "Low-Energy Elastic Electron Scattering by Acetylene," A. Gauf, C. Navarro, G. Balch, L. R. Hargreaves, M. A. Khakoo, C. Winstead, and V. McKoy, Phys. Rev. A **87**, 012710 (2013).

9. "Excitation of the 6 Lowest Electronic Transitions in Water by 9 to 20 eV Electrons," K. Ralphs, G. Serna, L. R. Hargreaves, M. A. Khakoo, C. Winstead, and V. McKoy, J. Phys. B **46**, 125201 (2013).

10. "Low-Energy Electron Interactions with Biomolecules," V. McKoy, Physics Department Seminar, Federal University of Amazonas, Manaus, Brazil, June 13, 2011.

11. "Low-Energy Electron Interactions with Biomolecules," C. Winstead, XXVII International Conference on Photonic, Electronic, and Atomic Collisions, Belfast, UK, July 27–August 2, 2011 *(invited talk)*.

12. "Anomalously Large Low-Energy Elastic Cross Sections for Electron Scattering from the CF_3 Radical," J, R. Brunton, L. R. Hargreaves, M. J. Brunger, S. J. Buckman, G. Garcia, F. Blanco, O. Zatsarinny, K. Bartschat, C. Winstead, and V. McKoy, XXVII International Conference on Photonic, Electronic, and Atomic Collisions, Belfast, UK, July 27–August 2, 2011.

13. "Cross Sections for Electronic Excitation of Water by Low-Energy Electrons," L. R. Hargreaves, K. Ralphs, M. A. Khakoo, C. Winstead, and V. McKoy, XXVII International Conference on Photonic, Electronic, and Atomic Collisions, Belfast, UK, July 27–August 2, 2011.

14. "Electron and Positron Scattering from Pyrimidine," P. D. Palihawadana, J. R. Machacek, C. Makochekanwa, J. P. Sullivan, M. J. Brunger, C. Winstead, V. McKoy, G. Garcia, F. Blanco, S. J. Buckman, XXVII International Conference on Photonic, Electronic, and Atomic Collisions, Belfast, UK, July 27–August 2, 2011.

15. "Absolute Cross Sections for Electron Collisions with Diacetylene: Elastic Scattering, Vibrational Excitation and Dissociative Attachment," M. Allan, O. May, J. Fedor, B. C. Ibanescu, L. Andric, C. Winstead, and V. McKoy, XXVII International Conference on Photonic, Electronic, and Atomic Collisions, Belfast, UK, July 27–August 2, 2011.

16. "Simulating Quantum Collisions," V. McKoy, School of Computing and Information Sciences, Florida International University, March 23, 2012 *(invited talk, Distinguished Lecture Series)*.

17. "Low-Energy Electron Interactions with Biomolecules," C. Winstead, Forty-Third Annual Meeting of the APS Division of Atomic, Molecular and Optical Physics, Orange County, California, June 4–8, 2012 *(invited talk)*.

18. "Low-Energy Electron Scattering from Water Vapor," K. Ralphs, G. Serna, L. Hargreaves, M. A. Khakoo, C. Winstead, and V. McKoy, Forty-Third Annual Meeting of the APS Division of Atomic, Molecular and Optical Physics, Orange County, California, June 4–8, 2012.

19. "Low-Energy Elastic Scattering and Electronic Excitation of Water and Methanol by Electron Impact," M. A. Khakoo, L. R. Hargreaves, K. Varela, K. Ralphs, C. Winstead, and V. McKoy, XVIII International Symposium on Electron-Molecule Collisions and Swarms, Kanazawa, Japan, July 19–21, 2013.

ELECTRON/PHOTON INTERACTIONS WITH ATOMS/IONS

Alfred Z. Msezane (email: amsezane@cau.edu)

Clark Atlanta University, Department of Physics and CTSPS**,** Atlanta, Georgia 30314

PROGRAM SCOPE

The project's primary objective is to gain a fundamental understanding of the near-threshold electron attachment mechanism as well as identify and delineate resonances. The complex angular momentum (CAM) methodology, wherein is embedded the crucial electron-electron correlations and the core polarization interaction, is used for the investigations. Regge trajectories allow us to probe electron attachment at its most fundamental level near threshold, thereby uncovering new manifestations, including the mechanism of nanocatalysis, and determine the reliable electron affinities (EAs).

The time-dependent-density-functional theory is utilized to investigate the photoabsorption spectra of encapsulated atoms. Methods are developed for calculating the generalized oscillator strength, useful in probing the intricate nature of the valence- and open-shell as well as inner-shell electron transitions. Standard codes are used to generate sophisticated wave functions for investigating CI mixing and relativistic effects in atomic ions. The wave functions are also used to explore correlation effects in dipole and non-dipole studies as well as in R-matrix calculations of the photoionization process.

SUMMARY OF RECENT ACCOMPLISHMENTS

Resonances in near-threshold electron elastic scattering cross sections for atoms and Wigner threshold law application

A strong motivation for this investigation is that our novel and unique CAM method (also known as the Regge pole method) [1] is capable of producing accurate EAs from the electron elastic scattering total cross sections (TCSs) independently of experiments and other theoretical calculations. The importance of this investigation lies in that many measurements such as those of Refs. [2, 3] use the Wigner Threshold Law to extract the EAs from the measured data. We argue that where there is a rich resonance structure in the near-threshold region, the use of the Wigner Threshold Law could lead to uncertain EAs and use our results for the electron elastic TCSs for W, Rh and Os as well as the recently measured EA for the Sn atom [4], which agrees excellently with our calculated value, as illustrations. In [5] we demonstrated using the CAM method that the measured EAs for the atoms Ce, Pr, Nd, Eu, Tb and Tm were incorrect. Most of the theoretical EAs for the lanthanide atoms were riddled with uncertainties and therefore unreliable (see Table II of [5]). The recently obtained EA value for the complex Ce atom from the combined tunable infrared laser photodetachment spectroscopy and Relativistic Configuration Interaction Continuum formalism [6] is now converging to our CAM-calculated EA value [5]. We have identified three stable bound states of the Tl^- anion, with binding energy (BE) values of 0.0664, 0.281 and 2.415eV [7]. The experiment [8] and sophisticated theoretical calculations incorrectly identified the EA of Tl close to the 0.281 eV value. However, this value corresponds to the BE of the first excited state of the Tl^- ion and certainly not to the EA of Tl, which we calculated to be 2.415 eV.

Here we have investigated using the CAM method the near threshold electron elastic TCSs for the W, Rh, Os and Sn atoms to identify and delineate the resonances in the TCSs and extract the EAs, shape resonances (SRs), Ramsauer-Townsend (R-T) minima and BEs of their negative ions formed during the collisions as resonances. **Table 1**: Summarizes our calculated SRs, R-T minima and BEs for the ground and excited W^-, Rh^- and Os^- ions, all in eV. For the ground state of the W atom our SR and the measured EA [9] are very close together, namely 0.86 eV and 0.816 eV, respectively. Furthermore, for the excited Rh^- ion our calculated BE is 0.35 eV while the measured value is less than 0.385 eV [2]. Our SR for Rh is 1.70 eV while the measured EA is 1.143 eV [2]. For the complex Os atom our SR is close to the measured BE of the Os^- ion while our BE of the first excited state, 0.353 eV is close to the measured BE [3]. Consequently, we conclude that the measured EAs for the W, Rh and Os atoms appear to correspond to their shape resonances and certainly not to the EAs as claimed.

Atom	Z	1st R-T Minimum	SR	2nd R-T Minimum	EA Present	EA Expt.	BE (1st Extd) Present	BE(Extd) Expt.
Rh	45	0.88	1.70	3.06	3.12	1.143 [2]	0.35	< 0.385 [2]
W	74	0.58	0.86	1.56	1.59	0.816 [9]	0.61	

Bound states of the ground, first excited and second excited states of the Os^- negative ion

State	1st minimum	SR	2nd minimum	BE	BE, Expt. [3]
Ground	0.631	0.944	1.826	1.910	1.07780(12)
1st excited	0.082	0.353	1.079	1.230	0.553(3)
2nd excited	---	0.024	2.037	0.224	

A very important revelation in the comparisons is the appearance of the bound-state resonances of the negative ions together with the SRs of the ground and the excited states. Both theoretical calculations and experimental measurements could easily mistake one for the other. This could also be problematic in the use of the Wigner Threshold Law in high precision measurements of BEs of valence electrons using photodetachment threshold spectroscopy. We believe that the knowledge of the near-threshold structure of the elastic TCS of the relevant atoms is a useful guide for experimentalists when using the Wigner threshold law. It is also recommended to check the measurement of the EAs also through the DCSs.

Atomic Negative Ions Catalysis: Application to Methane Oxidation without CO_2 Emission

The role of atomic particles and nanoparticles in catalysis continues to attract extensive investigations from both fundamental and industrial perspectives. Recently, we have added the novel atomic negative ions to the study of catalysis at the atomic scale. The fundamental mechanism of negative ion catalysis in the oxidation of water to peroxide catalyzed by the atomic Au^- ion has been attributed to the anionic molecular complex $Au^-(H_2O)_{1,2}$ formation in the transition state [10], with the atomic Au^- ion breaking up the hydrogen bond strength in the water molecules, permitting the formation of the peroxide in the presence of O_2 usually provided by the support. Similarly, in the conversion of methane to methanol using the atomic Au^- ion catalyst, the anionic molecular complex $Au^-(CH_4)$ formation, weakens the C-H bond in the transition state [11].

From our CAM calculated low-energy electron scattering data, we have selected the atomic Y^-, Ru^-, At^-, In^-, Pd^-, Ag^-, Pt^-, and Os^- ions and investigated their catalytic activities using the atomic Au^- ion as the benchmark for the selective partial oxidation of methane to methanol without CO_2 emission. Dispersion-corrected density-functional theory has been used for the investigation. From the energy barrier calculations and the thermodynamics of the reactions, we conclude that the catalytic effect of the atomic Ag^-, At^-, Ru^-, and Os^- ions is higher than that of the atomic Au^- ion catalysis of CH_4 conversion to methanol [12]. By controlling the temperature around 290, 300, 310, 320 and 325 K methane can be completely oxidized to methanol without the emission of the CO_2 through the atomic Os^-, Ag^-, At^-, Ru^- and Au^- ion catalysts, respectively. We conclude by recommending the investigation of the catalytic activities of combinations of the above negative ions for significant enhancement of their catalysis.

Off-center effect on the photoabsorption spectra of encapsulated Xe atoms

The differential oscillator strengths (DOSs) for the photoabsorption spectra of the Xe atoms encapsulated at different locations of the C60 have been evaluated using the time-dependent-density-functional theory [13]. The calculations are performed in the energy region of the Xe 4d giant resonance. The results demonstrate that the main confinement resonances can result only when the Xe atom is located within a very small sphere of radius 0.3 °A around the center of the fullerene. The photoabsorption spectrum will be similar to that of the free Xe atom if the encaged Xe atom is located far away from the center such as at 2.0 °A off the center. The small resonance peak between two main confinement resonances has now been identified as a shape resonance of the free Xe 4d; it is not a confinement resonance.

Effect of C_{60} giant resonance on the photoabsorption of encaged atoms

The absolute differential oscillator strengths (DOSs) for the photoabsorption of the Ne, Ar, and Xe atoms encapsulated in the C_{60} have been evaluated using the time-dependent density-functional theory [14], which solves the quantum Liouvillian equation with the Lanczos chain method. The calculations are performed in the energy regions both inside and outside the C_{60} giant resonance. The photoabsorption spectra of the atoms encaged in the C_{60} demonstrate strong oscillations inside the energy range of the C_{60} giant resonance. This type of oscillation cannot be attributed to the confinement resonances, but is due to the energy transfer from the C_{60} valence electrons to the photoelectron through the intershell coupling.

Fine-structure energy levels, oscillator strengths and lifetimes in Al-like Chromium

Emission lines due to allowed and intercombination transitions in multiply ionized Al-like ions are observed in solar corona and laser produced plasmas. The lines arising from intercombination transitions, in particular, have been shown to be very useful, for instance, in understanding density fluctuations and elementary processes which occur in both interstellar and laboratory plasmas. Here we have calculated [15], using extensive configuration-interaction (CI) wave functions in intermediate coupling scheme constructed using Program CIV3, excitation energies from ground state for 97 fine-structure levels as well as of oscillator strengths and radiative decay rates for all electric-dipole-allowed and intercombination transitions among the fine-structure levels of the terms belonging to the (1s22s22p6)3s23p, 3s3p2, 3s23d, 3p3, 3s3p3d, 3p23d, 3s3d2, 3s24s, 3s24p, 3s24d, 3s24f, and 3s3p4s configurations of Cr XII. The relativistic effects in intermediate coupling are included through the Breit-Pauli approximation. The radiative lifetimes of the fine-structure levels have also been calculated.

Energy levels and radiative rates for transitions in Ti VI

Energy levels, radiative rates, oscillator strengths and line strengths for transitions among the lowest 253 levels of the (1s22s22p6) 3s23p5, 3s3p6, 3s23p43d, 3s3p53d, 3s23p33d2, 3s23p44s, 3s23p44p and 3s23p44d configurations of Ti VI have been calculated [16]. The general-purpose relativistic atomic structure package and flexible atomic code are adopted for the calculations. Radiative rates, oscillator strengths and line strengths are reported for all electric dipole (E1), magnetic dipole (M1), electric quadrupole (E2) and magnetic quadrupole (M2) transitions among the 253 levels, although calculations have been performed for a much larger number of levels. Comparisons are made with existing available results and the accuracy of the data is assessed. Additionally, lifetimes for all 253 levels are listed, although comparisons with other theoretical results are limited to only 88 levels. Our energy levels are estimated to be accurate to better than 1%, whereas results for other parameters are probably accurate to better than 20%. We recommend a reassessment of the energy level data on the NIST website for Ti VI.

CONTINUING RESEARCH

We continue with the theoretical investigations of low-energy electron scattering from simple and complex atoms, photoabsorption of endohedral fullerenes, strongly correlated systems and atomic structure calculations as delineated above. New accurate EAs for complex atoms will be obtained and nanocatalysts will be investigated and identified as well. Our recent CAM method [1] will be employed as well as extended to investigate Feshbach resonances.

REFERENCES AND SOME PUBLICATIONS ACKNOWLEDGING GRANT 2012-2013

[1] D. Sokolovski et al, Phys. Rev. A **76**, 012705 (2007)
[2] M. Scheer, C. A. Brodie, R. C. Bilodeau and H. K. Haugen, Phys. Rev. A **58**, 2015 (1998);
R. C. Bilodeau, M. Scheer, H. K. Haugen and R. L. Brooks, Phys. Rev. A **61**, 012505 (1999)
[3] R. C. Bilodeau and H. K. Haugen, Phys. Rev. Lett. **85**, 534 (2000)
[4] M. Vandevraye, C. Drag and C. Blondel, J. Phys. B **46**, 125002 (2013)
[5] Z. Felfli, A. Z. Msezane and D. Sokolovski, Phys. Rev. A **79,** 012714 (2009); Z. Felfli, A. Z. Msezane, and D. Sokolovski, J. Phys. B **41**, 041001 (2008)

[6] C. W. Walter, N. D. Gibson, Y. G. Li, D. J. Matyas, R. M. Alton, S. E. Lou, R. L. Field, D. Hanstorp, P. L. Lin and D. R. Beck, Phys. Rev. A **84,** 032514 (2011)
[7] Z. Felfli, A.Z. Msezane and D. Sokolovski, J. Phys. B **45,** 045201(2012)
[8] D. L. Carpenter, A. M. Covington and J. S. Thompson, Phys. Rev. A **61** 042501 (2000)
[9] A.O. Lindahl, P. Andersson, C. Diehl, et al, Eur. Phys. J. D **60**, 219 (2010)
[10] A. Tesfamichael, K. Suggs, Z. Felfli, X –Q Wang and A. Z. Msezane, J. Phys. Chem. C **116,** 18698 (2012)
[11] A. Z. Msezane, Z. Felfli, K. Suggs, A. Tesfamichael and X-Q Wang, Gold Bull. **45**, 127 (2012)
[12] A. Tesfamichael, K. Suggs, Z. Felfli, and A. Z. Msezane, J. Nano Research, Submitted (2013)
[13] "Off-center effect on the photoabsorption spectra of encapsulated Xe atoms", Zhifan Chen and Alfred Z. Msezane, Phys. Rev. A, At Press (2013)
[14] Zhifan Chen and Alfred Z. Msezane, Phys. Rev. A **86**, 063405 (2012)
[15] G. P. Gupta and A. Z. Msezane, Indian Journal of Physics, At Press (2013)
[16] "Energy levels and radiative rates for transitions in Ti VI", K. M. Aggarwal1, F. P. Keenan and A. Z. Msezane, Phys. Scr. **88**, 025302 (2013)
[17] "Self-intersecting Regge trajectories in multi-channel scattering", D. Sokolovski, Z. Felfli, A.Z. Msezane, Physics Letters A **376,** 733-736 (2012)
[18] "Photoabsorption spectrum of the Xe@C60 endohedral fullerene", Zhifan Chen and Alfred Z. Msezane, Euro. Phys. J. D **66**, 184, (2012)
[19] "Interference in Molecular Photoionization and Young's Double-Slit Experiment", A. S. Baltenkov, U. Becker, S. T. Manson and A. Z. Msezane, J. Phys. B **45**, 035202 (2012)
[20] "Identification of strongly correlated spin liquid in Herbertsmithite", V. R. Shaginyan, A. Z. Msezane, K. G. Popov, G. S. Japaridze and V. A. Stephanovich, Euro. Phys. Lett. **97,** 56001 (2012)
[21] "Fine-structure energy levels and radiative rates in Si-like Chlorine", G. P. Gupta, Vikas Tayal and A. Z. Msezane, Indian Journal of Physics, IDOI 10.1007/s12648-012-0006-5
[22] "A Mathematical Model of Negative Molecular Ion", A. S. Baltenkov, S. T. Manson, and A. Z. Msezane, Proceedings of Dynamic Systems and Applications **6** (Dynamic Publishers, 2012), pp. 53- 57
[23] "Fine-Structure energy levels, radiative rates and lifetimes in Si-like Nickel", G. P. Gupta and A. Z. Msezane, Phys. Scripta **86**, 015303 (2012)
[24] "Excitation energies, oscillator strengths and lifetimes in Mg-like Vanadium", G. P. Gupta and A. Z. Msezane, Physica Scripta **88,** 025301 (2013)
[25] "Scaling in dynamic susceptibility of herbertsmithite and heavy-fermion metals", V. R. Shaginyan, A. Z. Msezane, K.G. Popov and V.A. Khodel, Physics Letters A **376**, 2622 (2012)
[26] "Atomic Gold and Palladium Negative Ion-Catalysis of Water to Peroxide: Fundamental Mechanism", A. Tesfamichael, K. Suggs, Z. Felfli, Xiao-Qian Wang and A. Z. Msezane, J. Nanoparticles Research **15**, 1333 (2013)
[27] "Photoabsorption spectrum of the Sc3N@C80 molecule", Zhifan Chen and Alfred Z. Msezane, J. Phys. B **45**, 235205 (2012)
[28] "Magnetic field dependence of the residual resistivity of the heavy-fermion metal $CeCoIn_5$", V. R. Shaginyan, A. Z. Msezane, K. G. Popov, J. W. Clark, M. V. Zverev, and V. A. Khodel, Phys. Rev. B **86**, 085147 (2012)
[29] "Slow electron scattering from Ag, Pd, Pt, Ru and Y atoms: Search for nanocatalysts", A. Z. Msezane, Z. Felfli, and D. Sokolovski, Journal of Physics: Conference Series **388**, 042002 (2012)
[30] "Common quantum phase transition in quasicrystals and heavy-fermion metals", V. R. Shaginyan, A. Z. Msezane, K. G. Popov, G. S. Japaridze, V. A. Khodel, Phys. Rev. B **87**, 245122 (2013)
[31] "Innershell Photoionization of Atomic Chlorine," W. C. Stolte, Z. Felfli, R. Guillemin, G. Ohrwall, S.–W. Yu, J. A. Young, D. W. Lindle, T. W. Gorczyca, N. C. Deb, S. T. Manson, A. Hibbert, and A. Z. Msezane, Phys. Rev. A, Submitted (2013).

Theory and Simulation of Nonlinear X-ray Spectroscopy of Molecules

Shaul Mukamel
University of California, Irvine, CA 92697
Progress Report 2013, September 11, 2013
DOE DE-FG02-04ER15571

Program Scope

Sequences of coherent broadband X-ray pulses can reveal the dynamics of nuclei and electrons in molecules with attosecond temporal, and nanometer spatial resolution. These experiments, made possible by new X-ray free electron laser (XFEL) and high harmonic generation (HHG) sources provide a unique window into the motions of electrons, holes and excitons in molecules and materials. This program is aimed at the design of novel X-ray pulse sequences for probing valence electronic excitations, developing computational approaches for describing core-excited states, and the application of these techniques to specific molecular systems. Nonlinear spectroscopy techniques commonly applied in the visible and infrared regimes are extended to study all-X-ray as well as combined optical/UV and X-ray experiments on the same footing. Methods for visualizing the electronic coherences and currents underlying time resolved X-ray signals are explored. Applications are made to energy transfer in porphyrin arrays, long range electron transfer between metal centers, mixed-valence Mn complexes in the water-splitting light-harvesting complex PSII, and delocalized carbon core excitations in conjugated hydrocarbons. Signatures of vibrational motions and nonadiabatic dynamics in photo excited molecules are identified.

Recent Progress

To demonstrate the capacity of stimulated X-ray Raman processes to prepare electronic wavepackets with electron and hole densities local to the resonant core atom we have calculated the charge densities of superposition states prepared in the amino acid cysteine by impulsive X-ray excitation immediately following an excitation at the nitrogen, oxygen and sulfur K-edges. Movies of the time-evolving natural orbitals, the reduced electron and hole densities, and their degree of entanglement (natural orbital participation ratio) illustrate the correlated many-body dynamics of quasiparticles. In Fig. 1 we show the projection of the electron and hole densities onto three spatial regions of the cysteine molecule, following a Raman excitation at one of the heavier elements in the molecule. The time-dependent participation ratios show a rapid decay of the single particle-hole character of the excitation and the buildup of electron-hole entanglement. Time-dependent particle-hole occupations carry additional information on these correlations through the reduced electron and hole densities and the cross-correlation between them. Identifying other measures of these correlations, and designing the optimal experimental techniques for measuring them constitutes an interesting future challenge.

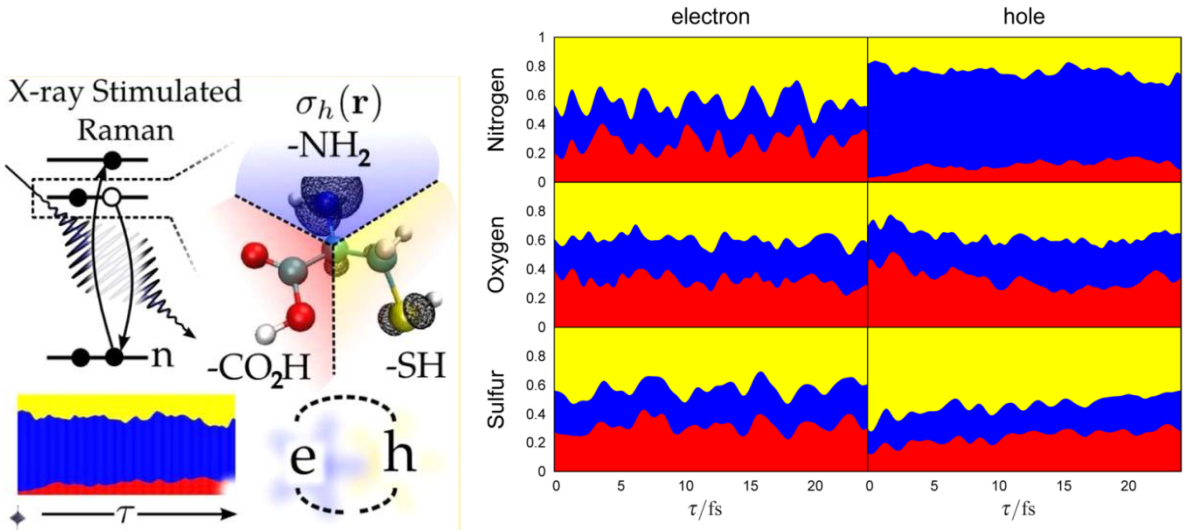

Fig 1: (left) schematic of the X-ray Raman process, and the division of cysteine into three spatial regions. (right) the projection of the electron and hole densities onto these regions as a function of time, following impulsive excitation at the oxygen, nitrogen and sulfur K-edges[P37].

We have further simulated the coherent and incoherent spontaneous light emission spectra triggered by an impulsive stimulated X-ray Raman excitation. In the semiclassical theory (quantum matter/classical field), spontaneous emission originates from the time-dependent charge-density and may be calculated with the Larmor formula. We have developed a more rigorous and complete description where both matter and field are treated quantum mechanically. The radiation back-reaction, missing in the semiclassical approach, causes inelastic scattering. This approach was applied to study the nonlinear light scattering caused by the time-evolving superposition of electronic excitations created by a coherent, broad-band X-ray source. The resulting time- and/or frequency-gated signals provide direct information on valence electronic motions, coherences and correlations. Difference-frequency generation and stimulated-Raman-induced fluorescence were compared.

Doubly core-excited states (DCES) can be prepared by short and intense X-ray laser pulses, and be studied by nonlinear X-ray signals. We have demonstrated the power of the X-ray double-quantum-coherence (XDQC) spectroscopy technique which preferentially targets doubly excited states in formamide at the nitrogen and oxygen K-edges.

Future Plans

Measuring electron and charge migration in multiporphyrin arrays is fundamental for understanding natural as well as artificial light-harvesting complexes. Linear, cyclic or dendrimeric multiporphyrin arrays differ in the linking groups, distances, angles, and degrees of conjugation between monomers. The effects of these changes on the charge and energy transfer efficiency will be studied by nonlinear X-ray spectroscopy at the metal edges. Simulations for dimers will be extended to larger aggregates. Stimulated X-ray Raman is uniquely suited to study energy and charge transfer due to its ability to create localized electronic states and to monitor electronic motion through localized spatial windows on the same or different monomers. The signals can be either one-color, when the pump and probe are identical, or two-color, when the pump and the probe are resonant with different core transitions. A localized wave-packet created on one monomer can have one of three possible fates: it can remain on the initially excited monomer, undergo coherent back and forth energy transfer, or become delocalized and spread across the whole dimer. Each of these scenarios should result in distinct signatures in the SXRS signals.

Charge transport between transition metal complexes occurs naturally in proteins and photosynthetic systems and in man-made solar cell materials. We shall study how ultrafast X-ray techniques may be used to characterize the charge separation dynamics after excitation. This will help the design of optimal experiments for measuring the transmission properties of organic molecular wires connecting different photoactive complexes. The spectra of Mn clusters in various oxidation states which are responsible for water splitting in Photosystem II (PS II) will also be simulated.

Our current work had covered the N1s, O1s, and S2p edges in molecules where only one core hole is created at a time. In most organic molecules the carbon K-edge has contributions from several atoms and is more complex. Contributions of different cores to the XANES spectra are additive but nonlinear signals are expected to be nonadditive due to interactions among carbon atoms, *i.e.* the valence orbitals are different for different core states. Simulations will be carried out on Furan, which has two types of carbon atoms.

We shall develop a quantum electrodynamic treatment of off-resonant X-ray scattering with several objectives: (i) to predict the ratio of elastic to inelastic scattering and how the latter can affect single molecule experiments. (ii) to extend this analysis to a molecule initially in an electronic superposition state. (iii) to predict new multidimensional diffraction signals obtained by photon coincidence measurements with multiple attosecond pulses.

Publications Resulting from the Project

P1. "Dissecting bi-exciton wavefunctions of Self-assembled Quantum Dots by Double Quantum Coherent Optical Spectroscopy". B. Fingerhut, M. Richter, J.W. Luo, A. Zunger, and S. Mukamel. Phys Rev B, 86, 235303 (2012).

P2. "Photosynthetic Reaction Centre Operates as a Quantum Heat Engine ", K. Dorfman, D.V. Voronine, S. Mukamel and M.O. Scully. PNAS, DOI/10.1073/pnas.1212666110 (2013).

P3. "Quantum Heat Engines: A Thermodynamic Analysis of Power and Efficiency", U. Harbola, S. Rahav and S. Mukamel. EPL, 99, 50005 (2012).

P4. " Theory of Coherent Raman Scattering Microscopy", E.O. Potma and S. Mukamel, in Coherent Raman Scattering Microscopy, J. X. Cheng and X. S. Xie (Eds.), pg. 3 (CRC Press, Boca Raton, 2013).

P5. "Simulations of the 2-dimensional Electronic Spectroscopy of the Photosystem II Reaction Center", K.L.M. Lewis, F.D. Fuller, J.A. Myers, C.F. Yocum, S. Mukamel, D. Abramavicius and J.P. Ogilvie. J. Phys. Chem. A, 117, 34 (2013).

P6. " Heat Fluctuations and Coherences in a Quantum Heat Engine", S. Rahav, U. Harbola and S. Mukamel. Phys Rev. A. 86, 043843 (2012).

P7. " Manipulating One-and Two-dimensional Stimulated X-ray Resonant Raman Signals in Molecules by Pulse Polarizations", D. Healion, J. Biggs, and S. Mukamel. Phys. Rev. A. 86, 033429 (2012).

P8. "Manipulation of Two-photon-induced Fluorescence Spectra of Chromophore Aggregates with Entangled Photons: A Simulation Study", F. Schlawin, K. Dorfman, B.P. Fingerhut, and S. Mukamel. Phys Rev A. 86, 023851 (2012).

P9. " Multidimensional Measures of Response and Fluctuations in Stochastic Dynamical Systems", M. Kryvohuz and S. Mukamel. Phys Rev A. 86, 043818 (2012)

P10. " Multidimensional Attosecond Resonant X-ray Spectroscopy of Molecules; Lessons from the Optical Regime", J. Biggs, D. Healion, Y. Zhang, and S. Mukamel. Ann. Rev. Phys. Chem. , 64, 101 (2013).

P11. " 2D optical photon echo spectroscopy of self assembled quantum dots", B. Fingerhut, M. Richter, J.W. Luo, A. Zunger, and S. Mukamel. Ann. Phys., 525, 31-42 (2013)

P12. "Two dimensional stimulated ultraviolet resonance Raman spectra of tyrosine and tryptophan; A simulation study". H. Ren, J.D. Biggs, D. Healion, and S. Mukamel. J. Raman Spectrosc. 44, 544-559 (2013).

P13. "Using Localized Double Quantum Coherence Spectroscopy for Reconstructing the Two Exciton Wave Function of Coupled Emitters", F. Schlosser, A. Knorr, S. Mukamel and M. Richter. New J. Phys. 15, 025004 (2013).

P14. "Broadband Infrared and Raman Probes of Excited-state Vibrational Molecular Dynamics; Simulation Protocols Based on Loop Diagrams", K. E. Dorfman, B.P. Fingerhut, and S. Mukamel. Phys Chem Chem Phys,15, 12348 (2013).

P15. " Suppression of Population transport and Control of Exciton Distributions in Photosynthetic Complexes by Entangled Photons, " F. Schlawin, K.E. Dorfman, B.P. Fingerhut, and S. Mukamel. Nat. Comm., 4:1782:DOI:10.1038/ncomms2802 (2013).

P16. "Core and Valence Excitations in Resonant X-ray Spectroscopy Using Restricted Excitation Window Time-dependent Density Functional Theory (REW-TDDFT)," Y. Zhang, J.D. Biggs, D. Healion, N. Govind, and S. Mukamel. J. Chem. Phys. 137, 194306 (2012)

P17. " Multidimensional X-ray Spectroscopy Valence and Core Excitations in Cysteine," J.D. Biggs, Y. Zhang, D. Healion, and S. Mukamel. J. Chem. Phys. 138, 144303 (2013)

P18. " Double Core-Excitations in Formamide can be probed by X-ray Double-quantum Coherence Spectroscopy ", Y. Zhang, D. Healion, J.D. Biggs, and S. Mukamel. J. Chem. Phys. 138, 144301 (2013).

P19. "Nonlinear Light Scattering in Molecules induced by Impulsive X-ray Raman Process", K.E. Dorfman, K. Bennett, Y. Zhang and S. Mukamel. Phys Rev. A, 87, 053826 (2013)

Nonlinear Photoacoustic Spectroscopies Probed by Ultrafast X-Rays

Keith A. Nelson
Department of Chemistry
Massachusetts Institute of Technology
Cambridge, MA 02139
Email: kanelson@mit.edu

Margaret M. Murnane
JILA
University of Colorado and National Institutes of Technology
Boulder, CO 80309
E-mail: murnane@jila.colorado.edu

Program Scope

In this project, ultrashort electromagnetic pulses in the visible, extreme ultraviolet (EUV), and x-ray spectral ranges are all used in complementary efforts to gain experimental access to elementary material excitations and fundamental condensed matter processes on ultrafast time scales and mesoscopic length scales. Of primary interest are heat transport, whose non-diffusive character at short length scales plays important roles in thermoelectric materials and nanoscale devices, and structural evolution in disordered media, which shows dynamics on wide-ranging time scales that have long eluded first-principles description. Central to these phenomena are acoustic phonons, which mediate both thermal transport and the compressional and shear components of structural relaxation. In addition to direct time-resolved observation of thermal transport, longitudinal, transverse, and surface acoustic wave generation and detection are key elements of our experiments in all spectral ranges.

We develop and use a variety of methods to excite and monitor acoustic waves and thermal transport on a wide range of length and time scales. For length scales in the roughly 1-100 micron range, we use crossed optical pulses to form an interference or "transient grating" (TG) pattern, directly generating thermoelastic responses with the grating period Λ (i.e. with wavevector magnitude $q = 2\pi/\Lambda$). The responses are monitored by time-resolved diffraction of probe laser light, revealing damped acoustic oscillations (from which acoustic speeds and attenuation rates, and elastic and loss moduli, are determined) and showing the kinetics of thermal transport from the heated interference maxima (the transient grating "peaks") to the unheated minima ("nulls"). The acoustic frequencies at these wavelengths are in the MHz or low GHz range. When the crossed pulses are perpendicularly polarized, transverse rather than longitudinal acoustic waves are generated. Therefore we have access to both compressional and shear material responses including elastic and loss moduli and the underlying structural relaxation dynamics that determine their frequency dependences. In order to reach higher acoustic frequencies and to monitor heat transport on length scales far less than 1 μm, we are working to extend transient grating methods to EUV wavelengths, taking advantage of ever-increasing EUV pulse energies produced through high harmonic generation (HHG), and to hard x-ray wavelengths using the LCLS facility at Stanford. In parallel with these long-term efforts, we have developed several approaches to provide experimental access to higher wavevectors than those reached through the interference patterns (or the coherent scattering) of visible light. Spatially periodic structures can be deposited onto substrate surfaces so that optical irradiation produces thermoelastic responses at the specified periods which may be as small as a few tens of nanometers. Time-resolved diffraction of variably delayed EUV pulses reveals the corresponding surface acoustic wave oscillations and thermal transport kinetics with extremely high sensitivity. Alternatively, a superlattice structure of alternating layers that have different optical absorption spectra (e.g. absorbing and transparent at an optical excitation pulse wavelength) can be irradiated to generate a thermoelastic response including a bulk compressional acoustic wave with the superlattice period. The acoustic wave may be detected in a variety of ways including measurement of acoustic modulation of the optical

absorption strength or interferometric measurement of time-dependent displacements at a sample interface when the acoustic wave arrives there. Alternatively, a thin opaque layer may be irradiated by a sequence of femtosecond optical pulses so that its periodic thermal expansion launches a multiple-cycle acoustic wave into a substrate. In this case it is not the acoustic wavevector that is specified experimentally but the frequency which is determined by the temporal period of the optical pulse sequence. The wave may be detected by coherent Brillouin scattering within the substrate for moderate acoustic frequencies, or by monitoring motion at the back of the substrate or at an interface. The use of an opaque layer that is crystallographically canted relative to the substrate plane yields a shear component to the thermoelastic response, thus permitting generation of GHz-frequency transverse as well as longitudinal acoustic waves.

Recent Progress

Nanoscale thermal transport and acoustics with EUV pulses

Nanoscale thermal transport: Understanding energy flow in nanostructures is very challenging because a fundamental understanding of how to model ballistic and quasi-ballistic transport are still under development. Thermal energy is carried by phonons that travel ballistically away from a nanoscale heat source for a significant distance before undergoing scattering, leading to non-local (i.e. non-diffusive) thermal energy distributions. Two simple models were developed for nanoscale thermal energy flow in 1D, but no models exist for 2D or 3D geometries. In past work in collaboration with CXRO at LBL, we used ultrafast coherent high harmonic (HHG) beams to measure the ballistic contribution to 1D thermal transport from a nanoscale heat source into its surroundings. We found a significant (as much as 3 times) decrease in energy transport away from the nanoscale heat source compared with Fourier law predictions. This work resolved a controversy in the field, because two different theories were proposed, but only one agreed with our measurements.

Intuitively, 2D confinement of heat flow from square hot spots should be stronger than for 1D wires of comparable size, and thus should lead to stronger ballistic effects. However, our initial measurements compared 1D and 2D heat flow on samples fabricated at different times. Since small changes in interfacial resistance could lead to different behavior, in the past year we repeated our measurements of nanoscale heat flow from 2D and 1D nanostructures that were fabricated on the same substrate at the same time. This allowed us to precisely compare nanoscale 1D and 2D heat flow, and to report our experimental findings (see Figure 1) with a high degree of confidence. Comparing 1D and 2D thermal transport for a series of nanostructure sizes with feature sizes ranging from 500 nm to 60 nm, we found that although in general smaller nanostructures show faster thermal decay kinetics, the rate of change is smaller in 2D, indicating a slower cooling rate in 2D than in 1D. Moreover, on longer timescales, where thermal dissipation in the substrate dominates the signal, thermal decay is identical for 1D and 2D, verifying that the substrate properties determine the heat flow kinetics. We thus can definitively state that we have observed strong ballistic effects in 2D nanoscale heat flow for the first time, and that they are significantly more pronounced than in 1D. Since no model of 2D nanoscale heat flow exists, we are developing a finite element simulation code using COMSOL to fully interpret our results.

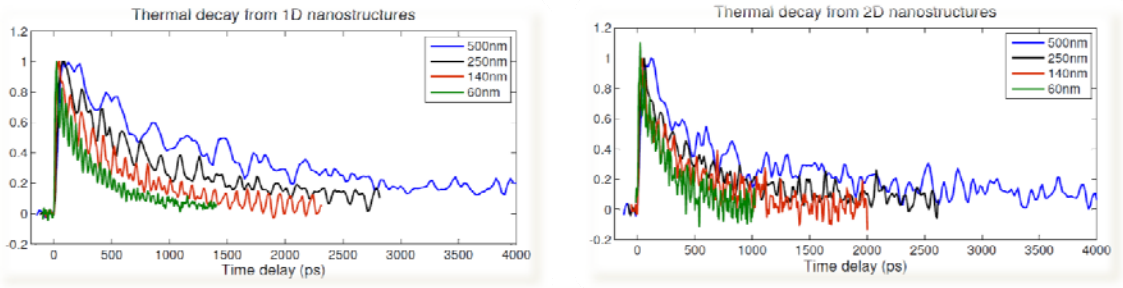

Figure 1: Thermal relaxation from 1D and 2D nanostructures of dimension 500 to 60 nm. The rate of increase of heat flow as the size of the nanostructure decreases is faster in 1D (top) than in 2D (bottom). The 1D and 2D nanostructures were fabricated at the same time on the same substrate at CXRO/LBL.

Optical measurements of GHz-THz acoustics: structural relaxation dynamics & thermal transport

Structural relaxation dynamics: A multiyear, collaborative experimental effort to measure elastic and loss moduli of supercooled liquids and glasses across an unprecedented 13-decade frequency range, from millihertz to hundreds of GHz with less than three decades of gaps, was continued in order to compare the results to the predictions of mode-coupling theory (MCT), the only (and far from universally accepted) first-principles theory of viscoelastic liquid behavior. Our effort was designed to address the extremely wide range of structural relaxation time scales exhibited by viscoelastic materials, which even at a single temperature T show distinct multiexponential relaxation kinetics including relaxation components on disparate time scales. As T is varied, the range of time scales spanned by the primary, or alpha, relaxation dynamics (the slow relaxation that we associate with familiar viscous behavior including diffusion and flow in liquids like honey) is extraordinary, with low viscosity (picosecond-nanosecond relaxation dynamics) at high temperatures and glassy behavior (many-second relaxation dynamics) at low temperatures. We measured longitudinal and transverse GHz-frequency acoustic waves that were generated at thin absorbing layers and MHz-frequency acoustic waves in bulk transient grating experiments, while our collaborators conducted dynamic mechanical measurements in the kHz, Hz, and mHz ranges. This is by many decades the most comprehensive study of viscomechanical dynamics ever performed on a single material (the single-component organic van der Waals liquid tetramethyl-tetraphenyl-trisiloxane, sold as a commercial oil with the trade name DC704). Our effort required the DOE-supported development of new measurement methodologies in the GHz range to overcome challenges including the very short (often submicron) propagation length for ~ 100-GHz acoustic waves (with wavelengths of ~ 30 nm) through viscous liquids before essentially complete attenuation. The data show agreement over all 13 decades with a result that has been observed empirically for many years over limited frequency ranges and often has been assumed to hold more broadly, namely "time-temperature scaling" (TTS) of the alpha relaxation spectrum which moves from GHz frequencies (corresponding to fast structural relaxation dynamics) at high T to millihertz (slow relaxation dynamics) at low T. TTS means that the relaxation spectrum, plotted on a log(frequency) scale, appears identical at all temperatures, with the same frequency-dependent form and width, and simply shifts from high to low frequency without any other change as the sample temperature is reduced. Our results provide the first truly comprehensive test of TTS through measurements of structural relaxation dynamics. Our results for the high-frequency limiting value of the shear modulus at the glass transition temperature T_g also yielded good agreement with a model of glass formation that associates the T-dependent change in activation energy for structural relaxation at temperatures near T_g, or the "fragility" of the liquid, with the activation barrier for local shear displacements of molecules relative to each other.

Our results also permit unique testing of mode-coupling theory which predicts a dynamic criticality at a critical temperature T_c (well above T_g) below which, in the idealized version of the theory, the supercooled liquid becomes nonergodic - the slow alpha relaxation dynamics become frozen and the liquid loses access to some configurations that would be accessible thermodynamically but that become cut off kinetically. A key theoretical prediction is that at $T > T_c$ there is a connection between the alpha relaxation dynamics and the nearly temperature-independent, faster (picosecond) "beta" relaxation dynamics that represent small-scale rearrangements among intermolecular configurations at multiple local potential energy minima without the larger-scale, slower interchanges of molecular center-of-mass positions that are necessary for diffusion and flow. The low-frequency side of the beta relaxation spectrum and the high-frequency side of the alpha relaxation spectrum are both predicted to show power-law behavior, with the exponents predicted to obey relations that are reminiscent of those describing critical exponents associated with phase transitions. Direct testing of this crucial MCT prediction, which directly connects the seemingly disparate (and at low temperatures, temporally disparate) alpha and beta relaxation kinetics, has been elusive because it requires measurement of the beta structural relaxation dynamics of picoseconds as well as the much slower alpha relaxation dynamics. Our DOE-supported methods have enabled the first measurements of GHz-frequency acoustic responses that give us the beta

relaxation dynamics. The results appear to support the MCT prediction. However, our comparison to theory has employed an approximate interpolation formula to describe the intersection between the alpha and beta relaxation spectra. The interpolation is highly questionable in the crucial temperature region above T_c where the wings of the two spectra overlap. The interpolation is used commonly, but its limitations have never been examined since no structural relaxation measurements in the key frequency and temperature ranges were possible before. Now we are working on a reformulation of the theoretical description that does not involve the approximate interpolation. We also have collected additional data in the beta relaxation (GHz) frequency range to completely fill in one of our previous frequency gaps, now that we have seen how crucial the comparison to theory is in this particular range.

GHz-THz acoustic phonon-mediated thermal transport: We are working toward a convergence of experimental results and fundamental understanding of nondiffusive thermal transport and the acoustic phonons that mediate it. Nondiffusive thermal transport in high-quality crystals is measurable at room temperature on micron length scales, indicating that significant amounts of thermal energy are transported by phonons with mean free paths on this length scale or longer. We have developed methods for optical generation and detection of coherent acoustic phonons throughout the GHz frequency range and extending in some cases up to > 1 THz frequencies. In room-temperature single crystalline silicon, we have compared nondiffusive thermal transport measured at 1-10 μm length scales, phonon mean free paths measured up to 640 GHz acoustic frequencies, modeling of phonon damping mechanisms, and numerical calculations of phonon damping rates. The results yield a consistent understanding of the thermal transport results in terms of the measured and modeled phonon mean free paths.

Future Plans

We have been experiments aimed at direct conversion of strong GHz-THz electromagnetic pulses into transverse and longitudinal acoustic waves in the same frequency range at piezoelectric crystal interfaces and thin layers. We also have planned TG measurements with EUV excitation and probe pulses which will foreshadow hard x-ray TG measurements at the LCLS. These efforts if successful will enable versatile generation and measurement of high-frequency surface and bulk acoustic waves extending throughout much of the Brillouin zone and measurement of very short-range thermal transport without fabricated surface patterns or metal photoacoustic layers.

References

1. M. Siemens et al., “Measurement of quasi-ballistic thermal transport from nanoscale interfaces using ultrafast coherent soft x-ray beams” *Nature Materials* **9**, 26 (2010).
2. D. Nardi et al., “Probing Thermomechanics at the Nanoscale: Impulsively Excited Pseudosurface Acoustic Waves in Hypersonic Phononic Crystals”, *Nano Letters* **11**, 4126 (2011).
3. Q. Li et al., “Generation and Detection of Very Short-Wavelength 35nm Surface Acoustic Waves at Nano-interfaces”, *Physical Review B* **85**, 195431 (2012).
4. Q. Li et al., “Photoacoustic characterization of ultrathin films using femtosecond coherent extreme-ultraviolet beams”, *Proc. SPIE* 8324, doi:10.1117/12.916866 (2012).
5. Kathleen Hoogeboom-Pot et al., “Ballistic thermal transport from 1D and 2D nano-interfaces”, in prep'n (2013).
6. A.A. Maznev et al., “Lifetime of sub-THz coherent acoustic phonons in a GaAs-AlAs superlattice,” *Appl. Phys. Lett*. **102**, 041901 (2013).
7. C. Klieber, T. Hecksher, T. Pezeril, D.H. Torchinsky, J.C. Dyre, and K.A. Nelson, “Mechanical spectra of glass-forming liquids. II. Gigahertz-frequency longitudinal and shear acoustic dynamics in glycerol and DC704 studied by time-domain Brillouin scattering,” *J. Chem. Phys*. **138**, 12A544, pp. 1-12 (2013).
8. F. Hofmann et al., “Intrinsic to extrinsic phonon lifetime transition in a GaAs-AlAs superlattice,” *J. Phys.: Cond. Matter* **25**, 295401, pp. 1-8 (2013); arXiv:1303.4413 [cond-mat] (2013).
9. K.J. Manke et al., “Detection of shorter-than-skin-depth acoustic pulses in a metal film via transient reflectivity,” AIP Conf. Proc. **1506** (Phonons 2012: XIV Intl. Conf. Phonon Scat. in Cond. Mat.), 22-27 (2013).
10. K. J. Manke et al., “Measurement of shorter-than-skin-depth acoustics pulses in a metal film via transient reflectivity,” *Appl. Phys. Lett.* (submitted).

Electron and Photon Excitation and Dissociation of Molecules

A. E. Orel
Department of Chemical Engineering and Materials Science
University of California, Davis
Davis, CA 95616
aeorel@ucdavis.edu

Program Scope

This program will study how energy is interchanged in electron and photon collisions with molecules leading to excitation and dissociation. Modern *ab initio* techniques, both for the photoionization and electron scattering, and the subsequent nuclear dynamics studies, are used to accurately treat these problems. This work addresses vibrational excitation and dissociative attachment following electron impact, and the dynamics following inner shell photoionzation. These problems are ones for which a full multi-dimensional treatment of the nuclear dynamics is essential and where non-adiabatic effects are expected to be important.

Recent Progress

Isomerization of C_2H_4: Snapshots of a chemical reaction continued
Although the results on the MFPADs for the isomerization of acetylene were interesting (Publication #10 and #11), experiments on this system may be very difficult to perform. The experiment for this molecule requires two photoionization events; one to first ionize the neutral acetylene to produce a signifant population of excited monocation and another to actually photionize the monocation. Therefore, there would exist a background noise from the first ionization process affecting the detection of the second photoionization event. In addition, the MFPADs in the vinylidene configuration vary rapidly with photon energy and do not image the molecule. We therefore carried out calculations on C_2H_4, a system which is currently being studied at LBL by the AMO experimental group. For this system, the first step is a photoabsorptionto produce an excited state of the neutral. The probe pulse then ionizes this state. We computed molecular frame photoangular distributions (MFPADs) from k-shell photoionization along the isomerization path. Calculations on the MFPADs from the ground state showed excellent agreement with previous experiment. Calculations for the excited state gave snapshots of the path to products. These results were published in Physical Review A, Publication #14.

Electron Impact Excitation of Water
Motivated by recent experiments, we began studies on the electron impact excitation of water. We studied excitation of the $\tilde{a}\ ^3B_1$, $\tilde{A}\ ^1B_1$,$\tilde{b}\ ^3A_1$, $\tilde{B}\ ^1A_1$, $1\ ^3A_2$ and $1\ ^1A_2$ states of water by low energy electron impact. The calculations are carried out in an eight-channel close-coupling approximation using the complex Kohn variational method. Particular attention is paid to the elimination of pseudoresonances that can occur when correlated target states are employed. We calculated both differential and integral cross sections and compared with the most recent experimental and theoretical results. These results were published in Physical Review A, Publication #13.

Future Plans

Electron Impact Excitation of Methanol
There is also experimental data available on low energy electron impact excitation of methanol. We have begun to study this system using similar methods as that used in our water calculation.

Mechanism for Dissociative Electron Attachment from Formic Acid
Experimental work has shown that low-energy electrons (<2 eV) can fragment gas phase formic acid (HCOOH) molecules through resonant dissociative attachment processes. The principal reaction products of such collisions were found to be formate ions (HCOO-) and hydrogen atoms. Previously we have carried out ab initio calculations for elastic electron scattering from formic acid using the complex Kohn variational method. We found a π^* resonance with the electron temporarily trapped in the CO antibonding π orbital. We also presented evidence, obtained from the low-energy behavior of the cross section and its dependence on target geometry, that there must necessarily exist a virtual state in this system. The OH bond must be broken to form the formate ion. Also, since the products have A' symmetry and the resonance is A", symmetry considerations dictate that the associated dissociation dynamics are intrinsically polyatomic. We proposed a mechanism in which the reaction follows a complicated path, first stretching both CO bonds, followed by a rotation of the hydrogen atom attached to the carbon out of plane, and then the OH bond starts to dissociate. A second anion surface, connected to the first by a conical intersection, is involved in the dynamics and the transient anion must necessarily deform to nonplanar geometries to couple to this state, before it can dissociate to the observed stable products. These calculations were at a level to show the qualitative behavior not the actual reaction path. However more recently it was proposed that the dissociative attachment occurs via direct attachment to a σ^* orbital. New experiments have indicated a small isotope effect in the dissociation process. A strong isotope effect would favor the π^* mechanism, but the magnitude of effect was not large enough to rule either mechanism out. We propose to revisit this system carrying out higher level calculations in non-planar geometry to determine the position of the conical intersection between the two anion surfaces and an accurate path to dissociation.

Highly correlated processes in diatomic photoionization
An analog to dissociative attachment is dissociative recombination which has been well-studied due to its importance in applications such as planetary atomospheres, chemistry in interstellar clouds and combustion. Each electronic state of the molecular ion can support a series of neutral Rydberg states. Many of these states lie above the ground state of the ion and therefore are autoionizing resonant states. They appear in electron scattering calculations as resonances. These states can also be seen in photoionization. However, these generally carry little oscillator strength, have narrow widths and have potential energy curves that simply track their parent ion states. Some systems have non-Rydberg doubly excited states which are expected to have much larger oscillator strengths, since their spatial overlap with the initial state is large. The N_2, CO and O_2 cases are particularly interesting since their doubly excited valence states, near the equilibrium target geometry, can decay into many open electronic channels. Moreover, some of the states are expected to be steeply dissociative. We propose to carry out high-level electronic structure and coupled-channel, fixed-nuclei electron-ion scattering calculations to obtain the energies and lifetimes of these states as a function of nuclear geometry. We will also compute photoionization cross sections and study the branching ratios into different final ion states and how these vary with internuclear distance. The primary motivation for undertaking these studies is to see if these states are interesting candidates for XUV pump/probe experiments, which we expect they will be, especially if the calculations show a rapid change in the branching ratios with increasing internuclear distance. This work will also form a basis for further time-dependent studies of these states in the ultrafast program.

Publications

1. Isotope effect in dissociative electron attachment to HCN, S. T. Chourou and A. E. Orel, Phys. Rev. A **83** 032709 (2011)

2. Dissociative Electron Attachment to HCN, HCCH and HCCCN, S. T. Chourou and A. E. Orel, J. Phys.: Conf. Ser. **300** 012014 (2011)

3. Electron diffraction self-imaging of molecular fragmentation in two-step double ionization of water, H. Sann, T. Jahnke, T. Havermeier, K. Kreidi, C.Stuck, M. Meckel, M. Schöffler, N. Neumann, R. Wallauer, S. Voss, A.

Czasch, O.Jagutzki, Th. Weber, H. Schmidt-Böcking, S. Miyabe, A. E. Orel, T. N. Rescigno and R. Dörner, Phys. Rev. Lett. **106** 133001 (2011).

4. Vibrational Feshbach resonances in near threshold $HOCO^-$ photodetachment; a theoretical study, S. Miyabe, D. J. Haxton, K. V. Lawler, A. E. Orel, C. W. McCurdy and T. N. Rescigno, Phys. Rev. A **83** 043401 (2011).

5. The role of Jahn-Teller couplings in the DR of H_3O^+ and H_3^+ ions, N Douguet, A. Orel, I Mikhailov, I Schneider, C H Greene and V Kokoouline, J. Phys.: Conf. Ser. **300** 012015 (2011).

6. Dissociative electron attachment to carbon dioxide via the 8.2 eV Feshbach resonance, D S Slaughter, H Adaniya, T N Rescigno, D J Haxton, A E Orel, C W McCurdy and A Belkacem, J. Phys. B: At. Mol. Opt. Phys. **44** 205203 (2011).

7. Dynamic modification of the fragmentation of autoionizing states of O_2^+, W. Cao, G. Laurent, S. De, M. Schoffler, T. Jahnke, A. Alnaser, I. A. Bocharova, C. Stuck, D. Ray, M. F. Kling, I. Ben-Itzhak, Th. Weber, A. Landers, A. Belkacem, R. Dorner, A. E. Orel, T. N. Rescigno, and C. L. Cocke, Phys. Rev. A **84** 053406(2011).

8. Dissociative Recombination of Highly Symmetric Polyatomic Ions, Nicolas Douguet, Ann E. Orel, Chris H. Greene, and Viatcheslav Kokoouline, Phys. Rev. Lett. **108** 023202 (2012).

9. Breaking a tetrahedral molecular ion with electrons: study of NH_4^+, N. Douguet, V. Kokoouline and A. E. Orel, J. Phys. B: At. Mol. Opt. Phys. **45** 051001 (2012).

10. Time-resolved molecular-frame photoelectron angular distributions: Snapshots of acetylene-vinylidene cationic isomerization, N. Douguet, T. N. Rescigno, and A. E. Orel, Phys. Rev. A **86**, 013425 (2012).

11. Imaging Molecular Isomerization Using Molecular-Frame Photoelectron Angular Distributions, T. N. Rescigno, Nicolas Douguet and A. E. Orel, J. Phys. B: At. Mol. Opt. Phys. **45** 194001(2012).

12. Resonant enhanced electron impact dissociation of molecules, D S Slaughter, H Adaniya, T N Rescigno, D J Haxton, C W McCurdy, A Belkacem, Å Larson and A E Orel, J. Phys.: Conf. Ser. **388** 012016 (2012).

13. Theoretical study of excitation of the low-lying electronic states of water by electron impact, T. N. Rescigno, and A. E. Orel, Phys. Rev. A **88** 012703 (2013).

14. Carbon-K-shell molecular-frame photoelectron angular distributions in the photoisomerization of neutral ethylene, N. Douguet, T. N. Rescigno, and A. E. Orel, Phys. Rev. A **88** 013412 (2013).

"Low-Energy Electron Interactions with Liquid Interfaces and Biological Targets"

Thomas M. Orlando
School of Chemistry and Biochemistry and School of Physics,
Georgia Institute of Technology, Atlanta, GA 30332-0400
Thomas.Orlando@chemistry.gatech.edu, Phone: (404) 894-4012, FAX: (404) 894-7452

Project Scope: The primary objectives of this program are to investigate the fundamental physics and chemistry involved in low-energy (1-250 eV) electron and (25-200 eV) x-ray interactions with complex targets. There is a particular emphasis on understanding correlated electron interactions and energy exchange in the deep valence and shallow core regions of the collision targets. The energy loss channels associated with these types of excitations involve ionization/hole exchange and negative ion resonances. Thus, the energy decay pathways are extremely sensitive to many body interactions and changes in local potentials. Our proposed investigations should help determine the roles of hole exchange via interatomic and intermolecular Coulomb decay and energy exchange via localized shape and Feshbach resonances in the non-thermal damage of biological interfaces. The targets we will examine range in complexity from defined molecular thin films of biologically relevant bio-molecules (nucleotides, amino acids, DNA and RNA), aqueous solution interfaces and epitaxial graphene.

Recent Progress:

Project 1. Low-energy electron induced damage of DNA

Novel materials and devices that probe the dynamics and structure of biomolecules under non-equilibrium conditions are necessary to advance our understanding of processes such as radiation-induced carcinogenesis. Development of effective radiotherapy strategies also relies upon the ability to control low-energy electron induced DNA breakage *in vitro*. We have used a sensitive chemical vapor deposited graphene platform for controlled and enhanced sequence dependent DNA damage studies. The use of p-doped graphene substrates enhances DNA breakage due to phosphate mediated parallel adsorption geometries and direct ballistic electron transfer to phosphate σ* levels. Graphene adsorbed on Au-thin films also provides enhanced electric fields for Surface Enhanced Raman micro-spectroscopy. The combination of these effects allows direct and fast assessment of ≤ 1 eV electron induced DNA damage as a function of base sequence without separations and amplification steps. The results demonstrate that sequences containing guanine and adenine are most susceptible to damage using electron enegies <

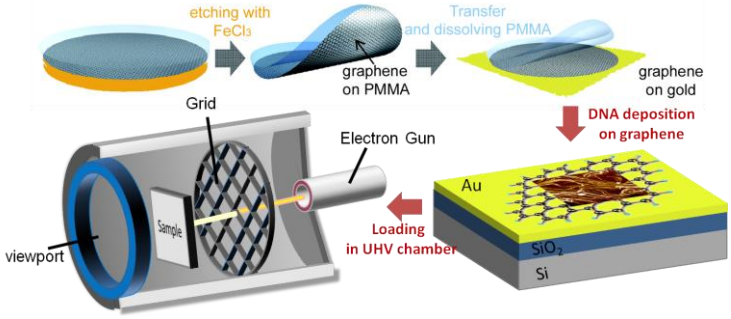

Figure 1. Schematic diagram of the experimental setup. The etching and transferring of a large area of graphene monolayer onto gold covered Si/SiO_2 substrate is followed by deposition of single strained DNA suspended in nanopure water. (Note: The AFM image of the DNA film on graphene is not to scale with the graphene and supporting substrate). The sample was then loaded in UHV chamber and irradiated by low energy electrons.

1 eV. In addition, the presence of interfacial water seems to enhance the damage probability.

We have also contributed to an experimental and theoretical study of the kinetic energy dependence of spin filtering of electrons by organized layers of DNA adsorbed on a gold substrate. The work was carried out in collaboration with Dr. Rosenberg of ANL. Using synchrotron radiation excitation, XPS CD measurements were made of electrons with energies in the range 30 to 760 eV. In all cases there was no evidence of any significant dichroism. These results are explained by a model in which the longitudinal polarization is strongly dependent on the k-vector, and hence the energy or the de Broglie wavelength. For a helix with a fixed number of turns, this dependence is due to a coherent process associated with multiple scattering. This model predicts that there is a window of energies where changes in the polarization should be expected. Two competing effects determine this window: the de Broglie wavelength must be small enough to be comparable to the spatial extension of the helix and it must be large enough so that the residence time of the electron in the scattering region allows for at least double scattering to take place.

Finally, our collaboration with Rosenberg has recently focused on examining x-ray damage of DNA adsorbed on Au in two different conformations. The first is a thiolated form which binds via a S bond and the other is direct adsorption via the bases. Differences in the damage cross sections are observed which can be related to the degree of charge exchange with the surface.

Project 2. Intermolecular Coulomb decay (ICD) and Coulomb explosions.

We are examining whether ICD occurs at weakly coupled molecular interfaces such as those present at hydrated DNA and protein "complexes". Initial work has focused on model systems such as ethane overlayers on water and tetrahydrofuran, a simple sugar, on water.

.

Project 3. Attosecond angle resolved photoemission studies of epitaxial graphene.

We have continued collaborating with Profs. H. Kapteyn and M. Murname on static, time- and angle-resolved photoemission of graphene substrates. To date, data has been obtained from epitaxial graphene grown on both the Si and C terminated faces of SiC(0001). We are carrying out these studies as a function of graphene thickness and are focusing on understanding the nature and carrier recombination rates at the so-called buffer layer. We have also begun studies on CVD graphene grown on Au.

Future Work

- The program will focus on ICD of mixed interfaces containing water and molecules representative of DNA backbones (i.e. sugars, phosphates and nucleosides). In addition, we will begin examining resonance Auger-ICD in DNA:Au clusters.

- The program will also continue low-energy electron induced damage of DNA by examining the sequence dependence of the break probability co-adsorbed with simple amino acids to address the role of protection by proteins.

- We will also carry out density functional and multiple scattering calculations to determine the binding interactions and excited states of DNA adsorbed on graphene. Longer term we plan to probe these interactions with time-resolved ARPES.

Presentations acknowledging support from this program during 2011-2013

1. T. M. Orlando, "The role of resonances and low energy electrons in the damage of DNA", Texas Tech., Lubbock, TX, April 20, 2011.
2. T. M. Orlando, "The interaction of low-energy electrons with complex biological targets", Gordon Research Conference on Photoions, Photoionization and Photodetachment, Galveston, TX, Feb. 12-17, 2012.
3. T. M. Orlando, "Stimulated Desorption and Dynamics at Weakly Coupled Heterogeneous Interfaces", International Workshop on Desorption Induced by Electronic Transitions XIIIE, Stratford-upon Avon, UK, July 2-6, 2012.
4. T. M. Orlando, "Very low-energy electron-induced damage of DNA", University of Rome, LaSapienza, July 10, 2012.
5. "Very low-energy electron-induced damage of DNA", Gaseous Electronics Conference, Univ. of Texas, Austin, Oct., 2012.
6. "The interaction of very low-energy electrons with complex biological targets", Institute of Theoretical Atomic and Molecular Physics Symposium, Harvard, University, Dec. 4-6, 2012.
7. "The interaction of very low-energy electrons with complex biological targets", Dept. of Physics, Vanderbilt, University, Feb. 2013.

Publications acknowledging support from this program during 2011-2013

1. B. O. Olanrewaju, J. Herring-Captain, A. Aleksandrov, G. Greives, and T. M. Orlando, "Probing the interaction of HCl on low-temperature water ice using thermal and non-thermal desorption", *J. Phys. Chem.* 115, 5936 (2011).
2. G. A. Greives and T. M. Orlando, "Intermolecular Coulomb decay at weakly coupled heterogeneous interfaces", *Phys. Rev. Lett.* 107, 016104 (2011).
3. B. O Olanrewaju, Ph.D. Thesis (2011), "Non-thermal processes on ice and liquid microjet surfaces".
4. A. N. Sidorov and T. M. Orlando, "Monolayer graphene platform for the study of DNA damage by low-energy electron irradiation", *J. Phys. Chem. Lett*., 4 (14), 2328–2333 (2013).
5. R. Rosenberg, J. M. Symonds, T. Z. Markus, T. M. Orlando and R. Naaman, "The lack of spin selectivity in low-energy electron induced damage of DNA films", *J. Phys. Chem. C.* doi: 10.1021/jp402387y (2013).

Structure from Fleeting Illumination of Faint Spinning Objects in Flight

A. Ourmazd, R. Fung, A. Hosseinizadeh, and P. Schwander
Dept. of Physics, University of Wisconsin Milwaukee
1900 E. Kenwood Blvd, Milwaukee, WI 53211
ourmazd@uwm.edu

It is now possible to interrogate molecules and their assemblies "in flight" with intense short pulses of radiation, and record "snapshots" before they are destroyed. We are developing a new generation of powerful algorithms to recover structure *and dynamics* from such ultra-low-signal random sightings. Combining concepts from differential geometry, general relativity, graph theory, and diffraction physics, these techniques promise to revolutionize our understanding of key processes in biological machines, such as enzymes, and ultrafast breaking of bonds in molecules. We report progress in two areas.

1. Spectroscopic movies of bond-breaking in N_2 with time resolution beyond pump-probe timing jitter (with P. Bucksbaum et al., and T. Seideman et al.)

Time-of-flight (ToF) spectra from pump-probe experiments using femtosecond IR-optical and X-ray pulses from the LCLS X-ray Free Electron Laser were analyzed to investigate the detailed processes underlying the Coulomb explosion of N_2 (Fig. 1). The temporal resolution of these experiments is limited by pump-probe timing jitter, measured to be ~300fs FWHM (*1*). We have succeeded in recovering dynamical information from such experimental data on timescales substantially below that set by pump-probe jitter.

The analysis proceeds as follows. We use graph-theoretic manifold-embedding techniques to determine the degrees of freedom open to the system. In order to determine the *dynamics*, i.e., the specific trajectory traversed by the molecule on the manifold during Coulomb explosion, we combine time-lagged embedding (*2*) with nonlinear singular value decomposition on the manifold (*3*). The resulting spectra reveal the characteristic (singular) modes of the ToF spectra, and the dynamics followed by each mode. Fig. 2 shows the time evolution of one of the characteristic modes resulting from this analysis. In essence, this spectral movie reveals the ultrafast dynamics of bond breaking in N_2 on timescales much shorter than the pump-probe timing jitter.

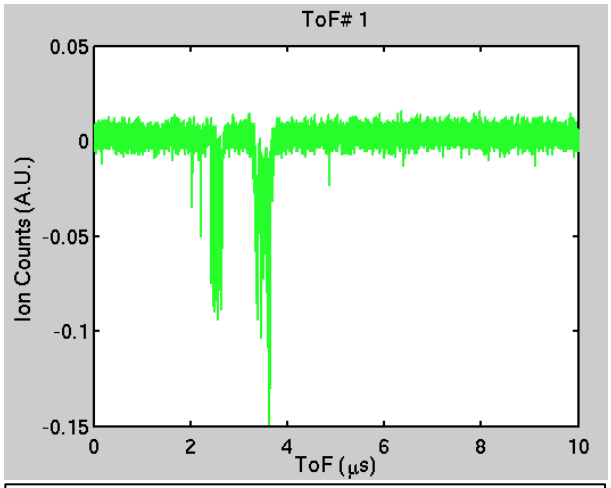

Fig. 1. Typical time-of-flight spectrum obtained from the Coulomb explosion of ~30 nitrogen molecules.

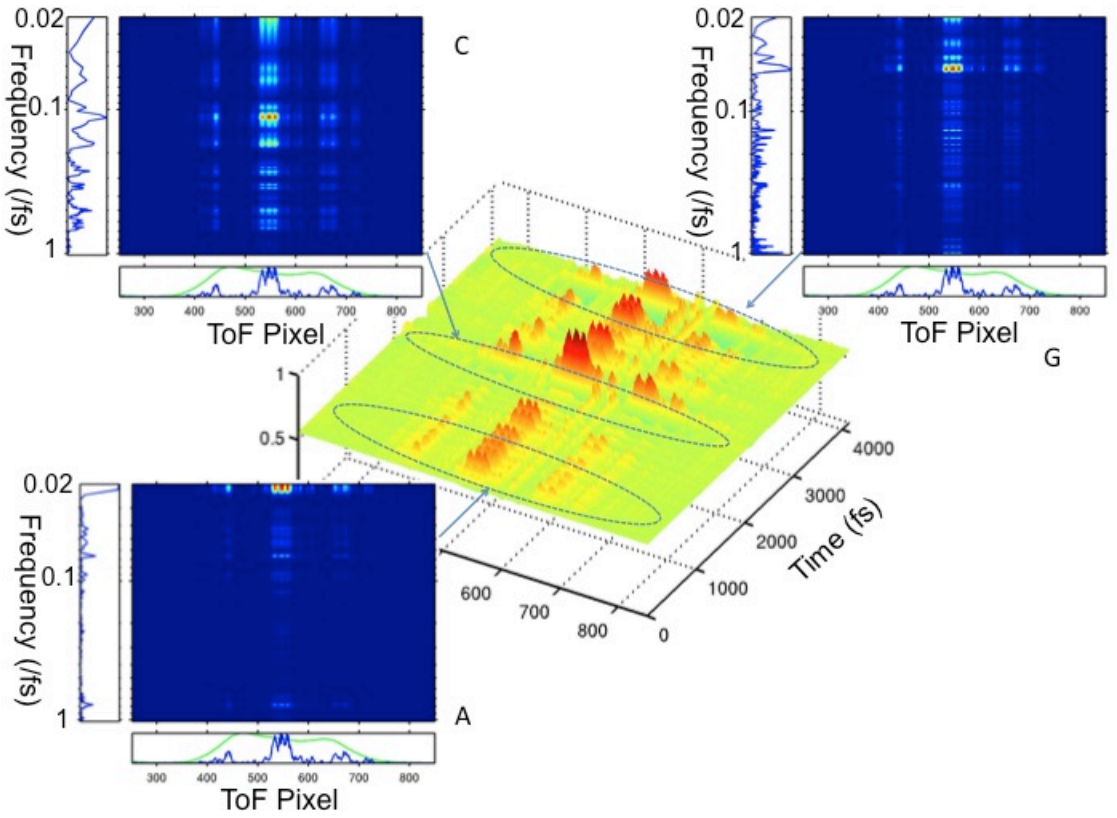

Fig. 2. The ToF movie obtained from a characteristic (SVD) mode, and Fourier power spectra for 500fs regions of the movie. The vertical and horizontal plots on each power spectrum represent column and row averages. The vertical plots quantify the frequency content of the rapid oscillations, and the fine structure along the horizontal ToF (energy) axis identifies the states involved.

As jitter represents a key limit for pump-probe experiments, particularly impacting the capability of SASE X-ray Free Electron Lasers for time-resolved work, our approach may substantially facilitate the study of ultrafast phenomena.

2. High resolution structure of viruses from random snapshots (with A. Hosseinizadeh, P. Schwander, A. Dashti, R. Fung, and R.M. D'Souza)

The advent of the X-ray Free Electron Laser (XFEL) has made it possible to record diffraction snapshots of biological entities injected into the X-ray beam before the onset of radiation damage. Algorithmic means must then be used to determine the snapshot orientations and thence the three-dimensional structure of the object. Existing Bayesian approaches are limited in reconstruction resolution typically to $1/10^{th}$ of the object diameter, with the computational expense increasing as the eighth power of the ratio of diameter to resolution. We have developed an approach capable of exploiting object symmetries to recover three-dimensional structure to $1/100^{th}$ of the object diameter, and

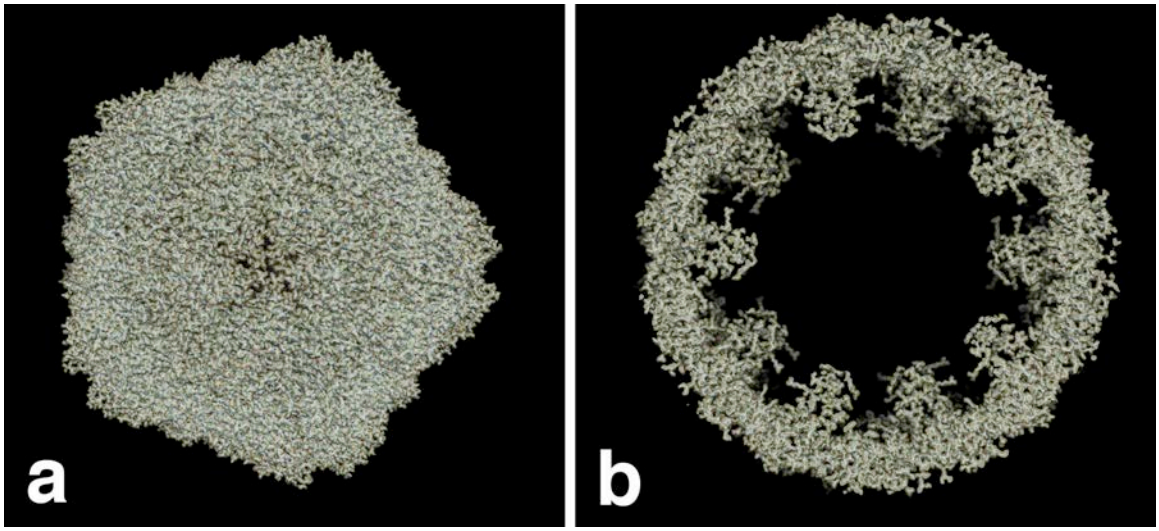

Fig. 3. Recovered structure of the satellite tobacco necrosis virus to atomic resolution. (a) The three-dimensional electron density extracted from 1.32 million diffraction snapshots of unknown orientation, demonstrating structure recovery to a resolution 1/100th of the object diameter (0.2nm). (b) A slice of the electron density showing atomic resolution. The known structure is shown as a ball-and-stick model without adjustment.

thus reconstructed the structure of the satellite tobacco necrosis virus to atomic resolution (Fig. 3). Combined with the previously demonstrated capability to operate at ultralow signal, our approach offers the highest reconstruction resolution for XFEL snapshots to date, and provides a potentially powerful alternative route for analysis of data from crystalline and nanocrystalline objects.

Publications from DoE sponsored research

1. C.H. Yoon et al., Unsupervised classification of single-particle X-ray diffraction snapshots by spectral clustering, Optics Express **17**, 16542 (2011).
2. D. Giannakis, P. Schwander, and A. Ourmazd, Symmetries of image formation: I. Theoretical framework, Optics Express **20**, 12799 (2012).
3. P. Schwander, D. Giannakis, C.H. Yoon, and A. Ourmazd, Symmetries of image formation: II. Applications, Optics Express **20**, 12827 (2012).
4. J.M. Glownia, A. Ourmazd, R. Fung, J. Cryan, A. Natan, R. Coffee, and P.H. Bucksbaum, CLEO Technical Digest, QW1F.3 (2012).
5. A. Hosseinizadeh, P. Schwander, A. Dashti, R. Fung, R.M. D'Souza, and A. Ourmazd, High resolution structure of viruses from random snapshots; under review.

References

1. J. M. Glownia *et al.*, *Optics Express* **18**, 17620 (Aug 16, 2010).
2. T. Sauer, J. A. Yorke, M. Casdagli, *Journal of Statistical Physics* **65**, 579 (1991).
3. D. Giannakis, A. J. Majda, *PNAS* **109**, (2011).

Control of Molecular Dynamics: Algorithms for Design and Implementation

Herschel Rabitz and Tak-San Ho

Princeton University, Frick Laboratory, Princeton, NJ 08540

hrabitz@princeton.edu, tsho@princeton.edu

A. Program Scope:

This research is concerned with the conceptual and algorithmic developments addressing control over quantum dynamics phenomena. The research is theoretical and computational in nature, aiming at developing a deeper understanding of quantum control and providing new algorithms to extend the laboratory control capabilities.

B. Recent Progress:

In the past year, a broad variety of research topics were pursued in the general area of controlling quantum dynamics phenomena. A summary of these activities is provided below.

1. **Discovering predictive rules of chemistry from property landscapes [1]**: This work introduced a novel method to reveal predictive chemical rules based on analysis of the chemical property landscape, which specifies the functional relationship between a measured property and an appropriate set of molecular variables. As an illustration, we considered landscapes for chemical shift and IR vibrational frequency with respect to the moieties attached to a carbonyl group. Implications of this Chemscape formulation for general molecular property prediction were discussed.

2. **Controllability analysis of quantum systems immersed within an engineered environment [2]**: In this work, we studied the problem of controllability of quantum systems interacting with an engineered environment, whose dynamics are described by a non-Markovian master equation. The manipulations of the dynamics was realized with both a laser field and a tailored nonequilibrium, and generally time-dependent, state of the surrounding environment. We used Lie algebra theory to characterize the structures of the reachable state sets and to prove controllability. The theoretical results were supported by examples.

3. **Topology of classical molecular optimal control landscapes in phase space [3]**: In this study, we considered the objective of steering a molecular system from an initial point in phase space to a target point, subject to the dynamic constraint of Hamilton's equations. The classical control landscape corresponding to this objective is a functional of the control field, and the topology of the landscape was analyzed through its gradient and Hessian with respect to the control. Under specific assumptions on the regularity of the control fields, the classical control landscape was found to be free of traps that could

hinder reaching the objective. We found that the Hessian associated with an optimal control field had finite rank, indicating the presence of an inherent degree of robustness to control noise. Extensive numerical simulations were performed to illustrate the theoretical principles, and to confirm the absence of traps in the classical control landscape.

4. **Maximum attainable field-free molecular orientation of a thermal ensemble with near-single-cycle THz pulses [4]**: This work examined the maximum attainable field-free molecular orientation with optimally shaped linearly polarized near-single-cycle THz laser pulses of a thermal ensemble. Large-scale benchmark optimal control simulations were performed, including rotational energy levels with quantum numbers up to J = 100 for OCS. The simulations were made possible by an extension of the recently formulated fast search algorithm to treat mixed-states optimal control problems. We showed that a very high degree of field-free orientation could be achieved by strong, optimally shaped near-single-cycle THz pulses.

5. **Dynamic homotopy and landscape dynamical set topology in quantum control [5]**: In this study, we examined the topology of the subset of controls taking a given initial state to a given final state in quantum control, where state may mean a pure state, an ensemble density matrix, or a unitary propagator. The analysis consisted in showing that the endpoint map acting on control space is a Hurewicz fibration for a large class of affine control systems with vector controls. Exploiting the resulting fibration sequence and the long exact sequence of basepoint-preserving homotopy classes of maps, we showed that the indicated subset of controls is homotopy equivalent to the loopspace of the state manifold.

6. **Exploring constrained quantum control landscapes [6]**: This work employed simulations to explore the topology and features of the control landscape for pure-state population transfer with a constrained class of control fields. The fields were parameterized in terms of a set of uniformly spaced spectral frequencies with the associated phases acting as the controls. Optimization results showed that the minimum number of phase controls necessary to assure a high yield in the target state had a special dependence on the number of accessible energy levels in the quantum system. Specifically, when an insufficient number of controls and/or a weak control fluence were employed, trapping extrema and saddle points were observed on the landscape. Moreover, when the control resources were sufficiently flexible, solutions producing the globally maximal yield became connected level sets of continuously variable control fields that preserve the yield. These optimal yield level sets shrank to isolated points on the top of the landscape as the control field fluence was decreased, and further reduction of the fluence turned these points into suboptimal trapping extrema on the landscape. The overall results show that progressive limitations placed on control resources lead an associated systematic reduction in system performance (i.e., rather than a sudden crash), which has importance practical experimental implications.

7. **Control in the Sciences over vast length and timescales [7]:** This work drew together experimental and theoretical findings from control landscapes in several domains of science with a particular focus on quantum control and manipulation in

chemical synthesis and property optimization. Strikingly similar landscape topology was found in these diverse domains for observables placed under optimal control. The collective behavior suggests that simultaneous control utilizing electromagnetic fields and chemical composition should lead to the best performance as well as enhanced ease of optimization.

C. Future Plans: The research in the coming year will focus on the formulation of new optimal control algorithms to allow for laboratory constraints, including on the fluence or the removal of dc and high frequency components of the control fields. Moreover, we plan to study the foundation for further understanding of control landscape structure, for example, by examining the linearity of gradient-based optimization trajectories through the space of control fields. We also plan to extend the current redundant landscape study on closed quantum systems to open quantum systems. Finally, we plan to continue our study on various atomic and molecular dynamics control problems, including molecular dynamics control in phase space, molecular isomerization control, laser-assisted ion-atom collisions, photo-association processes, and molecular alignment/orientation controls..

D. References

1. Discovering predictive rules of chemistry from property landscapes, K. W. Moore Tibbetts, R. Li, I. Pelczer, and H. Rabitz, Chem. Phys. Lett. 572, 1 (2013).
2. Controllability analysis of quantum systems immersed within an engineered environment, A. Grigoriu, H. Rabitz, and G. Turinici, J. Math. Chem. 51, 1548 (2013).
3. Topology of classical molecular optimal control landscapes in phase space, C. Joe-Wong, T.-S. Ho, R. Long, H. Rabitz, and Rebing Wu, J. Chem. Phys. 138, 124114 (2013).
4. Maximum attainable field-free molecular orientation of a thermal ensemble with near-single-cycle THz pulses, S.-L. Liao, T.-S. Ho, H. Rabitz, and S.-I Chu, Phys. Rev. A 87, 013429 (2013).
5. Dynamic homotopy and landscape dynamical set topology in quantum control, J. Dominy and H. Rabitz, J. Math. Phys. 53, 082201 (2012).
6. Exploring constrained quantum control landscapes, K. W. Moore and H. Rabitz, J. Chem. Phys. 137, 134113 (2012).
7. Control in the Science Over Vast Length and Time Scales, H. Rabitz, Quant. Phys. Lett. 1, 1 (2012).
8. Singularities of quantum control landscapes. Re-Bing Wu, Ruixing Long, Jason Dominy, Tak-San Ho, and Herschel Rabitz, Phys. Rev. A 86, 013405 (2012).
9. Critical Points of the Optimal Quantum Control Landscape: A Propagator Approach, Tak- San Ho, Herschel Rabitz and Gabriel Turinici, Acta Appl. Math. 118, 4956 (2012).
10. Laser-driven direct quantum control of nuclear excitations, Ian Wong, Andreea Grigoriu, Jonathan Roslund, Tak-San Ho, and Herschel Rabitz, Phys. Rev. A 84,

053429 (2011).
11. Fast-kick-off monotonically convergent algorithm for searching optimal control fields, Sheng-Lun Liao, Tak-San Ho, Shih-I Chu, and Herschel Rabitz, Phys. Rev. A 84, 031401(R) (2011) .
12. Bounds on the curvature at the top and bottom of the transition probability landscape, Vin- cent Beltrani, Jason Dominy, Tak-San Ho and Herschel Rabitz, J. Phys. B: At. Mol. Opt. Phys. 44, 154009 (2011).
13. Exploring quantum control landscapes: Topology, features, and optimization scaling, Katharine W. Moore and Herschel Rabitz, Phys. Rev. A 84, 012109 (2011).
14. Laser-assisted molecular alignment in a strongly dissipative environment, Dmitry Zhdanov and Herschel Rabitz, Phys. Rev. A 83, 061402(R) (2011).
15. Control of quantum phenomena, Constantin Brif, Raj Chakrabarti, and Herschel Rabitz, Adv. Chem. Phys. 148, 1-76 (2011).
16. Attaining persistent field-free control of open and closed quantum systems, E. Anson, V. Beltrani, and H. Rabitz, J. Chem. Phys. 134, 124110 (2011).
17. Exploring the top and bottom of the quantum control landscape, V. Beltrani, J. Dominy, T.-S. Ho and H. Rabitz, J. Chem. Phys. 134, 194106 (2011).
18. Volume fractions of the kinematic near-critical sets of the quantum ensemble control land- scape, J. Dominy and H. Rabitz, J. Phys. A, 44, 255302 (2011).
19. Optimal laser control of molecular photoassociation along with vibrational stabilization, E. F. de Lima, T.-S. Ho, and H. Rabitz, Chem. Phys. Lett. 501, 267 (2011).
20. Why is chemical synthesis and property optimization easier than expected? K. W. Moore, A. Pechen, X.-J. Feng, J. Dominy, V. J. Beltrani, and H. Rabitz, Phys. Chem. Chem. Phys. 13, 10048 (2011).
21. A general formulation of monotonically convergent algorithms in the control of quantum dynamics beyond the linear dipole interaction, T.-S. Ho, H. Rabitz, and S.-I Chu, Comp. Phys. Comm. 182, 14 (2011).
22. Search complexity and resource scaling for the quantum optimal control of unitary trans- formations, K. W. Moore, R. Chakrabarti, G. Riviello, and H. Rabitz, Phys. Rev. A 83, 012326 (2011).
23. Fidelity between unitary operators and the generation of robust gates against off-resonance perturbations, R. Cabrera, O. M. Shir, R. Wu, and H. Rabitz, J. Phys. A 44, 095302 (2011).

"Coherent and Incoherent Transitions"

F. Robicheaux
Purdue University, Department of Physics, 525 Northwestern Ave, West Lafayette IN 47907 (robichf@purdue.edu)

Program Scope

This theory project focuses on the time evolution of systems subjected to either coherent or incoherent interactions. This study is divided into three categories: (1) coherent evolution of highly excited quantum states, (2) incoherent evolution of highly excited quantum states, and (3) the interplay between ultra-cold plasmas and Rydberg atoms. Some of the techniques we developed have been used to study collision processes in ions, atoms and molecules. In particular, we have used these techniques to study the correlation between two (or more) continuum electrons and electron impact ionization of small molecules.

Recent Progress 2012-2013

Multiphoton ionization: We performed a large series of calculations to explore the role of the Keldysh parameter versus the frequency of the laser. Because most strong laser experiments use frequencies much smaller than the electronic frequencies in the atom, research has mainly focused on the role of the Keldysh parameter and its role in distinguishing between the multiphoton or tunneling regimes in this regime. We performed a large number of fully quantum calculations for a range of frequencies and found that the multiphoton vs. tunneling regime also strongly depends on the frequency of the laser. We used both the ionization rates and the final momentum distributions of the electrons to show how the divide between the two regimes depends on both the laser intensity and frequency. We found that scaling the laser frequency by the electron frequency provided a more meaningful measure of how to characterize the dynamics.

Extreme Rydberg system: We were part of a joint experimental/computational study of a time dependent two electron system.[18] We investigated the time-dependent evolution of wave packets where two electrons were excited to states just below the threshold for three-body breakup. We created the states using two short laser pulses: the first pulse put an electron into a Rydberg wave packet and the second pulse excited a second valence electron into a Rydberg wave packet of nearly the same size. The measurements and calculations found substantial energy exchange between the two electrons is nearly immediate upon the launch of the second electron. Calculations also showed very fast angular momentum exchange and sensitivity to the relative binding energies of the two electrons.

Two-electron ionization: For over a decade, we have made the calculation of two electron processes a high priority; calculations were performed for a wide variety of processes (for example, photo-double ionization, electron-impact ionization, etc) and for a variety of atomic and molecular systems. This undertaking is worth the long term effort because the correlations that develop as the two electrons leave the atom/molecule are important for understanding how energy and angular momentum can be transferred between two or more quantum degrees of

freedom. In Ref. [19], we extended the time dependent close coupling method to use model potentials with projection on orbitals of filled shells to enable calculations for heavier alkaline earth atoms. A key feature was to use an implicit propagator for the wave function which allowed the use of a variable mesh which gives accurate core orbitals. By projecting out the closed shell orbitals, we could prevent scattering into unphysical states. Calculations for Be and Mg illustrated the accuracy of these extensions.

Imaging of quantum state inside atom: We were involved in two experimental/computational projects to image a part of the wave function inside an atom.[20,21] The experiments used photoionization microscopy to image the variation in the wave function perpendicular to the electric field. The calculations involved a direct solution of the time dependent Schrodinger equation in a region ~30,000 Bohr radii by using a mixture of spherical harmonics (up to 300) and time dependent radial functions on a grid of points; the calculations were difficult both due to the large region of the wave function but also for the long times (6 ns) that needed to be simulated. In Ref. [20], we used Li atoms to image the transverse part of the wave function. We found characteristic resonant features, such as (i) the abrupt change of the number of wave function nodes across a resonance and (ii) the broadening of the outer ring of the image associated with tunnel ionization. The electron spatial distribution measured by the microscope is a direct macroscopic image of the projection of the microscopic squared modulus of the electron wave. In Ref. [21], we performed a similar measurement and calculation using H atoms. The H atom is unique, since it only has one electron and, in a dc electric field, the Stark Hamiltonian is exactly separable in terms of parabolic coordinates. Thus, the nodal structure near the nucleus is exactly preserved to macroscopic distances where we directly observed them.

Finally, this program has several projects that are strongly numerical but only require knowledge of classical mechanics. This combination is ideal for starting undergraduates on publication quality research. Since 2004, twenty three undergraduates have participated in this program. Most of these students have completed projects published in peer reviewed journals. Two undergraduates, Michael Wall in 2006 and Patrick Donnan in 2012, were one of the 5 undergraduates invited to give a talk on their research at the undergraduate session of the DAMOP meeting. There were 6 students doing research during the 2012-13 school year, but there will be few, if any, during the 2013-14 year due to starting research at a new university where I have not built up the infrastructure needed to recruit high quality undergrads and effectively train them in computational science.

Future Plans

Attosecond ionization: Experiments on ionization of atoms by attosecond laser pulses have been able to probe the dynamics of near ground state electrons. Investigations have focused on processes involving a single attosecond photon due to the weakness of the laser source. In anticipation of higher power in the future, we will perform calculations of two photon processes (e.g. hole burning in the initial wave function, Raman transitions, 2 photon absorption through a Cooper minimum, etc) and possible implications for three photon processes.

Rydberg Physics Recently published (and some unpublished) measurements from T. F. Gallagher's group show startling behavior of Rydberg atoms in very strong microwave fields. In particular, they find that atoms that are laser excited to near threshold (and above threshold!) energies while the microwaves are on can survive to extremely long times. We will perform quantum and classical calculations for this system to understand the mechanisms that lead to survival. This is a difficult problem because the interesting quantum physics extend to distances of $\sim 10^6$ a_0.

Two electron physics We have recently developed a method for dealing with the quantum mechanics when two electrons extend over very large regions and/or interact for a long time.[15,16,18] We will use our fully quantum method to test the range of validity of some of the approximations that are standard in PCI. We are also interested in further pursuing the time dependent double Rydberg system[18] but explicitly putting in quantum defects for the electrons and exploring the case where the two electrons have unequal excitation.

DOE Supported Publications (7/2010-8/2013)

[1] T.-G. Lee, M.S. Pindzola, and F. Robicheaux, J. Phys. B **43**, 165601 (2010).
[2] T. Topcu and F. Robicheaux, J. Phys. B **43**, 205101 (2010).
[3] F. Robicheaux, S.D. Loch, M.S. Pindzola, and C.P. Ballance, Phys. Rev. Lett. **105**, 233201 (2010).
[4] S.D. Bergeson, A. Denning, M. Lyon, and F. Robicheaux, Phys. Rev. A **83**, 023409 (2011).
[5] M.S. Pindzola, S.D. Loch, and F. Robicheaux, Phys. Rev. A **83**, 042705 (2011).
[6] M.S. Pindzola, J.A. Ludlow, C.P. Ballance, F. Robicheaux, and J. Colgan, J. Phys. B **44**, 105202 (2011).
[7] T. Topcu and F. Robicheaux, Phys. Rev. E **83**, 046607 (2011).
[8] I. Yavuz, Z. Altun, and T. Topcu, J. Phys. B **44**, 135403 (2011).
[9] K. Niffenegger, K. A. Gilmore, and F. Robicheaux, J. Phys. B **44**, 145701 (2011).
[10] P.H. Donnan, K. Niffenegger, T. Topcu, and F. Robicheaux, J. Phys. B **44**, 184003 (2011).
[11] M.S. Pindzola, Sh. A. Abdel-Naby, J.A. Ludlow, F. Robicheaux, and J. Colgan, Phys. Rev. A **85**, 012704 (2012).
[12] I. Yavuz, E.A. Bleda, Z. Altun, and T. Topcu, Phys. Rev. A **85**, 013416 (2012).
[13] P.H. Donnan and F. Robicheaux, New. J. Phys. **14**, 035018 (2012).
[14] M.S. Pindzola, Sh. A. Abdel-Naby, F. Robicheaux, and J. Colgan, Phys. Rev. A **85**, 032701 (2012).
[15] F. Robicheaux, J. Phys. B **45**, 135007 (2012).
[16] F. Robicheaux, M.P. Jones, M. Schoffler, T. Jahnke, K. Kreidi, J. Titze, C. Stuck, R. Dorner, A. Belkacem, Th. Weber, and A.L. Landers, J. Phys. B **45**, 175001 (2012).
[17] T. Topcu and F. Robicheaux, Phys. Rev. A **86**, 053407 (2012).
[18] X. Zhang, R. R. Jones, and F. Robicheaux, Phys. Rev. Lett. **110**, 023002 (2013).

[19] M. S. Pindzola, C. P. Balance, Sh. A. Abdel-Naby, F. Robicheaux, G. S. J. Armstrong, and J. Colgan, J. Phys. B **46**, 035201 (2013).
[20] S. Cohen, M. M. Harb, A. Ollagnier, F. Robicheaux, M. J. J. Vrakking, T. Barillot, F. Lepine, and C. Bordas, Phys. Rev. Lett. **110**, 183001 (2013).
[21] A. S. Stodolna, A. Rouzee, F. Lepine, S. Cohen, F. Robicheaux, A. Gijsbertsen, J. H. Jungman, C. Bordas, and M. J. J. Vrakking, Phys. Rev. Lett. **110**, 213001 (2013).

Generation of Bright Soft X-ray Laser Beams

Jorge J. Rocca
Department of Electrical and Computer Engineering and Department of Physics
Colorado State University, Fort Collins, CO 80523-1373
rocca@engr.colostate.edu

Program description

This project addresses the challenge of the efficient generation of bright x-ray laser beams. In table-top experiments conducted at Colorado State University during this grant period we extended gain-saturated table-top lasers to a λ= 8.8 nm laser emitting pulses of > 2 μJ energy, and have demonstrated 100 Hz repetition rate soft x-ray laser operation to produce a record average power of 0.15 mW at λ=18.9 nm. Recently we measured the wavefront of an injection-seeded soft x-ray laser at this wavelength using a Hartmann wavefront sensor with an accuracy of λ/32. A significant improvement in wavefront aberrations to 0.23±0.01λ was observed as a function of plasma column length. The measurements were used to reconstruct the soft x-ray source and confirm its high peak brightness We have also collaborated in an experiment at LCLS that demonstrated strong stimulated x-ray Raman scattering by resonantly exciting a dense gas target with femtosecond high-intensity x-ray pulses from an x-ray free-electron laser (XFEL). A small number of lower energy XFEL seed photons drive an avalanche of stimulated resonant inelastic x-ray scattering processes that amplify the Raman scattering signal by several orders of magnitude until it reaches saturation. Despite the large overall spectral width, the internal spikey structure of the XFEL spectrum determines the energy resolution of the scattering process. This is demonstrated by observing a stochastic line shift of the resonance Raman scattered x-ray radiation. In conjunction with statistical methods, XFELs can hence be used for stimulated resonant inelastic x-ray scattering, with spectral resolution smaller than the natural width of the core-excited, intermediate state.

Wavefront improvement of table-top soft x-ray laser by injection-seeding

A dramatic improvement in both spatial and temporal coherence of plasma-based soft x-ray lasers (SXRLs) was demonstrated from injection-seeding of SXRL plasma amplifiers with high harmonic pulses. We have measured the wavefronts of an injection-seeded SXRL created by irradiation of a solid target for the first time using a soft x-ray Hartmann wavefront sensor. The experimental set-up is schematically represented in Fig. 1(A). The plasma amplifier and seed pulses were generated using pulses from the table-top Ti:Sa laser were used to heat the plasma, and an additional pulse split from the same laser was used to generate the HHG seed. The Hartmann wavefront sensor has accuracy of λ/32 root mean square (rms) at 18.9 nm. It comprises an array of 51 × 51 square holes 80 μm in size over a 19 × 19 mm 2 area placed at about 310 mm in front of a back-illuminated x-ray CCD. The main conclusion of this experiment is that although SXRL plasma amplifier from solid targets are significantly denser than gas-based SXRL amplifiers for which wavefront was previously measured, they produce a good wavefront with distortions reaching λ/5 rms. As previously observed in the case of the gas amplifier case, the small size of gain zone acts as an spatial filtering of the incoming beam, that results in a reduction of the wavefront aberration by a factor of up to 2.5. The statistical studies we conducted observe that the wavefront of the SSXRL beam is more stable than that of the HHG seed, opening the possibility to implement static or active wavefront correction. The wavefront sensor allows for independent measurement of the different aberrations. In Fig.1(B) we plotted the values of the three strongest aberrations over 25 shots. The strongest improvement is observed for coma, with values improved by more than a factor of 2, from 0.4lλ to 0.18λ rms. Coma generates a central spot surrounded by many rays extending far from it . This spot is selectively amplified while the surrounding rays are much less

amplified, generating the observed drop of coma aberration. In comparison, astigmatism at 0 or 45 degrees tends to slightly increase the focal spot size in the region of "least confusion", meaning that the active spatial filtering effect of the gain zone is less effective, agreeing well with the measured values of astigmatism. Indeed, for 0 degree astigmatism the wavefront drops from about 0.10λ rms to the detection limit, while 45 degrees astigmatism being already low before amplification does not show significant changes. We also reconstructed the beam intensity distribution near the plasma location. Wavefront changes were observed when the seed pulse injection time was varied, which result from the different hydrodynamic and gain conditions. This measurement of the source size of a seeded solid target SXRL confirms the high brightness of about 1×10^{26} photons/ s•mm^2•mrad^2 .

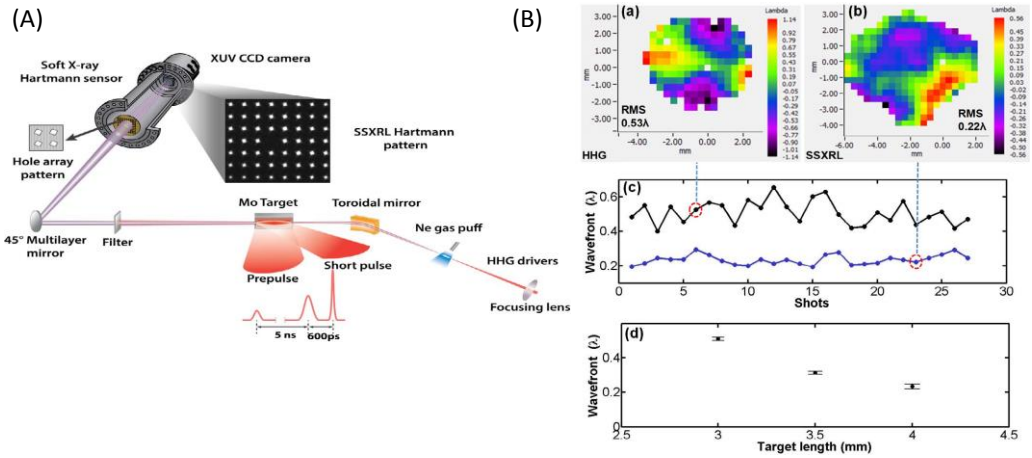

Fig. 1 (A) Schematic diagram of the experimental set-up used to measure the wavefront of an injection-seeded SXRL based on solid target plasma with a Hartmann sensor.: (B) 2D map of the wavefront after correction of tilt and spherical aberrations for: (a) HHG seed, (b) SSXRL. (c) Residual wavefront values of HHG seed (black line) and SXRL (4mm target). (d) Residual wavefront error values for the SSXRL from plasma lengths of 3.0mm, 3.5mm and 4.0mm.

Stimulated electronic x-ray Raman scattering

The high penetration depth of x-rays, combined with the element and chemical sensitivity of the x-ray Raman scattering process, could open pathways to temporally resolve complex dynamical processes. However, the cross section for x-ray Raman scattering is small compared to that in the visible spectral domain. This difficulty could be overcome by stimulating the Raman scattering process to produce a strong coherent amplification of the signal. We realized the first demonstration of stimulated resonant electronic x-ray Raman scattering (SRXRS) in an atomic gas with a self-amplified spontaneous emission (SASE) XFEL. These XFELs provide x-ray pulses of a spiky, noise-like spectrum with a bandwidth of several eV, a range that typically covers the excitation energy of several transitions. Despite the broad spectral bandwidth, the intrinsically incoherent, spectrally structured SASE XFEL pulses give high energy-resolution of the scattering process in a statistical sense. Compared to the spontaneous RXRS process, a signal enhancement of 7-9 orders of magnitude was achieved. SRXRS is positioned to become a powerful method for pump-probe studies at XFELs.

In the experiment, pulses from the LCLS XFEL of ≈40 fs duration were focused into a neon gas cell filled with a pressure of ≈500 Torr (Fig. 2 A). The on-axis x-ray radiation was analyzed with a flat-field grazing incidence spectrograph (see raw image in Fig. 2B). The XFEL photon energy was varied across the K edge (870.2 eV). For photon energies below the K edge, neutral atoms are core excited by resonant

excitation of the 1s shell. Due to the high intensities of the focused XFEL beam (~10^{17} W/cm^2), the resonant population transfer happens on a fs timescale. Thereby, a sizeable, but transient population inversion between the 1s and the valence shell is achieved. Despite the small branching ratio of radiative versus Auger decay of ≈1.7 %, a few seed photons at the 1s-2p emission frequency suffice to drive an avalanche of stimulated scattering events, which results in exponential amplification of the Raman signal. The geometry of this single-pass SRXRS amplifier is determined by the tight (1-2 µm, determined by the focus spot size) and long (2 mm) longitudinally pumped gain medium.

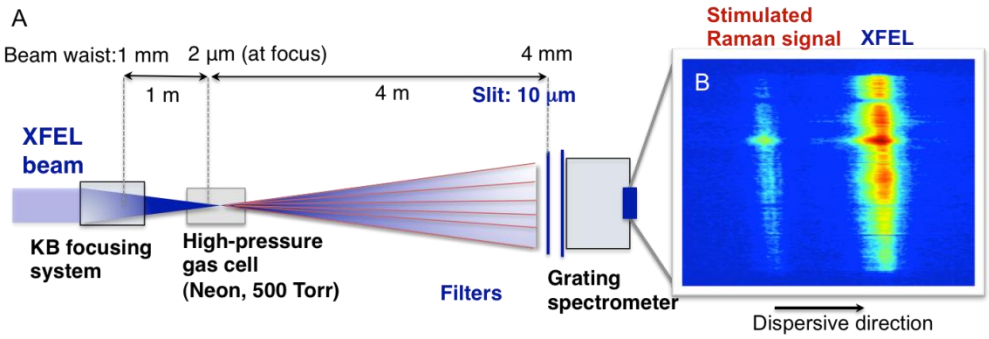

Fig. 2. (A) Stimulated X-ray Raman scattering experimental set up. The XFEL pulses are focused into a gas cell of 9.5 mm length filled with neon to spot sizes of ≈2 µm. A grating spectrometer of ≈1 eV energy resolution is fielded downstream. (B) Typical raw spectrum.

We measured an emission in the forward direction in a narrow cone of ≈1 mrad divergence. The strongest x-ray scattering channel involves the intermediary $1s^1 3p\ ^1P_1$ level (867.5 eV) and the final $2p^1 3p\ ^1S$ level, resulting in an emission at 849.3 eV. The process is stimulated by the spectral tail of the XFEL pulse, providing ~10^2-10^4 seed photons of ≈850 eV for a central incoming photon energy of ≈867 eV Fig. 3 A shows the recorded emission spectra for XFEL photon energies, ω_{in}, ranging from 862 to 880 eV. The XFEL pulse follows the diagonal. The amplified line emission corresponds to the vertical structure at around 850 eV, which was detected for ω_{in} as low as 866 eV. Due to the broad XFEL bandwidth (7 eV FWHM), covering the whole Rydberg series and part of the continuum, the SRXRS emission is not well separated from the Kα emission above the edge.

A systematic analysis of the measured line shape as a function of the XFEL photon energy shown in Fig. 3A demonstrates that the emission for ωin<870 eV stems from SRXRS. Whereas for ω_{in}>870 eV the peak position (849.2 ± 0.1eV) and the line shape are very reproducible from shot to shot, for ω_{in}<870 eV the lines show a stochastic shift of ± 0.4 eV, broadening, and sometimes a multi-peak structure that can be linked to stochastic detuning of the multiple spectral spikes of the SASE XFEL from resonance. Each spectral spike can be seen as a monochromatic x-ray pulse of a specific detuning **Δ**, resulting in detuning of the emission energy. The SRXRS process is dominated by one or a few of such spikes for each shot. Since the positions of the XFEL spectral spikes vary from shot to shot, this results in a stochastic line shift of the SRXRS signal. To support this interpretation, the SRXRS spectra was simulated by solving master equations for the multi-component atomic and ionic density matrix self-consistently coupled to one-dimensional Maxwell equations for an ensemble of numerically generated SASE XFEL pulses with varying incoming XFEL photon energy ω_{in}. Fig. 3D shows calculated single-shot emission spectra as a function of the incoming photon energy. In agreement with the experiment (Fig. 3E), the emitted line shows stochastic detuning for ω_{in}<870 eV and evolves into a reproducible form for ω_{in}>870. To demonstrate the exponential signal amplification, we studied the SRXRS signal strength as a function of the incoming XFEL pulse energy and compared to the theoretical model. Varying the pulse energy from 0.08 to 0.35 mJ results in a signal increase by almost 4 orders of magnitude. It is noteworthy that the spontaneous RXRS process in the experimental geometry would yield ~100 photons in the plane of the spectrometer

slit, compared to the measured 10^9-10^{11}. Compared to the spontaneous RXRS process, a signal enhancement up to a factor of $e^{16} – e^{21}$ was recorded, reaching saturated amplification. Looking forward, SRXRS might enable time-domain spectroscopy and non-linear techniques in the x-ray domain with broad applications to study ultrafast chemical and materials dynamics.

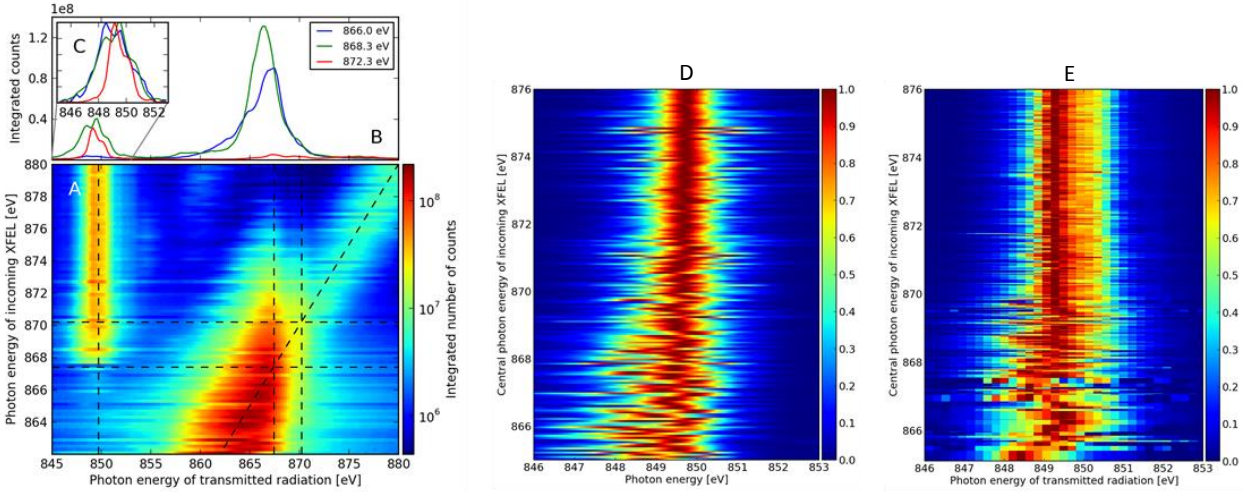

Fig. 3. (A) Experimental spectra as a function of the incoming XFEL photon energy. The plot has been assembled from 984 single-shot spectra.. The positions of the $1s^{-1}3p$ (867.5 eV) and the K edge (870.2 eV) and the emission line (849.7 eV) are marked by dashed lines. (B) Three measured single-shot spectra for central XFEL photon energies at 866 eV, 868.3 eV and 872.3 eV. (C) Zoom of the normalized emission lines. (D)) Simulated SRXRS emission spectra emission line profiles as a function of the XFEL photon energy. (E) Measured 819 single-shot emission line profiles normalized to their intensity maximum.

Journal publications resulting from DOE-BES supported work (2011-2013)

1. Lu Li. Y. Wang. S. Wang, E. Oliva, L.Ying, T.T. Thuy Le, S. Daboussi, D. Ross, G. Maynard, S. Sebban, B. Hu, J.J. Rocca P. Zeitoun, "Wavefront improvement in injection-seeded soft x-ray laser based on solid-target plasma amplifier" , Optics Letters (in press, September 2013).
2. C. Weninger, M. Purvis, D. Ryan, R.A. London, J.D. Bozek, C. Bostedt, A. Grapf, G. Brown, J.J. Rocca, N. Rohringer, "Stimulated electronic X-ray Raman scattering", submitted Phys. Rev. Lett. (2013).
3. Y. Wang, S. Wang, E.Oliva, L. Lu, M. Berrill, L. Ying, J. Nejdl, B.M. Luther, C. Proux, T.T.T Le, J. Dunn, D. Ros, Ph. Zeitoun, J.J. Rocca, "Gain dynamics in soft X-ray laser amplifier perturbed by a strong injected X-ray field", submitted, September 2013.
4. N.Rohringer, D. Ryan, R. London, M. Purvis, F. Albert, J. Dunn. J.D.Bozek, C.Bostedt, A. Graf, R. Hill, S.P. Hau-Ridge, J.J. Rocca,, "Inner-shell X-ray laser at 1.46 nm pumped by an X-ray free electron laser", Nature, **481**,488, (2012).
5. L. Urbanski, M.C. Marconi, L.M. Meng, M. Berrill, O. Guilbaud,A. Klisnick, J.J. Rocca, "Spectral linewidth of a capillary discharge Ne-like Ar soft X-ray laser and its dependence on amplification beyond gain saturation", Physical Review A, **87**, 033837, (2012).
6. S. Carbajo, I.D. Howlett, F. Brizuela, K.S. Buchanan, M.C. Marconi, W. Chao, E.H. Anderson, I. Artioukov, A. Vinogradov, J.J. Rocca and C.S. Menoni, "Sequential single-shot imaging of nano-scale dynamic interactions with a table-top soft x-ray laser", Optics Letters, **37**, 2994 (2012).
7. B. Reagan, K. Wernsing, A. Curtis, F. Furch, B. Luther, D. Patel, C.S. Menoni ,J.J. Rocca, " Demonstration of a 100 Hz repetition rate gain-saturated diode-pumped soft x-ray laser". Optics Letters ,**37**, 3624 (2012).
8. H. Bravo , B.T. Szapiro , P. Wachulak,, M.C. Marconi, W. Chao , E.H. Anderson, D.T. Attwood, C.S. Menoni, J.J. Rocca, " Demonstration of nanomachining with focuses EUV laser beams", IEEE J. of Selec Top. in Quant. Elect, **18**, 443, (2012).
9. D. Alessi, Y. Wang, D. Martz, B. Luther, L.Yin, D. Martz, M. Woolston, Y. Liu, M. Berrill, J.J. Rocca, "Efficient excitation of gain-saturated sub-9 nm wavelength table-top soft X-ray lasers and lasing down to 7.36 nm", Phys.Rev. X, **1**, 021023 (2011).
10. L.M. Meng, D. Alessi, O. Guilbaud, Y. Wang, M. Berrill, B.M. Luther, S.R. Domingue, D.H. Martz, D. Joyeux, S. De Rossi, J.J. Rocca , A. Klisnick, "Temporal coherence and spectral linewidth of an injection-seeded transient collisional soft x-ray laser", Optics Express , **19**, 12087, (2011).

Spatial Frequency X-ray Heterodyne Imaging of Micro and Nano structured Materials and their Time-resolved Dynamics

Christoph G. Rose-Petruck

Department of Chemistry, Box H, Brown University, Providence, RI 02912
phone: (401) 863-1533, fax: (401) 863-2594, Christoph_Rose-Petruck@brown.edu

1 Program Scope

This program focuses on the development of a novel imaging modality called Spatial Frequency Heterodyne Imaging (SFHI), which enables the quantification of nanoscopic changes inside of sample objects. SFXHI uses the x-radiation scattered off the sample to form an image. A related method using single-crystal x-ray mirrors is known as diffraction-enhanced imaging. In SFXHI however, the deflection of x-rays from the primary beam direction is detected by placing an absorption grid between the sample and the camera. The logarithm of the detected image intensity is approximately proportional to the product of the transmittances of the sample and the grid. Fourier transformation of the acquired images converts this product into a convolution, which results in heterodyning of the spatial frequencies of the sample and that of the grid. This effect permits the numerical separation of the acquired images into one with absorption information and two images with orthogonal small-angle scatter information. As a result, the density and orientation of nanostructures can be measured. In the future chemical sensitivity will additionally be possible.

We applied SFHI to measure the Gibbs Free Energy changes of water phase transitions inside of carbon nanotubes (CNTs). Comparative imaging measurement of samples using SFHI and Magnetic Resonance Imaging (MRI) allowed benchmarking the sensitivity of SFHI to the nanoparticle densities in objects. We performed the first soft x-ray SFH imaging experiments using a laser-driven plasma x-ray source. The theoretical description was tested in the 400-eV regime. Based on these data, we can extrapolate possibilities for future lens-less x-ray microscopic applications.

During the last year we also continued our work at the Advanced Photon Source, 7ID-C with specific focus in the improvement of the signal-to-noise of our measurements. During this time we used our assigned beamtime as APS Partner-users, which was granted for the period from the fall 2011 to the fall 2013 for the development of an ultrafast XAFS beamline endstation. 2-ps resolution XAFS measurements of the charge-transfer to solvent (CTTS) of $Fe(CN)_6^{4-}$ were measured.

12 published papers acknowledge this DOE grant.[1-12] In 2012 - 2013, one paper on hard-x-ray SFHI was published[6] and four papers (ultrafast XAFS at the APS[13], soft x-ray SFHI with plasma source[14], SFHI of water phase transitions in carbon nanotubes[15], SFHI and MRI sensitivity comparison[16]) are currently being written or have been submitted.

2 Recent Progress Details

2.1 SFHI of water phase transitions in carbon nanotubes

Water in confined spaces can show unusual properties that are not observed in the bulk. Carbon Nanotubes are made of hydrophobic graphene sheets. Despite the hydrophobic nature of the grapheme sheets, experimental studies have revealed that water can be confined in CNTs. Transmission Electron Microscopy and x-ray diffraction have been used to probe the behavior of water in CNTs. Our objective is to develop SFHI as an X-ray detection method suitable for studying phase transitions in nanomaterials.

We observed wetting and capillary filling of CNTs by water through the small angle x-ray scattering distribution as a function of temperature obtained by SFHI. In principle, the intensity of the x-ray scatter images has been used, after appropriate calibration and data processing, as a measure of the hydration of the CNTs.

Multi-walled carbon nanotubes (MWCNTs) produced by chemical vapor deposition were obtained from Nano Lab. Inc. The MWCNTs were reported to have an inner diameter of 7±2 nm, outer diameter of 15 ±5 nm and lengths of 1-5 microns. A portion of the as purchased MWCNTs were placed in a Pyrex tube, and heated to 500 °C in air for twenty four hours in order to uncap the ends of the CNTs through annealing and partial oxidation. Two heat-treated and two as-purchased 60-mg samples of MWCNTs were vacuum sealed in NMR tubes. Prior to sealing the samples one of the as-purchased and one of the heat-treated samples each had 250 ul of nano-pure water added to them. The four samples were then placed in an aluminum holder fitted with two heating elements and a thermocouple. The CNTs were packed in one end of the sealed NMR tube such that the vacant opposite end extended well beyond the end of the aluminum holder. This allowed for one end of the evacuated NMR tubes to remain near room temperature throughout the experiment, establishing a thermal gradient within the tube at elevated temperatures. The gradient promoted water to condense outside of the field of view during heating. The volume

occupied by the CNTs did not exceed the dimensions of the holder. Many SFH images were measured at various sample temperatures.

Before each experiment the samples were heated to 80 °C for 30 minutes in order to expel excess water from the sample to the vacant end of the NMR tubes. These average pixel values were then averaged between those measured from the vertical and horizontal second harmonics. The intensities were then plotted as a function of temperature (Figure 1). The two curves show the heat treated (HW) and original samples (OW) that had water added to them. The error bars are one standard deviation of the mean. Clearly the method of heat-treatment used that uncapped the ends of the CNTs produces a difference in the interaction of water and the CNTs. The HW tubes show two transitions, while the OW tubes show only one. The first transition common to both samples occurs at about 40 °C, while the second transition only seen in the HW sample occurs at 120 °C. The first transition is taken to be the expulsion of water from the exterior surface of the carbon nanotubes. The second transition is identified as the removal of water from within the CNTs. This evaporation at elevated temperatures has also been observed in the literature to occur from approximately 110 °C to 260 °C. The temperature-dependent scatter intensities were used to calculate the thermodynamics data for the transitions. These data are listed in Table 1. SFHI is very powerful in measuring thermodynamic data because the imaging modality simultaneously samples a large ensemble of particles by virtue of imaging a large sample area. In the future this study will be expended to measurements of the wetting properties of multi-layer graphene membranes.

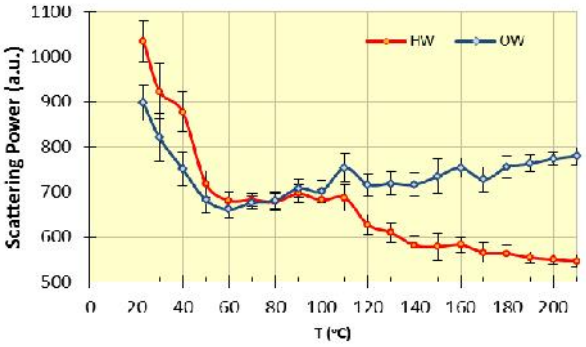

Figure 1: Scatter power of wet CNTs vs. temperature. One phase transition at about 40 °C and one at 120 °C are visible for the heat-treated (HW) CNTs. The second phase transition is absent for the original, untreated (OW) CNTs.

	ΔG (kJ/mol)	Error (kJ/mol)
First Transition	**-5.01**	**±0.90**
Second Transition	**-1.46**	**±0.29**

Table 1: Thermodynamic data of heat-treated, wet CNTs.

2.1.1 SFH imaging and Magnetic Resonance Imaging (MRI) of nanomaterials

Nanoparticles scatter x-rays very effectively. We have demonstrated this effect with gold nanoparticles (AuNPs), superparamagnetic iron oxide nanoparticles (SPIONs), as well a carbon nanoparticles. The purpose of this activity is to compare the scatter intensity of AuNPs to that of SPIONs. 10-nm FeNPs scatter as well as (or better than) AuNPs, as shown in Table 2. We measured that relative to their absorbing power, SPIONs are better scatterers than gold nanoparticles. Scatter images show about 10x enhancement over absorption images on average. We found similar results for 50-nm AuNPs versus 40-nm SPIONs.

	Absorption	Scatter	Scatter/abs ratio
1000 ppm AuNPs	1.2 +/- 0.2%	7.0 +/- 2.3%	5.8
1000 ppm SPIONs	0.6 +/- 0.2%	6.2 +/- 4.5%	10.3

Table 2: Measured hard x-ray properties of 10-nm AuNP and 10-nm SPION suspensions with 1000 ppm concentration. SPIONs scatter as much x-rays as AuNPs but have less absorption.

In order to demonstrate that the x-ray scatter is specific to the presence of NPs and not simply the average electron density of the sample, we compared the signals of the NP suspensions to that of solutions of $AuCl_3$ and $K_4Fe(CN)_6$ with the same metal atom densities. The results are shown in Table 3. When solutions are prepared with matching electron density, we measured very similar enhancements in absorption images but very different enhancements in scatter images: nanoparticle solutions always scatter significantly more than bulk solutions. This indicates that 1) SFHI is more sensitive than conventional absorption-based imaging to the presence of nanostructures and can show features not easily seen in absorption-based imaging and 2) the scattering power of

		Absorption	**Scatter**
10 nm AuNPs	signal enhancement over water (%)	2.75 ± 0.23	16.28 ± 0.99
$AuCl_3$		2.59 ± 0.06	10.31 ± 7.65
Ratio of AuNP to solution		1.06	1.58
		Absorption	Scatter
10 nm SPIONs	signal enhancement over water (%)	0.47 ± 0.27	5.33 ± 3.36
$Fe(CN)_6$		0.54 ± 0.06	1.24 ± 4.46
Ratio of SPION to solution		0.88	4.31

Table 3: Measured hard x-ray properties of 10 nm AuNP and 10 nm SPION suspensions compared to their respective solutions with equal metal concentration.

the nanoparticles is due to more than simply the electron density of the metals in solution; the structure of the particles is the important contributing factor. We also compared size effects of NPs of the same material: small vs. large AuNPs (10 nm vs. 50 nm) and small vs. large SPIONs (10 nm vs 40 nm). The results depended on the material of the nanoparticle. For AuNPs we see that larger particles tend to scatter more, for SPIONs we see that smaller particles scatter more. The reasons where subsequently determined by measuring the sensitivity of SFHI to x-rays scattered into various small angles off the sample.

The ability to utilize SPIONs with this technique is important, as it allows us to benchmark SFHI with MRI and could eventually lead to the development of a dual-modality imaging technique combining MRI and SFHI. Our results indicate that the sensitivity of SFHI approaches that of MRI when used in biomedical imaging applications albeit the much less complex and much less costly imaging delivery. Since this application transcends the interest of the DOE-supported research the implication are not further discussed here.

2.2 Time resolved XAFS endstation at 7ID-C, Advanced Photon Source

In collaboration with Dr. Bernhard Adams, Argonne National Laboratory, we improved the signal-to-noise of the streak camera end stations at sector 7 of the APS. We can now routinely measure XAFS data with a noise of less than 0.1% of the absorption signal of only the excited molecules. We took all data needed for characterization of the temporal resolution and detection efficiency of the entire system.

1) We replaced the entire systems with a back-illuminated CCD camera that directly detects the streaked electrons. The detection efficiency is very high while guaranteeing minimal noise close to the Poisson limit.
2) The upgraded streak camera now produces well-aligned streak images with 2-ps resolution. Figure 2 show a composite image of 50 streaks of 50-fs, 266-nm laser pulses. The delay steps between these pulses are 6.6 ps. These pulses allow us to calibrate the temporal resolution of the systems and the relation between streak time and position of the CCD camera.

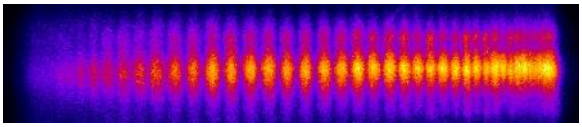

Figure 2: Composite image of streaks of 50-fs, 266nm laser pulses at various pump probe delays.

3) The deflection system of the streak camera was replaced. Steaking is now based on microwave deflection. The camera can streak at <u>any</u> repetition rate. Triggered by the laser oscillator in Hutch E of the 7ID, the camera currently streaks at 88 MHz. The pump laser amplifier operates at 5 kHz. Each CCD image contains two streaks, one with the laser exciting the sample and one measured in between laser shots. Thus data are acquired at 10 kHz repetition rate. With an upgrade of the laser system higher detection rates are of course possible.
4) We currently are analyzing the data taking with this upgrade in June of 2013. We are able to achieve a noise of less than 0.08% for 3 hours of data acquisition time per streak. Three streaks for the reactions of $Fe(CN)_6^{4-}$ photoexcited with 266-nm, 50-fs laser pulses are shown in Figure 3. The x-ray energies center on the 1st absorption maximum of the XANES spectrum at the iron K-edge. The data interpretation is still in its infancy but the 1st peak close to time-zero is likely due to molecular orbital shifting during the pump-laser pulse illumination of the sample solution with an intensity of about 5×10^{13} W / cm^2. The rise time of this peak is instrument-limited and serves as a cross-correlation between the laser and x-ray pulses. CTTS product ($Fe(CN)_6^{(4-x)-}$) formation should occur within less than 100 fs. The subsequent changes are likely due to vibrational cooling and formation of photoaquation products such as $[Fe(CN)_5H_2O]^{3-}$. Transmittance maxima at 7, 17, 27, and 37 ps indicate coherent vibrations. Their molecular origin has not been identified yet.

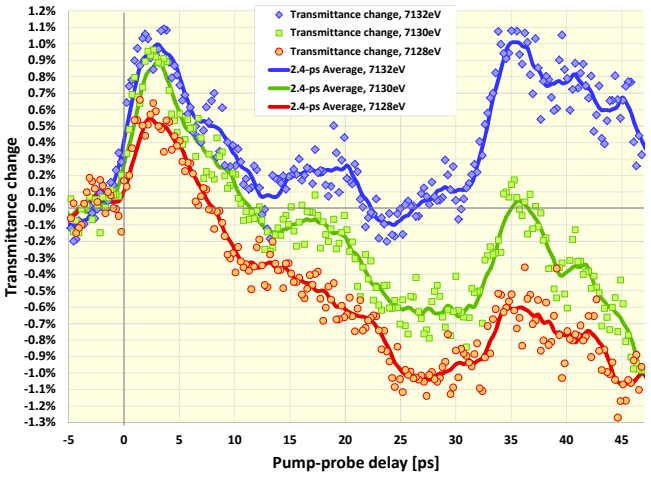

Figure 3: XAFS transmittance changes of $[Fe(CN)_6]^{4-}$ after 266-nm, 50-fs excitation.

Future plans

We will continue the research on Spatial Frequency Heterodyne Imaging and related techniques and further use the ultrafast XAFS endstation at 7ID-C for chemical dynamics studies. Specifically, we will

1. continue the development of the theoretical framework of X-ray Spatial Frequency Heterodyne Imaging,
2. continue hard x-ray SFHI experiments at Brown University. Primary application: phase transitions in

nanoparticle suspensions and in clathrate hydrate slurries.

3. Extend the studies of the phase transitions in CNTs to water penetration of grapheme sheets.
4. Continue to carry out ultrafast XAFS studies at 7 ID-C. The next beamtime will be used to measure streaks in the entire XANES and iron pre-edge region of photoexcited $[Fe(CN)_6]^{4-}$ and related charged complexes with the goal to delineate level-shifting, CTTS, ligand substitution product and observe the solvent responses for laser-induced transition of solutes from hydrophilic to hydrophobic.
5. We will seek a collaboration providing theoretical support for the ultrafast chemical dynamics research.

3 Papers acknowledging this DOE grant

1. "Picosecond x-ray absorption measurements of the ligand substitution dynamics of Fe(CO)5 in ethanol," B. Ahr, M. Chollet, B. Adams, E. M. Lunny, C. M. Laperle and C. Rose-Petruck, Phys. Chem. Chem. Phys. **13 (Also PCCP Cover Page, April 2011)** (13), 5590 (2011).

2. "2-ps Hard X-Ray Streak Camera Measurements at Sector 7 Beamline of the Advanced Photon Source (invited)," M. Chollet, B. Ahr, D. A. Walko, C. Rose-Petruck and B. Adams, Selected Topics in Quantum Electronics, IEEE Journal of **PP** (99), 1 (2011).

3. "Hard X-ray streak camera at the advanced photon source," M. Chollet, B. Ahr, D. A. Walko, C. Rose-Petruck and B. Adams, Nuclear Instruments and Methods in Physics Research Section A: Accelerators, Spectrometers, Detectors and Associated Equipment **649** (1), 70 (2011).

4. "X-ray spatial harmonic imaging of phase objects," Y. Liu, B. Ahr, A. Linkin, J. D. Gerald and C. Rose-Petruck, Optics Letters **36**, 2209 (2011).

5. "Nanomaterials for X-ray Imaging: Gold Nanoparticle Enhancement of X-ray Scatter Imaging of Hepatocellular Carcinoma," D. Rand, V. Ortiz, Y. Liu, Z. Derdak, J. R. Wands, M. Taticek and C. Rose-Petruck, Nano Letters **11** (7), 2678 (2011).

6. "Spatial frequency x-ray heterodyne imaging," B. Wu, Y. Liu, C. Rose-Petruck and G. J. Diebold, Applied Physics Letters **100**, 061110 (2012).

7. "X-ray Phase Contrast Imaging: Transmission Functions Separable in Cartesian Coordinates," G. Cao, T. Hamilton, C. Rose-Petruck and G. J. Diebold, J. Am. Optical Soc. A **24**, 1201 (2006).

8. "X-ray elastography: modification of x-ray phase contrast images using ultrasonic radiation pressure," T. Hamilton, S. Gehring, J. R. Wands, C. Rose-Petruck and G. Diebold, J. Appl. Phys. **105** (10), 102001 (2009).

9. "X-ray elastography: Modification of x-ray phase contrast images using ultrasonic radiation pressure," T. J. Hamilton, C. Bailat, S. Gehring, C. M. Laperle, J. Wands, C. Rose-Petruck and G. J. Diebold, Journal of Applied Physics **105** (10), 102001 (2009).

10. "X-ray Phase Contrast Imaging: Transmission Functions Separable in Cylindrical Coordinates," G. Cao, T. Hamilton, C. M. Laperle, C. Rose-Petruck and G. J. Diebold, J. Appl. Phys. **105**, 102002 (2009).

11. "X-ray spatial harmonic imaging of phase objects," Y. Liu, B. Ahr, A. Linkin, G. J. Diebold and C. Rose-Petruck, Optics Letters **36**, 2209 (2011).

12. "Nanomaterials for X-ray Imaging: Gold Nanoparticle Enhancement of X-ray Scatter Imaging of Hepatocellular Carcinoma," D. Rand, V. Ortiz, Y. Liu, Z. Derdak, J. R. Wands, M. Tatíček and C. Rose-Petruck, Nanoletters **11** (7), 2678 (2011).

13. "Hybrid lens/mirror x-ray focusing scheme and beam stabilization," B. Adams and C. Rose-Petruck, Review of Scientific Instruments **to be submitted** (2013).

14. "Soft x-ray spatial frequency heterodyne imaging," P. Bruza, D. Panek, M. Vrbová and C. Rose-Petruck, TBD, **to be submitted** (2013).

15. "Water phase transitions in carbon nanotubes," F. Schunk, D. Rand and C. Rose-Petruck, TBD, **to be submitted** (2013).

16. "Spatial Frequency Heterodyne and Magnetic Resonance Imaging," D. Rand, F. Schunk, E. Welch and C. Rose-Petruck, PNAS, **submitted** (2013).

4 Publications and theses related to this DOE grant

1. "Chemical Dynamics in the Condensed Phase: Time-resolved X-ray Imaging and Ultrafast X-ray Absorption Spectroscopy " B. Ahr, Brown University, 2011.
2. "A fickle molecule caught in the act," D. Bradley, 2011 Annual Report of the Advanced Photon Source (2012).

Tamar Seideman
Department of Chemistry, Northwestern University
2145 Sheridan Road, Evanston, IL 60208-3113
t-seideman@northwestern.edu

Strong-Field Control in Complex Systems

1. Program Scope

Our AMOS-supported research during the past year can be broadly categorized into two conceptually and practically related topics: (1)the design and control of complex material system with strong field concepts developed in our earlier AMOS work, including alignment, 3D alignment, torsional alignment and molecular focusing; and (2)the physics, implications, and potential applications of high harmonics generated from aligned molecules. Whereas the first topic is a generalization of the thrust of our original application, the second has been motivated by the intense interest of the AMOS Program in attosecond science and rescattering electrons physics, and has been carried out in collaboration with AMOS experimentalists colleagues.

Our work during the past year within the first part is summarized in Secs. 2.1–2.6 and ranges from a new and fascinating field-driven assembly mechanism (2.1) and a nanoscale, ultrafast current switch (2.2) to a variety of phenomena in torsional control (2.3) and spectroscopic applications of rotational wavepacket dynamics (2.6). Completion of this research, in the next year (Sec. 3.1), will hopefully accomplish our ultimate goal of extending alignment from the domain of physics and optics to make a tool in material science, solution chemistry, and possibly engineering. Within the second part of our AMOS-supported research during the past year, we collaborated with the Bucksbaum, Martinez and Guehr groups on the problem of HHG from aligned asymmetric top molecules (Sec. 2.9) and with the group of Murnane and Kapteyn on two projects in the field of HHG from aligned linear molecules (Secs. 2.7, 2.8). In addition, we continued our efforts to develop improved numerical methods to compute the electronic dynamics underlying HHG. Our plans for further research in the area of attosecond physics and HHG during the next year is outlined in Sec. 3.2. Citations refer to the list of AMOS-supported publications from the 2011–Aug. 2013 period, Sec. 4.

2. Progress during the past year

2.1 Laser-induced molecular assembly:

In recent work,[1] we illustrate a new phenomenon in the dynamics of molecular ensembles subjected to moderately intense, far-off-resonance laser fields, namely, field-driven formation of perfectly ordered, defect-free assembly. Interestingly, both the short range order of the constituting molecules within the individual assembly and the long-range translational and orientational order of the assembly with respect to one another are subject to control through choice of the field polarization. Relying on strong field induced dipole-induced dipole interactions that are established in dense molecular media, the effect is general. Our work suggests intriguing applications in material design. An article was published in *Phys. Rev. Lett.*[1]

2.2 Toward coherent control in the nanoscale: An ultrafast, nanoscale current switch:

In previous AMOS-supported research, we proposed a molecular switch based on extension of the concept of nonadiabatic alignment to surface-adsorbed molecules (M. Reuter, M. Sukharev and T. Seideman, *Phys.Rev.Lett.* **101**, 208303 (2008); *Nature Photonics* **3**, 4–5 (2009)). A recent extension[2] of the ultrafast, nanoscale switch concept generalizes laser orientation to the case of surface-adsorbed molecules, where the polarizability is enhanced by the substrate, the field is plasmon-focused and -enhanced by a tip, and a host of new applications open up. Here we also construct a multidimensional potential surface, develop efficient approaches to compute the associated multimode orientation dynamics and plasmonic response, and explore the interplay between the tip location and the laser field. An experimental realization has been initiated.

2.3 Torsional coherences and torsional control subject to a dissipative medium:

The concept of torsional alignment was introduced in our earlier AMOS-supported research (S. Ramakrishna and T. Seideman, *Phys. Rev. Lett.* (2007)) and has been subsequently the topic of considerable experimental and numerical activity by several groups world-wide. Our own work during the past year has led to

significant advancement of this research field,[3–6] pointing also to several exciting future directions (*vide infra*). In particular, in Ref. 3, we propose a strong-field based method to control the chirality of molecules that exhibit torsion, illustrating the possibility of converting a racemate into a pure enantiomer at elevated temperatures. Optimal control theory is applied to design a laser pulse that will maximize the enantiomeric ratio achieved, considering both the case of a fixed, linear polarization and the case of a tunable polarization. Our simulations show the possibility of converting 99% and 99.5% of the population into a desired enantiomer for the fixed and tunable polarization solutions, respectively, deriving interesting insights regarding the conversion dynamics from the optimized pulse shape. Reference 4 combines torsional alignment with group theoretical arguments to develop an approach for separating nuclear spin isomers. In Ref. 5 we unravel several interesting phenomena in the dynamics of strong field-triggered torsional wavepackets, which carry implications for the problem of torsional control. Our results point to the origin and consequences of the fundamental differences between rotational and torsional coherences. In addition, we provide design guidelines for torsional control experiments, and propose several potential applications of coherent torsional control in chemistry, physics, material science and engineering.

A recently published manuscript[6] explores the controllability of molecular torsions subject to dissipative media, providing insights into how phase information is exchanged between torsional modes and a dissipative environment. Our results point to several new and interesting phenomena in wavepacket dissipation dynamics that are unique to torsions but enrich our general understanding of wavepacket phenomena.

2.4 Alignment as a probe of the multielectron ionization dynamics of mixed-bonding Van der Waals clusters:

In a collaborative study with an experimental group, we studied the order in which a strong laser field removes multiple electrons from an aligned multicenter molecular cluster. The N_2Ar, with an equilibrium T-shaped geometry, contains both a covalent and a van der Waals (vdW) bond, and serves as a simple, yet rich and prototypical example. Interestingly, the fragmenting double and triple ionizations of N_2Ar with vdW bond breaking are favored when the vdW bond is aligned along the laser field polarization vector. However, the orientation of the covalent bond with respect to the laser field rules the triple ionization when both the covalent and vdW bonds are simultaneously broken. Electron-localization-assisted enhanced ionization and molecular orbital profile-dominated, orientation-dependent ionization are discussed to reveal the sequence of electron release from different sites of N_2Ar. Our numerical results explain the experimental findings and substantiate their conclusions. Our theory illustrates the way in which multielectron ionization experiments probe the electronic distribution within molecules. An article appeared in *Phys. Rev. Lett.*[7]

2.5 Rotational wavepacket imaging:

The vast majority of studies of rotational wavepackets have focused on applications of the associated sharp alignment, but the interest in rotationally-broad wavepackets as such has been noted. In particular, our earlier work illustrated that rotational coherences can serve to explore intramolecular coupling mechanisms, such as rotation-vibration coupling, and contain unique information regarding the interaction of solvated molecules with their environment, hence, potentially, a route to the dissipative properties of exotic media.

In a recent publication[8] we propose and illustrate numerically the possibility of imaging rotational wavepackets in angular space and time using different pump-probe spectroscopic techniques. A general theoretical framework to perform such rotational mapping is derived and three specific spectroscopies are numerically explored. All three approaches are shown to provide direct mapping of the rotational coherences of molecules but they are not equivalent; comparison of their results yields interesting insights into their relative merits.

2.6 Microwave Spectroscopy in the Time Domain:

In collaborative work with experimental groups at DESY, we introduced a new, time-domain approach to explore rotational dynamics caused by intramolecular coupling or the interaction with dissipative media.[9] The approach pushes the time resolution toward the ultimate limit determined by the rotational period. Femtosecond pulses create a coherent superposition of two rotational states of carbon monoxide. The wave packet motion predicted by quantum mechanical calculations is probed experimentally by Coulomb explosion, which results in a time-dependent asymmetry of spatial fragmentation patterns. The asymmetry oscillation prevails for at least 1 ns covering more than 300 periods with no decoherence. Long time scans will allow weak perturbations, of the order of $\delta E/E = 10^{-4}$.

2.7 Extracting continuum electron dynamics from high harmonic signals
Our previous AMOS-supported research developed a theory of HHG from aligned molecules that illustrated that harmonic signals exhibit much higher order rotational fractional revivals than hitherto explored probes of rotational wavepacket dynamics, providing also a sensitive probe of rotational coherences. Experimental data at the time of publication, however, showed only the standard half and quarter fractional revivals, familiar from other alignment-sensitive probes. Recent experiments by the group of AMOS colleagues Murnane and Kapteyn, where much improved signal-to-noise ratio was achieved, observed as high order fractional revivals as the 1/16 and 1/6 in CO_2 and N_2O, respectively, in agreement with the theory. By fitting the high-quality experimental data to our theory of HHG from aligned molecules, we extracted the electronic dipole moment elements that underly high harmonic emission and contain detailed information regarding the dynamics of the field-driven continuum electron. For the considered molecules, we found that the electron gains angular momentum from the photon field as it is accelerated. An joint article with the JILA group appeared in *Phys. Rev. Lett.*[10]

2.8 Ultrafast elliptical dichroism as a probe of molecular structure and electron dynamics:
Molecules illuminated by an elliptically polarized, high intensity laser field emit elliptically polarized high-order harmonics. Our recently submitted research in collaboration with AMOS experimental collaborators Murnane and Kapteyn[11] explains surprising experimental observations of ultrafast elliptical dichroism in the harmonic emission as the ellipticity of the driving field and the molecular alignment are scanned. Our analysis ties the observed elliptical dichroism to the journey of the continuum electron in the field and the underlying bound state of the molecular ion. These results show how to use molecular structure and alignment to manipulate the polarization state of high-order harmonics, and also present a potential new attosecond probe of the underlying molecular system. An article was submitted for publication in *Phy. Rev. Lett.*[11]

2.9 HHG from aligned asymmetric tops as a route to electronic structure and reaction dynamics
The above studies, and likewise other experimental and theoretical studies of HHG from aligned molecules by different groups, our own group included, have been able to obtain valuable information about molecular orbitals and continuum electron dynamics for simple linear molecules. Asymmetric tops, however, comprise the widest class of molecules, as well as the configurations underlying the vast majority of transition states. Here the emission from different molecular directions interfere, concealing individual angular signatures. In a recent collaborative study with the groups of AMOS colleagues Bucksbuam, Guer and Martinez, we introduce an orientational decomposition method for obtaining both the angle-dependent amplitude and phase of harmonic emission in the molecular frame. Using the quantum revivals as spectral markers, we fit single-axis alignment patterns to experimental data to decompose the HHG signal into the amplitude and phase from each molecular axis. Our analysis allows reconstruction of the fundamental harmonic emissions in the molecular frame by separating each harmonic energy into three distinct signals. A joint article was submitted for publication in *Nature Photonics*.[12]

3. Future Plans

3.1 Alignment, Orientation, and Torsional Alignment in Complex systems. Toward Applications in Material Science

During the next funding period, we will explore three new applications of intense laser alignment in material science. The first study, in collaboration with a Northwestern experimental group, will establish long-range orientational order in an assembly of semiconductor nanorods. The theoretical component will involve a molecular dynamics study using analytical polarizabilities and two-body interactions. The second study will apply torsional alignment of an adsorbed biphenyl derivative to introduce an approach to ultrafast electron spin flipping. Here, use will be made of the recent experimental illustration that chiral molecules adsorbed onto a gold surface can serve as a spin filter for electrons that are photoejected from the metal substrate and are transmitted through the molecules. A third study will establish an approach, based on torsional alignment, to enhance desired forward electron transfer processes while suppressing undesired back transfer processes, which hamper charge separation. One example where such selective torsional control may find important applications is artificial photosynthesis-like solar cells. Another is charge transfer from a semiconducting quantum dot into a bulk semiconductor via a bridge, relevant, for instance, to the problem

of designing efficient quantum-dot-sensitized solar cells and to the application of quantum dots in catalysis.

3.2 HHG and Attosecond Science. Method Development and Applications

One goal of our research in the area of HHG and attosecond science during the coming year is to continue and extend our already fruit bearing collaborative work with the group of Murnane and Kapteyn and with the groups of Bucksbaum, Martinez and Guehr while initiating a joint project with the group of Kumarappan and Kansas State collaborators. The latter research will generalize the theory of Ref. 10 and combine it with measurements of HHG from aligned N_2 molecules that will complement our earlier results for a different molecular symmetry[10] and provide needed insights on the question of angular momentum exchange between the continuum electron and the incident photons.

A second goal of this research is to develop a new numerical method for calculation of HHG signals that will extend our current capabilities in a significant way. Our approach will be based on a real time time-dependent density functional theory (TDDFT), currently under development in our group. We will test the new method by application to the case of simple linear molecules, for which we currently have reliable results from solutions of the Schrödinger equation. It will be our main goal, however, to extend the method to polyatomic molecules. Here we will combine our (already tested) approach to establishing 3D alignment by means of elliptically polarized fields with a TDDFT solution of the driven electronic dynamics. These studies will be complemented by semiclassical trajectory calculations that will serve both to provide qualitative insights and to simplify aspects of the calculation.

4. Publications from DOE sponsored research(2011–August 2013, in citation order)

1. M. Artamonov and T. Seideman, *Predicted Ordered Assembly of Ethylene Molecules Induced by Polarized Off-Resonance Laser Pulses*, *Phys. Rev. Lett.* **109**, 165408 (2012).
2. M. Reuter, M. A. Ratner and T. Seideman, *Laser Alignment as a Route to Ultrafast Control of Electron Transport through Junctions Phys. Rev. A* **86** 013426 (2012).
3. S. M. Parker, M. A. Ratner and T. Seideman, *Coherent Optimal Control of Axial Chirality*, Special Issue of *Mol. Phys.* **110**, 1941 (2012) (**invited**).
4. J. Floss, T. Grohmann, M. Leibscher, and T. Seideman, *Nuclear Spin Selective Torsional Control*, *J. Chem. Phys.* **136**, 084309 (2012).
5. B. Ashwell, S. Ramakrishna and T. Seideman, *Laser-Driven Torsional Coherences*, *J. Chem. Phys.* **138**, 044310 (2013).
6. B. Ashwell, S. Ramakrishna and T. Seideman, *Laser-Driven Torsional Coherences in Dissipative Environments*, Special Issue of *J. Phys. Chem.* , in press (**invited**).
7. J. Wu, X. Gong, M. Kunitski, L. Ph. H. Schmidt, T. Jahnke, A. Czasch, T. Seideman, and R. Dorner, *Sequencing Strong Field Multiple Ionization of a Multicenter Multibond Molecular System*, *Phys. Rev. Lett.* **111**. 083003 (2013)
8. S. Ramakrishna and T. Seideman, *Rotational Wave Packet Imaging of Molecules*, *Phys. Rev.* A **87**, 023411 (2013).
9. A. Przystawik, A. Al-Shemmary, S. Dusterer, M. Harmand, A. Kickermann, H.Redlin, L. Schroedter, M. Schulz, N. Stojanovic, S. Toleikis, T. Laarmann, A. M. Ellis, K. von Haeften, F. Tavella, J. Szekely and T. Seideman, *Generation of the Simplest Rotational Wave Packet in a Diatomic Molecule: Microwave Spectroscopy in the Time Domain without Microwaves*, *Phys. Rev. A* **85**, 052503 (2012).
10. R.M. Lock, S. Ramakrishna, X. Zhou, H.C. Kapteyn, M.M. Murnane, and T. Seideman, *Extracting Continuum Electron Dynamics from High Harmonic Emission from Molecules*, *Phys. Rev. Lett.* **108**, 133901 (2012).
11. P. A. J. Sherratt, R. M. Lock, X. Zhou, H. C. Kapteyn, M. M. Murnane, and T. Seideman, *Ultrafast Elliptical Dichroism in High-Order Harmonics as a Probe of Molecular Structure and Electron Dynamics*, submitted for publication in Phys. Rev. Lett.
12. L. S. Spector, M. Artamonov, S. Miyabe, Todd Martinez, T. Seideman, M. Guehr, and P. H. Bucksbaum, *High Harmonic Generation in Rotating Quantum Asymmetric Tops Reveals New Aspects of Electronic Structure*, submitted for publication in *Nature Physics*.
13. S. Ramakrishna and T. Seideman, *On the Information Content of Time- and Angle-Resolved Photoelectron Spectroscopy*, Special Issue of *J. Phys. B* **45**, 194012 (2012) (**invited**).
14. M. Artamonov and T. Seideman, *Three-Dimensional Laser Alignment of Polyatomic Molecular Ensembles*, Special Issue of *Mol. Phys.* **110**, 885 (2012) (**invited**).
15. S. M. Parker, M. A. Ratner and T. Seideman, *Coherent Control of Molecular Torsion* J. Chem. Phys. **135**, 224301 (2011).
16. P. Sherratt, S. Ramakrishna and T. Seideman, *Signatures of the Molecular Potential in the Ellipticity of High-Order Harmonics from Aligned Molecules*, *Phys. Rev. A* 053425 (2011).
17. S. L. Chin, T. J. Wang, C. Marceau, J. Wu, J. S. Liu, O. Kosareva, N. Panov, Y. P. Chen, J-F Daigle, S. Yuan, A. Azarm, W. W. Liu, T. Seideman, H. P. Zeng, M. Richardson, R. Li, and Z. Z. Xu, *Advances in Intense Femtosecond Laser Filamentation in air*, *Laser Physics* **16**, 1 (2011) (**invited**).

Inelastic X-ray Scattering Under Extreme and Transitional Conditions

Gerald T. Seidler, seidler@uw.edu,
Department of Physics
University of Washington
Seattle, WA 98195-1560

Program Scope

The goal of this program is to expand the scope and scientific potential of time-resolved inelastic x-ray scattering (IXS). First, we are using x-ray spectroscopies, soon to include resonant inelastic x-ray scattering, to gain new insight into the energy transfer mechanisms of lanthanide-based phosphors and related luminescent materials and to study the time dynamics of the electronic and structural changes at metal-insulator transitions. Second, we are performing combined theoretical and experimental work to critically test, and substantially improve, the use of IXS methods in the study of dense plasmas, such as in the transitional, 'warm dense matter' regime. Third, we are continuing several collaborations based on IXS instrumentation and methods developed by the PI, including studies of the time-dynamics of energy transfer in photosynthetic proteins and of the *f*-electron physics of lanthanide elements and compounds at high pressures. Finally, as a side-project based on our need for a small in-house test system for x-ray optics for inelastic x-ray scattering, we are re-assessing the scientific role of laboratory-based x-ray emission spectroscopy and x-ray absorption spectroscopy.

Recent Progress and Future Directions

II. Time-resolved Studies of Energy Transfer and Electron Correlations

First, lanthanide compounds and coordination complexes are responsible for a wide range of light-gathering and light-emitting applications, including as commercial phosphors in lighting applications, as tools to better match the solar spectrum to the function of photovoltaic devices, and as a critical component in many bioassays. In this lattermost role, an organic 'antenna' acts as a strong near-UV photoabsorber before nonradiatively transferring energy to a chelated, trivalent lanthanide ion via a 4*f*-4*f* intrashell excitation. This dipole-forbidden excitation subsequently decays through the so-called 'hypersensitive' pseudo-quadrupolar decay, giving light at delays of order msec after the initial excitation due to the long lifetime for the 4*f* excitation. This long time-delay allows simplest time-gate filtering of the emission from the luminescent lanthanide complex from that of the host biological system.

The microscopic physics underlying each step in the energy transfer pathway in the luminescent lanthanides, and indeed in all materials used for the applications described above, remain incompletely understood. Our recent work at the Advanced Photon Source on luminescent lanthanide complexes may have high impact in this field by demonstrating an unexpected, but clear expression of the 4*f* instrashell excitation in the time-resolved x-ray absorption near-edge spectrum (XANES) of the lanthanide ion.[3] While a conclusive explanation of this feature will require repeating the experiment with life-time broadening suppression by high-energy resolution fluorescence detection (HERFD), the leading explanations require either an unexpectedly large local structural conformation upon excitation or else a surprisingly dynamic coupling between

the 4*f* and 5*d* orbitals of the lanthanide ion. [3] In any event, this discovery opens up new opportunities to use the LCLS to directly monitor the energy transfer onto the lanthanide species, giving an important complement to studies of the de-excitation of multiple ligand states by transient optical absorption.

Second, also at the Advanced Photon Source, we have continued our investigation of the time-dynamics of the local structure of unstrained, single-crystal VO_2 nanobeams when forced through the metal-insulator transition by photoabsorption in the valence band. This study follows our completed study of the ambient condition, polarization-dependent XANES of the same samples. [4] Given the uncertain influence of strains on the dynamics of the metal-insulator transition, this study may provide the first unbiased perspective on the linkage between electronic and structural degrees of freedom at this purportedly pure Mott-like transition.

II. The electronic structure of warm dense matter

Matter at solid-like and higher densities that is also at temperatures of order a few eV to somewhat past the Fermi energy is frequently referred to as 'warm dense matter' (WDM). In this regime, all but the lightest species will still be partially (rather than fully) ionized, resulting in a highly complex admixture of the physics typical of plasmas and that of condensed phases. This regime, whose fundamental interest is seasoned by strong technical relevant for fusion science and direct representation of the thermodynamic conditions of several astrophysical and planetary phenomenon, is seeing emergent interest from both the plasma and condensed phase communities.

However, the highly transient nature of such experiments at large-scale laser facilities and x-ray free electron lasers poses unique challenges for the determination of even the most basic state variables (*e.g.*, pressure, temperature, density, and ionization state). This limitation is critically impeding progress toward understanding of the equation of state or toward any consequent, comprehensive microscopic treatment. As a case in point, WDM thermometry is in a uniquely difficult situation compared to any other regime of quasi-equilibrium matter: no thermometry from other fields of science is applicable to WDM, and the dominant methods used in WDM (specifically, based on inelastic x-ray scattering) are extremely sensitive to models of electronic structure.

We have developed improved theoretical tools whose treatment of all atomic and condensed-phase effects can be validated against ambient-condition, high-resolution IXS results collected at synchrotron light-sources and then applied to LCLS/MEX results and to the much poorer-quality IXS spectra that are typical of WDM studies at large-scale laser-plasma facilities. Our work includes a real-space Green's function treatment of the valence contribution to the IXS spectrum [8], a reinvestigation of methods used to treat the core contribution to IXS in WDM experiments,[5] and the recent identification of the fundamental importance of orthogonalization of the free- and bound-electron wavefunctions for any correct treatment of the electronic structure of WDM. [1]

III. Synchrotron Instrument development and Instrument-related Collaborations

The PI's group has a long record in x-ray instrument development and in sharing new experimental technology with facilities and other teams. Under this award, we have further developed the 'miniXES' x-ray emission spectrometers [10,11] and also continued to work on polycapillary-coupled spectrometers for experiments with more modest needs in energy resolution. [6, 17] The miniXES instruments continue to provide

a stream of solid collaborations [*e.g.*, 7, 9, 13]. We have also invested considerable effort to optimize the performance of polycapillary-coupled Bragg spectrometers by enhancing the integral reflectivity of the analyzer crystal by as much as a factor of five through programmed crystallographic damage. [6] The resulting instruments dramatically enhance the options for x-ray emission spectroscopy as a tool to understand the local electronic and magnetic structure of 4*f* species in diamond anvil cells, allowing critical distinction between different theoretical models of 4*f* delocalization at the volume collapse transition. [2] Other collaborations that are enabled by instrumentation or technical expertise are reported in [12, 14, 15, 16].

IV. A Reassessment of Laboratory-based X-ray Emission Spectroscopy and X-ray Absorption Spectroscopy Using Modern Analyzer Optics

We have constructed an inexpensive, low-flux x-ray spectroscopy system at the UW to allow rapid diagnostic of the spherically-bent crystal analyzers (SBCA's) that we need to develop for the above time-resolved XAFS studies of experiments on energy transfer in lanthanide-based systems. Commissioning of the in-house test facility will occur in October 2013.

In addition to serving its intended purpose, we anticipate that a side-project based on this equipment will demonstrate two unexpected results that could have high impact in the synchrotron community. First, high-resolution, nonresonant x-ray emission spectroscopy (XES) -- a technique that is with only the rarest exceptions always performed at synchrotron light source -- will now be possible using only an inexpensive lab-based system with measurement times intermediate between that of a monochromatized 3rd-generation BM and ID. Second, we anticipate that the use of modern optics (SBCA's) will more generally yield a laboratory hard x-ray monochromator with sub-eV energy resolution and fluxes 10-100 times higher than what was achieved (with poor energy resolution) in laboratory XAFS systems in the 1980's. If correct, these types of modern, laboratory-based instruments can assist with synchrotron user-base development, can be used for prototype studies for sample validation prior to synchrotron access, could fully support research programs that only require transmission-mode XANES (e.g., *in situ* studies of electrical energy storage), and may have important applications for *in situ* studies of catalysis or active synthesis where the necessary support equipment cannot be easily transported to the synchrotron.

References

1. Brian A. Mattern, Gerald T. Seidler, Joshua J. Kas, "Condensed Phase Effects on the Electronic Momentum Distribution in the Warm Dense Matter Regime," *submitted*, Physical Review Letters (2013).
2. D. Mortensen, J.A. Bradley, M. Lipp, B.A. Mattern, G.T. Seidler, P. Chow, and Y. Xiao, "Toward a general understanding 4f delocalization in Rare Earth systems," *in preparation*, (2013).
3. Joseph I. Pacold, David S. Tatum, Gerald T. Seidler, Kenneth N. Raymond, Xiaoyi Zhang, Andrew B. Stickrath, and Devon R. Mortensen, "Direct Observation of 4f Intrashell Excitation in Luminescent Lanthanide Complexes by Time-Resolved X-ray Absorption Near Edge Spectroscopy," *submitted*, Journal of the American Chemical Society (2013).

4. J.I. Pacold, G.T. Seidler, and D. Cobden, “Polarization-dependent X-ray absorption near edge structure across the VO_2 metal-insulator transition,” *in preparation*, (2013).
5. Brian A. Mattern and Gerald T. Seidler, "Theoretical Treatments of the Bound-Free Contribution and Experimental Best Practice in X-ray Thomson Scattering from Warm Dense Matter," Physics of Plasmas 20, 022706 (2013) (doi: 10.1063/1.4790659).
6. S.M. Heald, G.T. Seidler, D. Mortensen, B. Mattern, J.A. Bradley, N. Hess, M. Bowden, "Recent Tests of X-ray Spectrometers Using Polycapillary Optics," in Advances in X-Ray/EUV Optics and Components VII, edited by Shunji Goto, Christian Morawe, Ali M. Khounsary, Proc. of SPIE Vol. 8502 (2012), article number 85020I (doi: 10.1117/12.929960).
7. K.M. Davis, B.A. Mattern, J.I. Pacold, T. Zakharova, D. Brewe, I. Kosheleva, R.W. Henning, T.J. Graber, S.M. Heald, G.T. Seidler, Y. Pushkar, “Fast Detection Allowing Analysis of Metalloprotein Electronic Structure by X-ray Emission Spectroscopy at Room Temperature,” *accepted*, journal of Physical Chemistry Letters **3**, 1858 (2012).
8. B.A. Mattern, G.T. Seidler, J.J. Kas, J.I. Pacold, J.J. Rehr, “Real-Space Green’s Function Calculation of Compton Profiles,” Phys. Rev. B **85**, 115135 (2012).
9. J.A. Bradley, K.T. Moore, M. J. Lipp, B.A. Mattern, J.I. Pacold, G. T. Seidler, P. Chow, E. Rod, Y. Xiao, and W. J. Evans, “4*f* electron delocalization and volume collapse in praseodymium metal, ” Phys. Rev. B **85**, 100102 (2012).
10. J.I. Pacold, J.A. Bradley, B.A. Mattern, et al., “A miniature X-ray emission spectrometer (miniXES) for high-pressure studies in a diamond anvil cell,” J. Synch. Rad. **19**, 245 (2012).
11. B.A. Mattern, G.T. Seidler, M. Haave, J.I. Pacold, R.A. Gordon, J. Planillo, J. Quintana, B. Rusthoven, “A Plastic Miniature X-ray Emission Spectrometer (miniXES) based on the Cylindrical von Hamos Geometry,” Rev. Sci. Instrum. **83**, 023901 (2012).
12. Steven D. Conradson, et al., "Bose condensate-type behavior from a collective excitation in the chemically and optically doped Mott-Hubbard system, UO2+x," accepted, Physical Review B (2013).
13. K.M. Davis, I. Kosheleva, R.W. Henning, G.T. Seidler, Y. Pushkar, "Kinetic Modeling of the X-ray-induced Damage to a Metalloprotein," accepted, Journal of Physical Chemistry B (2013).
14. Matthew Gliboff, Hong Li, Kristina M. Knesting, et al., "Competing Effects of Fluorination on the Orientation of Aromatic and Aliphatic Phosphonic Acid Monolayers on ITO," accepted, Journal of Physical Chemistry C (2013).
15. Matthew Gliboff, Lingzi Sang, et al,, "Orientation and Order of Phenylphosphonic Acid Self-assembled Monolayers on Transparent Conductive Oxides: A Combined NEXAFS, PM-IRRAS and DFT Study," Langmuir 29, 2166 (2013).
16. Stefan G. Minasian, Jason M. Keith, Enrique R. Batista, et al., "Covalency in Metal-Oxygen Multiple Bonds Evaluated Using Oxygen K-edge Spectroscopy and Electronic Structure Theory", Journal of the American Chemical Society 135, 1864 (2013) (DOI: 10.1021/ja310223b)
17. D.R. Mortensen, G.T. Seidler, J.A. Bradley, M.J. Lipp, W.J. Evans, P. Chow, Y.-M. Xiao, G. Boman, and M.E. Bowden, "A Versatile Medium-Resolution X-ray Emission Spectrometer for Diamond Anvil Cell Applications," Review of Scientific Instruments 84, 083908 (2013).

DYNAMICS OF FEW-BODY ATOMIC PROCESSES

Anthony F. Starace, P.I.
The University of Nebraska, Department of Physics and Astronomy
855 North 16th Street, 208 Jorgensen Hall, Lincoln, NE 68588-0299

Email: astarace1@unl.edu

PROGRAM SCOPE

The goals of this project are to understand, describe, control, and image processes involving energy transfers from intense electromagnetic radiation to matter as well as the time-dependent dynamics of interacting few-body, quantum systems. Investigations of current interest are in the areas of strong field (intense laser) physics, attosecond physics, high energy density physics, and multiphoton ionization processes. Nearly all proposed projects require large-scale numerical computations, involving, e.g., the direct solution of the full-dimensional time-dependent or time-independent Schrödinger equation for two-electron (or multi-electron) systems interacting with electromagnetic radiation. In some cases our studies are supportive of and/or have been stimulated by experimental work carried out by other investigators funded by the DOE AMOS physics program. Principal benefits and outcomes of this research are improved understanding of how to control atomic processes with electromagnetic radiation and how to transfer energy optimally from electromagnetic radiation to matter.

RECENT PROGRESS

A. Evidence of the 2s2p(^{1}P) Doubly-Excited State in the Harmonic Generation Spectrum of Helium

We have solved the full-dimensional time-dependent Schrödinger equation for a two-active-electron system (helium) in an intense and ultrashort laser field in order to study the role of electron correlation in the resonant enhancement of some harmonics in the HHG spectrum. Our non-perturbative numerical calculations have identified signatures of the well-isolated He 2s2p(^{1}P) autoionizing state on the 9th, 11th, and 13th harmonics for a range of driving laser frequencies ω_L that put these harmonics in resonance with that state (from the ground state). Despite the fact that He is the simplest and most fundamental multi-electron system, our results show that isolating the resonant enhancement of the particular harmonics we investigated is complicated by both low-order multiphoton resonances with singly-excited states and also by resonant coupling between different autoionizing states. Nevertheless, our results show that when resonant coupling between doubly-excited states is absent, the resonant enhancement of the He 2s2p(^{1}P) autoionizing state on the 9th and 13th harmonics is clearly observable when one examines the ratio of the harmonic powers of these two harmonics with those of their lower order neighboring harmonics. These ratios serve to remove the effect of low-order multiphoton resonances with singly-excited states and thus isolate the effect of the resonance with the autoionizing state. Experimental observation of our predicted results seems feasible for experiments employing a spatially-shaped (flat-top) focus as the predicted results appear to be reasonably insensitive to variations of intensity. In particular, the energy shifts of the resonance maxima with driving laser intensity appear to be smaller in magnitude than the widths of the resonance profiles. (*See reference [2] in the publication list below*.)

B. Perturbation Theory Analysis of Ionization by a Chirped Few-Cycle Attosecond Pulse

The angular distribution of electrons ionized from an atom by a chirped few-cycle attosecond pulse has been analyzed using the perturbation theory (PT) approach developed in *Phys. Rev. A* **80**, 063403 (2009), keeping terms in the transition amplitude up to second order in the pulse electric field. The dependence of

the asymmetries in the ionized electron distributions on both the chirp and the carrier-envelope phase (CEP) of the pulse are explained physically using a simple analytical formula that approximates the exactly-calculated PT result. This approximate formula (in which the chirp dependence is explicit) reproduces reasonably well the chirp-dependent oscillations of the electron angular distribution asymmetries found numerically by solving the time-dependent Schrödinger equation, as in *Phys. Rev. A* **80**, 013407 (2009). It can also be used to determine the chirp rate of the attosecond pulse from the measured electron angular distribution asymmetry. (*See reference [3] in the publication list below*.)

C. Attosecond Streaking in the Low-Energy Region

We have analyzed few-cycle XUV attosecond pulse carrier-envelope-phase effects on ionized electron momentum and energy distributions in the presence of a few-femtosecond IR laser pulse. Whereas attosecond streaking usually involves high-energy photoelectrons, when photoelectrons have low initial kinetic energies, the IR field can provide a remarkable degree of control of the continuum-electron dynamics. Specifically, a short IR laser pulse can guide some initially-ionized electrons back to the parent ion, from which they can rescatter and interfere with directly-ionized electrons, thus providing a kind of holographic image of the ionic potential. By increasing the IR laser pulse length, multiple returns of low energy continuum electrons are shown to arise. Using a semiclassical model, we show that the various possible trajectories of the photoelectrons in the continuum can be revealed by the interference patterns exhibited in the low-energy photoelectron spectrum. Our analysis explains the unusual asymmetric structures we predicted previously [*New J. Phys.* **10**, 025030 (2008)] by direct solution of the time-dependent Schrödinger equation. (*See reference [4] in the publication list below*.)

D. Two-photon double ionization of helium: Evolution of the joint angular distribution

By directly solving the time-dependent, full-dimensional, two-electron Schrödinger equation for He in the field of a laser pulse, we investigate the two-photon double-ionization (TPDI) process for the case of XUV laser pulses in both the nonsequential and the sequential regimes. We have carried out a systematic analysis of the joint angular distribution (JAD) of the two ionized electrons as a means to elucidate the role of electron correlations in TPDI. In direct (nonsequential) double ionization, the back-to-back emission pattern always dominates, indicating the importance of electron correlations in the intermediate state (i.e., during the interaction of the electrons with the laser pulse). Such a pattern in the JAD is found to be a general one for any energy sharing for photon energies less than 54.4 eV. This distribution pattern thus serves as a hallmark of electron correlation in the intermediate state. In the sequential double-ionization regime, if the two electrons share the excess energy equally, the dominant correlation mechanism is similar to that of the nonsequential double-ionization regime. However, for extremely unequal energy sharing, the Coulomb repulsion between the electrons in the final state (after the end of the laser pulse) becomes the dominant electron correlation effect. Finally, for both the nonsequential and sequential regimes, initial-state electron correlation effects have been identified in the JAD patterns. Namely, an uncorrelated initial state produces only a few angular momentum partial waves in the TPDI process, whereas a correlated ground state produces a richer number of partial waves. The number of partial waves has been shown to greatly affect the pattern of the JAD. These various investigations have thus demonstrated the value of the JAD as a means of elucidating two-electron dynamics. (*See reference [5] in the publication list below*.)

E. Validity of Factorization of the High-Energy Photoelectron Yield in Above-Threshold Ionization of an Atom by a Short Laser Pulse

We have derived quantum mechanically an analytic result for the above-threshold ionization (ATI) probability that is valid in the high-energy part of the ATI plateau for a short laser pulse of any shape and

duration. Factorization of this probability in terms of an electron wave packet function (dependent primarily on laser field parameters) and the field-free cross section for elastic electron scattering (EES) (dependent primarily on the target atom) is shown to occur only for the case of an ultrashort pulse. In general, the probability involves interference of different EES amplitudes involving laser-field-dependent electron momenta. These analytic results allow one to describe very accurately the left-right asymmetry as well as the large-scale (intracycle) and fine-scale (intercycle) oscillations in ATI spectra. In fact, agreement with results of accurate numerical solutions of the time-dependent Schrödinger equation is excellent. To use our results, only the field-free EES amplitude for the target atom and the solutions of certain classical equations describing the active electron motion for a given short laser pulse are needed. Our analytic formulas thus provide an efficient tool for the quantitative description of short-pulse ATI spectra, both elucidating the physics of the process and allowing experimentalists to plan and/or control the processes they investigate. (*See reference [6] in the publication list below*.)

F. Enhanced Asymmetry in Few-Cycle Attosecond Pulse Ionization of He in the Vicinity of Autoionizing Resonances

By solving the two-active-electron, time-dependent Schrödinger equation in its full dimensionality, we have investigated the carrier-envelope-phase (CEP) dependence of single ionization of He to the $He^+(1s)$ state triggered by an intense few-cycle attosecond pulse with carrier frequency ω corresponding to the energy $\hbar\omega = 36$ eV. Effects of electron correlations were probed by comparing projections of the final state of the two-electron wave packet onto (i) field-free highly-correlated Jacobi matrix wave functions with (ii) projections onto uncorrelated Coulomb wave functions. Significant differences are found in the vicinity of autoionizing resonances. Owing to the broad bandwidths of our 115-as and 230-as pulses and their high intensities (1-2 PW/cm^2), asymmetries are found in the differential probability for ionization of electrons parallel and antiparallel to the linear polarization axis of the attosecond laser pulse. These asymmetries stem from interference of the one- and two-photon ionization amplitudes for producing electrons with the same momentum along the linear polarization axis. Whereas these asymmetries generally decrease with increasing ionized electron kinetic energy, we find a large enhancement of this asymmetry in the vicinity of two-electron doubly-excited (autoionizing) states on an energy scale comparable to the widths of the autoionizing states. The CEP-dependence of the energy-integrated asymmetry agrees very well with the predictions of time dependent perturbation theory [*Phys. Rev. A* **80**, 063403 (2009)]. (*See reference [7] in the publication list below*.)

G. Asymmetries in Production of $He^+(n=2)$ with an Intense Few-Cycle Attosecond Pulse

By solving the two-electron time-dependent Schrödinger equation, we studied carrier-envelope-phase (CEP) effects on ionization plus excitation of He to $He^+(n=2)$ states by a few-cycle attosecond pulse with a carrier frequency of 51 eV. For most CEPs the asymmetries in the photoelectron angular distributions with excitation of $He^+(2s)$ or $He^+(2p)$ have opposite signs and are two orders of magnitude larger than for ionization without excitation. These results indicate that attosecond pulse CEP effects may be significantly amplified in correlated two-electron ionization processes. (*See reference [8] in the publication list below*.)

FUTURE PLANS

Our group is currently carrying out research on the following additional projects:

(1) ***Potential Barrier Features in Three-Photon Ionization Processes in Atoms***

We are currently calculating an extensive set of model potential results on the frequency dependence of three-photon ionization cross sections from inner subshells of rare gas and other closed-shell atoms.

These results show that the potential barrier effects we discovered for two-photon ionization processes in the XUV regime [1] persist also for three-photon processes. We have used third order perturbation theory in the X-ray field and sum intermediate states using the well-known Dalgarno-Lewis method (A. Dalgarno and J.T. Lewis, *Proc. R. Soc. A* **233**, 70 (1955)). When one or more photons are above threshold, we employ a complex coordinate rotation method to calculate the three-photon amplitude (B. Gao and A.F. Starace, *Computers in Physics* **1**, 70 (1987)).

(2) Carrier-Envelope-Phase-Induced Asymmetries in Double Photoionization of He by an Intense Few-Cycle XUV Pulse

We have carried out an analytic parametrization of double ionization of He by an intense few-cycle attosecond pulse in terms of the pulse polarization and carrier-envelope phase and the momentum vectors of the two ionized electrons.

(3) High-Order Harmonic Generation of Be in the Multiphoton Regime

We have discovered a novel plateau structure in the harmonic generation spectrum of Be despite being well in the multiphoton regime, so that rescattering is not involved.

PUBLICATIONS STEMMING FROM DOE-SPONSORED RESEARCH (2010 – 2013)

[1] L.-W. Pi and A.F. Starace, "Potential Barrier Effects in Two-Photon Ionization Processes," *Phys. Rev. A* **82**, 053414 (2010).

[2] J.M. Ngoko Djiokap and A.F. Starace, "Evidence of the $2s2p(^1P)$ Doubly Excited State in the Harmonic Generation Spectrum of He," *Phys. Rev. A* **84**, 013404 (2011).

[3] E.A. Pronin, A.F. Starace, and L.-Y. Peng, "Perturbation Theory Analysis of Ionization by a Chirped, Few-Cycle Attosecond Pulse," *Phys. Rev. A* **84**, 013417 (2011).

[4] M. Xu, L.-Y. Peng, Z. Zhang, Q. Gong, X.-M. Tong, E.A. Pronin, and A. F. Starace, "Attosecond Streaking in the Low-Energy Region as a Probe of Rescattering," *Phys. Rev. Lett.* **107**, 183001 (2011).

[5] Z. Zhang, L.-Y. Peng, M.-H. Xu, A. F. Starace, T. Morishita, and Q. Gong, "Two-Photon Double Ionization of Helium: Evolution of the Joint Angular Distribution with Photon Energy and Two-Electron Energy Sharing," *Phys. Rev. A* **84**, 043409 (2011).

[6] M.V. Frolov, D.V. Knyazeva, N.L. Manakov, A.M. Popov, O.V. Tikhonova, E.A. Volkova, M.-H. Xu, L.-Y. Peng, and A.F. Starace, "Validity of Factorization of the High-Energy Photoelectron Yield in Above-Threshold Ionization of an Atom by a Short Laser Pulse," *Phys. Rev. Lett.* **108**, 213002 (2012).

[7] J.M. Ngoko Djiokap, S.X. Hu, W.-C. Jiang, L.-Y. Peng, and A.F. Starace, "Enhanced Asymmetry in Few-Cycle Attosecond Pulse Ionization of He in the Vicinity of Autoionizing Resonances," *New J. Phys.* **14**, 095010 (2012). [*Published in the Focus Issue on "Correlation Effects in Radiation Fields."*]

[8] J.M. Ngoko Djiokap, S.X. Hu, W.-C. Jiang, L.-Y. Peng, and A.F. Starace, "Asymmetries in Production of $He^+(n=2)$ with an Intense Few-Cycle Attosecond Pulse," *Phys. Rev. A* **88**, 011401(R) (2013).

FEMTOSECOND AND ATTOSECOND LASER-PULSE ENERGY TRANSFORMATION AND CONCENTRATION IN NANOSTRUCTURED SYSTEMS

DOE Grant No. DE-FG02-01ER15213

Mark I. Stockman, PI

Department of Physics and Astronomy, Georgia State University, Atlanta, GA 30303

E-mail: mstockman@gsu.edu, URL: http://www.phy-astr.gsu.edu/stockman

Current year Grant Period of 2012-2013 (Publications 2011-2013)

1 Program Scope

The program is aimed at theoretical investigations of a wide range of phenomena induced by ultrafast laser-light excitation of nanostructured or nanosize systems, in particular, metal/semiconductor/dielectric nanocomposites and nanoclusters. Among the primary phenomena are processes of energy transformation, generation, transfer, and localization on the nanoscale and coherent control of such phenomena.

2 Recent Progress and Publications

Publications resulting from the grant during the period of 2011-2013 are [1-17]. During the current grant period of 2012-2013, the following articles with this DOE support have been published [9-12, 14-17]. Additionally, the following major articles are submitted during period of 2012-2013: [8, 13]. Review article [6] is currently the top download in Optics Express. Below we highlight the articles that we consider most significant.

2.1 Ultrafast Dynamic Metallization of Dielectric Nanofilms by Strong Single-Cycle Optical Fields [1]

This is a significant development and generalization of our recent work [18] on the adiabatic metallization. The system under consideration is a dielectric (or, wide-band semiconductor such as diamond, zinc oxide, or gallium nitride) film of several nanometer thickness. Nanofilms of this thickness are used, in particular, as gate oxide insulators in field-effect transistors. In Ref. [1], we have predicted a dynamic metallization effect where an *ultrafast* (single-cycle) optical pulse with a $\lesssim 1$ V/Å field causes plasmonic metal-like behavior of such a dielectric nanofilm. This manifests itself in plasmonic oscillations of polarization and a significant population of the conduction band evolving on a $\sim$1 fs time scale. These phenomena are due a combination and mutual influence of both adiabatic (reversible) and diabatic (irreversible) pathways. The underlying adiabatic phenomena are Wannier stark localization and the related formation of Wannier-Stark ladder of electronic states spaced by the Bloch oscillation frequency and the appearance of the localized states (quantum bouncers) at the surfaces of the nanofilm. In ultrafast fields, the metallization is related to anticrossing of the quantum-bouncer levels originating from the valence and conduction band. This article stimulated experimental and theoretical research published recently in Nature [15, 16].

2.2 Nanoplasmonics: The Physics behind the Application [3]

Nanoplasmonics is a relatively young science but it has already but it is reach in phenomena that lead to important applications in physics, chemistry, biomedicine, environmental monitoring and national security. In this feature article [3] in the most widely read professional physics journal, Physics Today, we have considered the fundamental phenomena of nanoplasmonics in their relation to the applications that they have inspired and are underlying.

2.3 Spaser Action, Loss Compensation, and Stability in Plasmonic Systems with Gain [4, 5]

This work deals with one of the most important problems in nanooptics and nanoplasmonics: extremely high optical losses in existing plasmonic metamaterials render them practically unusable. One of the ways proposed to mitigate or even completely eliminate those losses is based on adding a gain medium and using quantum amplification to compensate those looses [19, 20]. This approach is based on our idea of spaser [21-23]. We have developed [4, 5] a general analytical theory of the loss compensation in dense resonance metamaterials, which all the existing optical metamaterials are. We have demonstrated that the conditions of spaser generation and the full loss compensation in a dense resonant plasmonic-gain medium (metamaterial) are identical. Consequently, attempting the full compensation or overcompensation of losses by gain will lead to instability and a transition to a spaser state. This will limit (clamp) the inversion and lead to the limitation on the maximum loss compensation achievable. The criterion of the loss overcompensation, leading to the instability and spasing, is given in an analytical and universal (independent from system's geometry) form.

2.4 Nearfield Enhanced Electron Acceleration from Dielectric Nanospheres by Intense Few-Cycle Laser Fields [7]

This work has been inspired to a significant degree by our recent work on metallization of dielectrics by intense optical fields [1, 18]. Collective electron motion in condensed matter typically unfolds on a sub-femtosecond timescale. The well-defined electric field evolution of intense, phase-stable few-cycle laser pulses provides an ideal tool for controlling this motion. The resulting manipulation of local electric fields at nanometer spatial and attosecond temporal scales offers unique spatio-temporal control of ultrafast nonlinear processes at the nanoscale, with important implications for the advancement of nanoelectronics. In this article [7] we have demonstrated the attosecond control of the collective electron motion and directional emission from isolated dielectric (SiO_2) nanoparticles with phase-stabilized few-cycle laser fields. A novel acceleration mechanism leading to the ejection of highly energetic electrons is identified by the comparison of the results to quasi-classical model calculations. The observed lightwave control in nanosized dielectrics has important implications for other material groups, including semiconductors and metals.

2.5 Optical-Field-Induced Current in Dielectrics [15]

The time it takes to switch on and off electric current determines the rate at which signals can be processed and sampled in modern information technology. Field-effect transistors are able to control currents at frequencies beyond ~100 GHz, but electric interconnects hamper progress towards the terahertz (THz) frontier. In reality, charging of these interconnects limits processor speed to 2-4 GHz only. All-optical injection of currents via interfering photo-excitation pathways or photoconductive switching of THz transients has permitted controlling electric current on a subpicosecond time scale in semiconductors. Insulators have been deemed unsuitable for both concepts, because of the need for either UV light or high fields, which induce either slow damage or ultrafast breakdown, respectively. In this article [15], we report the feasibility of electric signal manipulation in a dielectric. A few-cycle optical waveform increases reversibly – free from breakdown – the (ac) conductivity of amorphous silicon dioxide (fused silica) by more than 18 orders of magnitude within 1 femtosecond, allowing electric currents to be driven, directed, and switched by the *instantaneous field of light*. This work opens a route to extending electronic signal processing and high-speed metrology into the petahertz domain.

2.6 Attosecond Control of Dielectrics [16]

The control of the electric and optical properties of semiconductors with microwave fields forms the basis of modern electronics, information processing and optical communications. The extension of such control to optical frequencies calls for wideband materials such as dielectrics, which require strong electric fields to alter their physical properties. Few-cycle laser pulses permit damage-free exposure of dielectrics to electric fields of several volts per ångström and significant modifications in their electronic system.

Fields of such strength and temporal confinement can turn a dielectric from an insulating state to a conducting state within the optical period. However, to extend electric signal control and processing to light frequencies depends on the feasibility of reversing these effects approximately as fast as they can be induced. In this article [16], we study the underlying electron processes with sub-femtosecond solid-state spectroscopy, which reveals the feasibility of manipulating the electronic structure and electric polarizability of a dielectric reversibly with the electric field of light. We irradiated a dielectric (fused silica) with a waveform-controlled near-infrared few-cycle light field of several volts per ångström and probed changes in extreme-ultraviolet absorptivity and near-infrared reflectivity on a timescale of approximately a hundred attoseconds to a few femtoseconds. The field-induced changes follow, in a highly nonlinear fashion, the turn-on and turn-off behavior of the driving field, in agreement with the predictions of a quantum mechanical model developed in the article. The ultrafast reversibility of the effects implies that the physical properties of a dielectric can be controlled with the electric field of light, offering the potential for petahertz-bandwidth signal manipulation.

2.7 Theory of Dielectric Nanofilms in Strong Ultrafast Optical Fields [9]

We have theoretically predicted that a dielectric nanofilm subjected to a normally incident strong but ultrashort (a few optical oscillations) laser pulse exhibits deeply nonlinear (nonperturbative) optical responses which are essentially reversible and driven by the instantaneous optical field. Among them is a high optical polarization and a significant population of the conduction band, which develop at the peak of the pulse and almost disappear after its end. There is also a correspondingly large increase of the pulse reflectivity. These phenomena are related to Wannier-Stark localization and anticrossings between the Wannier-Stark ladders originating from the valence and conduction bands leading to optical "softening" of the dielectric. Theory is developed by solving self-consistently the Maxwell equations and the time-dependent Schrödinger equation. The results point out to a fundamental possibility of optical-field effect devices with the bandwidth on the order of optical frequency.

3 Directions of Work for the Next Period

We will develop the present success in the optics of ultrastrong and ultrafast fields on the nanoscale. We will extend the existing theory to metals and semimetals, graphene in particular. We will invoke more realistic models for the crystal structure of the materials involved, in particular using tight-binding model with experimentally known geometry of the unit cell. We will extend theory to describe photoelectron emission caused by the strong ultrashort pulses and probe attosecond XUV pulses. In ultrafast plasmonics, we will study properties of the spaser with electric pumping trough quantum wires. We will examine ultrafast dynamics of such spasers, which stems from their extreme nanoscale sizes.

References

1. M. Durach, A. Rusina, M. F. Kling, and M. I. Stockman, *Predicted Ultrafast Dynamic Metallization of Dielectric Nanofilms by Strong Single-Cycle Optical Fields*, Phys. Rev. Lett. **107**, 086602-1-5 (2011).
2. I.-Y. Park, S. Kim, J. Choi, D.-H. Lee, Y.-J. Kim, M. F. Kling, M. I. Stockman, and S.-W. Kim, *Plasmonic Generation of Ultrashort Extreme-Ultraviolet Light Pulses*, Nat. Phot. **5**, 677-681 (2011).
3. M. I. Stockman, *Nanoplasmonics: The Physics Behind the Applications*, Phys. Today **64**, 39-44 (2011).
4. M. I. Stockman, *Spaser Action, Loss Compensation, and Stability in Plasmonic Systems with Gain*, Phys. Rev. Lett. **106**, 156802-1-4 (2011).
5. M. I. Stockman, *Loss Compensation by Gain and Spasing*, Phil. Trans. R. Soc. A **369**, 3510-3524 (2011).
6. M. I. Stockman, *Nanoplasmonics: Past, Present, and Glimpse into Future*, Opt. Express **19**, 22029-22106 (2011).

7. S. Zherebtsov, T. Fennel, J. Plenge, E. Antonsson, I. Znakovskaya, A. Wirth, O. Herrwerth, F. Suessmann, C. Peltz, I. Ahmad, S. A. Trushin, V. Pervak, S. Karsch, M. J. J. Vrakking, B. Langer, C. Graf, M. I. Stockman, F. Krausz, E. Ruehl, and M. F. Kling, *Controlled near-Field Enhanced Electron Acceleration from Dielectric Nanospheres with Intense Few-Cycle Laser Fields*, Nature Physics **7**, 656-662 (2011).
8. V. Apalkov and M. I. Stockman, *Metal Nanofilm in Strong Ultrafast Optical Fields*, arXiv:1209.2245 [cond-mat.mes-hall], 1-5 (2012).
9. V. Apalkov and M. I. Stockman, *Theory of Dielectric Nanofilms in Strong Ultrafast Optical Fields*, Phys. Rev. B **86**, 165118-1-13 (2012).
10. S. H. Chew, F. Sussmann, C. Spath, A. Wirth, J. Schmidt, S. Zherebtsov, A. Guggenmos, A. Oelsner, N. Weber, J. Kapaldo, A. Gliserin, M. I. Stockman, M. F. Kling, and U. Kleineberg, *Time-of-Flight-Photoelectron Emission Microscopy on Plasmonic Structures Using Attosecond Extreme Ultraviolet Pulses*, Appl. Phys. Lett. **100**, 051904-4 (2012).
11. D. Li and M. I. Stockman, *Electric Spaser in the Extreme Quantum Limit*, arXiv:1211.0366 [cond-mat.mes-hall], 1-5 (2012).
12. A. Schiffrin, T. Paasch-Colberg, N. E. Karpowicz, V. Apalkov, D. Gerster, S. Mühlbrandt, M. Korbman, M. Schultze, S. Holzner, J. Reichert, J. Barth, R. Kienberger, R. Ernstorfer, V. Yakovlev, M. I. Stockman, and F. Krausz, in Laser Science (LS), *Subfemtosecond Photoconductive Switching in Dielectrics* (Optical Society of America, Rochester, NY (USA), 2012), p. LW4H.3.
13. V. Apalkov and M. I. Stockman, *Graphene Spaser*, arXiv:1303.0220 [cond-mat.mes-hall], 1-5 (2013).
14. D. Li and M. I. Stockman, *Electric Spaser in the Extreme Quantum Limit*, Phys. Rev. Lett. **110**, 106803-1-5 (2013).
15. A. Schiffrin, T. Paasch-Colberg, N. Karpowicz, V. Apalkov, D. Gerster, S. Muhlbrandt, M. Korbman, J. Reichert, M. Schultze, S. Holzner, J. V. Barth, R. Kienberger, R. Ernstorfer, V. S. Yakovlev, M. I. Stockman, and F. Krausz, *Optical-Field-Induced Current in Dielectrics*, Nature **493**, 70-74 (2013).
16. M. Schultze, E. M. Bothschafter, A. Sommer, S. Holzner, W. Schweinberger, M. Fiess, M. Hofstetter, R. Kienberger, V. Apalkov, V. S. Yakovlev, M. I. Stockman, and F. Krausz, *Controlling Dielectrics with the Electric Field of Light*, Nature **493**, 75-78 (2013).
17. M. I. Stockman, *Spaser, Plasmonic Amplification, and Loss Compensation*, in *Active Plasmonics and Tuneable Plasmonic Metamaterials*, edited by A. V. Zayats and S. Maier (John Wiley and Sons, Hoboken, NJ, 2013).
18. M. Durach, A. Rusina, M. F. Kling, and M. I. Stockman, *Metallization of Nanofilms in Strong Adiabatic Electric Fields*, Phys. Rev. Lett. **105**, 086803-1-4 (2010).
19. V. M. Shalaev, *Optical Negative-Index Metamaterials*, Nat. Phot. **1**, 41-48 (2007).
20. S. Xiao, V. P. Drachev, A. V. Kildishev, X. Ni, U. K. Chettiar, H.-K. Yuan, and V. M. Shalaev, *Loss-Free and Active Optical Negative-Index Metamaterials*, Nature **466**, 735-738 (2010).
21. D. J. Bergman and M. I. Stockman, *Surface Plasmon Amplification by Stimulated Emission of Radiation: Quantum Generation of Coherent Surface Plasmons in Nanosystems*, Phys. Rev. Lett. **90**, 027402-1-4 (2003).
22. M. I. Stockman and D. J. Bergman, *Surface Plasmon Amplification by Stimulated Emission of Radiation (Spaser) [US Patent 7,569,188],* USA Patent No. 7,569,188 (August 4, 2009).
23. M. I. Stockman, *The Spaser as a Nanoscale Quantum Generator and Ultrafast Amplifier*, Journal of Optics **12**, 024004-1-13 (2010).

Laser-Produced Coherent X-Ray Sources

Donald Umstadter, Department of Physics and Astronomy, 257 Behlen Laboratory, University of Nebraska, Lincoln, NE 68588-0111, donald.umstadter@unl.edu

Program Scope

The development of x-ray synchrotrons has transformed x-ray science. The latest generation of synchrotrons, x-ray free-electron-lasers, is now transforming ultrafast x-ray science. As part of our DOE-funded project, we developed a novel all-laser-driven x-ray synchrotron light source,[1] which, like an x-ray free-electron-laser, can produce femtosecond-duration x-ray pulses, and thus enable spatial and temporal resolutions that are simultaneously on the atomic scalelength.

This table-top light source currently produces quasi-monoenergetic, and tunable hard x-ray beams (50 keV $\leq$ $h\nu \leq$ 7 MeV), which have high-brightness and low-divergence angle (10 mrad). The source is based on the mechanism of Thomson (or inverse-Compton) back-scattering of intense laser light from a laser-accelerated electron beam. One near-term objective is to adapt the current x-ray source characteristics for use in ultrafast studies. We will first tune the x-ray photon energy to the sub-angstrom range (10 to 100 keV) and then measure the x-ray pulse duration (predicted to be < 10 fs). Numerical modeling will be employed to simulate expected results, guide experimental design, and be used to compare experiment with theory.

Another objective of this program is to equip the source with a user end-station configured for pump-probe experiments. An advantage of an all-laser-driven source is that its component pulses, x-rays, electrons, and optical photons, are all femtosecond in duration, and all synchronized to the same clock. Thus, any of these pulses can function as either pump or probe with minimal time jitter. Laser light will be used for the pump, and x-ray light for the probe. Transient changes to the diffraction efficiency will be resolved on the 10-fs timescale in order to identify novel physical mechanisms in the interactions of light with matter.

The all-laser-driven x-ray synchrotron has an additional advantage, in that it can ultimately be used to merge ultrafast x-ray science with high-field science. Its femtosecond x-rays can be combined with ultrahigh intensity light (up to 10^{22} W/cm^2), from our existing petawatt-power laser, for the study of the ultrafast dynamics of extreme states of matter. For instance, at such high intensity, atoms can be ionized to extremely high charge states (up to hydrogen-like gallium). In this case, the tightly bound electron is highly relativistic, and thus its spin, as well as its spin-coupling to the ultra-high laser fields, both play much greater roles in the interaction dynamics. The latter could be resolved on the angstrom length scale and fs time scale.

Recent Results

Ultrashort pulses of x-rays with photon energy within the range of 1 keV and 100 keV are of particular interest for the study of dynamics of atomic or molecular structures.[i] All-laser-driven Thomson x-ray sources are good candidates for such studies since they can achieve pulse durations as low as a few fs. In a counter-propagation geometry, the x-ray pulse duration is determined by that of the electron pulse.[ii,iii]

In Compton scattering, the x-ray energy scales as $E_\gamma = 4\gamma^2 E_L$, where γ is the electron relativistic factor, and E_L is the laser photon energy. In order to generate 10 keV to 100 keV x-rays with 800-nm laser light

(E_L =1.5 eV), an electron beam with energy ranging from 20 MeV to 65 MeV is required. We currently generate, by means of laser-wakefield acceleration, stable and monoenergetic electron beams with central energy in 50-300 MeV range. For this project, a series of experiments were conducted at the lower end of the electron beam range, and the resulting x-rays were measured.

Experimental characterization of the x-ray light source

Synchronized high-intensity laser pulses

Both of the required laser pulses, one to drive the electron accelerator, and one for Compton scattering, were generated from the same laser system: Diocles, at the University of Nebraska, Lincoln. The 1.9-J, 35-fs drive laser pulse was focused by a 1-m focal length parabolic reflector onto a 2-mm supersonic gas target (mixture of 99% helium and 1% nitrogen) with a Gaussian full-width half maximum (FWHM) focal spot size of 20 μm. Thirty-three percent of the laser energy of the driven pulse was enclosed in the FWHM width, and it corresponded to a peak intensity of 7.4×10^{18} W/cm^2 (normalized vector potential of $a_0 = 1.9$). The plasma density of the target was 1.0×10^{19}/cm^3.

Electron accelerator

The laser wakefield accelerator was operated in the ionization-injected, self-guided, and bubble regime. The energy and the charge of the *e*-beam were measured with a magnetic spectrometer, consisting of a calibrated LANEX screen, and imaged by a 12-bit CCD camera on every shot. The electron beam is optimized in the experiment, in terms of energy and charge, by controlling both the plasma density and the focal position of the driving laser beam (relative to the gas target). Electron beams were produced with cut-off energy ~250 MeV, and total integrated charge of ~0.1 nC (for energies > 50 MeV).[2,3]

Counter-propagating Compton-scattering geometry

The 0.5-J, 90-fs scattering laser beam was focused by a 1-m focal length lens. The measured focal spot was 22 μm FWHM (RMS spot size σ_L = 9 μm) with 16% of its energy enclosed in the FWHM width, corresponding to a peak focused intensity of 3.4×10^{17} W/cm^2 (a_0 = 0.4). The scattering laser beam counter-propagates at an angle of Φ=170° (in the horizontal plane) to the *e*-beam. The interaction point was located in the vacuum region 1-mm downstream from the exit of the laser plasma accelerator.

X-ray beam measurements

To detect and characterize the high energy x-ray beam generated in this experiment with optimal response and high spatial resolution, we used a CsI-crystal scintillator, which consisted of a 1-cm deep, 40×40 array of 1.0×1.0×10-mm "voxels" (3D pixels), with a 0.2-mm epoxy layer between voxels. The CsI(Tl) scintillator, which was imaged by a CCD camera, was placed on-axis (Φ=180°) at a distance of 1.72 m from the interaction point. The x-ray beams have a ~10-mrad divergence angle, near-circular shape, and Gaussian profile. The number of x-ray photons per shot was found to be $1.7\text{x}10^6$. The photon number, and thus photon flux, depends on three factors: scattering-laser beam intensity, degree of beam overlap, and *e*-beam charge.

X-ray spectral measurements

To characterize the x-ray spectrum, we utilized a Ross-filter measurement technique, based on the use of consecutive pairs of K-edges for a set of different materials placed in front of the pixelated CsI detector.

The x-ray spectrum was found to be Gaussian-shaped, with the central energy of 65 keV, and energy width of 50% (FWHM).

X-ray source size

Another important parameter of the x-ray source is the source size. We exploit the spatial cross-correlation technique to measure the radiation source size, in which the scattering beam focal spot was scanned vertically across the e-beam over a spatial range of 90 μm. With the measured focal spot size of the laser pulse, σ_L = 9, and width of the cross-correlation trace, the *e*-beam size was estimated, by deconvolution of the cross-correlation curve, to be σ_e =6 ± 3μm. The x-ray source size is found to be σ_x = 5 ± 3 μm.

Numerical modeling

We have also developed a fully relativistic and three dimensional inverse-Compton scattering model that calculates and quantifies radiation emitted when an intense laser pulse interacts at an arbitrary angle with a relativistic electron beam.[4] This code also takes into account the polarization (linear/circular/elliptical) of the scattering laser pulse. The electron beam is represented with a realistic 6-dimensional phase space distribution (constructed using measured electron beam parameters), and the laser pulse is described to a high degree of accuracy, exceeding the commonly used paraxial approximation.

The developed code has already been used to quantify emitted radiation in a counter-propagating geometry, and the calculations benchmarked against our recent experimental results. Recent effort has also involved implementation of co-propagating and orthogonal scattering geometries into the code, enabling the design of the future experiments and analysis.

Future Plans:

Ultrashort x-ray pulse generation

The electron bunch duration, which controls the x-ray pulse duration, can be minimized by either controlling the wakefield generation process, or by minimizing the duration of the drive-laser pulse. An upper limit on the x-ray pulse duration will be determined by means of cross-correlation between laser and electron pulses in the orthogonal scattering geometry.

Ultrafast pump-probe experiments

An x-ray beam-line end-station will be built for femtosecond diffraction studies using the all-laser synchrotron x-ray source. Extreme states of matter can be created with our petawatt (PW) laser system, and studied with femtosecond temporal resolution and sub-angstrom spatial resolution, merging high-field physics with ultrafast science. With a peak intensity of 10^{22} Wcm^{-2}, hydrogen-like atoms up to gallium can be produced through photo-ionization. The remaining tightly bound electron is highly relativistic, and the high magnetic field should have considerable effects on the dynamics. Moreover, the spin of the electron, and its coupling with the laser field, becomes important.[v, vi]

DOE-Sponsored Publications (published within last three years)

1. Chen et al., "MeV-energy x-rays from inverse Compton scattering with laser-wakefield accelerated electrons," Phys. Rev. Lett. **110**, 155003 (2013).
2. S. Banerjee et al., "Stable, tunable, quasimonoenergetic electron beams produced in a laser wakefield near the threshold for self-injection," Phys. Rev. ST Accel. Beams **16**, 031302 (2013).
3. S. Banerjee et al., "Generation of tunable, 100-800 MeV quasi-monoenergetic electron beams from a laser-wakefield accelerator in the blowout regime," Phys. Plasmas **19**, 056703 (2012).
4. I. Ghebregziabher et al., "Spectral bandwidth reduction of Thomson scattered light by pulse chirping," Rev. ST Accel. Beams **16**, 030705 (2013).
5. J. Silano et al., "Selective activation with all-laser-driven Thomson γ-rays," forthcoming in Proceedings of the 2013 *IEEE* International Conference on Technologies for Homeland Security (Waltham, MA, 2013).
6. B. M. Cowan et al., "Computationally efficient methods for modeling laser wakefield acceleration in the blowout regime," J. Plasma Phys. **78**, 469 (2012).
7. S. Y. Kalmykov et al., "Electron self-injection into an evolving plasma bubble: quasi-monoenergetic laser-plasma acceleration in the blowout regime," Phys. Plasmas **18**, 056704 (2011).
8. V. Ramanathan et al., "Submillimeter-resolution radiography of shielded structures with laser-accelerated electron beams," Phys. Rev. Spec. Top.- Accel. Beams **13,** 104701 (2010).

DOE-Sponsored Publications (under review)

9. C. Liu et al., "Adaptive-feedback spectral-phase control for interactions with transform-limited ultra-short high-power laser pulses," Opt. Lett. (In review 9/2/2013).
10. N. D. Powers et al., "Tunable and quasi-monoenergetic x-rays from a laser-driven Compton light source," Nature Photonics (In review 6/3/2013).

---

[i] L. X. Chen, "Probing transient molecular structures in photochemical processes using laser-initiated time-resolved X-ray absorption spectroscopy," Annu. Rev. Phys. Chem. **56**, 221 (2005).

[ii] Alexander Buck et al., "Real-time observation of laser-driven electron acceleration," Nature Phys. **7**, 543 (2011).

[iii] O. Lundh et al., "Few femtosecond, few kiloampere electron bunch produced by a laser-plasma accelerator," Nature Phys. **7,** 219 (2011).

[iv] I. Ghebregziabher et al., "Spectral bandwidth reduction of Thomson scattered light by pulse chirping," Phys. Rev. ST Accel. Beams **16**, 030705 (2013).

[v] F. M. H. Faisal and S. Bhattacharya, "Spin assymetry in intense field ionization process," Phys. Rev. Lett. **93**, 053002 (2004).

[vi] R. Santra et al., "Spin orbit effect on the strong field ionization of Krypton," Phys. Rev. A **74**, 043403 (2006).

New scientific frontiers with ultracold molecules

Jun Ye

JILA, NIST and University of Colorado

PROGRAM SCOPE

In a March 2013 PRL paper, we reported the first realization of a two-dimensional magneto-optical trapping for molecules. Currently our group is collaborating with John Doyle's group at Harvard to work on the implementation of a fully three dimensional MOT for molecules. Of course we know that the development of atomic magneto-optical traps revolutionized the field of atomic and quantum physics by providing a simple method for the rapid production of ultracold atoms. A similar breakthrough for molecules will have a huge impact to a diverse set of fields including quantum physics, condensed matter, precision measurement, and physical chemistry. We have currently prepared a slow YO molecule beam of 60 m/s , which will be cooled and loaded into a 3D MOT.

On the front of dipolar molecules in the quantum regime, we have recently realized a lattice spin model. We use two rotational states of the molecules to encode spin, and we pin the molecules in a deep 3D optical lattice. This system is in stark contrast to previous work with atomic lattices, where pinning the atoms turns off all spin-exchange interactions. For polar molecules, however, the long-range dipolar interaction allows the spin dynamics to be decoupled from motion. This hugely relaxes the requirements for extremely low temperature and entropy that have plagued attempts to realize quantum simulators for magnetism. By initializing and probing the system with microwaves that drive a coherent rotational excitation, we have observed spin-exchange interactions due to direct dipolar interactions, which manifest in a strongly density-dependent coherence time as well as in clear oscillations of the Ramsey contrast vs. time. We have also studied tunneling-induced loss for weaker lattices in order to determine the lattice filling. Here, we provide compelling evidence for the quantum Zeno effect, where increasing the on-site chemical reaction rate actually lowers the overall loss rate in the lattice.

FY 2013 HIGHLIGHTS

In a Nature paper published in September 2013 (in collaboration with Debbie Jin), we report a major step towards the experimental realization of a realistic quantum magnetism model. Polar molecules are promising candidates for realization of novel strongly interacting quantum systems. Their unique capability arises from the long-range and anisotropic dipolar interactions. We have made the first observation of this long-range dipolar interaction of polar molecules pinned in a deep three-dimensional optical lattice. Molecules located in the neighboring lattice sites can resonantly exchange their rotational angular momentum, providing a foundation for the realization of a lattice spin model to explore quantum magnetism. This work paves the ground for future explorations of many-body spin dynamics with direct and long-range spin interactions.

List of Participants

Andreas Becker
University of Colorado
440 UCB
Boulder, CO 80027
Phone: 303-492-7825

Ali Belkacem
Lawrence Berkeley National Laboratory
1 Cyclotron Road
Berkeley, CA 94720
Phone: 510-486-6382

Itzik Ben-Itzhak
Kansas State University
116 Cardwell Hall,
Department of physics, KSU
Manhattan, Kansas 66506
Phone: 785-532-1636

Nora Berrah
Western Michigan University
Physics Department
Kalamazoo, MI 49024
Phone: 269-387-4955

John Bohn
University of Colorado
UCB 440
Boulder, CO 80309
Phone: 303-492-5426

Philip Bucksbaum
SLAC National Accelarator Laboratory
2575 Sand Hill Road
Menlo Park, Ca 94025
Phone: 650-926-1726

Michael Casassa
U.S. Department of Energy
19901 Germantown Rd
Germantown, MD 20874
Phone: 301-903-0448

Martin Centurion
University of Nebraska
855 North 16th Street
Lincoln, NE 68588
Phone: 402-472-5810

Shih-I Chu
University of Kansas
Dept. of Chemistry,
Malott Hall, 1251 Wescoe Hall Drive,
Room 2010
Lawrence, Kansas 66045
Phone: 785-864-4094

Lew Cocke
Kansas State University
Physics Departmen, Kansas State Univ.
Manhattan, KS 66506
Phone: 785-532-1609

Robin Côté
University of Connecticut
2152 Hillside Road, U-3046
Storrs, CT 06269
Phone: 860-486-4912

Steven Cundiff
University of Colorado
440 UCB
Boulder, CO 80309
Phone: 303-417-0586

Marcos Dantus
Michigan State University
578 S. Shaw Lane, Room 58
East Lansing, MI 48824
Phone: 517-355-9715 x314

Matthew DeCamp
University of Delaware
217 Sharp Lab
Newark, DE 19716
Phone: 302-831-2671

David DeMille
Yale University
PO Box 208120
New Haven, CT 06520
Phone: 203-432-3833

Louis DiMauro
Ohio State University
Physics Bldg. 191 W. Woodruff Ave
Columbus, OH 43210
Phone: 614-688-5726

Todd Ditmire
University of Texas
2515 Speedway Stop C1600
Austin, TX 78712
Phone: 512-471-3296

Gilles Doumy
Argonne National Laboratory
9700 S. Cass Ave.
Argonne, Illinois 60439
Phone: 630-252-2588

John Doyle
Harvard University
17 Oxford Street
Cambridge, MA 02138
Phone: 617-945-4250

Robert Dunford
Argonne National Laboratory
9700 S. Cass Ave
Lemont, IL 60439
Phone: 630-252-4052

Joseph Eberly
University of Rochester
600 Wilson Blvd.
Rochester, NY 14627
Phone: 585-275-4351

Veit Elser
Department of Physics
524 Clark Hall
Cornell University
Ithaca, NY 14853
Phone: 607-255-2340

Brett Esry
Kansas State University
116 Cardwell Hall
Manhattan, KS 66506
Phone: 785-532-1620

Roger Falcone
Lawrence Berkeley National Laboratory
One Cyclotron Road, MS:80R0114
Berkeley, CA 94720
Phone: 510-486-6692

Jim Feagin
California State University
325 Dover Ave
Brea, CA 92821
Phone: 714-504-7581

Christopher Fecko
U.S. Department of Energy
19901 Germantown Rd
Germantown, MD 20874
Phone: 301-903-1303

Mette Gaarde
Louisiana State University
Dept of Phys & Astronomy, LSU
Baton Rouge, LA 70803
Phone: 225-400-2528

Kelly Gaffney
Stanford University
2575 Sand Hill Road
Menlo Park, CA 94303
Phone: 650-926-2382

Thomas Gallagher
University of Virginia
Department of Physics
Charlottesville, VA 22904
Phone: 434-924-6817

Oliver Gessner
Lawrence Berkeley National Laboratory
1 Cyclotron Road
Berkeley, CA 94720
Phone: 510-486-6929

Phillip Gould
University of Connecticut
Physics Dept. U-3046,
2152 Hillside Rd.
Storrs, CT 06269
Phone: 860-486-2950

Chris Greene
Purdue University
Department of Physics
West Lafayette, IN 47907
Phone: (765) 496-1859

Markus Guehr
SLAC National Accelerator Laboratory
2575 Sand Hill Road
Menlo Park, CA 94025
Phone: 650-926-5550

Daniel Haxton
Lawrence Berkeley National Laboratory
1 Cyclotron Road
Berkeley, CA 94720
Phone: 510-495-2508

Robert Jones
University of Virginia
382 McCormick Road
Charlottesville, VA 22904
Phone: 434-924-3088

Elliot Kanter
Argonne National Laboratory
9700 S. Cass Ave.
Argonne, IL 60439
Phone: 908-617-1622

Henry Kapteyn
University of Colorado
440 UCB
Boulder, CO 80309
Phone: 303-492-8198

Victor Klimov
Los Alamos National Laboratory
MS-J567
Los Alamos, NM 87545
Phone: 505-665-8284

Bertold Kraessig
Argonne National Laboratory
9700 S. Cass Avenue
Argonne, Illinois 60439
Phone: 630-252-9230

Jeffrey Krause
U.S. Department of Energy
19901 Germantown Rd.
Germantown, MD 20874
Phone: 301-903-5827

Vinod Kumarappan
Kansas State University
328 Cardwell Hall
Manhattan, KS 66506
Phone: 785-532-3415

Allen Landers
Auburn University
206 Allison Lab
Auburn, AL 36849
Phone: 334-844-4048

Anh-Thu Le
Kansas State University
Department of Physics,
Kansas State University
Manhattan, Kansas 66502
Phone: 785-532-1635

Stephen Leone
University of California
209 Gilman Hall, Department of Chemistry,
University of California, Berkeley
Berkeley, CA 94720
Phone: 510-643-5467

Chii-Dong Lin
Kansas State University
2101 Hillview Dr
Manhattan, KS 66502
Phone: 785-532-1617

Robert Lucchese
Texas A&M University
Department of Chemistry
College Station, TX 77842
Phone: 979-412-0910

Stephen Lundeen
Colorado State University
Dept. of Physics , CSU
Fort Collins, CO 80523
Phone: 970-491-6647

Joseph Macek
University of Tennessee
401 Nielsen Physics Bldg.
Knoxville, TN 37996
Phone: 865-975-0770

Steven Manson
Georgia State University
Dept. of Physics & Astronomy
Atlanta, GA 30030
Phone: 404-413-6046

Diane Marceau
U.S. Department of Energy
19901 Germantown Road
Germantown, MD 20874
Phone: 301-903-0235

Anne Marie March
Argonne National Laboratory
9700 S. Cass Ave.
Argonne, Illinois 60439
Phone: 630-252-4099

Todd Martinez
SLAC National Accelerator Laboratory
2575 Sand Hill Rd
Menlo Park, CA 94025
Phone: 650-736-8860

Spiridoula Matsika
Temple University
315 New Street
Philadelphia, USA 19106
Phone: 215-204-7703

William McCurdy
University of California
One Shields Avenue
Davis, CA 95616
Phone: 520-599-7071

Vincent McKoy
California Institute of Technology
Pasadena, CA 91125
Phone: 626-437-3445

Alfred Msezane
Clark Atlanta University
223 James P Brawley Drive, SW
Atlanta, GA 30314
Phone: 404-880-8663

Shaul Mukamel
University of California
1102 Narural Sciences II
Irvine, CA 0
Phone: 949-824-7600

Margaret Murnane
University of Colorado
440 UCB
Boulder, CO 80309
Phone: 303-589-8984

Daniel Neumark
University of California
Department of Chemistry
Berkeley, CA 94720
Phone: 510-642-3502

Ann Orel
University of California
CHMS, UC Davis,
One Shields Ave.
Davis, CA 95616
Phone: 925-980-9245

Thom Orlando
Georgia Institute of Technology
901 Atlantic Drive NW
Atlanta, GA 30332
Phone: 404-385-6047

Abbas Ourmazd
University of Wisconsin
1900 E Kenwood Boulevard
Milwaukee, WI 53211
Phone: 414-229-2610

Enrique Parra
Air Force Office of Scientific Research
875 North Randolph Street, Suite 325
Arlington, VA 22203
Phone: 703-696-8571

Erwin Poliakoff
Louisiana State University
Chemistry Department
Baton Rouge, LA 70803
Phone: 225-578-2933

Herschel Rabitz
Princeton University
Frick Chemistry Laboratory,
Washington Road
Princeton, NJ 8544
Phone: 609-258-3917

David Reis
Stanford University
2575 Sand Hill Rd
Menlo Park, CA 94025
Phone: 650-926-4192

Tom Rescigno
Lawrence Berkeley National Laboratory
1 Cyclotron Rd. MS 2-100
Berkeley, CA 94720
Phone: 510-486-8652

Francis Robicheaux
Purdue University
525 Northwestern Avenue
West Lafayette, IN 47907
Phone: 765-494-3029

Jorge Rocca
Colorado State University
Fort Collins, Colorado 80523
Phone: 970-491-8371

Christoph Rose-Petruck
Brown University
324 Brook Street
Providence, RI 2912
Phone: 401-863-1533

Artem Rudenko
Kansas State University
116 Cardwell Hall
Manhattan, Kansas 66506
Phone: 785-532-4470

Norbert Scherer
University of Chicago
929 E. 57th St.
Chicago, Illinois 60637
Phone: 773-702-7069

Robert Schoenlein
Lawrence Berkeley National Laboratory
1 Cyclotron Rd. MS: 80-114
Berkeley, CA 94720
Phone: 510-486-6557

Tamar Seideman
Department of Chemistry
Northwestern University
2145 Sheridan Road
Evanston, IL 60208-3113
Phone: 847-467-4979

Gerald Seidler
University of Washington
1644 21st Ave
Seattle, Washington 98122
Phone: 206-427-8045

Steve Southworth
Argonne National Laboratory
Bldg 401
Argonne, IL 60439
Phone: 630-252-3894

Claudiu Stan
Stanford University
2575 Sand Hill Road
Menlo Park, California 94025
Phone: 650-926-5306

Anthony F. Starace
University of Nebraska
855 North 16th Street,
208 Jorgensen Hall
Lincoln, Nebraska 68588
Phone: 402-472-2795

Mark Stockman
Georgia State University
29 Peachtree Center Ave
Atlanta, GA 30303
Phone: 678-457-4739

Uwe Thumm
Kansas State University
Department of Physics
Manhattan, KS 66506
Phone: 785-532-1613

Carlos Trallero
Kansas State University
116 Cardwell Hall
Manhatan, KS 66503
Phone: 785-532-0846

Donald Umstadter
University of Nebraska
500 Stadium Dr. Rm. 257
Lincoln, NE 68588
Phone: 402-472-8115

Thorsten Weber
Lawrence Berkeley National Laboratory
1 Cyclotron Road
Berkeley, CA 94720
Phone: 510-486-5588

Thomas Weinacht
Stony Brook University
Dept of Physics and Astronomy
Stony Brook, NY 11776
Phone: 631-632-8163

Jun Ye
University of Colorado
JILA, 440 UCB, University of Colorado
Boulder, Colorado 80309
Phone: 303-735-3171

Linda Young
Argonne National Laboratory
9700 S. Cass Ave
Argonne, IL 60439
Phone: 630-252-8878